

Lecture Notes in Civil Engineering

Osman Gencel
M. Balasubramanian
T. Palanisamy *Editors*

Sustainable Innovations in Construction Management

Select Proceedings of ICC-IDEA 2023

 Springer

Lecture Notes in Civil Engineering

Volume 388

Series Editors

Marco di Prisco, Politecnico di Milano, Milano, Italy

Sheng-Hong Chen, School of Water Resources and Hydropower Engineering,
Wuhan University, Wuhan, China

Ioannis Vayas, Institute of Steel Structures, National Technical University of
Athens, Athens, Greece

Sanjay Kumar Shukla, School of Engineering, Edith Cowan University, Joondalup,
WA, Australia

Anuj Sharma, Iowa State University, Ames, IA, USA

Nagesh Kumar, Department of Civil Engineering, Indian Institute of Science
Bangalore, Bengaluru, Karnataka, India

Chien Ming Wang, School of Civil Engineering, The University of Queensland,
Brisbane, QLD, Australia

Zhen-Dong Cui, China University of Mining and Technology, Xuzhou, China

Lecture Notes in Civil Engineering (LNCE) publishes the latest developments in Civil Engineering—quickly, informally and in top quality. Though original research reported in proceedings and post-proceedings represents the core of LNCE, edited volumes of exceptionally high quality and interest may also be considered for publication. Volumes published in LNCE embrace all aspects and subfields of, as well as new challenges in, Civil Engineering. Topics in the series include:

- Construction and Structural Mechanics
- Building Materials
- Concrete, Steel and Timber Structures
- Geotechnical Engineering
- Earthquake Engineering
- Coastal Engineering
- Ocean and Offshore Engineering; Ships and Floating Structures
- Hydraulics, Hydrology and Water Resources Engineering
- Environmental Engineering and Sustainability
- Structural Health and Monitoring
- Surveying and Geographical Information Systems
- Indoor Environments
- Transportation and Traffic
- Risk Analysis
- Safety and Security

To submit a proposal or request further information, please contact the appropriate Springer Editor:

- Pierpaolo Riva at pierpaolo.riva@springer.com (Europe and Americas);
- Swati Meherishi at swati.meherishi@springer.com (Asia—except China, Australia, and New Zealand);
- Wayne Hu at wayne.hu@springer.com (China).

All books in the series now indexed by Scopus and EI Compendex database!

Osman Gencel · M. Balasubramanian ·
T. Palanisamy
Editors

Sustainable Innovations in Construction Management

Select Proceedings of ICC-IDEA 2023

 Springer

Editors

Osman Gencil
Bartın University
Bartın, Türkiye

M. Balasubramanian
SRM Institute of Science and Technology
Kattankulathur, Tamil Nadu, India

T. Palanisamy
National Institute of Technology Karnataka
Mangalore, India

ISSN 2366-2557

ISSN 2366-2565 (electronic)

Lecture Notes in Civil Engineering

ISBN 978-981-99-6232-7

ISBN 978-981-99-6233-4 (eBook)

<https://doi.org/10.1007/978-981-99-6233-4>

© The Editor(s) (if applicable) and The Author(s), under exclusive license to Springer Nature Singapore Pte Ltd. 2024

This work is subject to copyright. All rights are solely and exclusively licensed by the Publisher, whether the whole or part of the material is concerned, specifically the rights of translation, reprinting, reuse of illustrations, recitation, broadcasting, reproduction on microfilms or in any other physical way, and transmission or information storage and retrieval, electronic adaptation, computer software, or by similar or dissimilar methodology now known or hereafter developed.

The use of general descriptive names, registered names, trademarks, service marks, etc. in this publication does not imply, even in the absence of a specific statement, that such names are exempt from the relevant protective laws and regulations and therefore free for general use.

The publisher, the authors, and the editors are safe to assume that the advice and information in this book are believed to be true and accurate at the date of publication. Neither the publisher nor the authors or the editors give a warranty, expressed or implied, with respect to the material contained herein or for any errors or omissions that may have been made. The publisher remains neutral with regard to jurisdictional claims in published maps and institutional affiliations.

This Springer imprint is published by the registered company Springer Nature Singapore Pte Ltd. The registered company address is: 152 Beach Road, #21-01/04 Gateway East, Singapore 189721, Singapore

Paper in this product is recyclable.

Contents

Construction Engineering and Management

Comprehensive Review on Recycled Aggregate Concrete Using Scientometric Analysis Approach	3
Anmol Basnett, Anandh Sekar, and S. Sindhu Nachiar	
Performance of Concrete by the Addition of Bio-Cement on Ultrasonic Pulse Velocity	13
K. Chandramouli, R. Santhi Kala, and N. Pannirselvam	
Effects of Staggered Openings on Response Reduction Factor of Frames with Shear Wall	21
C. V. Samyuktha and T. M. Jeyashree	
Load-Bearing Masonry: A Review of FE Numerical Analysis Approach	31
Piyushkumar Vachhani, Payal Desai, and Nirav Patel	
Comparison of Reinforced Cement Concrete Versus Steel Structures in Health Industry	43
R. Kavitha, V. Rajeshkumar, S. Sabarinathan, V. Vijai Anand, and J. Ajithkumar	
Experimental Investigation on Concrete by Partial Replacement of Fine Aggregate with Olivine Sand	51
G. Akash Kanna and N. Parthasarathi	
Optimum Study of Friction Pendulum Isolated Building in Response Mitigation under Near Fault Excitation	63
Dasari Sreeman and Bijan Kumar Roy	
Flexural Behaviour of Cold-Formed Steel Built-Up Beams Using Sigma and Channel Sections	75
C. Manoj Kumaar, Venus David Rayan, K. Govarthini, Nemat Bano, Marnadu Dinesh Kumar, and M. Saran Kumar	

Evaluation of Surface-Coated Recycled Coarse Aggregate in Concrete Using Alccofine	89
J. Rajprasad, Akshaya ram, and Jeeva Prasanth	
Analysis and Experimental Feasibility Study on Bio-mimicked Non-developable Shell Model	103
Nelson Takhellambam and K. S. Satyanarayanan	
Composite Behavioural Study on GI Wire Mesh and PVA Fibre Reinforced Concrete Slabs	119
S. Govindasami and S. Inthumathi	
Review on Partially Replacement of Cement with Industrial Waste in Manufacturing of Concrete and Bricks	125
R. Akash Nevel, R. Dinesh Kumar, and M. Surendar	
Effect of Slope, Cross-Section of Pile and Eccentricity in Calculating the Modulus of Laterally Loaded Single Pile	135
S. V. Sivapriya	
Investigation on Plastic Hinge in Non-prismatic Beam with Circular Openings	143
Venumadhav Guligari, C. Arunkumar, and N. Umamaheswari	
Analysis of Ergonomics Risk During Plastering in Construction Sites	159
Aleena Josey, M. S. Ameer Suhail, Nazneen Niyas, and Sahimol Eldhose	
Quality Assessment of Building and Infrastructure Project Using Taguchi Methodology	169
D. Harish, S. Manikandaprabhu, S. Prakash Chandar, and N. Pavithra	
Constructive Project Management System in Construction Industry	183
R. Balamurugan, R. Sivakumar, K. Srinivasan, Ravi sankar, and M. Anand	
Scheduling Time and Cost by Integrating Quality and Risk in Construction Projects	191
N. Sai Krishna and S. M. Renuka	
Flexural Behavior of Reinforced Beam Mixed with Copper Slag and Jute Fiber	203
V. Swaminathan, R. Ramasubramani, P. T. Ravichandran, and Rakshit Srivastava	
An Ergonomic Risk Evaluation of the Construction Industry Based on Specific Factors	217
G. Nakkeeran, V. Kamala, and L. Krishnaraj	

Urban Planning and Design

Structural Analysis and Design of Solar Car Park in College of Engineering-Dawadmi: A Move Toward Energy Efficient Campus 229
 Mohammad Abdur Rasheed and Yazeed Saud Alotaibi

Development of Sustainable Earthquake Resistant Building for Future Generations 239
 V. Chandrikka and D. Shoba Rajkumar

Study on Risk Allotment for Public Private Partnership in Indian Infrastructure 251
 S. Vedha Varshini, S. Anandh, S. Sindhu Nachiar, and B. Hemanth Sai Kalyan

Adopting the Low-Cost Housing Technology in Residential Buildings in Chennai 259
 K. T. Murali Krishnan, S. Manikandaprabhu, and D. Nigitha

Building Energy Conservation and Green Architecture

Seismic Response Control Strategies for Buildings 271
 J. Jestalt Srisanth, G. V. Rama Rao, and D. Senthil Velan

Study on Sustainable Building Materials to Develop Block for Net Zero Carbon Building 281
 Abishek Rauniyar and L. Krishnaraj

Green Building Rating Systems: A Comparative Study of Global and Indian Standards 293
 K. S. Anandh, M. G. Soundarya Priya, S. Senthamizh Sankar, and K. Prasanna

Integrating BIM with Energy Analysis and Green Building Certification System to Design Sustainable Building 303
 G. S. Mahaaraja and S. M. Renuka

Cost-Benefit Analysis of Adoption of Green Materials in Conventional Building to Improve Green Rating 317
 Srihari Vedartham, J. S. Sudarsan, Vijay Narayan, K. Prasanna, and S. Mohanakrishna

Impacts of Natural Disasters on the Performance of Residential Construction Projects of Kashmir, J&K 325
 J. Rajprasad and Hilal Ahmad Wani

Quantifying the Trends and Impacts of Solid Waste Generation in Chennai City: A Study of Current Management Practices and Future Needs	337
E. Mugesesh and D. Justus Reymond	
A Path Towards Sustainable Transport Research and Policy: A Case Study from Metropolitan City in India	345
Ali Shkera and Vaishali Patankar	
Scientometric Analysis of Building Energy Analysis in the Construction During 2005–2022	353
G. Nakkeeran and L. Krishnaraj	
Impact of Green Construction Management Study on the Quality of G+6 Offices Building at Kochi, Kerala	361
Balasubramanian Murugesan	
Materials Science and Engineering	
Regression Analysis on the Behaviour of Thin Spherical Shells with Various Parameters	375
G. Pennarasi, S. Sindhu Nachiar, and S. Anandh	
Parametric Study of Steel Pipe rack	385
Jatan Patel, Aditi Sheth, and Yogesh Kulkarni	
Experiment Investigation of Protecting the R.C. Structure from Heat Exposure by Using Composite Materials	397
K. Sandhya, S. Barath Raj, and S. Muthu Kumar	
The Impact of Glass Fiber on Controlled Permeable Formwork Self-Compacting Concrete	409
S. Kandasamy, S. Syed Ibrahim, and N. Pannirselvam	
Ramifications of Payment Delays on Contractors in the Construction Industry	421
B. Hemanth Sai Kalyan, S. Anandh, and S. Sindhu Nachiar	
Mechanical Properties and Microstructural Analysis of Banana Stem Fibre in M40 Grade Concrete	429
S. Prakash Chandar, D. Murugan, and R. Ramasubramani	
Comparative Study on the Performance of RC Frame Multistorey with Three Different FRP Reinforcements	445
Raj Dhruvkishor Patil and N. Pannirselvam	
Analytical Study of Plastic Hinge Formation in Beams Strengthened with CFRP Sheets	459
Anand Mehta, R. Ravi, and S. Sivakamasundari	

Influence of Basalt Fiber and Slag on the Moduli of Elasticity of Fine-Grained Concrete 469
 Alein Jeyan Sudhakar and Bhuvaneshwari Muthusubramanian

Analytical Investigation of Cold-Formed Steel Build-Up Sigma-Shaped Section 481
 A. Yogesh Kumar and S. A. Vengadesh Subramanian

Innovation in Construction Materials

A Novel XGBoost and RF-Based Metaheuristic Models for Concrete Compression Strength 495
 Manish Kumar, N. Zainab Fathima, and Divesh Ranjan Kumar

Analytical Study on 3D-Printed Concrete Wall with Different Wall Configurations When Exposed to High Temperature 505
 B. Vignesh and N. Parthasarathi

Seismic Response Analysis of Reinforced Concrete Chimneys with Tuned Mass Damper 517
 Ashish Kumar Gupta, Sudhir Singh Bhadauria, and Aruna Rawat

Experimental Study on the Mechanical Properties of the Agro Waste as a Partial Replacement of the Binder Material 527
 S. Vighash and L. Sabarigirivasan

Development of Sustainable Bricks by Industrial By-Product 539
 Harresh Jagadeesan, R. Balaraman, and G. Senthil Kumar

Experimental Investigation and Comparative Study on Self-healing Concrete with Superabsorbent Polymer and Bacteria 549
 R. Kaviraja, N. Ganapathy Ramasamy, R. Suriyapakash, S. Prakash Chandar, and A. Siranjeevinathan

An Effective Approach on Implementation of Scrum in the Construction Industry for an Increased Productivity 563
 S. Manikandaprabhu, Bommireddy Hruday Reddy, and Sachikanta Nanda

Investigation on the Mechanical Properties of Marine Algal Concrete in High Strength Concrete 575
 R. Ramasubramani, M. Murali, and P. T. Ravichandran

Feasibility Assessment on Electronic Waste (EW) as a Partial Reduction for Coarse Aggregate (CA) in Concrete 591
 R. Padmapriya, J. S. Sudarsan, N. Sunmathi, and Srihari Vedartham

Information Technology in Civil Engineering

Review of Robotics’ Role in Unsafe Site Conditions in the Construction Industry	601
Sourav Kumar, Balasubramanian Murugesan, Aishwarya Sathyanarayanan, and Mukilan Poyyamozhi	
Perception of Proposed Bridge Using Augmented Reality of BIM in Educational Institute—Case Study	613
V. Kavithanjali, A. Meenachi, and M. Soundararajan	
Machine Learning-Based Dynamic Cost Estimation Model for Construction Projects	625
Sheema Shah and S. Gopinath	
Effectiveness of Multicriteria Decision-Making for Ongoing Construction Projects—AHP Method	635
S. Antony Kevin and A. Arokiaprakash	
House Price Prediction in Southern Chennai Using Machine Learning Algorithms	645
J. Prasanna Kumar, M. B. Sridhar, R. Sathyanathan, and B. Divya	
Access the Prospect of Automation in Inventory Management of Construction Projects	657
B. Pavan Kumar and A. Arokiaprakash	

About the Editors

Dr. Osman Gencel is working as a professor in the Civil Engineering Department faculty of Engineering, Architecture, and Design Bartın University, 74100 Bartın, Turkey. He graduated B.Sc. at Firat University, a Master's from Afyoun Kocatepe University, a Ph.D. at Suleyman Demirel University, a Ph.D. in Studies, and a Post-doctorate from the University of North Texas. He listed the world's top 2% of scientists as 275 in 2020, 174 in 2021, and 117 in 2022 at Stanford University. According to Web of Science, he had an H-index of 33. He has research interests in cement-based composites, foam concrete, lightweight concrete, radiation shielding concrete, polymer concrete, geopolymers, fiber-reinforced concrete, mortar, Gypsum-based composites, phase change materials, energy storage, smart buildings, recycling and sustainability, 3D printing concrete, and nanomaterials. He had published more than 170 papers in SCI and SCI-E journals and published 5 books and has duties in 4 respective scientific journals.

Dr. M. Balasubramanian has fourteen years of diverse experience in academics and industrial projects. He completed his B.E. in Civil Engineering at Annamalai University, Chidambaram, M. Tech, in Construction Engineering and Management, and Doctorate of Philosophy in SRM Institute of Science and Technology. He has published more than 50 research articles in SCI and Scopus-indexed journals, he filed and published eight patents, and he has four funded projects for the various research streams, such as special concrete, energy efficiency buildings, and construction project management, and his current research topics include the energy efficiency construction material, IoT in construction, and artificial Intelligence in smart buildings. He served as the panel member of international and national conferences, an editorial board member, and a reviewer of several journals. He is a member of Institution of Engineers (M.I.E), Indian Concrete Institute (ICI), Indian Society for Technical education, and other technical membership communities.

Dr. T. Palanisamy is currently working in the Department of Civil Engineering, National Institute of Technology Karnataka (NIT K), Surathkal, India. He specialized in Structural Engineering and areas of interest in bio-concrete, concrete battery,

micro-characterization of concrete, beam-column joint, and artificial intelligence and machine learning applications in beam-column joint. He obtained B.E. (Civil) at Government College of Engineering Erode from Bharathiyar University, Coimbatore, India, an M.E. (Structural Engineering) at Government College of Engineering, India, and a Ph.D. in Civil Engineering–Structural Engineering from Government College of Technology, Coimbatore, Tamil Nādu, under Anna University, Chennai, India. He has a total of 20 years of teaching experience and has published 35 research articles in journals and 45 in conferences. He published 7 books/chapters and E-learning materials developed. He acts as an editor of two international publication books. He has registered 17 patents and 3 have been granted. He has received 16 awards for his contribution including the “Young Concrete Engineer and Vishwakarma Award” and completed three R&D-sponsored projects with a total value of around 55 lakhs.

Construction Engineering and Management

Comprehensive Review on Recycled Aggregate Concrete Using Scientometric Analysis Approach



Anmol Basnett, Anandh Sekar, and S. Sindhu Nachiar

1 Introduction

On a worldwide scale, concrete is the most often used building material [1]. There are several reasons why it is so popular, including its inexpensive cost and resistance to heat and water, as well as its versatility [2]. Concrete is used in almost every civil engineering structure [3, 4]. Concrete is made up of three fundamental ingredients: aggregates, cement, and water. After water, concrete is the material that is utilised the most globally, according to estimations. The most important of these components is aggregate, which makes up around 60–75% of the overall concrete volume [5]. Aside from this, due to its high demand on natural resources and its growing industrialisation and urbanisation as the economy and people grow in tandem, concrete has become the least sustainable building material. Its annual raw material use is estimated at roughly 20 billion tonnes (aggregates) [6]. The extraction and crushing of natural aggregate (N-A) also result in significant energy use and increased CO₂ emission. As a result, the rapid depletion of natural resources and an increase in environmental contamination are caused by the extensive use of concrete. For the modern building business, the depletion of natural resources and the rise in CDW are serious issues. Both of these issues could be solved at the same time by recycling CDW for new construction purposes. As an aggregate supplier, N-A has been replaced by recycled concrete from the CDW [7, 8]. Demolitions and precast members that have been abandoned are only two examples of the many causes that contribute to a build-up of waste concrete [9]. Recycled aggregates (R-As) are a low-cost and ecologically sustainable solution to reduce the amount of CDW produced during construction. The construction of the demolished structure, as well as the process used to create the resources, will determine whether or not the structure is classified as R-A. In contrast,

A. Basnett · A. Sekar (✉) · S. Sindhu Nachiar
Department of Civil Engineering, SRM Institute of Science and Technology, Kattankulathur,
Tamil Nadu 603203, India
e-mail: anandhs@srmist.edu.in

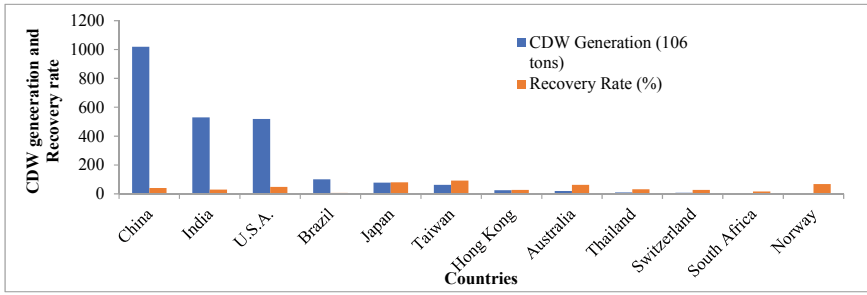


Fig. 1 Indexes of total CDW production and CDW recovery, 2017 [20]

R–As are made of a broad range of materials, such as wood and glass blocks, as well as plastics and waste [10–12]. Replacing N–As in concrete with R–As from CDW would improve the environmental sustainability of construction.

Given that the volume of CDW generated globally is anticipated to increase steadily over the coming years, novel methods for CDW recycling and reusing are necessary. Data on CDW production and recovery/recycling rates for nations throughout the world can be found in Fig. 1. A non-hazardous CDW reduction target of at least 70 per cent of its weight by 2020 was stipulated by the EU Waste Framework Directive (2008/98/EC) according to the European Union’s final study [13].

From 2000 to 2022, bibliometric data will be analysed in a scientometric study, since the development of recycled aggregate has been on the rise over this time period. A scientometric evaluation can examine big data without bringing new obstacles. In order to connect disparate fields of knowledge, traditional literature evaluations fall short. The most difficult components of current study are co-occurrence and citation mapping. Goal of this study is to improve traditional reviews by utilising scientometric analysis to identify and correct faults. It is possible to find the most frequently referenced authors and articles, as well as areas that are particularly interested in using R-A concrete for environmentally friendly building using a scientometric study that looks for these things. Graphic portrayal will help future academics develop scientific partnerships, create joint venture papers, and exchange new approaches or notions. It has also been emphasised and researched the most crucial parts of the R-A concrete field. Recycled aggregate concrete’s practical application and improvement methods are investigated. We then identify and propose new research avenues for the future of this investigation.

2 Research Significance

Recent research has gone a long way towards figuring out how to make building more environmentally friendly, and the results are noteworthy. There have been a large number of manual review studies completed so far. Scientific visualisation

and bibliographic co-occurrence are two of the most difficult issues in modern research. Scientists from around the world can now use the scientometric analysis-developed mapping of different areas of the literature to build research collaborations, joint ventures, and exchange new ideas and technology. Research gaps and crucial concerns in R-A concrete acceptance and application are also highlighted in this study. New paths for research are also recommended.

3 Methodology

The seven steps of the review study are depicted in Fig. 2, which shows the various levels of the review process.

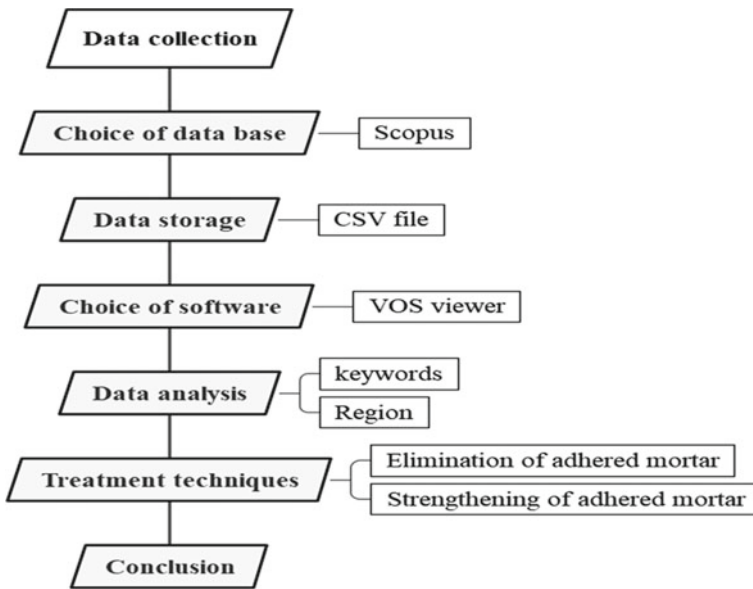


Fig. 2 Methodology adapted in this article

4 Data Analysis on Scientometric Analysis

4.1 Keyword Analysis

The review that was undertaken for this work was centered on recycled aggregate concrete, and an analysis of relevant keywords was carried out. There can be a maximum of five instances of each term in the phrase. Following these guidelines, a mapping technique was utilized to capture the co-occurrences of terms as well as their overall frequency. As a result, 764 out of 6830 of the articles satisfied the criteria. Recycled aggregate is referred to by many other names in R-A concrete articles, including concrete aggregates, compressive strength, aggregate, and recycled aggregate concrete. Figure 3 shows how keyword networks are visualised, along with the links and intensity related with the frequency of co-occurrence correlation. The size and location of a keyword circle indicate how often the term appears in different articles. Additional evidence that these keywords are important in R-A concrete research was provided by a scientific visualisation that displayed larger circles around some key terms. Various colours of circles reflect different clusters of keywords that appear together in a variety of articles.

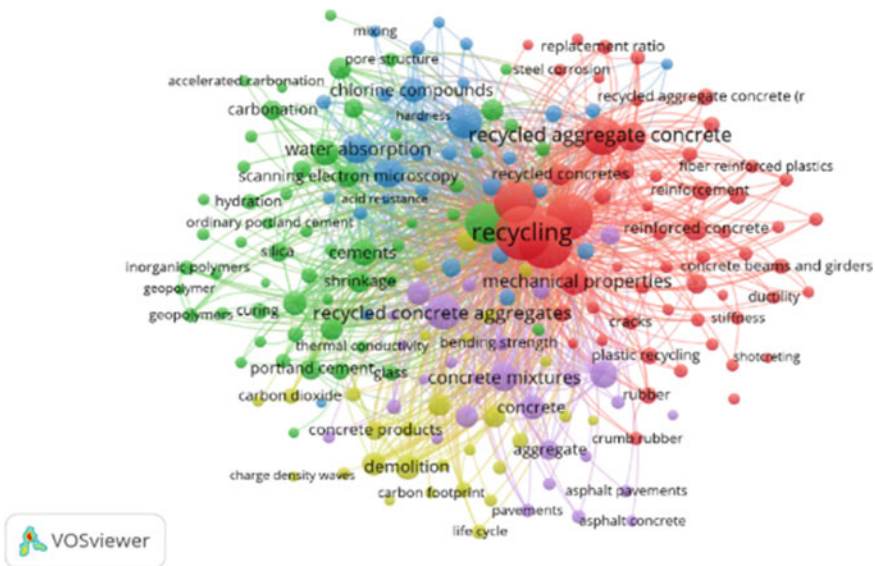


Fig. 3 Occurrence’s map of keywords

Table 1 Clusters of nations

Cluster no	Country
1	Bangladesh, Egypt, Malaysia, the Netherlands, Nigeria, Pakistan, Palestine, Poland, Saudi Arabia, Thailand
2	Algeria, Argentina, Belgium, Canada, France, Jordan, Kuwait, Lebanon, Qatar
3	South Africa, South Korea, Singapore, Hong Kong, China, and the United Kingdom
4	Brazil, Chile, Colombia, Germany, Italy, Switzerland
5	Czech Republic, Ethiopia, Japan, Taiwan, Vietnam
6	Australia, Iran, Turkey, UAE, USA
7	Iraq, Portugal, Serbia, Spain

4.2 Regions Analysis

In the study, the maximum number of nations per document was limited to 25 and the lowest to 5. Co-production groups' overall strength and the country's total bandwidth among the 72 countries are used to determine whether countries fit the requirement. National cooperation is depicted as a network of collaboration. As illustrated in Table 1, there are seven clusters in the region that have conducted comparable research, with cluster 1 comprising 10 nations, 2-nine, 3-seven, 4-six, 5-five, 6-five, and 7-four.

5 Treatment Techniques of RCA

Various strategies and methods have been proposed to enhance the features of recycled concrete aggregate (RCA) due to the wide range of impacts that attached mortar has on RCA quality. There are two broad classes into which these methods and strategies fall. It begins with scraping, sanding, or otherwise removing the mortar that has stuck to the RCA surface. Second, it entails enhancing the quality of the adhering mortar to change and enhance RCA's qualities. Figure 4 depicts a range of methods that can be employed to enhance the quality of RCA.

5.1 Eliminating the Adhered Mortar

The widespread presence of poorly adhering mortar is blamed for diminishing RCA's overall quality. Low density, excessive water absorption, and porosity are all characteristics that suffer as a result of the linked weak mortar. Using heat, mechanical abrasion, or chemicals, the poorly adhering mortar can be scraped from the RCA

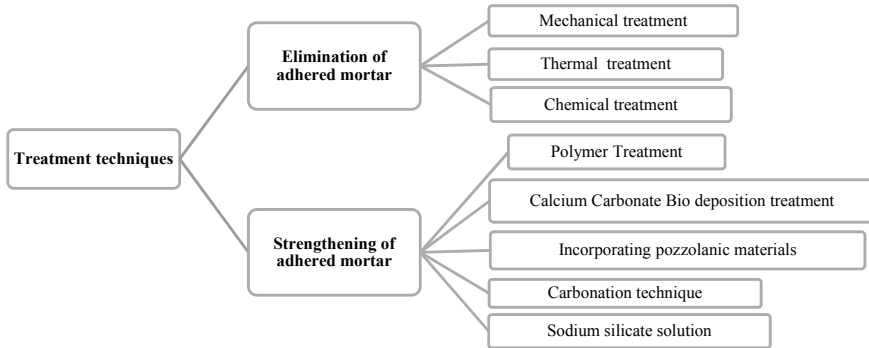


Fig. 4 Treatment methods of recycled coarse aggregate

surface. In the following paragraphs, we will go through each of these therapies in further depth.

Mechanical Treatment. High-quality RCA can be produced by mechanical treatment, which involves removing attached mortar from the N-A. Here, the mortar adhesions are broken apart and scraped away by mechanical means [14]. Mechanical grinding and the eccentric-shaft rotor technique have both been offered for this operation. The RCA lumps are transferred between two cylinders, one of which rotates at a high eccentricity compared to the other, using a process called eccentric-shaft rotor. This process may be used to clean RCA of any mortar that has stuck to it. However, the method has the potential to damage the RCA particles, resulting to micro-cracks, due to impact and grinding activities that alter the geometric features of RCA particles [15].

Thermal Treatment Technique. Treatment options for eliminating the linked weak adhering mortar are limited; however, heat treatment is often favoured due to its simplicity of operation and low cost. This method involves subjecting RCA particles to high temperatures for around 2 h. Differential thermal expansion between the original aggregate and the attached mortar produces thermal stresses that weaken the adhering mortar and allow it to pull away from the surface. Shima et al. [16] found that when RCA is heated over 300 degrees Celsius, the aggregate-mortar interface dries out, which makes the connection brittle and easy to break. After treatment, just 2% of the cement paste remained attached to the natural aggregate particles. The results were consistent with those of Ma et al. [17]. The aggregates in C&D waste concrete were separated from the mortar by heating the concrete at 750 degrees Celsius. The findings revealed that the removal of mortar becomes easier with increasing heating.

5.2 *Quality Improving the Adhered Mortar*

These techniques reinforce the current mortar on the original aggregate rather than first removing the weak mortar and then recycling the original aggregate. Two of the best ways to boost quality are to reinforce ITZs by filling in and solidifying the weak spots. Carbonation is only one of several methods that may be used to improve the binding that exists among the RCA and the new mortar. Additional examples include pozzolanic reaction, pozzolanic treatment, and the inclusion of pozzolanic compounds as surface coating binders.

Polymer Treatment. The hydration products of connected mortar can chemically react with some polymers, increasing the concrete's strength, while other polymers can create a coating over the concrete, shielding it from the environment [18]. The resulting calcium complexes can effectively seal the RCA surface by filling up the cracks and crevices of the adhering mortar. In other words, lowering water absorption and porosity might improve durability performance. Both water-repellent polymers based on silicon and water-soluble polymers, such as polyvinyl alcohol (PVA), have been used to enhance RCA's properties. Water-soluble polymers have advantages including their adhesive properties and their speed of solidification. Soaking RCA in a water-soluble polymer allows the polymer molecules to penetrate the porous, poorly adhering cement and strengthen the connection. Water absorption in RCA, a porous material, might be decreased by using PVA solution, a water-soluble polymer [19]. Kou and Poon [20] tested the mechanical and physical characteristics of PVA-treated RCA with concentrations of 6, 8, 10, and 12%. Water absorption by PVA-treated RCA was shown to diminish with increasing PVA content; a 10% PVA solution was found to be optimal for impregnating RCA.

Calcium Carbonate Biodeposition. Biodeposition of calcium carbonate is another method under development for bettering the quality of RCA, especially with regard to lowering water absorption in the adhering mortar. This method employs bacteria, and it is predicated on the negative zeta potential of the cell wall surface to expedite calcium carbonate production at the aggregate's outermost layer [21]. Furthermore, the biodeposition process is a more organic approach than previous theories. All of the materials required for seeding the substrates exist naturally; thus, there is less of an impact on the environment when using this technique. Grabiec et al. [22] proposed use of *Sporosarcina pasteurii* bacteria grown in a liquid media produced by hydrolysing urea to treat RCA. Additionally, the precipitated CaCO_3 showed strong binding in the aggregate surface by filling holes and gaps in the adhering mortar.

Incorporating Pozzolanic Materials. To better enhance the qualities of adhering mortar, pozzolanic ingredients like fly ash or silica fume are used. When RCA is immersed in pozzolanic material slush or treated with pozzolanic materials (surface coating), a hydrated calcium silicate (C-S-H) gel is generated. This is because the pozzolanic materials come in contact with the calcium hydroxide (CH) left in the adhering mortar. By changing the surface of the RCA and the characteristics

of the connected mortar, these hydrated compounds may improve RCA's bonding capabilities [23].

Carbonation Technique. Carbonation occurs when carbon dioxide CO_2 penetrates adhering mortar and reacts with the resulting hydration products [24]. When CO_2 combines with calcium hydroxide in the adhering mortar, a thick layer develops around the reacted calcium hydroxide crystals and fills the pores and spaces of the cement paste, initiating the carbonation of calcium hydroxide [25]. At a CO_2 concentration of 50%, the results showed that RCA was capable of absorbing as much as 65% of the gas, with the absorption rate increasing when the particle size of the RCA was smaller than 2 mm and the water saturation was less than 0.4 [26, 27]. Studied the carbonation treatment of RCA by subjecting to a carbonation chamber with different durations of 6, 12, 24, 48, and 72 hours under low-pressure circumstances, specifically 0.1 Bar above atmospheric pressure. This experimental setup aimed to examine the impact of carbonation treatment on the properties of RCA. Physical and mechanical characteristics of treated RCA were shown to be enhanced by carbonation treatment regardless of curing time or particle size.

Sodium Silicate Solution. Cheng et al. [28] Immersed RCA in sodium silicate solutions with concentrations of 0.05 M, 0.1 M, 0.2 M, 0.3 M, and 0.4 M for durations of 1 hour, 5 hours, and 24 hours. The results revealed that the water absorption of RCA was drastically reduced by using sodium silicate. This is because the pores and spaces of RCA are filled by the silicic acid gel precipitated from the sodium silicate solution. In addition, the C-S-H gel created by the sodium silicate and calcium hydroxide reaction strengthened the binding between the mortar and RCA.

6 Conclusion

This study's goal was to provide an overview of the state of the art for recycled aggregate concrete (RAC) by using a large-scale data mining method of scientometric analysis of the literature and by presenting an in-depth discussion of the findings. Based on bibliometric data taken from the Scopus database from 2001 to 2021, we conducted a scientometric analysis of R-A concrete articles. Scientists investigated the most popular terms and locations for publishing as part of their scientometric investigation. Furthermore, important issues in this field of research were highlighted and discussed. In this study, we found the following results:

- Recycling, concrete aggregates, concretes, aggregates, compressive strength, and recycled aggregate concrete were the most often used keywords in the field of study, according to a scientometric examination of the enormous bibliographic data. Additionally, it was discovered that the top nations that publish a big number of journals are China, the USA, Australia, Spain, and Portugal.

- To totally recover demolition debris, employ reclaimed mortar in a variety of ways, and improve the structural performance of recycled concrete aggregates. Considering the time and money invested in treatment, decisions about which treatments to employ should be based on these criteria.
- Fibre, mineral materials, and other components are now used as admixtures, but they are expensive, scarce, and harmful to the environment. The future of research will focus on developing cost-effective admixtures, which is a crucial step towards engineering applications of RAC in the real world.
- Most therapeutic studies have only been conducted on a tiny scale in labs. More investigation into the efficacy and feasibility of these therapies on an industrial and commercial scale may be warranted in the light of the findings of this study.

References

1. Dong W, Li W, Tao Z (2021) A comprehensive review on performance of cementitious and geopolymeric concretes with recycled waste glass as powder, sand or cullet. *Resour Conserv Recycl* 172:105664
2. Baturkin D, Hisseine OA, Masmoudi R, Tagnit-Hamou A, Massicotte L (2021) Valorization of recycled FRP materials from wind turbine blades in concrete. *Resour Conserv Recycl* 174:105807
3. Yu J, Mishra DK, Hu C, Leung CKY, Shah SP (2021) Mechanical, environmental and economic performance of sustainable Grade 45 concrete with ultrahigh volume Limestone-Calced Clay (LCC), Resources. *Conserv Recycl* 175:105846
4. Hu H, He Z, Shi J, Liang C, Shibro T, Liu B, Yang S-Y (2022) Mechanical properties, drying shrinkage, and nano-scale characteristics of concrete prepared with zeolite powder pre-coated recycled aggregate. *J Clean Prod*: 128710; Zhang B et al (2022) *J Build Eng* 46:103679, 27
5. Golafshani EM, Behnood A, Hosseinikebria SS, Arashpour M (2021) Novel metaheuristic-based type-2 fuzzy inference system for predicting the compressive strength of recycled aggregate concrete. *J Clean Prod*: 128771
6. Mikhailenko P, Piao Z, Kakar MR, Bueno M, Poulidakos LD (2021) Durability and surface properties of low-noise pavements with recycled concrete aggregates. *J Clean Prod* 319:128788
7. Kazmi SMS, Munir MJ, Wu Y-F (2021) Application of waste tire rubber and recycled aggregates in concrete products: a new compression casting approach. *Resour Conserv Recycl* 167:105353
8. Khan M, Cao M, Ali M (2020) Cracking behaviour and constitutive modelling of hybrid fibre reinforced concrete. *J Build Eng* 30:101272
9. Khan M, Cao M, Xie C, Ali M (2021) Efficiency of basalt fiber length and content on mechanical and microstructural properties of hybrid fiber concrete, fatigue & fracture of engineering materials & structures
10. Khan M, Cao M, Chaopeng X, Ali M (2021) Experimental and analytical study of hybrid fiber reinforced concrete prepared with basalt fiber under high temperature, fire and materials
11. Hosseini P, Booshehrian A, Delkash M, Ghavami S, Zanjani MK (2009) Use of nano-SiO₂ to improve microstructure and compressive strength of recycled aggregate concretes. In: *Nanotechnology in construction*, vol 3. Springer, pp 215–221
12. Limbachiya M, Meddah MS, Ouchagour Y (2012) Use of recycled concrete aggregate in fly-ash concrete. *Construct Build Mater* 27(1):439–449
13. Deloitte. Study on resource efficient use of mixed wastes, improving management of construction and demolition waste—final report. *Prep Eur Comm DG ENV 2017 2*:152–162
14. Pandurangan K, Dayanithy A, Om Prakash S (2016) Influence of treatment methods on the bond strength of recycled aggregate concrete. *Constr Build Mater* 120:212–221

15. Savva P, Ioannou S, Oikonomopoulou K, Nicolaidis D, Petrou MF (2021) A mechanical treatment method for recycled aggregates and its effect on recycled aggregate-based concrete. *Materials* 14:2186
16. Shima H, Tateyashiki H, Matsuhashi R, Yoshida Y (2005) An advanced concrete recycling technology and its applicability assessment by the input-output analysis. *J Adv Concr Technol* 3(1):53–67
17. Ma XW, Han ZX, Li XY, Meng FN (2009) Thermal treatment of waste concrete and the rehydration properties of the dehydrated cement paste. *J Qingdao Technol Univ* 3(4):93–97
18. Singh NB, Rai S (2001) Effect of polyvinyl alcohol on the hydration of cement with rice husk ash. *Cem Concr Res* 31(2):239–243
19. Mansur AAP, Santos DB, Mansur HS (2007) A microstructural approach to adherence mechanism of poly vinyl alcohol modified cement systems to ceramic tiles. *Cem Concr Res* 37(2):270–282
20. Kou SC, Poon CS (2010) Properties of concrete prepared with PVA-impregnated recycled concrete aggregates. *Cem Concr Compos* 32(8):649–654
21. Achal V, Mukherjee A, Basu PC, Reddy MS (2009) Lactose mother liquor as an alternative nutrient source for microbial concrete production by *Sporosarcina pasteurii*. *J Ind Microbiol Biotechnol* 36(3):433–438
22. Grabiec AM, Klama J, Zawal D, Krupa D (2012) Modification of recycled concrete aggregate by calcium carbonate biodeposition. *Constr Build Mater* 34:145–150
23. Katz A (2004) Treatments for the improvement of recycled aggregate. *J Mater Civ Eng* 16(6):597–603
24. Castellote M, Fernandez L, Andrade C, Alonso C (2009) Chemical changes and phase analysis of OPC pastes carbonated at different CO₂ concentrations. *Mater Struct* 42(4):515–525
25. Thierry M, Villain G, Dangla P, Platret G (2007) Investigation of the carbonation front shape on cementitious materials: effects of the chemical kinetics. *Cem Concr Res* 37:1047–1058
26. Borges PHR, Costa JO, Milestone NB, Lynsdale CJ, Streatfield RE (2010) Carbonation of CH and C–S–H in composite cement pastes containing high amounts of BFS. *Cem Concr Res* 40(2):284–292
27. Kou SC, Zhan BJ, Poon CS (2014) Use of a CO₂ curing step to improve the properties of concrete prepared with recycled aggregates. *Cem Concr Compos* 45:22–28
28. Cheng HL, Wang CY (2004) Improvement of recycled aggregate quality by pre-soaking with water glass. *Gypsum Cem Build* 12:12–14

Performance of Concrete by the Addition of Bio-Cement on Ultrasonic Pulse Velocity



K. Chandramouli, R. Santhi Kala, and N. Pannirselvam

1 Introduction

Concrete is frequently employed for infrastructure construction. Concrete has a very high load-bearing capability when it is compressed. Nevertheless, this same substance weakens when put under tension. Steel bars are therefore included into the concrete to allow the structures to withstand tensile loads. When the concrete fractures under tension, the steel reinforced bars help to disperse the stress, preventing structural damage [1–4]. As matrix cracking begins to occur at higher stress levels, elasticity decreases and stability is compromised [5]. Concrete is a high-maintenance material that can quickly deteriorate due to wear and tear. It typically cracks and shows signs of wear after only a few decades in service.

In order to reconstruct concrete structures, a cement mortar must typically be applied and adhered to the damaged surface. Sometimes, in order to prevent it from moving, this mortar needs to be fixed into position with steel rods. Due to the structure's difficulties in being accessed and the possibility that repairs will need to be conducted on upper levels or at considerable heights, repairs can be time-consuming and expensive [6]. Concrete cracks and fissures can now be automatically repaired using a novel process called microbologically induced calcite or calcium carbonate precipitation (MICP) [7–13]. As certain bacteria produce secret calcite precipitations,

K. Chandramouli

Department of Civil Engineering, NRI Institute of Technology, Visadala (V), Medikonduru (M), Guntur, Andhra Pradesh, India

R. Santhi Kala

Department of Civil Engineering, KKR & KSR Institute of Technology and Sciences, Vinjanampadu, Vatticherukuru (M), Guntur, Andhra Pradesh, India

N. Pannirselvam (✉)

Department of Civil Engineering, Faculty of Engineering and Technology, SRM Institute of Science and Technology, Kattankulathur, Tamil Nadu 603203, India
e-mail: pannirsn@srmist.edu.in

doing this will help the structure last longer. These fissures can be fixed naturally by adding specific bacteria species into concrete [14]. These bacteria have the potential to secrete calcite precipitations, which will eventually seal the fissures and boost structural stability.

A non-destructive test method using ultrasonic pulse velocity. Cube specimens were cast, cured, and tested at 7, 28, 56, and 90 days [14–21].

2 Experimental Program

The experiment was conducted over a 28-day period to examine the various facets of how microbiological concrete develops its strength [22–26]. Following is a list of the materials used and variable parameters examined:

2.1 Materials

2.1.1 Bacteria

It is the blend of bacteria (*Bacillus pasteurii*) along with nutrients such as calcium and urea. Each gram contains 5% *B. pasteurii* and 95% urea and calcium lactate. After the reaction, it will auto-fill the pore spaces present in concrete through the process of microbiologically induced calcite precipitation (MICP) [27–30].

Cement: Ordinary Portland Cement (OPC), which is sold in the locality, was employed as the binding substance. The normal consistency of cement is 30% with initial and final settings of 53 and 245 min, respectively. Soundness determined as 4.5 mm and specific gravity of 3.15. The cement mortar was casted, cured, and tested at 7 and 28 days and obtained 35 and 55 MPa.

Aggregate: Locally available fine aggregate, naturally occurring passing through 4.75 mm sieve was used. The 12.5 mm nominal size crushed stone is used as the coarse aggregate. Table 1 lists the attributes of the aggregate.

Table 1 Aggregate physical properties

Properties	Fine aggregate	Coarse aggregate
Specific gravity	2.56	2.58
Unit weight (kg/m^3)	1585	1565
Fineness modulus	2.56	6.67
Absorption capacity (%)	1.40	0.5
Moisture content (%)	1.11	0.55

Water: A sample of water that met IS 456–2000 specifications and had a pH of 7, and no turbidity was taken.

2.2 Variables

- Concrete quality: Concrete was used, namely M40 and M60 grades of bio-concrete, which include 1% bio-cement. For the purpose of comparing the qualities of bio-concrete to conventional concrete, it was cast.
- Exposure period: Following the stipulated cure period of 7, 28, 56, and 90 days in plain water, specimens were analyzed on a regular basis.
- Cube specimens: Specimen of size 100 mm × 100 mm × 100 mm was used in accordance with ASTM standard procedure.
- Environment for curing: In the lab, 48 cube-shaped concrete specimens were cast. After casting, specimens were stored at 27 °C and 90% relative humidity for 24 h before being cured in water at room temperature.
- Concrete quality: Concrete was used, namely M40 and Mix proportion: The characteristics of the material were used to design concrete. Cement, fine aggregate, and coarse aggregate proportions for an M40 concrete mix design were determined to be 1: 1.47: 2.84 with w/c of 0.35 by mass. The mix ratio for M60 concrete was 1: 1.06: 2.19, and the water–cement ratio was 0.28 [31, 32].

3 Results and Discussion

3.1 Compressive Strength

Compressive strength is a critical mechanical property used to assess the performance of concrete. Compressive strength is typically determined through standardized testing procedures which involve subjecting a material specimen to an applied load or force until it fails. The compressive strength of conventional and bio-concrete for M40 and M60 grades is shown in Table 2.

Table 2 Compressive strength values for with and without bio-cement

Grade of concrete	% of bio-cement (%)	Curing period in days			
		7	28	56	90
M40	0	32.88	49.29	53.83	56.69
	1	36.84	56.48	61.81	65.16
M60	0	44.21	69.67	76.13	81.17
	1	49.7	76.15	82.62	86.61

Table 3 UPV values for conventional and bio-concrete

Grade of concrete	% of bio-cement	Curing period in days			
		7	28	56	90
M40	0%	4895	4912	4934	4978
	1%	5014	5032	5067	5091
	Concrete quality	Excellent	Excellent	Excellent	Excellent
M60	0%	4943	4965	4986	5019
	1%	5003	5112	5124	5149
	Concrete quality	Excellent	Excellent	Excellent	Excellent

3.2 Ultrasonic Pulse Velocity Test

Ultrasonic pulse velocity (UPV) is a non-destructive testing (NDT) to measure the speed of ultrasonic waves through a material. It is commonly used to assess the quality and integrity of concrete and other construction materials, as well as to estimate their mechanical properties. In a UPV test, a pair of transducers, typically piezoelectric transducers, are used to generate and receive ultrasonic pulses in a material. One transducer acts as a transmitter, which emits a high-frequency ultrasonic pulse, and the other transducer acts as a receiver, which detects the pulse after it has traveled through the material. The pulse velocity is calculated by dividing the distance between the transducers by the time it takes for the UP to travel through the material [32]. The UPV determined for M40 and M60 grades of conventional and bio-concrete and results are tabulated in Table 3.

3.3 Empirical Relation Between Compressive Strength and Ultrasonic Pulse Velocity

Empirical relations formed between compressive strength and UPV for M40 and M60 grades of concrete for values at curing periods of 7, 28, 56, and 90 days (Figs. 1, 2, 3 and 4).

Empirical relation from Figs. 1, 2, 3 and 4.

- Conventional concrete for M40 grade: $Y = 244.68 \times - 1158, R2 = 0.6819$.
- Bio-concrete for M40 grade: $Y = 323.25 \times - 1577.6, R2 = 0.7781$.
- Conventional concrete for M60 grade: $Y = 451.48 \times - 2178.3, R2 = 0.7906$.
- Bio-concrete for M60 grade: $Y = 256.52 \times - 1233.7, R2 = 0.9926$.

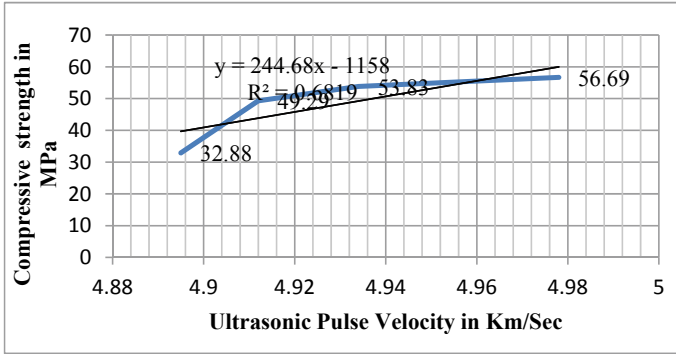


Fig. 1 Empirical relation between compressive strength and UPV for conventional concrete of M40 grade

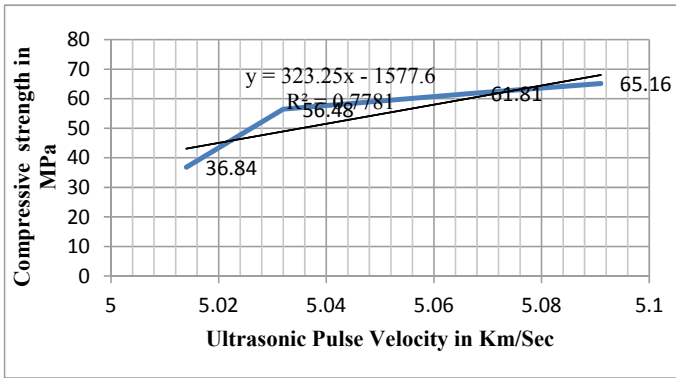


Fig. 2 Empirical relation between compressive strength and UPV for bio-concrete of M40 grade

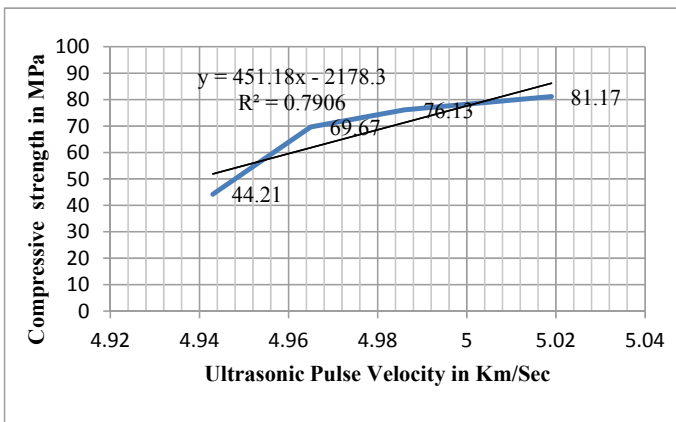


Fig. 3 Empirical relation between compressive strength and UPV for conventional concrete of M60 grade

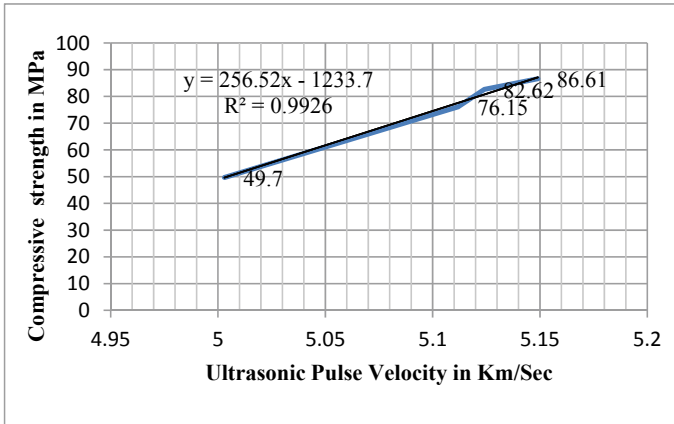


Fig. 4 Empirical relation between compressive strength and UPV for bio-concrete of M60 grade

4 Conclusion

- (i) Because of its eco-friendliness, self-healing powers, and increased durability of structural real as creating materials, bacterial real tech has already been shown to be superior to numerous conventional technologies.
- (ii) This method of cementing has proven straightforward and practical. However, additional effort is required to increase the viability of this technology.
- (iii) The pulse velocity value in mt/s was excellent, and its value decreases with age and grade of concrete as the concrete becomes dense and also decreases for bio-concrete when compared to conventional concrete.
- (iv) The percentage decrease in UPV value ranges from 0.51 to 2.65% and decreases for bio-concrete when compared to conventional concrete, which classifies it as excellent concrete in terms of strength and durability of concrete.
- (v) An empirical relation between “compressive strength and UPV” is proposed for conventional concrete and bio-concrete, and it is in the form of $f_{ck} = 244.68V_d - 1158$, $R^2 = 0.6819$, $f_{ck} = 323.25V_d - 1577.6$, $R^2 = 0.7781$ for M40 grade of concrete.
- (vi) An empirical relation between “compressive strength and UPV” is proposed for conventional concrete and bio-concrete, and it is in the form of $f_{ck} = 451.48V_d - 2178.3$, $R^2 = 0.7906$, $f_{ck} = 256.52V_d - 1233.7$, $R^2 = 0.9926$ for M60 grade of concrete.

References

1. Algaifi HA, Bakar SA, Sam ARM, Ismail M, Abidin ARZ, Shahir SA (2020) Insight into the role of microbial calcium carbonate and the factors involved in self-healing concrete. *Constr Build Mater* 2020(254):119258
2. Pawar AP, Mulya SB (2020) Bacterial concrete—solution for micro cracks, 2020 JETIR July 2020, vol 7, Issue 7. www.jetir.org. ISSN-2349-5162
3. Castro-Alonso MJ, Montanez-Hernandez LE, Sanchez-Munoz MA, Macias Franco MR, Narayanasamy R, Balagurusamy N (2019) Microbially induced calcium carbonate precipitation (MICP) and its potential in bioconcrete: microbiological and molecular concepts. *Front Mater* 6:126
4. Sharma D, Kumar V, Sain H (2021) A review of bio-concrete in modern construction era. *Int Res J Mod Eng Technol Sci* 03(08):406–409
5. Chaurasia L, Bisht V, Singh LP, Gupta S (2019) A novel approach of bio mineralization for improving micro and macro-properties of concrete. *Constr Build Mater* 195:340–351
6. Camara LA, Wons M, Esteves ICA, Medeiros-Junior RA (2019) Monitoring the self-healing of concrete from the ultrasonic pulse velocity. *J Compos Sci* 3:16. <https://doi.org/10.3390/jcs3010016>, www.mdpi.com/journal/jcs
7. Jagannathan P, Satyanarayanan, Kantadevi Arunachalam KS (2018) Studies on the mechanical properties of bacterial concrete with two bacterial species. *Maters Today Proc* 5:887
8. Priyom SN, Islam M Islam S (2018) An experimental investigation on the performance of bacterial concrete. In: 4th international conference on advances in civil engineering 2018 (ICACE 2018), 19–21 Dec 2018, CUET, Chittagong, Bangladesh
9. Hedjazi S, Castillo D (2020) Relationships among compressive strength and UPV of concrete reinforced with different types of fibers. *Sci Direct Heliyon* 6:e03646
10. Santhosh Kumar K, Prithivi Raj C, Ushman Batcha S, Mohamed Azarudeen S (2019) Performance evaluation of bacterial concrete. *Int J Eng Res Technol*. ISSN: 2278-0181. Published by www.ijert.org; CONFCALL—2019 conference proceedings.
11. Jose S, Reshma George V, Rodrigues A, John J, Venu D (2018) A study on strength characteristics of bacterial concrete. *IRJET* 05(03). e-ISSN: 2395-0056
12. Raina SS, Singla S, Batra VS (2018) Evaluation of *Bacillus. Subtilis* bacterial concrete with normal concrete. *IOSR J Mech Civ Eng (IOSR-JMCE)* 15(5):01–06. e-ISSN: 2278-1684, p-ISSN: 2320-334X, Ver. III
13. Srinivasan G, Saravanan J (2020) A study on strength characters of bacterial concrete. *Mater Sci Eng IOP Conf Ser*: 993012043
14. Joshi S, Goyal S, Sudhakara Reddy M (2018) Influence of nutrient components of media on structural properties of concrete during bio cementation. *Constr Build Mater* 158:601–613
15. Achal V, Li M, Zhang Q (2014) Bio-cement, recent research in construction engineering: status of china against rest of world. *Adv Cem Res* 26(5):281–291
16. Nodehi M, Ozbakkaloglu T, Gholampour A (2022) A systematic review of bacteria-based self-healing concrete: biomineralization, mechanical, and durability properties. *J Build Eng* 49:2352–7102
17. Grino AAM, Daly MK, Ongpeng JMC (2020) Bio-influenced self-healing mechanism in concrete and its testing: a review. *Appl Sci* 10(15):5161
18. Bhina MR, Wibowo AH, Liu KY, Khan W, Salim M (2021) An overview on bioconcrete and the utilization of microbes in civil engineering. Preprints, 2021040019
19. Ahmed SO, Nasser AA, Abbas RN, Kamal MM, Zahran MA, Sorour NM (2021) Production of bioconcrete with improved durability properties using Alkaliphilic Egyptian bacteria. *3 Biotech* 11(5)
20. Chithambar A, Ganesh M, Muthukannan R, Malathy C, Ramesh Babu C (2019) An experimental study on effects of bacterial strain combination in fibre concrete and self-healing efficiency. *KSCE J Civ Eng* 23:4368–4377
21. Kala RS, Chandramouli K, Pannirselvam N, Varalakshmi TVS, Anitha V (2019) Strength studies on bio cement concrete. *Int J Civ Eng Technol* 10(3):1300–1307

22. Khan MBE, Shen L, Dias-da-Costa D (2021) Self-healing behaviour of bio-concrete in submerged and tidal marine environments. *Constr Build Mater* 277:122332
23. Al-Tabbaa A, Litina C, Giannaros P, Kanellopoulos A, Souza L (2019) First UK field application and performance of microcapsule-based self-healing concrete. *Constr Build Mater* 208:669–685
24. Mohammed H, Ortoneda-Pedrola M, Nakouti I, Bras A (2020) Experimental characterisation of non-encapsulated bio-based concrete with self-healing capacity. *Constr Build Mater* 256:119411
25. Sidiq A, Gravina R, Giustozzi F (2019) Is concrete healing really efficient? A review. *Constr Build Mater* 205:257–273
26. Meraz MM, Mim NJ, Mehedi MT, Bhattacharya B, Reduan Aftab M, Mustakim Billah M, Musfike Meraz M (2023) Self-healing concrete: fabrication, advancement, and effectiveness for long-term integrity of concrete infrastructures. *Alexandria Eng J* 73:665–694
27. Guo YC, Wang X, Yan Z, Zhong H (2015) Current progress on biological self-healing concrete. *Mater Res Innov* 19:S8–S750
28. Wang XF, Yang ZH, Fang C, Han NX, Zhu GM, Tang JN, Xing F (2019) Evaluation of the mechanical performance recovery of self-healing cementitious materials—its methods and future development: a review. *Constr Build Mater* 212:400–421
29. Sonali Sri Durga C, Ruben N, Sri Rama Chand M, Venkatesh C (2020) Performance studies on rate of self healing in bio concrete. *Mater Today Proc* 27:158–162
30. Jeon S, Hossain MS, Han S, Choi P, Yun K-K (2022) Self-healing characteristics of cement concrete containing expansive agent. *Case Stud Constr Mater* 17:e01609
31. IS 10262 (2009) Guidelines for concrete mix proportioning, 1st rev. Bureau of Indian standards, New Delhi
32. IS 13311-1 (1992) Method of Non-destructive testing of concrete—ultrasonic pulse velocity. Bureau of Indian standards, New Delhi, India

Effects of Staggered Openings on Response Reduction Factor of Frames with Shear Wall



C. V. Samyuktha and T. M. Jeyashree

1 Introduction

The tall buildings are different from common buildings in terms of resistance to lateral load due to wind, earthquake, etc. in addition to vertical loads. This results in demand for providing both lateral strength and stiffness to the building to meet the strength and serviceability criteria under lateral loads. Normally, a tall building is provided with a horizontal load-resisting system apart from a vertical load-resisting system. A lateral load-resisting system is required to safeguard the tall building under lateral loads. Horizontal loads on buildings increase with the increase in height of buildings. Depending on the type of building, different structural systems are used to resist lateral loads. The shear wall is the one which is most frequently utilized in structures. By providing the necessary lateral strength and stiffness to resist horizontal stresses, the shear walls in a building are a structurally effective method to strengthen the construction [1]. It is common practice for shear walls to begin from the basement and continue up the entire height of the structure, and they can be located along the building's sides or clustered together to form a core. Shear walls may need to incorporate one or more openings due to the need to accommodate a variety of functional requirements. It is crucial to have shear walls, but their size and placement matter a great deal. A plan's symmetry is crucial for minimizing twisting effects in structures. Shear walls in buildings that have been carefully planned and detailed have proven to be effective in reducing damage during previous earthquakes. Many countries, like New Zealand and the USA, are prone to earthquakes; thus, buildings are provided with shear walls to reduce the earthquake damage to both permanent and temporary parts of a building. In addition, the historical strong earthquakes that have been recorded all over the world have demonstrated that several elements,

C. V. Samyuktha · T. M. Jeyashree (✉)

Department of Civil Engineering, Faculty of Engineering and Technology, SRM Institute of Science and Technology, Kattankulathur, Tamil Nadu 603203, India

e-mail: jeyashrm@srmist.edu.in

including plan shape, wall and opening dimensions, reinforcing and openings layout, site condition, earthquake type, and strain rates, all have a role in determining the extent of damages and the specific failure mechanisms of shear walls. For practical purposes, doors, windows, skylights, and other openings in shear walls are possible. Understanding the seismic responses and behaviour of structural systems is essential for making an appropriate configuration of openings in shear walls, as it is knowledge of the effects of openings sizes and configurations on stiffness.

Based on the literature review, it is observed that many research works focused on shear walls with different types of openings and sizes. Past observations on the response of a shear wall with an opening to seismic forces were identified using finite element simulation ETABS software [2]. When the opening area is less than 20% of the shear wall area, the stiffness is determined by the size of the opening rather than its location. Openings in shear walls that are greater than 20% have a significant impact on the stiffness of the system [3]. When compared to a vertical opening, the staggered one performed better. Compared to uniform openings, staggered ones experience less shear at the foundation [4]. Staggered openings are better as compared in reducing displacement, drift, and shear in irregularly shaped buildings (H-shaped and T-shaped). Displacement in the Y -axis was satisfactory in an irregular L -shaped building with vertical openings [5]. As much as 50% of the shear wall's stiffness, the ultimate load could be lost due to openings, though the strength and ductility of the reduction would vary depending on the type and shape of openings [6]. The present study makes an attempt to study the effect of openings on the behaviour of shear wall system and response reduction factor (R) is determined. Code recommendations for various types of structural systems vary in how they define the reducing factor for responses (R). The factor of ductility, the strength factor, and the structural redundancy all play a role in determining the value of R . Using the finite element analysis ETABS software, nonlinear static pushover analysis is performed on the analytical models. The response reduction factor (R factor) is computed based on the nonlinear static pushover analysis findings.

2 Analytical Investigation Using ETABS

For the present study, a three-dimensional structure is modelled in ETABS. The analysis of three different building heights: 56, 72, and 88 m is carried out. In the post-analysis of the building, parameters like maximum storey displacement, the building's response to seismic forces, and storey drift are determined. Linear static analysis is used to estimate the equivalent static forces utilized to calculate inter-storey drift and the serviceability criterion. This study examines the seismic response of the RC building frame in terms of performance and the impact of seismic forces on multi-storey building frames. The study involves the design of a building's framework according to Indian standards (specifically, IS 456:2000 and IS 1893:2000). The seismic parameters considered are zone IV, medium soil condition, response

reduction factor = 5, and importance factor = 1. The members are designed as per the limit state method of design by the code IS 456 [7] and IS 1893 [8].

2.1 Frame Model

Dimension of the bay is 15 m, and the height of the building is as follows: “H1” series is 56 m height with a 14 storey, the “H2” series is 72 m height with an 18-storey, and the “H3” series is 88 m height with a 22 storey. Different height of the building is considered to study the effect of storey height on response of the building with shear wall system. Figure 1 shows the layout of different shear wall positions, and the plan shape of shear wall is varied to study its effect on behaviour of building under seismic load.

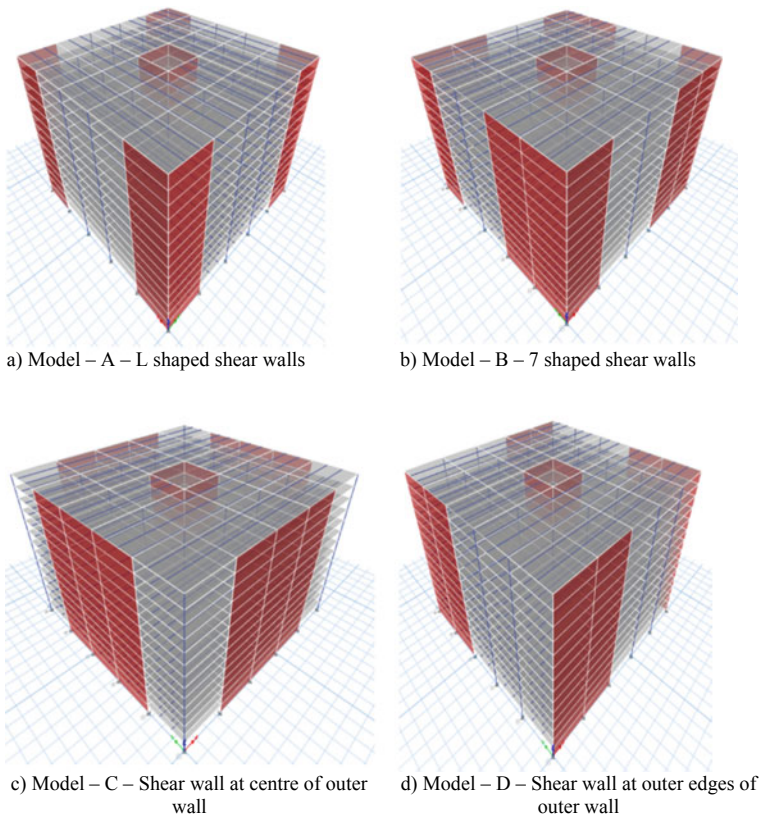


Fig. 1 Layout of different shear wall positions

2.2 Effects of Storey Height and Shear Wall Position

Several studies have been implemented to reduce the complexity of the precise seismic analysis of the building, which is necessary for the building design for seismic activity to be done in a refined and easy manner. Especially, in this study, four models (A, B, C, D) with different heights of structures are designed. Table 1 shows the size of the structural elements considered for the present study. The analysis output of the 56 m height of the building (*H1*), 72 m height of the building (*H2*), and 88 m height of buildings (*H3*) is shown in Figs. 2 and 3.

As per the analytical results, the storey displacement and storey drift are well within the allowable range of H (Height of building)/250 and 0.004 as per IS code in all the systems, as specified by IS 1893 [8]. Edge-provided shear walls increase the maximum storey displacement of buildings relative to centre-provided shear walls. Providing more shear walls is not a guarantee for better seismic behaviour of buildings, as their effectiveness is not dependent on the number of shear walls [4]. Forces acting on the structural element are significantly affected by shear walls. From the analytical investigation, it is clear that Model C with 72 m height of the building performs well under seismic load compared to other configurations of shear wall. This can be attributed to the fact that symmetry of the shear wall orientation plays a vital role in deciding the behaviour of building under seismic load. Model A is also symmetrically placed but the provision of shear wall at the centre of the outer wall results in lesser displacement and drift.

Table 1 Size of structural elements

S. No.	Elements	Cross-section (mm)
1	Primary beam	450 × 600
2	Secondary beam	250 × 300
3	Column	1000 × 1000
4	Thickness of slab	250
5	Thickness of shear wall	230

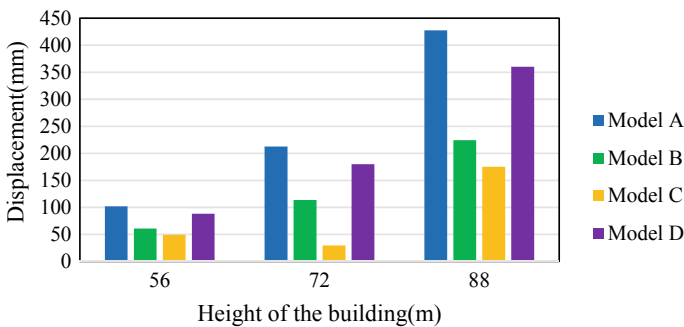


Fig. 2 Effect of different shear wall positions on lateral displacement for *H1*, *H2*, and *H3*

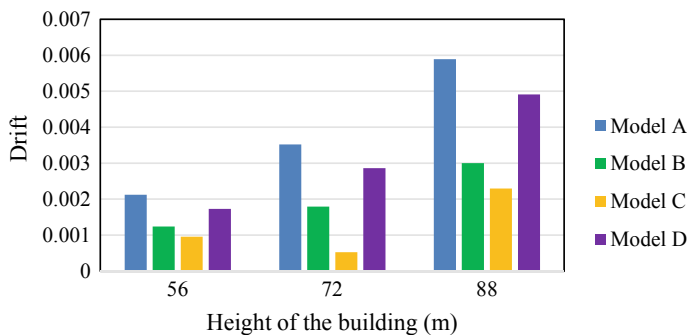


Fig. 3 Effect of different shear wall positions on drift for $H1$, $H2$, and $H3$

2.3 Effect of Openings in Shear Wall

5, 10, and 15% openings in the shear wall are considered for 56, 72, and 88 m heights of the building with the varying size of opening ($R1$, $S1$, $R2$ and $S2$). Table 2 shows the size of opening considered for the present study. The model's name R is indicated for buildings with rectangular openings, and S is indicated for buildings with square openings.

Table 3 shows the outcomes of the results by comparing the analytical output for 15% of opening, and it is observed that the vertical and staggered openings produce nearly identical values. The trend in increase of lateral displacement and lateral drift for shear wall with 5 and 10% of opening remains similar to shear wall with 15% of opening. When compared to walls with vertical openings, the performance and rigidity of walls with staggered openings are significantly higher.

According to Table 3, displacement in the building model with different shapes of openings at different heights of the building is greater in vertical openings than in staggered openings because staggered openings appear to make the shear wall more rigid and ductile, while vertical openings make the shear wall more brittle. The displacement in the square opening is less than a rectangle opening for the 56 and 88 m heights of the building. Analysis shows that staggered openings of both rectangle and square shapes in shear walls perform well against seismic loads.

Storey drift refers to the movement of one storey in relation to another. The maximum drift value follows the same pattern as the lateral displacement, and the

Table 2 Size of opening considered for the present study

S. No.	Model no.	Size of opening (m)
1	$R1$	1.25×2
2	$S1$	1.35×1.35
3	$R2$	1.5×2
4	$S2$	2×2

Table 3 Displacement and drift of vertical and staggered openings for varying sizes (15% of opening) at different heights of the building

Height of the building (m)	Model	Lateral displacement (mm)		Lateral drift		% of reduction	
		Vertical	Staggered	Vertical	Staggered	Displacement	Drift
56	R1	61.81	59.33	0.0011	0.00106	4.01	3.64
	R2	66.75	64.28	0.00119	0.00115	3.70	3.36
	S1	57.36	53.4	0.00102	0.00095	6.90	6.86
	S2	61.81	60.82	0.0011	0.00109	1.60	0.91
72	R1	119.61	110.04	0.00166	0.00153	8.00	7.83
	R2	127.86	115.07	0.00178	0.0016	10.00	10.11
	S1	126.21	112.32	0.00225	0.00201	11.01	10.67
	S2	138.58	123.34	0.00247	0.0022	11.00	10.93
88	R1	227.91	205.12	0.00259	0.00233	10.00	10.04
	R2	243.69	229.06	0.00277	0.0026	6.00	6.14
	S1	219.14	214.76	0.00391	0.00383	2.00	2.05
	S2	238.43	214.58	0.00426	0.00383	10.00	10.09

values for buildings with staggered openings are smaller compared to buildings with vertical openings.

3 Response Reduction Factor

The amount of energy lost due to inelastic deformation during a seismic excitation is measured by a factor known as the R factor. In this investigation, the R factor is evaluated in terms of ductility and over-strength factor. The R factor is calculated by selecting the lowest value of vertical and staggered openings from Table 3. Response reduction factor is determined using Eq. (1) as follows:

$$\text{Response reduction factor}(R) = R_s \times R_\mu. \quad (1)$$

The over-strength factor (R_s) is calculated by comparing the actual ultimate lateral load to the lateral load calculated from IS: 1893 [8] as given in Eq. (2):

$$R_s = V_o/V_b, \quad (2)$$

where

V_o actual base shear coefficient at the performance point of the structure and the value is determined by pushover analysis.

V_b total base shear calculated as per current standard code IS 1893:

$$V_b = W \times A_h, \quad (3)$$

where

W seismic weight of the structure,

A_h design horizontal acceleration coefficient.

The ductility factor (R_μ) is a measure of a material's (or a structure's) ability to withstand significant strain without breaking. The ductility factor is determined using the following Eq. (4):

$$R_\mu = \frac{\mu - 1}{\phi} + 1, \quad (4)$$

where μ = displacement ratio, ϕ = soil condition.

3.1 Pushover Analysis

A pushover analysis determines how far a building can go into the inelastic range before it is about to fail in whole or in part and is therefore subjected to a static analysis. Dead loads and average live loads are applied to the building with the force–deformation relationships of all load-resisting parts before and after yielding. To predict seismic force and deformation requirements, the inelastic static pushover analysis can be used. This study uses inelastic static pushover analysis to investigate the effect of seismic stresses on building models with shear walls. The steps followed to perform a pushover analysis on three-dimensional building are as follows:

- The standard method is used to create the model (without the pushover data).
- The desired qualities and limits for the pushover hinges are specified.
- The frame elements are specified and assigned with one or more hinge attributes and hinge locations to locate the pushover hinges in the model.
- The load cases for defined.
- A nonlinear static pushover analysis is performed.
- The pushover curve is obtained from the analysis.
- The value of V_o is determined from the pushover analysis.

Table 4 shows the response reduction factor calculated for models with vertical and staggered openings. From Table 4, it is observed that the response reduction factor is lesser for vertical openings compared with staggered openings. Staggered openings are preferred to vertical openings since it has similar values to the shear walls without openings.

Table 4 Comparison on the values of response reduction factor

Models	V_o (kN)	R_s	T (s)	R_μ	“R” factor
With a shear wall and no openings	31,269.94	1.96	0.57	1.84	3.60
With shear walls and vertical openings	30,158.85	1.89	0.42	1.48	2.79
With shear walls and staggered openings	31,532.0	2.04	0.50	1.69	3.44

4 Conclusion

The analytical study on building with various shear wall positions, varying sizes of openings, varying percentages of openings, and their influence on the seismic behaviour of the building is carried out. The observations are made and compared for maximum storey displacement and drift for those configurations. From the study, the following conclusions have been made.

1. The shear wall model (Model C) has better performance than the other models because the building is stiffer.
2. Staggered openings have a slightly better arrangement based on displacement and drift than vertical openings.
3. A minimum of 5, 10, and 15% of the openings have lateral displacements for 56 m height of the building (49.94, 51.92, and 53.40 mm), 72 m height (91.15, 94.65, and 110.04), and 88 m height (182.6, 194.86, and 214.58 mm).
4. Staggered openings appear to make the shear wall more rigid and ductile, while vertical openings make the shear wall more brittle.
5. The most rigidity failure occurs in walls with vertical openings due to coupling beam failure.
6. The R factor is greater in staggered shear wall openings than in uniform shear wall openings. As a result, the staggered shear wall improves building performance.

Based on the analysis above, it would be preferable to provide staggered openings than vertical openings. A staggered opening shear wall is the better choice for providing the opening, as it gives better performance against earthquakes.

References

1. Hame VR (2014) Comparative study of strength of RC shear wall at different locations on a multi-storied residential building. *Int J Civ Eng Res* 5(4):341–400
2. Aarthi Harini T, Kumar GS (2015) Behavior of RC shear wall with staggered openings under seismic loads. *Int J Res Emerg Sci Technol* 2(3):91–96
3. Ali Mohammadi H, Esfahani MD, Yaghin ML (2019) Effects of openings on the seismic behaviour and performance level of concrete shear walls. *Int J Eng Appl Sci* 9(1):34–39
4. Bush RC, Shirkol AI, Sruthi JS, Kumar A (2022) Study of seismic analysis of asymmetric buildings with different shapes of staggered openings and without openings in Shear Walls. *Mater Today Proc* 64:964–969

5. Chavan JM, Tupe DH, Gandhe GR (2020) Study of seismic behaviour of staggered opening shear wall in multistorey building. *Int Res J Eng Technol* 7(7):593–598
6. Agarwal P, Shrikhand M (2011) Earthquake resistant design of structures kindle edition. PHI Learning Private Limited, New Delhi
7. IS 456 (2000) Indian standard code of practice of plain and reinforced concrete. BIS, New Delhi
8. IS 1893 (Part 1) (2002) Criteria for earthquake resistant design of structures. BIS, New Delhi

Load-Bearing Masonry: A Review of FE Numerical Analysis Approach



Piyushkumar Vachhani, Payal Desai, and Nirav Patel

1 Introduction

Most current constructions and a substantial amount of the world's-built heritage are mainly composed of existing structures, most of which have walls made of structural (load-bearing) unreinforced masonry (URM) or non-structural (non-load-bearing) infill masonry panels encased in reinforced concrete frames. Also, load-bearing masonry is one of the earliest materials used in structures. Many massive historic structures throughout the world, like temples, forts, churches, water retaining structures, etc., are made of load-bearing masonry. The significant differences between historic and ordinary load-bearing masonry structures are of material used, geometry, and structural composition of the masonry construction. Even though load-bearing masonry has a very long and time-tested record of withstanding immense vertical loadings, it lacks ductility. Earthquake damages have brought attention to the possible earthquake-loading vulnerability of load-bearing unreinforced masonry (URM) structures. Even with low-intensity tremors, cracks could appear in load-bearing masonry construction.

The other probable reasons for cracks to appear in load-bearing masonry constructions can be due to strength degradation because of ageing, weathering, loss of mortar, uneven loading, wind and temperature loadings, and differential settlement. Recent years have seen continual growth in the number of techniques for examining masonry structures due to the increased interest in historical architectural heritage and the desire to preserve historic structures. Although the historic monuments are generally load-bearing masonry construction, physical characteristics and structural behaviour are relatively unexplored. Lack of scientific and experimental understanding and the slow construction process of load-bearing masonry construction have immensely contributed to the development and implementation of innovative

P. Vachhani (✉) · P. Desai · N. Patel
Civil Engineering, Navrachana University, Vadodara 391410, India
e-mail: piyudex@gmail.com

materials and technologies in the construction field like steel and concrete. Although steel and concrete have almost nullified the usage of load-bearing masonry, the total built mass of this planet still has a significant amount of masonry in a variety of forms. Health, safety, stability, and integrity analysis of masonry structures became a critical area of research, and to accurately predict and analyze the mechanical behaviour of masonry structures, numerous numerical techniques have been developed over a period. Experimental and analytical investigation for vast typologies of masonry structures, that are associated with historical structures, with different complex geometries is time-consuming as well as uneconomical. Implementing available scientific evaluation techniques, like finite element numerical modelling approaches which can simulate the behaviour of masonry structures near the actual structural response, predicting and analyzing the health, safety, stability and integrity of the masonry structures. The paper showcases a comprehensive analysis of the difficulties in the numerical modelling of masonry structures. It also overviews two primary numerical approaches—macro (a continuous mechanics model) and micro (discontinuous mechanics model) modelling approaches for the analysis of masonry structures along with an exploration of each strategy and field of application.

2 Structural and Mechanical Challenges

Masonry is a complex material considering that it consists of a variety of different materials used as units and vast mortar compositions along with a different structural geometry. The numerical analysis of masonry structures is a complex task. Along with the uncertainties in mechanical characteristics, the mechanical behaviour of masonry structures is highly unpredictable. For historical structures, the level of complexity increases due to large variations and uneven geometry. The accurate mechanical parameters of masonry and its constituents, which were obtained through destructive and non-destructive laboratory experimental and in situ testing, play a pivotal role in the development of reliable numerical tools with accurate simulation capabilities. While deriving mechanical parameters, one may face two major challenges. First, lack of resources available to investigate the mechanical response of old masonry structures. Second, the analysis of historical structures is constrained by inadequate knowledge and understanding. This section briefly addresses the main structural and mechanical challenges which occur while dealing with historical as well as ordinary masonry structures. More details can be found on this in [1, 2].

2.1 Structural Challenges

Masonry structures largely consist of walls and lintels' arrangements. Structural details of these components play a pivotal role in the mechanical response of the masonry structures. The mechanical response of the wall depends on its structural

details like the type of arrangements of masonry units (masonry bonds line stretcher, header, English, Flemish, etc. [3], connection (toothing or not) between orthogonal walls [4]. In the case of the lintel arrangement, mechanical response depends on the type of lintel (arch, wooden, stone, etc.). When these components form a structure, the strength of the connection with the horizontal diaphragm [5] and interaction with the adjacent building [6] also play an important role in the mechanical response. Structure-related details are also influenced by historical development and the centuries-long overlap of alterations. With a lengthy building time and an uncertain construction sequence, a lot of information is unclear which includes geometry, the inner core of structural elements, the level of present damage, and many more [4]. A thorough geometrical and structural survey is needed in these contexts. Another concern is whether structural details and geometry can be used for structural analysis based on geometrical and structural surveys. As proposed in [7], the CAD drawings can be directly import for simple structural analysis tool. However, it could be difficult to import CAD drawings in mesh-based structural analysis tool. These CAD drawings usually have compatibility issues in terms of mesh errors during numerical process. To address these issues, some methods have been suggested in [8–11].

2.2 *Mechanical Challenges*

Masonry refers to an assembly of components made with blocks bonded with mortar. These blocks usually present quasi-brittle mechanical behaviour and are made of natural stones, fired and unfired clay bricks, calcium silicate bricks, etc. The heterogeneity of masonry is attributed to masonry bond, i.e. assembly of masonry units in a certain pattern, whereas the complexity of masonry is attributed to the large variety of constituent materials with different mechanical properties [1]. Masonry is an anisotropic material [12]. There are three anisotropies that can be observed in masonry. First, strength anisotropy as it shows different strengths with respect to different directions. Second, elastic anisotropy as it exhibits different elastic properties along different directions. And third, brittleness anisotropy is based on its post-peak response. Brick masonry exhibits significant anisotropic properties than stone masonry since there is no periodicity in the material [4].

The mechanical response of masonry is governed by the mechanical properties of its constituents. Masonry components usually exhibit quasi-brittle behaviour under both compressive and tensile loads. Although in comparison to the tensile response, the compressive response exhibits significantly higher values of strength and fracture energy [8]. Figure 1a, b depict the behaviour of quasi-brittle materials under uniaxial tensile and compressive loads, respectively.

In addition to the nonlinearity demonstrated by the masonry constituents, it also exhibits typical stress-dependent cohesive-frictional behaviour in shear and a cohesive behaviour in tension, both of which include softening of the cohesion [2]. Two separate phenomena, tensile and shear failure, can be seen at the unit–mortar

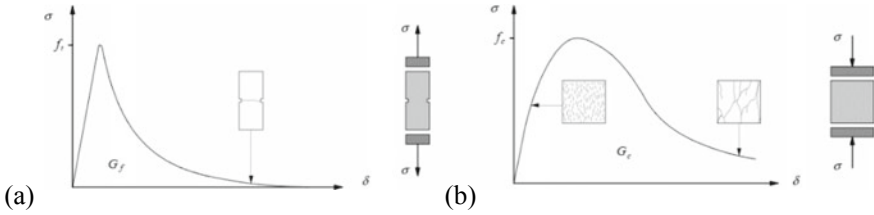


Fig. 1 Behaviour of quasi-brittle materials; **a** uniaxial tensile loading; **b** uniaxial compressive loading [13]

interface. Although, strength, ductility, and stiffness are the defining factors of the mechanical behaviour of masonry.

2.3 Masonry Characteristics

Although masonry can be constructed using a variety of materials, structural details, and geometries, it is extremely difficult to characterize the mechanical properties experimentally. However, over the years, experimental setups and tests have been proposed by various researchers, but the accuracy of those is still debatable [15, 16]. Also, Masonry exhibits different maximum strength and failure modes at different scales as shown in Fig. 2. Masonry could be characterized experimentally at different scales, like masonry components, small-scale masonry wallets, full-scale masonry wall panels, and full-scale masonry structures [17].

Although laboratory testing is considered to be more reliable than the in situ testing. For existing and historical masonry structures, non-destructive and semi-destructive in situ methods can be employed for the characterization of the masonry [18, 19].

2.4 Failure Mechanism

Masonry walls are susceptible to in-plane loading. Some of the common failure patterns observed in the masonry walls are sliding, diagonal cracking, and crushing. Figure 3 depicts typical masonry failure patterns. Sliding occurs due to the low strength of mortar and low pre-compression, whereas diagonal cracking depends on the relative strength of the unit and mortar. Crushing happens due to high loading in the normal direction, whereas diagonal cracking may occur due to high axial load and low aspect ratio.

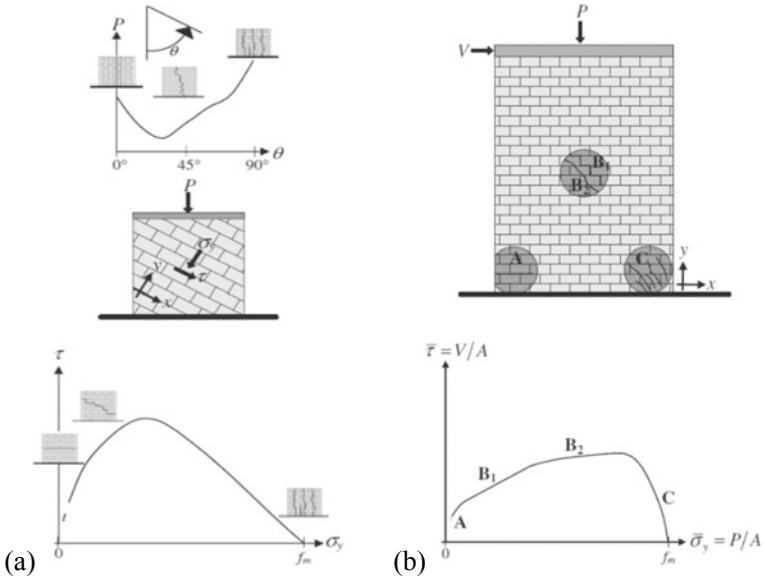


Fig. 2 Maximum strength and failure modes of masonry **a** at material scale, **b** at structural element (pier) scale [14]

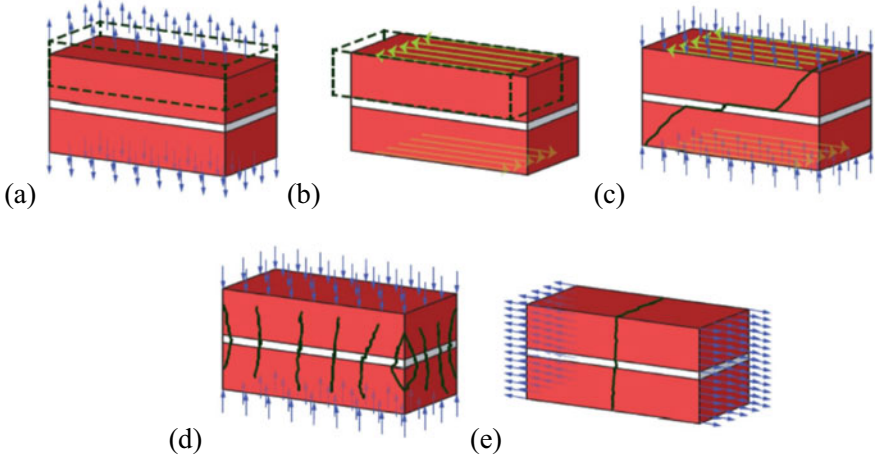


Fig. 3 Masonry failure [20]: **a** bond tensile failure, **b** bond shear sliding, **c** diagonal masonry cracking, **d** masonry crushing, and **e** tensile cracking

3 Masonry Analysis Approaches

To understand the behaviour and damage of masonry structures, it is extremely necessary to develop a reliable advanced structural modelling technique. This modelling approach also aids in developing design principles and comprehending experimental programmes [21]. To model the behaviour of masonry structures, the displacement-based FE method is mostly used. Two basic approaches can be used to explore a masonry structure's collapse or near-collapse response: incremental analyses and limit analysis-based methods [4].

3.1 Incremental Analysis Approaches

Generally, incremental analysis can be based on displacement or loading, in which the loads are divided into several increments. Load and displacement are increased in each step in the load-based incremental and the displacement-based incremental analysis approaches, respectively. These methods make it possible to consider both geometrical and mechanical nonlinearities. It can be classified into two types as follows [22].

First, nonlinear static analysis, with simulations in either load control or displacement control, as well as event-by-event damage control [23, 24]. This type of analysis is used to conduct the pushover analysis, a widely used and standardized method to evaluate the seismic response of masonry structures [4].

Second, nonlinear dynamic analyses can take damping and inertial effects into consideration while gradually applying the time-dependent loading or displacement on the structure [25]. It can simulate how earthquakes, collisions, explosions, and other dynamic events will affect masonry structures.

3.2 Limit Analysis Approaches

Limit analysis estimates the collapse load of a specific structural model based on a set of theorems instead of iterative or incremental analysis [4]. Static theorem (lower bound limit analysis) underestimates the required force to be applied to cause a specific deformation, whereas the kinematic theorem (upper bound limit analysis) overestimates the force to be applied to cause a specific deformation. The two methods are collectively referred to as "limit analysis" since the actual loads needed will fall between the lower and upper boundaries. It only provides information on the mechanism of collapse; it does not provide information regarding the ultimate displacement or post-peak reaction, which are essential to widely used displacement-based seismic evaluation procedures [4].

4 Modelling Strategies

Brick units and mortar joints combine to form the composite material known as masonry. Because mortar joints serve as weak points or planes of weakness, masonry exhibits specific directional characteristics. To define the characteristics of masonry, several constitutive models are used. The definition of the constitutive model is given in [4]. Constitutive models have been created in such a way that simulations and experiments may reasonably agree with each other. As discussed in the previous section, displacement-based FE calculations have been carried out by dividing the structure into elements and assigning the material properties individually [20].

As shown in Fig. 3, it is clear that (a) and (b) are joint mechanisms, (c) and (d) are mechanisms that involve units and joints together, and (e) is a unit mechanism. To consider all these modes of failure in the masonry model is an interesting challenge. Over the years, many researchers have pursued including all these failure modes in a constitutive model. Like [26, 27] have considered the shear and tensile failures of the joints. By limiting the compressive/shear stress combinations, [13] has incorporated diagonal tensile cracking of the units and masonry crushing, along with the shear and tensile crackings of joint failure mechanisms in the model. Two different modelling strategies, micro (discontinuous mechanics model) modelling and macro (continuous mechanics model) modelling, are suggested by [13] to model masonry and all the above-described failure modes using the constitutive models.

4.1 *Micro (Discontinuous Mechanics Model) Modelling*

In the micro-modelling approach, the individual components, unit, mortar, and unit–mortar interface of the masonry are modelled discretely. There are two micro-modelling strategies based on the accuracy required as follows [21].

First, the detailed micro-modelling, in which the units, mortar modelled as a continuum element and the unit/mortar interface is modelled as a discontinuum element [13] Fig. 4a; second, the simplified micro-modelling, in which units are expanded, to maintain overall geometry Fig. 4b, is modelled as continuum elements and the behaviour of the mortar and the unit/mortar interface is combinedly modelled as discontinuum elements [13].

As shown in Fig. 5, units are modelled with continuum elements that expanded in both directions by the mortar thickness [13].

Micromodels can produce load–displacement paths and crack patterns of a masonry structure [13, 21]. The various tests utilized to find the material characteristics necessary for the micro-model are described in [29].

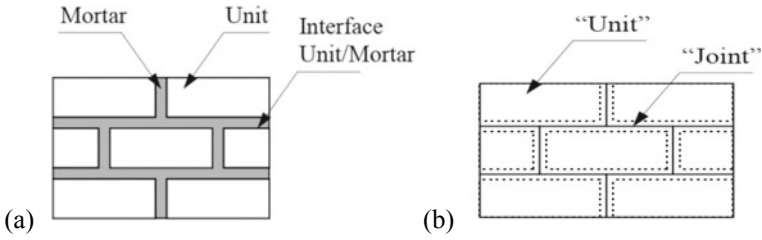
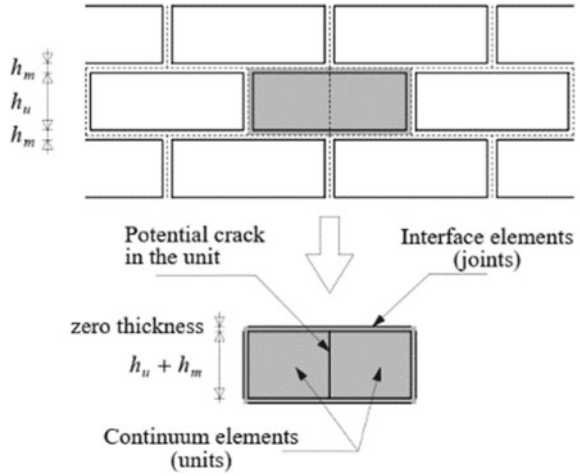


Fig. 4 Modelling strategies **a** detailed micro-modelling, **b** simplified micro-modelling [28]

Fig. 5 Zero-thickness interface element [13]



4.2 Macro (Continuous Mechanics Model) Modelling

In the macro-modelling approach, unit, mortar, and unit/mortar interface are considered and modelled as a homogeneous continuum [13] (Fig. 6a).

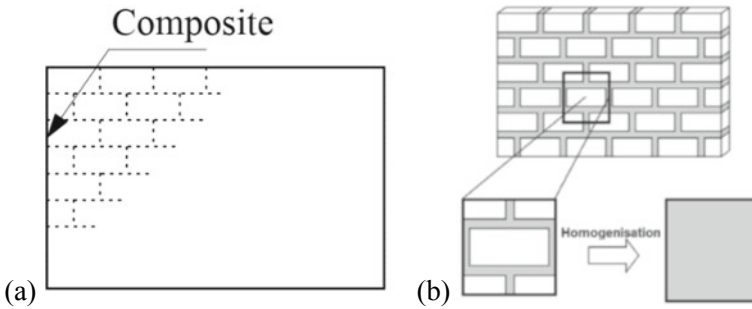


Fig. 6 **a** Macro-modelling strategy [28]; **b** homogenization [29]

It is assumed in [13] that internal parameters associated with a fracture energy in tension and compression can be used to simulate the internal damage related to each failure mechanism, and that micro-level crack development controls the failure mechanism of masonry loaded in tension and compression. These assumptions are made to model a continuum that behaves like the orthotropic material. The material stress–strain behaviour is determined from experimental tests that are conducted on masonry assemblages in [30] or using a process known as homogenization (Fig. 6b). A review of homogenization techniques is provided in [13].

5 Conclusion

The micro-model accounts for the coupling between cracking and decohesion and softening the friction and dilatancy angles. A full pre- and post-failure zone can be tracked, which is in good agreement with experimental observations [13].

Small-scale masonry assemblages, like small structures or structural components, where the interaction between units and mortar is of major importance are particularly well suited for the micro-model. Time and memory requirements are massive for large structures. The macro-model can predict completely diverse behaviour along the material axis. It also can reproduce the biaxial behaviour of all masonry types. The macro-modelling technique does not allow for the modelling of local failure mechanisms (unlike the micro-modelling technique). Since local failure modes are less significant, it is helpful for modelling huge masonry sections. Additionally, it demonstrates significant agreement with the experimental findings [13]. Local masonry failure modes, notably cracking, are significant for historic structures. An accurate local crack pattern may not be replicated by a macro-model [31]. Conversely, a micro-model could imitate local debonding behaviour since it can capture detailed local crack patterns.

It can be concluded that the numerical tool developed using these FE numerical modelling approaches has accurate predictive capabilities in analyzing masonry ranging from historic to modern structures, which can be applied in engineering practices.

References

1. Como M (2013) Statics of historic masonry constructions. Springer, Berlin
2. Hendry A (1998) Structural masonry. Macmillan Education, London
3. ICETEC Homepage, <https://www.lceted.com/2021/05/types-of-bonds-used-in-brick-masonry.html>. Last accessed 2022/01/21
4. D'Altri AM, Sarhosis V, Milani G et al (2020) Modeling strategies for the computational analysis of unreinforced masonry structures: review and classification. Arch Computat Methods Eng 27:1153–1185

5. Solarino F et al (2019) Wall-to-horizontal diaphragm connections in historical buildings: a state-of-the-art review. *Eng Struct* 199:1–20
6. Tondelli M et al (2012) Evaluation of uncertainties in the seismic assessment of existing masonry buildings. *J Earthq Eng* 16 (sup a):36–64
7. Chiozzi A, Grillanda N, Milani G, Tralli A (2018) An adaptive limit analysis NURBS-based program for the automatic assessment of partial failure mechanisms in masonry churches. *Eng Fail Anal* 85:201–220
8. Castellazzi G, D’Altri A, Bitelli G, Selvaggi I, Lambertini A (2015) From laser scanning to finite element analysis of complex buildings by using a semi-automatic procedure. *Sensors* 15(8):18360–18380
9. Castellazzi G, D’Altri AM, de Miranda S, Ubertini F (2017) An innovative numerical modeling strategy for the structural analysis of historical monumental buildings. *Eng Struct* 132:229–248
10. Korumaz M, Betti M, Conti A, Tucci G, Bartoli G, Bonora V, Korumaz AG, Fiorini L (2017) An integrated terrestrial laser scanner (TLS), deviation analysis (DA) and finite element (FE) approach for health assessment of historical structures. A minaret case study. *Eng Struct* 153:224–238
11. D’Altri AM, Milani G, de Miranda S, Castellazzi G, Sarhosis V (2018) Stability analysis of leaning historic masonry structures. *Autom Constr* 92:199–213
12. Page AW (1981) The biaxial compressive strength of brick masonry. *Proc Inst Civ Eng* 71(3):893–906
13. Lourenco PB (1996) Computational strategies for masonry structures. Delft University of Techno, Delft, The Netherlands
14. Calderini C, Cattari S, Lagomarsino S (2009) In-plane strength of unreinforced masonry piers. *Earthq Eng Struct Dyn* 38(2):243–267
15. Sassoni E, Mazzotti C, Pagliai G (2014) Comparison between experimental methods for evaluating the compressive strength of existing masonry buildings. *Constr Build Mater* 68:206–219
16. Kržan M, Gostič S, Cattari S, Bosiljkov V (2015) Acquiring reference parameters of masonry for the structural performance analysis of historical buildings. *Bull Earthq Eng* 13(1):203–236
17. Esposito R, Messali F, Ravenshorst GJP, Schipper HR, Rots JG (2019) Seismic assessment of a lab-tested two-storey Dutch terraced house. *Bull Earthq Eng* 17(8):4601–4623
18. Borri A, Castori G, Corradi M, Speranzini E (2011) Shear behavior of unreinforced and reinforced masonry panels subjected to in situ diagonal compression tests. *Constr Build Mater* 25(12):4403–4414
19. Lumantarna R, Biggs DT, Ingham JM (2014) Compressive, flexural bond, and shear bond strengths of in situ New Zealand unreinforced clay brick masonry constructed using lime mortar between the 1880s and 1940s. *J Mater Civ Eng* 26(4):559–566
20. D’Altri AM, de Miranda S, Castellazzi G, Sarhosis V (2018) A 3D detailed micro-model for the in-plane and out-of-plane numerical analysis of masonry panels. *Comput Struct* 206:18–30
21. Lourenço PB (2008) Structural masonry analysis: recent developments and prospects. In: *Proceedings of 14th international brick and block masonry conference*. University of Newcastle, Callaghan, NSW, Australia
22. Reddy JN (2004) *An introduction to nonlinear finite element analysis*. Oxford University Press, Oxford
23. DeJong MJ, Belletti B, Hendriks MA, Rots JG (2009) Shell elements for sequentially linear analysis: lateral failure of masonry structures. *Eng Struct* 31(7):1382–1392
24. Rots JG, Belletti B, Invernizzi S (2008) Robust modeling of RC structures with an “event-by-event” strategy. *Eng Fract Mech* 75(3–4):590–614
25. Clough RW, Penzien J (2003) *Dynamics of structures (revised)*. Computers and Structures Inc., Berkeley, Calif
26. Page AW (1978) Finite element model for masonry. *J Struc Div ASCE* 104(8):1267–1285
27. Rots JG, Berkers WGJ, Heuvel HA, Van Den JG (1994) Towards fracture mechanics-based design rules for movement-joint spacing. In: *Shrive NG, Huizer A (eds) 10th international brick and block masonry conference*. University of Calgary, Calgary, Alberta, Canada, pp 707–717

28. Angelillo M, Lourenco P, Milani G (2014) Masonry behaviour and modelling. CISM International Centre for Mechanical Sciences, Courses and Lectures, pp 1–26
29. Rots JG (1997) Structural masonry: an experimental/numerical basis for practical design rules. Balkema, Rotterdam
30. Page AW (1983) The strength of brick masonry under biaxial compression-tension. *Int J Masonry Constr* 3(1):26–31
31. Grande E, Milani G, Sacco E (2008) Modelling and analysis of FRP-strengthened masonry panels. *Eng Struct*: 30, 1842–1860

Comparison of Reinforced Cement Concrete Versus Steel Structures in Health Industry



R. Kavitha, V. Rajeshkumar, S. Sabarinathan, V. Vijai Anand, and J. Ajithkumar

1 Introduction

Medical equipment rooms required service trenches to provide cables. Higher floor height is required at operation theatre locations to install high ventilation air conditioning plenums and lighting. Sufficient space should be available between the ceiling and the false ceiling to run all the service lines. It needs radiation insulation for the computed topography simulator, MRI scan, X-ray, linear accelerator, and other medical equipment rooms. Noise insulation should be provided for air handling units and other electrical equipment rooms as a functional requirement. The life of the structure shall be considered to be 100 years. Steel is used as an alternative material for construction is gaining acceptance around the world due to many reasons fabricated steel materials are kept in the factory yard. Material for construction is stored on site. Consequently, there is less congestion on site, which improves site management. Concrete structures have better fire resistance than steel. RCC construction will result in lower project costs overall than steel buildings [1].

1.1 Merits of RCC Structures

RCC structures need unskilled labour, not like steel structures, which require skilled labour. RCC structures are economical, so the overall cost of the projects will be lower in the case of RCC structures compared to steel structures. RCC materials are easily available. Outweigh is an advantage for structures, which is critical to wind load and flood load conditions to satisfy the stability of structures. Since service coordination

R. Kavitha (✉) · V. Rajeshkumar · S. Sabarinathan · V. Vijai Anand · J. Ajithkumar
Department of Civil Engineering, KPR Institute of Engineering and Technology, Coimbatore,
Tamil Nadu 641407, India
e-mail: kavitha.r@kpriet.ac.in

is more important in healthcare projects, core cutting in RC slabs is easier compared to composite deck slabs. RCC has less thermal expansion capacity than steel, so it is affected by high temperatures [2]. Reinforced concrete structures have better thermal expansion and sound insulation than steel structures. RCC structures are good enough to absorb radiation from medical equipment such as linear accelerators, X-rays, CT simulators, MRI scans, brachytherapy, and nuclear plants. RCC structures are weatherproof, allowing them to withstand the most severe effects of climate change. It can be cast to take the shape required by the architect because of its fluidity. RCC structures withstand noise insulation for air handling units and other medical equipment rooms. RCC structures can easily withstand earthquake loads and are designed with an important factor for seismic load conditions of 1.5.

1.2 Merits of Steel Structures

Steel has many advantages and is becoming more popular in India as a substitute for other building materials due to many reasons. Due to the faster construction schedule, the construction time on site is reduced since the steel framework is manufactured off-site and is merely welded together. In comparison with concrete structures, steel frames may be constructed in less than 50% of the time. Material is fabricated off-site in a highly precision-engineered condition. Hence, better quality can be achieved. The entire production process is automated, with input from Tekla that becomes the CNC machine's input data and is directly fabricated, reducing the involvement of humans. Quality control can be planned, executed, and monitored easily in steel. Fewer labours are required at the site, so less administrative people are required, which results in fewer accidents happening at the site. The majority of workers are highly trained and skilled, making construction in steelwork much safer than reinforced concrete. Steel adds to the green building concept in terms of the reusability of steel after the life cycle of the project. Steel frames can be 100% recycled and reused. Steel frames can be demountable and reusable. It needs fewer well-trained and skilled labours, and accidents will be fewer to achieve safety. Steel has the advantage of being compatible with modification after construction. Steel better addresses modification issues as compared to concrete. Steel frames can achieve much longer spans. Office floors can achieve long spans of up to 18 m. Wide column spanning implies better utilisation of space and reduced area due to internal columns. Hence, it produces better-quality spaces [3]. Long spans provide more flexibility for future changes in use. Parallel activity is possible when the structure can be done at the top and glazing work can be done at the bottom. Architectural features can be easily accommodated in steel structures. The erection process will be safe when compared to RCC structures. Less storage space is required at the site, and material is fabricated and stored at the factory yard. Material for a construction is stored at the site. Hence, less clogging of space is required at the site. Steel construction is quiet and dust-free. A steel structure can be built in a commercial area with little hindrance to the public. Complicated design and fabrication can be simplified, and accuracy can be guaranteed.

2 Modelling and Analysis

The building described is a 24-storey hospital with three basement levels and a ground floor. The original structural system is made up of a reinforced concrete flat slab with a drop, peripheral beams, and column construction. The columns are spaced at 11.7×8.7 m and 8.7×8.7 m centres, and lateral stability is provided by reinforced concrete walls located in the lifts, stairwells, and edges. For comparison, a steel frame building was modelled by replacing the reinforced concrete flat slab with composite deck sheets, the reinforced concrete peripheral beams with steel beams, and the reinforced concrete columns with steel columns. The steel beams and columns would need to be designed to support the same loads as the previous reinforced concrete structure. Lateral stability would need to be provided by the steel frame and bracing system. The foundation, which is a raft foundation with pedestals, as determined by the soil report, would also be used in steel frame buildings. 3D structural modelling and analysis were carried out using a finite element software package for dead load, live load, wind load, earthquake load, and load combinations [4–6].

2.1 Dead Imposed Load

The imposed loads are intended to act permanently (wherever applicable) as listed in Table 1. This load includes the self-weight of every frame and shell element built into the structure, as well as the self-weight of slabs applied to beams as trapezoidal, triangular, or uniform loads depending on the yield line pattern. This example consists of toilet waterproofing, ceiling-hung loads, and floor finishes. Solid brick walls that are either 230 or 115 mm thick make up every interior and exterior wall. Calculated loads are applied when necessary as either an evenly distributed load on the beams or a uniform pressure on the slab. This load also takes into account parapet loads [6, 7].

Table 1 Dead imposed load

Description	Intensity in kN/m ² of plan area
Weather-proof course	Depends on the thickness and slope
False ceiling and MEP services	0.5
Floor finish	1.2

Table 2 Live load

Occupancy classification	Udl kN/m ² of plan area
X-ray rooms	3.0
Operating rooms, general storage area, ICU	3.0
Office rooms and OPD rooms	2.5
Wards and dressing rooms	2.0
Records/files store rooms and storage space	5.0
Corridors, passages including staircases	4.0

2.2 Live Load

The live loads based on the occupancy classification as per IS: 875 (Part 2) are mentioned in Table 2 [8–10].

2.3 Wind Load

The wind load and pressure on the structure are calculated based on the provisions in IS: 875 (Part 3)—2015. The basic wind speed is 44 m/s, risk coefficient is 1.07, terrain category is 2, structure class is Class C, and the topography factor is 1.0. These inputs are used to determine the static design wind pressure, which is then applied to the model for the load analysis. The joint loads for each floor are calculated based on the contributory areas and applied in the respective diaphragms [11, 12].

2.4 Seismic Load

The loading due to earthquakes is calculated based on IS: 1893. Seismic Zone III is considered, and an importance factor of 1.5 is applied for the hospital building. The response spectrum method is used for the dynamic analysis of earthquake forces in both *X* and *Y* directions. The response spectrum values are calculated using *T* versus *Sa/g* equations, and the base shears are adjusted by a factor of (\sqrt{B} bar/ \sqrt{B}). The effect of torsion is considered by applying eccentricity overrides in the software [13].

3 Result and Discussion

A typical foundation design done for a 24-storey building in RCC and steel requires a reinforced concrete frame of 78 m³ and a steel frame of 24 m³, which shows steel buildings are 40% lighter than equivalent reinforced concrete and hence require

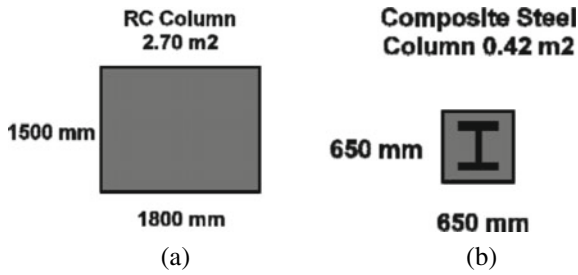


Fig. 1 a Reinforced concrete frame. b Steel frame

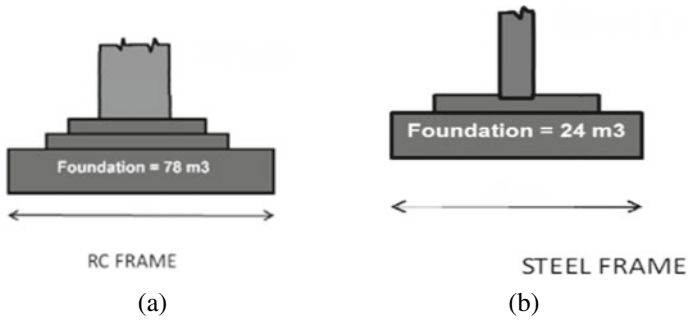


Fig. 2 a Carpet area for reinforced concrete frame. b Carpet area for steel frame

70% less concrete, resulting in smaller foundations and lesser site work. This saves time and money on groundwork. The approximate foundation size for reinforced concrete frames and steel frames is shown in Fig. 1. A typical column design for a 24-storey building requires a column size of 1500 mm by 1800 mm. The composite steel column size required is 650 mm by 650 mm. The carpet area required for the typical column design of a 24-storey building is shown in Fig. 2. The size of steel columns is much smaller than RCC columns, and the sleek nature of steel enables more carpet area. Steel columns take up less space; they can be 85% smaller than equivalent RC columns. This results in an increase in net lettable floor space and is more architecturally pleasing. The approximate RC column size for reinforced concrete frames and steel frames is shown in Fig. 2.

4 Conclusion

The cost of the steel structures is mainly based on the RC foundation, RC basement, structural steel for column, beam, profile deck sheeting, steel erection, fire protection coating, reinforced cement concrete slab over deck slab, concrete to encase the steel column, RC core wall for staircase and lift location, lintel and sunshade, elevation

features, staircase, water tanks, pedestals, and the addition width of the expansion joint between two buildings. If the steel structure is built for both dead load and live load, the cost will increase by 40–50% compared to RCC buildings and by 70% if the steel structure with bracing is intended for lateral load. Steel buildings are 40% lighter than equivalent reinforced concrete and hence require 70% less concrete, resulting in smaller foundations and lesser site work. Steel columns take up less space; it can be 85% smaller than equivalent RC columns. The type of structure is to be considered based on the optimisation of:

- Due to the return on investment—Steel structures can be erected much faster than concrete structures. Steel components are prefabricated off-site, allowing for efficient assembly on-site. This reduces labour costs and overall construction time, resulting in cost savings.
- Labour availability—Conduct a thorough assessment of the project requirements and create a comprehensive workforce plan. This plan should consider the required skills, experience levels, and labour quantities for each phase of the project.
- Completion time—Construction time can vary depending on project size, complexity, and other factors; steel structures generally offer shorter construction durations compared to concrete structures. The ability to prefabricate steel components, the ease of assembly, reduced curing time, and weather independence are key factors that contribute to the faster completion time of steel structures. Construction time was almost reduced to 50%.
- In the healthcare industry, buildings should be fire-proof and radiation-insulated to satisfy functional requirements.
- Air and noise pollution control needs to satisfy the statutory requirements.

References

1. Kavitha R, Logeshwaran S, Sabarinathan S, Vijaijanand V (2023) Structural analysis and design for a warehouse using STAADPRO. <https://doi.org/10.1016/j.matpr.2023.04.479>
2. Kavitha R, Sundaraja MC, Ram Vivekananthan M, Vinodhini C, Thiruvishnu P, Deepan P (2023) Seismic analysis and design of multilevel car parking using ETABS. <https://doi.org/10.1016/j.matpr.2022.04.212>
3. Kavitha R, Sundaraja MC, Indhiradevi P, Manikandan P, Archana Vaishnavi S, Karthikeyan G, Abdul Rahman A, Akash E (2021) Flexural and compressive behaviour of I Steel Section strengthened by stainless steel plate. *Mater Today Proc*
4. Sameer P (2016) Study of seismic analysis and design of multi storey symmetrical and asymmetrical building. *Int Res J Eng Technol* 03(01):732–737. ISSN: 2395-0056
5. Balaji U (2016) Design and analysis of multi-storied building under static and dynamic loading conditions using ETABS. *Int J Tech Res Appl* 4(4):1–5. ISSN: 2320-8163
6. Balaji, Selvarasan (2016) Design and analysis of multi-storeyed building under static and dynamic loading conditions using ETABS. *Int J Tech Res Appl* 4(4):1–5. e-ISSN: 2320-8163, www.ijtra.com
7. Geethu SN, Depthi M, Abdul Nasir NA, Izzudeen KM (2016) Comparative study on design and analysis of multi storied building by STAAD. Pro and ETABS softwares

8. Patil MN, Sonawane YN (2015) Seismic analysis of multi-storied building. *Int J Eng Innov Technol* 4(9):123–129. ISSN: 2277-3754
9. Varalakshmi V, Shivakumar G, Sarma RS (2014) Design of G+5 residential building by ETABS. In: International conference on advance in engineering and technology
10. Kumawat MS, Kalurkar LG (2014) Analysis and design of multistory building using composite structure. *Int J Struct Civ Eng Res* 3(2):125–137. ISSN 2319–6009, www.ijscer.com
11. Ambadkar SD, Pajgade PS (2012) Design of steel frame industrial building compared with reinforced cement concrete industrial building. *Int J Sci Eng Res* 3(6). ISSN 2229-5518
12. Panchal DR, Marathe PM (2011) Comparative study of RCC, steel and composite (G+30 storey) Building. ICCTT
13. IS: 1893:2000, Part 1 (2002) Criteria for earthquake resistant design of structures—general provisions for buildings. Bureau of Indian Standards, New Delhi

Experimental Investigation on Concrete by Partial Replacement of Fine Aggregate with Olivine Sand



G. Akash Kanna and N. Parthasarathi

1 Introduction

Concrete is widely regarded as one of the most commonly utilized building materials worldwide. It is notable for its great compressive strength and a considerably lower environmental impact when compared to steel. However, since concrete is used in such large quantities during construction, the main concern regarding its use is the environmental impact. A recent study indicated that concrete is responsible for up to 8% of global CO₂ emissions [1]. A Lancet study also estimated that 1.7 million of India's registered fatalities in 2019 were premature, accounting for 17.8% of all deaths that year which were largely caused by particulate matter (PM) pollution. Hence, this is a compelling argument for creating greener concrete that has a better influence on the environment, in this case, carbon absorption [1].

According to the above considerations, this paper focuses on investigating the behaviour of partial replacement of fine aggregate using olivine sand. In 2022, Frank Winnefeld proposed that magnesium silicate-based rocks such as olivine are sufficiently abundant and are significantly capable of sequestering all the carbon emissions for the next few centuries [2]. The usage of these materials will not only sequester higher amounts of CO₂ but also open up possibilities for generating construction materials with a carbon-negative impact.

Olivine sand is utilized as a substitute for fine aggregate since it has proven to have strong carbon absorption qualities and because utilizing waste materials and readily available resources is a growing trend in the building industry. This will not only lower the atmospheric CO₂ level but also improve the concrete's tensile and compressive strengths, making it a preferable alternative to fine aggregate. In addition, olivine

G. Akash Kanna · N. Parthasarathi (✉)

Department of Civil Engineering, Faculty of Engineering and Technology, SRM Institute of Science and Technology, Kattankulathur, Tamil Nadu 603203, India

e-mail: parthasn@srmist.edu.in

sand has a high thermal resistance capacity which makes the concrete resistant to thermal attacks up to 850 °C [3].

2 Materials Used

2.1 Cement

Cement plays an essential role in the field of construction, serving as a fundamental component for various structures including buildings, bridges, dams, roads, and many others. In this paper, Ordinary Portland Cement (OPC) of grade 53 was utilized. As per IS4031 part 11-1988 [4], the specific gravity of cement typically falls within the range of 3.10–3.16, while the recommended fineness should be around 10%. The cement employed in this study exhibits a specific gravity of 3.15 and a fineness of 8%.

2.2 Olivine Sand

Olivine sand is a naturally occurring mineral obtained by crushing a type of rock known as dunite. The mineral is notable for its high melting point and high relative density [5–7]. This makes it one of the best substitutes when compared to other sands [2]. Olivine sand is primarily used for making moulds in the manufacture of large steel and iron castings which provides a cleaner surface when demoulded than using quartz sand.

The specific gravity of olivine sand ranges from 3.2 to 3.4 and the fineness modulus ranges from 2.2 to 3.2. In this project, the variation in percentage of olivine sand as a fine aggregate replacement is done.

2.3 M-Sand

Manufactured Sand (M-Sand) is a type of sand which is used as a substitute for conventional river sand. These are made by crushing hard rocks and granites. The M-Sand has a particle size of 4.75 mm. The rapidly expanding construction sector has caused a significant rise in sand demand, which has resulted in a global shortage of adequate river sand. The usage of M-Sand has grown due to the over-exploitation of high-quality river sand for construction. As per IS383-2016 [8], the specific gravity of M-Sand ranges from 2.4 to 2.9 and the fineness modulus ranges from 2.2 to 3.2. In this paper, M-Sand was utilized as a fine aggregate.

2.4 Coarse Aggregate

Coarse aggregate refers to the granular material used in construction, primarily for creating concrete and other composite materials. The primary role of coarse aggregate in concrete is to provide volume and stability to the mixture. By combining with cement, water, and fine aggregates (such as sand), coarse aggregates form the framework that binds the concrete together. In this study, coarse aggregates measuring 12 mm in size were employed. The physical characteristics of the coarse aggregate were assessed in accordance with IS383-2016 [8] and IS2386 part 1-1963 [9], revealing a specific gravity of 2.51 and a fineness modulus of 4.89.

3 Preparation of Specimens

Concrete mix of grade M30 was prepared as per IS456-2000 [10] and IS10262-2019 [11] for the desired fine aggregate replacement proportions. A special care should be taken while mixing the concrete as it may affect the workability and structural integrity of the concrete. Preliminary tests such as specific gravity and fineness modulus were done to evaluate the characteristics of the materials used prior mixing of concrete. Machine mixing is adopted to get an efficient and uniform mixing.

After the mixing process, the concrete mix is poured into a variety of moulds as per requirement. The compressive strength test utilized cubical moulds measuring 100 mm × 100 mm × 100 mm, while the flexural strength test employed cuboidal moulds measuring 500 mm × 100 mm × 100 mm. Lastly, for the split tensile strength test, cylindrical moulds with dimensions of 200 mm × 100 mm were utilized. In this study, 100 mm cubical moulds and 200 mm cylindrical moulds were used instead of 150 mm cubical and 300 mm cylindrical moulds due to their convenience in handling and storage. Another reason for adopting these mould sizes is for easy comparison and reference to past studies and projects using the same cube size, enhancing the comparability of test results. After the concrete mixture is carefully poured into the moulds, it is crucial to maintain a state of uninterrupted rest for a duration of 24 h to allow the concrete to dry. Then the concrete specimens are demoulded and transferred to the curing tank. Subsequently, the cured concrete undergoes testing at intervals of 7 days, 14 days, and 28 days to assess their respective strengths.

4 Experimental Study

4.1 Compressive Strength Test

Compressive strength stands as a fundamental characteristic of concrete. In this study, the primary objective was to determine the maximum load-carrying capacity of concrete specimens. The test was carried out in accordance with IS516-1959. The experiment involved casting seven different concrete mix proportions, including a conventional mix, into cube moulds sized at 100 mm × 100 mm × 100 mm. For each curing period, three sample specimens were casted for each mix proportion such that 9 cubes per proportion which sums up to a total of 63 concrete cubes. Following the designated curing time, the cubes were dried and carefully positioned within a compression testing machine (CTM) capable of handling 2000 kN. Gradually, an increasing load was applied to the surface of each specimen until it ultimately failed, allowing for the recording of the maximum load endured.

4.2 Split Tensile Strength Test

The split tensile strength test was conducted to determine the hardened concrete's capacity to withstand tension. This test was performed in accordance with IS5816-1999. In general, concrete is not expected to resist direct stress and tends to develop cracks when the tensile force surpasses its inherent tensile strength, primarily due to its brittle characteristics. For this experiment, cylindrical moulds of size 200 mm × 100 mm were used. The cylindrical concrete specimens were positioned horizontally in a CTM of 2000 kN capacity and subjected to a uniform load until it failed vertically. The resulting failure load was recorded, and the concrete's tensile strength was determined.

4.3 Flexural Strength Test

The flexural strength test is a widely employed method for evaluating the capacity of concrete to resist bending or flexural forces. The size of the beam mould used in this experiment is 500 mm × 100 mm × 100 mm. To prevent any reduction in flexural strength due to surface drying, the specimens were promptly tested upon removal from the curing environment. The specimens were marked with a line of 5 cm from both ends of the beam and a line of 7 cm on both sides from the midpoint of the beam. For this test, a Universal Testing Machine (UTM) with a capacity of 2000 kN was used. The specimens were loaded without shock at a constant rate of 1800 N/m until the specimen gets failed. The failure load was noted, and the flexural strength of the concrete was evaluated.

Table 1 Properties of hardened concrete

Percentage of olivine sand in concrete (%)	Compressive strength of concrete (MPa)			Split tensile strength of concrete (MPa)			Flexural strength of concrete (MPa)		
	7 days	14 days	28 days	7 days	14 days	28 days	7 days	14 days	28 days
0	24.23	31.07	33.06	1.32	1.71	2.16	7.11	8.69	9.41
10	24.82	31.35	34.32	2.02	2.74	2.98	8.30	8.77	9.72
20	25.16	32.27	35.57	2.47	3.12	3.44	8.63	9.36	9.81
30	27.03	33.41	38.14	2.84	3.57	3.60	9.61	9.95	11.02
40	25.30	32.28	34.44	2.59	3.37	3.38	8.66	9.52	9.84
50	25.31	31.81	34.23	2.48	3.23	3.34	7.91	9.41	9.75
60	24.62	30.97	34.05	2.36	3.09	3.28	7.61	9.19	9.41

5 Results and Discussion

5.1 Compressive Strength of Concrete

The compressive strength of concretes of various replacement proportions was examined and compared [12, 13]. Table 1 gives the compressive strength of concrete at various fine aggregate replacement proportions. Results show that the compressive strength of concrete improves when the fine aggregate is substituted with olivine sand up to 30% and gradually decreases after further replacement proportions. This may be due to the finer particle size of olivine sand which slows down the formation of the water-cement gel matrix, a crucial factor in determining the strength of concrete. The concrete mixture utilizing M30 grade and replacing 30% of fine aggregate with olivine sand demonstrates a peak compressive strength of 38.14 MPa, surpassing the conventional mix's strength of 33.06 MPa after 28 days. These findings indicate that incorporating 30% olivine sand as a replacement for fine aggregate yields the optimum strength. Figure 1 shows the graph of compressive strength versus percentage of olivine sand in concrete.

5.2 Split Tensile Strength of Concrete

The splitting tensile strength of concrete at different fine aggregate proportions is given in Table 1. A similar response was obtained from the results which indicates that the strength of concrete gradually increases up to 30% of olivine sand in concrete and decreases with further replacement proportions. Cylindrical specimens made of M30 grade concrete were fabricated in order to assess the splitting tensile strength. Based on the findings, the optimal splitting tensile strength of 3.60 MPa was attained

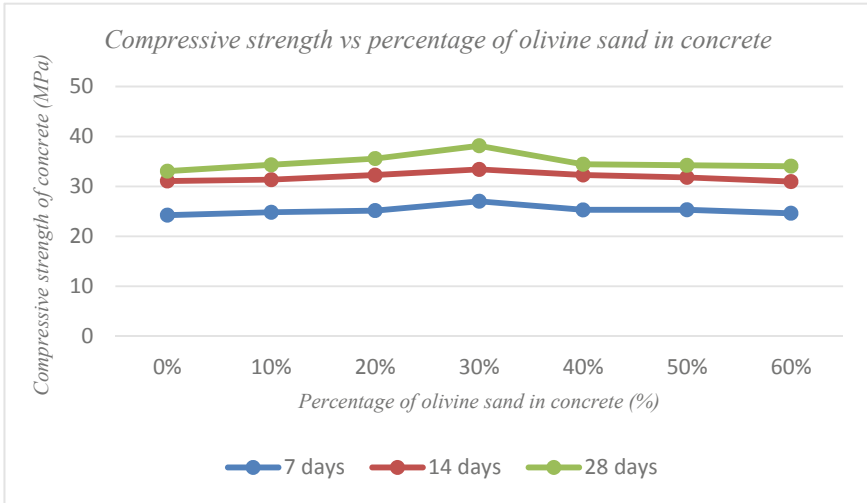


Fig. 1 Compressive strength versus percentage of olivine sand in concrete

from 28 days of curing by incorporating 30% olivine sand as a replacement for M-Sand, surpassing the tensile strength of conventional concrete, which measures at 2.16 MPa. Figure 2 shows the graph of split tensile strength versus percentage of olivine sand in concrete.

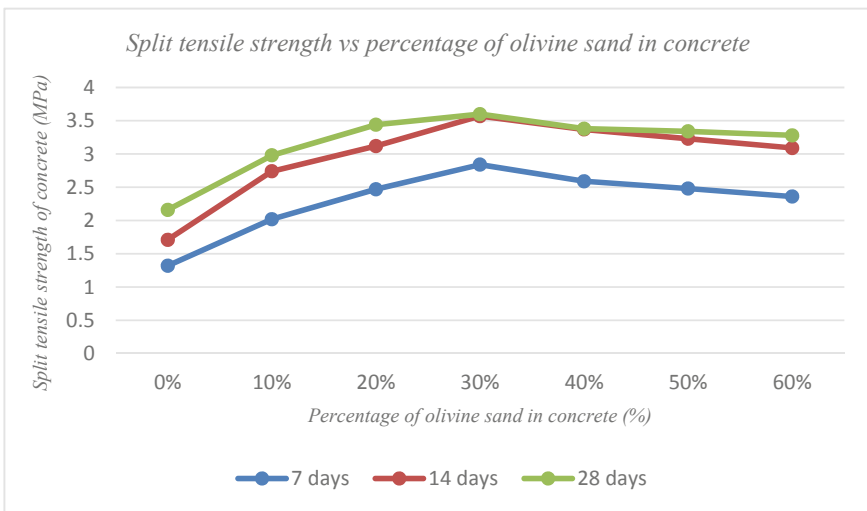


Fig. 2 Split tensile strength versus percentage of olivine sand in concrete

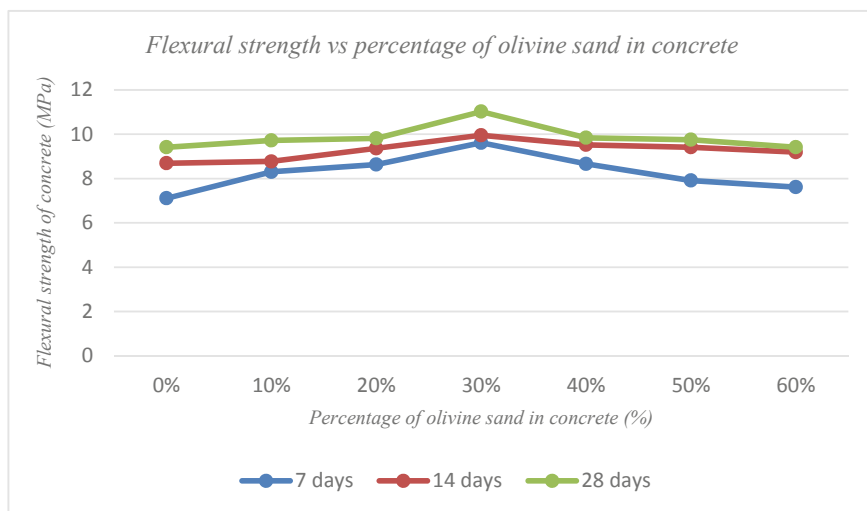


Fig. 3 Flexural strength versus percentage of olivine sand in concrete

5.3 Flexural Strength of Concrete

The flexural strength results of different fine aggregate proportions in concrete are given in Table 1. To determine the flexural strength, flexure beams were casted and subjected to curing. Following the curing period, three-point loading was applied to the specimens to check the failure load. The flexural strength of the specimen exhibits a proportional increase of up to 30% fine aggregate replacement with olivine sand, similar to the patterns observed in compressive and tensile strength. However, upon further addition of olivine sand, the flexural strength experiences a decline. The flexural strength of the concrete incorporating 30% olivine sand was assessed at the end of 28 days and determined to be 11.02 MPa. This value surpassed the flexural strength of conventional concrete, which measured at 9.40 MPa. Based on the results obtained, 30% replacement of M-Sand with olivine sand provides better performance and gives the optimum flexural strength. Figure 3 shows the graph of flexural strength versus percentage of olivine sand in concrete.

5.4 Microstructural Studies on Concrete Samples

The microstructures of the optimum concrete and conventional concrete were analysed and compared [3]. Based on the development of hydration components in the microstructure of the samples, the reason behind the strength of concrete was determined. Pores, residual hydrated cement, Calcium Silicate Hydrate (C-S-H), and calcium hydroxide (CH) are the most important elements to be considered during

the microstructural study of concrete [14]. The HRSEM microstructural images of the conventional and optimum concrete powder samples are shown in Figs. 4 and 5.

The HRSEM images give detailed information on the elements present in concrete's surface structure and microstructure [14]. The powdered concrete samples were sieved to get uniform size distribution and then subjected to the analysis. For this project, microstructural images of the concrete samples at a magnification of 5000 and 15,000 μm were obtained. The fundamental factor responsible for the practical hardness of conventional concrete was found to be the widespread distribution of C-S-H gel over the wet cement paste mixture [6]. A variety of hydration products including CSH and CH were formed in all concrete samples. Calcium hydroxide (CH) is represented by the bright portion in the HRSEM image whereas Calcium Silicate Hydrate (CSH) is represented by the grey spherical portion. The finer the aggregate, concrete will exhibit more compact surface with minimum voids.

XRD analysis is one of the techniques to identify the mineral composition like Calcium Silicate Hydrate (CSH), calcium carbonate (C), calcium hydroxide (CH), ettringite present in concrete. As illustrated in Fig. 6, the X-ray diffraction (XRD) analysis revealed prominent peaks of quartz (SiO_2) in both concrete samples. The detection of CSH indicates the formation of hydration products in concrete, which play a crucial role in conferring strength to cement-based concretes [6]. The peaks of calcium-bearing minerals are linked to cement, whereas the peaks of quartz are linked to aggregates. The presence of peaks indicating calcium hydroxide (CH) and carbon

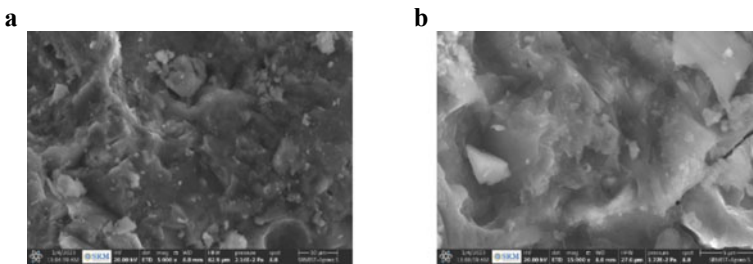


Fig. 4 Microstructural image of conventional concrete **a** 5000 μm ; **b** 15,000 μm

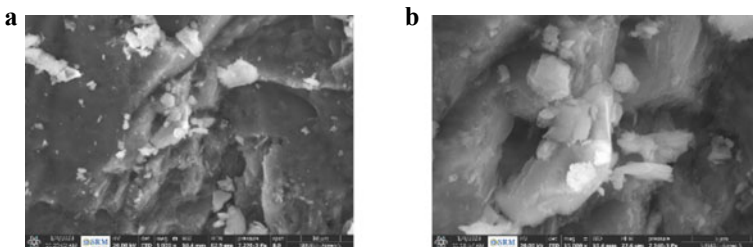


Fig. 5 Microstructural image of optimum concrete **a** 5000 μm ; **b** 15,000 μm

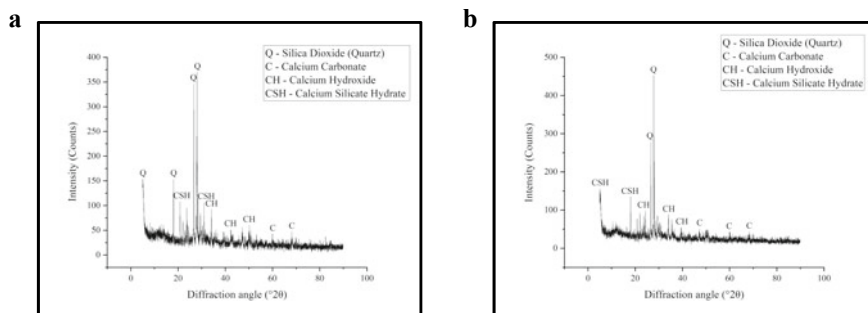


Fig. 6 XRD pattern of **a** conventional concrete; **b** optimum concrete

(C) in the XRD pattern implies an abundance of unreacted lime in the cement, potentially caused by the lack of amorphous components within the concrete [15]. Notably, Fig. 6 demonstrates that the optimum concrete sample exhibited sharp peaks of SiO_2 along with significant CSH peaks [3]. Apart from this, other mineral peaks were found weaker. The presence of hydration products suggests that the calcium minerals were almost entirely converted, leading to the formation of a well-developed microstructure. This, in turn, contributes to the reinforcement of the concrete's strength [14]. Ettringite, which could have transformed into monosulfaluminate hydrates during subsequent hydration phases, was not detected in either of the concrete samples due to the presence of tricalcium aluminate (C3A) in the cement. Figure 6 shows the XRD pattern of both conventional and optimum concrete samples.

6 Conclusions

In this study, the optimum percentage of olivine sand in concrete was determined using various mechanical and analytical techniques. The results were compared with conventional concrete and led to the following conclusions.

- The compressive strength of concrete cubes at 28 days was observed. From the observation, it was found that concrete with 30% of fine aggregate as olivine sand achieved a compressive strength of 38.14 MPa which is comparatively higher than conventional concrete whose compressive strength is 33.06 MPa.
- This concrete with a fine aggregate proportion of 70:30 (M-Sand: Olivine sand) also performed better in flexural and splitting tensile test which makes it as the optimum replacement proportion.
- The microstructures of both conventional and optimum concrete samples indicate the development of hydration components. In both cases, a well-developed and evenly distributed microstructure was apparent. Minor traces of CH in all the concrete samples show its maximum utilization in the hydration process of cement.

- Quartz (SiO₂) and CSH were the dominant peaks in all the concrete samples, and minor peaks of C and CH were also found.
- The optimum concrete showed 15.36% greater compressive strength, 66.66% greater splitting tensile strength, and 17.20% greater flexural strength when compared to the conventional concrete at 28 days.
- The cost of olivine sand is comparatively higher than that of usual fine aggregates such as M-Sand and river sand. But the benefits of adopting olivine sand in concrete outshine its disadvantages. In addition, the recommended amount of olivine sand replacement from the project results is 30%, which would not make the concrete more expensive and can still be affordable.
- It was suggested that concrete manufactured using the application of olivine sand can be utilized for both commercial and industrial applications.

Acknowledgements The authors sincerely acknowledge the Management and the Department of Civil Engineering of SRM Institute of Science and Technology, Kattankulathur for their support towards this project.

References

1. Senguttuvan K (2021) Impact of M sand and olivine sand in geo polymer concrete at ambient temperature synthesis and processing parametric studies on geopolymer concrete using recycled aggregates, ceramic waste and bamboo aggregates. View project Parametric Studies on Geopolymer Concrete View project
2. Papayianni I, Patsiou V, Petrohilou V (2013) Development of fire resistance shotcrete with olivine aggregates. Upgrading and Refurbishment of Infrastructures Congress Report, pp 114–115
3. Bureau of Indian Standards B (1988) IS 4031-11: Methods of physical tests for hydraulic cement, Part 11: Determination of density
4. Lu Y, Spencer-Williams I, Frizzell N, Bungler AP (2019) Evidence for self-healing of carbonated olivine for wellbore cementing and plugging under high temperature high pressure (HTHP) reservoir conditions
5. Malathy R, Rajagopal Sentilkumar SR, Prakash AR, Das BB, Chung IM, Kim SH, Prabakaran M (2022) Use of industrial silica sand as a fine aggregate in concrete—an explorative study. Buildings 12
6. Furlani E, Tonello G, Aneggi E, Maschio S (2012) Preparation and characterization of sintered ceramics made with spent foundry olivine sand and clay
7. Schuiling RD (2013) Olivine: a supergreen fuel
8. Bureau of Indian Standards B (2016) IS 383: Coarse and fine aggregate for concrete—specification
9. Bureau of Indian Standards B (1963) IS 2386-1: Methods of test for aggregates for concrete, Part I: Particle size and shape
10. Bureau of Indian Standards B (2000) IS 456: Plain and reinforced concrete—Code of practice
11. Bureau of Indian Standards B (2009) IS 10262: Guidelines for concrete mix design proportioning
12. Rajamane NP, Annie Peter J, Ambily PS (2007) Prediction of compressive strength of concrete with fly ash as sand replacement material. Cem Concr Compos 29
13. Narendran RB, Rajkumar U (2017) Recyclable perlite concrete using olivine sand

14. Reddy PN, Naqash JA (2019) Experimental study on TGA, XRD and SEM analysis of concrete with ultra-fine slag. *Int J Eng Trans B* 32:679–684
15. Furlani E, Magnan M, Mingone E, Deison M, Aneggi E, Andreatta F, Fedrizzi L, Maschio S (2019) Waste olivine and silica sands boost geopolymers' performances: experimental investigation. *Int J Environ Stud* 76:491–506

Optimum Study of Friction Pendulum Isolated Building in Response Mitigation under Near Fault Excitation



Dasari Sreeman and Bijan Kumar Roy

1 Introduction

Numerous studies have demonstrated that base isolation systems can effectively reduce the structural damage during seismic excitations [1]. In practice, the widely used seismic isolators are lead rubber bearings (LRB) and friction pendulum bearings (FPS). During the last few decades, the FPS has been employed widely in the seismic design of buildings and bridges due to its notable characteristics [2]. The unique behaviour of the FPS system is its ability to exhibit pendulum like motion in the presence of friction and enables it to effectively dissipate a significant amount of energy through self-recentring and sliding, thereby it reduces torsional effects by eliminating mass eccentricity in the structure [3]. Number of researchers have conducted analyses on the parameters of FPS bearings in order to optimize their performance and achieve optimal seismic effectiveness [4]. In order to minimize the seismic response of building in terms of displacement, researchers have derived optimal ranges for the frictional coefficient [5]. Jangid [6] examined an optimum design of FPS bearings subjected to near fault (NF) excitations. Earthquake records from NF excitations exhibit significant differences compared with records from far fault (FF) excitations, especially when the site is located within a distance of 20 km from the fault rupture [7]. Under such excitations, the behaviour of buildings could be significantly different. Primarily, two significant effects characterize NF excitations, namely the fling step and directivity effect. These effects are based on three main characteristics which are residual ground movement, the rupture direction corresponding to the land site and the rupture mechanism. Fling step corresponds to

D. Sreeman (✉) · B. K. Roy
Department of Civil Engineering, National Institute of Technology Silchar, Silchar,
Assam 788010, India
e-mail: dasari_rs@civil.nits.ac.in

B. K. Roy
e-mail: bijan@civil.nits.ac.in

one-sided velocity pulse, whereas the directivity effect shows a two-sided pulse in its time domain velocities of the normal fault [8].

The study on NF excitations considering forward directivity and fling step effects has attracted significant research interest. Under such excitations, well-designed and constructed buildings can also get damaged [9]. According to studies, these velocity pulses can induce high inelastic demands on multi-storey buildings [10]. Kalkan and Kunnath [11] evaluated by comparing the behaviour of steel structure subjected to FF excitations and NF excitations with fling step and directivity motions and concluded that earthquakes with directivity characteristics excited higher modes, whereas ground motion with fling effects led to a dominant first-mode response. Vafaei and Eskandari [12] performed dynamic response of steel buildings by comparing FF excitations to NF excitations with fling step and directivity characteristics and found that NF earthquakes contribute to higher seismic demands than FF earthquakes, and more dispersion in the results for NF with fling motions. Beiraghi et al. [13] evaluated the impacts of FF and NF earthquakes with directivity effect on tall reinforced concrete buildings. They concluded that NF earthquakes with a directivity effect induce significant displacement demands, ductility deformations and inter-storey drift ratio than FF earthquakes. Xi and Liu [14] evaluated the response of intake tower to NF excitations considering the fling step and forward directivity effects. The findings revealed that these effects resulted in large curvatures and significant nodal displacements, particularly in the lower portions of the structure.

Seismic isolated structures are designed and analyzed mostly for FF excitations. The superstructure remains linear under design level earthquake, but the isolator goes into nonlinear behaviour. Despite the considerable reduction in the building's response achieved through the implementation of isolation system, the structural response of long period buildings may experience amplification due to presence of velocity pulse found in NF events accompanied by directivity and fling motions. The velocity pulses with a longer duration may distress the resisting force of the friction pendulum isolators because it enhances the velocity to a certain constant value [15]. Furthermore, Petti et al. [16] concluded that if the isolated buildings are close to the vibration period of NF excitations, they may induce resonance at low seismic isolation frequencies. Ismail et al. [17] showed that NF ground motions could cause considerable residual displacements in isolation systems with insufficient restoring capabilities. The effect of LRB isolated structures subjected to bidirectional FF and NF seismic excitations and observed that NF seismic excitations result in higher seismic demands in the bearing system and superstructure [18]. Bhandari et al. [19] examined the LRB isolated structure under FF excitations and NF excitations with directivity and fling pulses and noticed that NF earthquakes with fling pulses impose higher structural demands on the isolated structure than other seismic excitations. Rong [20] studied the dynamic behaviour of five-storey buildings implemented with LRB isolators under NF earthquakes to determine the optimal yield shear coefficient and optimal LRB of pre- to post-yield stiffness ratio. Ozuygur [21] investigated the storey acceleration of LRB isolated structure with different seismic force resistant systems subjected to FF and NF excitations. It is observed that increasing the stiffness of the superstructure may effectively reduce floor accelerations, but excess damping

is detrimental. Bhagat et al. [22] evaluated the performance of LRB isolated building subjected to NF excitations with directivity and fling motions. The investigation also considered the influence of artificial pulses and examined the effect of pulse characteristics on the system. The study observed that the presence of pulses in NF excitations induces significant seismic demands on LRB isolated building. Furthermore, pulses with fling step effects exhibit larger responses in superstructure and isolator compared with those with forward directivity characteristics. More research is needed to investigate the impact of directivity and fling motions observed in NF earthquakes.

Several researches have been conducted to examine the behaviour of LRB isolated buildings under FF and NF seismic excitations, limited studies have been done on directivity and fling motions. However, the influence of building's response on pulse characteristics of directivity and fling effects are not explored to the best of authors' knowledge by using FPS. A total of fifteen numbers of ground motion records are considered in this study, which includes three different categories of excitations, namely FF and NF with directivity and fling seismic excitations. Under each category, five earthquake records are considered with which the time history response of the structure and isolator is evaluated. Furthermore, a parametric investigation is performed by varying different values of the frictional coefficient and time period of the isolator to assess the response behaviour of isolated building under these earthquakes. The findings reveal that certain values of frictional coefficient mitigate the acceleration of the superstructure and improve its isolation efficiency. Consequently, the parameters such as frictional coefficient in FPS are taken as design variables in order to conduct gradient-based optimization of top storey acceleration as an objective function.

2 Seismic Response Evaluation of Building Using FPS Isolation System

Figure 1a depicts the multi-storey building frame implemented on the FPS as base isolator. The governing equations of an N-storey superstructure under ground motion \ddot{z}_g can be represented in matrix form as

$$[M]\{\ddot{z}\} + [C]\{\dot{z}\} + [K]\{z\} = -[M]\{r\}(\ddot{z}_g + \ddot{z}_b), \quad (1)$$

where $[M]$, $[K]$ and $[C]$ are the matrices of size $N \times N$ representing the superstructure's mass, stiffness and damping, respectively. Here $\{z\} = \{z_1 \ z_2 \ z_3 \ \dots \ z_n\}^T$ represents the displacement vector that contains the lateral displacement of each storey with respect to the isolator, \ddot{z}_b is the isolator mass acceleration and \ddot{z}_g is the acceleration of ground motion.

The governing isolator mass equation (Fig. 1b) is given as follows:

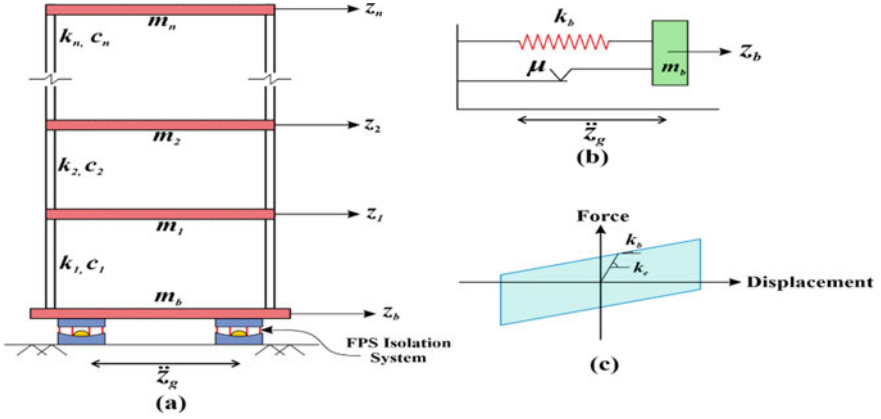


Fig. 1 a Flexible building with FPS; b Mechanical model of FPS; c Hysteresis cycle of FPS

$$m_b \ddot{z}_b + F_b - c_1 \dot{z}_1 - k_1 z_1 = -m_b \ddot{z}_g, \quad (2)$$

where k_1 indicates stiffness and c_1 signifies damping of the building's first storey, respectively, m_b is the base mass and F_b is the lateral resisting force mobilized in the FPS. The term F_b in the FPS base isolated system is expressed as

$$F_b = k_b z_b + F_x, \quad (3)$$

in which k_b refers to the lateral stiffness of the FPS and given as $k_b = W/R$, where W denotes weight sustained by the isolators and R signifies the radius of spherical surface. F_x denotes the friction force generated at the sliding interface and expressed as $F_x = \mu W Z$, where μ represents coefficient of friction of FPS and Z is a non-dimensional parameter given as $Z = \text{sgn}(\dot{z}_b)$, where $\text{sgn}(\cdot)$ is the signum function. By combining Eqs. (2) and (3), the adjusted isolator equation given as

$$m_b \ddot{z}_b + k_b z_b + F_x - c_1 \dot{z}_1 - k_1 z_1 = -m_b \ddot{z}_g. \quad (4)$$

The fundamental time period of the isolated structure, $T_b = 2\pi\sqrt{R/g}$, which corresponds to the pendulum component, is associated only with the curvature of the spherical surface and is independent of superstructure's mass. Consequently, the governing Eqs. (1) and (4) are solved using Newmark's beta method and analyzed in the MATLAB computer program.

3 Numerical Study

In this study, linear five-storey shear building is analyzed using FPS as a base isolator. For simplicity, damping ratio, mass (m_i) and stiffness (k_i) of all the floors are kept identical. The structural properties examined in this study are time period of super-structure (T_s) and structural damping ratio (ξ_s) taken as 0.5 s and 2%, respectively. The isolator properties are taken as $\mu = 0.05$ and $T_b = 2.5$ s. For this analysis, 15 number of actual ground motion records are sourced from PEER strong motion database as given in Table 1 with relevant peak ground velocity (PGV) and peak ground acceleration.

Figure 2a–c depicts a top storey acceleration response of FPS isolated for FF ground motion (Beverly hills), directivity motion (Elcentro array #5) and fling motion (TCU068), respectively. The maximum top storey accelerations of the building are 0.39, 0.53 and 0.93 g for FF (GM-5), forward directivity (GM-6) and fling step (GM-15), respectively. Furthermore, compared with forward directivity motions, the records of fling motion exhibit higher values of acceleration. Due to the influence of the velocity pulse period, the NF earthquakes mostly impose higher accelerations than FF earthquakes.

A typical isolator response for FF ground motion (GM-5), directivity motion (GM-6) and fling step (GM-15), respectively, are depicted in Fig. 3a–c. It can be noticed

Table 1 Real earthquake data

S. No:	Year	Earthquake	PGA (g)	PGV (cm/s)
<i>Far fault data</i>				
1	1940	El Centro (GM-1)	0.318	22
2	1952	Taft Lincoln school (GM-2)	0.18	17
3	1983	Parkfield (GM-3)	0.27	32
4	1992	Baker fire (GM-4)	0.12	9
5	1994	Beverly hills (GM-5)	0.42	56
<i>Near fault data with directivity motion</i>				
1	1979	El Centro array # 5 (GM-6)	0.38	100
2	1979	El Centro array # 7 (GM-7)	0.46	113
3	1987	Parachute test site (GM-8)	0.43	135
4	1994	Rinaldi (GM-9)	0.87	173
5	1994	Sylmar converter (GM-10)	0.85	117
<i>Near fault data with fling motion</i>				
1	1999	Izmit (GM-11)	0.23	40
2	1999	TCU072 (GM-12)	0.47	80
3	1999	TCU067 (GM-13)	0.49	95
4	1999	TCU052 (GM-14)	0.36	153.2
5	1999	TCU068 (GM-15)	0.51	247.3

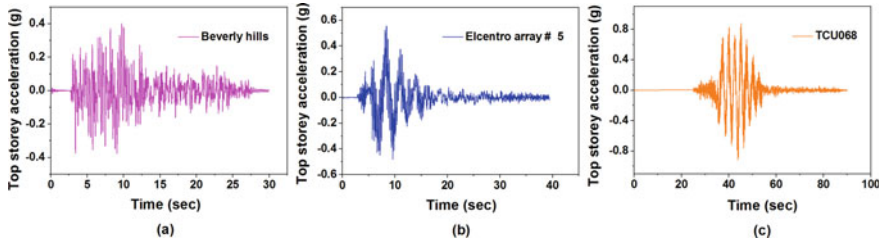


Fig. 2 Top storey acceleration of FPS isolated building under **a** FF ground motion (GM-5); **b** NF with directivity motion (GM-6); **c** NF with fling motion (GM-15)

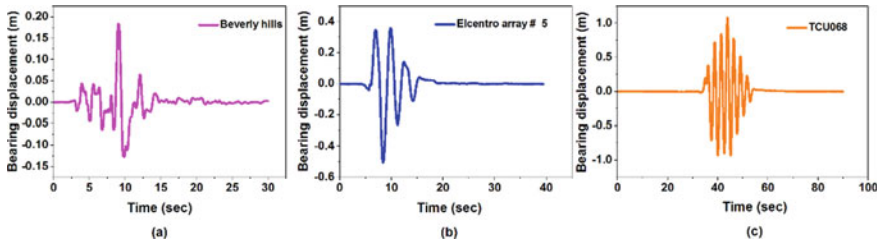


Fig. 3 Isolator displacement of FPS isolated building under **a** FF ground motion (GM-5); **b** NF with directivity motion (GM-6); **c** NF with fling motion (GM-15)

from Fig. 3b, c that fling step and forward directivity earthquakes induce significant displacement demand. The maximum isolator displacement increases by 2.6 times for directivity motion and 5.77 times for fling motion compared with FF ground motion. Even though the NF ground motion with directivity effect (0.38 g, GM-6) has less PGA value than FF ground motion (0.42 g, GM-5), it imparts significantly higher demands in NF earthquakes due to inherent velocity pulses.

For this study, the maximum acceleration at the top storey and bearing displacement are conducted by changing different frictional coefficient values considering different FF earthquakes (GM-1 to GM-5), NF with directivity effect (GM-6 to GM-10) and NF with fling motion (GM-11 to GM-15). The individual responses within each category are combined to obtain the average responses, as illustrated by the bold line in the respective figures.

Figures 4 and 5 as a whole show the impact of frictional coefficient on the performance of FPS system. The frictional coefficient substantially impacts the response as it causes the energy to be dissipated through coulomb damping. The variation of top storey acceleration against the coefficient of friction is depicted in Fig. 4a–c. In contrast, Fig. 5a–c depicts the variation of bearing displacement against coefficient of friction for various FF and NF with directivity and fling step seismic excitations, which shows the effect of frictional coefficient ranging from 0.01 to 0.20. It can be observed in Fig. 4 that as the frictional coefficient increases, the average top storey acceleration initially decreases and reaches a minimal value, and subsequently increases, in contrast the displacement in the isolator decreases (as shown in

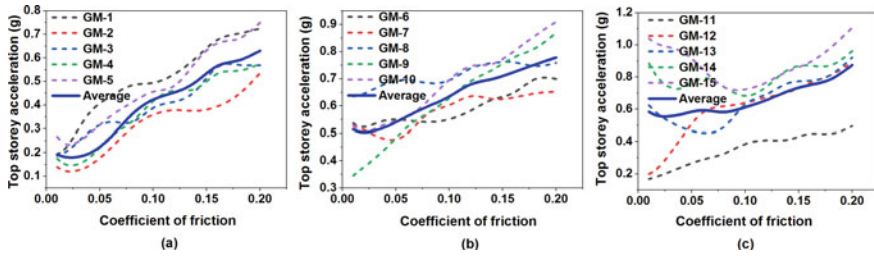


Fig. 4 Variation of maximum top storey acceleration with respect to frictional coefficient of FPS for all records of **a** FF earthquake; **b** NF with directivity motion; **c** NF with fling motion

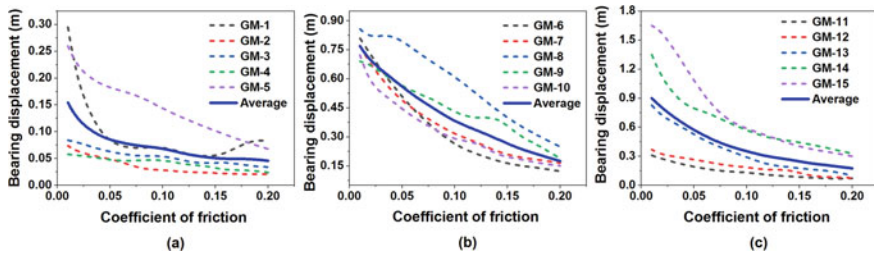


Fig. 5 Variation of maximum bearing displacement with respect to frictional coefficient of FPS for all records of **a** FF earthquake; **b** NF with directivity motion; **c** NF with fling motion

Fig. 5) as the coefficient of friction increases for various earthquakes. By increasing the frictional coefficient values in the isolation system restricts mobility and leads to higher seismic energy entering the superstructure. However, FF ground motion is less sensitive than NF with directivity and fling motions due to large seismic demands.

4 Optimization of FPS Isolation System

The FPS isolated building has some particular coefficient of friction values that minimizes superstructure accelerations and improves its isolation efficiency. For this, gradient-based optimization technique is used to solve optimal parameter such as coefficient of friction that is taken as design variable of FPS isolation system. It is worth noting that the objective function for FPS system corresponds to minimization of top storey accelerations.

For varying levels of isolator time period, the optimized values of acceleration and corresponding frictional coefficient are shown in Fig. 6a–c for different FF and NF excitations, considering directivity and fling motions. It can be found that the optimal parameter of frictional coefficient value increases with the increasing isolation time period of FPS isolation system. To prevent additional bearing displacement the frictional coefficient must be increased. Consequently, as the isolator time period

increases, the top storey acceleration reduces and the isolator displacement increases. The mean of top storey acceleration and bearing displacement for NF with directivity motion impose, respectively, about 49 and 73% higher demands than those of FF ground motions and for NF with fling motion are 59 and 85% higher demands than FF ground motions for varying isolator time period. Figure 7a, b depicts the optimized values of acceleration and corresponding frictional coefficients by varying superstructure flexibilities, as well as the corresponding bearing displacement as shown in Fig. 7c. The findings indicate that the time period of superstructure increases, and the optimal frictional resistance decreases because lower values of frictional coefficients are required to maintain to keep efficiency of the isolation system. Thus, the top storey acceleration increases and the bearing displacement decreases with increasing values of superstructure flexibilities. From the results, the mean of top storey acceleration and bearing displacement for NF with directivity motion impose, respectively, about 42% and 75% higher demands than those of FF ground motions and for NF with fling motion are 63% and 83% higher demands than FF ground motions for different levels of superstructure flexibilities. As NF excitation involves pulses with a substantial release of seismic energy in short duration, resulting in higher seismic demands than FF excitations. However, FPS isolated building subjected to fling step effect achieves significant bearing displacement than directivity effect. This is due to the fling step that typically characterizes a unidirectional velocity pulse of large amplitude and produces a monotonic step in its time domain displacements. Thus, the large residual ground displacements corresponding with rupture mechanism are caused by these monotonic steps.

5 Conclusions

This study examines the efficacy of FPS in reducing the seismic response of isolated building during FF and NF excitations considering fling step and directivity effects. The study conducts a parametric investigation and optimal analysis to access the influence of FPS parameters on building responses. Comparative evaluation of FPS isolated building to FF and NF with directivity and fling motions is carried out to emphasize its relative importance. From this study, the response parameters of the isolated building under each NF excitations are much higher than those under corresponding FF excitations. Despite having a smaller PGA value for NF excitations than FF excitations, the top acceleration and bearing displacement amplify significantly due to directivity and fling motions. As the frictional coefficient increases, larger seismic loads are transmitted to the superstructure through frictional action, resulting in an increase in top storey acceleration, whereas the bearing displacement decreases. The optimum frictional coefficient decreases and increases with increasing structural time period as well as isolator time periods, respectively, but the differences remain relatively consistent for all FF and NF considering fling step and directivity ground motions. Even though the top storey acceleration values under directivity

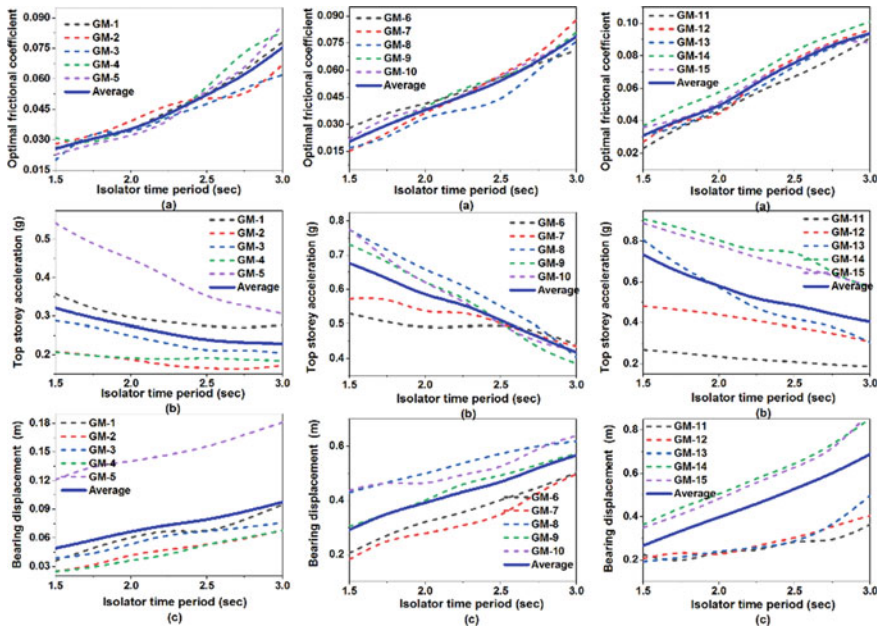


Fig. 6 Optimal **a** frictional coefficient, **b** top storey acceleration, **c** bearing displacement against time period of isolator for all FF and NF with directivity and fling step earthquake data

effect are lower than fling step effect, the disparities between them are not substantial for different levels of structural and isolator time periods. However, the impact of directivity effect on the reductions in bearing displacement are less pronounced than fling step effect, as the structural and isolator time periods increase. The demands in the above response quantities are considerably higher than FF ground motions, indicating that FPS isolation system induce significant bearing displacement, and thereby the FPS isolators are severely damaged, especially under NF with fling step effects have been purposely neglected. Thus, employing an optimized FPS isolation system can improve the building’s response over FPS system without optimization subjected to FF and NF, considering directivity and fling step seismic ground motions. In particular, some caution is required in designing the FPS isolation system, especially when the structure is subjected to fling step pulses.

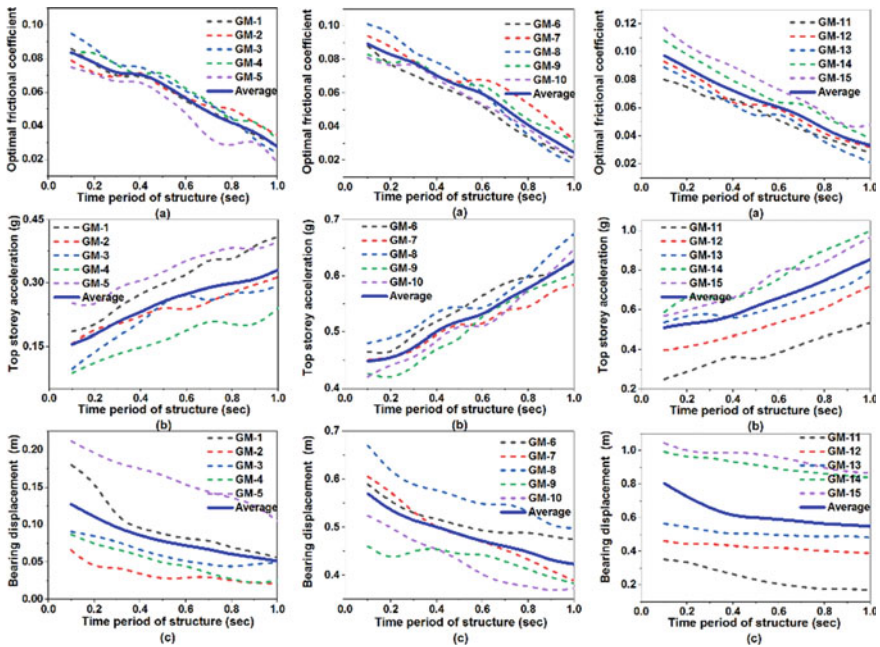


Fig. 7 Optimal **a** frictional coefficient, **b** top storey acceleration, **c** bearing displacement against time period of structure for all FF and NF with directivity and fling step earthquake data

References

1. Buckle IG, Mayes RL (1990) Seismic isolation: history, application, and performance—a world view. <https://doi.org/10.1193/1.1585564>
2. Zayas VA, Low SS, Mahin SA (1990) A simple pendulum technique for achieving seismic isolation. *Earthq Spectra* 6:317–333. <https://doi.org/10.1193/1.1585573>
3. Mokha A, Constantinou M, Reinhorn A (1990) Teflon bearings in base isolation I: testing. *J Struct Eng* 116:438–454. [https://doi.org/10.1061/\(ASCE\)0733-9445\(1990\)116:2\(438\)](https://doi.org/10.1061/(ASCE)0733-9445(1990)116:2(438))
4. Bucher C (2009) Probability-based optimal design of friction-based seismic isolation devices. *Struct Saf* 31:500–507. <https://doi.org/10.1016/j.strusafe.2009.06.009>
5. Castaldo P, Ripani M (2016) Optimal design of friction pendulum system properties for isolated structures considering different soil conditions. *Soil Dyn Earthq Eng* 90:74–87. <https://doi.org/10.1016/j.soildyn.2016.08.025>
6. Jangid RS (2005) Optimum friction pendulum system for near-fault motions. *Eng Struct* 27:349–359. <https://doi.org/10.1016/j.engstruct.2004.09.013>
7. Somerville PG, Smith NF, Graves RW, Abrahamson NA (1997) Modification of empirical strong ground motion attenuation relations to include the amplitude and duration effects of rupture directivity. *Seismol Res Lett* 68:199–222. <https://doi.org/10.1785/gssrl.68.1.199>
8. Payyappilly LJ, Karthik Reddy KSK, Somala SN (2021) Impact of directivity on seismic risk assessment: rupture distance, component and propagation length. *Asian J Civ Eng* 22:1361–1375. <https://doi.org/10.1007/s42107-021-00388-7>
9. Elnashai AS (2000) Analysis of the damage potential of the Kocaeli (Turkey) earthquake of 17 August 1999. *Eng Struct* 22:746–754. [https://doi.org/10.1016/S0141-0296\(99\)00104-2](https://doi.org/10.1016/S0141-0296(99)00104-2)
10. Alavi B, Krawinkler H (2004) Behavior of moment-resisting frame structures subjected to near-fault ground motions. *Earthq Eng Struct Dyn* 33:687–706. <https://doi.org/10.1002/eqe.369>

11. Kalkan E, Kunnath SK (2006) Effects of fling step and forward directivity on seismic response of buildings. *Earthq Spectra* 22:367–390. <https://doi.org/10.1193/1.2192560>
12. Vafaei D, Eskandari R (2015) Seismic response of mega buckling-restrained braces subjected to fling-step and forward-directivity near-fault ground motions. *Struct Des Tall Spec Build* 24:672–686. <https://doi.org/10.1002/tal.1205>
13. Beiraghi H, Kheyroddin A, Kafi MA (2016) Forward directivity near-fault and far-fault ground motion effects on the behavior of reinforced concrete wall tall buildings with one and more plastic hinges. *Struct Des Tall Spec Build* 25:519–539. <https://doi.org/10.1002/tal.1270>
14. Chen X, Liu Y, Zhou B, Yang D (2020) Seismic response analysis of intake tower structure under near-fault ground motions with forward-directivity and fling-step effects. *Soil Dyn Earthq Eng* 132:106098. <https://doi.org/10.1016/j.soildyn.2020.106098>
15. Cardone D (2012) Re-centring capability of flag-shaped seismic isolation systems. *Bull Earthq Eng* 10:1267–1284. <https://doi.org/10.1007/s10518-012-9343-1>
16. Petti L, Polichetti F, Palazzo B (2013) Analysis of seismic performance of fps base isolated structures subjected to near fault events. *Int J Eng Technol* 5:5233–5240
17. Ismail M, Rodellar J, Pozo F (2014) An isolation device for near-fault ground motions. *Struct Control Heal Monit* 21:249–268. <https://doi.org/10.1002/stc.1549>
18. Bhagat S, Wijeyewickrema AC (2017) Seismic response evaluation of base-isolated reinforced concrete buildings under bidirectional excitation. *Earthq Eng Eng Vib* 16:365–382. <https://doi.org/10.1007/s11803-017-0387-8>
19. Bhandari M, Bharti SD, Shrimali MK, Datta TK (2018) The numerical study of base-isolated buildings under near-field and far-field earthquakes. *J Earthq Eng* 22:989–1007. <https://doi.org/10.1080/13632469.2016.1269698>
20. Rong Q (2020) Optimum parameters of a five-story building supported by lead-rubber bearings under near-fault ground motions. *J Low Freq Noise Vib Act Control* 39:98–113. <https://doi.org/10.1177/1461348419845829>
21. Özüygür AR (2021) A comparative study of floor accelerations of different structural systems with lead-rubber-bearing (LRB) isolators. *Can J Civ Eng* 48:482–493. <https://doi.org/10.1139/cjce-2019-0382>
22. Bhagat S, Wijeyewickrema AC, Subedi N (2021) Influence of near-fault ground motions with fling-step and forward-directivity characteristics on seismic response of base-isolated buildings. *J Earthq Eng* 25:455–474. <https://doi.org/10.1080/13632469.2018.1520759>

Flexural Behaviour of Cold-Formed Steel Built-Up Beams Using Sigma and Channel Sections



C. Manoj Kumar, Venus David Rayan, K. Govarthini, Nemat Bano, Marnadu Dinesh Kumar, and M. Saran Kumar

1 Introduction

Steel plates, sheets, and strips are frequently used to create cold-formed steel structural elements. The material is rolled and bent at room temperature to create the desired forms and shapes. In building structures, floor decks, wall panels, and steel wall studs are constructed using cold-formed steel material. The most commonly adopted shapes for beams are I, channel, Zed, and hat sections. Apart from building construction, cold-formed steel members are also utilized to construct grain bins, automobile bodies, and storage racks. The green material, cold-formed steel, is made up of 67% recycled materials, and it is 100% recyclable and reusable. The strength of cold-formed steel sections is 20% more than that of hot-rolled steel sections [1]. The non-combustible and strong cold-formed steel has longer durability to endure structural damage from fire accidents and natural calamities including earthquakes, cyclones, and heavy rainfall and snowfall. Cost-effectiveness as per the study lumber cost increases 60% in 2021 and cold-formed cost increases only 20%. So cold-formed steel is cost-effective for building or other structures compared to other materials. A comprehensive study was carried out to analyse the flexural strength of box sections. The research involved conducting a series of experimental and analytical tests on a total of 30 specimens. The tests focused on evaluating factors such as the yield strength of cold-rolled steel, screw spacing, and the application of two different types of loads. Based on the findings, the researchers concluded that the existing

C. Manoj Kumar · V. D. Rayan (✉) · K. Govarthini · N. Bano · M. Dinesh Kumar · M. Saran Kumar

Department of Civil Engineering, Sathyabama Institute of Science and Technology (Deemed to be University), Chennai 600119, India

e-mail: davidvenu06@gmail.com

C. Manoj Kumar

e-mail: cmanoj1@gmail.com

design practices might overestimate the flexural strength of cold-formed steel (CFS) built-up box sections [2].

The flexural strength and buckling behaviour of cold-formed steel C-section is greatly influenced by edge stiffeners [3]. The cold-formed steel (CFS) sections are widely used nowadays due to their high strength-to-weight ratio, rigidity, recyclability, homogeneity, smoothness, aesthetic appearance, and ease of production of the lightweight materials. The past few decades have shown increased number of studies on the structural behaviour of cold-formed steel (CFS) beams [4]. One of the most intriguing and challenging topics in the research area is the interaction of instability phenomena, such as local, distortional, and lateral-torsional buckling [5].

The experiment involved seven different types of specimens, including single beams and built-up beams that were subjected to bending around both strong and weak axes. The built-up box beam components were able to withstand the bending moment integrally, thanks to the stress distribution at the mid-span cross-section. A numerical study was conducted on cold-formed T-shaped built-up steel sections [6] to establish a significant correlation between the moment carrying capacity, failure mechanisms identified through finite element analysis, and experimental results. To assess the bending strength, a validated finite element model was utilized by varying the thickness and length. A study was undertaken to examine the compressive and flexural behaviour of steel sections, comparing those with and without lips. Through a comparison of analytical and experimental results, the author concluded that the inclusion of a cover plate, enhancement of edge stiffness, and an increase in the overall beam depth led to a substantial 22% increase in the ultimate load-carrying capacity. Furthermore, it was observed that the presence of lips on the section effectively controlled local flange buckling [7]. These built-up sections frequently serve as members in steel trusses, space frames, and portal frames. Fasteners such as screws, bolts, welds, and clinches are commonly used to attach the components of these built-up sections. In the case of back-to-back built-up CFS channel sections [8], individual channel sections are secured from buckling in the longitudinal direction by intermediate screw fasteners.

Cold-formed steel beams with three different cross-sectional shapes, namely lipped channels, zed sections, and hat sections, were tested and exhibited distortional failure modes when subjected to uniform bending. Additionally, cold-formed steel I-beams with hollow tubular flanges were prepared and subjected to four-point bending tests [9]. In a recent study examining the flexural behaviour of channel and I sections, researchers found that the addition of angle stiffness resulted in a remarkable 90% increase in the load-carrying capacity [10].

Table 1 Properties of sigma sections

Specimen	Units	SSBB	SSTT	MSBB	MSTT
Height, H	mm	240	240	240	240
Upper flange height, A	mm	60	60	60	60
Lower flange height, B	mm	60	60	40	40
Upper lip width, C_1	mm	16	16	16	16
Lower lip width, C_2	mm	16	16	16	16
Connection surface, E	mm	65	65	65	$E_1 = 65$ $E_2 = 45$
Bending, F	mm	15	15	15	$F_1 = 21$ $F_2 = 9$
Depth, G	mm	25	25	25	$G_1 = 35$ $G_2 = 15$
Thickness, t	mm	2	2	2	2

2 Materials and Methods

2.1 Geometrical Properties of Sections Used

All specimens were created using sigma sections adhering to TS EN 1993-1-3, and their geometrical properties are mentioned in Table 1. Figure 1 shows the cross-section of a typical sigma section.

The chemical properties of cold-rolled steel sheet of grade CR2 are given in accordance with IS 513:2008 in Table 2. Figure 2 shows the cross-sectional views of all four specimens.

2.2 Modelling of Beam Sections Using Abaqus Software

All the beam sections are modelled in Abaqus CAE. The cold-formed built-up beams employ two channels and two sigma sections in four different forms, namely symmetric sigma sections connected back-to-back (SSBB), symmetric sigma sections connected toe-to-toe (SSTT), mono-symmetric sigma sections connected back-to-back (MSBB), and mono-symmetric sigma sections connected toe-to-toe (MSTT) (see Fig. 3). The plasticity and elasticity of the material should be included in the geometry of the deformable-shell-extrusion, and by assigning the section, the model will be established and ran for analysis by giving boundary conditions and appropriate loads.

Fig. 1 Cross-section of a typical sigma section

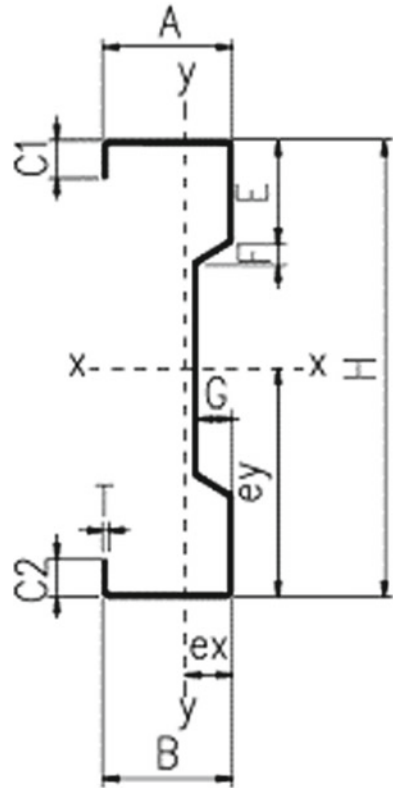


Table 2 Chemical composition of CR2

Chemical constituent	%
Carbon	0.7
Manganese	0.5
Phosphorus	0.4
Silicon	0.05

2.3 Material Property

A coupon test was carried out in order to determine the tensile properties of the steel used. The dimensions of steel coupon as shown in Fig. 4 are referred from ASTM-E8 [11]. The test results are listed in Table 3. The failure was observed in the web portion of the coupon as shown in Fig. 5. The stress-strain curve for a steel coupon is shown in Fig. 6.

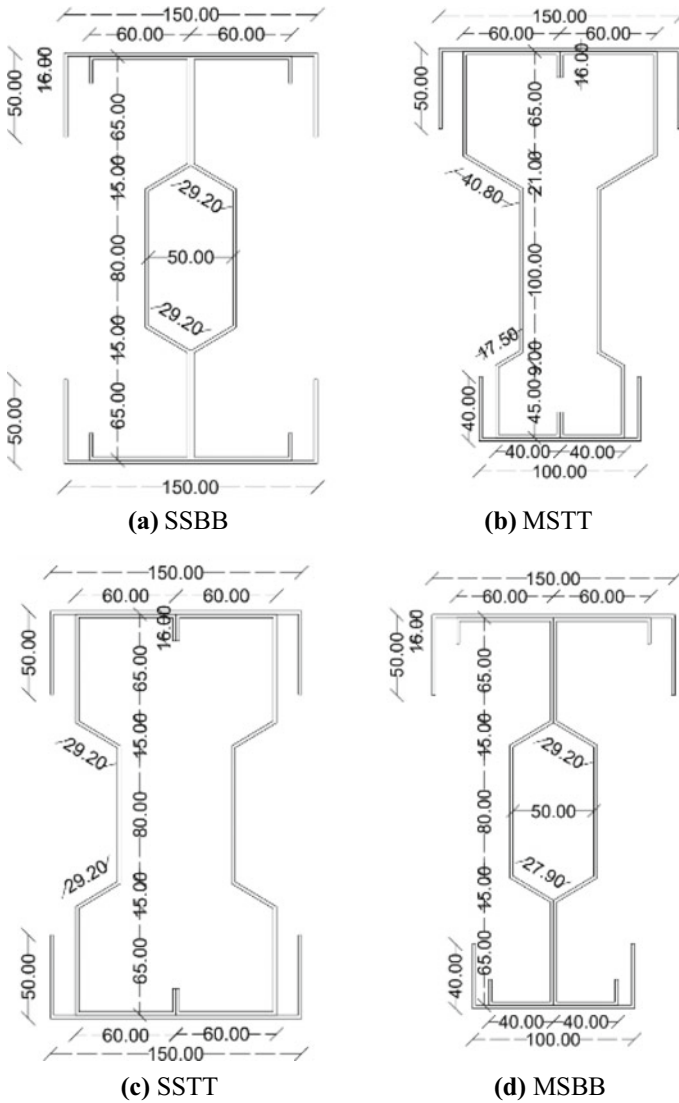


Fig. 2 Cross-section views. a SSBB, b MSTT, c SSTT, d MSBB

2.4 Modelling of Material

The sheets used to build the steel section are taken as solid parts in Abaqus. Each specimen was assigned with pinned support and roller support at a distance of 50 mm from each end. The load points are fixed at one-third spans from either support (See Fig. 7). The elastic modulus and Poisson’s ratio are assigned as 200 GPa and 0.3,

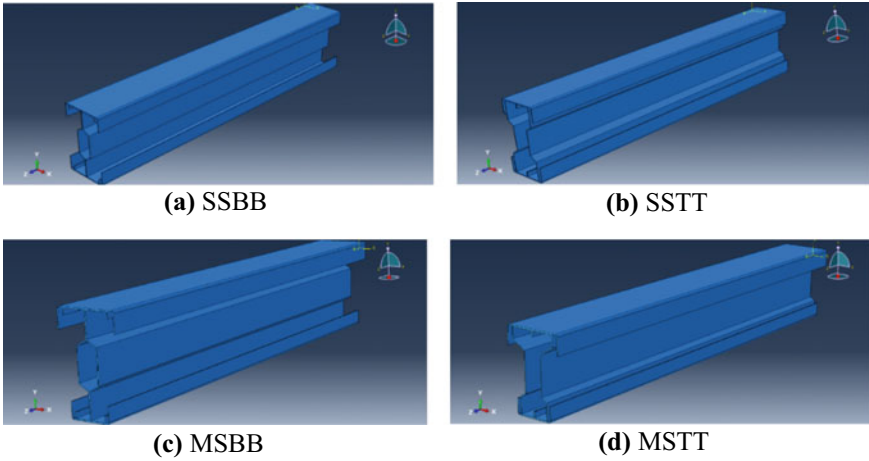


Fig. 3 Geometry of section. **a** SSBB, **b** SSTT, **c** MSBB, **d** SSTT

Fig. 4 Coupon dimensions

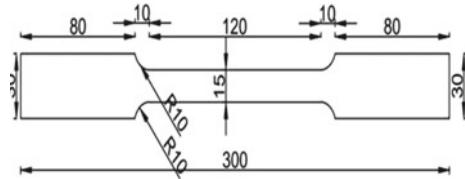


Table 3 Test results of tensile properties of CFS

Tensile property	Observed value
Load at yield	6.154 kN
Elongation at yield	2.686 mm
Yield stress	205.15 N/mm ²
Load at peak	10.384 kN
Elongation at peak	32.942 mm
Tensile strength	346.117 N/mm ²
Load at peak	8.658 kN
Elongation at peak	42.533 kN
Breaking strength	288.583 N/mm ²
% Reduction area	35.20%
% Elongation	32.94%

Fig. 5 Tensile testing strip



Fig. 6 Stress versus strain curve for CFS obtained from coupon test

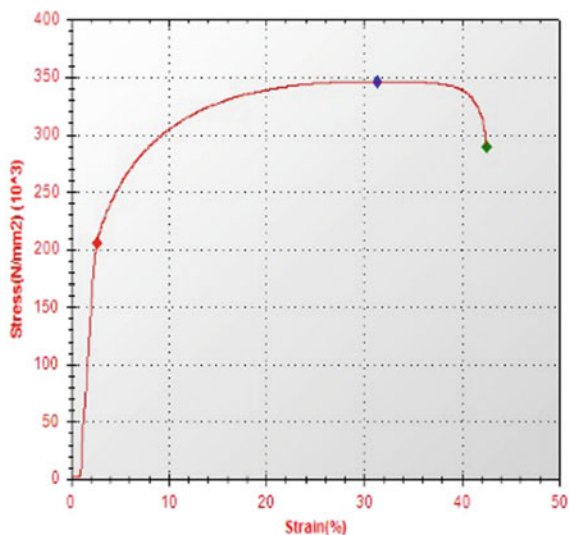
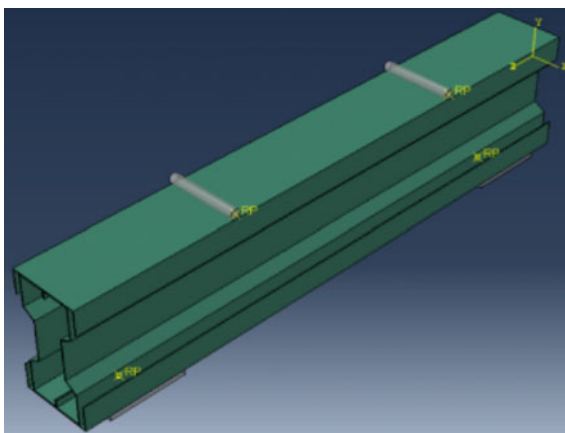


Fig. 7 Abaqus model for control beams

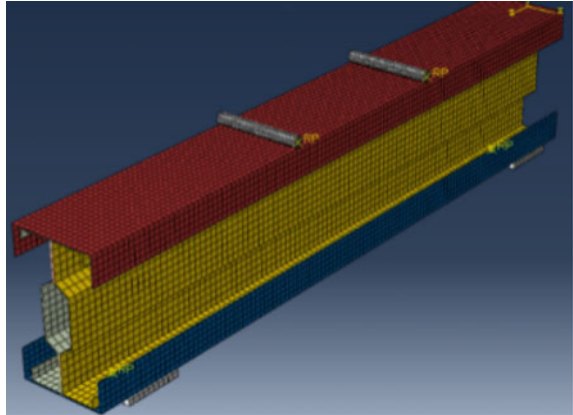


respectively. Then, the models are conducted with finite element analysis [12]. The buckling modes of the beams and the eigenvalues obtained from linear analysis are used to compute load versus deflection curve.

2.5 Mesh Optimization

A mesh size of 20 mm × 20 mm was finally optimized and adopted to create 1200 and 900 elements in sigma and channel sections respectively, as shown in Fig. 8.

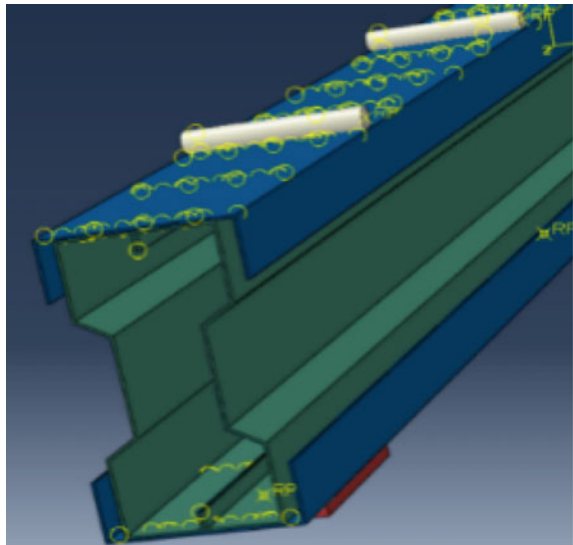
Fig. 8 Finite element model of SSBB



2.6 Interaction Contact Modelling

The connection between the web of channel section and flanges of the sigma sections and connection between the two sigma sections were established using “surface to surface” contact option (see Fig. 9). The stiffness was observed to be 100 KN/m, and the coefficient of friction was observed as 0.2 [13].

Fig. 9 Assigning surface-to-surface contact modelling



2.7 Numerical Results

The deformations and stress concentration diagrams for all sections are shown in Figs. 10 and 11.

Fig. 10 Total deformation diagram

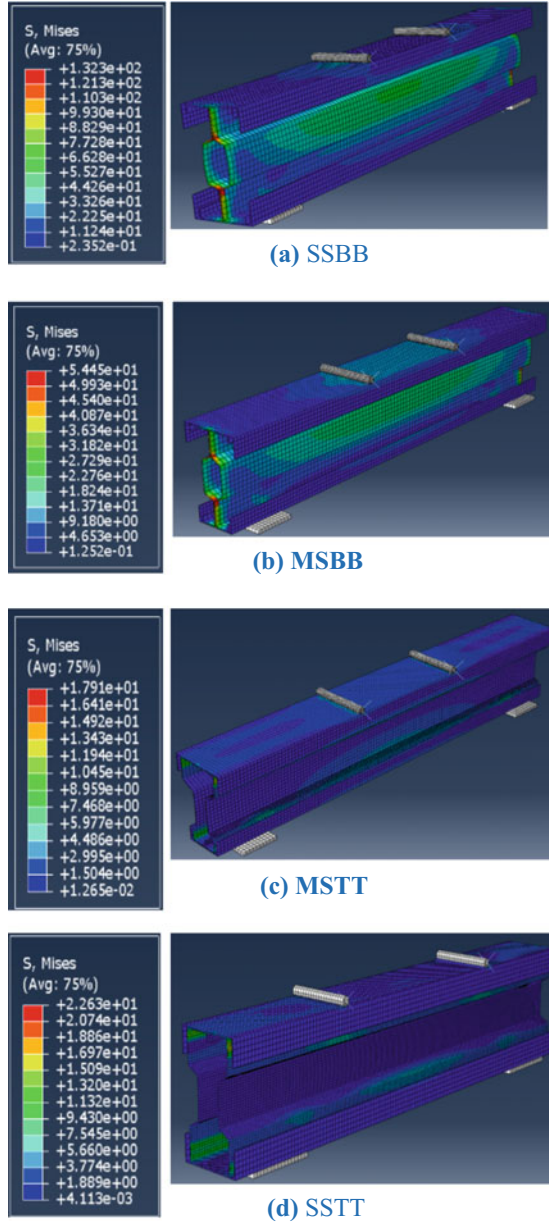
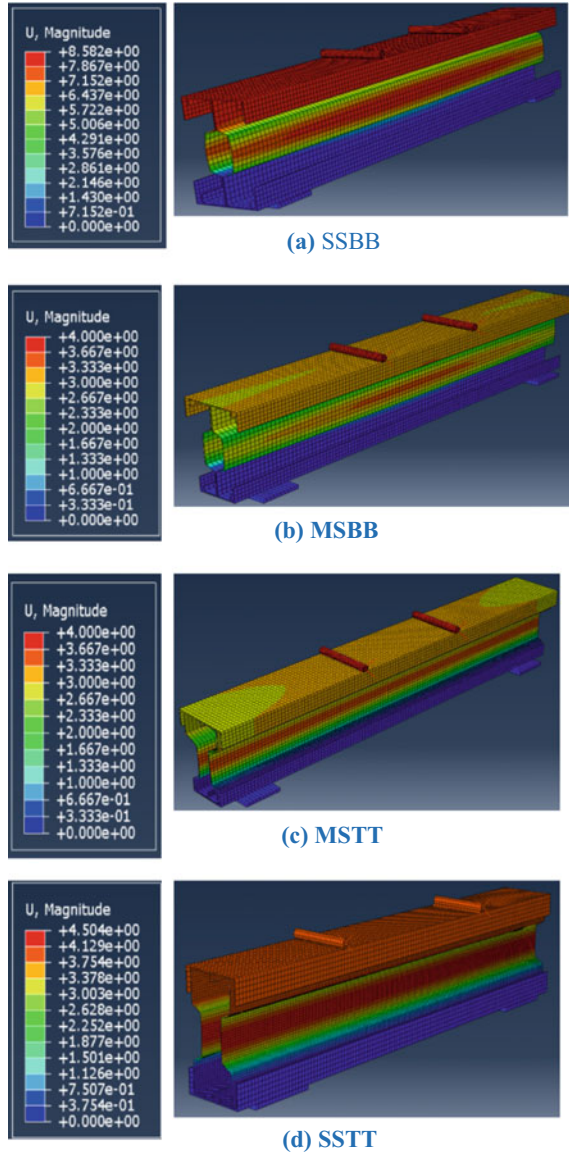


Fig. 11 Stress concentration diagram



Among all sections, SSBB has exhibited maximum stress concentration with larger deformations due to combining the webs, the shear transfer was quite easy and SSTT has exhibited least stress concentration with smaller deformations due to wider space between the webs.

3 Experimental Results

3.1 Fabrication

The IS 513 CR2 sheets of size 1200 mm × 2500 mm × 2 mm are cut and joined using tungsten inert gas (TIG) to fabricate all four beams [14]. The channel and sigma sections are connected using plug weld by created holes of diameter 5 mm at a pitch distance of 75 mm across the span. After the process of fabrication, the specimens are painted for the aesthetic look and undergone testing of specimen in loading frame, by applying the load the deformed structure of beams were clearly shown in Fig. 12.

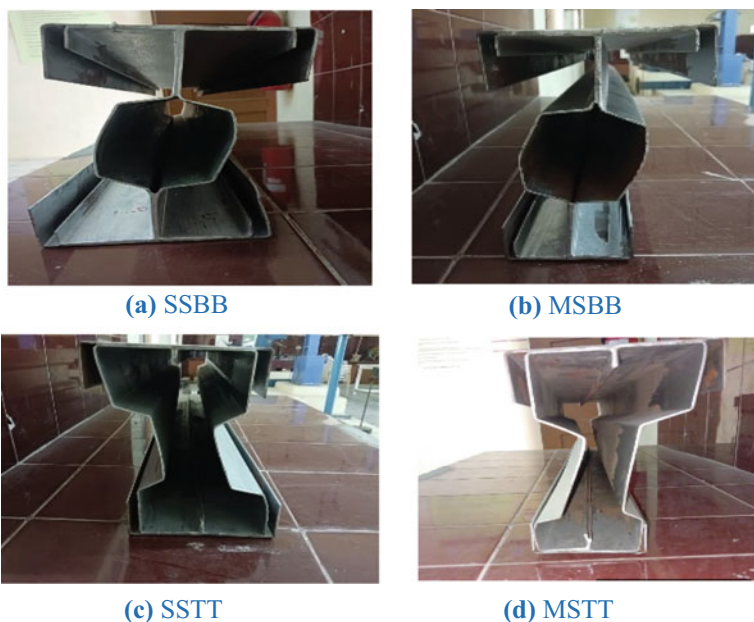


Fig. 12 Deformed sections

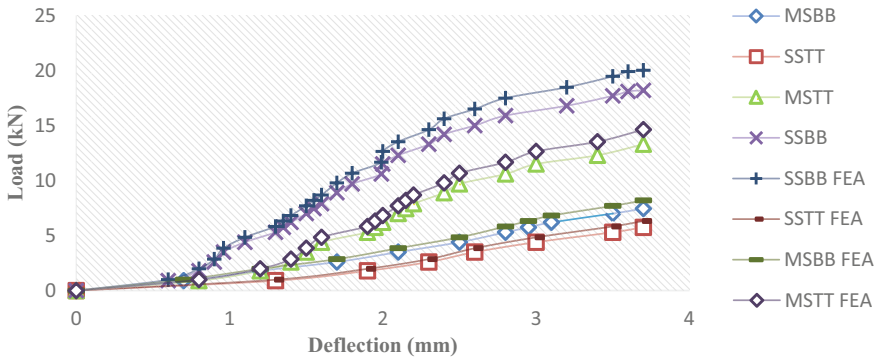


Fig. 13 Comparison of experimental and analytical results of SSBB, SSTT, MSBB, and MSTT

Table 4 Strength/weight ratio

Beams	Maximum load (kN)	Weight (kN)	Strength/weight ratio
MSBB	7.45	0.222687	33.45503
SSTT	5.75	0.242601	23.70144
MSTT	13.3	0.221608	60.01591
SSBB	18.2	0.242601	75.02021

4 Results and Discussions

4.1 Comparison of Experimental and Analytical Results

The load versus deflection curves for all the specimen obtained from experimental and analytical methods shown in Fig. 13 and the strength/weight ratio for all specimens are calculated as given in Table 4. The maximum load-carrying capacity has been analysed with respect to maximum permissible limit of span/325 as specified in IS 800-2007.

4.2 Discussion

All the beams were tested up to considerable formation of local buckling. However, the beams are compared by the load-carrying capacities with respect to permissible limit of vertical deflection as per IS 800:2007 [15]. In both experimental and analytical results, the load versus deflection curve is plotted up to permissible deflection of span/325. The mass of SSBB is 8.21% higher than that of MSBB, and it carried more load than MSBB by 144% as MSBB failed predominantly due to lateral buckling, which did not occur in SSBB. Even though the mass of MSTT is 8.65% lower than

that of SSTT, it carried more load than SSTT by 131% because of its deeper middle portion of web. The SSBB beam carried more load than SSTT by 216% having same mass due to combined action of web plates. Bulging and separation of web portion of sigma section has been observed as local buckling failure in SSBB. In MSBB, bulging of sigma section occurred along with the lateral distortional buckling in the top flange. With mass being constant, MSTT beam carried load more than that of MSBB by 78%. This is due to the opening of sigma sections in the box region of MSBB.

Provision of vertical stiffeners connecting the top and bottom flanges can able to resist the lateral distortion in MSBB and SSBB. In these sections, the load-carrying capacity can be further increased by providing spot welding along the top and bottom portions of webs. However, horizontal stiffeners can be provided in the tension and compression zones by connecting the webs of sigma sections in SSTT and MSTT to prevent the lateral-torsional buckling. The most economic section in terms of strength/weight ratio is SSBB, and the second most economic section is MSTT.

5 Conclusion

The structural behaviour of cold-formed, thin-walled closed built-up beams, which consists of sigma sections and channel sections was investigated to identify the most economic sections with respecting to load-carrying capacity under flexural action. The comparison showed good agreement between the analytical and experimental results for both buckling and load–deflection curves. The results of this study showed that two-channel sectional beams and two sigma sections can be employed successfully in applications such as primary and secondary beams. The findings dictate that the thickness of the web, strength-to-weight ratio, and degree of welding have a significant impact on the structural behaviour of built-up sections. In comparison with the SSTT and MSBB specimens, the SSBB and MSTT specimens demonstrated a higher load bearing capacity, and these can be utilized as primary beams in structures. Also, SSBB is found to be the most cost-effective section in terms of strength-to-weight ratio, MSTT is the second most cost-effective segment despite having a 36.8% lower load-carrying capacity. MSTT can be used as secondary beams in structures.

References

1. Zhen N, YQ Li (2016) Material properties of cold-rolled thin-walled steel plates at elevated temperatures. In: Proceedings of international speciality conference on cold-formed steel structures
2. Xu L, Sultana P, Zhou X (2009) Flexural strength of cold-formed steel built-up box sections. *Thin-Walled Struct* 47:807–815
3. Li YL, Li YQ, Zen Z-Y (2016) Investigation on flexural strength of cold-formed thin-walled steel beams with built-up box section. *Thin-Walled Struct* 107:66–79

4. Anbarasu M (2019) Simulation of flexural behaviour and design of cold-formed steel closed built-up beams composed of two sigma sections for local buckling. *Eng Struct* 191:549–562
5. Wang C, Li SS, Zhang Z, Qian H, Quo Y (2022) Experiments on perforated cold-formed built-up I-section beam-columns with longitudinal web and complex edge stiffeners. *Structures* 38:765–780
6. Aruna G, Ponraj Shankar L, Sudharshan N, Balakrishnan V (2021) Numerical simulation of cold-formed T-shaped built-up steel sections under bending. 46(Part 1):857–861
7. Babu SS, Selvan SS (2020) Study on the flexural and compressive behavior of cold-formed steel sections with and without lips. *Mater Today Proc*
8. Roy K, Lau HH, Ting TCH, Chen B, Lim JBP (2021) Flexural behaviour of back-to-back built-up cold-formed steel channel beams. *Structures* 29:235–253
9. Reza W, Selvan SS (2016) Experimental study on flexural behaviour of cold formed steel channel and I sections providing angle stiffener on the web. *Indian J Sci Technol* 9
10. Manikandan P, Sukumar S (2016) Behaviour of cold-formed steel built-up closed section with intermediate web stiffener under bending. *Mater Today Proc* 24:298–302
11. ASTM E8/E8M-13a standard test methods for tension testing of metallic materials 1. https://doi.org/10.1520/E0008_E0008M-13A
12. Laim L, Rodrigues JPC, da Silva LS (2013) Experimental and numerical analysis on the structural behaviour of cold-formed steel beams. *Structures*
13. Nguyen VB, Wang CJ, Mynors DJ, Castellucci MA, English MA (2013) Finite element simulation on mechanical and structural properties of cold-formed dimpled steel. *Thin-Walled Struct* 64:13–22. <https://doi.org/10.1016/j.tws.2012.11.002>
14. Górka J, Jamrozik W, Kiel-Jamrozik M (2023) The effect of TIG welding on the structure and hardness of butt joints made of Inconel 718. *Heliyon* 9(2)
15. IS 800 (2007) General construction in steel—code of practice

Evaluation of Surface-Coated Recycled Coarse Aggregate in Concrete Using Alccofine



J. Rajprasad, Akshaya ram, and Jeeva Prasanth

1 Introduction

Concrete is a crucial material in the construction industry, but many countries face scarcity in natural resources. To address this issue, recycling materials is important, and recycled aggregate concrete (RAC) has gained global attention for its environmental benefits [1]. RAC is made from recycled concrete aggregate (RA), which has been extensively studied, but its mechanical and durability characteristics fall short of those of natural aggregate concrete (NAC). However, using RA reduces the cost of aggregate, decreases excessive construction and demolition wastes, and preserves landfill space [2]. One major drawback of RA is its high porosity, which can absorb up to 4–6% water depending on the aggregate's nature and age. Simple and cost-effective coating techniques are used to overcome this hurdle, such as treating the coarse aggregate with alccofine-1203 (AF), a micro-fine material that fills the pores with glass particles or processed GGBS, hindering the flow of water. Preliminary tests showed that surface-treated recycled coarse aggregate has half the water absorption of untreated recycled aggregate [2]. Various strategies have been proposed to enhance RAC function, with the surface treatment of RA receiving the most attention. The authors of existing literature have suggested treating RA with pozzolanic materials, such as cement, cement with fly ash, and silica fume, which can react with the calcium hydroxide in old mortar to generate C-S-H gels, improving the strength and durability properties of RAC [4, 5]. Surface-treating RA in a cementitious slurry containing nano-silica and nano-CaCO₃ can greatly increase the mechanical performance of

J. Rajprasad (✉)

Department of Civil Engineering, Faculty of Engineering and Technology, SRM Institute of Science and Technology, Kattankulathur, Tamil Nadu 603203, India
e-mail: rajprasj@srmist.edu.in

Akshaya ram · J. Prasanth

Department of Civil Engineering, SRM Institute of Science and Technology, Kattankulathur, Tamil Nadu 603203, India

RAC [8]. This study focuses on enhancing the properties of recycled aggregate by surface treating it using alccofine-1203-AF to improve the mechanical properties of concrete. Various mechanical properties tests were conducted, and their results were compared with conventional concrete and untreated recycled aggregate concrete mixes [11]. Alccofine coating on recycled coarse aggregate increases its strength by filling in the pores and voids, reducing porosity and increasing density. This reduction in porosity leads to an increase in compressive strength, making it more suitable for construction applications where strength is critical [9]. Alccofine also contains silica fume, a highly reactive pozzolanic material that reacts with calcium hydroxide to form additional calcium silicate hydrate (CSH) gel, improving the mechanical and chemical bonds between the cement paste and aggregate particles. Therefore, the combination of reduced porosity and increased pozzolanic reaction contributes to the increased strength of recycled aggregate coated with alccofine [13].

1.1 Literatures Study

Zhang et al. [10], the purpose of this research is to discover an effective microbial carbonate precipitation technique for altering RA and to investigate the impact of RA on the properties of RAC. Laboratory made concrete cubes were first created as model RA to assess the efficacy of various precipitation operations, keeping calcium source addition techniques and rotating treatment methods into account. Based on the results of the tests, an effective precipitation technique was proposed. Second, the RA from factories was adjusted before being molded into concrete using the indicated precipitation technique. Because biomodification improved the microhardness of the interfacial transition zones, the RAC had a higher compressive strength.

Kavussi, RCA is being considered as a viable replacement for CA in asphalt formulations. Regardless of some contradictory findings, RCA treatment is expected to greatly improve the overall quality of recycled asphalt mixtures. In this investigation, coarse RCA materials were subjected to two treatments to improve their properties. The RCAs were treated by soaking them in HCl and then impregnating them using calcium metasilicate (CM). The pores of the RCAs contained CM particles. When virgin aggregates with varied quantities of coarse RCA materials were replaced for HMA in indirect tensile fatigue test (ITFT), the tensile properties of the mixes improved. The treatments made the mixtures less sensitive to moisture. The advantages were primarily linked to RCA materials' lower water absorption. The morphological parameters of the treated-coarse RCA materials were also determined using SEM (scanning electron microscopy) images.

Prasad et al., a unique bio-deposition process was utilized in this work to improve the properties of RCA. The experimental investigation was conducted in two stages. First, the physical properties of the bio-deposition-treated RCA, which includes as crushing value, crushing value, density and water absorption were determined. Then, it was determined how easily workable, water-absorbing, and compressive treated RCA mortars were. RCA treatment versus untreated was compared.

Qiu et al., this paper investigates microbial carbonate precipitation (MCP) as a novel approach for treating RCA surfaces. The effects of MCP RCA were investigated. MCP levels were shown to peak at pH 9.5 and increase with bacterial concentration, calcium content, or increasing temperature. Improved MCP on RCA can be created by properly managing the culture and precipitating conditions. The results reveal that MCP can be used to change the surface of RCA, as evidenced by the rise in mass and decreases in water absorption.

Santos, because of the material's high porosity, this study intends to analyze the properties of D&CW recycled aggregates treated with a silane-based water repellent agent in three separate ways: (a) immersion, (b) sprinkling, and (c) dripping. Wettability and water absorption were discovered by measuring apparent contact angles, evaluating water absorption following 24 h of saturation (standard approach), and recording the variance of immersed mass over a 24-h period. All treatments made it feasible to reduce water absorption and its dynamics. The treatment's outcomes were consistently hydrophobic, as evidenced by contact angle measurements. When the various techniques were compared, immersion yielded the best results regarding both measurement variability and absolute findings.

2 Materials

Materials of good quality are essential to create a concrete without any honeycombs, pores, and air voids. The procurement of material plays an important role and affects the strength and durability of concrete.

2.1 Cement

As per 12269:2013, OPC 53 grade cement was used, with a specific gravity of 3.15 and a surface area of 225 m²/kg. Tables 1 and 2 demonstrate the chemical composition and characteristics of cement. Cement with a proper chemical composition provides greater binding between particles, which is vital in building concrete durability and strength.

2.2 Alccofine-1203

Conventional Aggregate (CA)

In this research study, crushed stones with a specific gravity of 2.67 and a size between 10 and 20 mm were employed as coarse aggregates.

Table 1 Constituents of cement

Constituents	Percentage
Na ₂ O—sodium oxide	0.47
Al ₂ O ₃ —alumina	4.57
CaO—calcium oxide	68.64
SO ₃ —sulfur trioxide	3.14
MgO—magnesium oxide	1.39
Fe ₂ O ₃ —iron oxide	1.21
SiO ₂ —silica	19.35
Other oxides	1.23

Table 2 Properties of cement

Constituents	Result
Consistency	33%
Fineness	4%
Specific gravity	3.06
Initial setting	42 min
Final setting	133 n

M-Sand

M-sand with a specific gravity of 2.76 was utilized as the finer aggregate. M-sand is made by crushing hard granite rocks into fine particles and is a manufactured sand that is eco-friendly and cost-effective, unlike naturally occurring river sand extracted from riverbeds.

Recycled Coarse Aggregate (RCA)

The RA was sourced from a wrecked residential structure in Chennai’s West Mambalam. The aggregate obtained had a specific gravity value of 2.78 and was crushed to the necessary particle size of 10–20 mm. RA is created by crushing and sorting construction waste, such as concrete, brick, and asphalt, into sizes that are appropriate for use in new construction projects. This process of reusing construction materials is commonly referred to as RA.

The water absorption characteristics of both conventional and RAs were investigated by submerging three kilograms of oven-cooked aggregates in water for 24 h, as given in Table 3. After averaging the findings of three studies, it was observed that RA exhibits greater capacity to absorb water compared to surface and native treated aggregates. The most crucial aspects were the adhering mortar and the source of RA’s improved water absorption capacity (Fig. 1).

The addition of alccofine to RA enhanced test findings. The study discovered that RA absorbs more water than native aggregate, so it’s best to employ it in a fully saturated state of dryness for concrete preparation. This can be accomplished by wetting coarse aggregate particles and then drying the surfaces. Concrete waste is

Table 3 Properties of aggregate

Description	Aggregate (Conventional)	Aggregate (Recycled)	Aggregate (Surface coated)
Specific gravity	2.67	2.78	2.8
Impact value, %	8.5	12.6	9.6
Abrasion, %	30	45	37
Water absorption, %	2.5	5.48	4.7
Crushing value, %	25	38	32

**Fig. 1** Recycled aggregate

collected from the site, manually hammered to remove cement mortar, and fed into a jaw crusher for initial crushing. The fragments detained from the crusher vary from 10 to 50 mm. They are then further crushed using an impact crusher to achieve a size of 10–21.5 mm. The resulting conventional is used for casting the concrete. ASTM C33 sets a 50% limit for crushing and impact values for concrete aggregates made of gravel, crushed gravel, and crushed stone. Testing showed that CA had a crushing value of 22%, while RA had 38%. RA also had higher impact and abrasion values (34% and 41%, respectively) compared to CA (15% and 25%, respectively). RA of size 10–21.3 mm. However, treating the RA with alccofine improved its strength, with a 30% increase in crushing value and 30% and 33% improvements in impact resistance and abrasion value, respectively, over run treated RA. It is clear that the quality of RA is inferior to that of CA.

Mixing Approaches

Two surface mixes of aggregate were involved. Trail A involved adding RA to an alccofine mortar with a water–alccofine ratio of 0.8, while Trail B used a ratio of 0.6. Both mixes were created using a 40 kg pan mixer. In each mix, the initial half of the water used for mixing (W) was mixed for 100 s with alccofine (AF) to generate a slurry which had a water–binder ratio. The RA was then stirred into the slurry for one hundred seconds in order to coat the RA surfaces. The coated aggregates were

surface-dried for 48 h before use in concrete in a saturated surface dry condition (SSD). For Trail B, the total water–binder ratio was kept constant at 0.6 throughout the coating process. Trail B exhibited superior surface coating on the RA compared to Trail A. The coated aggregate look slight gray in color.

Concrete Mixture

Four separate types of concrete mixtures were made utilizing both surface-treated recycled material and M25 graded RA. These mixtures were then compared to conventional concrete. The labels RCA-100, RCA-75, RCA-50, and RCA-25 indicate RA concrete compositions with replacement amounts of 100%, 75%, 50%, and 25%, respectively. Similarly, surface-coated recycled aggregate (SCRA)-100, SCRA-75, SCRA-50, and SCRA-25 denotes concrete mixtures with surface-coated recycled-aggregate replacement levels of 100%, 75%, 50%, and 25%. Finally, TC denotes traditional concrete. The varying blended proportions were given in Tables 4 and 5. The above mixed designs were designed according to IS10262:2009. The concretes were cast into mold for the ages 3, 7, and 28.

Specimen Preparation

The specimens are mixed using mixing equipment with a maximum weight of 100 kg. The coarse aggregate and small aggregates are mixed for 1 min to begin the operation. The mixture is then stirred for another minute with a water–cement ratio of 0.49 retained throughout the specimen production process. Finally, the amount that’s required of water is progressively incorporated into the mixture and stirred for 5 min. Before the concrete was cast into the molds, the molds were oiled or greased. Within 10 min, the mixes of concrete are cast into molds, and the surface of the concrete is

Table 4 Proportions of traditional concrete and recycled coarse aggregate concrete

Constituents (kg/m ³)	TC	RCA-25	RCA-50	RCA-75	RCA-100
Cement	383	383	383	383	383
Water	191	191	191	191	191
Fine aggregate	636	636	636	636	636
Coarse aggregate	118	886.5	591	295.5	0
Recycle aggregate	0	295.5	591	886.5	1182

Table 5 Mix proportion of surface-coated recycled aggregate concrete

Constituents (kg/m ³)	SCRA-25	SCRA-50	SCRA-75	SCRA-100
Cement	383	383	383	383
Water	191	191	191	191
Fine aggregate	636	636	636	636
Coarse aggregate	886.5	591	295.5	0
Surface-coated recycled aggregate (SCRA)	295.5	591	886.5	1182

smoothed and leveled with a trowel or float. During this operation, make sure that any extra concrete has been removed off at top of the mold. To keep the concrete from air drying out too rapidly, wrap it with a sheet of plastic or keep it in a humid environment. Moreover, it is essential to let the concrete cure for 24 h by placing the concrete in curing tank. Prior to testing, the samples are removed from the curing tank and dried to prevent damage; the sample should be managed with care. Tests can be done on the finished concrete specimen to determine its durability, tensile strength, and compressive strength. These tests are crucial to make sure that the concrete used in a construction project will be strong enough to meet the project's requirements and be able to resist the environmental conditions it will be exposed to. The material was batched prior to the casting and aggregates undergone various tests listed above. The mortar should be compacted properly into the mold to avoid any honeycombs and voids which might affect the durability and strength of the concrete.

3 Results and Discussion

Slump Cone Test

The value of the slump for conventional concrete was 40 mm, and the slump values for 100%, 75%, 50%, and 25% CA replacement were 20 mm, 25 mm, 30 mm, and 35 mm, respectively. The increased water absorption of RA causes a decreasing slump when replacing natural material. When compared to RAC, the slump values of surface-coated aggregate concrete were 25, 35, 40, and 45 mm. This is due to the low water absorption of SCRA. It is due to the low porosity of the aggregate due its surface treatment the pores are filled with alccofine and hinders the capillary action inside the aggregate, whereas the in RA and harsh surface and some of the old mortar present in its surface poses more water and increases the water absorption. The high-water absorption due to its uneven surface reduces the binding properties with the binding materials. There is an increase in SCR25 compared with RC25 by 28.5%; comparing the SCR50 and RC50, there is an increase of 33.3%, and for SCR75 and SCR100 with RC75 and RC100, there is an increase of 40% and 25%, respectively. Among all the above values, the SCR25 exhibits superior workability (Fig. 2).

Compression Test

The study's findings are given in Table 6. In terms of strength, the results show that surface-coated aggregate concrete surpasses both traditional mixed and RAC. SCR100, SCR75, SCR50, and SCR25 compressive strengths are 29.4, 31.3, 33.6, and 34.5 (N/mm²), while RC100, RC75, RC50, and RC25 compressive strengths are 18, 20, 22, and 24 (N/mm²). The compressive strength of conventional concrete is 31.4. SCRA-25 has the highest compressive strength.

Figure 3 displays the compressive strength progression of various combinations of RA, SCRA and CA over time. The study showed that lower RAC strength than CAC regardless of age. The presence of attached mortar in RA was discovered to be

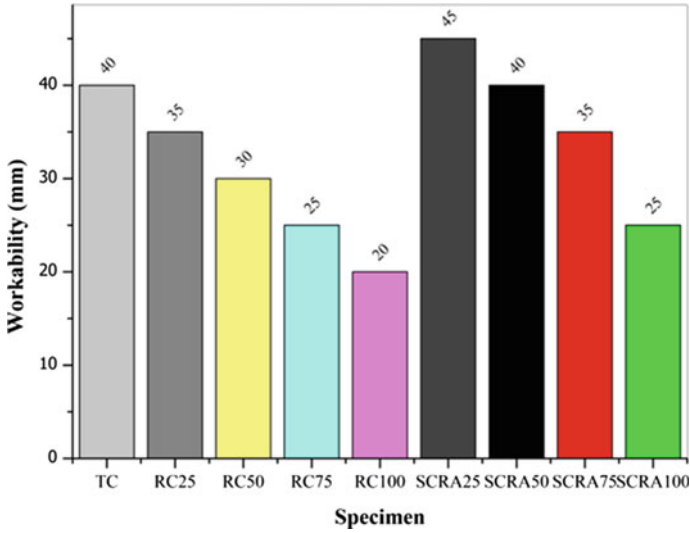


Fig. 2 Workability results

Table 6 Compression test results

Mix code	Compressive strength, N/mm ²		
	3 days	7 days	28 days
TC	12.3	20.2	31.4
RCA-25	12	19.5	24
RCA-50	15.86	17.8	22
RCA-75	9.76	15.86	20
RCA-100	9.11	14.8	18
SCRA-25	19.76	29.91	34.5
SCRA-50	18.5	28.44	33.6
SCRA-75	15.59	24.88	31.3
SCRA-100	14.32	22.04	29.4

a factor impacting concrete strength, as RAC had 25% lower compressive strength at 28 days than CAC. When compared to untreated RAC at 28 days, treating the RA with alccofine improved the surface quality and resulted in a 40% rise in compressive strength. The strength improvement of treated RAC was found to be good in later ages.

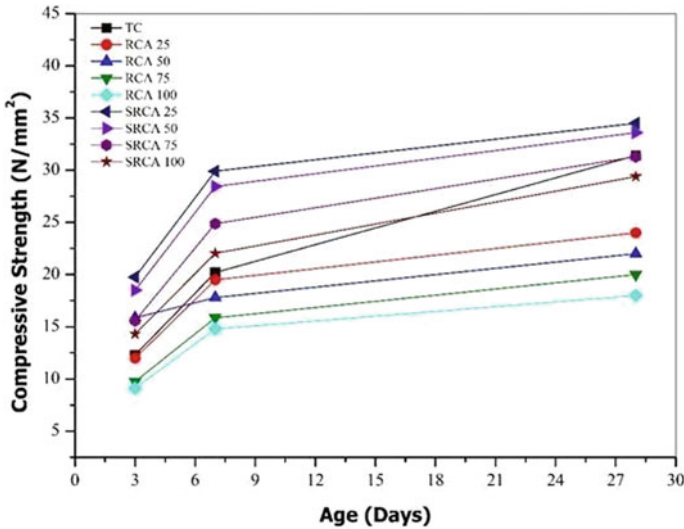


Fig. 3 Compression test results

3.1 Split Tensile Test

The tensile strength for SCR25, SCR50, SCR75, and SCR100 are 3.49, 2.89, 2.79, and 2.71 (N/mm²) and tensile strengths for RC25, RC50, RC75, and RC100 are 2.44, 2.34, 2.23, and 2.12 (N/mm²) and 2.8 (N/mm²). The tensile strength of surface-coated RAC exhibits high strength compared to untreated RAC and CAC, from Fig. 4. Surface-treated RA with alccofine greatly improved tensile strengths of SRC25 and SRC50, surpasses the intent value (3.35 N/mm²) at 28 days. RC75 and RC100 had notably lowered tensile strengths (3.27 and 3.14 N/mm²) compared to SCR75 and SCR100. At 28 days, SCR75 and SCR 100 had improved tensile strengths by 34.56% and 38.93% compared with RC75 and RC100, respectively, under the same curing conditions (Table 7).

3.2 Flexural Test

The flexural strength for SCR25, SCR50, SCR75, and SCR100 are 3.49, 2.89, 2.79, and 2.71 (N/mm²) and for RC25, RC50, RC75 and RC100 are 2.74, 2.56, 2.43, and 2.26 and 3.14 (N/mm²) for TC its recorded as 3.28 (N/mm²) from Fig. 5 it has been discovered as there has been a gain in strength of 27.37 and 33.98% for SCR25 and SCR50 compared with RC25 and RC50 and for SCR75 and SCR100

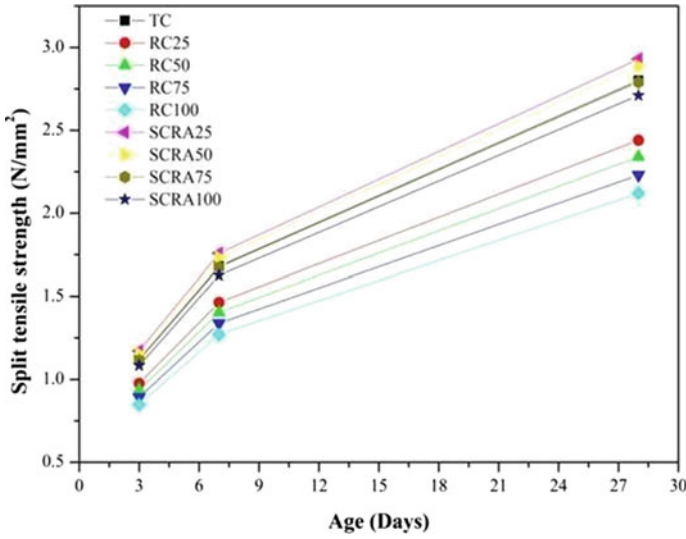


Fig. 4 Split tensile test results

Table 7 Split tensile test results

Mix code	Split tensile, N/mm ²		
	3 days	7 days	28 days
TC	1.12	1.68	2.8
RCA-25	0.976	1.464	2.44
RCA-50	0.936	1.404	2.34
RCA-75	0.892	1.338	2.23
RCA-100	0.848	1.272	2.12
SCRA-25	1.05	1.57	3.49
SCRA-50	1.156	1.734	2.89
SCRA-75	1.116	1.674	2.79
SCRA-100	1.084	1.626	2.71

there is an increase of 34.56% and 38.9 relative to TC75 and RC100. Surface-treated aggregates exhibit higher flexural strength than untreated aggregates, especially at 28 days. Alccofine-coated specimens show significant improvements in flexural strength compared to RC25 and SCR25. Coating RA with alccofine at a 0.6 alccofine–water ratio is recommended, although it is equally effective for traditional application. Figure 5 shows that SCR25 and SCR50 have the highest flexural strength at 28 days. The alccofine’s ultra-fine properties exhibit high consistency which leads to better binding ability leading to adhere well with the aggregate and used for surface coating the RA.

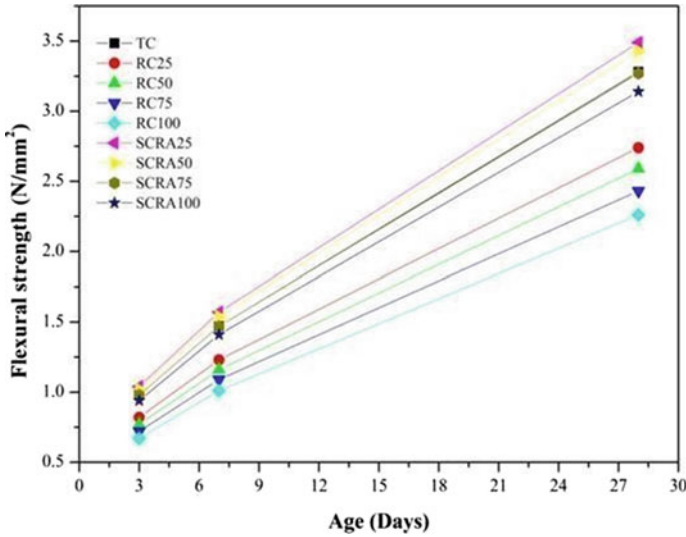


Fig. 5 Flexural test results

4 Conclusion

As the world’s population continues to grow, so does the demand for sustainable building materials. The construction industry has been exploring the use of recycled materials in the production of concrete. One such material is recycled aggregate, which is produced by crushing concrete and other construction waste. While recycled aggregate has been used in construction for some time, there are concerns about its mechanical properties and durability. To address these concerns, researchers have been exploring various methods of enhancing the properties of recycled aggregate concrete. One promising method is the use of surface coatings. Surface coatings can be used to improve the mechanical properties of concrete by reducing the porosity of the aggregate, enhancing its bonding with cement paste, and reducing the water absorption of the concrete. One such coating material that has been explored is alccofine, a type of pozzolanic material that is known for its ability to improve the strength and durability of concrete. This allowed for a comprehensive assessment of the mechanical properties of each type of concrete, both with and without the alccofine coating on the recycled aggregate. The results of the study indicate that SCRA-25 and SCRA-50 are the optimal mixes for increasing the strength of the concrete. These mixes were found to be most effective in improving the mechanical properties of the recycled aggregate concrete when compared to traditional concrete and non-coated recycled aggregate concrete. This suggests that the use of surface-coated recycled aggregate can be an effective way of enhancing the properties of concrete.

In addition to improving the mechanical properties of concrete, the use of surface-coated recycled aggregate also has other potential benefits. For example, by treating the recycled aggregate, the depletion of natural aggregate can be reduced, which is important given the limited availability of natural resources. Additionally, the use of recycled aggregate can reduce the amount of waste that is sent to landfills, which is both cost-effective and environmentally friendly. Another benefit of surface coating recycled aggregate is that large quantities of the material can be treated with relatively small amounts of alccofine and water. This is because the coating process is able to penetrate the aggregate and bind with the cement paste, thereby reducing the amount of material that is needed. This can make the use of surface-coated recycled aggregate more cost-effective than other methods of enhancing the properties of concrete.

The use of surface-coated recycled aggregate can also lead to concrete with greater slump values. Slump refers to the degree to which concrete settles or slumps after being poured into a mold. A greater slump in value can make it easier to work with concrete, which is important in construction applications where precise pouring and leveling are necessary. In the study discussed above, greater slump values were obtained for the concrete containing the surface-treated recycled aggregate with alccofine compared to that of untreated aggregate and natural aggregate. Despite the potential benefits of surface-coated recycled aggregate, there are some challenges that need to be addressed. One such challenge is the issue of compatibility between the coating material and the recycled aggregate. The coating material needs to be able to bond effectively with the aggregate, which can be difficult given the variability in the size and shape of the aggregate particles. Additionally, there is the potential for the coating material to negatively impact the workability of the concrete if it is not applied properly.

References

1. Rajprasad J, Pannirselvam N (2020) Experimental investigation on concrete using treated recycled aggregate. *IOP Conf Ser Mater Sci Eng* 912(6):062059. <https://doi.org/10.1088/1757-899x/912/6/062059>
2. Rajprasad J, Pannirselvam N (2020) Optimizing the properties of treated recycled aggregate concrete. In: 1st international conference on mathematical techniques and applications ICMTA2020. <https://doi.org/10.1063/5.0025258>
3. Medina C, Zhu W, Howind T, de Rojas MIS, Frías M (2014) Influence of mixed recycled aggregate on the physical-mechanical properties of recycled concrete. *J Clean Prod* 68:216–225
4. Duan ZH, Poon CS (2014) Properties of recycled aggregate concrete made with recycled aggregates with different amounts of old adhered mortars. *Mater Des* 58(6):19–29
5. Silva RV, Neves R, de Brito J, Dhir RK (2015) Carbonation behaviour of recycled aggregate concrete. *Cem Concr Compos* 62:22–32
6. Kou SC, Poon CS (2013) Long-term mechanical and durability properties of recycled aggregate concrete prepared with the incorporation of fly ash. *Cem Concr Compos* 37:12–19
7. Huda SB, Alam MS (2015) Mechanical and freeze-thaw durability properties of recycled aggregate concrete made with recycled coarse aggregate. *J Mater Civ Eng* 27(10):04015003
8. Tam VW, Tam CM, Le KN (2007) Removal of cement mortar remains from recycled aggregate using pre-soaking approaches. *Constr Build Mater* 50:82–101

9. Pepe M, Filho RDT, Koenders EAB, Martinelli E (2014) Alternative processing procedures for recycled aggregates in structural concrete. *Constr Build Mater* 69:124–132
10. Zhang J, Shi C, Li Y, Pan X, Poon CS, Xie Z (2015) Influence of carbonated recycled concrete aggregate on properties of cement mortar. *Constr Build Mater* 98:1–7
11. Zhang H, Zhao Y, Meng T, Shah SP (2016) Surface treatment on recycled coarse aggregates with nanomaterials. *J Mater Civ Eng* 28:04015094
12. Grabiec AM, Klama J, Zawal D, Krupa D (2012) Modification of recycled concrete aggregate by calcium carbonate bio-deposition. *Constr Build Mater* 34:145–150
13. Kou SC, Zhan BJ, Poon CS (2014) Use of a CO₂ curing step to improve the properties of concrete prepared with recycled aggregates. *Cem Concr Compos* 45:22–28
14. Kou SC, Poon CS (2010) Properties of concrete prepared with PVA-impregnated recycled concrete aggregates. *Cem Concr Compos* 32:649–654
15. Kong D, Lei T, Zheng J, Ma C, Jiang J, Jiang J (2010) Effect and mechanism of surface-coating pozzalanic materials around aggregate on properties and ITZ micro-structure of recycled aggregate concrete. *Constr Build Mater* 24(5):701–708
16. Shi C, Li Y, Zhang J, Li W, Chong L, Xie Z (2016) Performance enhancement of recycled concrete aggregate—a review. *J Clean Prod* 112:466–472
17. Katz (2004) Treatments for the improvement of recycled aggregate. *J Mater Civ Eng* 16(6):597603
18. Shayan AX (2003) Performance and properties of structural concrete made with recycled concrete aggregate. *ACI Mater J* 100(5):371–380
19. Du T, Li HQ, Wu XG (2002) Experimental study on enhancement of recycled aggregate. *New Build Mater* 3:6–8
20. Zhang H, Zhao Y, Meng T, Shah SP (2015) The modification effects of a nano-silica slurry on microstructure, strength, and strain development of recycled aggregate concrete applied in an enlarged structural test. *Constr Build Mater* 95:721–735
21. Tam Vivian WY, Gao XF, Tam CM (2006) Environmental enhancement through use of recycled aggregate concrete in a two-stage mixing approach. *Human Ecol Risk Assess* 12(2):277–288
22. Li Q, Li Y, Zhu C (2005) Influence of a particle shape correcting technique in properties of recycled coarse aggregate. *CailiaoKexueyuGongyi/Mater Sci Technol* 13(6):579–81 (2005)
23. Du T, Li H, Wu X et al (2005) Compression-deformation behaviour of concrete with various modified recycled aggregates. *J Wuhan Univ Technol Mater Sci Edition* 20(2):127–9
24. Tsuji M, Sawamoto T (2000) New technique producing recycled aggregate concrete for conservation of resources and energy. *Trans Japan Concr Inst* 22:77–84
25. Katz A (2004) Treatments for the improvement of recycled aggregate. *J Mater Civil Eng* 16(6):597–603
26. Sawamoto T, Tsuji M (2000) Technique to produce recycled aggregate concrete with crushed concrete waste. *Zairyo/J Soc Mater Sci* 49(10):1079–1084 [in Japanese]
27. Zaharieva R, Buyle-Bodin F, Skoczylas F et al (2003) Assessment of the surface permeation properties of recycled aggregate concrete. *Cem Concr Comp* 25(2):223–232
28. Buyle-Bodin F, Hadjieva-Zaharieva R (2002) Influence of industrially produced recycled aggregates on flow properties of concrete. *Mater Struct/Materiaux et Constr* 35(252):504–509
29. De Larrard F (1999) Concrete mixture proportioning: a scientific approach. E&FN Spon, London
30. Bentz DP (2000) Influence of silica fume on diffusivity in cement-based materials (II). Multi-scale modeling of concrete diffusivity. *Cem Concr Res* 30(7):1121–9 (2000)
31. Paulon VA, Dal MD, Monteiro PJ (2004) Statistical analysis of the effect of mineral additives on the strength of the interfacial transition zone. *Interf Sci* 12(4):399–410
32. Kobayashi K, Hattori A, Miyagawa T et al (1996) Characters of interfacial zone of cement paste with additives around aggregate. *Zairyo/J Soc Mater Sci* 45(9):1001–1007 [in Japanese]
33. Zheng JJ, Li CQ, Zhou XZ (2005) Thickness of interfacial transition zone and cement content profiles around aggregates. *Magaz Concr Res* 57(7):397–406
34. Poon CS, Shui ZH, Lam L (2004) Effect of microstructure of ITZ on compressive strength of concrete prepared with recycled aggregates. *Constr Build Mater* 18(6):461–468

35. Montgomery DG (1998) Workability and compressive strength properties of concrete containing recycled concrete aggregate. In: Dhir RK, Henderson NA, Limbachiya MC (eds) Proceedings of international symposium: sustainable construction: use of recycled concrete aggregate. Thomas Telford, London, pp 289–96
36. Tateyashiki H, Shima H, Matsumoto Y et al (2001) Properties of concrete with high quality recycled aggregate by heat and rubbing method. Proc JCI 23(2):61–66
37. Tam VWY, Tam CM, Le KN (2007) Removal of cement mortar remains from recycled aggregate using pre-soaking approaches. Resour Conserv Recycle 50(1):82–101

Analysis and Experimental Feasibility Study on Bio-mimicked Non-developable Shell Model



Nelson Takhellambam and K. S. Satyanarayanan

1 Introduction

The dome's design and development were influenced by the arch. The dome has a hemi-spherical structure by definition. The word 'dome' refers to an upward or outward swelling that forms a roof or ceiling. A dome is a thin shell structure that is produced when an arc curve revolves around one of its axes. Domes are those kind of space structures that offer significant net valuable column-free spaces. Culture-wise, dome architecture has changed, both in terms of its construction and significance. It served as a crucial building for storage and shelter in antiquity. Architecturally speaking, it evolved from having basic utilitarian utility for homes and cemeteries to having symbolic, religious, and artistic value. As a representation of the sky and the boundless, it took on symbolic and theological significance (Fig. 1).

The study of emulating and mimicking nature for various structural elements to solve complex human problems is termed as bio-mimicry. Bio-mimics in structures helps in the flow and adaptation of natural stability and material used strategies and broadens the design solution space to bring new solutions to the design table.

2 Literature Study

Prabhavati et al. [1] applied the shell theory analysis approach for shell analysis and working stress method design in accordance with IS 800-2007. Domes are optimized using the dynamic programming method. Bar charts are used to display the results. It is possible to create and receive a low-cost design for an RCC dome.

N. Takhellambam (✉) · K. S. Satyanarayanan

Department of Civil Engineering, Faculty of Engineering and Technology, SRM Institute of Science and Technology, Kattankulathur, Tamil Nadu 603203, India

e-mail: nt6426@srmist.edu.in



Fig. 1 Dome structures: **a** Tomb display of Geodesic dome in Changnyeong, **b** National Museum of Brazil

Sharma et al. [2] have gathered, grouped, and displayed scientific data on bio-mimicry up to this point. Despite the fact that bio-mimicry is a dispersed field, they also classify the uses of bio-mimicry in various ways. There have also been discussions about other bio-mimicry gaps, tools, and difficulties.

Saltik et al. [3] have done the experiment on form finding of the shell structure. TNA method and Rhino Vault plugin were used in the design of the forms. The Karamba (finite element analysis) plugin converted the produced form into structural models. The results in the study are focused on deformations related to load. They also studied the effects of shell when the openings were removed according to the loads; thus, the weight was reduced and form alternatives were created. The resulting forms were analysed again, and the structures stayed in the structural safe zone.

Wani et al. [4] have analysed the behaviour and strength of modern-day thin spherical shell domes made of concrete with and without rib beams using finite element technique with the help of SAP2000 software. The work consists of the erection of round domes with a massive diameter of 50, 100, and 150 m with and without rib beams and a shell thickness of 15 cm.

Gohnert et al. [5] have developed the membrane theory for a catenary dome with a linear variation in wall thickness. Furthermore, the theory is extended to catenary domes with an oculus, or a dome with a concentric hole at the apex. A finite element analysis (FEA) was also performed to determine the accuracy of the proposed theory.

3 Methodology

Various literature papers were studied to understand shape and size of jasmine flower, about 100 flowers were collected, measured, and their average was taken into consideration for modelling the bio-mimicked shell structure. A pilot model has been developed using steel wires and analysed in a finite element analysis software (Abaqus V 6.14). Scaled model has been developed comparing the size of jasmine flower with ferrocement and ring beam; and comparison of the results with the experimental values has been done.

4 Dimensioning of Bio-Mimic Scaled Model

Jasmine flower has been considered as it has equivalent distribution of petals as well as depth of the petals. The jasmine flower resembles a dome structure when it is inverted. The mean value of D/h ratio is shown in Table 1.

So, the jasmine flower has been selected as a mimicking structure. The sample was collected from Potheri, Tamil Nadu, during monsoon season (Fig. 2).

Table 1 Dimensions of bio-mimicked model

S. No	Diameter (mm)	Height (mm)	D/h
1	30	8	3.75
2	31	7	4.43
3	36	4	9.00
4	35	8	4.38
5	34	5	6.80
6	35	5	7.00
7	35	8	4.38
8	35	6	5.83
9	35	6	5.83
10	35	6	5.83
11	35	6	5.83
12	35	6	5.83
13	30	8	3.75
14	35	6	5.83
15	33	7	4.71
		Average	5.55
	+5%–5%	Mean	5.83

Fig. 2 Flower. **a** Wild jasmine flower and **b** measurement of flower



(a)

(b)

5 Pilot Experiment of Shell Model

Pilot model of both conventional dome shell and bio-mimicked jasmine flower dome shell was made as shown in Fig. 3a, b, respectively. This pilot model has been developed to bring the idea of jasmine flower shape shell. It has been developed using the steel wires with the dimension of dome as 15 cm diameter and height of 4 cm. A member rod has also been attached to take point load for experimental purpose.

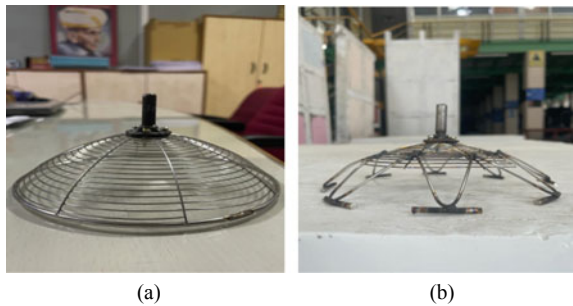
5.1 Testing of Pilot Shell Model

A compressive test has been conducted for the pilot shell model for both conventional and bio-mimicked shell as shown in Fig. 4a, b, respectively. The test was performed in order to study the load carrying capacity of the bio-mimicked shape. The failure of the conventional pilot shell model punches through and for the bio-mimicked pilot shell, it failed at very small load as there is no steel wire connected at the support area which will act as a circular beam but in the conventional shell circular wire the steel wire at the support acted as a circular beam. Therefore, there is no horizontal displacement. The respective load deflection comparison graph of pilot shell is shown in Fig. 5.

5.2 Numerical Study of Pilot Model

The analytical study for the pilot model was done using Abaqus V 6.14 as shown in Fig. 6; steel plate was used to model both conventional dome-shaped structure and bio-mimicked flower shape, and this particular dome does not include the design and analysis of ring beam model in it.

Fig. 3 a Conventional pilot dome and b bio-mimic pilot shell



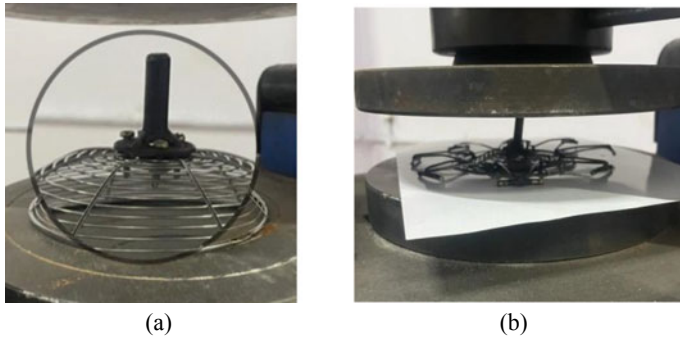


Fig. 4 Compression test: **a** conventional dome and **b** bio-mimic dome

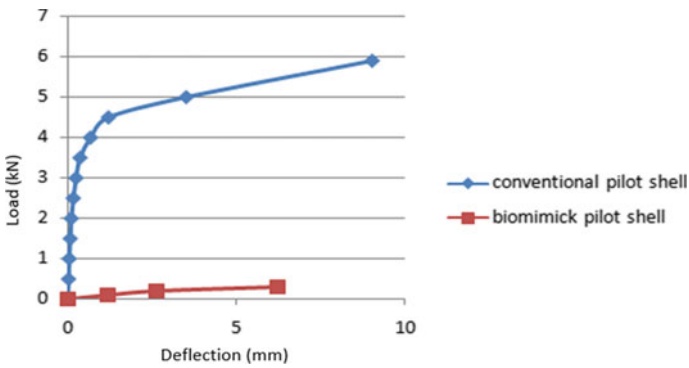


Fig. 5 Load versus deflection graph of conventional and bio-mimic pilot shell

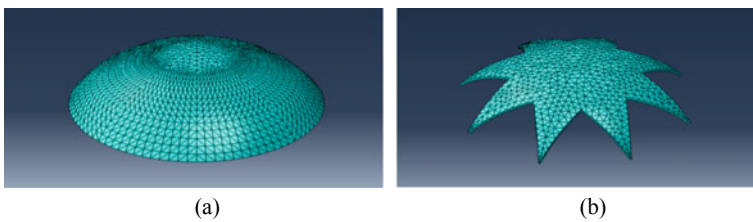


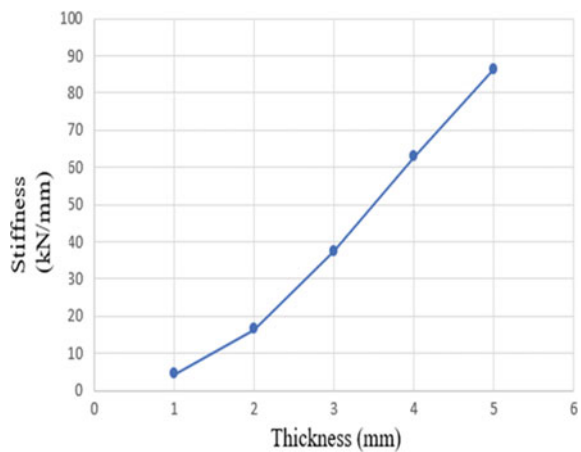
Fig. 6 **a** FEM modelling of conventional dome shell and **b** bio-mimic flower shell

5.3 Material and Properties of Pilot Shell and Stiffness

Table 2 shows the input parameter used in the FEM software. The thickness was determined from Stiffness and thickness graph shown in Fig. 7.

Table 2 Input parameters of Abaqus software for the pilot shell

Description		Parameters
Material		Steel plate
Dimension	Diameter	150 mm
	Height	40 mm
	Thickness	2 mm
Mesh	Type	C3d10—a 10 node quadratic tetrahedron
	Size	10 mm
Loading		Concentrated load of 5–50 kN
Support condition		Roller support

Fig. 7 Stiffness versus thickness of pilot shell model

5.4 Mesh Optimization

The analysis of conventional dome model was carried out by varying the mesh size under a constant point load of 10 kN. Finer the mesh the more accurate the results are; the deflection of the dome is inversely proportional to that of the mesh size until after a point where there is no change in deflection even there is increase in mesh size which will be considered as optimum mesh size of the model. There is no significance change in deflection after mesh size of 10 as shown in Fig. 8.

5.5 Displacement and Stress of Pilot Shell Analysis Model

The maximum principal stress of both conventional and bio-mimicked models have been shown in Figs. 9a, b and 10a, b, respectively.

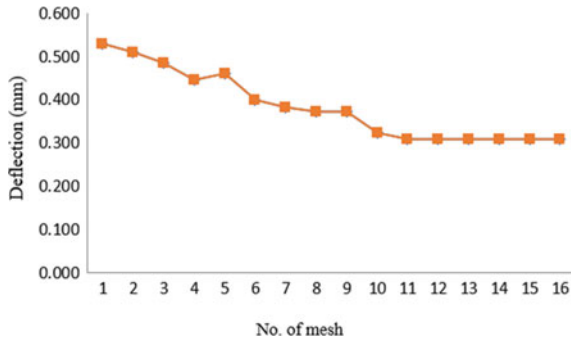


Fig. 8 Mesh convergence

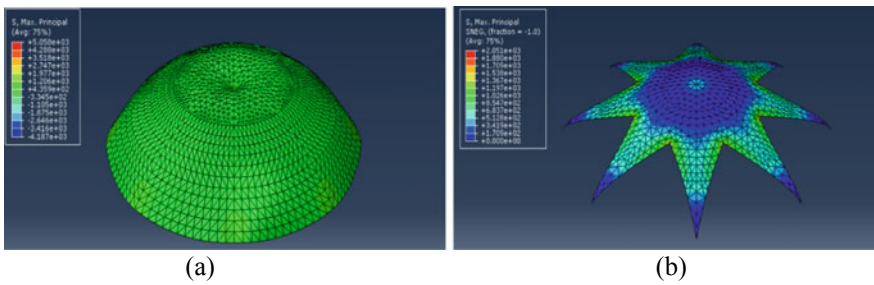


Fig. 9 Max principal stress **a** conventional dome and **b** bio-mimic shell

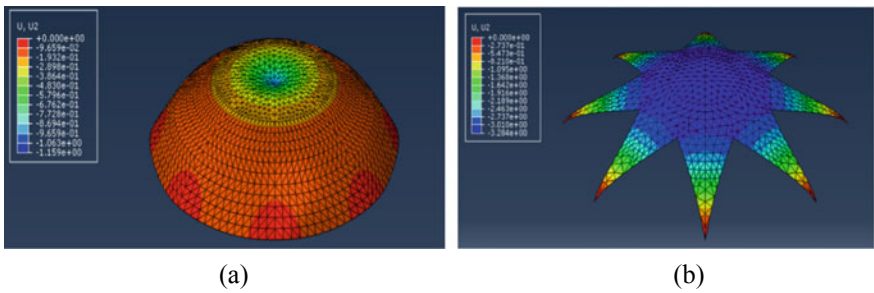


Fig. 10 Max displacement **a** conventional dome and **b** bio-mimic shell

The failure of the conventional pilot shell model punches through and for the bio-mimicked pilot shell it failed at very small load as there is no steel wire connected at the support area which will act as a circular beam but in the conventional shell circular wire at the support is acted as a circular beam. Therefore, there is no horizontal displacement; but in ferrocement model, we have considered the ring beam for analysis. The load deflection graph of respective pilot shell is shown in Fig. 11.

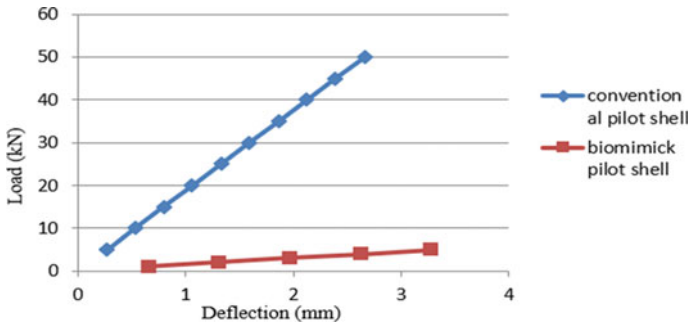


Fig. 11 Load versus deflection comparison between conventional dome and bio-mimic shell

5.6 Summary of Pilot Model Shell

An experimental and analytical study was done on the pilot shell model.

- The difference in the stiffness is very vast in the experimental values due to absence of ring beam in the bio-mimicked shell. But in the conventional pilot shell experiment, there is a thicker wire element at the support area which act as a ring beam.
- The failure of the conventional pilot shell was punches through the shell and flatten out for the bio-mimicked pilot shell.
- Therefore, from the above conclusion, a ring beam has been considered for the scaled model.

5.7 Representation Model of Bio-Mimicked Pilot Shell

- A representation model has been prepared for the shape visualization of the bio-mimicked jasmine shell as shown in Fig. 12.
- The height of the shell is 1/6th of its diameter ($h = d/6$).
- Diameter of the shell is 2 m, and height is 0.35 m.
- There are eight petals structure which are all connected to a ring beam. These ring beam help the structure's stability while connecting to column in each petal.

6 Casting

Slabs, conventional dome, and bio-mimicked shell have been casted and properly cured.



Fig. 12 Model of bio-mimicked shell

6.1 Casting of Ferrocement Slabs

Three slabs of 600 mm × 300 mm × 20 mm were casted using wire mesh of 10 mm × 10 mm with 0.51 mm diameter and 2:1 mortar. These slabs were casted in order to determine the modulus of elasticity of the ferrocement.

6.2 Casting of Conventional Dome and Bio-Mimicked Shell

For casting of the dome shell, firstly, a dome mould has been casted. This dome is casted by using a ply wood which is cut in a desired curve and pinned at the centre of the dome. To bring the curvature of the dome, the wooden tool rotates around the concrete. The conventional dome was casted above the dome mould, a layer of 6 mm mortar was casted at first then a wire mesh was kept above that, and another layer of 6 mm mortar was casted for a total thickness of 12 mm shown in Fig. 13.



Fig. 13 Casting of conventional and bio-mimicked shell with ferrocement

6.3 Testing of Conventional Slab

Flexure testing is a common method used to evaluate the strength and performance of ferrocement slabs under bending loads. This test was performed on the ferrocement slabs of 600 mm × 300 mm × 20 mm after curing for 28 days, and the values were compared. Three-point bending test has been done in the Compression Testing Machine (CTM) shown in Fig. 14.

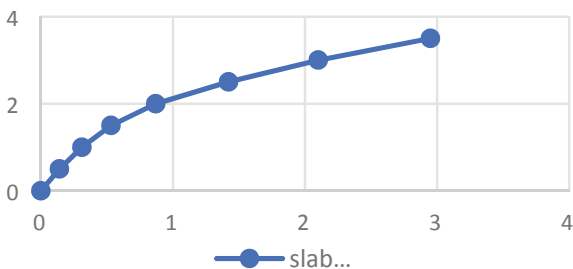
Under CTM machine, two roller supports were kept 5 cm from each end, and a steel ball was kept at the centre of the slab for the concentrated load. From the above graph (Fig. 15), an initial slope has been determined which will be used in calculating the modulus of elasticity of the ferrocement shell.

$$k = \frac{L}{d} = \frac{2500 - 1500}{1.42 - 0.53} = 1123.59 \text{ N/mm.}$$

Fig. 14 Testing of ferrocement slab



Fig. 15 Load versus deflection of the ferrocement slab



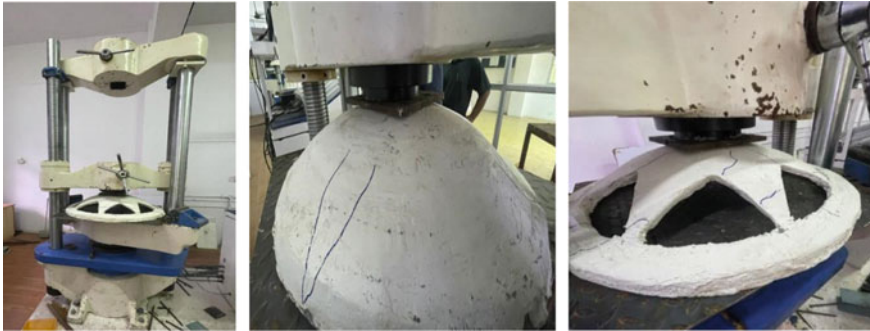


Fig. 16 Conventional and bio-mimicked models under UTM machine

6.4 Calculation of Modulus of Elasticity

The calculation of Young’s Modulus was done from the flexure test of slab with three-point bending test. Deflection of a three-point flexure bending test at the centre of the slab is

$$E = \frac{PL^3}{48D\Delta},$$

$$E = 35,164.8 \text{ N/mm}^2.$$

Therefore, modulus of elasticity of ferrocement slab (E) is 35,164.8 N/mm². Normal range is given in literature as 10–30 GPa [5].

6.5 Testing of Conventional Dome and Bio-Mimicked Shell

The testing of conventional and bio-mimic is done under UTM machine as shown in Fig. 16 and Comparison of experimental and analytical failure is shown in Fig 17.

7 Analysis and Result of Conventional and Bio-Mimicked Scaled Model with Ferrocement

From the load deflection graph shown in Fig. 18 of ferrocement conventional and bio-mimicked shell, the deflection varies by 30%. The specific stiffness of conventional shell is 0.8 and 0.7 for the bio-mimicked shell. Though the stiffness is similar, analysis of the bio-mimicked shell by increasing the thickness is done to have more idea.



Fig. 17 Failure of conventional and bio-mimicked dome model

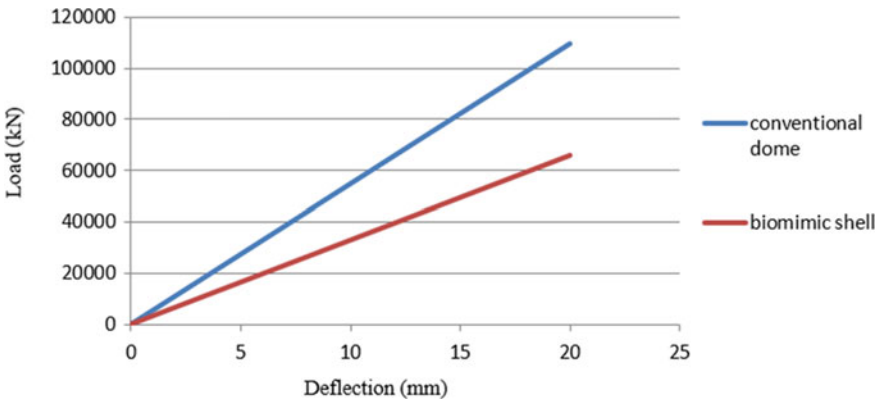


Fig. 18 Load versus deflection graph of ferrocement conventional and bio-mimicked shell

After analysing different variations of thickness in the scaled ferrocement bio-mimicked shell model. It is found that by increasing the thickness 1.5 times of the scaled conventional shell, the load carrying capacity of scaled ferrocement bio-mimicked shell model is almost equivalent as shown in Fig. 19.

8 Analysis Based on Thickness

After optimizing the thickness in FEM analysis with different variation of thickness in the scaled ferrocement bio-mimicked shell model, is found that by increasing the thickness of bio-mimicked shell by 1.5 times of the scaled conventional shell, i.e. adopting 20 mm thickness for bio-mimicked shell while thickness of conventional shell is 12 mm as shown in Fig. 20. The stiffness of scaled ferrocement bio-mimicked shell model is almost similar. Therefore, thickness of 12 and 20 mm was adopted for conventional and bio-mimicked shell model, respectively as shown in Fig. 21 and experimental results of conventional and bio-mimic shell is shown in Fig. 22.

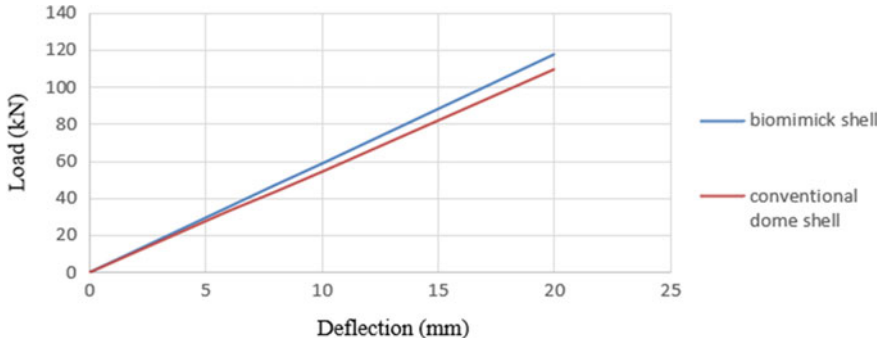


Fig. 19 Load versus deflection by increasing thickness of scaled bio-mimicked shell model

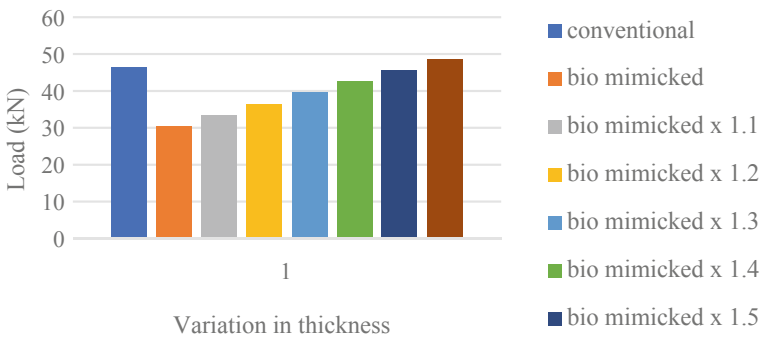


Fig. 20 Thickness optimization of the bio-mimicked model

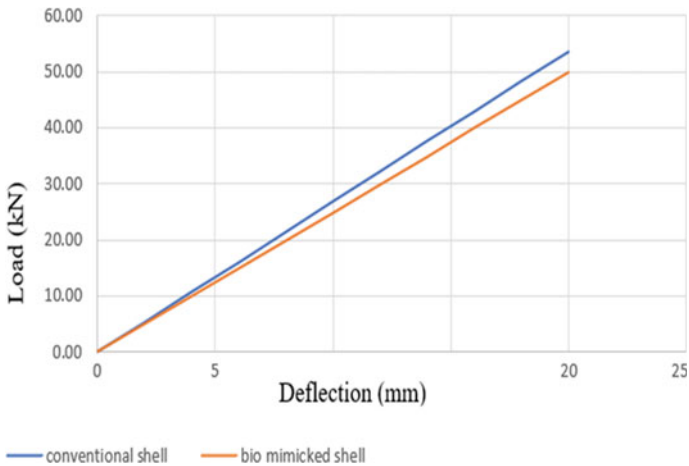


Fig. 21 Load versus deflection by optimizing the thickness

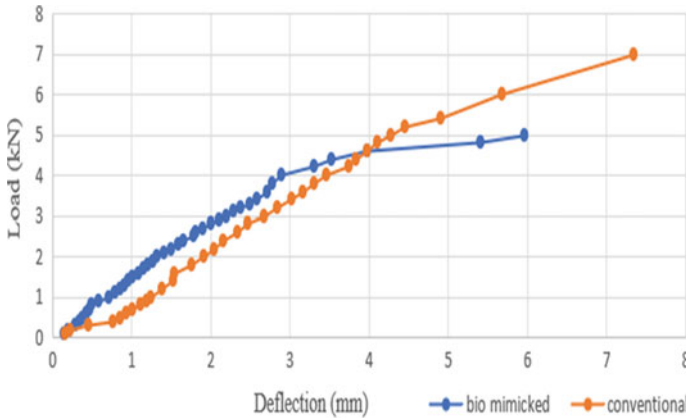


Fig. 22 Load versus deflection for conventional and bio-mimicked shell model using experiment

9 Conclusion

Dimensioning of the scaled model has been done by measuring the 15 specimens of jasmine flower by taking average within its $\pm 5\%$. The height of the shell is recommended as $1/6$ th of its diameter. Failure of pilot model was due to the absence of ring beam, conventional beam failed by punching through and for the bio-mimicked shell, it failed at very small load by flattened out. From the pilot experiment and analysis, ring beam has been considered for the conventional and bio-mimicked shell in scaled model. From the flexure test of ferrocement slab, modulus of elasticity was calculated as $35,164.8 \text{ N/mm}^2$.

When comparing the scaled models, the load versus deflection of bio-mimicked shell is lower than the conventional dome by 30%. The specific stiffness of conventional shell is 0.8 and 0.7 for the bio-mimicked shell. Thus, it is also lighter than conventional shell. After increasing the scaled bio-mimicked flower shell thickness 1.5 times, the stiffness is increased in the bio-mimicked shell than the scaled conventional shell model. In the experimental graph, the stiffness of the both the shells is similar till 4 mm deflection, but the ultimate load of bio-mimicked shell is less than the conventional shell due to the localized failure during testing. The stiffness of ferrocement bio-mimicked shell is found to be more than the conventional shell by 5%.

10 Declaration of Interest

The authors declare that they have not known competing financial interests or personal ties that could have influenced the research presented in this study.

References

1. Prabhavati P, Vankudre SB, Melinamani SD (2014) Optimization of RCC dome using genetic algorithm. *Int J Sci Technol* 2(7):54
2. Sharma S, Sarkar P (2019) Bio-mimicry: exploring research, challenges, gaps, and tools. *Smart Innov Syst Technol* 134:87–97
3. Saltik E, Alacam S (2020) Experiments for design and optimization of thin shell structures
4. Wani SB (2020) Analytical study on the influence of rib beams on the stability of RCC dome structures. *Int J Innov Technol Interdisc Sci* 3(3):480–489
5. Gohnert M, Bradley R (2022) Membrane stress equations for a catenary dome with a variation in wall thickness. *Eng Struct* 253:113793

Composite Behavioural Study on GI Wire Mesh and PVA Fibre Reinforced Concrete Slabs



S. Govindasami and S. Inthumathi

1 Introduction

The globe is functioning with natural systems, and the world is engaged with numerous of activities with infrastructural facilities. So, the mankind is in need of construction materials, and steel is playing a major role on providing infrastructural facilities. This research is focussing towards reducing the quantity of steel by introducing the fibres in concrete for reducing the brittleness of concrete as a sustainable construction technology based on the following investigations which were carried out on introducing PVA fibre in concrete as reinforcement. Researchers investigated the mechanical properties of composites with polyvinyl alcohol fibre [1], behaviour of beams with polyvinyl alcohol [2], performance of polypropylene and ferro-fibre slabs [3], properties of polypropylene concrete [4], characters of polyvinyl alcohol fibre pervious concrete [5], effect of recycled fibre on mechanical properties of concrete [6], behaviour of polypropylene concrete slabs [7], polyvinyl alcohol fibre concrete with slag powder and fly ash [8], flexural properties of polyvinyl alcohol fibre concrete [9], durability of polyvinyl alcohol fibre concrete [10], ductility index [11] and mechanical properties of polyvinyl alcohol fibre [12]. So, this research was aimed to introduce wire mesh in polyvinyl alcohol fibre concrete slabs and to determine the energy absorption capacity of such slabs.

S. Govindasami (✉)

Civil Engineering, Vel Tech High Tech Dr. Rangarajan Dr. Sakunthala Engineering College (Autonomous), Avadi, Chennai 600062, India
e-mail: drsgovindasami@gmail.com

S. Inthumathi

M.E Structural Engineering, Vel Tech High Tech Dr. Rangarajan Dr. Sakunthala Engineering College (Autonomous), Avadi, Chennai 600062, India

2 Materials and Methodology

The slab specimens were casted as circular and square of size 300 mm diameter and 25 mm thickness and 300 mm × 300 mm × 25 mm with polyvinyl alcohol fibre, cement. The specimen slabs of M30 concrete were casted with two layers (2L) of mesh and 0.5% PVA fibre, 2L-PVA 1.0%, 2L-PVA 1.5% and 2L-PVA 2.0% in terms of volume fraction. In addition to the slab, specimens were casted as square cylinder and prism to determine the compressive and split tensile strength of concrete.

3 Results and Discussions

Experiments were carried out to determine the compressive strength, split tensile strength and flexural strength. Impact strength and energy absorption capacity were determined. All tests were conducted for various percentages of PVA, and the results are presented in Tables 1, 2, 3, 4, 5, 6, 7 and 8.

Table 1 reveals that there is a slight increase (1.3%) in the compressive strength by adding 0.5% of PVA. But there was no percentage of increase of compressive strength while increasing the PVA from 0.5 to 2.0%.

Table 1 Compressive strength of PVA concrete at 28 days

S. No	Composition	Compressive strength (N/mm ²)	Percentage of increase with conventional concrete	Percentage of decrease with conventional concrete
1	CS PVA 0%	37.5	–	–
2	PVA 0.5%	38	1.3	–
3	PVA 1.0%	30	–	20
4	PVA 1.5%	29.33	–	21.7
5	PVA 2.0%	22.66	–	39.5

Table 2 Split tensile strength of PVA concrete at 28 days

S. No	Composition	Split tensile strength (N/mm ²)	Percentage of increase with conventional concrete	Percentage of decrease with conventional concrete
1	CS PVA 0%	4.244	–	–
2	PVA 0.5%	4.566	7.58	–
3	PVA 1.0%	3.395	–	20
4	PVA 1.5%	3.183	–	25
5	PVA 2.0%	3.501	–	17.5

Table 3 Flexural strength of PVA concrete at 28 days

S. No	Composition	Split tensile strength (N/mm ²)	Percentage of increase with conventional concrete	Percentage of decrease with conventional concrete
1	CS PVA 0%	5.121	–	–
2	PVA 0.5%	6.315	23.3	–
3	PVA 1.0%	6.416	25.3	–
4	PVA 1.5%	6.895	34.6	–
5	PVA 2.0%	5.771	12.7	–

Table 4 Impact strength on PVA concrete square slab without mesh at 28 days

Composition	First crack (N ₁)	Ultimate failure (N ₂)	Energy absorption at first crack (J)	Impact strength effectiveness ratio (ISER)	Energy absorption at ultimate failure (J)	Impact strength effectiveness ratio (ISER)
CS PVA 0%	2	3	11.772	–	17.658	–
PVA 0.5	3	6	17.658	1.5	35.316	2.0
PVA 1.0	4	7	23.544	2.0	41.202	2.33
PVA 1.5	5	7	29.43	2.5	41.202	2.33
PVA 2.0	6	8	35.316	3.0	47.088	2.66

Table 5 Impact strength on PVA concrete square slab with mesh at 28 days

Composition	First crack (N ₁)	Ultimate failure (N ₂)	Energy absorption at first crack (J)	Impact strength effectiveness ratio (ISER)	Energy absorption at ultimate failure (J)	Impact strength effectiveness ratio (ISER)
CS PVA 0%	2	67	11.772	–	394.29	–
PVA 0.5	5	75	29.43	2.5	441.45	1.11
PVA 1.0	8	97	47.088	4.0	570.942	1.44
PVA 1.5	10	101	58.86	5.0	594.486	1.50
PVA 2.0	12	104	70.632	6.0	612.144	1.55

Table 6 Impact strength on PVA concrete circular slab with mesh at 28 days

Composition	First crack (N ₁)	Ultimate failure (N ₂)	Energy absorption at first crack (J)	Impact strength effectiveness ratio (ISER)	Energy absorption at ultimate failure (J)	Impact strength effectiveness ratio (ISER)
CS PVA 0%	3	52	17.658	–	306.072	–
PVA 0.5	4	61	23.544	1.33	359.046	1.17
PVA 1.0	5	68	29.43	1.66	400.248	1.31
PVA 1.5	10	71	58.86	3.33	417.906	1.37
PVA 2.0	11	76	64.746	3.66	447.336	1.46

Table 7 Initial energy absorption on PVA concrete square and circular slab at first crack

Composition	PVA concrete Square slab without mesh (N)	PVA concrete Square slab with two-layer mesh (N)	PVA concrete Circular slab with two-layer mesh (N)
CS PVA 0%	11.772	11.772	17.658
PVA 0.5	17.658	29.43	23.544
PVA 1.0	23.544	47.088	29.43
PVA 1.5	29.43	58.86	58.86
PVA 2.0	35.316	70.632	64.746

Table 8 Initial energy absorption on PVA concrete square and circular slab at ultimate failure

Composition	PVA concrete Square slab without mesh (N)	PVA concrete Square slab with two-layer mesh (N)	PVA concrete Circular slab with two-layer mesh (N)
CS PVA 0%	35.316	394.29	306.072
PVA 0.5	35.316	441.45	359.046
PVA 1.0	41.202	570.942	400.248
PVA 1.5	41.202	594.486	417.906
PVA 2.0	47.088	612.144	447.336

It is observed from the Table 2 that there is a slight increase (7.58%) in the split tensile strength by adding 0.5% of PVA. But there was no percentage of increase of split tensile strength while increasing the PVA from 0.5 to 2.0%. Similar results were obtained by the researchers on their investigations [9, 10].

The flexural strength of PVA concrete is presented in Table 3, and the results shows that the flexural strength is increased from 23.3 to 34.6% for the PVA percentages from 0.5 to 2.0%.

The results of impact strength on PVA concrete square slab without mesh at 28 days are presented in Table 4. It is learnt from the results that the impact strength effectiveness ratio [ISER] is increased from 2.0 to 2.66 for the PVA percentages from 0.5 to 2.0%.

The results of impact strength on PVA concrete square slab with mesh at 28 days are presented in Table 5. It is learnt from the results that the impact strength effectiveness ratio [ISER] is increased from 1.11 to 1.55 for the PVA percentages from 0.5 to 2.0%.

The results of impact strength on PVA concrete circular slab with mesh at 28 days are presented in Table 6. It is learnt from the results that the impact strength effectiveness ratio [ISER] is increased from 1.17 to 1.46 for the PVA percentages from 0.5 to 2.0%.

It is learnt from Table 7 that the initial energy absorption on PVA concrete square slab at first crack is increased from 29.43 to 70.632 N for the PVA percentages from 0.5 to 2.0%.

It is observed from Table 8 that the initial energy absorption on PVA concrete square slab at ultimate failure is increased from 441.45 to 612.144 N for the PVA percentages from 0.5 to 2.0%.

4 Conclusions

There was no percentage of increase of compressive strength and split tensile strength of composite concrete while increasing the PVA from 0.5 to 2.0%. Flexural strength composite concrete increased from 23.3 to 34.6% for the PVA percentages from 0.5 to 2.0%. Impact strength effectiveness ratio [ISER] of composite square slab increased from 2.0 to 2.66 for the PVA percentages from 0.5 to 2.0% without mesh. Impact strength effectiveness ratio [ISER] of composite square slab increased from 1.11 to 1.55 for the PVA percentages from 0.5 to 2.0% with mesh. Impact strength effectiveness ratio [ISER] of composite circular slab increased from 1.17 to 1.46 for the PVA percentages from 0.5 to 2.0% with mesh. Initial energy absorption on PVA concrete square slab with two-layer mesh at first crack increased from 29.43 to 70.632 N for the PVA percentages from 0.5 to 2.0%. Initial energy absorption on PVA concrete square slab with two-layer mesh at ultimate failure increased from 441.45 to 612.144 N for the PVA percentages from 0.5 to 2.0%. It is concluded that the ductile behaviour of concrete is increased by PVA and enhanced the energy absorption capacity of concrete.

References

1. Zhang P, Zhang P, Wu J, Zhang Y, Guo J (2022) Mechanical properties of polyvinyl alcohol fiber-reinforced cementitious composites after high-temperature exposure. *Gels* 8(10):662–679
2. Du W, Yang C, De Backer H, Wang C, Pan Y (2022) Investigation of the flexural behavior of reinforced concrete beams strengthened with a composite reinforcement layer: polyvinyl alcohol fiber-reinforced ferrocement cementitious composite and steel wire mesh. *Struct Concr* 1–15. <https://doi.org/10.1002/suco.202100894>
3. Saeed HZ, Saleem MZ, Chua YS, Vatin NI (2022) Research on structural performance of hybrid ferro fiber reinforced concrete slabs. *Materials* 15(19):6748. <https://doi.org/10.3390/ma15196748>
4. Amran M, Lesovik V, Tolstoy A, Fediuk R, Rusinov R, Rusinova N, Qader DN, Mohammed K, Rashid RSM (2022) Properties and performance of polypropylene fibered high-strength concrete with an improved composite binders. *Case Stud Constr Mater* 17:e01621
5. Feng L, Xia Y, Xu F (2022) Characterization of PVA fibre reinforced pervious concrete with blended recycled ceramic aggregates and natural aggregate. *Adv Mater Sci Eng.* <https://doi.org/10.1155/2022/4375043>
6. Balea A, Fuente E, Monte MC, Blanco A, Negro C (2021) Recycled fibers for sustainable hybrid fiber cement based material: a review. *Materials (Basel)* 14(9):2408. <https://doi.org/10.3390/ma14092408>
7. Sadowska-Buraczewska B, Szafranec M, Barnat-Hunek D, Łagód G (2020) Flexural behavior of composite concrete slabs made with steel and polypropylene fibers reinforced concrete in the compression zone. *Materials* 13(16). <https://doi.org/10.3390/ma13163616>

8. Liu FY, Ding WQ, Qiao Y (2020) Experimental investigation on the tensile behavior of hybrid steel-PVA fiber reinforced concrete containing fly ash and slag powder. *Constr Build Mater* 241(3):118000. <https://doi.org/10.1016/j.conbuildmat>
9. Arulmurugan P (2018) Evaluation of FRC beams using steel and PVA fibres in concrete. *Int J Adv Res Innov* 6(4):121–124
10. Devi M, Kannan L, Ganeshkumar, Venkatachalam TS (2018) Durability studies on polyvinyl alcohol fibre reinforced concrete. *Int J Eng Res Technol* 7(2):94–98
11. Devi M, Kannan L, Ganeshkumar M, Venkatachalam TS (2017) Flexural behaviour of polyvinyl alcohol fibre reinforced concrete. *SSRG Int J Civil Eng* 4(6):27–30
12. Noushini A, Samali B, Vessalas K (2013) Effect of polyvinyl alcohol (PVA) fibre on dynamic and material properties of fibre reinforced concrete. *Constr Build Mater* 49:374–383

Review on Partially Replacement of Cement with Industrial Waste in Manufacturing of Concrete and Bricks



R. Akash Nevel, R. Dinesh Kumar, and M. Surendar

1 Introduction

Cement is a commonly used building material that is essential for constructing durable and long-lasting structures. It is a fine powder made by heating a mixture of limestone, clay and other minerals in a kiln at high temperatures. Cement is primarily used as a binding agent in concrete, mortar, and stucco. Cement is the most important ingredient in the field of construction, starting from foundation to plastering of the buildings. Due to this, the production of cement reached up to 4.2 billion tonnes in the year 2020. This leads to increase in the release of greenhouse gases and environmental pollution; greenhouse gases such as nitrogen oxide causes various health problems, while sulphur dioxide is the major reason for acid rain and carbon monoxide can cause harmful health effects by reducing oxygen supply to the various organs and tissues. Reduction of the manufacturing and usage of cement will help in controlling the pollution on a large scale. While exploitation of river sand is also one of the major environment affecting act, an alternative material needs to be brought into use in the construction field. Blocks which have both cement and sand as the major parts of it, replaced of the material can help in reduce the environmental effect and cost of the manufacture of the blocks by 30–60%. Ground granulated blast furnace slag, a cementitious material that is a by-product of the iron-making blast furnaces, is mostly utilised in concrete. Blast furnace slag's primary constituents are CaO (30–50%), SiO₂ (28–38%), Al₂O₃ (8–24%), and MgO (1–18%). Up to respective values of 10–12% and 14%, the MgO and Al₂O₃ concentration exhibit the similar pattern, and after such values no further advancement is possible. The manufacturing of high slag blast furnace cement and Portland blast furnace cement both of which have GGBS contents that typically range from 30 to 70%, as well as the creation of ready mixed or site batched durable concrete, are two important uses

R. Akash Nevel · R. Dinesh Kumar (✉) · M. Surendar
Department of Civil Engineering, Easwari Engineering College (Autonomous), Chennai, India
e-mail: dineshkumar.r@eec.srmrmp.edu.in

of GGBS. It is commonly used as a pozzolan to make hydraulic cement or hydraulic plaster as well as to fully or partly replace Portland cement in the creation of concrete, with about 43% of it being recycled. Concrete and plaster are strengthened against moisture and chemical assault by pozzolans, which also ensure that the two materials set. When coal used in power plants is burned, a heterogeneous by-product called fly ash is created. It is a fine, glassy powder with a grey colour that rises with the exhaust gases. Fly ash contains pozzolanic elements, which when combined with lime, produce cementitious materials. The usage of fly ash is in concrete, mining, landfills, and dams [15, 17]. RHA is a by-product of the milling of rice. Its usage as a soil stabiliser is an environmentally advantageous substitute for final disposal. RHA is not naturally cementitious, cements must be created by adding a hydraulic binder, such as lime, to the RHA in order to reinforce the soil. An active pozzolana with numerous uses in the cement and concrete industries is rice husk ash. RHA is less expensive because it reduces the amount of cement required and lowers the total cost of making concrete. Reduced cement requirements lead to decreased cement plant pollution, which benefits the climate and the economy. They also provide a useful way to get rid of this farming waste product, which has few other applications.

2 Literature Review

A literature review is an evaluation report of information found in earlier literature which related to my project study. This chapter is explained briefly about the various literatures contained of the study of industrial waste materials and its physical and chemical properties.

Muleya et al. [8] made experimental study on RHA, which is used to make cement in small amounts, was used to test the integrity of concrete made in Zambia. The main objective was to evaluate the costs and benefits of using RHA in concrete. RHA was utilised in ratios of 10, 20, and 30% to replace cement in some places. The 20% cement replacement mix at a 0.5 water/binder ratio resulted in the optimal concrete strength 18 MPa. This resulted in a 12.5% decrease in the price of concrete, which is especially important for bigger concrete volumes.

Divahar et al. [3] made experimental examination on the compressive strength and physical characteristics of clay with GGBS brick is described in detail. Six various brick ratios, including 0, 5, 10, 15, 20, 25, and 30%, were examined. According to the findings, 5% of lime was continuously added to promote stability, and 5% of GGBS was increased and added in varied ratios. 20% of the entire amount of clay is now only used. The bricks are made using a straightforward manufacturing process that doesn't include any additional equipment, plant, or machinery for autoclaving or fire. Consequently, compared to ordinary burnt clay bricks and calcium silicate bricks, the energy consumption will be significantly lower.

Vijaya et al. [13] evaluated that the potential effects of mineral admixtures on the compressive and flexural properties of cements including silica smoulder, fly ash, and rice husk ash. The current project uses concrete of M60 grade with a midway

substitution made of fly debris, rice husk debris, and silica seethe (FA + RHA + SF = 30%) for three different proportions: 18:5:5, 18:6:6, 16:7:7. For M60 grade concrete, for blend construction, the actual water concrete percentage is 0.29 for a 50–75 mm droop. Increased pozzolanic action to stop concrete corrosion in coastal locations is an advantage of utilising FA, RHA, and SF.

Seevaratnam et al. [7] used earth cement blocks with RHA as a partial cement substitute are the subject of an experimental research in this work. RHA may only substitute 0–20% of the maximum binder in a cement block. For mechanical qualities, the investigations on earth cement blocks look at flexural tensile strength and compressive strength; for durability, they look at water absorption, sorption rate, and erosion against water spray. Up to 10% RHA content, a considerable improvement in the compressive and flexural tensile strength of earth cement blocks was noted due to the high SiO₂ content and strong reactivity of RHA. However, when the percentage of RHA replacement increases, the durability of earth cement blocks degrades, although only to a certain extent.

Phul et al. [11] describe about the compressive strength characteristics of concrete made with fly ash and GGBS in place of some of the cement. As a result of the use of waste materials as a cement substitute, the construction industry's greater demand for cement raises concerns about environmental deterioration. Using fly ash and GGBS. For various curing days, the optimal level of GGBS and fly ash was evaluated using different percentages ranging from 0 to 30%. When the compressive strength increased by 26.30% at 30% replacement compared to 0% control, and the slump value hit 30% compared to SF0, the workability of the substituted concrete improved. Results revealed that the addition increases the workability and compressive strength, which ultimately improves the mechanical properties of GGBS and fly ash.

Kumutha et al. [1] study involves the use of fly ash, GGBS, and manufactured sand (M-sand) to create bricks. Fly ash, GGBS, and cement are the main ingredients in the binder, which is used in a 1:2 mix ratio to create bricks. The test findings show that mix M1, which contains 75% fly ash, 15% GGBS, and 10% PPC, has a greater average compressive strength and minimum water absorption of 13.08%.

Manjunatha et al. [2] replaced a portion of the cement by GGBS up to 45%, this experiment aims to better understand the mechanical and fresh property strengths of concrete specimens, including compressive strength. Four different proportions of concrete mix-NC, Mix 1–15%, Mix 2–30%, and Mix 3–45% with and without GGBS were created. Our findings indicate that, for M35 and M40 grade concrete, a partial replacement of cement to GGBS up to 45% increased the degree of workability of the concrete.

Yogendra et al. [5] used concrete made with OPC and GGBS in various amounts ranging from 0 to 40% and looked at the compressive and flexural strength of the material. Compressive and flexural strength for 90 days of curing are only slightly reduced by 4% and 6%, respectively, when OPC is replaced by GGBS up to 20%.

Hossain et al. [10] included RHA with silicate, which is a component of pozzolanic materials. In an effort to substitute bricks and concrete, this RHA has been tried in place of cement. A standardised presentation of the experimental findings on bricks and concrete was made. The control specimen, or specimen without any RHA, was

used as the basis for normalisation. Concrete loses both compressive and cracking tensile strengths when RHA is added. Additionally, it has been discovered that adding RHA to brick does not modify the shape or size of the brick, keeping the volume constant. However, adding RHA to brick reduces its crushing capabilities and increases its water absorption.

Oyetola et al. [9] validated the suitability of the constituent materials for constructing hollow sandcrete blocks made of OPC and RHA, preliminary examination of the materials was done. The freshly made blend was also put to a physical test. For 1, 3, 7, 14, 21, and 28 days, hollow sandcrete blocks of 150 mm by 450 mm were cast, cured, and crushed at replacement levels of 0, 10, 20, 30, 40, and 50%. According to test results, the majority of the commercial sandcrete blocks in Minna town are subpar. The OPC/RHA sandcrete blocks' compressive strength improves with age at curing and declines as the amount of RHA material rises. 20% was determined to be the ideal replacement amount by the study.

Summary of Literature Review

From the study of various literature review it is summarised as follows:

- Fly ash and GGBS can be replaced up to 30% with the cement, where its compressive strength will be increased.
- RHA can be used as a replacement of cement 10–20%. Using RHA, the water absorption will be increased.
- The amount of cement that is used in the cement block can be reduced up to 50% by adding fly ash, GGBS, and RHA at the correct ratio.

3 Material Properties

Cement—Cement is a fine powder that is widely used in the construction industry due to its excellent binding properties. Its physical properties, including fineness, colour, setting time, strength, density, heat of hydration, soundness, and consistency, affect its performance and suitability for various applications. The particle size of cement affects its workability and setting time, while its colour can vary due to the addition of pigments. The setting time of cement determines how quickly it hardens after being mixed with water, and its compressive strength is crucial for load-bearing structures. IS code refers to the Indian Standards code, which provides specifications and guidelines for the use of cement in construction in India. The Indian Standard code for cement is IS 269:2015, which provides specifications for different types of cement, including ordinary Portland cement, Portland pozzolana cement, rapid hardening Portland cement, and low heat Portland cement. The generalised physical properties of cement are provided in Table 1 by referencing to the journal papers.

Fly Ash—Fly ash is a fine, powdery material that is a by-product of burning pulverised coal in electric power generating plants. It is composed primarily of silica, alumina, and iron with small amounts of calcium, magnesium, and other

Table 1 Physical properties of cement

Physical properties	Cement	Fly ash	GGBS	RHA
Fineness	< 90 micron	10–100 micron	20–250 micron	5–15 micron
Bulk density (kg/m ³)	1440	800	1200	150
Colour	Grey	Dark grey	Off-white	Greyish black
Specific gravity	3.15	2.52	2.9	2.15

metals. Fly ash is classified as a pozzolanic material because it contains reactive silica and alumina compounds that react with calcium hydroxide in the presence of water to form cementitious compounds. When added to concrete, fly ash improves its strength, durability, and workability [12, 14]. It also reduces the amount of cement needed, which results in cost savings and a lower carbon footprint [16].

GGBS—GGBS is a pozzolanic material that reacts with calcium hydroxide in the presence of water to form cementitious compounds, similar to fly ash. GGBS is a sustainable material because it reduces the amount of waste generated by the steelmaking industry and reduces the carbon footprint of concrete production [4]. In addition, it has a lower embodied energy than Portland cement, which means that it requires less energy to produce.

Rice Husk Ash—Rice husk is a major agricultural waste product in many countries, and its disposal can create environmental problems. However, when burned at high temperatures, rice husk produces a fine, powdery ash that has a range of useful properties. RHA contains high levels of amorphous silica, which makes it a valuable material for use in various industries [6]. For example, it can be used as a partial replacement for cement in concrete to improve its strength, durability, and workability. RHA can also be used as a source of silica in the production of high-grade glass, ceramics, and refractory materials.

The chemical components of cement, GGBS, fly ash, and rice husk ash are given in Table 2.

4 Compressive Strength

Table 3 shows the compressive strength of GGBS, fly ash, and RHA with replacement for different proportions.

The values were obtained by varying the percentage of the GGBS in the concrete. From Fig. 1 it can be inferred that 20% replacement of GGBS attained high compressive strength.

The values were obtained by varying the percentage of the fly ash in the concrete. From Fig. 2 it can be inferred that 20% replacement of GGBS attained high compressive strength.

Table 2 Chemical components

Chemical component	Cement	GGBS	Fly ash	Rice husk ash
Calcium oxide (CaO)	64.97	40	3.58	0.87
Silica (SiO ₂)	19.71	30.3	59.94	88.32
Ferric oxide (Fe ₂ O ₃)	3.26	10.2	4.67	0.671
Alumina (Al ₂ O ₃)	4.52	9.2	22.87	0.56
Sulphuric anhydride (SO ₃)	2.44	1.5	0.35	
Magnesium oxide (MgO)	1.71	6.2	1.55	0.84
Sodium oxide (Na ₂ O)	0.42	0.8	0.62	0.12
Potassium oxide (K ₂ O)	0.54	0.4	2.19	2.91
(TiO ₂)	0.13	0.8	0.94	–
(P ₂ O ₅)	0.8	0.1	–	–
(MnO)	–	0.5	–	–
LOI	1.50	–	3.34	5.81

Table 3 Compressive Strength of GGBS

Replacement material	% Replacement	Day-7	Day-14	Day-28
GGBS	0	21.25	28.5	31.5
	10	28.15	30.3	31.5
	20	31.1	33.5	35.1
	30	23	26.32	28.4
Fly ash	0	19.5	23	26
	10	20	24.4	28
	20	22.6	28.2	33
	30	21	25.9	29
RHA	0	16.5	21	26
	5	17.3	22	27
	10	18	23.5	29
	15	15	22.5	27
	20	10.5	18	23

The values were obtained by varying the percentage of the RHA in the concrete. From Fig. 3 it can be inferred that 10% replacement of RHA attained high compressive strength.

The values were obtained by varying the percentage of the fly ash, GGBS, and RHA in the concrete. From the above graph it can be inferred that 20% replacement of GGBS, 25% replacement of fly ash and 15% replacement of RHA attained high compressive strength (Fig. 4).

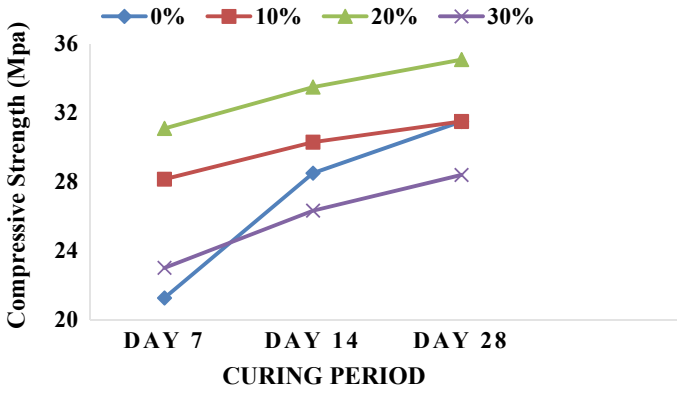


Fig. 1 Compressive strength for GGBS

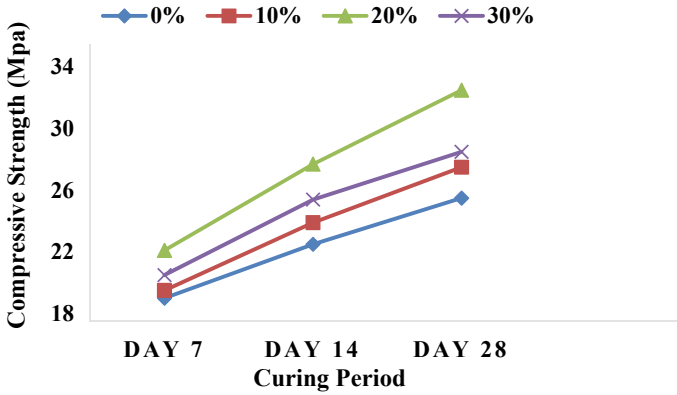


Fig. 2 Compressive strength for fly ash

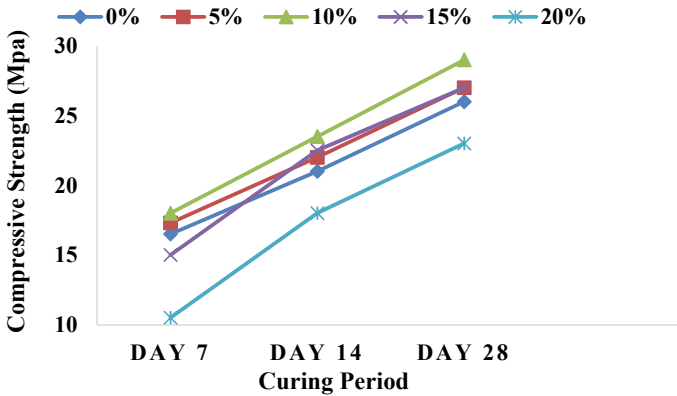


Fig. 3 Compressive strength for RHA

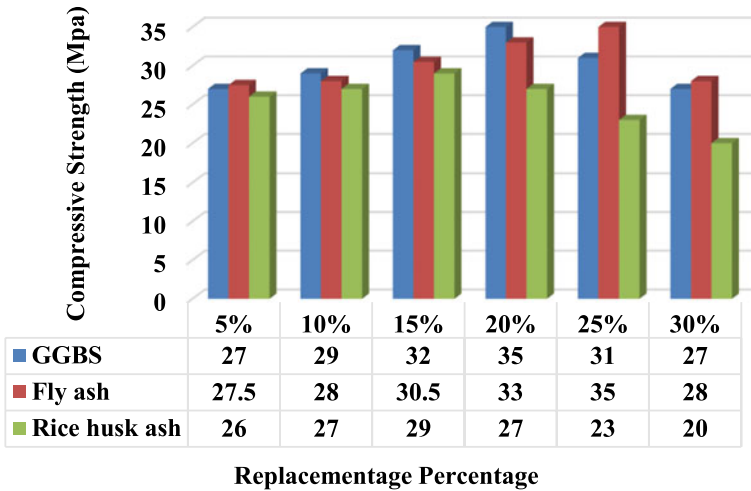


Fig. 4 Compressive strength comparison between fly ash, GGBS, and RHA

5 Conclusions

- The cost of GGBS is around 25–50% less than that of OPC, so replacing cement with it aids in lowering the cement content of concrete and lowering building costs.
- The current study demonstrates that using GGBS in place of traditional concrete can produce concrete with higher strengths. When 20% of the cement is replaced with GGBS.
- The earth cement blocks density was altered by the RHA replacement, rendering them lighter.
- The compressive and tensile strength of cement blocks significantly increased up to 10% RHA content due to the high SiO₂ content and strong reactivity of RHA.
- Fly ash and GGBS can be replaced up to 30% with the cement, where its compressive strength will be increased.
- RHA can be used as a replacement of cement 10–20%. Using RHA, the water absorption will be increased.
- The amount of cement is used in the cement block can be reduced up to 50% by adding fly ash, GGBS, and RHA at the correct ratio.

References

1. Kumutha R, Vijai K, Noor Nasifa S (2018) Experimental investigation on fly ash bricks incorporating M-Sand and GGBS. *Int J Constr Res Civil Eng* 4(2):1–6

2. Manjunatha M, Jeevan H (2015) Study of early age properties and behaviour of concrete with GGBS as partial replacement of cement. *Sci Technol Arts Res J* 4(4):148–155
3. Divahar R, Sangeetha SP (2020) Bricks manufacturing with partial replacement of clay with GGBS. *Int J Sci Technol Res* 9(2):6498–6501
4. Arya KC (2018) A comparative study of clay bricks with GGBS and laterite soil. *Int J Res Eng Appl Manage* 4(2):384–391 (2018)
5. Patil YO, Patil PN, Dwivedi AK (2013) GGBS as partial replacement of OPC in cement concrete—an experimental study. *Int J Sci Res* 2(11):189–191
6. Kishore R, Bhikshma V, Prakash PJ (2011) Study on strength characteristics of high strength rice husk ash concrete. *Procedia Eng* 14:2666–2672
7. Seevaratnam V, Uthayakumar D et al (2020) Influence of rice husk ash on characteristics of earth cement blocks. *Mater Res Soc* 1–13
8. Muleya F, Muwila N (2021) Partial replacement of cement with rice husk ash in concrete production: an exploratory cost-benefit analysis for low-income communities. *Eng Manage Prod Serv* 13(3):127–141
9. Oyetola EB, Abdullahi M (2006) The use of rice husk ash in low-cost sandcrete block production. *Leonardo Electron J Pract Technol* 58–70
10. Hossain T, Sarker Kumar S et al (2011) Utilization potential of rice husk ash as a construction material in rural areas. *J Civil Eng* 39(2):175–188
11. Phul AA, Memon MJ et al (2019) GGBS and fly ash effects on compressive strength by partial replacement of cement concrete. *Civil Eng J* 5(4):913–921
12. Herath C, Gunasekara C et al (2020) Performance of high volume fly ash concrete incorporating additives: a systematic literature review. *Constr Build Mater* 258:1–13
13. Vijaya SK, Jagadeeswari K, Srinivas K (2013) Behaviour of M60 grade concrete by partial replacement of cement with fly ash, rice husk ash and silica fume. *Mater Today Proc* 1–5
14. Krithika, Ramesh Kumar GB (2020) Influence of fly ash on concrete—a systematic review. *Mater Today Proc* 1–6
15. Shaw SK, Sil A (2020) Experimental study on cyclic loading characteristics of fly ash as partial replacement of cement in beam-column joint. In: *Case studies in construction materials*, vol 13, pp 1–19
16. Dinesh Kumar R, Ravichandran PT, Divya Krishnan K (2020) Use of quarry dust with recycled coarse aggregate in sustainable self compacting concrete. *J Green Eng* 10(4):1297–1311
17. Velraj Kumar G, Ajith J, Muthulakshmi S, Dinesh Kumar R, Nanthini Sri KV (2022) Characterization of carbon fibre reinforced polymers sheet bonded RC beam with end anchorage under static and cyclic response. *J Balkan Tribol Assoc* 28(4):522–536

Effect of Slope, Cross-Section of Pile and Eccentricity in Calculating the Modulus of Laterally Loaded Single Pile



S. V. Sivapriya

1 Introduction

As infrastructure development increases, the study of foundations gains a lot of attention. The type of foundation, whether it is a shallow or deep foundation is chosen in accordance with the super-structure and the prevailing soil–profile. When the load transmitted from the super-structure is more and the bearing obtained in the soil is at deeper depth—pile (deep) foundation is adopted. In case the structure faces a large lateral load, the analysis and design of the pile involves additional attention.

The study of a pile subjected to lateral load has seen its extent in understanding the nonlinear behaviour when placed at ground level with the maximum possible parameters such as length, diameter, soil profile, configuration of piles in a group and loading conditions [1–5]. As the cross-section, length, configuration of pile group increases, the capacity increases. The role of spacing and arrangement is dominant in a pile group subjected to lateral load [6]. The study is not only limited to a single layer; it is further extended to multiple layers. Salgado et al. proposed a decay function based on the deformation behaviour of pile [7] for calculating the displacement of single and group piles in layered soil.

The laterally loaded study was done experimentally and numerically, by considering wedge theory [8], gap theory [9] and p - y method [10]. The study of the laterally loaded pile in slope is gaining its attention from the research community recently. The lateral/horizontal load behaviour of the pile depends upon the properties of the soil, ground condition and pile material property [4]. The effect of the slope when the pile is placed in the embankment becomes negligible when it is kept beyond $2.5R$ (R —relative stiffness factor) in the embankment for cohesive soil [11], whereas in terms of diameter, the slope becomes insignificant as the pile is moved to a distance

S. V. Sivapriya (✉)

Department of Civil Engineering, Sri Sivasubramaniya Nadar College of Engineering,
Chennai 603110, India

e-mail: sivapriyavijay@gmail.com

Table 1 Soil properties

Soil type	Material property	Values
Clay	Unit weight (kN/m^3)	17.84
	Cohesive strength (kPa)	30
	Modulus (kPa)	8025
Sand	Relative density (%)	70
	Angle of internal friction ($^\circ$)	32
	Modulus (kPa) [16]	110,000

of 8D [12]. In sandy soil, the change in geometry of the slope becomes negligible when the pile moved beyond $15\text{--}20D$ (D —diameter) [13].

The soil–structure interaction properties like modulus and stiffness factor are not given much importance. Hence, this paper focuses on modulus calculation from load–deformation curve for the pile located at the crest position for positioned at the slope-crest of cohesive and cohesionless soil for a Ig model study conducted in the laboratory.

2 Soil Properties

In this study, two types of soil clayey from Siruseri [11, 14] and sandy soil [4] from Chennai, India, with their respective properties are considered. The basic and engineering properties of the soil considered are listed in Table 1. The parameters of the soil and soil–structure interaction properties were extracted from published literature by the author [4, 5, 11, 15].

3 Methodology

The clay soil is mixed with desired water content to attain desired shear strength to ensure the stability of the slope. The dry clay soil is mixed with water to achieve consistency and allowed to consolidate for more than 2 days before placing it in the tank. The soil is filled in the tank by kneading compaction technique layer by layer. The percentage of water present in the soil is checked frequently to ensure soils its consistency. The sand is filled in the tank to achieve a relative density of 70%. The formation of the slope in the tank is ensured. The parameters involved in this study are the slope angle and eccentricity for sandy soil and the effect of slope in clayey soil (Table 2).

Table 2 Parametric study

Type of soil	L/D ratio	Slope angle	Eccentricity
Sand	500/16	1V:1.5H (33.69°)	0
	500/16	1V:2H (26.56°)	0
	500/16	1V:2.5H (21.8°)	0
	300/25	1V:2H (26.56°)	0
	300/16	1V:2H (26.56°)	0
	300/12.5	1V:2H (26.56°)	0
	500/16	1V:2H (26.56°)	0.5 and 1T ^a
Clay	450/16	1V:2H (26.56°)	0
	450/16	1V:2.5H (21.8°)	0
	450/16	1V:3H (18.44°)	0

^a *T*—relative stiffness factor

3.1 Preparation of Sand Bed

The sand is filled in a tank of $1 \times 1 \times 0.5$ m depth of dimension with a relative density of 70% using the soil raining technique. The pile is placed in the slope-crest and loaded towards the slope. Using Matlock and Resse [17] formulae, the relative stiffness of the soil is found as 92 mm by maintaining the geometry of the ground as horizontal. Under eccentric loading conditions, the load is applied at a distance of 0.5 and 1*T* from the crest of the slope.

3.2 Preparation of Clay Bed

With clayey soil of 30 kPa as its cohesive strength is filled in the tank, and the unit weight of 17.84 kN/m^3 is obtained by kneading compaction technique.

The tank used in the experiments had one side as transparent which is to ensure the formation of the slope. The modulus is found as the initial slope of the lateral load–displacement behaviour of a laterally loaded pile [18] as shown in Fig. 1.

4 Results and Discussion

4.1 Influence of Slope

As the geometry of the slope goes steeper, the lateral capacity borne by the pile decreases which is due to the reduction in passive wedge area. This leads to a decrease in modulus value too (Fig. 2a). The modulus for horizontal ground terrain with the

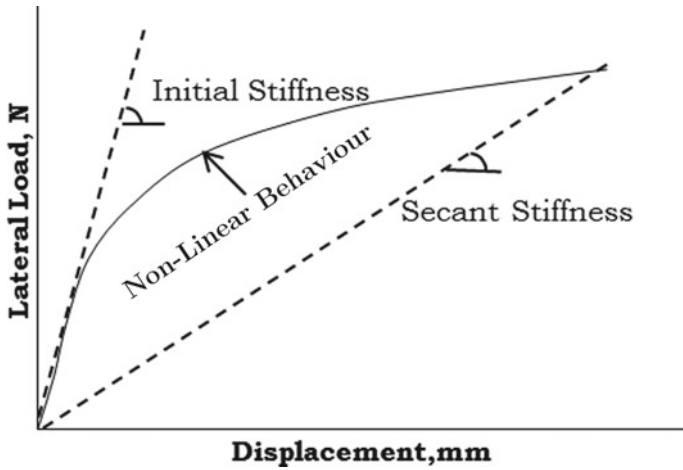


Fig. 1 Representation of stiffness behaviour

same L/D ratio and soil properties is 40.5 N/mm. The modulus reduces by 69.14, 58.84 and 35.01% for the slope angle 33.7° , 26.57° and 21.8° respectively in a sandy soil slope.

In a clayey slope, the load-bearing capacity is more for a stable slope; there is a huge variation in the change in the modulus value. As the slope-angle changes from 1V:3H to 1V:2H, the reduction in capacity from 40.4 to 74.29% compared to the horizontal ground (Fig. 2b).

This is mainly due to passive wedge formation. In sandy soil, there is a reduction in the formation of a passive wedge marking an angle of $45 - \phi/2$ and an active wedge of $45 + \phi/2$. Whereas in a clayey slope, the active and passive wedge formation remains the same due to the absence of friction. Moreover, the passive wedge formation is

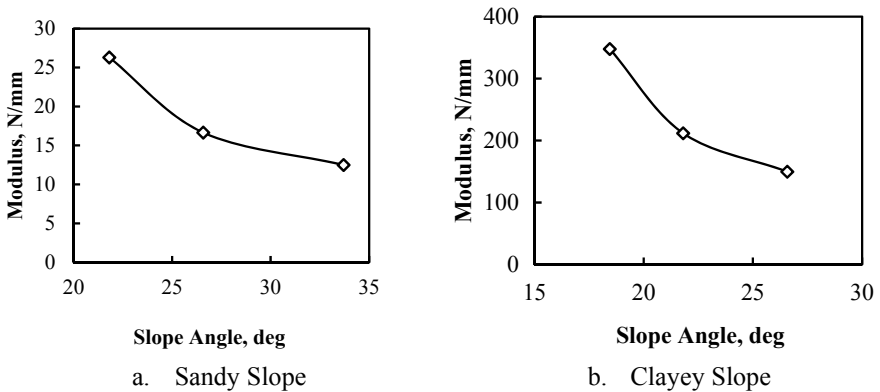
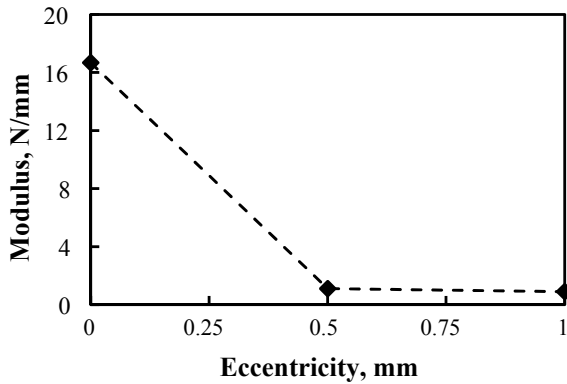


Fig. 2 Influence of slope angle

Fig. 3 Influence of eccentricity



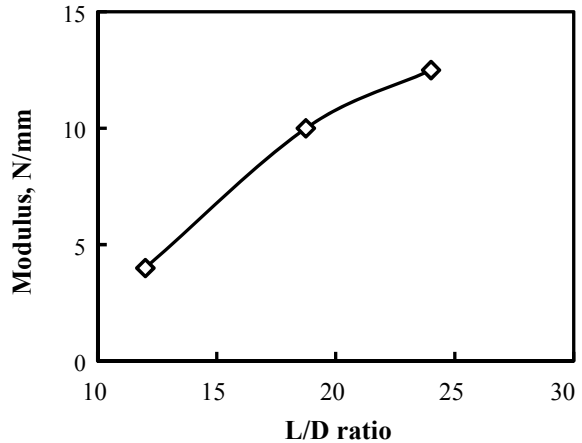
more for clayey slope for the same slope angle. This makes a stable-clayey slope bears' more lateral load. From the figures, it is understood that the cohesive soil has more modulus than that of cohesionless soil.

4.2 Influence of Eccentricity

The length of eccentricity defines here the free length above the slope-crest where the load is applied. The depth of embedment has major role in load-bearing capacity of the pile subjected to lateral load; as the embedded depth increases the capacity increases. The reduction in lateral capacity also reduces the modulus. From Fig. 3, we can see the sudden drop in the modulus; this is mainly due to the influence of the embedded depth of the pile [19]. When the free length increases with the total depth of the pile, the rigidity of the pile decreases and the soil–structure interaction reduces. This provokes a reduction in modulus. With the initial reduction in modulus because of the increase in free length, it starts decreasing and becomes almost linear. This also indicates that when the flexibility of pile, the module increases, but when it shifts to the behaviour of rigid the modulus reduces. As the passive resistance remains constant, the modulus behaviour of the pile almost remains linear. The effect of eccentricity is studied only for sandy/cohesionless soil.

4.3 Influence of L/D Ratio

By keeping the total length of the pile constant at 300 mm, the diameter is varied as 12.5, 16 and 25 mm making it a long, intermediate and short pile respectively for cohesionless soil. As there is an increase in length (L)/diameter (D), the modulus increases, as it majorly depends upon the length of the pile (Fig. 4).

Fig. 4 Influence of L/D ratio

With the change in behaviour of pile from short to intermediate, the modulus increases by 1.5 times; as the behaviour then shifted to long, the modulus value increases to 2.13 times. The increase in modulus is due to the fact that the pile transferred its behaviour of short rigid to long flexible behaviour [20]. It is also understood the head condition, i.e. free-head condition didn't have a restrained condition [21].

5 Conclusion

The soil–pile interaction study of a pile subjected to lateral load in the sloping ground with varied L/D ratio, slope angle, free-length and soil type are as follows:

1. The modulus of the cohesive soil is more than the cohesionless soil. As the slope angle increases, the modulus decreases for the condition of slope remains constant.
2. With an increase in the free length of the pile head with the same length of pile, the lateral load capacity decreases leading to a decrease in the modulus of the pile.
3. The increase in L/D ratio increases the capacity, and the modulus increases with the same slope angle.

From the experimental data, it is observed that the main factor influencing the modulus of the pile is the soil type and the geometry of the pile.




References

1. Haldar A, Yenumula VSNP, Chari TR (2000) Full-scale field tests on directly embedded steel pole foundations, pp 414–437
2. Thompson MJ, White DJ (2005) Lateral load tests on small-diameter piles for slope remediation (2005)
3. Rajagopal K, Karthigeyan S (2008) Influence of combined vertical and lateral loading on the lateral response of piles. In: 12th international conference on computer methods and advances in geomechanics, vol 5, pp 3272–3282
4. Sivapriya SV, Balamurukan R, Jai Vigneshwar A, Prathibha Devi N, Shrinidhi A (2019) Eccentricity effect in sandy slope of laterally loaded single pile. *Civ Environ Eng* 15(2):92–100
5. Sivapriya SV, Ramanathan R (2019) Load–displacement behaviour of a pile on a sloping ground for various L/D ratios. *Slovak J Civ Eng* 27(1):1–6. <https://doi.org/10.2478/sjce-2019-0001>
6. Rao N, Ramakrishna VGST, Babu Rao M (1998) Influence of rigidity on laterally loaded pile groups in marine clay. *J Geotech Geoenviron Eng* 124(6):542–549
7. Salgado R, Tehrani FS, Prezzi M (2014) Analysis of laterally loaded pile groups in multilayered elastic soil. *Comput Geotech* 62:136–153. <https://doi.org/10.1016/j.compgeo.2014.07.005>
8. Kim Y, Jeong S, Lee S, Asce M, Lee S (2011) Wedge failure analysis of soil resistance on laterally loaded piles in clay. *J Geotech Geoenviron Eng* 137(7):678–694. [https://doi.org/10.1061/\(ASCE\)GT.1943-5606.0000481](https://doi.org/10.1061/(ASCE)GT.1943-5606.0000481)
9. Brown DA, Shie CF (1990) Three dimensional finite element model of laterally loaded piles. *Comput Geotech* 10(1):59–79. [https://doi.org/10.1016/0266-352X\(90\)90008-J](https://doi.org/10.1016/0266-352X(90)90008-J)
10. Mahanta R, Ghanekar RK (1970) Influence of API p-y procedures on design of offshore piles in clay lateral loading on long offshore piles, pp 1–9
11. Sivapriya SV, Gandhi SR (2019) Soil–structure interaction of pile in a sloping ground under different loading conditions. *Geotech Geol Eng* 37(6):1–10. <https://doi.org/10.1007/s10706-019-01080-z>
12. Nimityongskul N, Kawamata Y, Rayamajhi D, Ashford SA (2018) Full-scale tests on effects of slope on lateral capacity of piles installed in cohesive soils. *J Geotech Geoenviron Eng* 144(1):04017103. [https://doi.org/10.1061/\(asce\)gt.1943-5606.0001805](https://doi.org/10.1061/(asce)gt.1943-5606.0001805)
13. Muthukkumaran K (2014) Effect of slope and loading direction on laterally loaded piles in cohesionless soil. *Int J Geomech* 14(1):1–7. [https://doi.org/10.1061/\(ASCE\)GM.1943-5622.0000293](https://doi.org/10.1061/(ASCE)GM.1943-5622.0000293)
14. Sivapriya SV, Gandhi SR (2013) Experimental and numerical study on pile behaviour under lateral load in clayey slope. *Indian Geotech J* 43(1):105–114. <https://doi.org/10.1007/s40098-012-0037-z>
15. Sivapriya SV, Muttharam M (2018) Behaviour of cyclic laterally loaded pile group in soft clay. *Indian Geotech J*. <https://doi.org/10.1007/s40098-018-0328-0>
16. Bowles JE (1997) *Foundation analysis and design*. The McGraw-Hill Companies Inc., Singapore
17. Reese LC, Matlock H (1956) Non-dimensional solutions for laterally loaded piles with soil modulus proportional to depth. In: *Proceedings of the 8th Texas conference on soil mechanics and foundation engineering*, pp 1–41
18. Poulos BHG, Asce F (2006) Analysis of residual stress effects in piles. *J Geotech Eng* 113(3):216–229
19. Sivapriya SV, Ganesh Kumar S (2022) Modulus of laterally loaded pile in cohesionless slope crest with varying condition. *Civ Environ Eng Rep* 32(3):133–142 (2022). <https://doi.org/10.2478/ceer-2022-0032>

20. Antony VJ, Chandrasekaran SS (2022) Effect of spacing and slenderness ratio of piles on the seismic behavior of building frames. *Buildings* 12(12) (2022). <https://doi.org/10.3390/buildings12122050>
21. Basak S (2009) Effect of L/D ratio on degradation of capacity of pile subjected to lateral cyclic load in clay. *Indian Geotechnical Society*, pp 712–715

Investigation on Plastic Hinge in Non-prismatic Beam with Circular Openings



Venumadhav Guligari , C. Arunkumar , and N. Umamaheswari 

1 Introduction

Non-prismatic beams, also referred to as variable section beams, are beams with varying cross-sectional shapes. Analysis of non-prismatic beams is a more complex procedure because of their geometric properties compared to prismatic beams but they are found to be suitable for structures like bridges, multi-storeyed buildings and offshore platforms. They must be studied and understood because the distribution of internal forces and moments is affected by the changing cross-sectional form of these materials, which in turn impacts how strong and stable they are. In order to properly design non-prismatic beams, one must have a thorough understanding of how they behave under various loading scenarios as well as the analytical and predicative skills to do so.

Overall, non-prismatic beams must be understood and studied in order to construct structures safely and effectively because of the complicated bending and stress distributions caused by non-prismatic beams' variable geometry, understanding and researching them is crucial to ensuring their strength and stability. Understanding non-prismatic beams is also helpful for making the best use of materials and lightening the weight of buildings, which can result in cost savings and increased sustainability. Non-prismatic beams can be modified to give increased strength and stiffness where it is needed while using less material overall by adjusting the cross-sectional dimensions along the length of the beam.

Non-prismatic beams can aid in distributing loads more uniformly down the length of the beam, lowering the possibility of isolated high stresses and boosting the structure's overall stability and safety. It is feasible to reduce the quantity of material used during construction, which will save money and increase sustainability, by

V. Guligari · C. Arunkumar · N. Umamaheswari (✉)
Department of Civil Engineering, SRM Institute of Science and Technology,
Kattankulathur 603203, India
e-mail: umamahen@srmist.edu.in

optimizing the cross-sectional dimensions of non-prismatic beams. Non-prismatic beams have been utilized in building from the time of the ancient Romans and Greeks, who also used curved arches and vaults in their projects. In the nineteenth and twentieth centuries, as engineering and construction techniques advanced, non-prismatic beams were used more frequently because they could be produced and installed more easily. Non-prismatic beams are gaining interest from academia and industry due to these benefits, in part because of the design freedoms provided by advancements in additive manufacturing, such as 3D printing. The shear stress is particularly impacted by the beam's form and any internal forces. Understanding the specimen's maximum load bearing capacity and maximum stress tolerance depends on determining the collapse load (a non-prismatic beam). Understanding the above problem requires understanding the location and length of the plastic hinge formation in the structure. The plastic hinge idea plays a significant role in the design of ductile structures, which are intended to bend in a controlled way in reaction to severe loads, lowering the likelihood of a catastrophic failure.

The position along a beam or any other structural part where material yields as a result of applied loads is referred to as a plastic hinge. As a result of this yielding, the beam loses stiffness and strength and develops a hinge-like mechanism that may disperse and absorb more energy. The plastic hinge idea is used in structural design to depict a structure's inelastic behavior when subjected to significant deformations, such as those that take place during earthquakes or other extreme loading events. Engineers may make sure that a structure can withstand the effects of severe loads and continue to support the desired loads even after yielding by precisely positioning and managing the production of plastic hinges. The cross-sectional measurements, loading conditions, and material qualities of the structural element are commonly used to determine the length of the plastic hinge. For instance, in reinforced concrete beams, the plastic hinge length which is related to the reinforcement ratio is commonly taken as the distance between the cross-sections, center of gravity, and the point of high concrete strain. Monotonic loading is a type of loading in which there is no reversal of the loading direction, and the load or force applied to the structure is constant or steadily increasing. Structures are frequently designed and tested using this kind of stress to assess their strength and stability in a controlled loading environment.

Numerous researchers investigated the non-prismatic beam, and the state of the art is discussed. Kaveh et al. [1] have investigated about three-dimensional steel frame seismic design. The frames are made in accordance with LRFD-AISC design guidelines and are loaded by gravity and earthquakes. Ordinary moment frames are seen as having lateral resisting systems in this context. Two types of frames consisting of prismatic frames and non-prismatic frames are optimized, and results are compared. Non-prismatic beams are good at resisting lateral sway moment. Zhou et al. [2], as theoretically put forth, a shear stress analytical expression for elastic tapered beams is derived based on the theory of elasticity. It demonstrates that shear stresses in tapered beams are dissimilar due to change in cross-section. It is important to consider the additional shear stress caused by the bending moment for the shear calculations of tapered beams. The accuracy of this is confirmed by numerical investigation of RC

beams. Kaveh [3] has examined the reduction of optimal cost and carbon dioxide reduction in non-prismatic beams. A 2, 4, and 8 story RC frames with long spans had considered five metaheuristic algorithms. ECBO showed the best result for optimal cost and less CO₂ emissions. Kaveh et al. [4] developed a computational method for the performance-based optimal seismic design of RC frames with prismatic beams and frames without prismatic beams. Five metaheuristic algorithms were used to determine the optimal CO₂ emission and optimal cost relation. Hence, in frames with prismatic beams the performance levels has increased from 2.2 to 4% for cost, and CO₂ emissions were reduced by 1.8–12%. Jolly et al. [5] analyzed about reinforced concrete haunched beams. The paper has documented that the design shear force was reduced by concrete compression chord because of the existence of vertical shear resistance component. Reinforced concrete haunched beams can redistribute cracks along haunch length, so brittle and sudden shear failure is reduced. Tan [6] designed the reinforcement for non-prismatic RC beams using strut-and-tie models. Seven beams are constructed and tested based on these models. The width and location of the recess, as well as the strengthening strategy, were considered. The impact of these parameters on the strength and behavior of beams were discussed after the test results were compared to design values. Resan [7] aims to create an in-plane non-prismatic flanged concrete beam and research the effects on improving strength, rotation capacity, and flexural ductility without significantly affecting ultimate load bearing capacity or plastic rotation capacity when subjected to three-point loading. Jabbar [8] investigates about effects of openings in hollow beams in web portion, where the behavior of the hollow beams with and without 100 mm openings was the same, when compared to 200 and 300 mm openings. Kim [9] study is based on the cross-sectional characteristics and material characteristics of RC beams; the study offers a method for choosing the proper diameter and spacing of the circular web holes. The linear strain distribution of the longitudinal reinforcing bars served as the basis for the calculation of the neutral axis depth is used in this study to assess the suitability of the planned web apertures. Additionally, to lessen the effect on the flexural strength of RC beams, the maximum diameter of the web opening is determined using a linear strain distribution at nominal strength. The net tensile strain in high tension reinforcement is used to get this dimension.

In the present research, an attempt has been made to find the plastic hinge length and location for different length of taper section (200, 300, 400 mm) with different circular openings of diameter 80, 100, and 120 mm. The adopted shape is a haunched-shaped beam with tapered sections near the ends of the beam.

Table 1 Model configuration for non-prismatic beam

Length of the tapered section (mm)	Size of the openings (mm)	No. of openings	No. of models
200	80	2 openings	3
	100		
	120		
300	80	2 openings	3
	100		
	120		
400	80	2 openings	3
	100		
	120		

2 Model Configuration

The parametric study was carried out by the Finite Element Analysis (FEA) of non-prismatic beam with different tapered section length (200, 300, and 400 mm) and different circular openings ($0.4H$, $0.5H$, and $0.6H$), where H = height of the beam. The openings of size 80 mm, 100 mm, and 120 mm were created for 200 mm, 300 mm, and 400 mm tapered beams, respectively. The model configuration is given in Table 1.

3 Numerical Investigation

FEA has been carried out using ABAQUS V.14. The analysis deals with the behavior of non-prismatic beams subjected to monotonic loading conditions. From the analysis using plastic strain, plastic hinge length and location were calculated.

3.1 Geometrical Modeling

The beam is having length 2000 mm with cross-section 100×200 mm. The concrete part is modeled with three-dimensional solid elements C3D8R. The circular hole has accomplished by extrude cut. The reinforcing bars are modeled as wire element. Four numbers of 12 mm Φ bar is used for main reinforcement, and 8 mm Φ bar is used for stirrups. Figures 1 and 2 show the assembled non-prismatic beam and its reinforcement details, respectively.



Fig. 1 Assembled non-prismatic beam

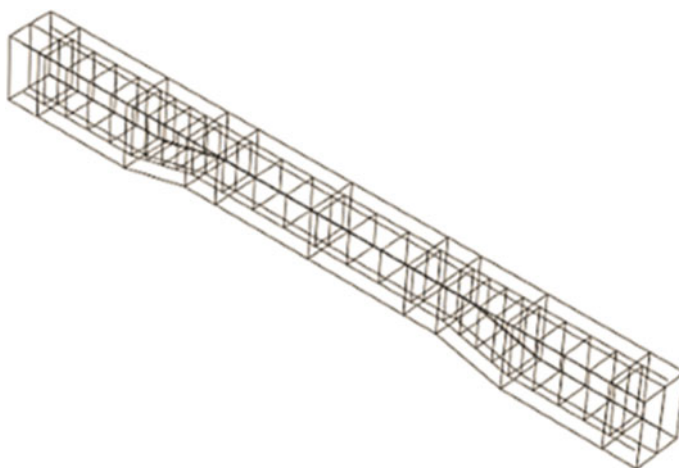


Fig. 2 Reinforcement detailing of non-prismatic beam

3.2 *Material Property*

Two different materials were used such as concrete and steel. The Young's modulus and poisson's ratio for the adopted M25 concrete is $15427.2973 \text{ N/mm}^2$ and 0.18, respectively. The elastic property of steel such as Young's modulus and Poisson's ratio is $2 \times 10^5 \text{ N/mm}^2$ and 0.3, respectively. The inelastic compressive and tensile strain behavior of M25 concrete is shown in Figs. 3 and 4, respectively.

Fig. 3 Compressive stress strain behavior of M25 concrete

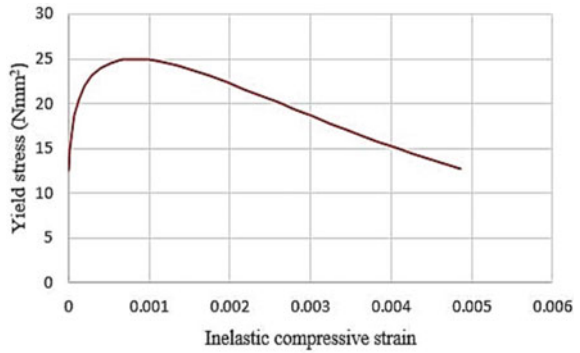
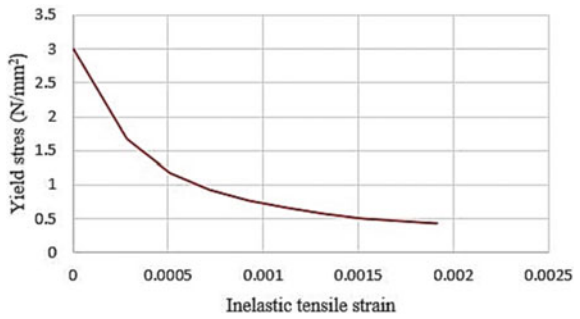


Fig. 4 Tensile stress strain behavior of M25 concrete



3.3 Interaction

Finite element parts are created independently in its own coordinate system. Interaction between concrete and reinforcement bars has done as ‘embedded region,’ and the same is shown in Fig. 5.

Fig. 5 Interaction between concrete and reinforcement bar

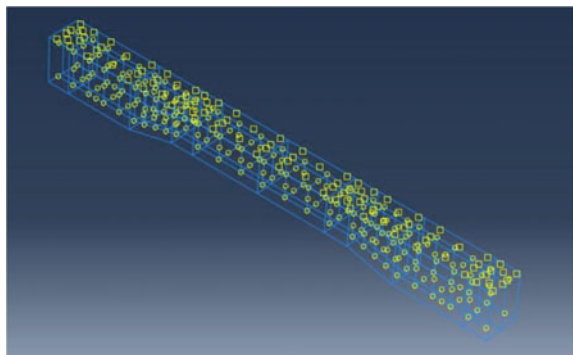
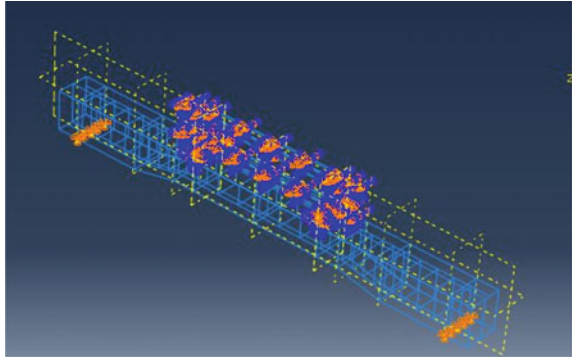


Fig. 6 Boundary conditions for non-prismatic beam



3.4 Boundary Condition and Load

The beam is supported with pinned ($U_1 = U_2 = U_3 = 0$) boundary condition. To avoid the lateral slip of the loaded I section, it is restrained only in the lateral directions ($U_1 = U_3 = 0$). Displacement approach was used for loading. The load was gradually increased with the initial step time 0.01 and incremented to the maximum of step time 0.1. The load was given as two-point load using I section as shown in Fig. 6.

3.5 Meshing

Structure meshing technique was used for meshing of the elemental parts as shown in Fig. 7. Meshing is done individually by part. The global seed sizes for concrete, main reinforcement, stirrup of size 150×200 mm, and stirrup of size 150×150 mm are 30, 50, 15, and 13, respectively.

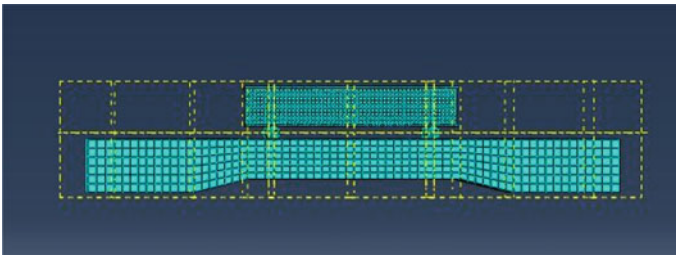
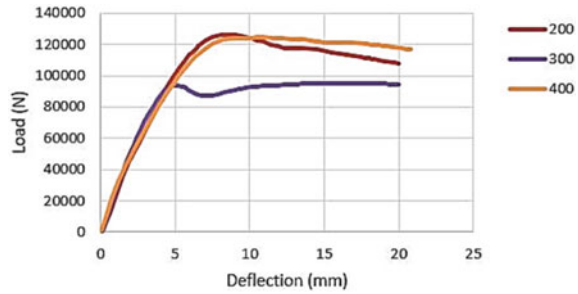


Fig. 7 Meshing of non-prismatic beam

Fig. 8 Load–deflection of tapered section-200 mm



4 Results and Discussion

Non-prismatic beam with different tapered sections with different diameter of circular openings were analyzed using ABAQUS. The results are discussed with respect to effect of length of the tapered section, effect of circular opening, plastic hinge length, and location.

4.1 Effects of Length of the Tapered Section

The ultimate load of 200 mm tapered section is 200 kN. It is 48 and 47% higher than that of 300 and 400 mm tapered section. It is depicted that the increase of the taper length increases the capacity of beam. The deflection obtained at the center of the beam is getting reduced due to increase of the taper section which is shown in Fig. 8.

4.2 Effects of Circular Opening in Non-prismatic Beam

The ultimate load of 200 mm tapered section with 100 mm opening is 120 kN. It is 2 and 3% higher than that of the same section with 80 and 120 mm opening, respectively. When increasing the size of the circular opening, the stiffness of the beam is reduced as shown in Fig. 9. It is depicted that the size of the opening is indirectly proportional to stiffness of the beam. Hence, the plastic hinge is formed faster in case of large openings.

The ultimate load of 300 mm tapered section with 120 mm opening is 90 kN. It is 2% higher than that of the same section with 80 and 100 mm opening, respectively. The difference in the ultimate load between the two sections (80 and 100 mm opening) is 0.75%. When increasing the size of the circular opening, the stiffness of the beam is reduced as shown in Fig. 10. The ultimate load of 400 mm tapered section with 100 mm opening is 105 kN. It remains the same for the same section with 80 and 120 mm opening also. When increasing the size of the circular opening, the stiffness

Fig. 9 Load–deflection of 200 mm tapered non-prismatic beam with circular openings

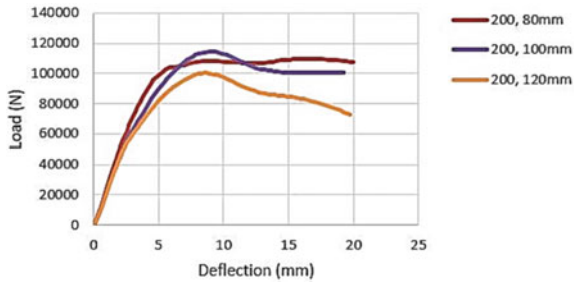


Fig. 10 Load–deflection of 300 mm tapered non-prismatic beam with circular openings

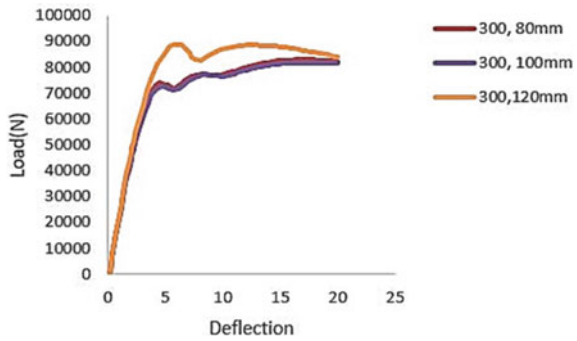
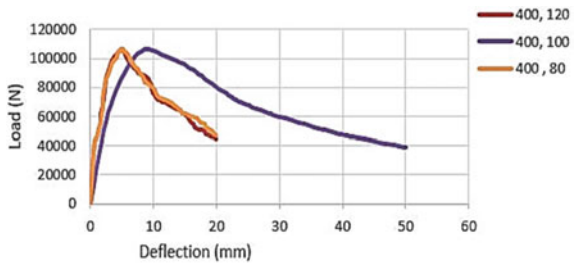


Fig. 11 Load–deflection of 400 mm tapered non-prismatic beam with circular openings



of the beam is reduced as shown in Fig. 11. It is depicted in all the cases that the size of the opening is indirectly proportional to stiffness of the beam. The ultimate load is (105 kN) obtained for larger tapered length irrespective of the opening size.

4.3 Plastic Hinge Length and Location

According to Zhao et al. [10], plastic hinge length and location can be calculated by using the rebar yielding zone, concrete crushing zone, curvature localization. Concrete strain ranging from 0.02 to 0.06 stays in a yield zone, where formation of

plastic hinges can be observed. The model specimens TB1, TB2, and TB3 representing the 200, 300, and 400 mm tapered section, respectively. The hinge location is represented by ‘a’ and ‘b’ for left and right side of the beam, respectively. The hinge length in the left and right side is $\perp a$ and $\perp b$, respectively. The hinge location and length are shown in Fig. 12.

The beam of tapered section 400 mm with 120 mm opening and 200 mm taper with 120 mm opening have plastic hinge formation in the compression zone of the concrete as shown in Fig. 13. In beam with circular openings, the plastic hinge was formed at tension zone of concrete, at a distance of 0–250 mm and 1750–2000 mm as shown in Fig. 14. The hinge location and calculated hinge length are given in Tables 2 and 3 for concrete compression and tension zone, respectively.

For the reinforcements, the rebar strain curve is used to locate the yield zone (strain range 0.02–0.086). The rebar placed in the tension region is having high tendency to form plastic hinge along its entire length. As shown in Fig. 15, along the beam length, the strain is maximum at 100–250 mm region and 1780–1970 mm region. The hinge length is varied between 41 and 230 mm. In tension rod 2, the high chance of formation of plastic hinge located at a distance of 19.6–255 mm and 1790–1970 mm

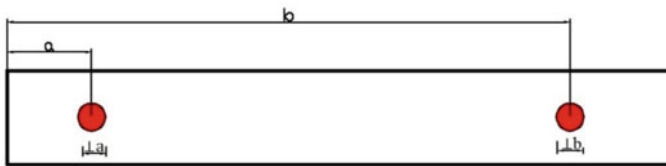


Fig. 12 Hinge locations and hinge length

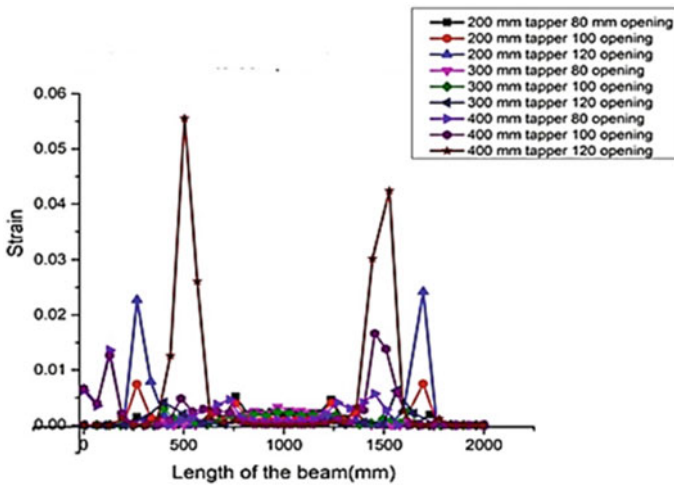


Fig. 13 Strain in concrete compression zone

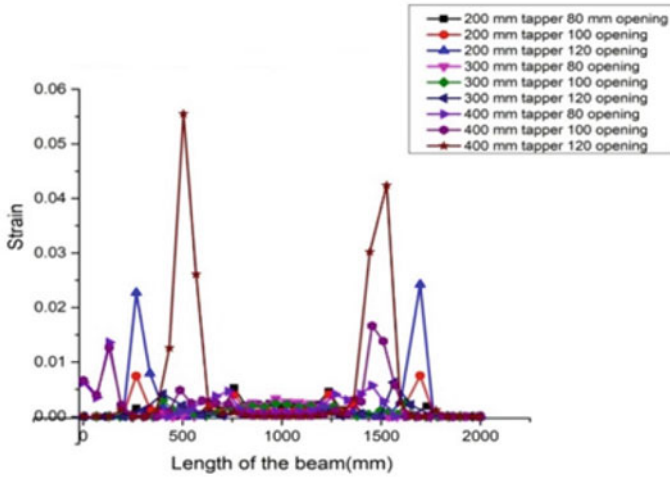


Fig. 14 Strain in concrete tension zone

Table 2 Strain in concrete compression zone

Specimen ID	Hinge location from one end (mm)		Hinge length (mm)	
	a	b	⊥a	⊥b
TB1a200, 80 mm	570–630	1200–1340	60	140
TB1b200, 100 mm	230–260	1720–1760	30	40
TB1c200, 120 mm	500–550	1600–1750	50	150
TB2a300, 80 mm	780–820	840–1100	40	260
TB2b300, 100 mm	450–600	1600–1650	150	50
TB2c300, 120 mm	400–500	1570–1650	100	80
TB3a400, 80 mm	0–250	1850–1915	250	65
TB3b400, 100 mm	0–250	1450–1620	250	170
TB3c400, 120 mm	375–600	1325–1500	225	175

as shown in Fig. 16. The hinge length is varied between 39.3 and 235 mm. The hinge location and calculated hinge length are given in Tables 4 and 5 for tension rods 1 and 2, respectively.

Table 3 Strain in concrete tension zone

Specimen ID	Hinge location from one end (mm)		Hinge length (mm)	
	a	b	⊥a	⊥b
TB1a200, 80 mm	125–145	1850–1900	20	50
TB1b200, 100 mm	125–145	1850–1900	20	50
TB1c200, 120 mm	150–300	1650–1850	150	200
TB2a300, 80 mm	66.6–160	1875–1900	93.4	25
TB2b300, 100 mm	70–170	1820–1900	100	80
TB2c300, 120 mm	69–170	1900–1950	101	50
TB3a400, 80 mm	67.1–175	1900–1950	107.9	50
TB3b400, 100 mm	67.5–120	1900–1970	52.5	70
TB3c400, 120 mm	67.4–175	1875–1925	107.6	50

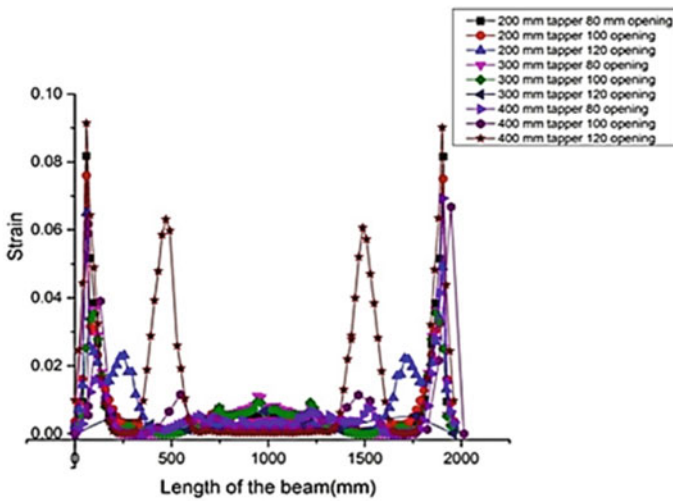


Fig. 15 Strain in tension rod I

4.4 Failure Assessment of Non-prismatic Beam

Failure of beam is observed inside the opening and around the supports because of high stress concentration near the opening and at the supports as shown in Fig. 17. Top surface is also taking a significant amount of stress due to two-point load. The portion inside the opening experienced more stress than supports because of the variation in stiffness. Hence, the opening region yielded more as shown in Fig. 18. When increasing the length of the taper section, the stress concentration is accumulated in

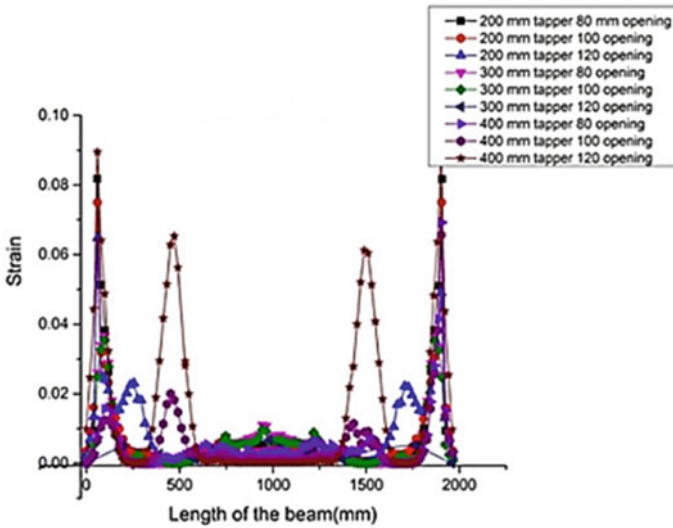


Fig. 16 Strain in tension rod 2

Table 4 Strain in steel tension rod 1

Specimen ID	Hinge location from one end (mm)		Hinge length (mm)	
	a	b	⊥a	⊥b
TB1a200, 80 mm	58–100	1790–1875	41	85
TB1b200, 100 mm	59–100	1790–1875	42	85
TB1c200, 120 mm	58.8–98.1	1910–1950	39.3	40
TB2a300, 80 mm	78–120	1800–1940	42	140
TB2b300, 100 mm	78–120	1800–1940	42	140
TB2c300, 120 mm	75–150	1800–1940	75	140
TB3a400, 80 mm	100–250	1850–1900	150	50
TB3b400, 100 mm	350–525	1864–1940	175	76
TB3c400, 120 mm	19.6–250	1780–1970	230	190

the mid span and the opening region as shown in Fig. 19. From the failure assessment, it is clear that the purpose of opening is justified. The hinge formation is occurred in the vicinity of the opening.

Table 5 Strain in steel tension rod 2

Specimen ID	Hinge location from one end		Hinge length	
	a	b	⊥a	⊥b
TB1a200, 80 mm	58.9–100	1790–1875	41.1	85
TB1b200, 100 mm	58.9–100	1790–1875	41.1	85
TB1c200, 120 mm	58.8–98.1	1910–1950	39.3	40
TB2a300, 80 mm	78–120	1800–1940	42	140
TB2b300, 100 mm	78–120	1800–1940	42	140
TB2c300, 120 mm	75–150	1800–1940	75	140
TB3a400, 80 mm	100–250	1850–1900	150	50
TB3b400, 100 mm	350–525	1864–1940	175	76
TB3c400, 120 mm	19.6–255	1790–1970	235	180

Fig. 17 Non-prismatic beam of tapered section TB1_c200, 120 mm

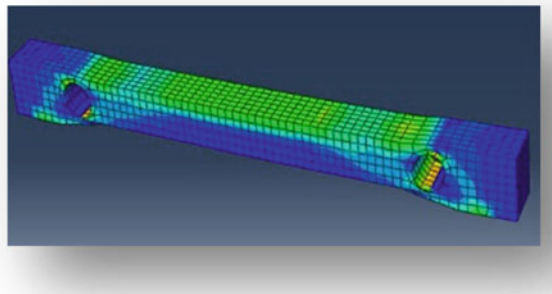


Fig. 18 Non-prismatic beam of tapered section TB2_b300, 100 mm

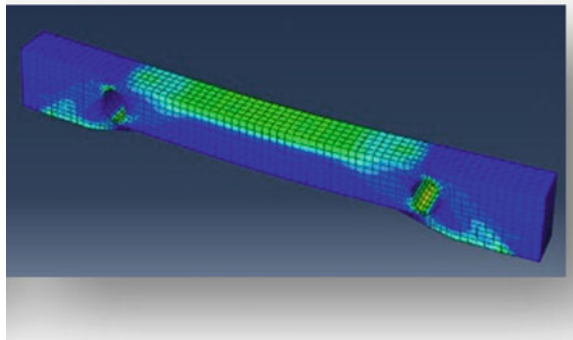
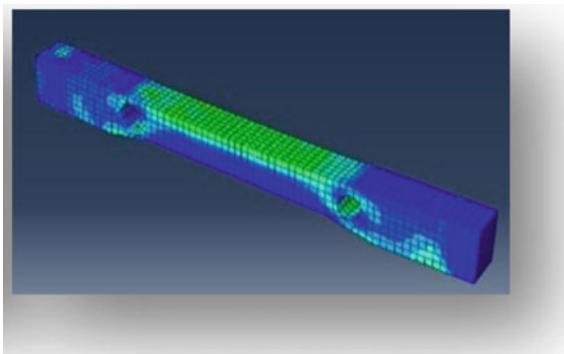


Fig. 19 Non-prismatic beam of tapered section TB3C400, 100 mm



5 Conclusion

The behavior of non-prismatic beam is studied with different length of tapered section and different diameter of circular openings. The plastic hinge length and location are explored for the non-prismatic beams, and the following conclusions have arrived from this research. The ultimate load of 200 mm tapered section is 200 kN. It is 48% higher than 300 mm taper section and 47% higher than 400 mm taper section. The increase of the taper length increases the capacity of beam. The size of the opening is indirectly proportional to stiffness of the beam. Hence, the plastic hinge is formed faster in case of large openings. Strain in concrete compression zone ranges between 0.02 and 0.06 and strain in concrete tension zone ranges between 0.02 and 0.086. As per concrete tension zone strain, the maximum hinge length of 200 mm is obtained in the non-prismatic beam with the specification of 200 mm taper length with 120 mm opening. From the detailed analysis, it is observed that the size of the opening exceeding 0.5 h (height of the beams) exhibited multiple plastic hinges in the beam due to less stiffness to mass ratio. Nevertheless, the size of the tapered section and location of the opening also plays a vital role in the formation of plastic hinges.

References

1. Kaveh A, Kabir MZ, Bohlool M (2020) Optimum design of three-dimensional steel frames with prismatic and non-prismatic elements. *Eng Comput* 36(3):1011–1027
2. Zhou M, Fu H, An L (2020) Distribution and properties of shear stress in elastic beams with variable cross section: theoretical analysis and finite element modeling. *KSCE J Civ Eng* 24(4):1240–1254
3. Kaveh A, Mottaghi L, Izadifard RA (2021) An integrated method for sustainable performance-based optimal seismic design of RC frames with non-prismatic beams. *Sci Iran* 28(5):2596–2612
4. Kaveh A, Mottaghi L, Izadifard RA (2022) An integrated method for sustainable performance-based optimal seismic design of RC frames with non-prismatic beams. *Eng Comput* 38:69–86

5. Jolly A, Vijayan V (2016) Structural behaviour of reinforced concrete haunched beam: a study on ANSYS and ETABS. *Int J Innov Sci Eng Technol* 3(8):495–500
6. Tan KH (2004) Design of non-prismatic RC beams using Strut-and-Tie models. *J Adv Concr Technol* 2(2):249–256
7. Zamel JK (2021) Flexural behavior of developed reinforced concrete beams of non prismatic flanges. *Mater Today: Proc* 42:2974–2983
8. Jabbar S, Hejazi F, Mahmood HM (2016) Effect of an opening on reinforced concrete hollow beam web under torsional, flexural, and cyclic loadings. *Latin Am J Solids Struct* 13:15761595
9. Kim HG, Lee YJ, Kim KH (2022) Cyclic flexural performance of RC beams with small circular openings in plastic hinge region. *Constr Build Mater* 321:126339
10. Zhao XM, Wu YF, Leung AYT (2012) Analyses of plastic hinge regions in reinforced concrete beams under monotonic loading. *Eng Struct* 34:466–482

Analysis of Ergonomics Risk During Plastering in Construction Sites



Aleena Josey, M. S. Ameer Suhail, Nazneen Niyas, and Sahimol Eldhose

1 Introduction

Ergonomics risk assessment is measure of the risk factors in work environment that may lead to musculoskeletal disorders among workers. Ergonomics risks can be caused by static, dynamic, changing, or unstable postures. It involves the evaluation of risk associated with occupational tasks. Musculoskeletal disorders are the most widely spread occupational problems for both developed and developing countries, in construction sector, which increase expenses of salary compensation, health costs, declining productivity, and lower quality of life.

1.1 Literature Review

Francis et al. [1], based on the analysis, it is found that biomechanical factors such as muscle tension and high muscle contact, poor posture, and repetitive movement were the most important ergonomic risk factors. In addition, psychosocial factors, including management and the environment, also affect the health of workers. Among management, pressure to meet deadlines and low training are the main problems of office workers. To solve these problems, it is important to follow the right management. Engineering controls include modifying the workplace or work environment to reduce ergonomic hazards. Control management focuses on the implementation of policies and procedures to address identified risks. Personal protective equipment

A. Josey (✉) · M. S. A. Suhail · N. Niyas
Toc H Institute of Science and Technology, Kochi, Kerala 682313, India
e-mail: aleenajosey15@gmail.com

S. Eldhose
Department of Civil Engineering, Toc H Institute of Science and Technology, Kochi,
Kerala 682313, India

(PPE) can be used to protect workers from ergonomic hazards. Finally, replacing known hazards with ergonomically designed tools or procedures can help reduce risk. By implementing engineering controls, regulatory controls, personal protective equipment, and reproducible equipment/processes, you can reduce the risk of development and provide a safe and healthy environment for employees.

Mustapha et al. [2] found out stating that maintaining an awkward posture can lead to decreased muscle efficiency, increased force exertion, muscle fatigue, and discomfort for workers. These issues can contribute to the development of musculoskeletal disorders (MSDs) among individuals performing repetitive tasks with heavy loads. However, implementing best practices such as job rotation, posture changes, and safety devices has been shown to be effective in reducing the occurrence of MSDs and promoting worker health. Job rotation involves periodically rotating workers among different tasks or job roles. This practice helps distribute the physical demands and stress on different muscle groups, preventing overuse and reducing the risk of developing MSDs. By allowing workers to perform a variety of tasks, job rotation also provides opportunities for rest and recovery for specific muscle groups. Posture changes are important in preventing prolonged exposure to awkward postures. Employers can encourage workers to maintain proper body mechanics and provide ergonomic training to promote correct posture during work activities. Additionally, regular breaks and stretching exercises can help alleviate muscle fatigue and reduce the negative effects of sustained awkward postures. The use of safety devices and ergonomic equipment is another effective strategy to minimize the risk of MSDs. Employers can invest in tools and equipment specifically designed to reduce the strain on workers' bodies. For example, lifting aids, adjustable workstations, and ergonomic tools can significantly decrease the physical stress associated with heavy loads and repetitive tasks. By implementing these best practices, organizations can achieve several benefits. First, it reduces the likelihood of work-related injuries and illnesses, which can lead to a decrease in absenteeism and workers' compensation costs. Second, it promotes the overall health and well-being of workers, improving job satisfaction and productivity. Finally, by preventing MSDs, organizations can avoid potential legal liabilities and associated expenses. Ergonomic assessments and consultations with professionals can help to identify and address potential risk factors and develop appropriate interventions to mitigate them.

Isabel Moreira-Silva, Azevedo et al. [3], according to the data and results of this study, the 7-day prevalence of musculoskeletal disease among the manufacturing company employees is 41.6%. The most common symptoms are back (18.8%), wrists/hands (17.3%), neck (15.8%), shoulder (15.3%), and ankle/foot (11.4%). The study also identified several factors associated with the development of musculoskeletal symptoms. The study found that job category was an important determinant of back and shoulder pain and showed that the type of work a person does affects the likelihood of experiencing pain symptoms. Also, older workers are more likely to have musculoskeletal symptoms than younger workers. In addition, gender was found to be an important marker of arthritis, suggesting that there may be differences in the presentation of musculoskeletal symptoms between men and women. To address these findings and prevent musculoskeletal symptoms in workers, the study

highlights the need for workplace interventions. By implementing intervention plans such as ergonomic improvements, training, and workplace changes, companies can reduce the incidence of musculoskeletal symptoms and improve the overall health, cleanliness, and well-being of their employees.

From the literature review, most significant ergonomics risk factors occur due to repetitive work and awkward posture. In all the above journals referred, they conducted the questionnaire, discussed with the workers, and collected the data history of musculoskeletal disorders to find the REBA scores. None of the journals quantify ergonomic risk in construction. In this study by using the software to find posture angles as well as repetitive risk to ergonomics hazard. In most of the cases, REBA techniques are applied for medical and IT Industry. In all the referred journal, whole body is considered; therefore, exact problem cannot be identified. In this part by part analysis is done which helps to identify the corrective measures.

2 Methodology

Methodology adopted for this project is follows:

1. Literature review: The data and information required for the project were collected from literature to understand various aspects of project.
2. Identification of risk factors: The most significant risk factors are repetitive work and awkward posture identified from PLIBEL and checklist method. It also referred that flooring and plastering works mostly deal with repetition and bad posture [4].
3. Analysis: The angles corresponding to the head, torso, pelvis, etc., of the workers are analyzed using the software POSTUREZONE [5].
4. Preparation of Worksheet: Data is collected about postures of workers that is placed into worksheet evaluator [6, 7] to differentiate the risk into low, medium, or high and prioritize the risk.
5. Validation: The values calculated using conventional method are validated using REBA [8, 9].
6. Results and discussion: Worksheet evaluator will the give the final risks score that represents the level of risk of the workers [10].

2.1 Identification of Factors

The main factors identified from review are:

Awkward posture • Repetitive work • Localized or whole body vibration • Static loading • Contact stress of muscles and tendon • Insufficient rest breaks • Lifting heavy items. Environmental related (physical and social) risk factors • Noise • Extreme temperature • Poor lighting • Poor ventilation • Chemical or dust exposure • Poor layout • Uneven surfaces • Lack of autonomy • Lack of control of work.

Table 1 T-Test result for plastering workers

On basis of	Mean	SD	SEM	P Value	Remarks
<i>(a) Health</i>					
Healthy	28.317	21.450	7.583	0.2981	Not statistically significant
Unhealthy	39.275	19.036	6.730		
<i>(b) Age</i>					
Age < = 35	39.012	16.395	3.864	0.2144	Not statistically significant
Age > 35	31.547	18.916	4.458		
<i>(c) Height</i>					
Height < = 175	26.286	15.450	3.544	0.0014	Statistically significant
Height > 175	43.151	14.646	3.360		
<i>(d) Experience</i>					
Experience < = 10	36.944	15.620	5.206	0.5706	Not statistically significant
Experience > 10	31.438	23.869	7.956		

2.2 Statistical Analysis of Physical Parameters

To determine whether there is a difference between two unrelated groups such as health, age, height, and experience, statistical test is done. It was done for 50 population based on two independent samples and compare the mean between two independent groups (Table 1).

2.3 Body Part Definition






Body parts is defined to the study the posture by dividing the human body into three (3) general movement areas: (i) head, (ii) torso, and (iii) pelvis as per posture zone software. This helps to observe risk exposure of these parts and helps to eradicate the musculoskeletal disorder. The values assigned to the body part postures is termed as risk scores relative to each observations.

2.4 Assign Risk Level

After assigning score, classify risk level is done with reference to REBA worksheet. The risk levels are given in Table 2.

The postures related to the corresponding works are found out by taking their live images during work using the Software Posture Zone. Posture Zone provides visual representation for improvement or decline in posture. It helps to measure inclinations in degrees to track postural changes, balance and symmetry of the head, torso, and

Table 2 Assigning risk levels

Score	Risk	Risk classification
0–50	Negligible	
50–100	Low	
100–150	Medium	
150–200	High	
200+	Very high	

Source Alexandra Gemitzi

pelvis over the center of the feet. For more accuracy, the same worker’s posture from different sides was found. The details were collected from various sites in Ernakulum district, Kerala (Fig. 1).

The angles observed from POSTURE ZONE software of plastering, are collected for further calculating risks score from postural hazard analysis sheet and the values obtained from the Table A scores are given below and from this hazard scores can evaluate the levels of risks such as low, medium, or high. The live image of the plastering work was taken using the posture zone software from which the angles

Fig. 1 Angles obtained during masonry works

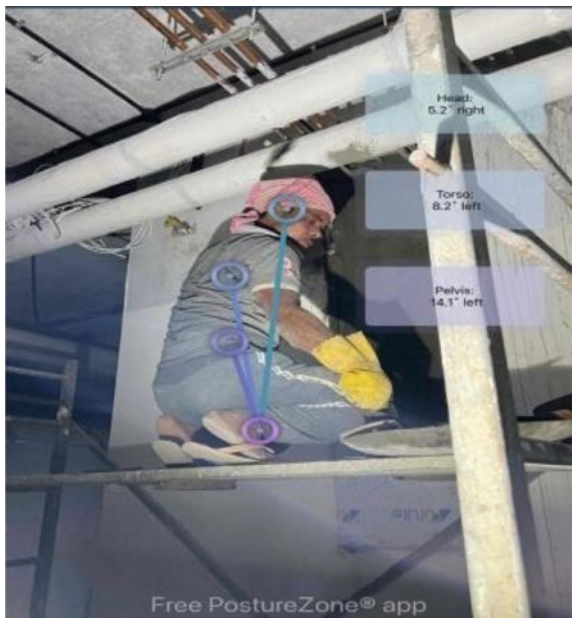


Table 3 Observations for plastering works

Worker		Observation 1			Worker		Observation 1		
No	Head	Torso	Pelvis	No	Head	Torso	Pelvis		
1	25.4	2.2	26.9	14	19.1	11.3	5.1		
2	15.2	11.2	2.3	15	0.6	4.1	12.3		
3	7.9	11.9	18.6	16	19.8	8.7	2.4		
4	7.1	40	16.1	17	1.9	2.2	7.9		
5	5.2	8.2	14.1	18	4.1	3.4	6.4		
6	80	9.7	11.9	19	90	8.6	2.5		
7	8.4	8.2	9.1	20	14.5	16.4	170		
8	12.5	11.4	90	21	21.7	26.5	30.8		
9	30	4.4	50	22	20	30	1.2		
10	5.9	2.8	3.9	23	150	16.9	170		
11	17.4	160	3.5	24	180	20.7	21.8		
12	12.7	11.9	18.6	25	4.7	5.9	4.4		
13	6.8	3.1	150	26	80	9.8	8.5		

of head, torso, and pelvis are identified. Using this angles obtained ergonomic risk level can be calculated (Table 3).

From all the observations taken, the max angles were found for bar plastering workers, and the angles corresponding to each workers posture were 43.6°, 37°, 30.7°, 30.9°, and 43.9° for head, torso, and pelvis, respectively.

2.5 Ergonomic Risk Score

The angles observed from POSTURE ZONE software of plastering activities are collected for further calculating risks score from postural hazard analysis sheet and the values obtained from the Table scores are given below and from this hazard scores can evaluate the levels of risks such as low, medium, or high. The model developed for calculating score using regression equation is as follows (Table 4):

$$\begin{aligned} \text{Total score} = & 56.786 + \text{PS} \times 6.496 \\ & - \text{EF} \times 29.623 + \text{OR} \times 18.35 \end{aligned} \quad (1)$$

where

- PS Posture score
- EF Environmental factors
- OR Organizational risk.

Table 4 Score for plastering workers

Site no (S)-Worker no (W)	Total Score	Site no (S)-Worker no (W)	Total Score	Site no (S)-Worker no (W)	Total Score	Site no (S)-Worker no (W)	Total Score
S1W1	122.5	S3W1	37	S2W5	147	S4W5	44.8
S1W2	50.4	S3W2	66	S2W6	116.3	S4W6	59
S1W3	75.6	S3W3	55.5	S2W7	126	S5W1	48.8
S1W4	84	S3W4	71	S2W8	44.4	S5W2	29.6
S1W5	165.6	S3W5	121.6	S2W9	55.5	S5W3	51.2
S1W6	225.4	S3W6	68.8	S2W10	95.4	S5W4	33.5
S1W7	114	S3W7	73.6	S2W11	48	S5W5	37
S2W1	80	S4W1	14.8	S2W12	40	S5W6	56
S2W2	80	S4W2	40	S2W13	55.5	S5W7	64
S2W3	66	S4W3	29.6	S2W14	240	S5W8	69.6
S2W4	44.4	S4W4	42.4	S2W15	48	S5W9	44.8

The given radar chart displays multivariate data of three or more quantitative variables like score of respective worker that is mapped onto an axis (Fig. 2).

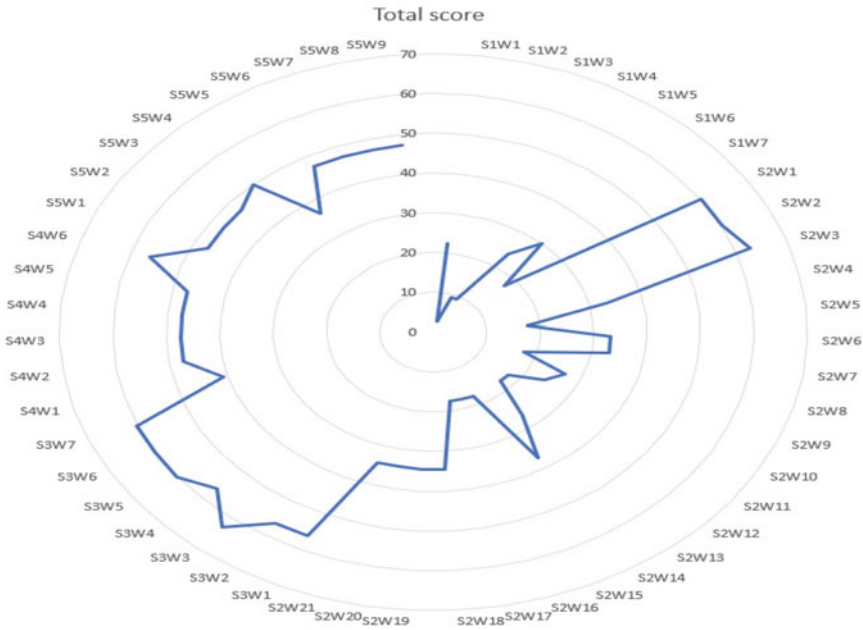


Fig. 2 Radar chart showing worker and score

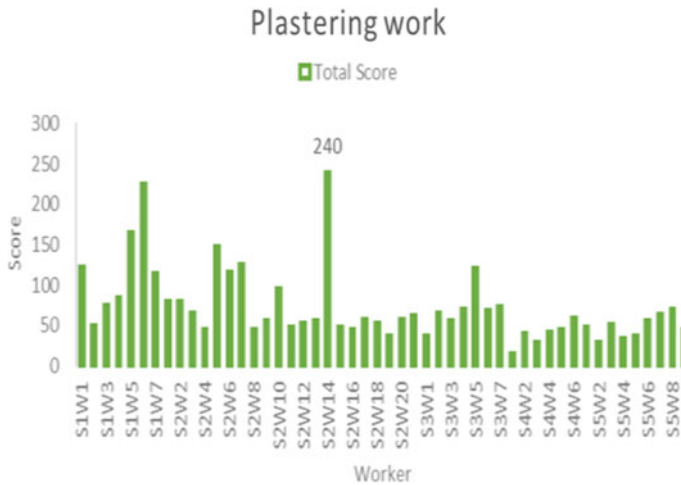


Fig. 3 Graph showing plastering score versus workers

3 Results and Discussion

The major factors were identified from literature review and checklist. The ergonomics risks of workers were calculated using POSTUREZONE, and their posture score was found out. The maximum posture angles were found out for plastering. The observed angles were 17.0°, 77.5°, 30.8° and 13°, 62.6°, 53° for head, torso, and pelvis, respectively. After that, the risk score corresponding to environmental factors, repetition, and duration was found out for each worker, and then the total score was found out. For plastering, 49.68% of angles are in danger. The scoring chart for plastering is given below (Fig. 3).

4 Conclusion

Awkward posture and repetitive work are the major factors that contribute ergonomic risk by literature survey [11, 12]. By the statistical analysis using T-Test height was found out to be statistically insignificant. The relation between various factors is modeled using regression analysis. The observations for posture were made from various plastering workers in Kerala construction sites using posture zone software. Out of 50 observations made for plastering work, it was found that 17 workers were in negligible risk zone, 6 workers in the medium risk zone, 1 worker in the high-risk zone and remaining 2 in the very high-risk zone, 24 workers in the low risk zone, 6 workers in the medium risk zone, and one worker was in the high-risk zone. Thereby from all observations made, 4 people needed immediate action. Therefore, an alert system can be introduced in sites for preventing musculoskeletal disorder [13, 14].

References

1. Francis JR et al. (2019) A study of plausible ergonomic risk factors in construction Industries, IRJET 06(03)
2. Mustapha Z et al. (2022) Impact of work-related musculoskeletal disorders among construction workers in Ghana, BJREECM 11 (10)
3. Azevedo J et al. (2020) Predicting musculoskeletal symptoms in workers of a manufacturing company, IJOSE 27(04).
4. Vensheeb P, Delin S, Roja RY, Karthika S (2020) Analysis of occupational risk factors for ergonomic design of construction work systems. Int Res J Eng Technol (IRJET) 07(08)
5. Yunus MNH, Jaafar MH, Mohamed ASA, Azraai NZ, Hossain MS (2021) Implementation of kinetic and kinematic variables in ergonomic risk assessment using motion capture simulation, a review. Int J Environ Res Publ Health 07(08)
6. Cheon W, Jung K (2020) Analysis of accuracy and reliability for OWAS, RULA and REBA to assess risk factors of work related musculoskeletal disorders. J Korea Saf Manag 22(2)
7. Brand C (2017) Ergonomics analysis of working postures using OWAS in semi-trailer assembly, applying an individual sampling strategy. Int J Occupancy Saf Ergonomics
8. Ansari NA, Sheikh MJ (2016) Evaluation of work posture using REBA and RULA. IOSR J Mech Civ Eng
9. Narendra S, Kumar S, Akarsh, Juhi V (2020) Ergonomics risk analysis using REBA and RULA. Int J Trend Res Dev (IJTRD) 7(1)
10. Satish MB (2018) Identifying and controlling ergonomic risk factors in construction. J Ergonomics 8(4)
11. Kulkarni VS, Devalkar RV (2019) Postural analysis of building construction workers using ergonomics. Int J Constr Manage 19(6)
12. Nor LBS, Mat SN, Zain FMY, Saidin MT (2019) Ergonomic risk factors (ERF) and their association with musculoskeletal disorders (MSDs) among Malaysian construction trade workers: concreters. Int J Acad Res Bus Soc Sci 9
13. Reza A, Amir BH, Nipun N (2017) Ergonomics analysis of construction worker's body postures using wearable mobile sensors. J Constr Eng 11(3)
14. Chukwuma N, Orcid, Awolus I, Park JWO, Alex A (2020) Wearable sensing devices: Towards the development of a personalized system for construction safety and health risk mitigation. Emerg Technol Tech Civ Constr Eng 21(3)

Quality Assessment of Building and Infrastructure Project Using Taguchi Methodology



D. Harish, S. Manikandaprabhu, S. Prakash Chandar, and N. Pavithra

Notations

P_{hi}	Very highly affects the construction quality value
P_{li}	Very low influencing on construction quality value
H_{li}	Signal to noise for smaller to better
H_{hi}	Signal to noise for larger to better
η	Taguchi signal-to-noise ratio

1 Introduction

The construction sector is vital to world financial growth and development, and it contributes significantly to economic development. The construction industry is India's second largest source of gross domestic product after agriculture (GDP). New and faster building procedures are being created as a result of the advancement of science and technology.

When it comes to project management, time, money, and quality are the three pillars that hold it all together. The success of the project is dependent on the effectiveness of the quality management system. Construction quality may be defined as the achievement of acceptable performance standards by construction operations. When a product or service satisfies all of the necessary criteria, it is considered to be of high quality. In the long term, attaining quality in the construction industry is challenging and has historically been a source of worry. Without the use or improper use of quality management systems in a firm, the project's time, cost of work,

D. Harish · S. Manikandaprabhu (✉) · S. P. Chandar · N. Pavithra
Department of Civil Engineering, Faculty of Engineering and Technology, SRM Institute of Science and Technology, Kattankulathur, Tamilnadu 603203, India
e-mail: saravanaprabhou@gmail.com

and productivity of progress are compromised. According to Adenuga, Olumide Afolarin discusses the challenges that limit effective quality assurance processes and to determine who should be largely liable for ensuring/enforcing effective quality assurance practises in public housing projects [1]. Polat et al. say the absence of top level support, dedication, and leadership, an underqualified workforce, and a lack of an effective team are the three most significant impediments to TQM adoption in building sector [2]. Modi finds that the lack of quality planning, inspection, delays in the delivery of supplies, labour, financial difficulties, execution, and the ignorance and lack of expertise of the project manager are the top most important causes in quality construction sector concerns [3]. Jha and Iyer speak about the absence of support from top-level management and less experienced project manager are the most important factors on the quality performance of a construction project are the major factors which affects the quality of construction [4]. Abas et al. discuss the poor quality of construction activities in Pakistan, that leads to cost overruns, delays, and unnecessary reworking, which are the factors has a negative influence on building projects [5]. Freddi and Salmon say that Genichi Taguchi's approach consists of three design steps which are system design, parameter design, and tolerance design [6]. The methodologies of Taguchi are founded on the notion of parameter design, which is an engineering method for product or process design that focuses on identifying the parameter (factor) settings that generate the optimum levels of a quality characteristic (performance measure) with the least variation [7]. Taguchi designs are a highly effective way for creating processes that run consistently and ideally under a wide variety of situations. To establish the optimal design, it is necessary to conduct a strategically designed experiment in which the process is exposed to a range of design parameters [8]. This Taguchi signal-to-noise ratio in a way that is more precise than other interpretations. The Taguchi s/n ratio is the most precise representation of the concept of quality, and it has influenced modern design processes significantly [9, 10]. While statisticians may argue, the signal-to-noise ratio simplifies statistical analysis, and it is a significant simplification that brings designers closer to statistics [11]. The objective of this research to find out the quality-related factors in construction projects and to analysis the impact of construction quality loss by Taguchi signal-to-noise ratio function. The study discusses based on nine main factors influencing quality of construction activity in south Indian region. The factors were ranked based on Taguchi signal to noise.

2 Data Collection

With South Indian standard construction companies as the subjects of the research, this study helped improve the current construction quality to satisfy customer demands for quality building. The primary objective of this study was to use the Taguchi signal-to-noise analysis technique on the questionnaire responses of South Indian construction businesses in order to account for variations in the work experience of quality officials from the civil sector's assessment of quality characteristics

and to combine highly affected factor and least affected factor data S/N ratios in order to analyse the factor that influences quality performance and to prioritise improvement efforts. The quality attributes of the construction sector are established in this study by referring to the literature and excepts pilot study. By using a questionnaire and randomly selected samples, the survey was conducted in various building organisations in the South Indian region. The obtained data was then analysed using the Taguchi signal-to-noise ratio approach to increase the quality standards of construction in the southern Indian region. In Table 1, the main nine factors which are affect the quality of construction are categorised under category A to I.

A direct personal interview and a literature review were used to gather information on the elements that impact quality and potential solutions. The results of the research were compared to those of the direct personal interview and the literature review. The questionnaires are framed by nine main factors which affecting the construction quality, in each factors having six sub-factors influencing aspects of quality in building and management. The Likert scale is used to evaluate all questions. Numerous aspects of a construction project are assessed on a five-point, two-point Likert scale with 1 being the least important and 5 the most significant, with 1 indicating no influence and 5 indicating a considerable impact on quality of construction. As a result of the size, it was required of the responders that they identify the aspects that have an impact on quality.

Table 2 shows the demographic information of the questionnaire survey taken in the Chennai region which includes the details like total number of organisations, designation of responded, experience, types of projects, and education qualification.

The top level organisation provided 7 responses, the medium level organisation provided 23 responses, and the low-level organisation provided 17 responses. Designer, structural engineer, site engineer, chief engineer (government), assistant engineer (government), project manager, owner, quality engineer, and supervisor were among the positions held by the participants. The 105 responses received from people with experience ranging from 0 to 5 years received 39 responses, persons with experience ranging from 5 to 10 years received 30 responses, peoples with experience ranging from 10 to 20 years received 18 and some with experience ranging from more than 20 years received 20. Projects undertaken by the participants include residential, commercial, industrial, and other developments. Some organisations are engaged in more than one project within their organisation. Among the respondents' educational qualifications shown in Fig. 1 include two doctorate candidates, 15 post graduate candidates, 57 under graduate candidates, and 31 diploma candidates.

3 Taguchi Signal-to-Noise Ratio

Dr. Taguchi recommended that great quality should meet the accompanying necessity, The average and target values of a quality characteristic should be constant, and the smaller the variation of a quality attribute characteristic would be better for industries [12]. Subsequently, quality evaluation ought to consider both the effect

Table 1 Categorisation of factor influencing construction quality

<i>Category A—Contractor factor</i>					
Lack of contractor supervision and site management—(A1)	Lack of management leadership—(A2)	Lack of contractor's involvement in quality—(A3)	Lack of management commitment to continual quality improvement—(A4)	Poor financial control on-site—(A5)	Reduced subcontractor responsibility—(A6)
<i>Category B—Management factor</i>					
Lack of top level management support—(B1)	Poor planning and scheduling of the project—(B2)	Lack of quality policy in the management—(B3)	Poor training system—(B4)	Lack of coordination between designers and contractors—(B5)	Lack of auditing system—(B6)
<i>Category C—Technical factor</i>					
Design complexity—(C1)	Low-quality drawing and specification—(C2)	Poor knowledge about new applications and software's of quality system—(C3)	Estimation error—(C4)	Change in design specifications during execution—(C5)	Lack of technical and professional expertise to perform task—(C6)
<i>Category D—Labour factor</i>					
Lack of skills (labours)—(D1)	Lack of communication—(D2)	Lack of concentration on work—(D3)	Poor productivity of labours—(D4)	Availability of required number of labours (shortage)—(D1)	Delay and low wages of labours—(D6)
<i>Category E—Material factor</i>					
Lack of inspection and testing—(E1)	Selection of poor quality material—(E2)	Water content—(E3)	Poor concrete mix design—(E4)	Increase cost of materials—(E5)	Availability of material in required stages—(E6)
<i>Category F—Equipment factor</i>					
Improper inventory management—(F1)	Unavailability of major equipment—(F2)	Improper selection of equipment—(F3)	Low-quality efficiency equipment—(F4)	Unawareness of equipment specification—(F5)	Lack of usage of advanced technology in construction—(F6)

(continued)

Table 1 (continued)

<i>Category G—Political factor</i>					
Corruption and bribery—(G1)	Poor law and regulation—(G2)	Prices fluctuation—(G3)	Changes in government policies—(G4)	Instability in governance—(G5)	Inflation—(G6)
<i>Category H—Political factor</i>					
Harsh climate condition—(H1)	Poor soil condition—(H2)	Natural disaster—(H3)	Uneven topography—(H4)	Project in congested area—(H5)	Unfriendly neighbourhood—(H6)
<i>Category I—Miscellaneous factor</i>					
Time scale of work (urgency)—(I1)	Client satisfaction —(I2)	Mistakes during construction and rework—(I3)	Lack of maintenance after construction—(I4)	Codes and standard—(I5)	Sudden Health issues of workers—(I6)

Table 2 Characteristic of respondent

Designation	Experience (years)			
	0–5	5–10	10–20	> 20
Design engineer	4	3	2	4
Structural engineer	5	7	2	1
Site engineer	12	5	3	1
Chief engineer	0	0	2	1
Assistant engineer	0	3	5	0
Project manager	2	1	2	4
Owner	4	1	0	1
Quality engineer	7	6	2	4
Supervisor	6	3	0	2

Respondent Qualification

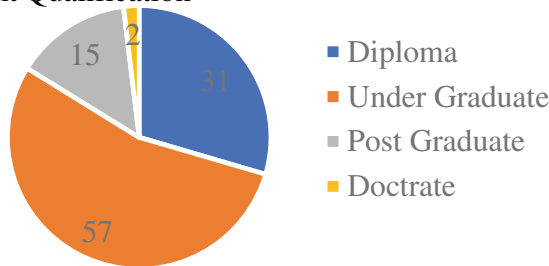


Fig. 1 Respondent qualification

of normal and difference simultaneously. Harmony showed that S/N proportion has thought about at the same time the effect of normal and change in the evaluation of value property and coordinated the investigation results from the two-layered model into the one-layered model [13]. Thus, S/N proportion has awesome added substance capacity in quality assessment and forecast. The benefit of S/N proportion is its capacity to mirror the varieties of the quality ascribes. While executing quality enhancements, S/N proportion can freely change normal qualities to the objective qualities [14]. During the process of making quality enhancements, the signal-to-noise ratio may independently change average values to desired levels. The implementation of a comparison of the quality’s performance is the goal of the S/N system. As a result, the S/N ratio may be used to gauge relative quality, and its use is both straightforward and capable of additive analysis [15]. Taguchi et al. pointed out that one of the benefits of using S/N ratio is its direct relationship with economy since S/N ratio is derived and varied into the ratio from loss function. This was mentioned as one of the advantages of using S/N ratio [16]. The ordered categorical data of count value data type was used as the measuring level for the satisfaction survey.

This allowed the researchers to differentiate count value S/N ratios into three categories: the smaller the better, the larger the better, and the ordered categorical data. In this study, the features of the count values known as “the larger the better” and “the smaller the better” were utilised to measure factors affecting the construction quality performance. These features were used while taking into consideration the influence of average and variation and combining data on highly influencing and very low influencing of quality [15]. In the assessment of experience stakeholders in construction industry, in the design of a questionnaire, a Likert scale is commonly used to prioritise the real stakeholder impression of factors impacting quality by level. This study employed the S/N ratio to describe the technique for factor of construction quality and summarise the questionnaire survey data of experienced employees in the building sector, using Likert five-point scale data, as given in Table 1, where if the 5-point scale $l = 1$ to 5, yt represented the number of collected valid questionnaires. Data on the priority level may be converted into the count value data type in order to differentiate between very strongly influence quality performance and very lowly influence quality performance [17]. Level 3 (neutral), level 4 (highly), and level 5 (very highly) as factors affect construction quality and level 2 (least) and level 1 (very low) as stakeholders’ opinion of factor influence construction quality attributes. Hence, among collected valid questionnaires, the factor quality attribute i ’s stakeholder very highly affect the construction quality value was $hi = yi4 + yi5$, while the factor quality attribute i ’s experienced personnel’s very low influencing on construction quality value was $li = yi1 + yi2$ [18]. Calculating the very highly impacting coefficient psi and the very low affecting coefficient pdi is required for the consideration of the very highly and very low factors information S/N ratio analysis. These coefficients may be found in Eq. 1

$$P_{hi} = \frac{(yi4 + yi5)}{yt} \quad P_{li} = \frac{(yi2 + yi1)}{yt}, \quad (1)$$

where $I = 1, 2, 3, \dots, n$ indicates n administration quality ascribes. As indicated by information transformation of Eq. (1), exceptionally low coefficient pdi was the smaller the better quality property, as partner assessment factors which is modest influence the nature of development in south India area; thus, the extremely low coefficient was the better; the exceptionally high coefficient psi is the bigger the better quality trait as bigger number addressed the component profoundly influences the structure quality [16]. After information change, I -th disappointment coefficient’s S/N proportion can be addressed by Eq. (2), while I -th fulfilment coefficient S/N proportion was addressed by Eq. (3). Conditions (2) and (3) thought about the distinctions in impression of various clients as well as considering of the typical qualities [19].

$$S/N_{hi} = \eta_{hi} = -10 \log \left(\frac{p_{hi}}{1 - p_{hi}} \right), \quad (2)$$

Table 3 Likert 5-point scale data summary

Levels	1	2	3	4	5	Total
Level	Very low	Low	Neutral	Highly	Very high	
Number of frequencies	y_{i1}	y_{i2}	y_{i3}	y_{i4}	y_{i5}	y_i

$$S/N_{li} = \eta_{li} = -10 \log \left(\frac{1 - p_{li}}{p_{li}} \right). \tag{3}$$

The purpose of the log functions of Eqs. (2) and (3) was to get the addition capability, and the “−” was to make the quality decision-making consistent while $i = 1, 2, 3, \dots, n$ represented n service quality attributes. The greater η_{li} value represented better quality, namely the experience person opinion factors highly affect quality of construction attributes [20]. Meanwhile, the greater η_{li} value represented least negative influencing factor on construction quality attributes. Fowlkes and Creveling suggested that the S/N has the advantage of addition [14]. Hence, when measuring two groups of data under same conditions and calculating their S/N ratios, the results can be added up when maximising S/N ratio [20]. As a result, Eq. (4) integrated with the i -th satisfaction and dissatisfaction data was applied to assess service quality performance.

$$\eta_{li} = \eta_{hi} + \eta_{li}. \tag{4}$$

If the value obtained from the Eq. (4) is higher, then it indicates the factor impact highly over the construction quality. Hence, this research used it to analyse the primary element that affects construction quality performance and establish the order of priority for improvement [17]. This study developed a total of 9 major elements and 54 sub-factors determining quality construction attributes through a literature analysis and expert interviews with industrial representatives, government officials, and scholars, as given in Table 2. We randomly selected samples based on the proportions of construction quality in the south India region to distribute 150 questionnaire copies and receive 105 copies back at a 70% recovery rate. We have $n = 105$ valid samples after deleting 45 invalid questionnaire copies. Table 3 shows the Likert 5-point scale for the number of frequencies.

4 Critical Factors

Through Taguchi signal-to-noise ratio formula, Fig. 2 provides information for analysis data. When A 1 in contractor factors gives a highest S/N ratio of 14.1088 among the six sub-factors which highly affecting quality of construction, followed by A 2 with the s/n ratio of 12.7055 in second place. A 3 and A 4 have s/n ratio of 12.6027

and 10.2593. In lower s/n ratio value, A 5 and A 6 have got 7.6098 and 3.6940 which are least value in these category A of contractor related factor.

In Category B, management related factor is shown in Fig. 3. B1 gives the higher S/N ratio and highly affects the construction quality with the value of 14.1044. B2 has the value of 9.8900 of S/N ratio and B3 value which is slightly lower than B2 of 9.7184. B4 and B5 with value of 9.5479 and 7.2231, B6 has got lower signal-to-noise ratio value of 6.6005 which is comparatively least sub-factor affecting the quality of construction. In Category C, as shown in Fig. 4, there is a technical issue to consider. With a score of 12.1424, C1 has a greater S/N ratio and has a significant impact on the overall construction quality. C2 has a S/N ratio of 11.3239, and C3 has a value of 9.7184, which is somewhat lower than C2's value of 11.3239. C4 and C5 have values of 8.3897 and 8.0536, respectively, while C6 has a lower signal-to-noise ratio of 0.7349, making it the sub-factor that has the least impact on the overall quality of the construction project. Figure 5 provides information for data analysis through the use of the Taguchi signal-to-noise ratio algorithm. When D1 in labour factors provides the highest S/N ratio of 13.4781 among the six sub-factors that have a significant impact on the quality of construction, D2 comes in second with a S/N ratio of 11.0016. The s/n ratios for D3 and D4 are 9.8900 and 9.2003, respectively. D5 and D6 had a lower s/n ratio of 6.6005 and 5.0212, respectively, which are the least significant values in the category D of labour-related factors. In Category E material-related factor, Fig. 6 demonstrates analysis value of signal-to-noise ratio value. Taguchi signal-to-noise value of E1 = 13.2968 which is overhead among other factors in category E. E2 = 12.3277 and E3 = 11.5173 denote second and third highest impact sub-factor in category E, E4 = 9.9156 is next significant factor. Finally, E5 = 8.6034 and E6 = 7.8867 with less signal-to-noise ratio value in category E factor.

Fig. 2 S/N ratio value of contractor factor

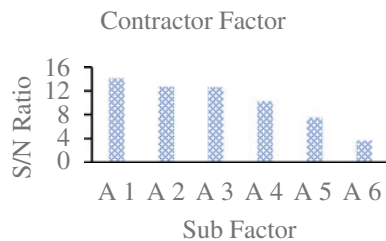


Fig. 3 S/N ratio value of management factor

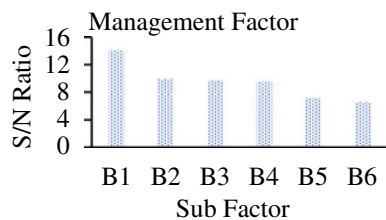


Fig. 4 S/N ratio value of technical factor

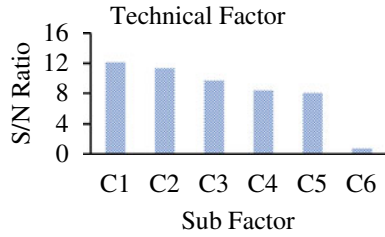


Fig. 5 S/N ratio value of labours factor

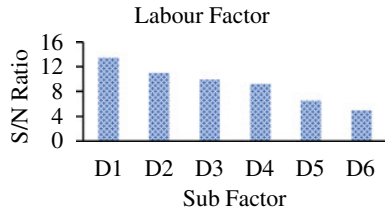
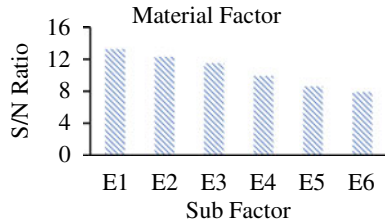


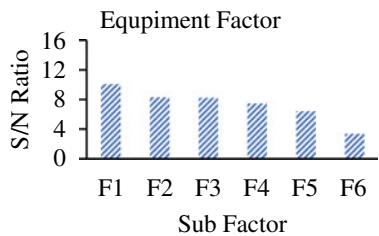
Fig. 6 S/N ratio value of material factor



The Taguchi signal-to-noise ratio technique is used in Fig. 7 to provide information or data analysis. When F1 in equipment factors has the highest S/N ratio of 10.0877 among the six sub-factors that have a massive impact on construction quality, F2 is second with a S/N ratio of 8.3184. F3 and F4 have s/n ratios of 8.2213 and 7.4707, respectively. F5 and F6 showed a lower s/n ratio of 6.4342 and 3.3648, respectively, which are the least severe values in the equipment-related factor category F.

In Category G material-related factor, Fig. 8, the signal-to-noise ratio is analysed. Taguchi G1 has a signal-to-noise ratio of 14.4185, which is above average when

Fig. 7 S/N ratio value of equipment factor



compared to other variables in category G. $G2 = 9.2448$ and $G3 = 8.0919$ signify the second and third most important sub-factors in category G, respectively, while $G4 = 7.9234$ signifies the next major factor. Finally, $G5 = 7.8068$ and $G6 = 7.3038$ have a low signal-to-noise ratio in category G. As seen in Fig. 9, there is an environment factor to address in Category H. H1 has a higher S/N ratio (13.3590) and has a substantial influence on the overall construction quality. H2 has a S/N ratio of 13.2968, whereas H3 has a value of 9.0309, which is somewhat less than H2's 13.2968. H4 and H5 have signal-to-noise ratios of 8.6660 and 4.1014, respectively; however, H6 has a signal-to-noise ratio of 1.6273, making it the sub-factor with the least influence on the overall quality of the building project. I1 has a greater S/N ratio and has a significant impact on construction quality, with a value of 16.2878. I 2 has a S/N ratio of 14.0346, whereas I 3 has a value of 11.7803, which is slightly less than I 2. I 4 and I 5 have values of 11.5361 and 3.7702, respectively, whereas I 6 has a lower signal-to-noise ratio of 0.5290, which is a relatively minor effect impacting the construction's quality.

Taguchi signal-to-noise analysis can identify all the factors that highly impact on construction quality. The overall impacting variable causing quality of construction in south Indian construction industry is seen from Fig. 10. Factors are time scale of the work due to urgency in construction, corruption, and bribery in construction has second high impact factor in construction, lack of contractor supervision and site management, lack of top level management support, client satisfaction, lack of skills (labours), harsh climate condition, lack of inspection and testing, poor soil condition, lack of management leadership, lack of contractors involvement in quality, selection of poor quality material, design complexity, mistakes during construction and rework. Figure 11 shows the top 10 factors that are identified as the most impacted and highly affecting the quality of construction.

Fig. 8 S/N ratio value of political factor

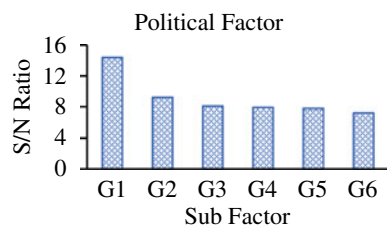
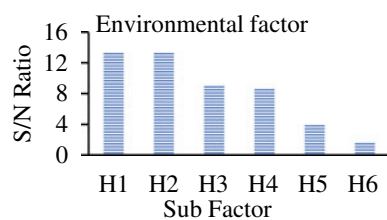


Fig. 9 S/N ratio value of environmental factor



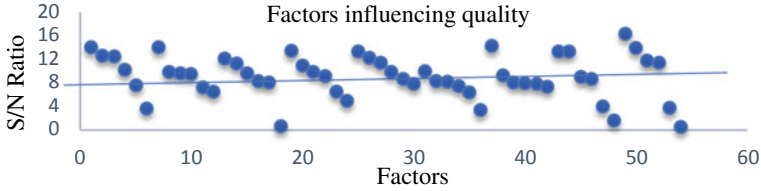


Fig. 10 Overall influencing factor in construction quality

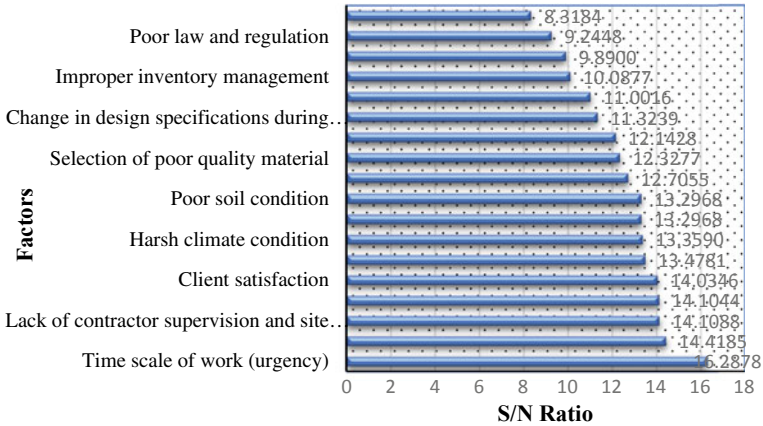


Fig. 11 Top influencing factors in construction quality

5 Conclusion

A successful building project requires high-quality performance. Increased performance may be achieved by examining and enhancing the aspects that have a major impact on the quality. We identified these parameters in our study and collected responses from construction experts via questionnaires. The top 10 impact factors found in Fig. 11 include the following time scale of work (urgency), corruption and bribery, lack of contractor supervision and site management, lack of top level management support, lack of skills (labours), harsh climate condition, lack of inspection and testing, design complexity, improper inventory management through analysed result from Taguchi signal-to-noise ratio. The identified factors pertain to general construction, which includes residential, transportation, and bridge construction, among others. Professionals should prioritise these elements when completing building projects. The construction company should use new technology and establish an effective risk and quality management team [21]. It is necessary to supervise both the material and work on a daily basis for better quality output [22]. The best way to increase the quality of construction projects is through introducing high-quality supply chain management in the project.

References

1. Adenuga OA (2013) Factors affecting quality in the delivery of public housing projects in Lagos state, Nigeria. *Int J Eng Technol* 3:332–344
2. Polat G, Damci A, Tatar Y (2011) Barriers and benefits of total quality management. In: 7th research/expert conference with international participations quality, pp 1115–1120
3. Modi HJ (2017) Analysis top crucial factors of contract clauses and quality in construction projects 4(05):239–243
4. Jha KN, Iyer KC (2006) Critical factors affecting quality performance in construction projects. *Total Qual Manag* 17(9):1155–1170. <https://doi.org/10.1080/14783360600750444>
5. Abas M, Khattak SB, Hussain I, Maqsood S, Ahmad I (2015) Evaluation of Factors affecting the Quality of Construction Projects. *Technical J Univ Eng Technol (UET) Taxila Pak* 20(2):115–120
6. Freddi, Salmon M (2019) Introduction to the Taguchi method, Springer tracts in mechanical engineering. 159–180 (2019). https://doi.org/10.1007/978-3-319-95342-7_7
7. Ealey LA (1994) *Quality by design: Taguchi methods and US industry*, 2nd edn. Irwin, Burr Ridge
8. Karna SK, Singh RV, Sahai R (2012) Application of Taguchi Method in Indian Industry. *Int J Emerg Technol Adv Eng* 2:387–391
9. Nawaz R, Hussain I, Noor S, Habib T, Omair M (2020) The significant impact of the economic sustainability on the cement industry by the assessment of the key performance indicators using Taguchi signal to noise ratio. *Cogent Eng* 7(1). <https://doi.org/10.1080/23311916.2020.1810383>
10. Lee Y, Yen T, Tsai C (2008) Modify IPA for quality improvement: Taguchi's signal-to-noise ratio approach. *TQM J* 20(5):488–501
11. Khattak SB (2020) Assessment of environment conscience construction practices in Pakistan using signal to noise ratio. *J Eng Appl Sci* 38(2):2518–4571
12. Taguchi G, Tsai SC (1995) Quality engineering (Taguchi methods) for the development of electronic circuit technology 44(2):225–229. <https://doi.org/10.1109/24.387375>
13. Peace GS (1992) Taguchi methods. <https://doi.org/10.1604/9780201563115>
14. Fowlkes WY, Creveling CM (1995) *Engineering methods for robust product design*. Addison Wesley Publishing Company, Boston, First Printing, pp 53–58
15. Taguchi G, Chowdhury S, Wu Y (2004) *Taguchi's quality engineering handbook*. Wiley Interscience. <https://doi.org/10.1604/9780471413349>
16. Taguchi G (1987) *System of experimental design: engineering methods to optimize quality and minimize costs*, 1st ed., American Suppliers Institute, Dearborn, MI
17. Kros JF, Mastrangelo CM (1998) Impact of nonquadratic loss in the Taguchi design methodology. *Qual Eng* 10(3):509–519
18. Taguchi G (1991) *Taguchi methods: Signal-to-noise ratio for quality evaluation*. 1st Edition, American Suppliers Institute, Dearborn, pp 78–80
19. Das D, Chatterjee A (2014) Taguchi and ANOVA approach for optimization of flow characteristics of self-compacting concrete. *Emerg Mater Res* 3(1):37–45. <https://doi.org/10.1680/emr.13.00016>
20. Lee J, Lamberson L (2003) Evaluation of the distribution of Taguchi's signal-to-noise ratio and the effectiveness of the signal-to-noise ratio for detecting changes in the mean and/or variance 1425304, pp 189–189
21. Joseph VR, Wu CFJ (2002) Operation window experiment: a novel approach to quality improvement. *J Qual Technol* 34:345–354
22. Hellard RB (1993) 4 General application of total quality management to construction projects. *Total Qual Constr Project* 81–89. <https://doi.org/10.1680/tqip.19515.0006>

Constructive Project Management System in Construction Industry



R. Balamurugan, R. Sivakumar, K. Srinivasan, Ravi sankar, and M. Anand

1 Introduction

The importance of project management is significant for all organizations, regardless of their size. As businesses undertake new projects, they often face challenges related to cross-functional expertise and the development of complex products, services, and processes within tight timeframes to maintain a competitive edge. Consequently, project management becomes a critical and powerful tool for businesses that possess the necessary understanding and skills to utilize it effectively. When organizations develop task management skills and implement records management systems, project management can evolve into a crucial mechanism. It enables enterprise teams to collaborate, define plans, and effectively manage their efforts to bring products and services to market. By synchronizing team-oriented tasks, schedules, and resources, organizations can streamline their operations and stay ahead in the market.

1.1 Construction Development

The building industry encompasses companies engaged in various activities such as designing, manufacturing, modifying, renovating, maintaining, managing facilities, demolishing, and recycling building and civil engineering projects. Additionally, the industry includes the supply of resources necessary for these activities. The

R. Balamurugan (✉) · K. Srinivasan · Ravi sankar
Department of Civil Engineering, Annamalai University, Cuddalore 608002, India
e-mail: pmbala1978@gmail.com

R. Sivakumar
Department of Business Administration, Annamalai University, Cuddalore 608002, India

M. Anand
Department of Civil and Structural Engineering, Annamalai University, Cuddalore 608002, India

overall success of this industry relies on the collaborative efforts of both internal and external stakeholders who adhere to the industry's regulations, practices, norms, and culture. In essence, the building industry thrives when all participants work together in alignment with the established guidelines and shared values.

Businesses that are engaged in the creation, manufacturing, refurbishment, upkeep, facility management, deconstruction, and recycling of buildings and civil engineering projects are included in the category of construction improvement businesses. These firms also provide the necessary resources. These businesses, along with a wide variety of stakeholders both internal and external, contribute to the formation and maintenance of the norms, practices, and culture of the industry.

A planned and methodical strategy that aims to improve the efficiency and potential of a sector is an example of what we mean when we talk about the growth of the building industry. This comprises efforts aimed at optimizing overall efficiency, as well as enhancing overall construction processes, promoting creativity, applying environmentally sustainable practices, and creating an innovative environment. It is absolutely necessary for the industry to make such development efforts in order to adapt to the ever-changing demands, technical breakthroughs, and societal expectations. The construction sector may expand its capacities, secure its continued sustainability over the long term, and make a contribution to the overall development and prosperity of the communities it serves if it places a priority on continual improvement.

2 Review of Literature

Bennett [1] conducted a research study to explore the concept of project control within the production process. The study's findings revealed that project control comprises two crucial elements. The first facet is strategic, and it entails gaining a grasp of the customer's desired outcomes, elaborating on the purpose, and coordinating this with the larger commercial enterprise. The second component concentrates on the necessary tasks that must be completed during the building process. This research places an emphasis on the significance of these ideas and draws attention to the interconnections that exist between them. The report comes to the conclusion that building projects should combine control, design, and production procedures, and then transform such integrations into clearly defined jobs.

In a separate piece of research, Akinradewo (2019) explores the influence that building project design has on the wages of contractors. The findings of this study highlight how critical planning is to the delivery of any project on time and within budget. It places an emphasis on the necessity of anticipating the nature of the assignment, identifying potential risks, and allocating the required resources in order to accomplish the goals of the organization. The investigation used both qualitative and quantitative approaches to research methodology. A well-structured questionnaire was used to validate the data acquired during the interviews that were done to collect essential information from respondents. The interviews themselves

were conducted to collect crucial information from respondents. Quantity surveyors, builders, engineers, and designers were some of the professionals who took part in the research.

The results of the study indicated that there is a considerable connection between construction planning and the earnings that may be made by a contractor on a particular project. Furthermore, the study emphasized the importance of carefully planned contracts in reducing waste at construction sites, maximizing labor efficiency, ensuring timely project completion, enhancing quality, and optimizing resource utilization. It highlighted that when these elements are effectively implemented, they collectively contribute to increased profitability for contractors.

3 Research Methodology

The research methodology that will be used for this study will be described in detail, which will shed light on the way the research will be carried out. This will include specifics on the methodology of data collecting, the framework for the sampling that will be used, and the overall design of the study. The method of conducting research can be efficiently structured, which will ensure that dependable and legitimate results are obtained, provided that these aspects are determined. In addition, the restrictions that were placed on the research will be discussed in great detail. For the sake of maintaining transparency and gaining an awareness of the bounds within which the findings of the study can be understood, it is essential to acknowledge the limitations and potential faults of the research. This will make it possible for researchers as well as readers to critically assess the findings and draw suitable conclusions based on the information that is currently accessible. This study intends to give valuable insights to the field of inquiry by outlining the research technique, resolving any limits, and giving a clear framework for data collecting and analysis. In general, these steps will help the study contribute to the field.

3.1 Objectives of the Study

The study aimed to assess two aspects related to project management. Firstly, it aimed to explore the extent to which respondents utilize project information. This would provide insights into how effectively project data is being utilized in decision-making and project execution. Secondly, the study aimed to examine the impact of construction development on project management income. By analyzing the relationship between construction development and project management income, the study sought to understand whether improvements in construction practices lead to financial benefits for project managers. These two objectives together formed the focus of the study.

3.2 Hypothesis

- Respondents drastically range in their stage of use of undertaking facts.
- There is not any great distinction between production improvement and undertaking control earning.

3.3 Sampling Technique

To acquire the important information, a random sampling technique could be followed.

3.4 Sample Size

50 samples have been selected based totally on the stratified random sampling technique.

3.5 Statistical Tools Used

Statistical tools which include the t-test and the F-test had been used.

4 Result and Discussion

The study provides comprehensive data on the average, standard deviation (SD), and F-value regarding the level of task record usage among the respondents. The calculated F-value indicates a significant difference in the respondents' level of venture information usage. Based on this, the alternative hypothesis is accepted, and the null hypothesis is rejected. The computed F-value of 4.20 is deemed significant at the 0.01 level. Therefore, it can be concluded that the respondents utilize project records to varying extents (Fig. 1; Table 1).

Table 2 provides a comprehensive overview of the implications, standard deviation (SD), and t-value regarding the influence of the respondents' stage of production development on project management earnings. The obtained t-value (3.16) demonstrates a significant difference in the impact of the respondents' level of construction development on project management income. The significance level of 0.01 further supports this finding. Consequently, the alternative hypothesis is accepted, while the null hypothesis is rejected. Based on these results, it can be inferred that the level of

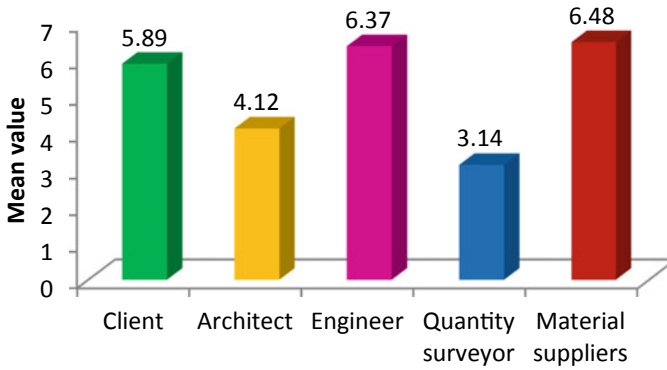


Fig. 1 Showing mean value for respondents level use of assignment facts

Table 1 Showing mean, S.D, and F-cost for respondents level use of assignment facts

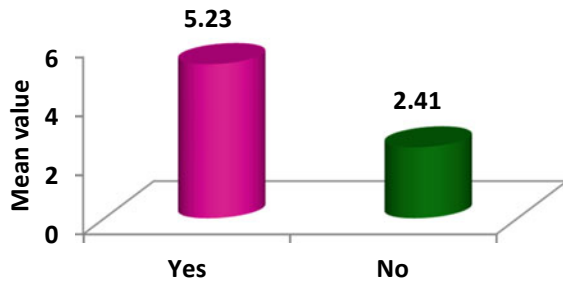
Information producer	Mean	S.D	F-value	P-value
Client	5.89	1.42	4.20	0.01 Significant
Architect	4.12	1.03		
Engineer	6.37	2.07		
Quantity surveyor	3.14	0.85		
Material suppliers	6.48	2.13		

production development among the respondents has a substantial impact on project management profit (Fig. 2).

Table 2 Showing mean, S.D, and t-price for respondents stage of construction development have an effect on in task management profit

Opinion	Mean	S.D	t-value	P-value
Yes	5.23	1.74	3.16	0.01 Significant
No	2.41	0.63		

Fig. 2 Showing mean of construction development have an effect on in task management profit



5 Conclusion

The evaluation of project management in relation to the enhancement of output is going to be carried out in the context of this present look at. Project management on a wide range of scales has been successfully implemented over the course of many years. The purpose of this study is to investigate the effect that creation development has on the earnings of project management. In the course of the research, a method known as stratified random sampling was utilized to collect fifty different samples. The researcher utilized statistical methods including t-tests and F-tests in their work. According to the findings, variations in the levels of production development of the respondents have an effect on the income generated by project management. In addition, the research indicates that project managers are in possession of distinctive skills and values that enable them to actively encourage creation improvement at many levels, including initiatives at the grassroots level. The project management team for the production improvement program has undergone essential training and possesses sufficient knowledge, skills, and experience to effectively manage a project.

Findings

The discovering of the study changed into that the outcomes found out that respondents differed of their diploma of use of challenge statistics. Further consequences propose that there may be a giant distinction inside the respondent's level of construction development's effect on assignment administration income. The calculated t-price (three.16) is widespread at the zero.01 degree. As a result, the exchange hypothesis is widely accepted and the aforementioned null hypothesis is disproved. Thus, it has been determined that respondents' levels of production development have an impact on their income from project management.

References

1. Bennett's J (2016) Observe on task control in production. *Int J Proj Manage* 6(2):Sixty nine–79
2. Kinradewo (2019) Impact of construction mission making plans on contractor income. *J Earth Environ Sci* 385(8):145–156

3. Ng TS, Chan APC, Wong JWM, Ng JWS (2007) The converting panorama of the unpublished MSc thesis. University of Salford
4. Walker A (2007) Project management in construction. Blackwell, Oxford
5. Johnson, Hall JE (2002) Integrated project management. Prentice Hall
6. Palestinian Contractors Union (2011) www.Pcu.Playstation
7. Committee, PMI Standards (1996) Guide mission management body of knowledge PMBOK. 1996. 0.33 edition
8. Kerzner H (2006) Project management a system approach to planning scheduling and controlling, vol 1. Willey, Ohio
9. Follett MP (1949) Freedom and Co-ordination: lectures in commercial enterprise corporation. Pitman, London
10. PMBOK (2006) Guide project management body of knowledge

Scheduling Time and Cost by Integrating Quality and Risk in Construction Projects



N. Sai Krishna and S. M. Renuka

1 Introduction

Construction projects involve many challenges such as the inflation of materials prices, accidents, reduced investment in the real estate sector, the effect of natural disasters, and improper estimation of the project budget. These challenges may be solved by properly taking care of quality and risk in any construction work. Risk and quality are important parameters for the good execution of a construction work [1]. Lack of risk and quality controls may have an impact on output and workmanship [2]. The cost and duration of a project may increase if these two criteria are balanced [3]. Thus, it is crucial to consider duration, expense, and value factors in tandem during the initial process. Instead of using MS Project's scheduling software, a technique to tackle multi-objective scheduling problems using Matlab's software can be used to build an optimized decision-making model. Although risk and quality exert significant role in enhancing productivity during implementation of the project, these two parameters together have not yet been undertaken in most of large scale scheduling problems [4]. Due to this, many defects occur in construction which is covered in Fig. 1a and b.

The study's main objectives are to construct a scheduling model to solve compromise issues between duration, expense and quality to (1) incorporate quality and risk into a scheduling model. The scope includes a framework model for quality and risk in a building project that was developed for scheduling problems with time and expense. This methodology enables multi-objective optimisation solutions and the resolution of large-scale scheduling problems.

N. S. Krishna · S. M. Renuka (✉)

Division of Structural Engineering, Department of Civil Engineering, CEGC, Anna University, Chennai 600025, India

e-mail: renuka@annauniv.edu

N. S. Krishna

e-mail: saik32383@gmail.com



Fig. 1 a Quality defects in construction, b Risk defects in construction

1.1 Literature Review

The review of the literature is presented subsequently along with development of model. After the analysis of results in detail, conclusions with findings have been done and presented.

1.2 Review of Trade-Off

When solving the multi-objective scheduling problem, Alavipour and Arditi [5] and Feng et al. [6] deal with time and cost in their main research. In most of the trade-off problems, quality and risk were taken as independent factors.

1.3 Trade-Off Time Cost Quality Models

Babu and Suresh [7] have told that quality may be affected by crashing the activity. So, he made a scale from 1 to 0 to measure the quality of the overall project, where 0 represents fully crashed activities and 1 represents normally crashed activities. In other study by Khang and Myint [8], three linear programming models that optimized one parameter and used other parameters as boundary conditions were used in a factory that made cement. Ghodsi and Skanderi [9] categorized the [8] dilemma as a continuous TCQ trade-off problem. El-Rayes and Kandil [10] developed a 3D model to solve the TCQ problem using a genetic algorithm. In his study, different quality indicators were taken into account to measure quality. Afshar et al. [11] used the quality indicators from research done by El-Rayes and Kandil [10] and developed a model using the ACO algorithm to generate Pareto optimal solutions with the minimum number of iterations.

1.4 Time Cost Risk Models that Trade-Off

Only a few studies have examined TCR trade-offs. Lakshminarayanan et al. [12] proposed a multi-objective optimization model (MOOM) to minimize the time and cost of projects (inclusive of risk) as a multi-objective optimization of time cost risk. From the results, it is found that the model proposed gives fine results when compared to MAWA and comparable results when compared to MOACO. Asadabadi and Zwikael [13] have integrated risk into estimations of time and cost through concept of stratification. The results provide a unique structure that is capable of considering uncertainty related to events and by determining specific activity's estimated time and cost, the project's estimated time and cost can also be calculated. Nwaneri and Anyaeche [14] suggest an optimization methodology for TCQR in trade-off projects utilizing a genetic algorithm with several targets. The findings of this study demonstrate that solutions with Pareto optimality were produced, from which the decision-maker can select a sample 18-activity project based on his preferences. A study titled integrating quality and safety in construction scheduling time–cost trade-off model was written by Panwar and Jha [15]. According to this study, an evolutionary algorithm was developed in an effective manner to optimize time and cost.

1.5 Multi-Objective Optimization Review

A work titled multi-objective optimization of time–cost–safety using genetic algorithm aims to design an optimization model that simultaneously reduces overall safety risk (OSR), total cost, and time. The OSR of non-dominated solutions is improved by assessing the risk techniques and applying it into TCO issues, according to the results. Quality and risk information had previously been presented independently in studies using trade-off models.

2 Methodology

2.1 Formulation of Problem for Scheduling the Project Involving Construction

Time: Time refers to a project's duration, which is commonly expressed in calendar days, weeks, or months. The length of the project as a whole plays a significant role in defining the project's cost, quality, and viability.

Objective 1: Optimization of Time:

$$T = \sum \text{ticp} \quad (1)$$

where T is the project's overall duration.

The duration associated with each activity on the critical path is known as ticp.

Cost: Cost in construction refers to the amount of money required to complete a construction project. This can include expenses related to materials, labour, equipment, permits, and contingencies.

Objective 2: Optimization of Cost:

$$C = (DCi + ICi), \quad (2)$$

where C is the project's overall cost.

DCi stands for direct project costs.

ICi stands for the overhead or indirect cost.

Quality: The level of perfection and consistency attained in the construction process and the final result is referred to as quality in construction.

Objective 3: Optimization of Quality

$$Q = \sum w_i \sum_{p=1}^P (w_p \times q_p) \quad (3)$$

where Q represents the project's quality and w_i is the activity's weight.

For the third quality indicator, w_p stands for the weight of the eighth activity.

q_i, p = performance of the i th activity's quality indicator value for the p th quality indicator.

Risk: Risk in construction refers to the uncertainty and potential for loss associated with a construction project.

Objective 4: Optimization of Risk:

$$R_i = \sum_{k=1}^K (L_k \times S_k) \quad (4)$$

where R_i is the risk posed by the action; L_k = Probability of k th risk

S_k is the k th risk's severity index.

In risk management, the likelihood of risk is often evaluated on a scale, such as remote, unlikely, possible, likely, probable, and highly probable to provide a qualitative assessment of the risk with values (1, 2, 3, 4, 5, 6). The impact of a risk is frequently assessed in risk management using a scale with categories like illness, minor injuries, accidents, serious injuries, and reportable injuries and fatality.

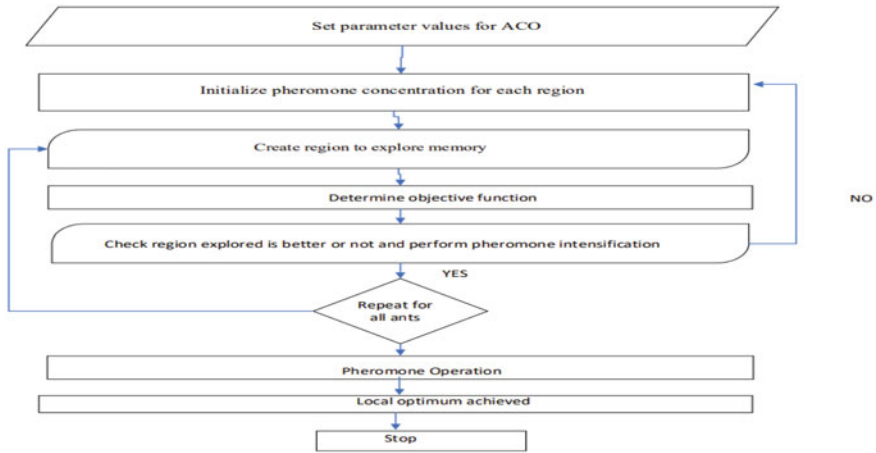


Fig. 2 ACO modelling for TCQR trade-off flow chart

2.2 Developed Multi-Objective ACO Model

The development process of the ACO model is shown in Fig. 2

2.3 List of Overall Data from Residential Buildings and from Large Scale Commercial, Industrial Buildings

Table 1 discusses the overall cost, time, risk, and quality obtained from five residential projects. Comparing the five projects, the project 1 has the lower time and cost. Project 5 has the higher quality, whereas the fourth project has the minimum risk. Table 2 discusses about the overall data obtained from twelve G+3 commercial, residential, and industrial projects. These data are calculated from the optimization equations. Comparing the twelve projects, the 7th project has lower time and cost, max quality than risk. The eighth project has the maximum quality and less risk. So, in both cases, the optimal solution is required to minimize time and cost with respect to maximizing the quality and minimizing the risk.

2.4 Optimal Solution Obtained from ACO Algorithm

The variations of TCQR for five residential projects and twelve large-scale residential, commercial, and industrial projects were shown in Figs. 3 and 4. The optimal solutions obtained using ACO algorithm is also represented in figures. From this, it can be interpreted that, among the 5 projects, the fourth project shows the optimal

Table 1 List of overall data collected from five residential projects

S. No	Time (in days)	Cost (in Rs)	Quality (in %)	Risk
1	105	1,794,000	85.73	293
2	185	5,152,000	80.83	254
3	257	34,500,000	88.14	268
4	150	46,500,000	82	151
5	178	2,774,614	94.42	312

Table 2 List of overall data

S. No	Time (in months)	Cost (in Rs)	Quality (in %)	Risk
1	18	30,000,000	82.28	186
2	12	30,000,000	85.76	208
3	10	17,662,880	94.23	150
4	12	29,100,000	79.72	200
5	12	42,300,000	93.5	172
6	8	32,850,000	86.81	208
7	7	4,049,526	92.4	116
8	28	13,623,537	94.36	75
9	29	15,920,975	93.24	94
10	24	9,227,991	85.24	94
11	18	32,500,000	93.56	84
12	30	11,006,984	90.81	94

solutions and among the 12 projects, the second project shows the optimal solutions regarding Time, cost, quality and risk.

A residential project data for 31 activities with sufficient data were collected and checked for optimizing time and cost with respect to constraints quality and risk in order to validate the model developed using ACO.

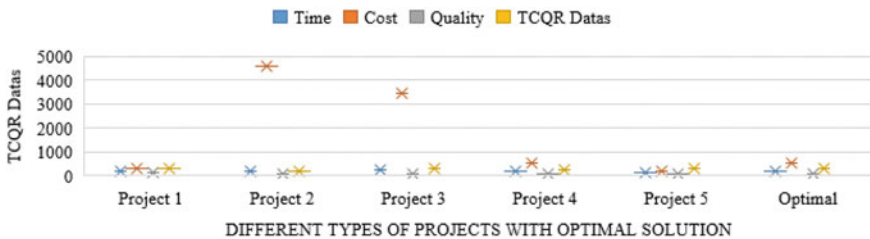


Fig. 3 TCQR plot of residential building

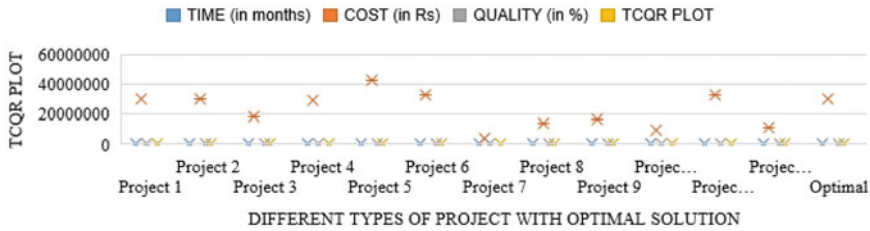


Fig. 4 TCQR plot of large-scale commercial, industrial buildings

3 Results and Discussions

The simulation findings are explained in this section using an example. This requires performing and fine-tuning the optimisation algorithm’s parameters, which include alpha, beta, rho, Q, and ants.

3.1 Verification of the Model

ACO is contrasted with SA and HC algorithms in Table 3. The optimal solutions found using ACO are 150 days, Rs.5152000, 94.42%, and 268. From SA algorithm, the values are 300 days, 30,105,510, 90.58, and 238.6. From Hill Climbing algorithm, the values are 150 days, Rs 44,953,504, 80.42%, and 138.76. From these comparisons, ACO has the best solutions regarding time, cost, and risk. In terms of quality, SA has the best solutions. So, our aim is to, with respect to constraints risk and quality, the time and cost must be reduced. So, ACO will be the best algorithm to be preferred compared to the other two regarding optimization of time and cost.

The optimal solutions at various stages of construction were interpreted in Fig. 5 using ACO algorithm as it is the best algorithm. From the Figure, it can be interpreted that, there is more time required in the planning and design stage with less quality and risk. So, if ACO is applied first itself in this stage, The TCQR variations in the next stage, i.e. substructure stage can be reduced. Thus, the optimal solutions can be obtained at all the stages.

Table 3 Comparison of ACO with other algorithms

Algorithm	Optimal Solution			
	Time (in days)	Cost (in Rs)	Quality (in %)	Risk
ACO	150	5,152,000	94.42	268
Simulated annealing	300	30,105,510	90.58	238.6
Hill climbing	150	44,953,504	80.42	138.76

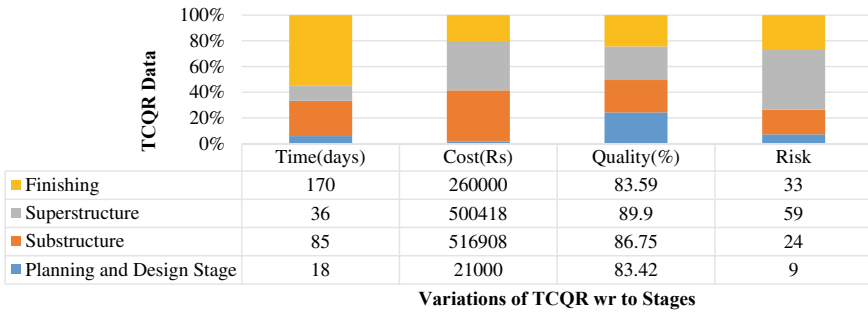


Fig. 5 Optimal solutions of TCQR for different stages of residential building

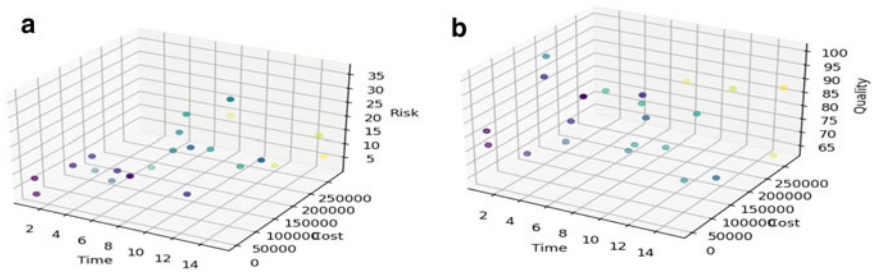


Fig. 6 **a** Trade-off curve for TCQ, **b** Trade-off curve for TCR

The TCQ and TCR trade-off graph depicts the link between time required to complete a project, its cost, and the quality and degree of risk involved. Time, money, and quality are the three axes of a graph. The cost of a project rises as it takes longer to finish, and depending on how the project is handled, the quality of the product may also rise or fall. Similarly, the level of risk involved with it may also rise or fall. In this case study, let us check the optimality of time and cost with respect to quality and risk through TCQ and

TCR trade-off graph shown in Fig. 6a and b. Interpreting these trade-off graphs is important because it helps project managers to make informed decisions about how to manage their projects.

3.2 Correlation Analysis

Correlation Analysis: The following steps can be used to analyse the correlation between variables using SPSS: Open your data set in SPSS after launching it. Choose “Correlate” from the “Analyse” menu in the top menu; Select “Bivariate” under “Correlate” in the menu. Using the arrow button, move the variables you want to correlate from the left column to the right column. If you want to use Pearson’s

correlation coefficient, which is suitable for continuous data, tick the box for “Pearson” under “Correlation Coefficients.” To carry out the correlation analysis, click “OK.” A correlation matrix that displays coefficients of correlation between each variable’s pairs will be produced by SPSS. You can also get the p-values for each correlation coefficient to determine the correlations’ statistical significance. A -ve correlation represented by -1 , + ve through 1 and no correlation by 0 . For this, select “Sig. (2-tailed)” from the “Options” drop-down menu in the “Bivariate Correlations” dialogue box. The correlation matrix will gain p-values as a result. The results are given in Table 4.

A 0.05 level of significance (2-tailed) for correlation.

The following conclusions can be drawn from the table:

Time and expense: Time and cost are not linked as indicated by -0.403 . There is a tendency, even though it is not at the proper level of 0.05 , that may suggest that cost tends to decline as time passes.

Time and Quality: Time and quality are + vely correlated, with a 0.194 . In this data set, there is a correlation between time and quality, although it is not significant. Hence, this association is not noteworthy.

Time and Risk: The inverse link between time and risk is too significant, with 0.703 . This shows that the safety risk score decline as time goes on.

Cost and Quality: There is a pattern that shows that quality tends to drop as expenses rise.

Cost and Risk: Cost and risk are positively correlated, as shown 0.648 . According to this, cost tends to drop as risk increases.

Quality and Risk: A correlation value of -0.617 shows a negative connection between quality and risk, indicating that as quality rises, the safety risk score tends to decline.

In general, these correlations shed light on how the variables are related to one another. For instance, increasing time may cause the safety risk score to fall, while increasing cost may cause the safety risk score to increase.

Table 4 Parameters of time, money, value, and danger for correlation

Parameters	Time	Cost	Quality	Risk
Time	1	-0.403	0.194	-0.70
Cost	-0.403	1	-0.236	0.648
Quality	0.194	-0.236	1	-0.617
Risk	-0.703	0.648	-0.617	1

4 Summary

The performance criteria that influence duration and expense of any project are quality and risk. A MOSP that incorporates these criteria offers a comprehensive building schedule. However, it wasn't noted in earlier research. This was because of the potential for exponential growth as activities rises. On the basis of ACO, a multi-objective optimisation model was developed to manage it. The trade-off between objectives is addressed by the model. A study on TCQ and TCR gathered from the literature was conducted to show the model's supremacy. The achieved solution shows that the model is capable of handling MOSPs. The proposed model also offers the ability for the construction stakeholders to include parameters of interest and can handle more than three objectives. It has been found that an approach with several schedules optimizes all four goals. This would make the makers of decision to utilize the optimized model throughout the project's actual planning phase. Construction projects in the real world are fraught with ambiguities and uncertainties; therefore, it would be exciting to see the model put to use in a scenario of probabilities and data sets with fuzzy logic for the TCQ trade-off.

Future research may focus on finding sensitivity analysis and to compare the solution with Pareto optimal solutions and hence optimize the cost.

Acknowledgements Thank construction professionals for providing data for doing research. This research doesn't have any financial support.

References

1. Ogwueleka AC (2013) A review of safety and quality issues in the construction industry. *J Constr Eng Proj Manage* 3(3), Jan 2013
2. Li H, Chan G, Skitmore M (2012) Multiuser virtual safety training system for tower crane dismantlement. *J Comput Civ Eng* 26(5), Sept 2012
3. Doloi H, Sawhney A, Iyer KC, Rentala S (2012) Analysing factors affecting delays in Indian construction projects. *Int J Proj Manage* 30(4):479–489
4. Jain H, Deb K (2014) An evolutionary many-objective optimization algorithm using reference-point based nondominated sorting approach. Part II: handling constraints and extending to an adaptive approach. *IEEE Trans Evol Comput* 18(4):602–622
5. Alavipour SM, Arditi D (2018) Time-cost tradeoff analysis with minimized project financing cost. *Autom Constr* 98:110–21, Nov 2018
6. Feng, H., Liu, L. and Burns, S.A. "Using genetic algorithms to solve construction time-cost trade-off" *J. Comput. Civ. Eng.*, July 1997.
7. Babu AJG, Suresh N (1996) Project management with time, cost, and quality considerations *Eur J Oper Res* Jan 1996
8. Khang DB, Myint YM (1999) Time, cost and quality trade-off in project management: a case study. *Int J Project Manage* Aug 1999
9. Ghodsi R, Skandari M (2009) A new practical model to trade-off time, cost, and quality of a project. *Aust J Basic Appl Sci* 3(4). ISSN 1991-8178
10. El-Rayes K, Kandil A (2005) Time-cost-quality trade-off analysis for highway construction. *J Constr Eng Manage* Apr 2005

11. Afshar A, Kaveh A, Shoghli OR (2007) Multi-objective optimization of time-cost-quality using multi-colony ant algorithm. *Fuzzy Sets Syst*
12. Lakshminarayanan S, Gaurav A, Arun C (2010) Multi-objective optimization of time-cost-risk using ant colony optimization. *Int J Proj Plann Finance* 1(1):2010
13. Asadabadi MR, Zwikael O (2021) Integrating risk into estimations of project activities' time and cost: a stratified approach. *Eur J Oper Res* 291:482–490
14. Nwaneri SC, Anyaeche CO (2015) Time-cost-quality-risk trade-off in engineering projects. *Int J Manag Appl Sci* 9:2394–7926
15. Panwar A, Jha KN (2021) Integrating quality and safety in construction scheduling time-cost trade-off model. *J Constr Eng Manag* 147:04020160

Flexural Behavior of Reinforced Beam Mixed with Copper Slag and Jute Fiber



V. Swaminathan, R. Ramasubramani, P. T. Ravichandran,
and Rakshit Srivastava

1 Introduction

In nowadays, structural concrete is widely employed in the construction of many types of structures, with approximately one tonne consumed for every living human being. Due to its flexibility, toughness, sustainability, and affordability, the world's most popular building material is concrete. The civil engineering industry dealt with material alteration by the substitution of industrial waste material and industrial by-products as a full or partial basis. In comparison to traditional cement, concrete constructed with such components showed improved usefulness and strength and has been used in the production of high intensity, artificial plant, and underground projects. "High performance concrete" is a concrete mixture that meets certain characteristics developed for a specific environment, such as high durability, high strength, and high workability, as well as the addition of additives such as chemical and mineral admixtures, and is designed to outperform ordinary concrete. The relative mixes of new materials under development in the qualities are referred to as high strength concrete. Fiber-reinforced concrete was developed after it was discovered that adding small, tightly spaced, and uniformly dispersed fibers to concrete would function as a crack arrester and significantly increase the concrete's compressive and flexural strength qualities [1].

V. Swaminathan · R. Ramasubramani (✉) · P. T. Ravichandran
Department of Civil Engineering, College of Engineering and Technology, SRM Institute of
Science and Technology, Kattankulathur, Tamil Nadu 603203, India
e-mail: ramasubr@srmist.edu.in

R. Srivastava
Saraswati Higher Education and Technical College of Engineering, Varanasi, Varanasi, India

1.1 Copper Slag

Sometimes copper slag can be used in place of some of the natural sand while making concrete. Stones made from copper slag are used in building. The interested parties' copper smelter produced crystalline copper slag that was heavily used for road construction in locations where burning was practiced. The heating and draining capabilities of granular slag can be used to prevent this winter's floor frost, which could result in pavement fractures [1]. The usage of this slag reduces the number of main raw materials used and the depth of development, lessening the structure's energy requirement. The manufacturing of grating equipment and the sand impacting sector both make extensive use of copper slag, with the remainder being wasted with no further use or recovery. A by-product of smelting and processing copper matte is copper slag [2].

1.2 Jute Fiber

Jute fiber is a multi-composite composite consisting predominantly of cellulose, glucans, and lignin, with traces of nutrients another inorganic. Jute has a high tensile strength in comparison to other fibers including sisal, bamboo, coir, and hemp. Apart from its tensile strength, jute fiber is also heat resistant. The natural fiber is 100% compostable as well as recyclable, offering it an environmentally friendly option. Jute is a golden-colored natural material with a smooth feel, earning it the moniker "golden fibers." The line with the basic nor skin of both the plant stem is used to make jute, the cheapest agricultural fiber [3]. Jute is ideal for agricultural commodity bulk shipment due to its high strength, moderate extensibility, and increased breathability of textiles. It helps to make growing industrial fiber fabric, meshes, and bags (Figs. 1 and 2).

Fig. 1 Copper slag



Fig. 2 Jute fiber**Table 1** Optimization of fibers

B1	Conventional beam
B2	Copper slag 20%, Jute fiber 0.5%
B3	Copper slag 30%, Jute fiber 1%
B4	Copper slag 40%, Jute fiber 1.5%

2 Materials Used and Mix Proportions

Copper slag was substituted for the fine aggregate in the mix in accordance with Indian Standard IS 12269:1987, along with regular Portland cement (53 grade), coarse aggregate, and water size is 10 mm aggregate and jute fiber is an overall addition, superplasticizer (Conplast SP430) to compare things. When combining and curing, water was utilized. And we are casted different mix proportions on M80 grade of concrete with conventional beam, (20%, 30%, 40%) of copper slag and (0.5%, 1%, 1.5%) of jute fiber (Table 1).

3 Design and Details of Beam

The details of the beams we are molded beam size of $2000 \times 200 \times 250$ mm. And we casted four beams for different mix proportions. Four beams were created in each case as single-reinforced beams (Fig. 3; Table 2).

And we have provided a main reinforcement 4 nos of 10 mm dia bar, 2-legged-8 mm dia bars as stirrups, vertical stirrups 2 legged-8 mm dia spacing @ 150 mm c/c. And nominal cover 25 mm (Fig. 4).

Fig. 3 Molded beam



Table 2 Mechanical properties of materials

S. No	Index of materials	Values
<i>Cement</i>		
1	Specific gravity of cement	3.14
2	Standard consistency	31%
3	Setting time and initial setting time	35 min
<i>Fine aggregate</i>		
4	Specific gravity	2.68
5	Fineness modulus	2.14
6	Sieve analysis zone	ZONE—II
<i>Coarse aggregate</i>		
7	Specific gravity	2.87
8	Fineness modulus	3.1
<i>Copper slag</i>		
9	Specific gravity	3.3
10	Fineness modulus	3



Fig. 4 Reinforcement of beam

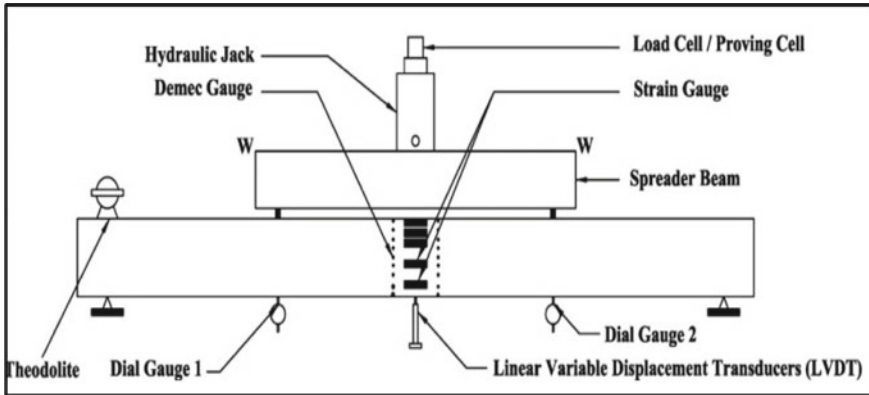


Fig. 5 Schematic diagram of flexural test beam arrangement

3.1 Properties of Concrete

In mechanical properties of materials as like, cement, fine aggregate, coarse aggregate, copper slag, jute fiber is tested a specific gravity, standard consistency, setting time and initial setting time, and fineness modulus.

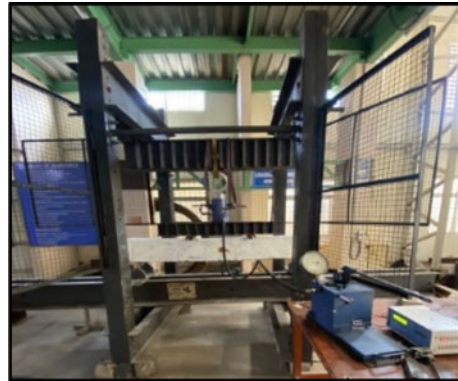
3.2 Specimen Preparation and Instrumentation

Molds made of plywood were constructed based on the anticipated beam size. And through a hydraulic jack, we lift a beam place it on testing frame. And we setup a beam in testing frame in support position. And making a beam it is $2000 \times 200 \times 250$ mm in that 10 mm cover, 600 mm from cover at both side marks at top of the beam [4–7]. And set a center of beam on testing frame, and set a hydraulic jack on a beam, set a proving ring, dial gauge, strain indicator on over a surface on the beam (Fig. 5).

3.3 Testing of Flexure Beam

The beam was painted white before testing, and a strain gauge’s mounting point was marked in exterior surface of concrete, effective span, and neutral axis (Fig. 6).

Fig. 6 Flexural testing frame



4 Results and Discussion

4.1 General

All of the beams' flexural behavior exhibited normal structural characteristics. The inside and outside margins of the beams or rod are the "extreme fibers." The greatest tensile stress a beam or rod can sustain before breaking is its ability to bend since nearly all substances fail with tensile stress earlier compressive stress [8, 9]. If the substance was homogenous, the flexural strength and tensile strength would remain the same. In actuality, most materials include minor or significant flaws that operate to concentrate pressures locally, resulting in a localized weakness. Only the extreme filaments of a material experience the greatest stress during bending; therefore, the substance's flexural strength will depend on how strong the intact "fibers" are. All of the material's fibers would be stressed equally if just bending forces were used, and failure would begin when the most fragile fiber reached its maximum tensile stress. As a result, flexural strengths are usually greater than tensile values for the same material. A homogenous material, on the other hand, may have a higher tensile strength than flexural strength if the only imperfections are on its surface (Fig. 7; Table 3).

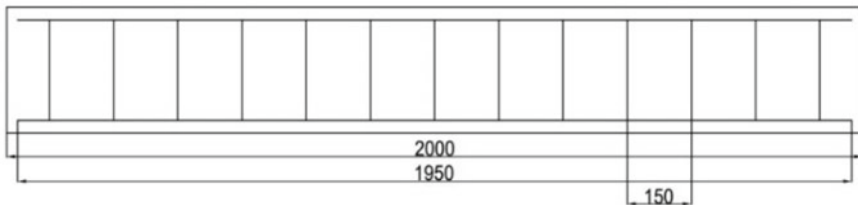


Fig. 7 Reinforcement of beam

Table 3 Beam details (2000 × 200 × 250 mm overall)

Beam no	Beam type	Tension reinforcement nos and size (mm)	Nominal /compressive reinforcement (mm)	Area of tensile, A_{st} (mm ²)	$P = A_{st}/bd$ (%)
B1	Singly reinforced (CC and CSJFC)	2Y10	2Y10	153.15	0.3
B2	Singly reinforced (CC and CSJFC)	2Y10	2Y10	153.15	0.3
B3	Singly reinforced (CC and CSJFC)	2Y10	2Y10	153.15	0.3
B4	Singly reinforced (CC and CSJFC)	2Y10	2Y10	153.15	0.3

CC–Concrete control, CSJFC–Copper slag jute fiber concrete, P–Percentage of reinforcement, Y–High yield strength deformed bar.

4.2 Ultimate Loads

Tables 4 and 5 provide the measured loads, moments, theoretically designed loads, and moments at the service stage and ultimate phases. As advised by and IS 456:2000, the theoretically calculated moment for the beam was anticipated [10]. It is discovered that the tests' last moment was approximately from B2, B3, B4 is higher than CC beams 20–70%. And compare to experimental loads and theoretical.

4.3 Deflection Behavior

Generally, the load–deflection patterns of all beams were comparable. In Table 6, comparison of deflection of beam on service stages in experimental deflection is taken through the reading test a beam permissible deflection as per IS 456:2000 [10]. Through these values, we calculated a ($\Delta_{exp}/\Delta_{per}$) and span/ Δ_{exp} . Through this, we can able to plot a graph load vs deflection for all the mix proportions and comparison graph of for all the mix proportions. And beam as high strength concrete

Table 4 Comparison between experimental and theoretical values at service stage

Beam no	Neutral axis depth in mm	Experimental values		Theoretical values		Capacity ratios of beam (exp/theo)
		Load in kN	Moment in kNm	Load in kN	Moment in kNm	
CC	11.64	110	55	86.79	36.54	1.27
B2	11.64	120	60	115.68	64.28	1.04
B3	11.64	130	65	126.87	88.74	1.02
B4	11.64	140	70	138.98	98.52	1.01

Table 5 Final stage comparison of experimental and theoretical values

Beam no	Neutral axis depth in mm	Experimental values		Theoretical values		Capacity ratios of beam
		Load in kN	Moment in kNm	Load in Kn	Moment in kNm	
CC	11.64	110	55	34.2	32.48	1.7
B2	11.64	120	60	59.54	55.38	1.08
B3	11.64	130	65	85.39	74.96	0.76
B4	11.64	140	70	98.67	92.45	0.8

Table 6 Comparative analysis of beam deflection at service stage

Beam no	Experimental deflection (Δ_{exp})	As per IS: 456 permissible deflection (mm)	$\Delta_{exp}/\Delta_{per}$	span/ Δ_{exp}
CC	18.43	8	2.304	109
B2	21.87	8	2.734	91
B3	19.13	8	2.391	105
B4	23.98	8	2.998	83

so deflection is maximum in B4 (Copper slag 40%, Jute fiber 1.5%) (Figs. 8, 9, 10 and 11).

4.4 Ductility Behavior

In this work, displacement ductility was looked at as well. Table 7 lists the beams' ductility values. The displacement ductility ratio is calculated using the equation $1 = u/y$, where y is the angle of deflection at the instant when steel gives and u is its deflection at the final moment. High ductility ratios often mean that a structural part can endure significant deflections before failing. In this analysis, it was found

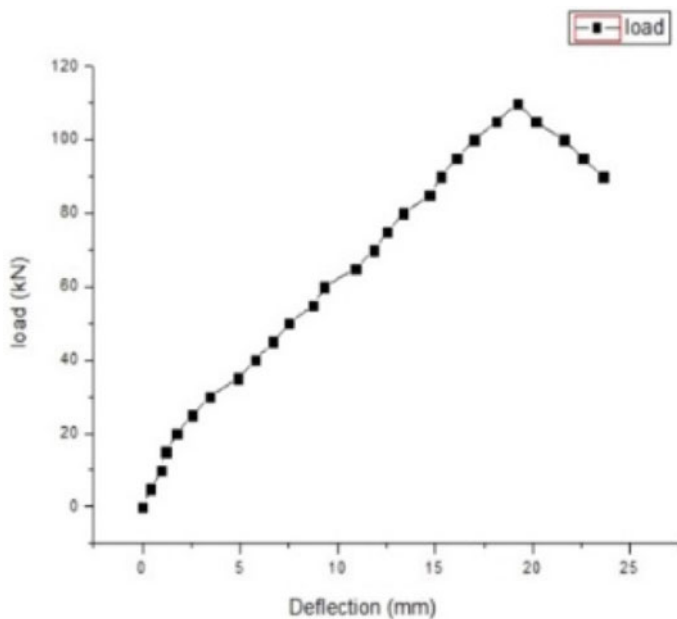


Fig. 8 Conventional beam

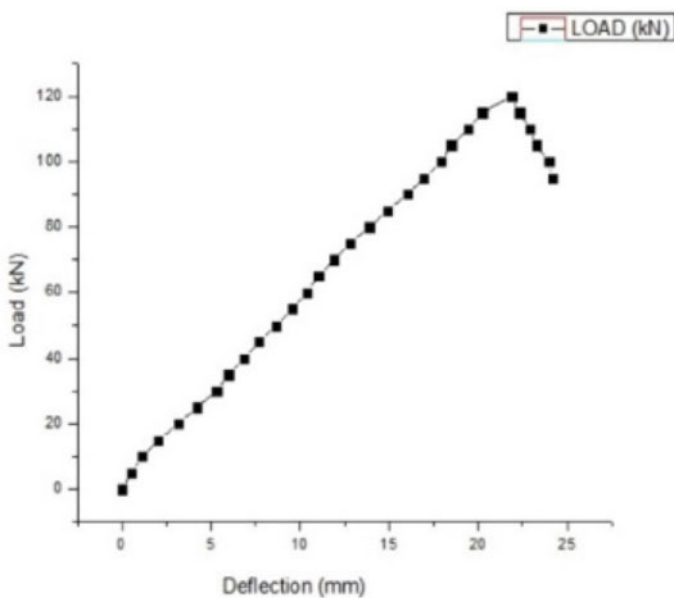


Fig. 9 B2 (Copper slag 20%, Jute fiber 0.5%)

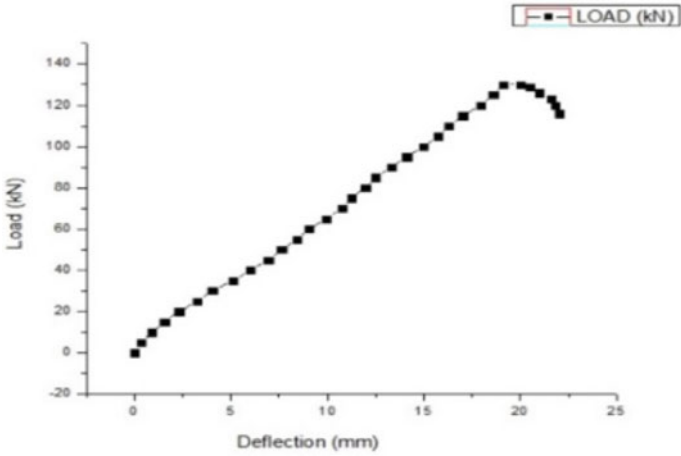


Fig. 10 B3 (Copper slag 30%, Jute fiber 1%)

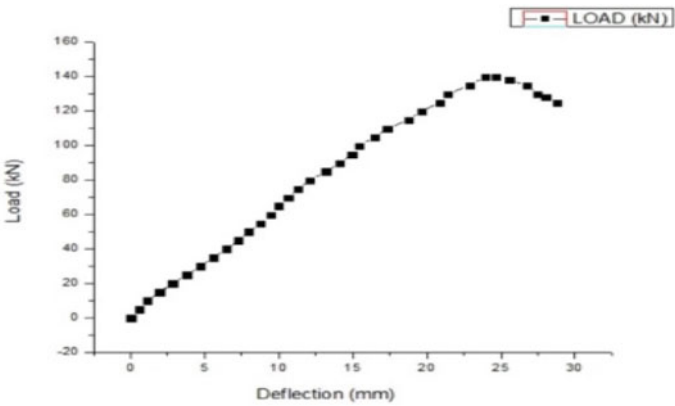


Fig. 11 B4 (Copper slag 40%, jute fiber 1.5%)

that each beam's ductility ratio was more than, suggesting very good ductility. This study suggests that structural elements exposed to significant displacements, such as sudden stresses from an earthquake, should be thought about using members with displaced ductility in a range of 3–5. As was predicted, it was shown that a greater tension reinforcement ratio (3.89%) causes less ductile behavior in this investigation as well. This agrees with the findings of other researchers.

Table 7 Experiment displacement ductility

Beam. No	Yield stage displacement Δy		Ultimate stage displacement Δu		Displacement ductility ratio $\mu = \frac{\Delta u}{\Delta y}$
	Moment (kNm)	Deflection (mm)	Moment (kNm)	Deflection (mm)	
CC	12.5	3.48	70.8	23.98	5.66
B2	15.6	4.19	65.4	19.13	4.19
B3	17.8	5.12	60.8	21.87	3.42
B4	18.2	6.46	55.2	18.43	3.03

Table 8 Beam cracking characteristics

Beam. No	Simulated crack size (mm)		Allowed crack width (mm) according to IS 456: 2000 0.4	Mean crack spacing (mm)	Crack count between loading points
	At service moment	At failure moment			
CC	0.28	1.58	0.4	78	4
B2	0.34	0.96	0.4	82	7
B3	0.57	1.42	0.4	94	9
B4	0.78	1.67	0.4	128	10

4.5 Cracking Behavior

The tension reinforcing level was used to measure the crack width at each load increment, and the crack forms were noted on the beam. The initial gradient of the moment-deflection curve is assumed to abruptly change at the first crack moment. In order for structural parts to function as intended, there shouldn't be a lot of cracking. Wide fissures make a member far less rigid, encourage the entry of dangerous chemicals into the material, are ugly, and might worry residents. Depending on the exposure circumstances, the maximum permitted crack widths specified by various codes of practice typically range between 0.1 and 0.4 mm IS 456:2000 [10]. It was observed that the first fracture consistently developed toward the middle of the beam's span. The surface on the beams developed vertical fissures, a sign that the failure mode of the beams is flexure. Refer from shown Table 8 (Figs. 12, 13 and 14).

5 Conclusions

Copper slag with jute fiber exhibits similar flexural behavior to other forms of concrete. All beams displayed typical structural behavior during flexure. There are no instances of bond failure, according to the horizontal fractures that were noticed. For ratios of reinforcement up to 3.14%, the IS 456:2000 can be used to produce

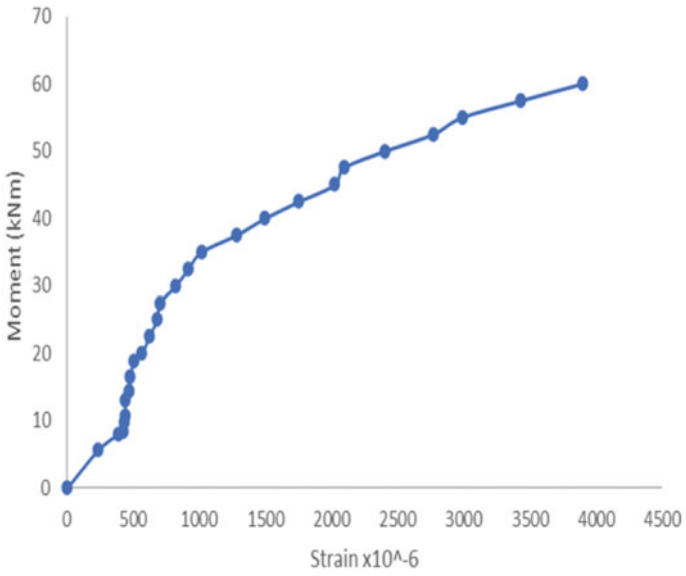


Fig. 12 Moment versus strain $\times 10^{-6}$

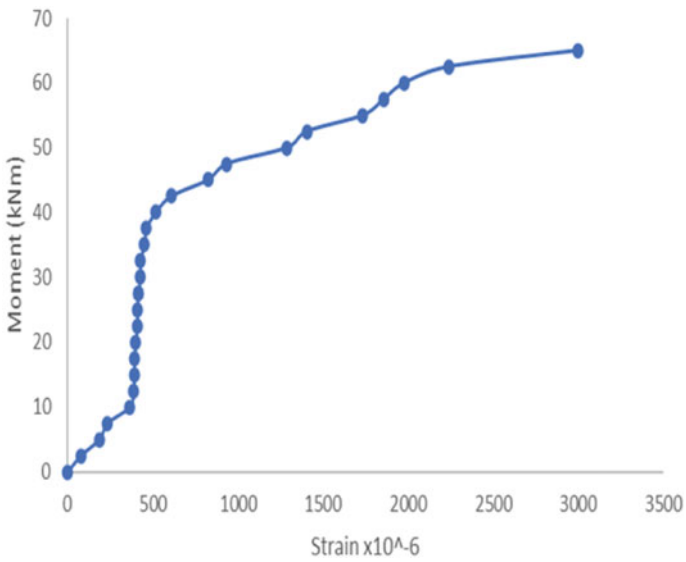


Fig. 13 Moment versus strain $\times 10^{-6}$

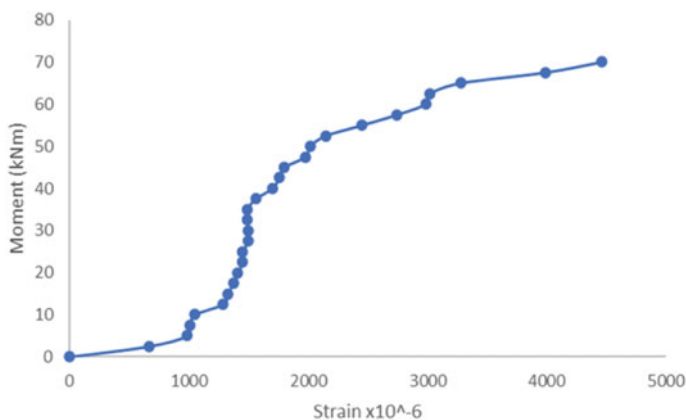


Fig. 14 Moment versus strain $\times 10^{-6}$

a suitable load factor against failure and a conservative estimate of the ultimate moment capacity. Under the planned service loads, the deflection is acceptable and falls within the permissible range specified by IS 456:2000. Larger beam depths may be used for concrete reinforcing ratios with high strengths. Fibers are frequently added to concrete to avoid cracks brought on by drying loss and plastic shrinkage. Concrete may be made using copper slag in place of some of the fine aggregate or cement. Concrete's density is increased by employing copper slag in place of fine aggregate, which also enhances the material's self-weight. In addition, strengthening of jute fiber increases a hardness and tensile strength. The average thickness of the jute fiber was 2.0 mm. Through this, study on flexural behavior on reinforced beam on different mix proportions on M80 grade of high strength concrete had been tested on ultimate loads, deflection, cracking, ductility of beam. So maximum loads and maximum deflection occur on B4 (Copper slag 40%, Jute fiber 1.5%). And any researches are going on investigated on copper slag as practical replacement of fine aggregate and jute fiber has as increase a tensile strength on concrete.

References

1. Suhas S (2020) Natural fiber reinforcement experimental study in polymer composite. *Mater Today* 45(2):6655–6659
2. Madhavi K (2020) External strengthening of concrete with natural and synthetic fiber. *Mater Today* 38(28):2803–2809
3. Jena B (2021) Influence of incorporation of jute fibre and ferrochrome slag on properties of concrete. *Aust J Civ Eng* 10(16):14488–18996, Apr 2021
4. Arun G (2018) Experimental investigation on flexural behavior of reinforced concrete beams containing copper slag, fly-ash and steel fibers. *Int Res J Eng Technol* 05(6). ISSN 2395-0072
5. Tamil Selvi P (2014) Experimental study on concrete using copper slag as replacement material of fine aggregate. *J Civil Environ Eng* 4(5):2165–7845

6. Mohd Areef DAS (2020) Flexural behaviour of steel fiber reinforced slabs made with copper slag as fine aggregate. *Int J Adv Res Eng Technol* 11(11):1565–1573, Nov 2020
7. Goel P (2013) Experimental study of jute fibre reinforced concrete. *Int J Adv Res Eng Technol* 5(7):2348–7550, July 2017
8. Dayakar Reddy MNV (2017) Mechanical properties of high strength concrete with copper slag as fine aggregate and partially replacing cement with nano silica. *Int J Innovative Res Sci Eng Technol* 6(2), Feb 2017
9. Chakravarthy M (2016) Experimental investigations on M80 grade concrete using supplementary cementitious materials. *Int J Latest Technol Eng Manage Appl Sci V(XI):2278–2540*, Nov 2016
10. IS: 456-2000. Plain and reinforced concrete – code of practice. Fourth revision

An Ergonomic Risk Evaluation of the Construction Industry Based on Specific Factors



G. Nakkeeran, V. Kamala, and L. Krishnaraj

1 Introduction

The term “ergonomics” is derived from the Greek terms “ERGON” and “NOMOS,” which represent “labour” and “principles or laws,” respectively. As a result, ergonomics literally means “the rules of labour” [1]. It is necessary to do scientific research that considers how humans perform their task in the workplace. Human behaviour, abilities, circumstances, working conditions, and the surrounding environment all play a role in this field of study. The application of this research is aimed at increasing worker well-being, safety, and health, as well as output and efficiency. It is the study of human behaviour in relation to his work that is the focus of ergonomics [2]. An individual at work in relation to his physical surroundings is the subject of this investigation. When it comes to ergonomics, the most fundamental principle is adapting tasks to the human body. A multidisciplinary field, ergonomics relies on physiology, psychology, and several technical disciplines to form its theoretical framework. “Designing the job to fit the worker, rather than forcing the worker to fit the job,” according to Occupational Safety and Health Administration’s definition of Ergonomics. Building construction equipment nowadays is the result of centuries of hard work by human beings. Although the use of professional tools is inevitable in building and construction, the methods of employing the body for completing tasks are critical [3]. Working conditions that are hazardous to workers’ health and the economy are exacerbated by subpar construction procedures. As a part of the IEA’s 13th triennial congress, Koningsveld and van der Molen presented

G. Nakkeeran (✉) · L. Krishnaraj

Department of Civil Engineering, Faculty of Engineering and Technology, SRM Institute of Science and Technology, Kattankulathur, Tamil Nadu 603203, India
e-mail: ng2683@srmist.edu.in

V. Kamala

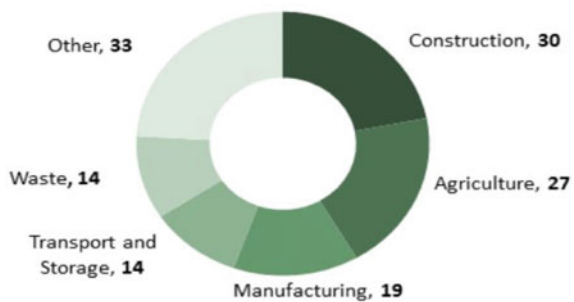
Department of Industrial Engineering, College of Engineering-Guindy, Chennai, Tamilnadu 600025, India

at Tampere's International Symposium on Ergonomics in Building and Construction on the history and future of this field [4]. International Ergonomics in Building and Construction Symposium outcomes might be taken as a major shift in work practises, conditions, and organisational structures is needed to ensure the long-term viability and health of the construction sector and its workforce. Ergonomics can aid in the development of a secure future. Ergonomics knowledge and principles are therefore crucial for improving working styles and creating a secure working environment for employees [5].

1.1 Statement of Issue

Figure 1 shows construction industry is risk industry compared to other industry. Keeping construction employees safe and healthy can be a challenge due to the industry's diversity, adaptability, and dynamic nature. Workplace accidents, diseases, disabilities, and even deaths are common in the construction sector due to the hazards posed by the projects' complexity and breadth of scope [7, 8]. From 1990 to 1998, Washington State's launched initiative ranked roofing, masonry, tile setting, plastering, and concrete construction among the top three jobs across all other industries. The Standard Industrial Classification has designated twelve high-risk industries based on their prevention index, which is a mix of musculoskeletal injury occurrence rate and total number of injuries. The construction business has the worst occupational safety and health records of any industry. 6% of the workforce is employed in the construction business, while 10% of occupational injuries and 21% of occupational deaths occur in this sector, according to accident (1998) [9, 10]. According to the Bureau of Labour Statistics (BLS) in terms of time away from work and lost time, construction workers ranked fourth in 2000 due of musculoskeletal ailments. While construction workers took an average of 10 days off every year, the rest of the workforce took an average of 7 days (BLS, 2000). Data collected from Scopus using the keyword "ergonomic in the construction industry" analysis done for future direction shown in Fig. 2.

Fig. 1 Injury rate in comparison with another industry to construction industry source from HSE [6]



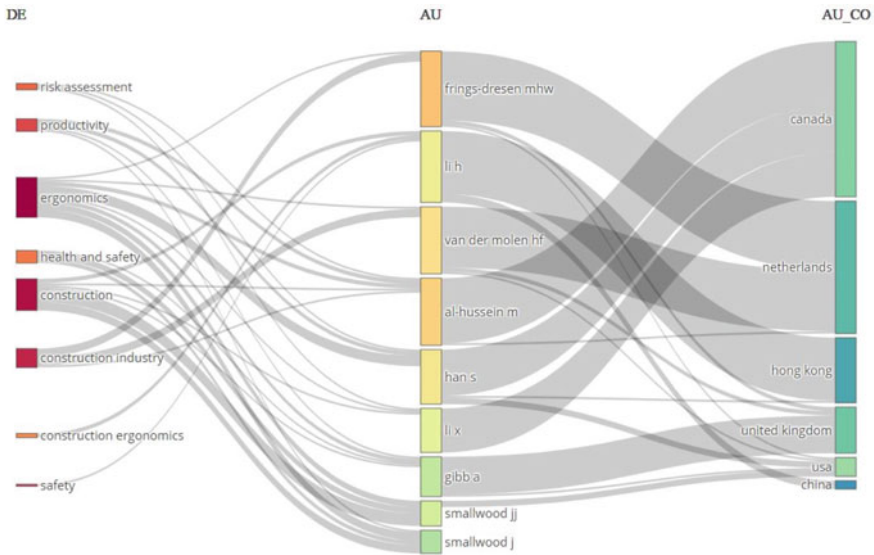


Fig. 2 Key finding map

1.2 HSE Dependent Variables Occupational Risk Factors for Remarks

➤ Anxiety (85.3%) Awkward postures due to the weather and physical exertion, such as climbing, stretching, kneeling, and reaching overhead 4 ➤ The area around the nose (91.8%) A stooped posture, a lack of rest, a climate that makes it difficult to move around, an abrupt change in position, and extended standing and sitting ➤ In the vicinity of the (87.8%) Lengthy periods of time spent sitting or standing in one position, as well as an uncomfortable posture, all contribute to poor posture. ➤ Distal portions of the body (81.6%) posture, climate, static posture, and standing for lengthy periods of time, and equipment all contribute to poor health. ➤ Roughly (83.7 per cent) Bending, stooping, and then rapidly rising to a standing posture ➤ The knuckles (83.7%) Sudden shifts in position and difficult posture, such as climbing, kneeling, or crouching ➤ The backbone (89.1%) static posture, rapid changes in position, stooping, bending, and other such physical adaptations ➤ Hip-hop (81.6%) instruments, rapid movement, extended sitting and standing, a static posture, as well as mountaineering ➤ A person’s knees (76.5%) Temperature, weather, and static posture are all factors in a climber’s ability to reach overhead. ➤ Legs, specifically the ankles (75.4%) Excessive bending, crouching, and kneeling, as well as extended sitting and standing [11, 12].

The construction industry is a major employer in the country many people in its workforce. Unfortunately, workers in this industry are victims of occupational disorders with hormonal dysfunctions and psychosocial stresses. Through the contractor’s

perspective, we aim to reduce the impact of ergonomic difficulties on construction employees and create healthy and successful workplaces [13, 14]. Every literature explains about an ergonomic risk in single factors affected safety in construction industry. Based on literature, collect a risk in basic factor to explain a collected physical, psychological, environmental, safety formed a risk assessment in construction industry solved by an RII in Relative Importance Index.

1.3 Objective and Scope

➤ To identify the ergonomic risk factors in the construction industry. ➤ To reduce worker issues and increase work efficiency. ➤ A construction sector focus is the primary focus of this study's research is to assess ergonomic risk factors in building construction. ➤ Proposing suggestions to mitigate ergonomic risk.

2 Methodology

The study was selected after the area was decided. Researchers looked at all the relevant material on the subject that has previously been published in journals articles, books and websites. Based on literatures, identify a risk assessment for construction industry. In addition to collected information of research was conducted by means of questionnaires and one-on-one interviews. Data was analysed through interviews and questionnaires using relative importance index (RII) [15]. Based on the findings of the investigation, the conclusions and recommendations were drawn show in Fig. 3.

2.1 Factors

Based on literature, ergonomic risk factors are identified in construction industry classified, 1. Physiological, 2. Psychological, 3. Environmental, 4. Safety factor [16–18].

2.1.1 Physiological Factors

Physiological ergonomics is one of three aspects of ergonomics: physical, cognitive, and organisational. Activity involving any ergonomic risk results in increased risk of strain and injury. Non-ionising UV light, such as that emitted by the sun and electric arc welding, and mechanical injuries and outcomes are examples of physical risks. 4 sub-factors are classified in physiological; (i) Basic Rate (iii) Organization (iii) Task Content (iv) Energy Expenditure (i) Basic Rate: In literature, Soumitry J. Ray explains

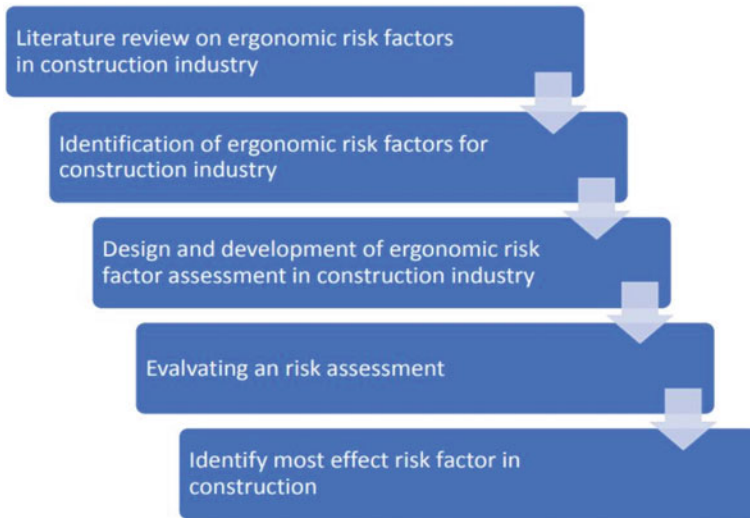


Fig. 3 Methodology

basic heart beat rate during a workplace compared to normal days, Respiration rate during a workplace, work acceleration in the workplace, skin temperature during work days. (ii) Organisation: In Tarek, Sobeih explains work an organisation to give a high physical task to complete in limit time, work responsibility of work comfort with body, organisation give a high level of work in manual (or) machine work separation in facility in work structure. 12 (iii) Task Content: In Alireza Ahankoob strength of human to do a work (or) handle capability of work, endurance of work in work place, work ask to suddenly handling without any proper information they capability to do it, repletion of work in work place to health issues, force exertion, awkward posture. (iv) Energy Expenditure: Load carrying during a working place, work moment is with a travel of work during a working time.

2.1.2 Psychological Factors

Psychological factors are the mental factors that helps or prevent self-motivating. To increasing an efficiency, workers encounter financial difficulties, health issues, illnesses, accidents, and even death. 4 sub-factors are classified in psychological; (i) Personal (ii) Work rest schedule (iii) Mental task content (iv) Skill and training. (i) Personal: Casual nature of employment (drink, drug, etc.). Drinking, smoking, and the use of other addictive substances can cause physical and emotional harm, lack of cooperation and self-satisfaction in work. (ii) Work rest schedule: Worker during body heat by using chemical material (or) place of work, work and rest of work time in work place. 13 (iii) Mental task content: Flow of information in high level to low level properly, memory loss to worker, uncertain work hours (limits of work are 8 h),

non-availability of raw material during working time. (iv) Skill and training: Training level of workers to handle without any fear (or) tension, storage (or) understanding capability, training of new workers helps to do work without illness.

2.1.3 Environmental Factors

Factors are in physical, biological, and chemical factors, which explain workplace. There are many factors that contribute to a good work environment, including a strong sense of self-worth and a desire to learn and contribute to the success of others. hazards such as dusts, fume, and mists. 3 sub-factors are classified in environmental factors; (i) Physical (ii) Biological. (i) Physical: Level of workplan from a sea level, work place in unsafe condition (slope, water base), temperature of work place (cold, hot), vibration in work place, noise problem both internal and external, lighting in work (internal, external) place, during work in outer and inner, cleanliness in work place. (ii) Biological: Occupation diseases handle a chemical (or) material, poor work area facility (water, sanitation). Because of poor sanitation and tainted water, workers are at danger of contracting diseases like malaria, dengue, and histoplasmosis (a lung infection caused by a common soil fungus).

2.1.4 Safety Factors

Rules and safety equipment to decrease a risk factor. Health and safety concerns for construction workers Safety experts should devote more time to developing innovative and successful health/wellness programmes. The effects of historical, economic, psychological, technical, procedural, frequency, and environmental issues are evaluated in terms of how these aspects are related to the level of site safety performance. Two sub-factors are classified in safety risk; (i) Management commitment (ii) Personal safety (i) Management commitment: Safety committee's formation, safety rules and accident investigation awareness, layout and design of work station for safety handle a machine, verbally communication (if any problem happened in process of flow convey an information faster) (ii) Personal safety: Personal protective equipment handles in work place, tool and handle design awareness in work, safety training to handle a working place.

Masons, Site Engineers, and Draftsmen working in construction are given a list of factors and sub-factors based on various literature questions. The questionnaire was created with a specific end goal in mind: Health, safety, and the environment were the subjects of a survey conducted by the company. When asked to answer the question, those who took the survey were instructed to use their own personal construction experience as a guide. Based on each factor, a liker scale method is used to form a question.

3 Analysis

Factors that affect health, safety, and the environment were examined, and the relative importance of each factor was ranked by the respondents using the relative importance index (RII). Equation was used to arrive at this result.

$$RII = \sum W/R * N (0 \leq RII \leq 1) \tag{1}$$

➤ *W*—weight given in each factors respondents and range from 1 to 5 (1-bad, 5—very good) ➤ *R*-highest weight (5) ➤ *N*-total number of respondents.

Calculation:

Physiological factors

$$\begin{aligned} \sum w &= 5216; R = 5; N = 100 \\ RII &= \sum W/R * N \\ RII &= 5216 / 5 * 100 = 10.432 \end{aligned}$$

Environmental factors

$$\begin{aligned} \sum w &= 2875; R = 5; N = 100 \\ RII &= \sum W/R * N \\ RII &= 2875 / 5 * 100 = 5.750 \end{aligned}$$

Psychological factors

$$\begin{aligned} \sum w &= 2796; R = 5; N = 100 \\ RII &= \sum W/R * N \\ RII &= 2796 / 5 * 100 = 5.5920 \end{aligned}$$

Safety factors

$$\begin{aligned} \sum w &= 1740; R = 5; N = 100 \\ RII &= \sum W/R * N \\ RII &= 1740 / 5 * 100 = 3.480 \end{aligned}$$

In risk factors, score in RII is total number of sample 100. RII in physiological factors is 10.432 mean value 0.6521, psychological factors score 5.5920 mean value 0.6213, environmental factors score value 5.750 mean value 0.6389, safety factors score 3.4800 mean value 0.5800 in Table 1.

Table 1 Score on risk factors in RII

Factors	Number of sample	Total score sample	RII	RII mean
Physiological	100	5216	10.432	0.6521
Psychological	100	2796	5.592	0.6213
Environmental	100	2875	5.575	0.6389
Safety	100	1740	3.48	0.58

Table 2 Result of RII

S. No	Factor	RII mean	Rank
1	Physiological	0.652	1
2	Psychological	0.6213	3
3	Environmental	0.6389	2
4	Safety	0.58	4

3.1 Result and Discussion

Relative important index (RII) and relative important index mean are computed for each factor, and the factors are ranked according to the RII mean score. As an illustration: For each of the two sub-factors, the RII value is calculated, and then the RII mean is calculated to determine the safety factor. In terms of average and rank, the safety factor has a mean of 0.5800. A complete breakdown of the factors is given in Table 2.

Workers from a variety of cultural backgrounds, who are ill-educated, and who have no awareness of ergonomics are the most likely to cause an accident in construction projects because of their unsafe reactions to the work environment. The safety of the operatives is critical in reducing their exposure to personal risk while on the job. Men’s jobs are largely driven by psychological factors as well. Safety supervisors, co-workers, and workers all play a role in reducing risk factors. Sub-factors that affect safety performance in the construction industry in addition to physiological factors include: union involvement, worker safety training deficiencies, and management expenditures on safety improvements. It is necessary to alter employees’ conceptions of safety if that environment is to be improved.

4 Conclusion

The construction industry exhibits a higher injury rate compared to other industries, primarily due to a lack of safety measures and the presence of ergonomic risk factors. This study work provides methodology for prioritising the risk factor influencing ergonomic in construction. Risk factors are classified as physiological, psychological, environmental, safety factors. Factors are form into questionnaires to score by

self-scoring method. Analysis by RII to rank the factor, sample size 100. RII in physiological factors score mean value 0.6521, psychological factors score mean value 0.6213, environmental factors score mean value 0.6389, safety factors score mean value 0.5800, physiological factor highly influence construction risk. Behaviour-based risk assessment is introduced to change workers perception of risk assessment. Consequently, the proposed method can be used to improve risk management in the construction industry. In physiological factors, basic rate, organisation, task content, energy expenditure ensure a risk contribution for workers.

References

1. Smallwood J, Allen C (2021) Construction ergonomics: can the challenges be overcome? Lect Notes Netw Syst 221 LNNS:337–344. https://doi.org/10.1007/978-3-030-74608-7_43
2. Smallwood JJ, Haupt TC (2009) Construction ergonomics: Perspectives of female and male production workers. In: Association of researchers in construction management, ARCOM 2009—Proceedings of the 25th annual conference, pp 1263–1271
3. Kathiravan S, Gunarani GI (2018) Ergonomic performance assessment (EPA) using rula and reba for residential construction in Tamil Nadu. Int J Civil Eng Technol 9(4):836–843
4. Abdul-Tharim AH, Jaffar N, Lop NS, Mohd-Kamar IF (2011) Ergonomic risk controls in construction industry—a literature review. Procedia Eng 20:80–88. <https://doi.org/10.1016/J.PROENG.2011.11.141>
5. Abaiean H, Inyang N, Moselhi O, Al-Hussein M, El-Rich M (2016) Ergonomic assessment of residential construction tasks using system dynamics. In: ISARC 2016—33rd international symposium on automation and robotics in construction, pp 258–266. <https://doi.org/10.22260/ISARC2016/0032>
6. Latest fatal injuries statistics issued by HSE | Safety Pass Alliance. <https://www.safetypassports.co.uk/news/latest-fatal-injuries-statistics-issued-by-hse/> (Accessed 09 Aug 2022)
7. Rodriguez FS, Spilski J, Hekele F, Beese NO, Lachmann T (2020) Physical and cognitive demands of work in building construction. Eng Constr Archit Manag 27(3):745–764. <https://doi.org/10.1108/ECAM-04-2019-0211>
8. Inyang N, Al-Hussein M (2011) Ergonomic hazard quantification and rating of residential construction tasks. Proc Annu Conf Can Soc Civ Eng 3:1885–1895
9. Torghabeh ZJ, Hosseini SS, Ressang A (2013) Risk assessment of ergonomic risk factors at construction sites. Appl Mech Mater 330:857–861. <https://doi.org/10.4028/WWW.SCIENTIFIC.NET/AMM.330.857>
10. Parida R, Ray PK (2015) Factors influencing construction ergonomic performance in India. Procedia Manuf 3:6587–6592. <https://doi.org/10.1016/J.PROMFG.2015.07.284>
11. Boschman JS, Frings-Dresen MHW, van der Molen HF (2015) Use of ergonomic measures related to musculoskeletal complaints among construction workers: a 2-year follow-up study. Saf Health Work 6(2):90–96. <https://doi.org/10.1016/J.SHAW.2014.12.003>
12. Village J, Ostry A (2010) Assessing attitudes, beliefs and readiness for musculoskeletal injury prevention in the construction industry. Appl Ergon 41(6):771–778. <https://doi.org/10.1016/J.APERGO.2010.01.003>
13. Inyang N, Al-Hussein M, El-Rich M, Al-Jibouri S (2012) Ergonomic analysis and the need for its integration for planning and assessing construction tasks. J Constr Eng Manag 138(12):1370–1376. [https://doi.org/10.1061/\(ASCE\)CO.1943-7862.0000556](https://doi.org/10.1061/(ASCE)CO.1943-7862.0000556)
14. Spielholz P, Davis G, Griffith J (2006) Physical risk factors and controls for musculoskeletal disorders in construction trades. J Constr Eng Manag 132(10):1059–1068. [https://doi.org/10.1061/\(ASCE\)0733-9364\(2006\)132:10\(1059\)](https://doi.org/10.1061/(ASCE)0733-9364(2006)132:10(1059))

15. Aravindh MD, Nakkeeran G , Krishnaraj L, Arivusudar N (2022) Asian journal of civil engineering evaluation and optimization of lean waste in construction industry. *Asian J Civ Eng* 1(3). <https://doi.org/10.1007/s42107-022-00453-9>
16. Qiu C, Li X (2023) Blended analysis of occupational safety hazards and risk assessment approach in the construction industry 499–511. https://doi.org/10.1007/978-981-19-1029-6_38
17. Golabchi A, Han S, Fayek AR, AbouRizk S (2017) Stochastic modeling for assessment of human perception and motion sensing errors in ergonomic analysis. *J Comput Civ Eng* 31(4):04017010. [https://doi.org/10.1061/\(ASCE\)CP.1943-5487.0000655](https://doi.org/10.1061/(ASCE)CP.1943-5487.0000655)
18. Golabchi A, Guo X, Liu M, Han SU, Lee SH, AbouRizk S (2018) An integrated ergonomics framework for evaluation and design of construction operations. *Autom Constr* 95:72–85. <https://doi.org/10.1016/J.AUTCON.2018.08.003>

Urban Planning and Design

Structural Analysis and Design of Solar Car Park in College of Engineering-Dawadmi: A Move Toward Energy Efficient Campus



Mohammad Abdur Rasheed and Yazeed Saud Alotaibi

1 Introduction

The Kingdom of Saudi Arabia has one of the highest solar radiation rates in the world. The study by Almarshoud [1] assesses the solar energy potential of various regions in Saudi Arabia by analyzing long-term solar radiation data obtained from meteorological stations across the country. The study concludes that Saudi Arabia has one of the highest solar energy potentials in the world, with an average annual solar radiation of 2100 kWh/m². In this context, Saudi Arabia's solar energy is enormous and can be exploited easily, and where it is considered clean energy, but efforts to benefit from it face some challenges, including the availability and low cost of oil compared to solar power generation and the impact of dust.

The Saudi Vision 2030 strategy, one of the key economic reforms in Saudi Arabia and the Middle East [2], sets out requirements such as the reduction of CO₂ emissions and sustainability in building construction and operation. The main objectives of the vision are to reduce energy consumption in all new buildings and significantly reduce the carbon footprint of transport and production in energy consumption. Tapping solar energy is considered to be one of the best solutions to reach the desired goals as it has a negligible environmental impact. Consequently, more and more houses and farms are increasingly becoming heavily dependent on solar energy, so solar panels are generally placed on roofs or backyards. Due to the high degree of external shading "optical systems" in urban areas, there is insufficient space for urbanization to install photovoltaic systems with vertical interfaces. Building surfaces, which are generally without external protection, are ideal for installing photovoltaic systems. Using the parachute area above parking spaces is appropriate for installing photovoltaic systems in road infrastructure. Because these shading surfaces are suitable for integrating solar

M. A. Rasheed (✉) · Y. S. Alotaibi
Department of Civil Engineering, College of Engineering, Shaqra University, Dawadmi,
Saudi Arabia
e-mail: marasheed@su.edu.sa



Fig. 1 Saudi Aramco's solar car park in Dhahran

PV and generating solar power [3] that can be used locally or exported to the grid, car parks are mostly executed as multi-story as fixed public transportation capacity is getting depleted in their open parking lots. Construction will be necessary in the future as part of parking spaces. It will be the optimal solution in terms of environmental impact as well as the capacity of the grid for electricity production to operate at the point of consumption. For example, on the roof of the building, but their use in parking is uncommon. In Saudi Arabia, some projects applied the concept of solar parking, e.g., "Aramco's building in Dhahran," [4] as shown in Fig. 1.

This study proposes implementing a solar car park lot system in the College of Engineering located in Dawadmi. The college ambience has ample space for car parking. The purpose is to make the existing parking lot a center for solar energy harvesting through which it is stored and can serve as a potential source for the supply of renewable energy.

2 Objectives

The main aim of this project is to provide a structural design of a solar car park using the existing car parking that can serve as a source of renewable energy for COE Dawadmi making it energy self-sufficient. Keeping in view the main aim of this project, the following objectives are to be achieved in the project:

1. To determine the electricity generated from solar car parking and compare it with actual electricity.

2. Structural analysis and design of solar car park lot including the various loads acting through its lifetime.
3. To be able to understand factors affecting the structural design of solar car park.

To achieve the objectives, the following methodology is adopted:

1. Review of available references.
2. Surveying and calculating all areas and dimensions required.
3. Analyze the economical costs.
4. Structural analysis and design using computer software.

Each step in the methodology will be explained briefly in the sections to be followed.

3 Literature Review

Solar car park lots are becoming increasingly popular due to their ability to generate electricity using renewable energy sources. However, the design and construction of these facilities must take into account the additional structural loads imposed by the solar panels and associated equipment. Various studies have been conducted to investigate the usage of car park lots for solar energy harvesting. The study by Nunes et al. [5] discusses the potential of using parking lots to solar-charge electric vehicles. The authors review the current state of the art and identify the main challenges, including the integration of renewable energy sources into the grid, the lack of standardization in charging protocols, and the high cost of energy storage systems. They propose a conceptual framework for the design and operation of a solar-powered parking lot, which includes the installation of photovoltaic panels, energy storage systems, and charging stations for electric vehicles. The authors also analyze the economic feasibility of this solution, taking into account the initial investment, operational costs, and potential revenue streams. A study by Yaseen and Nabil [6] proposes a solution to address the lack of charging point availability in the EVs market by utilizing existing gas stations for two purposes: installing PV solar systems and deploying them as charging points. An article by Saied et al. [7] discusses the challenges of energy management in urban electricity distribution networks. The authors attempt to integrate a smart parking lot (SPL), renewable energy sources (RESs), and local dispatchable generators (LDG) as a microgrid. In contrast, an energy management system is presented to consider uncertainties of wind speed, solar irradiation, and load consumption. A demand response program (DRP) based on a time-of-use tariff is used to reduce operational expenses. A new uncertainty modeling method based on Hong's two-point estimate method is employed to deal with the uncertainties of load consumption and wind generation. A study by Julieta et al. [8] showed that solar photovoltaic energy could be deployed without occupying additional land in regions with scarce land. A methodology has been developed to identify uncovered parking spaces and water deposits at the regional level and estimate how much of

these areas could be used to deploy solar photovoltaic energy, which could cover 9% of the regional electricity demand.

Critical literature review suggests that very limited studies have been carried out on the structural analysis and design of such structures. This study tries to address the research gap by combining the economic studies with the structural design aspect of solar car parking structure. The realization of the studies is expected to bring millions of Saudi Arab Riyal as benefit annually while being able to safely resist the loads of nature to which it is exposed.

SBC 301 [9] and SBC 306 [10] will be used in this study for the application of load and structural steel design, respectively. The load combinations applied to the structure in this study will be used as per Sect. 2.3.6 of SBC 301.

4 Surveying and Calculation of Shaded Areas

The College of Engineering premises contains three sections of parking as shown in Fig. 2. Each of these sections has parking portal frames slightly differing in size from each other as shown in Fig. 3. Manual surveying was carried out to find the dimensions of each type of frame, and the shading areas of the frame are calculated in the following sections.

Likewise, the dimensions of the existing structure were taken to model the structure geometry in the analysis and design software as shown in Fig. 4a. The existing structure is made of hollow structural steel circular tubes with an outside diameter of 130 mm and a thickness of 5 mm as shown in Fig. 4b.

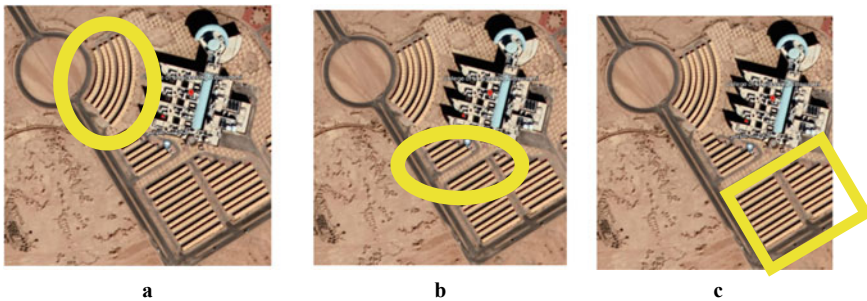


Fig. 2 **a** Back parking view from Google Earth. **b** Front parking view from Google Earth. **c** Left parking view from Google Earth

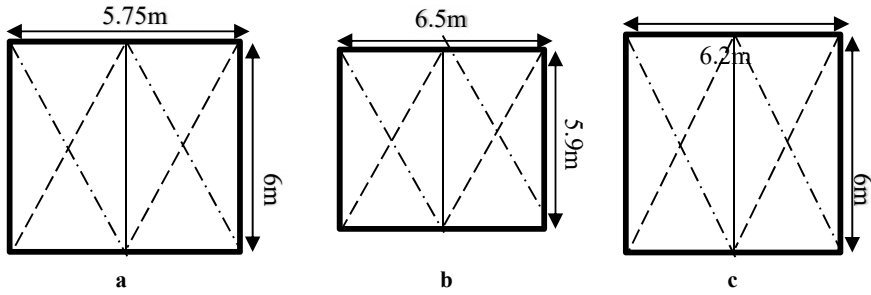


Fig. 3 **a** Back parking canopy dimensions, Back parking area calculations, Number of Car-parking canopies: 128, Area under one canopy= 34.5 m^2 , Total area of parking = 4416 m^2 . **b** Front parking canopy dimensions, Front parking area calculations, Number of Car-parking canopies: 48, Area under one canopy= 38.35 m^2 , Total area of parking = 1840 m^2 . **c** Left parking canopy dimensions, Left parking area calculations, Number of Car-parking canopies: 229, Area under one canopy= 38.35 m^2 , Total area of parking = 1840 m^2

5 Cost–benefit Analysis

Cost–benefit analysis can be used to assess the potential advantages and drawbacks of a proposed project or policy. When used in the context of solar car park lots, CBA can help determine the financial feasibility of investing in this type of infrastructure and provide decision-makers with valuable insight into the possible benefits and drawbacks of the project. A solar car park lot is a parking facility that harnesses solar panels to produce electricity, which can be used to power the parking lot's lighting and electrical systems. Furthermore, any extra energy generated can be supplied back to the grid, resulting in additional revenue.

To initiate this study, the monthly consumption of electricity in the College of Engineering was monitored over a period of twelve months. The price of the units consumed in this case comes under the public building category. The results of these monitoring are listed in Table 1. Average consumption monitored over a year was obtained as 756,953 kWh. Correspondingly, the monthly average price paid by the institution was obtained as 240,240 SAR.

To conduct a CBA of a solar car park lot, both the costs and benefits of the project must be identified and evaluated. Costs may include initial installation expenses, ongoing maintenance costs, and financing costs. Benefits may consist of reduced energy expenses, revenue from excess energy generation, and environmental benefits like decreased greenhouse gas emissions.

After the costs and benefits have been identified, they can be quantified and compared using financial metrics like net present value (NPV), internal rate of return (IRR), and payback period. These metrics can assist decision-makers in assessing the financial feasibility of the project and weighing the costs against the benefits. Hence, CBA can be used to evaluate a solar car park lot project and provide decision-makers with an accurate understanding of the potential financial benefits and drawbacks

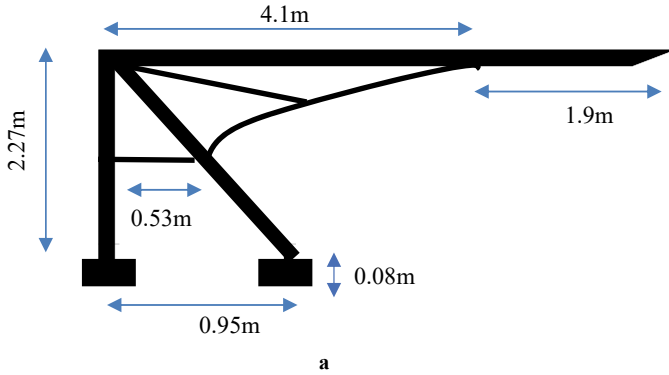
**b**

Fig. 4 **a** Parking structure dimensions (Back parking). **b** Surveying for parking structure dimensions

associated with investing in this type of infrastructure, enabling them to make well-informed decisions. Table 2 provides a summary of the economic analysis carried out. For the purpose of this study, panel-type monocrystalline with a capacity of 540 W is selected. The area covered by each panel is around 2 sq.m. Price per panel is obtained from local vendors. This is a conservative cost; considering the scale of the application, the same panels could be obtained at fairly lower prices from large-scale vendors. Also, the sunshine hours are assumed to be fairly conservative at 6.5 h a day. Earlier studies [11] have shown that the minimum amount of sunshine hours is around 7.26 h in Saudi Arabia during the winter. However, the maximum can also go up to 10.15 h during the month of June, which is summer. The total cost of the panels incurred can be recovered in 24 months, as mentioned in Table 2. As the car parking steel structure is already installed, the only additional components will be PV panel mounting to the structure. It is also evident that the average electricity

Table 1 Electricity consumption of COE Dawadmi

Month	Consumption (kWh)	Price (SAR)
August	760,358	240,863
September	756,184	239,093
October	760,016	240,349
November	767,807	239,969
December	773,470	243,296
January	752,762	244,068
February	747,198	239,714
March	738,253	240,099
April	740,287	239,118
May	759,005	236,521
June	776,383	242,465
July	751,716	237,325
Average	756,953	240,240

Table 2 Cost analysis

Month	Consumption (kWh)
Panel type	Monocrystalline, 540 W
Size of each panel	2 m × 1 m
Price per panel	760 SAR
Total shaded area available for PV installation	14775 m ²
Proposed total no. of panels to install	7387 panels
Total price for panels	5,614,120 SAR
Assumed sunshine hours	6.5 h
Average electricity generated per month	777,851.1 kWh
Average electricity consumed per month	756,953 kWh
Actual average monthly bill	240,240 SAR/month
No. of months to recover the cost	24 months

generated clearly surpasses the average electricity consumed in a month, making the premises energy self-sufficient.

6 Structural Analysis and Design of Proposed Model

The structure geometry has been modeled using the dimensions obtained in Sect. 5 of this paper. Figure 5a shows the geometric model of the structure. The sections used for the existing model contain a hollow circular section of diameter 130 mm and

5 mm thickness as shown in Fig. 5b. The base plate of the structure contains four bolts attached with the help of a rigid connection. The additional sections that are proposed for mounting the solar panels are shown in Fig. 5c. Several trial sections have been tested and finally, L35 × 25x4 has been selected to account for the additional loads due to panels. The demand-to-capacity ratio has been kept up to 90% to optimize the structure. Figure 5d shows the critical service load deflections diagram which are under permissible limits as per SBC 306 [10].

There are many commercial software used for the design of steel structures. Staad.pro is one of the most widely used software. The same has been used for the purpose of this study. However, it is not still integrated with Saudi Building Codes. Therefore, AISC 7-10 [12] has been selected in the software for the purpose of this study, which has parameters very close to what has been used for developing SBC.

Wind load has been carefully calculated as per the guidelines provided in SBC 301. The basic wind speed has been taken from the Fig. 6.4-1 of SBC 301. This figure provides basic 3-s gust wind speed in kmph for selected cities in Saudi Arabia. For the purpose of this study, wind speed is taken after interpolation from the nearest cities. A value of 170 kmph (47 m/s) is used in the study. Wind directionality factor is taken

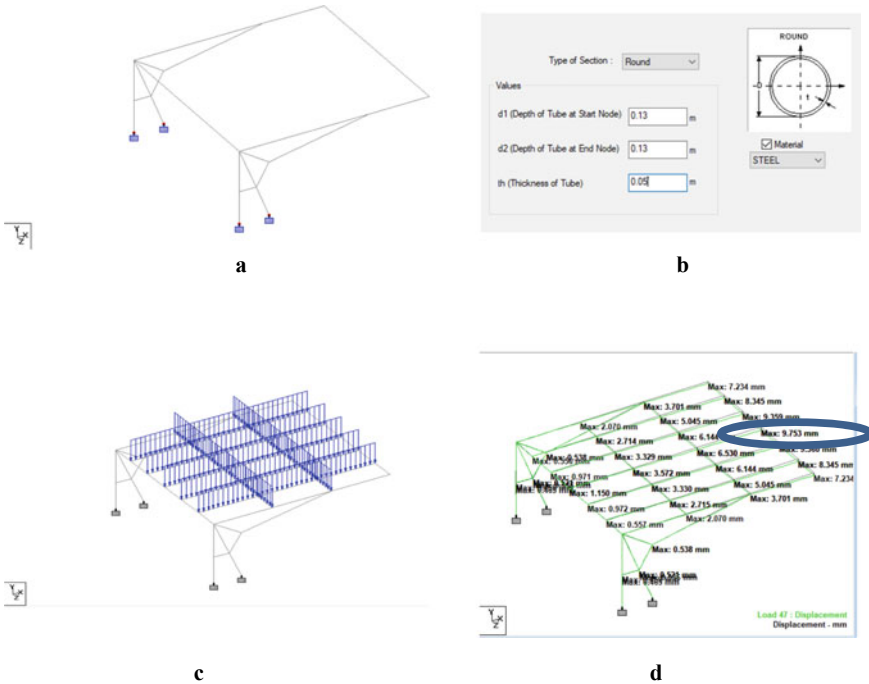


Fig. 5 a Geometric modeling of existing structure with fixed supports. b Sectional details of the existing structure. c Proposed additional sections for supporting solar panels. d Deflection diagram for critical service load combination

as 0.85 as the structure itself is main wind force resisting system as per Table 6.4-1 of SBC 301. Exposure category is considered as C category, as the terrain is mostly flat with unobstructed area. Topographic factor K_{zt} is considered to be 1, since the site location is not situated on a hill or 2d-escarpments. Gust effect factor is considered to be 0.85, assuming the structure to be rigid and having a fundamental natural frequency of less than 1.0 Hz.

Earthquake load parameters are provided in Fig. 9.4.1 of SBC 301. The 0.2 s spectral response acceleration S_s and 1 s spectral response acceleration S_1 for the Dawadmi region are now fed in the software.

The gravity loads expected to be acting on the car parking structure is mainly of two types, dead and live loads. The dead load predominantly coming from the self-weight of the structure and the PV panels. Minimum live load is taken from the SBC 301 to account for the regular maintenance and accidental loads.

7 Conclusions and Summary

The following are the conclusions based on the current study:

1. The study conducted proves that the college of engineering can be made 100% energy self-sufficient by implementing the proposed solar car park lot.
2. Various loads acting during the lifetime of the proposed structure have been carefully analyzed and applied to the structural model.
3. Cost–benefit analysis shows that the cost of installation will be recovered within 24 months of the start of operations.
4. By using the proposed structural model, a capacity-to-demand ratio of up to 90% was achieved by satisfying the strength and serviceability limits under different load combinations.

Based on the current study following, future studies are recommended:

1. Thermal analysis for the interaction between the structures and the parked vehicles.
2. CFD simulations interactions between the vehicles and the structure, to predict the pressure, velocity, and density response.

Acknowledgements The authors extend their appreciation to the deanship of scientific research at Shaqra University for funding this research work through the project number (SU-ANN-202229).

References

1. Almarshoud AF (2016) Performance of solar resources in Saudi Arabia. *Renew Sustain Energy Rev* 66:694–701. <https://doi.org/10.1016/j.rser.2016.08.040>
2. Bekhet HA, Matar A, Yasmin T (2017) CO₂ emissions, energy consumption, economic growth, and financial development in GCC countries: dynamic simultaneous equation models. *Renew Sustain Energy Rev* 70(2017):117–132. <https://doi.org/10.1016/j.rser.2016.11.089>
3. Deshmukh SS, Pearce JM (2021) Electric vehicle charging potential from retail parking lot solar photovoltaic awnings. *Renew Energy* 169:608–617. <https://doi.org/10.1016/j.renene.2021.01.068>
4. Steel International Contracting Company (2011) Saudi Aramco solar car park. In: Design and installation of 10.5 MW solar power farm in the parking lots of the North Park Office Complex. <https://www.siccltd.com/portfolio/saudi-aramco-solar-car-park/>
5. Nunes P, Figueiredo R, Brito MC (2016) The use of parking lots to solar-charge electric vehicles. *Renew Sustain Energy Rev* 66:679–693. <https://doi.org/10.1016/j.rser.2016.08.015>
6. Yaseen Alwesabi NM (2023) Self-sufficient solar power and electric vehicle penetration: A case study of New York State. *Renew Energy Focus* 45(2023):133–140. <https://doi.org/10.1016/j.ref.2023.03.001>
7. Saeid Shojaei HA, Beiza J, Abedinzadeh T (2022) Optimal energy and reserve management of a smart microgrid incorporating parking lot of electric vehicles/renewable sources/responsive-loads considering uncertain parameters. *J Energy Storage* 55 part b. <https://doi.org/10.1016/j.est.2022.105540>
8. Julieta S-R, José-Julio R-B, Pablo Y-R (2022) A methodology to estimate the photovoltaic potential on parking spaces and water deposits. The case of the Canary Islands. *Renew Energy* 189:1046–1062. <https://doi.org/10.1016/j.renene.2022.02.103>
9. Saudi Building Code National Committee, “Loads & forces requirements SBC 301,” Riyadh, Kingdom of Saudi Arabia
10. Saudi Building Code National Committee, “Steel structures requirements SBC 306,” Riyadh, Kingdom of Saudi Arabia
11. Rehman S, Ahmed MA, Mohamed MH, Al-Sulaiman FA (2016) Feasibility study of the grid connected 10 MW installed capacity PV power plants in Saudi Arabia. *Renew Sustain Energy Rev* 80(December 2016):319–329. <https://doi.org/10.1016/j.rser.2017.05.218>
12. ASCE (2017) Minimum design loads for buildings and other structures. <https://doi.org/10.1061/9780872629042>

Development of Sustainable Earthquake Resistant Building for Future Generations



V. Chandrikka and D. Shoba Rajkumar

1 Introduction

1.1 General

In India, there is a fast expanding collection of structures that are woefully unable to withstand earthquakes. This is something that may be seen in earthquake documentation. Therefore, it has become crucial to evaluate the safety of an existing structure's performance under seismic loads and, if necessary, to retrofit the building so that it satisfies the most up-to-date performance standards [1]. The placement and detailing of the reinforcement has a far greater impact on building behaviour during earthquakes than either the size of the members or the total quantity of reinforcement. The retrofitting engineer must take into consideration three potential causes of a building's defects:

(1) Poor planning and execution; (2) Material wear and tear through time and usage. (3) Earthquake or disaster-related damage.

The pushover analysis which is used to evaluate the reliability of a structure by determining its strength parameters and deformation criteria's required in the design of earthquake by using the analysis method of static inelastic. Forces caused by earthquakes may be represented by comparable static lateral loads. Any potential for early failure or weakness in a structure may be shown by the graphical representation between total base shear vs top displacement. Using nonlinear analysis, asymmetrical

V. Chandrikka (✉)

Research Scholar, Department of Civil Engineering, Government College of Engineering, Salem, Tamil Nadu, India

e-mail: chandrikkavinayakarao@gmail.com

D. S. Rajkumar

Professor & Head, Department of Civil Engineering, Government College of Engineering, Salem, Tamil Nadu, India

e-mail: gceshobarajkumar20@gmail.com

buildings built on flat ground and exposed to different loads is the focus of this research. All of the calculations were made using SAP2000 version 14. In this paper, the performance of a nonlinear static analysis (pushover) on a four-storey reinforced concrete structure in zone 5 using SAP 2000. The research demonstrated that in the beam members and column members, the hinges had evolved indicating the 3 phases of IO-immediate occupancy, LS-life safety, and CP-collapse prevention. These findings were used to refine the code-based design and make it more robust against earthquakes of the kind considered during the design process [2, 3].

1.2 Seismic Design

In order to prevent damage during dynamic loading, RC frame buildings as shown in Fig. 1 would have to be enormous, which might make the project unfeasible financially. The reality is that the structure must sustain earthquake-related damage in order to disperse the energy that is applied to it.

Accordingly, (a) structural damage is permissible under occasional significant shaking, as per seismic design philosophy. This means that (a) collapse is not an intended outcome of the design process, and (b) structural damage is negligible with semi-occasional moderate shaking, but non-structural damage is unacceptable [4–6].

Thus, structures are only constructed to endure a tiny proportion of the force they would experience if they were elastic during the predicted massive ground shaking. Seismic design balances cost and damage, making the project viable.

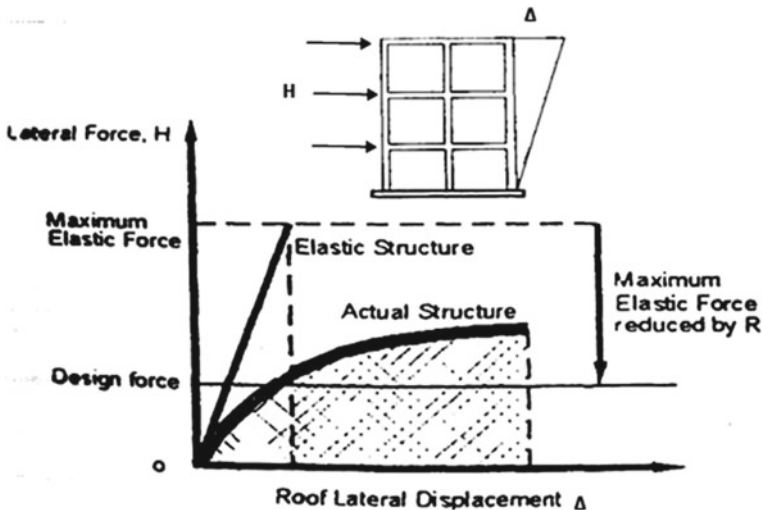


Fig. 1 Conceptual groundwork for earthquakes safety

1.3 Seismic Retrofitting

Potential sources for retrofitting include any building that was built more than 30 years ago, any building that was built within the past 30 years but was not properly designed, constructed, or maintained, and any building that was built within the past 30 years but was not properly designed, constructed, or maintained [7].

2 Pushover Analysis

The simplest performance in the field of nonlinear analysis is basically pushover analysis, the most elementary performance. Pushover analysis, the lateral load raised in small increments while keeping the established allocation pattern all along the altitude of the structure. When the weight on the structure increases, the points of failure and the weak spots also increase. The pushover analysis reveals the building's failure load, maximum deformation such as inelastic deflection, and its corresponding behaviour. When the structure is stressed until a mechanism for its collapse emerges. As load increases, a pushover curve is created by graphing the base shear against the roof displacement (Fig. 2). The pushover analysis calculates the structural limit states for base shear and roof displacement. It is also possible to estimate the building's global stiffness. Those user-designated points, called hinges, are where the nonlinear behaviour really takes place [8]. At the moment, hinges may only be added to frame objects and allocated anywhere along the frame object. Hinge types such as uncoupled moment, torsion, axial force, and shear may be found. The interplay of axial force and bending moments at the hinge position causes the linked P-M2-M3 hinge to yield. A single end of a frame object may have both a typeM3 (moment) and a V2 (shear) hinge. The true strength of the structure may be evaluated with the use of pushover analysis, which shows promise as a practical and effective method for performance-based seismic design. The ADRS format allows for the plotting of base shear against displacement at a given control joint, where the vertical axis is spectral acceleration and the horizontal axis is spectral displacement. The performance point may be determined by plotting the demand spectra on top of that graph. A visual depicting the pushover's step-by-step progression is available, with the development of each hinge and its corresponding colour code [9].

The procedure for doing a nonlinear static pushover analysis may be broken down into the following broad components. The reinforced concrete frame model is designed in three dimensions. To perform a pushover analysis, static load patterns must be created. The reinforced concrete framework models are specified for pushover loads. Elements of the model reinforced concrete frame have appropriate hinge qualities specified to them. It is decided to conduct a pushover study using a nonlinear static loading scenario. The outcomes of the push are analysed. An understanding of how different seismic retrofit solutions would affect the building's reaction may be gained via pushover analysis [10].

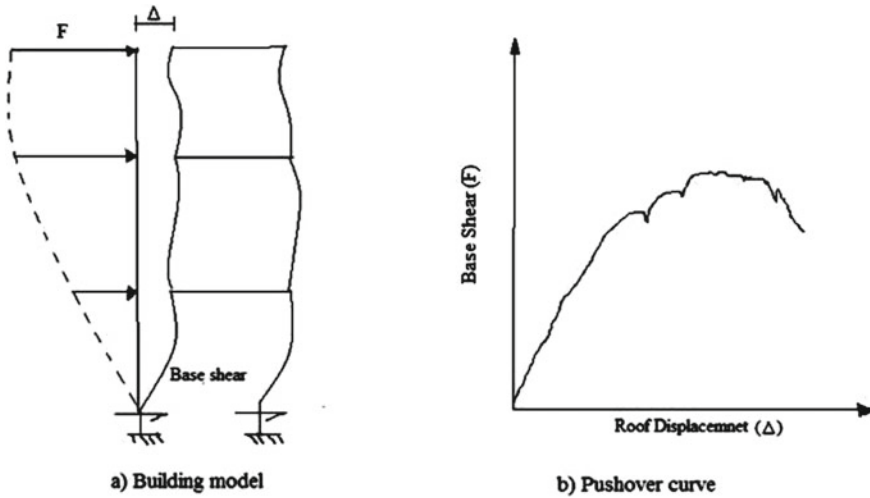


Fig. 2 Base shear versus roof displacement curve

In a performance-based design process, demand and capacity are two critical factors. The capacity of the building to withstand the seismic load is represented by this number. The output is proportional to the efficiency with which the capacity meets the demand.

If the structural components are not damaged beyond the allowable limits of the performance objective for the stresses and displacements projected by the displacement demand, then the capacity curve and demand curve have been successfully constructed, where the capacity and demand curves meet is where the system performs at its best (Fig. 3). In the presence of the performance point and an acceptable damage state, the structure performs as intended [11].

2.1 Advantages of Pushover Analysis

- Overall structural behaviour and performance qualities may be assessed.
- It allows us to study how plastic hinges develop in the various parts of a structure in order.
- It helps us to maximise cost effectiveness by reinforcing just the necessary elements of a building during a repair operation.
- Designed for structures that vibrates in the first and fundamental mode, the pushover analysis offers a fair approximation of global and local inelastic deformation needs.

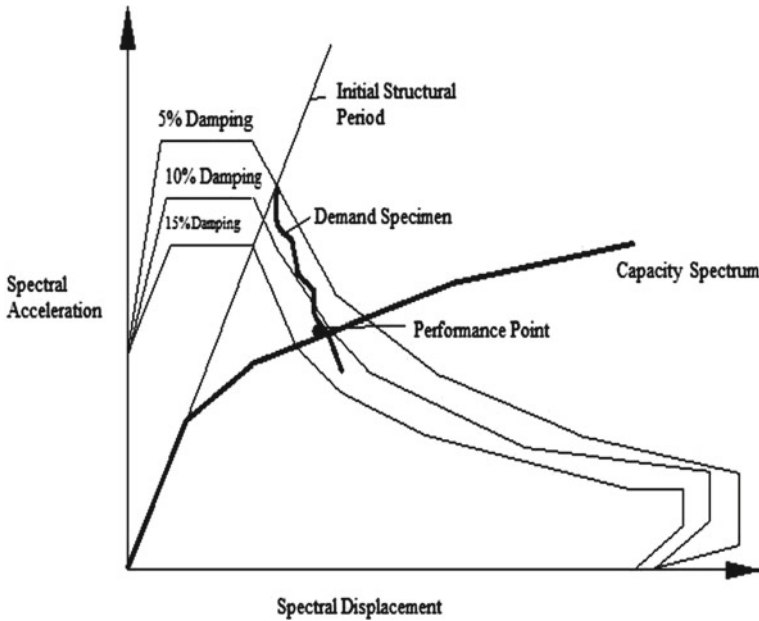


Fig. 3 Demand and capacity spectra

2.2 Limitations of Pushover Analysis

- Pushover study deformation estimations may be very off for structures with considerable higher mode special effects [12].
- On the evolution of elastic mechanism and P-delta effects, the maximum displacement linked with very ultimate +ve or -ve lateral stiffness, making it essential to conduct an analysis which uses displacements when compared to the force based methods.
- Without considering the impact of time, the number of stress reversals, or the cumulative energy dissipation requirement, pushover analysis provides an implicit guarantee that damage is proportional exclusively to the lateral displacement of the structure.
- The technique disregards the fact that a building's modal characteristics will evolve over time as it undergoes cyclic nonlinear yielding in the course of an earthquake.
- One bigger concern is that pushover analysis may only pick up on the initial local mechanism that forms during an earthquake, and might not reveal any further weaknesses that are developed as a result of changes in the dynamic properties of the structure [13].

3 Modelling and Analysis of Building

3.1 Introduction to SAP 2000

SAP 2000 was preferred in the analysis of the structures in this paper. Computers and structures (a company in Berkeley, California) created it. It is an all-inclusive software suite that has a unified user interface for model making, tweaking, running analyses, optimising designs, and reviewing the outcomes of such efforts. To analyse and construct civil structures, users may use SAP 2000, a stand-alone tool based on finite elements. In addition to providing the advanced modelling tools and methodologies required for even the most challenging tasks, its user-friendly interface makes working with it a delight.

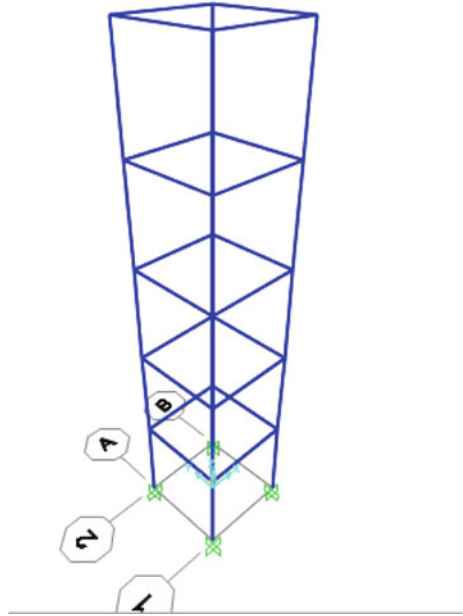
Since SAP 2000 is an object-based system, it follows that its models must include components that correspond to the actual world. Analysis and design results are given at the object level, making the data more accessible and more in line with the actual world.

Features of the SAP 2000 structural analysis software

- Frame and shell structural parts Linear and nonlinear analysis.
- Static (Linear) push over analysis and dynamic (Nonlinear) seismic analysis which were involved in the geometric nonlinearity such as P-Delta effects.
- Planar and solid geometry in two and three dimensions [14].

Table 1 Design consideration factors [14]

(i)	Zone	V
(ii)	Zone factor	0.36
(iii)	Response reduction factor	3
(iv)	Important factor	1
(v)	Soil condition	Medium
(vi)	Height of building	14 m
(vii)	Wall thickness	230 mm
viii)	Weight density of brick masonry	20 kN/m ³
(ix)	Weight density of RC material	25 kN/m ³
(x)	Storey	G + 4
(xi)	Floor to floor height	3.5 m
(xii)	Size of columns	230 mm × 450 mm
(xiii)	Size of beams	230 mm × 400 mm
(xiv)	Size of brace	50 × 50 × 6 mm
(xv)	Grade of steel	Fe-415
(xvi)	Grade of concrete	M20
(xvii)	Floor finish	1.0 kN/m ²
(xviii)	Imposed load	3.0 kN/m ²

Fig. 4 G+4 SAP 3D model

Figures 4, 5, and 6 show the x- and y-axis models' 3D representations, distorted shapes, and hinge patterns, respectively. Study of the model in the x-direction revealed hinges on the columns of the open ground storey, indicating poor performance under seismic excitation; likewise, analysis of the model in the y-direction revealed hinges on beams, indicating poor performance under seismic excitation.

4 Results and Discussions

In this investigation, SAP 2000 was used to analyse the nonlinear response of a pre-existing RC frame structure subjected to loads. The purpose of this research study is to confirm the structural x-axis and y-axis performance levels during seismic stimulation. The pushover curve can be seen in Figs. 7 and 8 once the analysis has been conducted. The models in both the x- and y-directions are shown in Figs. 7 and 8, which show the demand and capacity spectrum. Table 2 provides a frequency distribution of the studied models.

Fig. 5 Deformed shape of G+4 SAP 2D model

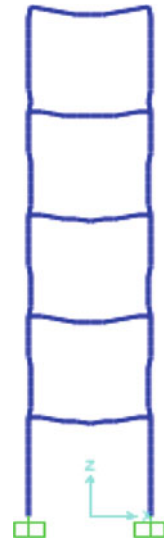
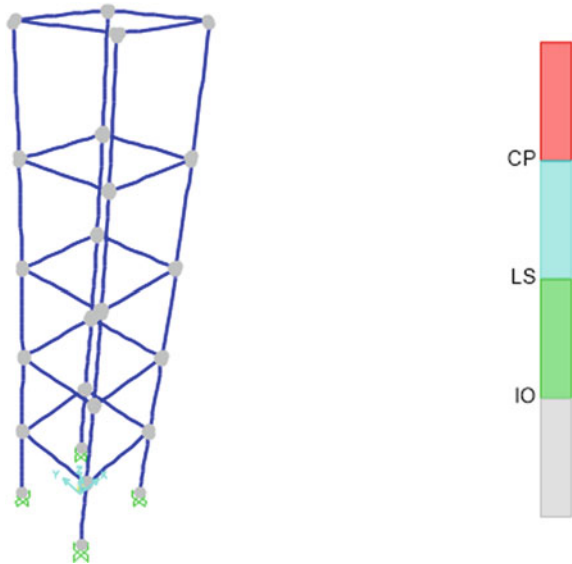


Fig. 6 Hinge patterns of the model based on performance analysis



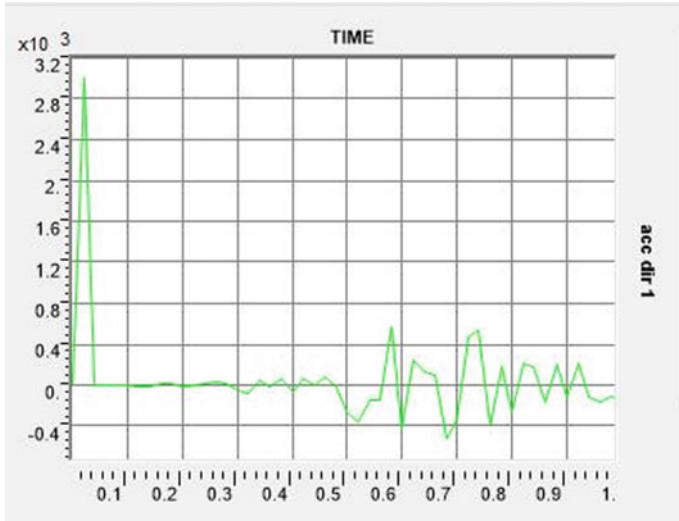


Fig. 7 Pushover curve

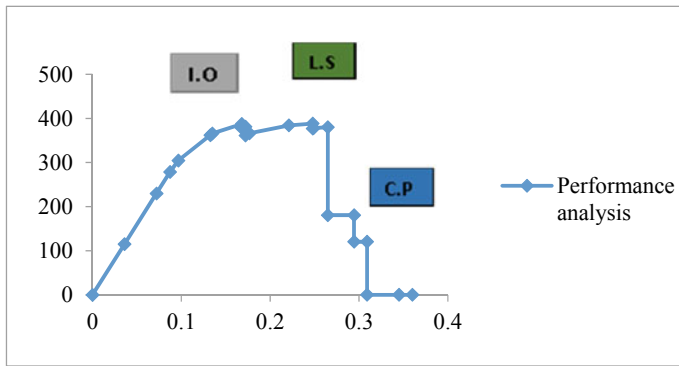


Fig. 8 Performance analysis chart. *I.O-immediate Occupancy, L.S-Life Safety and C.P-Collapse [15]

Table 2 Frequency of 3D RC frame model

Mode	SAP Analysis	
	Natural frequency, ω (rad/sec)	Natural period, T (sec)
Mode 1	3.309945561	0.30212
Mode 2	3.962748988	0.25235
Mode 3	4.057250408	0.246472
Mode 4	5.479999463	0.182482
Mode 5	5.808854733	0.172151
Mode 6	7.932040564	0.126071
Mode 7	10.28310238	0.097247
Mode 8	11.47377239	0.087155
Mode 9	11.92775844	0.083838
Mode10	12.95094653	0.083838
Mode11	13.55345405	0.073782
Mode12	13.71483523	0.072914

5 Conclusion

High-rise structures natural periods of vibration are determined using SAP analyses. In this context, a three-storey RC frame building is being considered. The natural periods and frequencies were determined and compared to the IS 1893: 2016 data using eigenvalue analysis in SAP. The study's results may be applied to even more massive buildings, such as skyscrapers. Modify the fundamental frequency by raising the height of the structure and softening its rigidity just a little. The column components' sizes have an effect on the building's stiffness and mass. Every adjustment in column size, therefore, has far-reaching consequences. According to the performance analysis chart, the numerical model yields results that are consistent with the theoretical model. There is no lumped-mass idealisation of material elasticity or structural stiffness in SAP. Significant features of this structure are modelled using nonlinear analytic techniques like pushover analysis. Increasing numbers of researchers and architects are using these methods for evaluating a structure's vulnerability to earthquakes.

References

1. Newmark NM, Rosenblueth E, Pao YH (1971) Fundamentals of earthquake engineering. Prentice-Hall, London
2. Saidi M, Sozen MA (1981) Simple nonlinear analysis of R/C structures. J Struct Div ASCE 107(5):937–952
3. Laogan BT, Elnashai AS (1999) Structural performance and economics of tall high strength RC buildings in seismic regions. Struct Des Tall Buildings 8(3):171–204

4. FEMA 356 (2000) Pre-standard and commentary for the seismic rehabilitation of buildings. American society of Civil Engineers, Reston, Virginia
5. Ghobarah A (2001) Performance-based design in earthquake engineering: state of development. *Eng Struct* 23(8):878–884
6. Rui J (2004) Application of SAP2000 in static elastoplastic analysis. *J Zhengzhou Univ*
7. GB 50352-2005 (2005) General principles for design of civil buildings. China Construction Industry Press, Beijing
8. Federal Emergency Management Agency (2005) FEMA-440: Improvement of nonlinear static seismic analysis procedures. Washington DC June 2005
9. GB 50011-2010 (2010) Code for seismic design of buildings. China Construction Industry Press, Beijing
10. Rahman MK, Ajmal M, Baluch MH (2012) Nonlinear static pushover analysis of an eight storey RC frame-shear wall building in Saudi Arabia. King Fahd University of Petroleum and Mineral, Dhahran, Saudi Arabia
11. Baraskar NB, Kawade UR (2015) Structural performance of RC Structural wall system over conventional beam column system in G+15 storey Building. *Int J Eng Res Gen Sci* 3(4), July-Aug 2015
12. Bajad MN, Shah RP, Ughareja HC (2016) A state of art review on aluminium formwork systems. *Int J Eng Res Online*, vol 4(2)
13. Hosur V, Earthquake—Resistant design of building structures. Wiley Precise Textbook
14. Nagaraju D, Venkateswarlu D, Lakshmaiah K (2016) Seismic analysis of multistorey building with bare frame, bare frame with slab element and soft storey at different levels of the building for various seismic zones. *Int J Civil Struct Eng Res* 4(1):374–391. ISSN 2348-7607 (Online)
15. IS 1893 (Part 1)-2016. Criteria for earthquake resistant design of structures. Bureau of Indian Standards, New Delhi, India

Study on Risk Allotment for Public Private Partnership in Indian Infrastructure



S. Vedha Varshini, S. Anandh, S. Sindhu Nachiar,
and B. Hemanth Sai Kalyan

1 Introduction

Public Private Partnership (PPP) are frequently utilized to undertake a variety of infrastructure projects across the world. The building of transportation systems, sports facilities, water conservation facilities, and waste-to-energy plants, among other types of infrastructure, is made possible by the PPP approach, which also raises the financial benefit of infrastructure outputs [1]. Private capital in public infrastructure may be dated back to the eighteenth century in European countries, even though the PPP concept was largely adopted in the late 1990s. The concession agreement that provided drinking the water to Paris is a prominent example [2]. Instead of native institutions, multinational corporations or foreign financial institutions have been engaged in PPP projects in China [3]. In addition to the lessons learnt through case studies, scholars have proposed the benefits of certain PPP-related elements, such as [4]: increased collaboration between the public and business sectors, improved risk taking, higher quality financial analysis, and improved contract maturation. PPPs are a product of the concept of enabling private companies to finance public sector infrastructure projects [5–13].

S. V. Varshini · S. Anandh (✉) · S. S. Nachiar · B. H. S. Kalyan
Department of Civil Engineering, Faculty of Engineering and Technology, SRM Institute of
Science and Technology, Kattankulathur, Tamil Nadu 603203, India
e-mail: anandhs@srmist.edu.in

S. V. Varshini
e-mail: Vs7984@srmist.edu.in

S. S. Nachiar
e-mail: sindhus@srmist.edu.in

B. H. S. Kalyan
e-mail: hb0040@srmist.edu.in

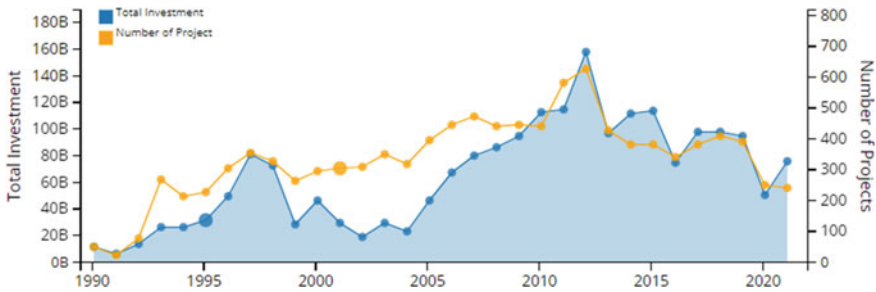


Fig. 1 Investment of projects

PPPs differ from traditional contracting or privatization in that the public and private sectors, who have distinct goals, interests, and risk preferences, share responsibility for the project's various stages [14]. PPPs divide the project's many phases among public and private duties. PPPs, particularly in the infrastructure sector, are subject to a wide range of hazards that have a significant influence on budget expenses, project performance, and service quality [15]. In PPP, services are done under specific terms and conditions [16–19]. Researchers should keep track of the PPP life cycle, spot possible problems, and offer solutions in order to support the growth of the expanding PPP infrastructure. A review of the literature is a quick and easy way to find knowledge gaps and get ideas for new research areas. It has been proven for a number of years that the life cycle viewpoint is effective in lowering the overall cost of construction projects [20–22]. A review of the literature is a quick and easy way to find knowledge gaps and get ideas for new research areas. This approach has been used by several academics to assess the pace of advancement in the PPP field. Over the years 1998 to 2008, the papers published, the contributions of key researchers, and various research interests were examined [23–25]. The evolution of PPP project execution from 1990 to 2014 is seen in Fig. 1. During this time, an upward tendency may be seen (i.e., 1990–2014).

The objective of this research is to study the different kind of PPP projects prevailing in India until 2019. Examine the status of different PPP in terms of infrastructure in PAN India. Assess the various risks associated with PPP and find suitable suggestion to overcome risk. Analyze the nature and magnitude of societal need and achieved under PPP in a particular project. Determine the critical factors responsible for success in the PPP project.

2 Research Methodology

Thematic maps have been created using ARC GIS software. The data of the public private partnership projects is taken from the website <https://www.pppinindia.gov.in/> which is controlled by the government. The data taken for this mapping is till 2019.

This map shows the different type of PPP project sectors in India. The major sectors are transportation, energy, water, and sanitation, social and commercial. Maharashtra has the highest PPP projects compared to other states. Chandigarh has only 1 project so far. The major sector which has more projects are in transportation.

This map gives the projects which are in stages of completion, operation and maintenance, pre-construction, and under construction till 2019. Operation and maintenance stage is predominant when compared to all other stages. Figure 2 gives the complete status of the PPP projects. The sector wise classifications are ports, transport, energy, water, and sanitation. Each sector has various project groups undertaken namely public private partnership, government sector, captive and private sector.

For PPP projects, risks are a constant study issue of interest. The methodology featured thorough scenario modeling of important project hazards and comprehensive expert professional judgment processing. Table 1 shows the different risk factors and bearers accordingly.

2.1 Risk Elements

Risks that have an impact on a project's desired results are detected, evaluated, and either prevented or minimized via the profession of risk management. Every project manager and team member must develop the ability to implement effective and organized risk mitigation methods. The risk factors and bearers are shown in Table 1. As a result, the entire organization will be able to manage its projects in the following ways. Predicting future expenses will help any resource planning.

- Upgrade businesses' project cost tracking systems.
- Increased ROI estimation accuracy.
- A more adaptable response to any upcoming issues.
- Increased ROI estimation accuracy.

3 Results and Discussion

3.1 Pre-operative Phase

During the pre-operative phase, design, project's strategic plan, procurement of permits or entitlements, and gathering of workers and construction-related materials are completed. This factor consists of updating of budget, updating of work schedule, motivation of workers, procurement of materials, meeting for design management, and meeting for construction management and it having 25.98% of variation.

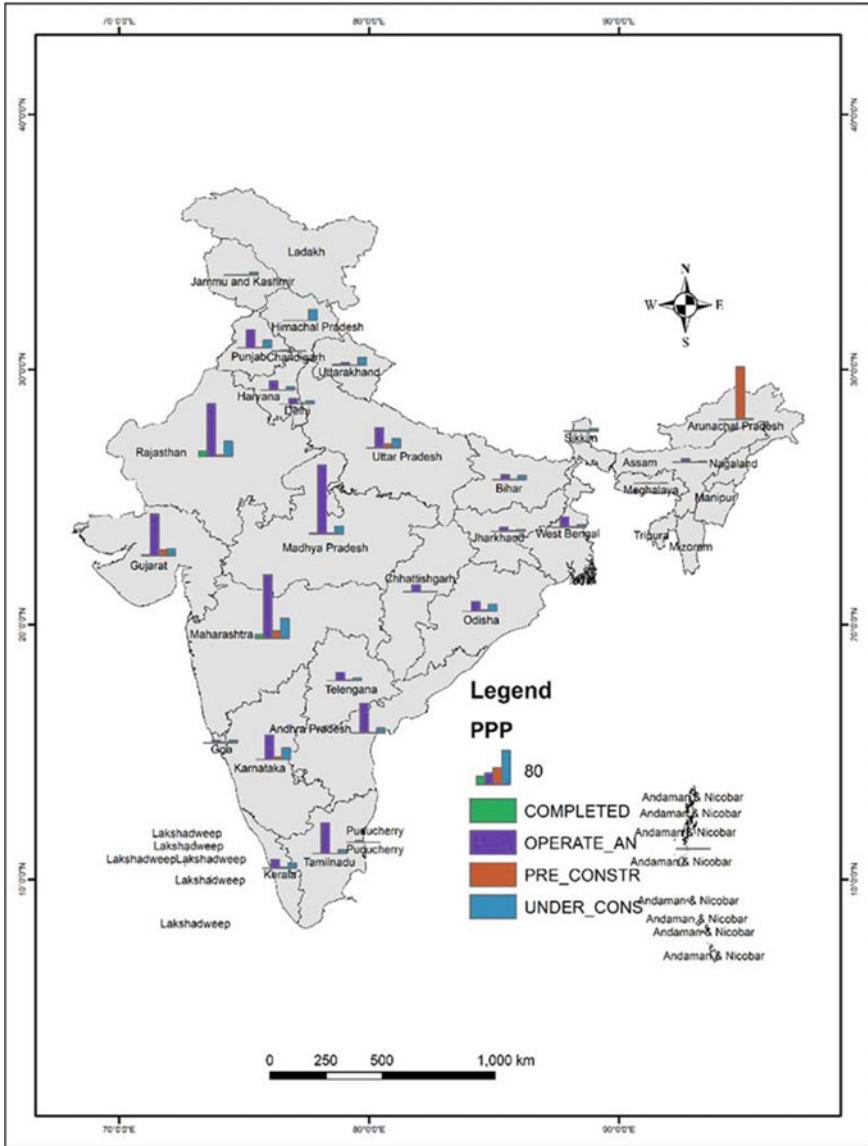


Fig. 2 Public private partnership status

Table 1 Risk factors and risk bearers

Risk factors	Primary risk bearers
<i>Pre-operative risk</i>	
Delay in land acquisition	Government
External linkages	Government
Financing	Private
Planning	Private
Approvals	Private
<i>Construction phase risk</i>	
Design risk	Private
Construction risk	Private
Approvals	Private
Operation phase risk	Private
Technology risk	Private
Operation risk	Private
Market risk	Private
Financial risk	Private
<i>Hand over risk</i>	
Terminal value risk	Private
<i>Other risk</i>	
Change in law	Private

3.2 Construction Phase

Construction phase responsibilities include clearing the site, landscaping, remodeling, demolition, and the actual building process. This factor comprises of involvement, capacity and obligation, alternative strategies, effective communication, and recognized schedules and it having 19.64% of variation.

3.3 Operation Phase

The monitoring phase, which advances concurrently, is when the concept and all operational decisions are assessed and improved. This factor includes market uncertainty, economic uncertainty, detection of risk, distribution of risk and diversification of risk and it having 15.35% of variation.

3.4 Handover Phase

The consumer gets back custody of the property to occupy during the handover phase of a construction project. When the agreement's tasks have been finished, as determined by the contract administrator, this happens. This factor contains size of the project, nature of work, complication, and clarity and it having 11.80% of variation.

3.5 Others

This factor covers technical competencies, monitoring, and feedback and it having 8.72% of variation. A factor analysis suggests that process interaction, human resource management, risk level, project characteristics, and process control are the main variables affecting effective risk in construction projects.

4 Conclusion

- The thematic maps are prepared using ARC GIS software which gives an idea of types of sectors under PPP, most used modes, and the status of projects which are in completed stage, operation and maintenance stage, pre-construction stage, and in under construction stage.
- Risk analysis is an essential part of PPP projects. It aids in the identification of possible risks and the development of methods to reduce them, so assuring the project's successful conclusion.
- Any public private partnership's success depends on achieving a financial equilibrium that enables the recovery of capital investments, whether for new construction or maintenance and operation.
- Several factors are considered in order to ensure the proper establishment of PPP, including the fairness of the deal for all parties, the clarity of the contract terms, the transparency between parties, the proper timing of the process, the appropriate communication tools, or the adequate monitoring schemes during the contract management.
- However, there are several issues that must be resolved, including the dearth of accurate information and the complex structure of PPP projects. PPP projects in the nation's port sector may realize their full potential while contributing to the nation's economic progress by resolving these issues and putting into place efficient risk management techniques.

References

1. Carter BC, Parra JD (2021) Structural impediments to policy learning: Lessons from Colombia's road concession programs. *Int J Publ Adm* 44(5):359–371. Kumaraswamy MM, Morris DA (2002) Build–operate–transfer type procurement in Asian megaprojects. *J Constr Eng Manage* 128(2):93–102
2. Koul P, Verma P, Arora L (2021) Road infrastructure development under PPP model in India: a credit rating perspective. *Built Environ Proj Asset Manage* 11(2):266–283
3. Mwesigwa R, Bagire V, Ntayi JM, Munene JC (2020) Contract completeness as a foundation to relationship building among stakeholders in public private partnership projects. *Int J Public Adm* 43(10):890–899
4. Nguyen HT, Le Thu H, Thach MQ, Pham Diem H (2022) Factors affecting public-private partnership preference in Vietnam Road infrastructure projects. In: CIGOS 2021, emerging technologies and applications for green infrastructure, vol 203. LNCE, pp 1525–1533
5. James AD, Cox D, Rigby J (2005) Testing the boundaries of public private partnership: the privatization of the UK defence evaluation and research agency. *Sci Publ Policy* 32(2):155–161
6. Li B, Akintoye A, Edwards PJ, Hardcastle C (2005) The allocation of risk in PPP/PFI construction projects in the UK. *Int J Proj Manage* 23(1):25–35
7. Li B, Akintoye A (2003) An overview of public–private partnership. In: Akintoye A, Beck M, Hardcastle C (eds), *Public–private part-heirships: managing risks and opportunities*. Blackwell Science Ltd., UK
8. Castelblanco G, Guevara J, Salazar J (2022) Remedies to the PPP crisis in the COVID-19 pandemic: lessons from the 2008 global financial crisis. *J Manag Eng* 38:04022017
9. Dansoh A, Frimpong S, Ampratwum G, Dennis Oppong G, Osei-Kyei R (2020) Exploring the role of traditional authorities in managing the public as stakeholders on PPP projects: a case study. *Int J Constr Manag* 20:628–641
10. Rybnicek R, Placolm J, Baumgartner L (2020) Risks in public-private partnerships: a systematic literature review of risk factors, their impact and risk mitigation strategies. *Publ Perform Manag Rev* 43(5):1174–1208
11. Kudtarkar SG (2020) Failure of operational PPP projects in India leading to private developer's apathy to participate in future projects: a case study-based analysis. *Indian J Fin Bank* 4(2):17–27
12. Chan WT, Chen C, Messner JI, Chua DK (2005) Interface management for China's build-operate–transfer projects. *J Constr Eng Manage* 131(6):645–655
13. Guo HL, Li H, Skitmore M (2010) Life-cycle management of construction projects based on virtual prototyping technology. *Manage Eng* 26(1):41–47
14. Ke Y, Wang S, Chan APC, Cheung E (2009) Research trend of public-private partnership in construction journals. *Constr Eng Manage* 135(10):1076–1086
15. Teasman GR, Klijn EH (2002) Partnership arrangements: Governmental rhetoric or governance scheme. *Publ Adm Rev* 62(2):189–198
16. Klijn E-H, Teisman GR (2003) Institutional and strategic barriers to public–private partnership: an analysis of Dutch cases. *Publ Money Manage* 23(3):137–146
17. Savas E (2000) *Privatization and public-private partnerships*. Seven Bridges Press, New York, NY
18. Hemanth B, Kalyan S, Sekar A, Nachiar SS, Ravichandran PT (2022) Discerning recurrent factors in construction disputes through judicial case studies—an Indian perspective. *mdpi.com* 2022. <https://doi.org/10.3390/buildings12122229>
19. Grimsey D, Lewis M (2002) Evaluating the risks of public private partnerships for infrastructure projects. *Int J Proj Manage* 20(2):107–118
20. Grimsey D, Lewis M (2002) Accounting for public private partnerships. *Account Forum* 26(3–4):245–270
21. Delmon J (2009) *Private sector investment in infrastructure: project finance*. PPP Projects and Risks, Kluwer Law International, The Netherlands

22. Grimsey D, Lewis M (2004) *Public private partnerships: the worldwide revolution infrastructure provision and project finance*. Edward Elgar, Cheltenham, Northampton
23. Demirag I, Khadaroo I (2008) Accountability and value for money in private finance initiative contracts. *Financ Acc Manag* 24(4):455–478
24. Chung D (2012) Contractual approach to optimising risk sharing: a quantitative study of the multidimensional nature of risk in private provision of road infrastructure”, available at: <http://ses.library.usyd.edu.au:80/handle/2123/8842> (Accessed 25 Apr 2014)
25. Hoppe E, Kusterer D, Schmitz P (2013) Public-private partnerships versus traditional procurement: an experimental investigation. *J Econ Behav Organ* 89:145–166

Adopting the Low-Cost Housing Technology in Residential Buildings in Chennai



K. T. Murali Krishnan, S. Manikandaprabhu , and D. Nigitha

1 Introduction

One of the most serious issues confronting emerging nations is the supply of sufficient housing, which is critical in people's lives. Housing has become a crucial component of daily life, yet only 20% of the population in emerging markets such as India has a high enough income to buy typical housing units. As a result, low-income residents in emerging nations find it difficult to enter the housing market. In India, the problem is compounded by population expansion and skyrocketing building prices, making housing a nightmare for many. The demand and supply dynamics exacerbate the problem, resulting in the spread of slums and unplanned urban layouts. Several causes contribute to this inequality, the most notable of which include rising material prices and restricted land availability. As India's population and economy expand, there is an increasing need to satisfy the housing requirements of low- and middle-income workers by offering affordable housing alternatives.

Despite efforts from both the public and commercial sectors to provide affordable housing alternatives, there is still a housing shortage. Furthermore, many existing housing units in India are of low quality and lack essential services such as power, running water, and sanitation. As a result, crowded and unsanitary slum homes have developed. To solve these concerns, the government has developed several housing

K. T. Murali Krishnan

Department of Civil Engineering, SRM Institute of Science and Technology, Kattankulathur, Chennai 603203, India

S. Manikandaprabhu (✉)

Department of Civil Engineering, Faculty of Engineering and Technology, SRM Institute of Science and Technology, Kattankulathur, Tamil Nadu 603203, India

e-mail: saravanaprabhou@gmail.com

D. Nigitha

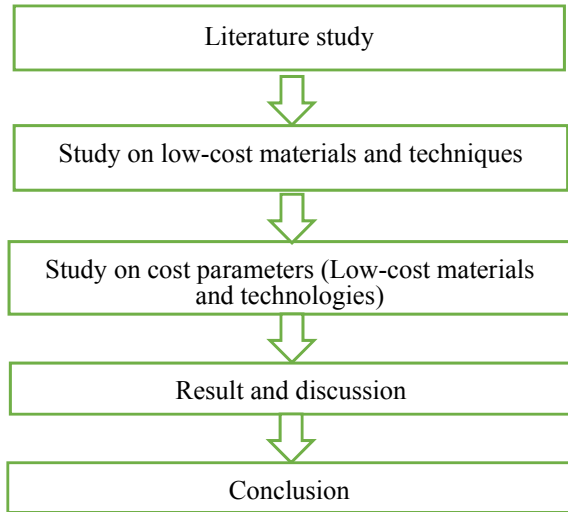
Department of Civil Engineering, SR University, Warangal, Telangana 506371, India

programs, including the Pradhan Mantri Awas Yojana, which seeks to provide affordable housing for everybody by 2022. However, administrative incompetence, corruption, and insufficient money have impeded the success of these programs. Overall, India's housing situation is a critical issue that demands ongoing efforts and financial commitment to guarantee that all citizens have access to safe, cheap, and high-quality housing. Low-cost home is a novel idea that makes the better budget control and utilizes the strategies that aid in decreasing the cost of building by using locally accessible materials as well as better skills and technology without sacrificing the structure's strength, performance, and longevity [1]. BMTPC, CBRI, IITD, IITR, IITM, IITK, and IPIRTI are just a few of the organizations responsible for developments in this field in India in the last few decades of time [1]. India has the second-largest urban population in the world. The nation requires a strategy for quick construction and land acquisition. 40% to 45% of people live in slums, and that number is increasing daily. India now has a shortfall of 17.6 million homes [2]. The cost control of a project involves the measuring and collecting the cost record of a project and work progress [3]. Finding locally accessible raw materials that can be utilized to manufacture construction materials that do not use regular cement is required to effectively finish low-cost housing projects and partially relieve the housing shortage [4]. The quality function deployment (QFD) is utilized to better understanding of client requirements, speed up the designing processes, and decrease execution time in order to attain continual improvement in affordable processing of housing schemes [5]. The construction sector uses 30–40% of all-natural resources and primary energy over its lifespan, accounting for 30% of global greenhouse gas (GHG) emissions and representing about 6% of the world's Gross Domestic Product (GDP) [6]. Creating novel technology and productivity-boosting methods is one strategy to lower the cost of building [7]. The monitoring of resource, managing the sub-contractor bills, and accounting modules aid in project cost control determination and show whether costs are within or exceeds budget [8]. This project aims to identify the most appropriate alternative materials and technologies which can be adopted for the low-cost housing. The alternative materials for wall material will be studied and technology adopted for this study is Mivan construction. The cost parameters of adopted materials and technologies will be worked on and compared with traditional construction method.

2 Methodology

The measures to address studying affordable housing are broken down into stages to better comprehend the necessity and work progress. The flow chart of Fig. 1 represents work methodology followed in this paper.

Fig. 1 Methodology flow chart



2.1 Materials

The cost of the materials is a crucial factor since it has an immediate impact on the budget. Site inspections are used to adopt alternative materials in order to assess their strength, quality, and durability. The cost parameters are studied together with the alternative low-cost materials. Both the new alternative materials and the traditional materials are worked out with cost analysis. The materials chosen for the wall masonry are AAC blocks, Fly ash bricks, and Porotherm bricks and compared with standard clay bricks.

2.1.1 Clay Bricks

When a clay brick reaches the end of its useful life, it may be recycled or used again since it is created from natural components like clay and water. As a result, choosing them for construction projects is sustainable. With a compressive strength that ranges from 10 to 40 N/mm², clay bricks are robust and long-lasting. This qualifies them for a variety of building applications, such as foundations and load-bearing walls.

2.1.2 AAC Blocks

Aerated concrete is a kind of lightweight concrete that eliminates the use of coarse materials and contains a significant amount of air voids AAC blocks weigh 12.23 kg, but CMU blocks weigh 15.4 kg. AAC blocks provide a wall area of 1.3 ft² (13.98 m²), while CMU blocks create a wall area of 0.88 ft² (9.46 m²). They are lighter than

Fig. 2 AAC blocks

conventional concrete blocks, have a higher wall area per block, and have less heat conductivity. Not appropriate for strong load bearing and its complicated manufacturing process is not suitable for small-scale production. AAC blocks are nowadays used widely for the construction of the walls in framed structures. In Chennai, the price of this blocks is Rs. 100 and if the volume is larger than the rates may reduce accordingly. The AAC blocks used in the site are represented in Fig. 2.

2.1.3 Fly Ash Bricks

Fly ash brick, typically masonry bricks, is made of class C or class F fly ash and water. The bricks can withstand more than 100 freeze–thaw cycles when compressed at 28 MPa, cured for 24 h in a 66 °C steam bath, and then toughened with an air entrainment agent [9]. In comparison to burnt clay bricks, fly ash bricks are consistent in shape and size; as a result, less mortar is needed during construction and finishing tasks, conserving cement mortar [10]. Compared to burnt clay bricks, fly ash bricks have greater quality control as they're machine-made. These bricks are manufactured in factory, and the dimensions are the same as the conventional bricks. The price of the fly ash bricks in Chennai is Rs. 6, and the strength is better than the bricks. Figure 3 represents the fly ash bricks.

2.1.4 Porotherm Bricks

Due to the 60% reduced weight of Porotherm Bricks compared to traditional walling materials, significant structural cost reductions are possible. The brick's perforated shape enables great thermal insulation, maintaining constant interior cooling. The fact that the blocks are entirely made of clay, as designated by the Green Building Council of India, makes Porotherm a natural walling material. Moreover, this makes building quicker and easy handling. These bricks are not the best option for the

Fig. 3 Fly ash bricks**Fig. 4** Porotherm bricks

building of foundation and base-slab works because of their lower density than clay bricks, which have a density of 1400–2100 kg/m³ and represented in Fig. 4.

These bricks are used in load-bearing and non-load-bearing structures. The price of these bricks is Rs. 95 and its weathering and construction time are very less.

2.2 Technologies

The construction technology adopted was Mivan construction, as it is popularly immersing and shares more benefits as well. The cost of construction of Mivan method is compared with traditional method.

2.2.1 Traditional Construction Method

The conventional process of construction involves laying the foundation, erecting the walls, roofing, and then starting to design the building's interior. This technique is applied with a framed construction using existing structures and employing common materials [11]. This technique is popular because it is reliable and durable, and it accommodates different building designs. These structures only need minimal care to last for many years in tough environments. One benefit of this approach is that adjustments may be made with little cost variation during or after construction. Workflow can be facilitated by integrating the activities. High labor requirements, difficult quality control, and lengthy and expensive construction are the drawbacks.

2.2.2 Mivan Construction Method

The construction of this method is done using aluminum formwork. This formwork is one of the most efficient methods available, requiring minimal maintenance and having a high level of durability [2]. Planning for the entire process is necessary initially. Wall, column, and slab can all be cast at the same time to save time. Aluminum panels are solid, lightweight, and convenient to handle. These can be repeated 250 times or more, and if not, it will be expensive. Its formwork's components include sheets, panels, and aluminum rail having a skin plate with a thickness of 4 and 6 mm ribbing to strengthen the panel.

2.3 Modeling of a Building

The Revit software was used to plan and design the G + 15 residential building, which has two stairs and four lifts. This is done as part of the research into low-cost materials and their cost parameters. The residential building's planning adheres to standards. This model is used to calculate the quantities of walls made of standard and low-cost materials. The scheduling of activities and the application of new cost saving technologies will be integrated to obtain low-cost construction framework. The building facing is west, and there are 8 units in a floor and each unit is of 580 ft².

The total buildup area is 8040 ft² per floor. The plan used in this study is represented in Fig. 5, typical floor plan of G + 15 residential building of 8 units in each floor. The section of the 1st floor of G + 15 residential building is shown in Fig. 6.

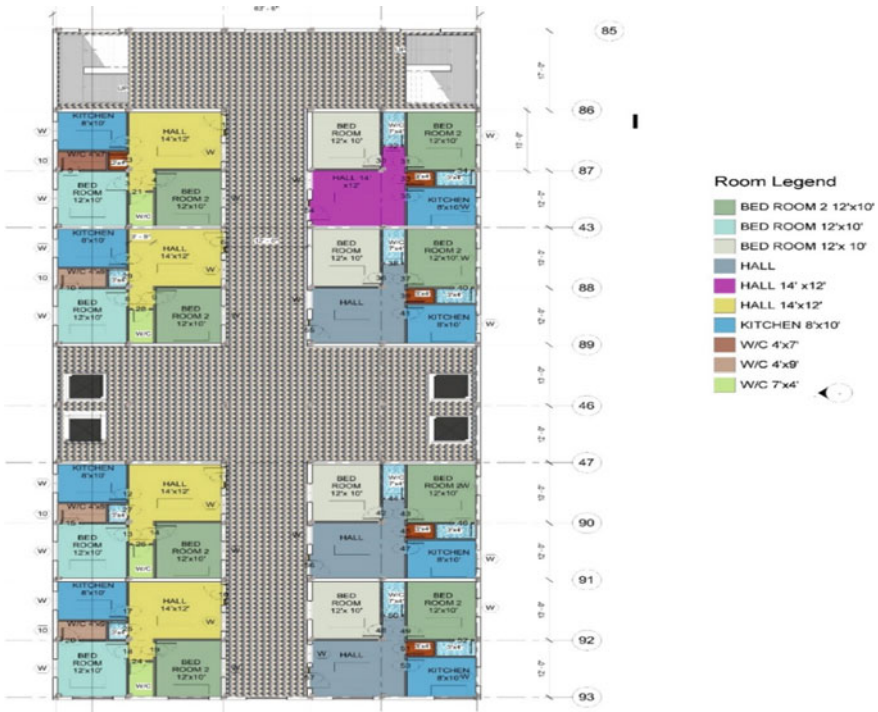


Fig. 5 Typical plan G + 15

Fig. 6 Sectional view



3 Results and Discussion

The low-cost materials used in walls are identified and their cost parameters are analyzed. This study confirms that use of eco-friendly and low-cost materials can lower the construction cost. The above chosen materials are good in strength and durable. Each has their own advantages and can be selected according to the availability and other conditions [12].

Table 1 Cost of wall materials

Materials	Volume of wall materials (m ³)	No. of bricks required	Cost of bricks/ blocks (INR)	Rate per 1 m ³
Bricks	3210	1,605,485	16,054,850	5002
AAC blocks	3210	106,676	10,667,671	3323
Fly ash bricks	3210	1,396,073	8,376,441	2609
Porotherm bricks	3210	178,387	13,379,025	4168

3.1 Materials

When the material cost of clay bricks is compared to the cost of AAC blocks, Fly ash bricks, and Porotherm bricks, the difference is 33, 47, and 16 respectively. Table 1 shows the material requirement and cost of the materials for the construction of the wall using various materials.

3.2 Technologies

The cost parameters are been worked out with traditional construction method for the adopted G + 15 residential building. The activities are identified and the quantities are calculated. The conventional materials and workflow are considered and the rates are taken as per the market rate (Chennai, Tamil Nadu, and India). The cost of construction of G + 15 residential building in this method is Rs. 305,853,000.00 (INR) and it is represented in Table 2. Brick, mortar, and other conventional building materials, such as timber and steel, are used in traditional construction to erect buildings. This approach takes a long time since it involves a lot of labor-intensive on-site construction of each building component.

The cost parameters are been worked out with Mivan construction method for the adopted G + 15 residential building. Less labor is used; the building process is quick; panels are reused; formwork is made to order; it is seismically resistant and requires less maintenance, and tower cranes are not needed. Finishing lines may be seen, planning should be done prior to construction, casting requires less alteration, and shrinkage cracks may occur are some drawbacks suitable for both low- and high-rise buildings. Estimated building time per floor is 6–8 days. The total budget for the G + 15 residential building is Rs. 384,042,000 (INR), and cost breakdown is represented in Table 3.

Table 2 Rate analysis abstract of traditional construction

Rate analysis of proposed building (traditional)		
S. No.	Description	Amount
1	Pile foundation up to a depth of 72'	121,380,131.55
2	Providing and laying RCC M20 grade for columns, beams, and slabs	27,449,493.75
3	Providing and laying brick masonry and plastering	32,936,512.50
4	Providing and applying 1 coat white + 1 coat interior primer + 2 coat emulsion on interior exterior and roof surface	36,194,253.75
5	Providing and laying flooring tiles	27,719,979.00
6	Carpentry works	21,492,000.00
7	Providing electrification	17,006,046.65
8	Construction of septic tank and sanitary arrangements	21,674,373.18
Total amount		305,852,790.38

Table 3 Rate analysis abstract of Mivan construction

Rate analysis of proposed building (Mivan technology)		
S. No.	Description	Amount
1	Pile foundation up to a depth of 72'	121,380,131.55
2	Providing and laying RCC M20 grade for columns, beams, and slabs	148,574,493.80
4	Providing and applying 1 coat white + 1 coat interior primer + 2 coat emulsion on interior exterior and roof surface	26,194,253.75
5	Providing and laying flooring tiles	27,719,979.00
6	Providing doors, windows, and painting	21,492,000.00
7	Providing electrification	17,006,046.65
8	Construction of septic tank and sanitary arrangements	21,674,373.18
Total amount		384,041,277.93

4 Conclusion

The papers discuss cost-cutting strategies and methods for increasing productivity. The design aspects are also reviewed because the customers intend to make changes and expand the house in the future. When the material cost of clay bricks is compared to the cost of AAC blocks, Fly ash bricks, and Porotherm bricks, the difference is 33, 47, and 16 in percentage respectively. AAC blocks require fewer bricks, reducing handling and wastage costs. Traditional construction methods often result in 20–30% brick wastage overall. Proper material selection can also reduce transportation and lifting charges. Mivan construction stands in stark contrast to traditional building methods, representing the latest developments in construction technology. Compared

to conventional shuttering techniques, the productivity of Mivan shuttering is significantly higher, with an average of 6.00 m²/man/day compared to 2.10 m²/man/day. This increased productivity translates into notable cost savings, with the construction cost of a G + 15 residential building being 25.11% lower when using Mivan construction. While the difference typically ranges from 15 to 20%, site conditions, location, and weather can cause variations. The rates used for these calculations are based on local market rates in the Chennai region.

Ultimately, the decision between traditional construction and Mivan construction depends on the specific project requirements, including budget, schedule, and desired quality level. Both approaches offer advantages and disadvantages, necessitating careful consideration before selecting one. Despite the higher initial expenditure, Mivan construction is often the preferred option for major projects, given its significant benefits. Integrating Mivan technology with precast technology can achieve affordable housing with efficiency and short duration, making it a suitable option for low-cost housing development.

References

1. Srivastava M, Kumar V (2018) The methods of using low-cost housing techniques in India. *J Build Eng* 15:102–108
2. Jasvi AH, Bera DK (2015) Sustainable use of low-cost building materials in the rural India. *Int J Res Eng Technol* 4(13):14
3. Hafez SM, Aziz RF, Elzebak HMM (2015) Optimal techniques for cost reduction and control in construction sites. *J Hum Resour Manag* 3(3):17–26
4. Taffese WZ (2012) Low-cost eco-friendly building material: a case study in Ethiopia. *Int J Civ Environ Struct Constr Archit Eng* 6(2):183–187
5. Salim AM, Alabdouli SH (2022) Application of quality function deployment method to design affordable houses in the United Arab Emirates. In: 2022 advances in science and engineering technology international conferences (ASET), Feb 2022. IEEE
6. Filho MV, da Costa BB, Najjar M, Figueiredo KV, de Mendonça MB, Haddad AN (2022) Sustainability assessment of a low-income building: a BIM-LCSA-FAHP-based analysis. *Buildings* 12(2):181
7. Formoso CT, Tillmann PA, Hentschke CDS (2022) Guidelines for the implementation of mass customization in affordable house-building projects. *Sustainability* 14(7):4141
8. Akhil RP, Das BB (2019) Cost reduction techniques on MEP projects. In: *Sustainable construction and building materials*. Springer, Singapore
9. Chowdhury S, Roy S (2013) Prospects of low-cost housing in India
10. Shinde SS, Karankal AB (2013) Affordable housing materials & techniques for urban poor's. *Int J Sci Res IJSR* 1:30–36
11. Sakin M, Kiroglu YC (2017) 3D printing of buildings: construction of the sustainable houses of the future by BIM. *Energy Procedia* 134:702–711
12. Gopalan K, Venkataraman M (2015) Affordable housing: policy and practice in India. *IIMB Manag Rev* 27(2):129–140

Building Energy Conservation and Green Architecture

Seismic Response Control Strategies for Buildings



J. Jestalt Srisanth, G. V. Rama Rao, and D. Senthil Velan

1 Introduction

An earthquake is a devastating natural disaster that potentially threatens life, destroys property, and disrupts essential services and public functioning. Natural catastrophes like earthquakes, floods, landslides, cyclones, and tsunamis frequently occur in India. Large-scale earthquakes have had an especially negative impact on India in recent decades. Therefore, there is an urgent need for an earthquake-resistance management strategy to minimize damage to buildings in the event of an earthquake.

The primary strategy for enhancing seismic performance and damage prevention of buildings is that of seismic response control strategies like passive, semi-active, and active control strategies. Addition of base isolation and shear wall as passive seismic response control system will help in controlling the seismic response of building. Structural response control is an emerging technology for seismic hazard mitigation in earthquake engineering and has been widely studied over the world. Whittaker [5] de-mystifies preliminary design of base-isolation systems in accordance with international earthquake design standard. Hadihosseini et al. [6] provide the structural performance of a framed building with shear wall. Rama Rao et al. [2] discuss the SAP2000 modeling of framed buildings with in-fills and supporting soil modeling. Rama Rao et al. [4] discuss a parametric study on the nonlinear ductile behavior of shear wall using ABAQUS finite element software. Rama Rao et al. [3] studied the nonlinear performance of three identical medium aspect ratio shear walls through application of monotonic and cyclic loading.

A number of research studies are available for each seismic response control strategy, however, comparative studies on the effectiveness of various seismic

J. Jestalt Srisanth (✉) · D. Senthil Velan
SRM IST Ramapuram, Chennai, India
e-mail: jestaltsrisanth@gmail.com

G. V. Rama Rao
CSIR-Structural Engineering Research Centre, Chennai, India

response control strategies are found to be scarce. A comparative study is conducted between these two control strategies. A five-storied building is considered for the present study and modeled in SAP2000 software using linear time history analysis. Newhall ground motion data, taken from SAP2000 database, is used for analyses. In one building, shear wall is designed and added, to resist seismic ground motions. In the other building with similar dimensions, base isolation is designed to resist seismic ground motions.

1.1 Base Isolation

The philosophy of seismic resistant design is undergoing a rapid change with emphasis on preserving the structure and its interiors intact and without letting them into nonlinear range. The best possible potential alternative is mounting of the structure on flexible elements which are replaced after a severe earthquake but the parent structure is prevented from damage. The fundamental idea is to extend the structure's time period such that the spectral acceleration is minimized. The inter-story drift is decreased since the superstructure essentially functions like a rigid body. The isolation moves the structure's position in the spectrum from the peak-plateau region to the lower regions by lowering the fundamental lateral frequency of the structure relative to its fixed base frequency (or lengthening the structure's time period). Because of this, higher damping is introduced at the base level as a result, and more damping is also produced, which further reduces the spectral acceleration. The benefit of using a base-isolation system is that in the event of an unexpected large-scale seismic activity, the damage is concentrated only on systems whose elements can be replaced.

1.2 Shear Wall

Shear walls are structural walls that are specifically built into structures to withstand lateral stresses that are created in the wall's plane by wind, earthquakes, and other factors. They are typically given in tall structures and have been found to be of great assistance in preventing the complete collapse of buildings under seismic forces. When designing shear walls, we should aim to load them with as much weight as they can safely support in order to minimize the bending tensile stresses brought on by lateral loads. In order to prevent torsional strains, they should also be laid symmetrically. Figure 2 shows the placement of shear wall symmetrically in a building to reduce torsion effects.

Shear walls are categorized by type: simple rectangular and with bounding elements, coupled shear walls, and boxed walls. A simple rectangular type is taken into consideration where normal gravity load and horizontal shear action along its length are subjected to bending and shearing. These latter types are called bar walls (rectangular walls with bounding elements) and are somewhat stronger and more

ductile. These walls must be designed so that they never fail under shear forces and do not fail due to deformation of the steel when bent. Shear failure is fragile and sudden. One of the disadvantages of this shear wall is that as these being rigid, during an earthquake, it attracts and dissipates a lot of energy by cracking, which is difficult in repair. This defect can be rectified in coupled shear walls. When two structural walls are connected by relatively short spandrel beams, the resulting wall becomes more rigid and the structure is able to release the majority of the energy by yielding the coupling beams without causing structural damage to the primary walls. It is easy to repair these coupling beams than the walls. In some buildings, the elevators and other service areas can be grouped in a vertical core which may serve as a device to withstand lateral forces. In most of the cases, moment-resisting frames are connected to stiffening walls. The interaction between rigid walls and moment frames of tall buildings is worth studying. Frame deflection occurs in shear mode and walls in bending mode. This interaction tends to reduce the maximum bending moment but increases the maximum shear force in the shear wall.

2 Analytical Study on Seismic Response Control Strategies

The above two control strategies (shear wall and base isolation) are taken into consideration and applied to a five-storied building. The reference in case one is a normal framed construction. In the other cases, shear walls are added in one case while base isolation is used in the other.

2.1 Case Study—1: Normal Framed Building

In this study, we consider a five-story square building with five spans in both X and Y directions. For this research, SAP2000 software is adopted. The structural model selected for the analytical study is designed as per IS 456:2000 [7] and linear time history analysis is performed. A 4 m bay width is common to all bays and a 3 m floor height is common to all floors. Beams and columns are modeled using 3D framing components. Figure 1 shows a 3D SAP2000 model of a normal frame building. The assumed beams and columns are given its cross-section dimensions, reinforcement details, and the type of material used. Material properties such as specific gravity, modulus of elasticity, Poisson's ratio, shear modulus of elasticity, specific compressive strength, yield strength, and ultimate stress of reinforcing steel and concrete are presented.

M25 grade concrete and Fe415 grade steel are the materials used. For all the simulations, a column with dimensions of 350 mm, 300 mm, and a 300 mm depth that is orientated in the X -direction is considered. Eight no's of 16 mm diameter bars are used for the column's longitudinal reinforcement, and 6 mm stirrups are used for the column's transverse reinforcement at 150 mm c/c. With six no's of 16 mm

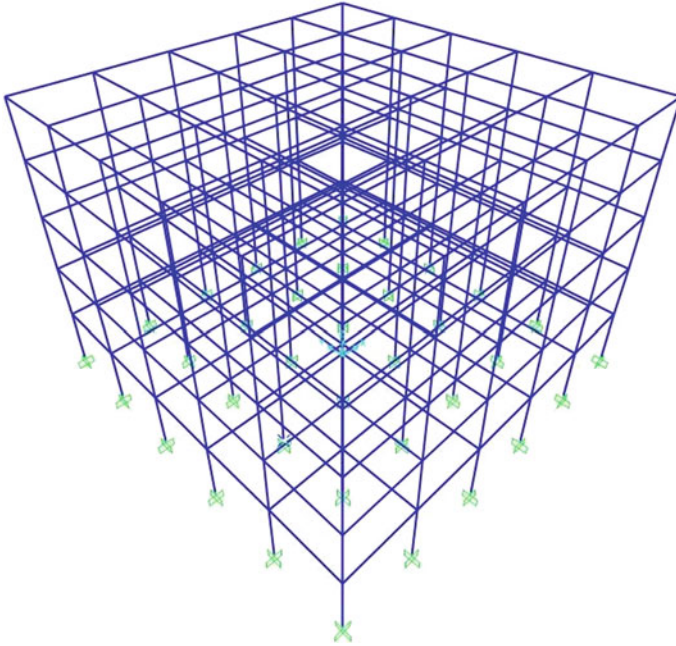
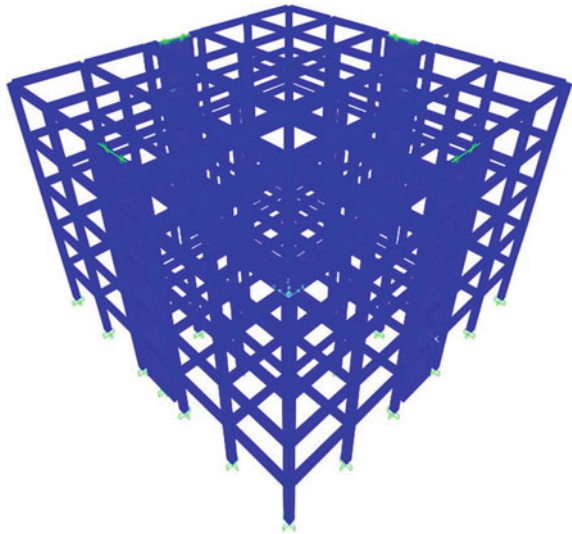


Fig. 1 SAP2000 model of 3D normal framed building

Fig. 2 SAP2000 model of framed building with addition of shear wall



diameter bars and 6 mm diameter (as per IS 456), stirrups at 150 mm center-to-center; 300 mm × 300 mm beam is used. To account for the impact of cracking, the moment of inertia of the beam and column have been modified by 0.5 and 0.7, respectively. The 120 mm slab thickness is taken into account. Outer brick infill walls are assumed to be 230 mm thick, while partition walls are assumed to be 115 mm thick. The infill wall is not modeled; however, the mass of the infill is considered and distributed on the beam. The unit weight of brick infill is taken as 20 kN/m³ where a 50% opening in the all-infill walls is considered.

The floor finish for typical floors is assumed to be 1.0 kN/m² and the imposed load on the ceiling is assumed to be 2.0 kN/m². According to IS 1893 Part 1 (2016) [1], live load is not considered for roof load. These structural data are listed in Table 1. In order to simulate the slab’s high in-plane stiffness, diaphragm constraint action is assigned at each floor level. Self-weight and loads acting on the slab are calculated separately as triangular loads and applied on the supporting beams. Beam and column connections were modeled by setting end length offsets for frame members. Dead load and live loads are applied as gravity loads. The importance factor is assumed to be 1.0, and the response reduction factor is assumed to be 3. Load combinations are considered as per IS 1893 (Part 1): 2016 [1]. A linear time history analysis has been performed in the X-direction (along the side of a 300 mm deep column) by applying Newhall earthquake data. Further, modal analysis is also performed. Table 2 shows the shear force, bending moment comparison of the critical column. The natural time period of the building is shown in Table 3. A comparison of inter-story drift is plotted in Fig. 6 and the top deflection of each floor is plotted in Fig. 5. The columns adopted for the study do not meet design seismic load calculations for zone-V, but only for the calculations for zone-III. To overcome this, a column size of 450 mm × 400 mm is used to meet the building design in zone-V with a depth of 400 mm oriented along the X axis where the longitudinal reinforcement in column is 12 no’s of 16 mm diameter reinforcements bars with 8 mm diameter stirrups at 150 mm c/c spacing.

Table 1 Structural data of the structure

Grade of concrete	M25	Column size	300 × 350
Grade of steel	Fe415	Beam size	300 × 300
Floor to floor height	3.0 m	Infill wall thickness	230 mm
Floor finish	1 kN/m ²	Partition-wall thickness	115 mm
Slab thickness	120 mm	Seismic zone	V
Live load	2 kN/m ²	Responsereduction factor	3
Soli type	Medium	Importance factor	1

Table 2 Critical column comparison

Case study number	Bending moment (kNm)	Shear force (kN)
Fixed frame	375.5	204.9
Shear wall	166.2	103
Base isolation	228.4	165

Table 3 Time period of the building

Case study number	Time period of the building (s)
Fixed frame	0.649
Shear wall	0.452
Base isolation	1.27

2.2 Case Study—2: Framed Building with Shear Wall

In case study 2, all the geometric and material properties of case study 1 are used and additionally, and shear wall is added. The design of shear wall is carried out with an assumption that the shear wall will resist 50% of the lateral moment and remaining 50% will be resisted by columns in the framed system. Four shear walls are added on the four sides middle, in such a way that torsional stress will not occur. Different modeling methods are used to represent shear walls, including combinations of shell and frame parts. The most popular modeling method, also known as the wide column method, consists of a mid-pier frame to reflect the stiffness of the shear wall and a horizontal frame (rigid arm) to allow proper couplings with intersecting beams and slab components.

Shear wall is designed as per IS 13920: 2016 [8]. The designed shear wall has a width of 2.5 m and a thickness of 200 mm, each direction with two numbers. The main reinforcement of 12 mm diameter with a spacing of 200 mm c/c and lateral reinforcement of 10 mm diameter with a spacing 200 mm c/c are used. The short beam connecting the column and shear wall has a higher depth of 400 mm to sustain the bending moment of the shear wall. The materials used for shear wall are M25 grade concrete and Fe415 grade of steel. Figure 2 shows the 3D SAP2000 model of the framed building with shear wall. Linear time history analysis is performed in *X*-direction (along 300 mm depth side of column). The shear force, bending moment, and inter-story drift of critical column are given in Table 2; and the time period of the building is tabulated in Table 3. Building with column size 350 mm × 300 mm with shear wall is able to withstand the seismic zone-V. The top deflection of each floor is plotted in Fig. 5.

2.3 Case Study—3: Framed Building with Base Isolation

Similar to case study 2, all the geometric and material properties of case study 1 is used in case study 3 and additionally, instead of shear wall, base isolation is added. The design of base isolation is made with an assumption of 50% reduction in the seismic response.

Laminated rubber bearing isolator is one type of isolators and is considered for the present study. It has a vertical load carrying capacity and is made of rubber in alternating layers. Steel laminated plates at the top and bottom of these layers distribute vertical loads and transmit shear force to the internal rubber layer. A rubber cover that protects the steel laminated plates is included on the top and bottom of the plate. This isolator with much lower horizontal stiffness is introduced between foundation and the superstructure. Spectral acceleration decreases with an increase in the system's natural period, which in turn reduces the force acting on the structure. But the system's displacement dramatically rises. This is due to the deformation of the rubber layer.

Base-isolation design includes determining the size of isolator, height of isolator, number of rubber layers and steel plates provided, mass of the isolator, horizontal stiffness and vertical stiffness of isolator. The provisions for evaluating these properties are stated in IS 1893 (Part 6): 2022. In this study, a framed building with base isolation is designed as per IS 1893 (Part 6): 2022 and is shown in Fig. 3. The isolators are modeled as link elements by giving relevant properties in SAP2000 software. Figure 4 shows the SAP2000 Elevation view of the Base Isolated structure. The isolators are placed on the pedestals to support the building. Linear time history analysis and modal analysis have been performed.

3 Comparative Study

By performing linear time history analysis, the model is analyzed in each case. The story deflection, bending moment, and shear force value of the critical column are compared for all three cases, and the time period of the three cases is also tabulated when performing modal analysis.

4 Conclusion

This study presents an analytical evaluation of the seismic response of three buildings using two alternative seismic response control techniques.

- By using linear time history analysis, the linear behavior of a framed building with a normal frame, a shear wall, and base isolation are compared.

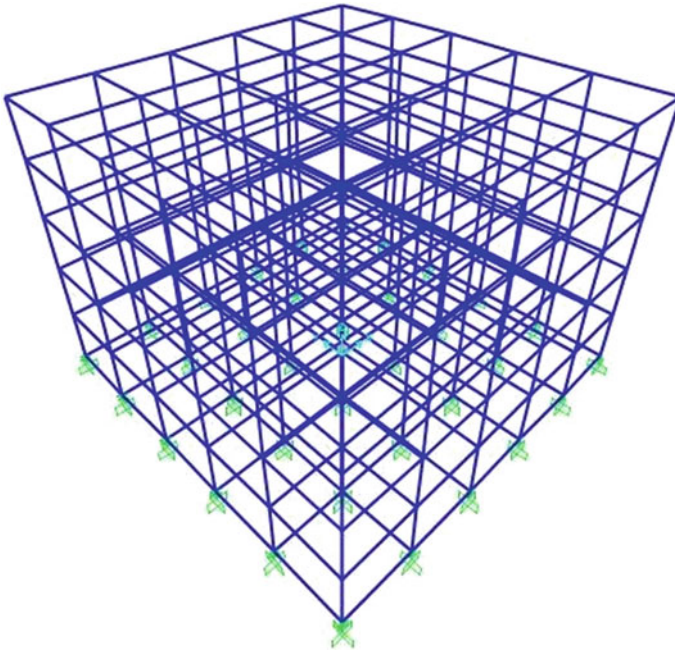


Fig. 3 SAP2000 model 3D framed building with addition of base isolation

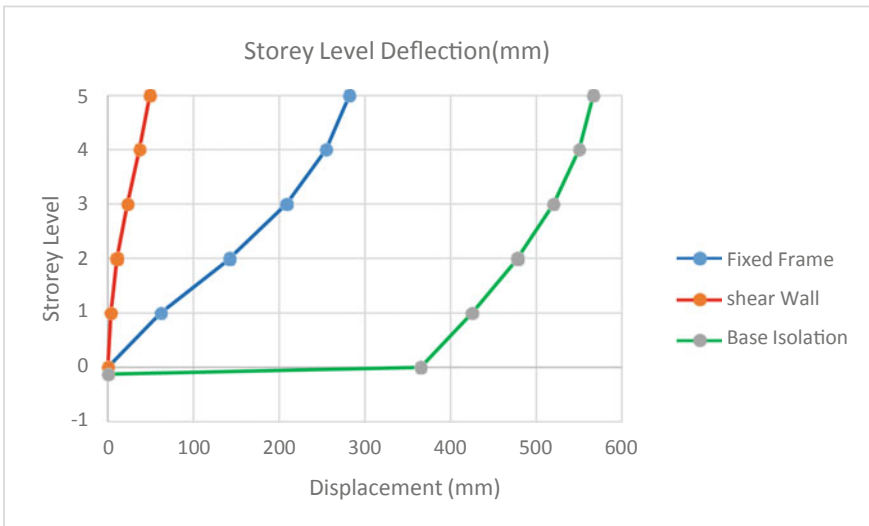


Fig. 4 Storey level deflection comparison

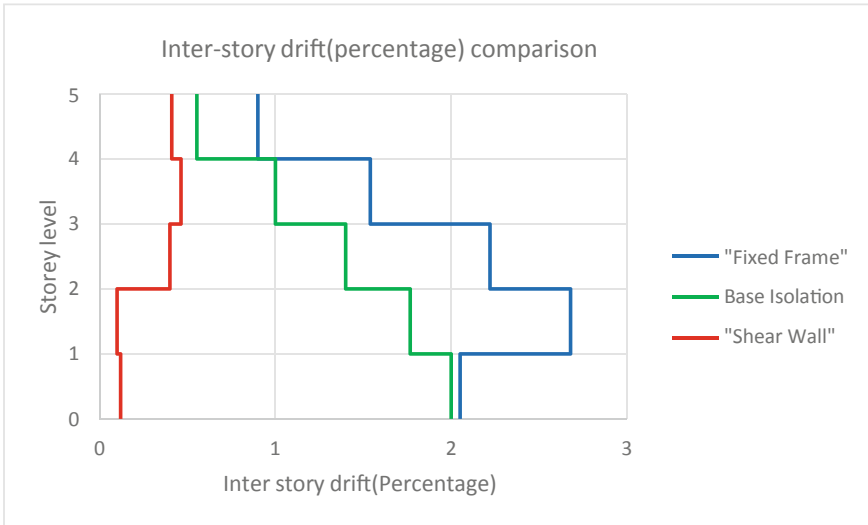


Fig. 5 Inter-story drift comparison

- From the study, it is observed that addition of shear wall has more effective and economical. Unlike base isolation, addition of shear wall doesn't require special construction technology. Because of the limitations in the base isolation, it may be ideal for all cases.
- We conclude that the construction of a shear wall reduces the natural period of the structure, increases lateral stiffness, and decreases bending moments and column shear stresses.
- Shear wall construction as a response control is a more practical choice and possesses better construction feasibility for low to medium rise buildings.

References

1. IS 1893 (Part 1): 2016, Indian Standard—Criteria for earthquake resistant design of structures, Part-1, General provisions and buildings. Bureau of Indian Standards, New Delhi
2. Rama Rao GV, Sunil JC, Vijaya R (2021) Soil-structure interaction effects on seismic response of open ground storey buildings. *Sadhana* 46(2):105, 1–17
3. Rama Rao GV, Gopalakrishnan N, Jaya KP, Muthumani K, Reddy GR, Parulekar YM (2016) Studies on nonlinear behavior of shear walls of medium aspect ratio under monotonic and cyclic loading. *ASCE J Perform Constr Facil* 30(1):04014201
4. Rama Rao GV, Gopalakrishnan N, Jaya KP, Dhaduk RJ (2015) Studies on ductility of shear walls. *J Struct Eng* 42(6):540–549
5. Whittaker D (2007) Base isolation design made simple. In: 10th world conference on seismic isolation, energy dissipation and active vibrations
6. Hadihosseini M, Hoseini AH (2014) Study the effective of shear wall on behavior of beam in frame structure. *Am J Eng Res* 03(10):188–202

7. IS 456 2000 Indian Standard Plain and reinforced concrete—code of practice. Bureau of Indian Standards, New Delhi
8. IS 13920 2016 Indian Standard Ductile design and detailing of reinforced concrete structures subjected to seismic forces—code of practice. Bureau of Indian Standards, New Delhi

Study on Sustainable Building Materials to Develop Block for Net Zero Carbon Building



Abishek Rauniyar and L. Krishnaraj

1 Introduction

The issue of climate change and the need to reduce carbon emissions has become a pressing concern for the building industry. Buildings are responsible for a significant portion of the world's energy consumption and greenhouse gas emissions, with the construction and operation of buildings accounting for nearly 40% of the world's energy usage and 36% of carbon emissions [1]. Considering this, there is a growing need to develop sustainable building materials and design strategies that can help to reduce the carbon footprint of buildings and move toward net zero carbon emissions [2]. Sustainable building materials refer to materials that are sourced, produced, and used in an environmentally responsible manner, and that have a lower environmental impact than traditional building materials. These materials can include, but are not limited to, materials such as bamboo, straw bale, rammed earth, and reclaimed wood [3]. They can also include products made from recycled materials, such as recycled steel, aluminum, and glass. The use of sustainable building materials can help to reduce the environmental impact of buildings by reducing the amount of energy required to produce and transport the materials, as well as by reducing the amount of waste generated during the construction process [4]. In addition to the use of sustainable building materials, the concept of net zero carbon building involves the integration of energy-efficient systems and technologies, such as solar panels, wind turbines, and geothermal systems, that can help to offset the carbon emissions associated with the building's energy usage [5]. This can be achieved through a combination

A. Rauniyar (✉)

Construction Engineering and Management, SRM Institute of Science and Technology,
Kattankulathur, Chennai 603203, India
e-mail: ar4677@srmist.edu.in

L. Krishnaraj

Department of Civil Engineering, Faculty of Engineering and Technology, SRM Institute of
Science and Technology, Tamil Nadu, Kattankulathur 603203, India

of energy conservation and the use of renewable energy sources. The goal of net zero carbon building is to produce as much energy as the building consumes, effectively eliminating its carbon footprint [6].

This paper aims to develop sustainable building materials to develop net zero carbon building, and here developed sustainable based Block which is made from natural waste for this project used sugar cane baggage and cornstalk through compaction forming technology, cornstalk CS and sugarcane baggage bio-composite (CMB) is developed as an eco-friendly sustainable-based block. The engineering properties of CMB were investigated by testing its physical, mechanical, and thermal insulation properties as a function of forming pressure (FP), concrete content (CS), and fly ash content (FA). A scanning electron microscope (SEM) was also used to examine the microstructural properties of typical CMB samples. As a result of these findings, the use of compaction forming technology for manufacturing CMB will become more widespread.

2 Literature Review

A recent literature review has examined the current state of research on sustainable building materials and their potential to contribute to the development of net zero carbon buildings [7]. The literature reviewed focused on materials such as bamboo, rammed earth, and reclaimed wood and how they can be used to reduce the embodied energy and carbon emissions associated with traditional building materials, such as concrete and steel. The literature reviewed found that bamboo, which is a fast-growing and renewable resource, has the potential to be a highly sustainable building material. It requires minimal energy input to process and has a high strength-to-weight ratio, making it suitable for use in construction. Rammed earth, which is made from locally sourced soil, can be created with minimal machinery, and has a low embodied energy, making it an environmentally friendly alternative to traditional brick or block construction. Reclaimed wood, meanwhile, reduces the demand for new wood products and can help to preserve old-growth forests [8]. The literature also highlighted the importance of considering the entire lifecycle of building materials, from extraction and production to disposal or reuse. It emphasized that the use of sustainable building materials in the construction of new buildings and retrofitting existing buildings can significantly reduce the carbon footprint of the built environment and move closer to achieving net zero carbon emissions. Additionally, the literature reviewed also discussed the importance of incorporating sustainable materials into the building design and construction process. It suggests that architects, builders, and designers should work together to ensure that sustainable materials are integrated seamlessly into the building design, to achieve the desired aesthetic and functionality. In conclusion, this literature review has demonstrated that sustainable building materials such as bamboo, rammed earth, and reclaimed wood have the potential to make a significant impact in the construction of net zero carbon buildings. The use of these materials can help to significantly reduce embodied energy and

carbon emissions, while also sequestering carbon, thus reducing the overall carbon footprint of buildings. It also emphasized the importance of considering the entire lifecycle of building materials and the need to incorporate them into the building design and construction process to achieve a sustainable built environment.

2.1 Cost–Benefit Analysis

The carbon benefit analysis of SBB compares the amount of CO₂ emitted when the blocks are utilized as a fuel source to the amount emitted when the blocks are not used as a fuel source. SBB is an organic energy source manufactured from wood chips, sawdust, and agricultural waste that is renewable and sustainable [5, 6]. SBB are carbon neutral as a fuel source because they do not emit carbon dioxide into the environment as they disintegrate. Rather than relying on nonrenewable energy sources, SBB retains and utilizes carbon as a source of energy, lowering the total carbon footprint. To quantify the carbon benefit of SBB, a lifecycle assessment may be performed, which comprises examining all carbon emissions created during the manufacture of SBB, from harvesting and shipping to manufacturing. The carbon footprint linked with nonrenewable energy sources, like coal and oil production and transportation, must also be evaluated as part of the carbon benefit analysis. A carbon benefit analysis suggests that SBB is a sustainable and ecologically friendly alternative to fossil fuels and can cut greenhouse gas emissions and prevent climate change. In India, agricultural waste management is a serious concern. Among the agricultural wastes produced each year are paddy straw, sugarcane bagasse, cotton stalks, and maize husks. The burning of agricultural waste in the fields pollutes the air, degrades the soil, and causes health concerns. Greenhouse gas emissions are created because of the combustion of agricultural waste. Agricultural waste, which is frequently utilized to manufacture biomass solid bricks, has grown in popularity in recent years. This substance can be used as fuel by the brickmaking industry, for example. By converting agricultural waste into solid bricks through biomass solid brick manufacture, the environmental effect of burning agricultural waste may be mitigated.

3 Materials and Methodology

3.1 Methodology

Research methodology is the process of locating, selecting, analyzing, and evaluating information on a certain topic. It is possible to evaluate a study's overall validity and reliability by looking at the methodology section of the article. Two critical difficulties were raised in the introduction, and both are addressed in the approaches

section. What methods were used to collect or create the data? As far as I know, that's how it was looked upon. Ultimately, the ultimate purpose of research is to find the truth that has been hidden and has not yet been disclosed by other ways of investigation. The purpose of research is to reveal answers to open-ended issues via the use of scientific techniques. The following general classifications may be used to categorize research objectives: To get acquainted with a phenomena or to obtain fresh insights into it is to familiarize oneself with it, to correctly depict the qualities of a certain person, circumstance, or group of people (studies with this object in view are known as descriptive research studies), for the purpose of determining the frequency with which something happens or with which it is connected with another (studies with this goal in mind are referred to as diagnostic research studies), a hypothesis about a causal link between two variables is being tested. Good research must be systematic, logical, empirical, and replicable. Keeping that in mind a research study must contain a solid and properly structured research methodology.

3.2 Materials

The raw materials used in this study include CS, sugarcane baggage, limestone powder, silica fume, gypsum powder, and FA. The CS was harvested at a farm in the northern India. CS was crushed and screened in the laboratory to a size of 5–15 mm, and we used CS and SCB for our samples. The materials used in the preparation of SBB are lime powder, fly ash, and silica fume. An Indian Refractory Plant supplied pellets of specific surface area of $230 \text{ m}^2 = \text{kg}$ and average particle size of 1.05 mm. Following calcination at $1500 \text{ }^\circ\text{C}$ for 6 h, MgO powder had a purity of 89.5%. Fine Chemical Plant of Northern Province, India supplied the glue and fiber used in the experiment. It was calcined using commercial MK with a $700 \text{ }^\circ\text{C}$ calcination temperature. Indian Power Plant supplied the SBB and FA as an admixture. Aggregates and fluid CS and sugarcane baggage are bonded together to form concrete, which hardens over time. Concrete made from Portland CS and sugarcane baggage is the most common type of concrete used today. CS and sugarcane baggage is a major constituent of concrete that is causing alarming environmental damage. For every ton of CS and sugarcane baggage produced, approximately 0.9 tons of carbon dioxide are released into the atmosphere. Greenhouse gases such as carbon dioxide are largely responsible for global warming. Thus, we need to investigate alternative concrete ingredients to reduce the environmental impact of concrete. Green concrete replaces hazardous materials in concrete with eco-friendly materials. Various industrial by-products are used to make green concrete, including fly ash, silica fume, metakaolin, and GGBS. Because these by-products are harmful to the environment, they are used in concrete in a way that ensures their safe disposal and that reduces CS and sugarcane baggage production, another threat to the environment. Researchers have worked on alternatives to CS and sugarcane baggage for years, but this paper examines their work. Lastly, various materials have been compared as alternatives or partial replace CS and sugarcane baggage s of CS and sugarcane baggage.

Table 1 Chemical properties of raw materials

Chemical composition	Lime powder (%)	Silica fume (%)	Fine gypsum powder (%)
CaO	38–42	0.25	18.86
SiO ₂	15–18	96	19.83
Al ₂ O ₃	3–5	0.25	11.63
MgO	0.5–3	0.56	5.75
Fe + Fe ₂ O ₃	1–1.5	0.55	6.20
Loss in ignition	30–32	0.15	35.24
SO ₃	3–5	0.89	0

3.3 Sample Preparation

The binder of Fly ash and gypsum consists of Limestone with a B1, B2, and B3 fixed mass ratio, determined from a preliminary test based on chemical properties of materials and shown in Table 1, the detail about procedure of making block. The premix total mass (TMP) was calculated based on sample size and CS content (defined as the mass ratio of CS to TMP). The FA content was determined by the mass ratio of FA to fly ash binder. Raw materials were weighed accurately (0.01 g) using an electronic balance. The mixing process involved adding dry cementitious materials (limestone, gypsum, silica fume, and FA) to a mixer, then mixing uniformly at low speed with a Los Angeles machine and vibration machine. Water was gradually added, and mixing continued during casting. The samples were cured in a standard room and tested after reaching the designated curing age.

4 Results

4.1 Mechanical Properties

Compression Strength

Unlike traditional structures, modern structures (such as masonry units) don't support loads. A minimum compressive strength requirement of 4.87 MPa was specified by ASTM for CS and sugarcane baggage blocks. The Indian standard, on the other hand, specifies a minimum compressive strength of 1.35 MPa. In addition to matrix strength and aggregate strength, CS and sugarcane baggage concentration and water-to-CS and sugarcane baggage ratio all influence the compressive strength of concrete. The compressive strength has been reported to decrease in several studies after agricultural waste was substituted for aggregates. A 15% replaces and sugarcane baggage of coarse aggregates with pistachio shells reduced the compressive strength of concrete by 24%. Waste material derived from periwinkle shells also

Table 2 Compressive strength for CS block

Mix type	Mix composition	Mix ID	Compressive strength in MPa		
			7 days	14 days	28 days
CS	(50, 30, 5 and 15%) (AW, L, SF, FS)	B1	3.63	3.83	4.62
	(30, 20, 10 and 30%) (AW, L, SF, FS)	B2	3.87	4.12	4.89
	(35, 25, 15 and 25%) (AW, L, SF, FS)	B3	4.12	4.52	4.80

Table 3 Flexible strength for CS block

Mix type	Mix composition	Mix ID	Flexible strength in MPa		
			7 days	14 days	28 days
CS	(50, 30, 5 and 15%) (AW, L, SF, FS)	B1	1.13	1.63	1.96
	(30, 20, 10 and 30%) (AW, L, SF, FS)	B2	1.29	1.79	2.13
	(35, 25, 15 and 25%) (AW, L, SF, FS)	B3	1.86	1.86	2.24

gave similar results. Concrete containing agricultural waste showed less strength than concrete containing coarse aggregate, even when farm waste was substituted for coarse aggregate (Table 2).

A test program was developed to demonstrate the compressive strength of CS blocks. Based on the results, the type of waste used, as well as the percentage of replaced CS and sugarcane baggage, significantly affect the block's compressive strength decreased as the waste content increased. This may be because agricultural residue has a lower mechanical resistance than sand, as well as the fact that the mortar with agricultural materials added has a greater share of water than CS and sugarcane baggage. The compressive strength of agricultural waste may also decrease, as shown in Table 3, because it is lighter than river sand. Since coconut husk is denser than other agricultural waste, CS and sugarcane baggage blocks containing coconut have greater compressive strengths than those containing sugarcane bagasse, as coconut husk is denser than other agricultural waste materials. Meanwhile, sugarcane yields the lowest compressive strength among the considered agricultural waste materials. In accordance with ASTM C129, most CS and sugarcane baggage blocks meet the specified minimum requirements, except for those with a B1 mix ratio. ASTM C129-compliant CS and sugarcane baggage blocks made with coconut husk may be made using a B1 mix ratio. There is no need to incorporate coconut husk in a B1 ratio for the density of the four types of CS and sugarcane baggage blocks that do not contain coconut husk. For example, pistachio shells, sawdust, and coconut husks are all thought to have a similar compressive strength as CS blocks.

Flexural Strength

The ability of a block to withstand flexural loads can be estimated by measuring the flexural stress. In general, a fracture occurs on the tensile side of the block that is closest to the middle of the cross-section. Figure 10 illustrates that flexural all have a

role in flexural strength. Similarly, the compressive and flexural strengths of agricultural material decreased. Table 4 represents the flexible strength of cornstalk block in different ratio of materials. Pistachio shells were also utilized, and it was recognized that decreasing their effective binding would decrease the flexural strength. When oil palm shells were used as coarse aggregates, the concrete lost 39% of its compressive strength compared to the control concrete at 30% replace and sugarcane baggage. The present findings are consistent with those obtained by adding coconut husk to the CS and sugarcane baggage mortar. The flexural strength was found to decrease by 23% and 46% at 20% and 50% substitution, respectively, compared with that of the control hardened mortar. The type of waste was considered in this experiment. CS and sugarcane baggage blocks containing coconut husk have higher flexural strength than those containing straw. The experimental results were evaluated using linear regression to generate a proportionality equation relating the flexural strength (f_t) of the CS and sugarcane baggage blocks to their compressive strength (f_{cu}) in the conventional form $f_t = a f_{cu} b$.

4.2 Micro-structure Analysis

Figure 11 shows the typical micro images with 10,000 magnifications of CMB, which has 20%, 25%, and 35% CS, respectively, because of SEM tests on SBB. In this study, strong adhesion and excellent biocompatibility of MPC binder were observed between MPC binder and CS. The bonding between MPC and CS was significantly weakened by the addition of CS to the MPC. Particularly after the CMB with 45% CS was cemented with MPC, the strength gain was decreased due to incomplete cemented CS [9]. During the testing of SBB, one of the main mechanisms of agglomeration was improved by the addition of struvite to the MPC, increasing the agglomeration effect between the two products. The microstructure of SBB with CS contents of 45, 10, 15, and 20% is presented under the CS content of 45%. In SBB, FA particles tend to fill the micropores between CS and MPC as the FA content increases. A conglomerate structure is formed inside the SBB by the production of struvite and FA [10]. Additionally, as the FA content exceeds 10%, the porosity also increases significantly. MPC may have weakened its bond with CS due to excessive FA particles delaying hydration. The scanning electron microscopy analysis for CS Block for 7 days casting minerals and it gives the same type of results for 14 days and 28 days, then only with the list of 7, 14 and 28 days results we can analyze the micro structural CS block.

4.3 Cost–Benefit Analysis

An overview of the estimated costs associated with each of the three mixtures developed in this study is provided in the following Table 5. As far as raw materials are

Table 4 Cost analysis of all mixtures (per m³)

S.No.	Mix ID	Proportions by weight %					Total cost (USD)	Cost increment (compared to control)
		Cornstalk (cost)	Modified fly ash (cost)	Lime powder	Silica fume	Water (cost)		
	Fly ash block		7.5	6.6	1.1	0.03	12.6	–
B1	(50, 30, 5 and 15%) (AW, L, SF, FS)	0.04	7.5	6.6	1.1	0.03	7.475	7.75
B2	(30, 20, 10 and 30%) (AW, L, SF, FS)	0.04	7.5	6.6	1.1	0.03	10.475	11.75
B3	(35, 25, 15 and 25%) (AW, L, SF, FS)	0.04	7.5	6.6	1.1	0.03	10.475	11.75

concerned, modified fly ash, silica fume, and lime powder are the only product that can be sold along with the cost of producing mixed cement. On the other hand, the remaining materials such as cornstalks, modified fly ash, and PPC cement were freely obtained since they are currently discarded in landfills in India and have not been recycled to date. During the time the raw materials for this research were purchased, the unit prices were based on the market prices on the local Indian market in January 2023. During the cost analysis, it was determined that the total cost per m³ varied between USD 11.75 and 12.6. Approximately 2200% more expensive (B2) was registered for the agriculture waste mixes as compared to the control mix, and the cost increased linearly with the increase in the agricultural waste dosage. However, when cornstalks, modified fly ash, and cement-admixed mixtures were substituted with a small dosage of 5%, their costs were comparable to those of the control mix. Based on their dosages from 5 to 20% and corresponding water requirements, cornstalk, modified fly ash, and cement mixes have a cost variation of 0–6%.

5 Discussion and Analysis

Based on the findings of the study on sustainable building materials to develop net zero carbon buildings, the following points can be discussed and analyzed:

- A net zero carbon footprint in buildings is achieved by using sustainable building materials [11].
- The study identified various sustainable building materials that can be used in construction, such as cornstalk, straw bale, and hempcrete, and 17% of Agricultural waste.
- These materials have lower embodied carbon and can also provide improved thermal insulation and air quality 11.2% is good as compared to clay bricks.
- The weight and cost of the biomass bricks were found to be 40% lighter than the normal clay bricks [12].
- The average compressive strength of the clay bricks was average 4.97 MPa and of the biomass bricks was 5.37 MPa, and the results show that the biomass bricks have higher compressive strength [13].
- The study suggests that the adoption of sustainable building materials in construction can significantly reduce carbon emissions up to 97%, which is essential to address the global climate crisis.
- The study highlights the need for policy interventions and market incentives to promote the adoption of sustainable building materials in construction.
- Several barriers have been identified as preventing the adoption of sustainable building materials in the construction industry, including the high cost of sustainable building materials, a lack of awareness of their benefits, and the lack of proper regulations.

- Building materials that are innovative and emerging are sustainable: Based on the study, it is evident that innovative and emerging sustainable building materials can reduce the carbon footprint of buildings, including cross-laminated timber, engineered wood, and bio-based materials. The effectiveness, scalability, and cost-effectiveness of these strategies require further investigation [14].

6 Conclusion

To conclude, the study on sustainable building materials to develop net zero carbon buildings has highlighted the importance of using environmentally friendly resources in the construction industry. Several studies have documented that the use of sustainable building materials, such as bamboo, cork, and recycled materials, can significantly reduce the carbon footprint of buildings. The study has also demonstrated that the use of these materials can improve the overall energy efficiency of buildings and contribute to the reduction of greenhouse gas emissions. A major aim of the study is to provide insights into the challenges and barriers that need to be overcome to increase the adoption of sustainable building materials in the construction industry. Sustainability materials are expensive, there is a lack of awareness and understanding of their benefits, and there are no proper regulations in place. The study has also provided a set of recommendations for further research and practical applications of sustainable building materials in the construction industry. There is a need for further research on the long-term performance of sustainable building materials, for the development of guidelines and standards, and for the creation of financial incentives aimed at encouraging the use of sustainable building materials. Based on the results of this study, it can be concluded that the use of sustainable building materials is an essential part of achieving net zero carbon buildings and reducing the carbon footprint of the construction industry. Researchers have published findings that can be used by architects, builders, and policymakers to make informed decisions regarding the development of the built environment and contribute to its sustainability.

References

1. Kazmi SMS, Munir MJ, Wu YF, Hanif A, Patnaikuni I (2018) Thermal performance evaluation of eco-friendly bricks incorporating waste glass sludge. *J Clean Prod* 172:1867–1880. <https://doi.org/10.1016/j.jclepro.2017.11.255>
2. Ahmed ATMF, Islam MZ, Mahmud MS, Sarker ME, Islam MR (2022) Hemp as a potential raw material toward a sustainable world: a review. *Heliyon* 8(1):e08753. <https://doi.org/10.1016/j.heliyon.2022.e08753>
3. Karić N et al (2022) Bio-waste valorisation: agricultural wastes as biosorbents for removal of (in)organic pollutants in wastewater treatment. *Chem Eng J Adv* 9. <https://doi.org/10.1016/j.cej.2021.100239>

4. Souza AB, Ferreira HS, Vilela AP, Viana QS, Mendes JF, Mendes RF (2021) Study on the feasibility of using agricultural waste in the production of concrete blocks. *J Build Eng* 42. <https://doi.org/10.1016/j.jobe.2021.102491>
5. Jannat N, Hussien A, Abdullah B, Cotgrave A (2020) Application of agro and non-agro waste materials for unfired earth blocks construction: a review. *Constr Build Mater* 254:119346. <https://doi.org/10.1016/j.conbuildmat.2020.119346>
6. Lang L, Duan H, Chen B (2020) Experimental investigation on concrete using corn stalk and magnesium phosphate cement under compaction forming technology. *J Mater Civ Eng* 32(12):1–11. [https://doi.org/10.1061/\(asce\)mt.1943-5533.0003487](https://doi.org/10.1061/(asce)mt.1943-5533.0003487)
7. Naga Sai MS, De D, Satyavathi B (2021) Sustainable production and purification of furfural from waste agricultural residue: an insight into integrated biorefinery. *J Clean Prod* 327:129467. <https://doi.org/10.1016/j.jclepro.2021.129467>
8. Odlare M, Lindmark J, Ericsson A, Pell M (2015) Use of organic wastes in agriculture. *Energy Procedia* 75:2472–2476. <https://doi.org/10.1016/j.egypro.2015.07.225>
9. Liberalesso T, Tassi R, Ceconi DE, Allasia DG, Arboit NKS (2021) Effect of rice husk addition on the physicochemical and hydrological properties on green roof substrates under subtropical climate conditions. *J Clean Prod* 315:128133. <https://doi.org/10.1016/j.jclepro.2021.128133>
10. Delhomme F, Prud'homme E, Julliot C, Guillot T, Amziane S, Marceau S (2022) Effect of hemp on cement hydration: experimental characterization of the interfacial transition zone. *Results Chem* 4:100440. <https://doi.org/10.1016/j.rechem.2022.100440>
11. Lahri A, Dixit S (2015) Alternatives to cement in concrete—a review. *Int J Sci Eng Res* 6(10):50–56 [Online]
12. Al-Jabri K, Hago AW, Al-Saadi S, Amoatey P, Al-Harthy I (2022) Structural and thermal performance of sustainable interlocking compressed earth blocks masonry units made with produced water from oilfields. *Case Stud Constr Mater* 17:e01186. <https://doi.org/10.1016/j.cscm.2022.e01186>
13. agro waste.pdf
14. Qaidi SMA, Tayeh BA, Isleem HF, de Azevedo ARG, Ahmed HU, Emad W (2022) Sustainable utilization of red mud waste (bauxite residue) and slag for the production of geopolymer composites: a review. *Case Stud Constr Mater* 16:e00994. <https://doi.org/10.1016/j.cscm.2022.e00994>

Green Building Rating Systems: A Comparative Study of Global and Indian Standards



K. S. Anandh , M. G. Soundarya Priya , S. Senthamizh Sankar ,
and K. Prasanna 

1 Introduction

The construction world is framed after decades of development, from basic brick walls to our advanced 3D printing. The construction industry is the leading industry in the world, giving new creations. Construction is the act of creating structures [1]. Also, the effects produced by this construction industry are good but still have an enormous impact on environmental degradation [2–6]. Here comes the aspect of pollution control caused by the construction industry. This leads to the responsibility of maintaining a deep-rooted balance of environmental, economic, and social health. It provides a set of rights for constructing environmentally friendly structures so that the adverse effects of buildings on the environment and occupants are mitigated. The vital aspect is adaptability to the upcoming advancements to establish required thermal, visual, and acoustic comfort with efficient energy usage. The act of living under a roof gave rise to the process of constructing structures. This leads to the well-known construction industry. Buildings have humongous and endlessly increasing effects on environmental issues about 0.4% of natural resources have been derived from industrial countries [1], utilizing about 0.7% of electric power and 0.12% of drinking water [7] and produce about 0.45–0.65% of the waste to

K. S. Anandh (✉) · M. G. Soundarya Priya · S. Senthamizh Sankar · K. Prasanna
Department of Civil Engineering, Faculty of Engineering and Technology, SRM Institute of
Science and Technology, SRM Nagar, Kattankulathur, Tamil Nadu 603203, India
e-mail: anandhk@srmist.edu.in

M. G. Soundarya Priya
e-mail: sm0295@srmist.edu.in

S. Senthamizh Sankar
e-mail: ss3069@srmist.edu.in

K. Prasanna
e-mail: prasannk@srmist.edu.in

landfills [6]. Further, they are reasonable for an enormous emission of harm. Considering about 0.3% of greenhouse gases are because of their operation, an additional 0.18% has been produced indirectly due to material waste and transportation [6–8]. Simultaneously, health problems are caused due to bad indoor environment quality, drastically reducing productivity [9]. GREEN BUILDING refers to both construction and operation of the building throughout its lifecycle, which positively impacts our climatic conditions and natural environment. GREEN BUILDING saves energy and resources and reduces toxic substances to provide occupants with a sustainable building and healthier space. The outlook of this paper is to expose a cluster of information available from technical manuals and official websites. This paper enriches the analysis of numerous building rating systems by collecting data from multiple sources, exposing the evolution of the considered rating systems over time, and providing a geographical representation of a global evaluation. In addition, the scoring credits for rating systems that are being analyzed are posted.

2 Methodology

The two most possible way for literature reviews is deductive and inductive paths [10]. The deductive path is employed here; whereas the literature identifies critical criteria, widely existing green building rating systems are used for analyzing those critical criteria. Here, a detailed review based on literature is accomplished to express the critical criteria. The resource data is obtained from the thesis, conference proceedings, journal papers, and manual books. After that, globally available rating systems were examined and denoted in further levels. The final phase of the paper involves a detailed discussion regarding the credit allocation of the considered rating systems. Globally significant GBRS (Green Building Rating System) to evaluate green buildings are recognized. Among those four rating systems are chosen, and a comparison is established. Existing comparison data are produced from various published papers, conference papers, and thesis. Compiling all these data, an overall comparison is shown. Chronological developments and their comparison to the convention are also obtained simultaneously. The research methodology of this paper is shown in Fig. 1. The major focus is given to Indian Green Building Council (IGBC), Building Research Establishment Environmental Assessment Method (BREEAM), Green Rating for Integrated Habitat Assessment (GRIHA), and Leadership in Energy and Environmental Design (LEED). Seven important themes are considered. Maximum and Mandatory Points of each theme have been calculated. Maximum Points of each theme have been analyzed and calculated as their Weightage in Percentage. Mandatory Points have also been calculated as per their Weightage in Percentage.

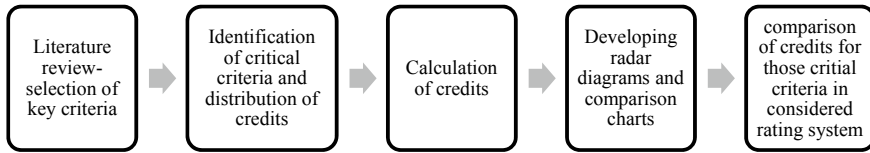


Fig. 1 Research methodology

3 Green Building

The Office of Federal Environmental Executive (OFEE) and the Environmental Protection Agency (EPA) defines GB as [11]—“the practise of increasing the efficiency with which buildings and their sites use energy, water, and materials and reducing building impacts on human health and the environment through better siting, design, construction, maintenance, and removal—the complete building life cycle” GB is a globally emergent new trend. The green building movement began when the built environment was transformed into one that is healthier, more sustainable, and more considerate of building occupants [12–14].

4 Rating Systems

A rating system provides a metric for designers, builders, and owners to evaluate their initiatives’ relative environmental and sustainability performance. Focusing on a sustainability stage using an existing rating system can aid in ensuring that initial objectives are met through the completion of construction. The most excellent intentions may be jeopardized as a project’s budget, schedule, and other pressures increase [13, 15]. Worldwide there are many GBRS (Green Building Rating Systems), such as:

BREEAM—Building Research Establishment Environmental Assessment Method, LBC—Living Building Challenge, BEAM PLUS—Building Environmental Assessment Method, HQE—High-Quality Environmental standard, TREE—Thailand Rating of Energy and Environmental Sustainability, GREENSHIP, IGBC—Indian Green Building Council, BCA—Building and Construction Authority, GRIHA—Green Rating for Integrated Habitat Assessment, BEE—Bureau of Energy Efficiency, LEED—Leadership in Energy and Environmental Design, GREEN MARK, CASBEE—Comprehensive Assessment System for Built Environment Efficiency, GPR—Green Point Rated, GS—Green Seal Standard, EDGE—Excellence in Design for Greater Efficiencies, LOTUS, DGNR—Deutsche Gesellschaft fur Nachhaltiges Bauen [16].

This paper uses four well-established GBRS (Green Building Rating Systems) from various countries. These rating systems were selected to compare globally used tools and those used in India. So, LEED, BREEAM, GRIHA, and IGBC are



Fig. 2 Globally existing GBRS [18]

chosen for this paper. Globally existing Green Building Rating Systems (GBRS) are shown in Fig. 2. The selected four rating systems are BREEAM (UK), LEED (USA), GRIHA, and IGBC (India). Many rating systems worldwide show the development of green buildings in sustaining the consumption of current energy for future use. This Rating System compiles thirty-four criteria classified into four sections. Some are as follows: Site selection, building planning and construction, building operation and maintenance, and innovation [17] (Fig. 3).

5 Main Features of the Above Rating System

The important features of the above-discussed four rating systems are listed in the following tabulation. The main features of the four rating systems, such as BREEAM, LEED, GRIHA, and IGBC, are listed in Table 1 [19]. The credit allocations of BREEAM, LEED, GRIHA, and IGBC with respect to categories are shown in Table 2.

6 Selection of Criteria

LEED, BREEAM, IGBC, and GRIHA are considered to compare. Comparison is made based on criteria, “attaining objectives by considering the analysis using the required parameters,” as defined by Munier [19]. The basic conditions used to analyze each rating system are designated below [21, 24]—Site selection, Energy, Water,

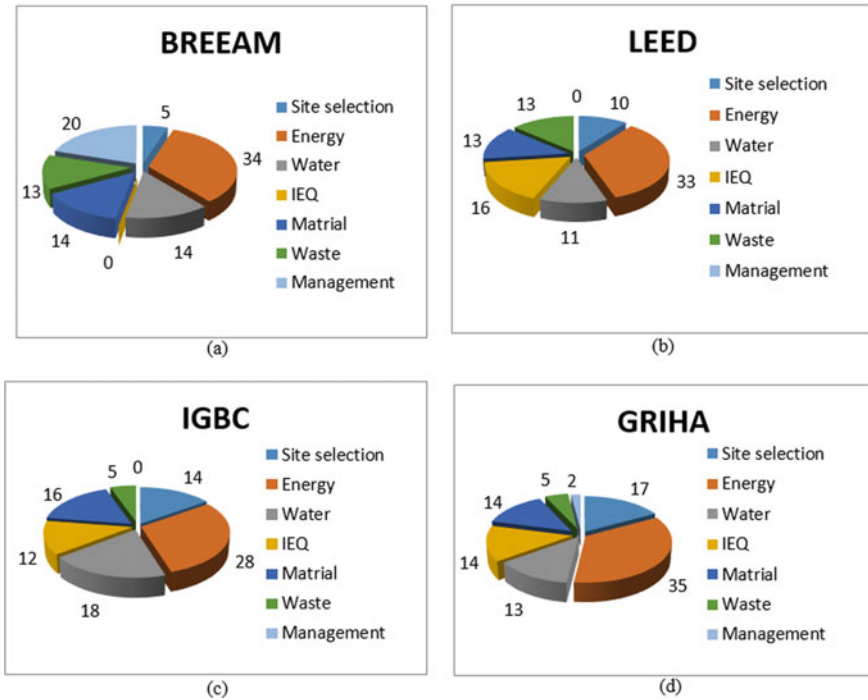


Fig. 3 a–d are the criteria allocated for BREEM, LEED, IGBC, and GRIHA

Indoor Environment Quality (IEQ), Material, Waste and pollution, and Management. The assessment scope of rating systems with respect to criteria is shown in Table 2.

Primary goals in site selection for green buildings include protecting sensitive sites, restoring and reusing previously developed sites, and minimizing transportation impacts on environmental and energy use. Reducing a building’s energy demand by designing it from the outset to consume less energy and be more efficient through equipment selection and high-quality construction. The selection of materials for green structures appears laborious. Green building materials favor renewable over non-renewable resources and are environmentally responsible because their impacts are evaluated over the lifecycle of the product. In addition, green buildings are constructed with reusable, eco-friendly materials that do not compromise the building’s durability or occupants’ health [18]. Minimizing the potential for water consumption by reducing the quantity of water used in the home through enhanced efficiency. Buildings can be designed to include more water catchment systems, such as cisterns, containers, and swales. The collected water can be routed and utilized for a variety of purposes, including evaporation in toilets, refrigerators, etc. Improving residents’ health by moderating the levels of indoor humidity, toxins, and pollutants. Greenhouse gases are not the only harmful pollutant that buildings emit. The levels of

Table 1 List of main features of four rating systems [18, 20, 21]

		BREEAM	LEED	GRIHA	IGBC
Full form		Building research establishment environment method	Leadership in energy and environment design	Green rating for integrated rating assessment	Indian green building council
Country		UK	USA	India	India
Organization		BRE	USGBC	TERI (The Energy and Research Institute)	CII (Confederation of Indian Industry)
Flexibility		77 countries	160 countries	India	India
First version		1990	1998	2000	2001
Last version		2016	2013	2015	2014
Rating criteria		Management Health and wellbeing Energy Transport Water Material Waste Land use and ecology Pollution Innovation	Integrative process Indoor Environment Quality Energy and Atmosphere Location and Transportation Water efficiency Material and Resources Sustainable Sites Regional Priority Innovation	Site parameters Maintenance and housekeeping Energy Water Human health and comfort Social aspects Innovation	Site selection and planning Water efficiency Energy efficiency Materials and resources Indoor environment quality Innovation in design
Rating level		Pass ≥ 30 Good ≥ 45 Very good ≥ 55 Excellent ≥ 70 Outstanding ≥ 85	Certified ≥ 40 Silver ≥ 50 Gold ≥ 60 Platinum ≥ 80	1star ≥ 25 2star > 40 3star > 55 4star > 70 5star > 85	Certified ≥ 50 Silver ≥ 60 Gold ≥ 70 Platinum ≥ 80 Super platinum ≥ 90
Rating scheme	Sections	10	8	7	7
	Criteria	57	57	36	42
	Total score	100	110	100	100

air pollution indoors are significantly higher than those outdoors. “Facilities management”—a discipline that plays a vital role in engineering, construction engineering, architectural, and management knowledge, particularly for maintaining or running commercial, institutional, and industrial buildings. The vital role of the facilities

Table 2 Assessment scope [22, 23]

Rating systems	Site	Water	Energy	IEQ	Materials	Waste	Management
LEED	✓	✓	✓	✓	✓	×	×
BREEAM	✓	✓	✓	×	✓	✓	✓
IGBC	✓	✓	✓	✓	✓	✓	×
GRIHA	✓	✓	✓	✓	✓	✓	✓

manager is to care existing building inventory as well as future planning and risk-based maintenance [23]. Growing waste generation and disposal rates will increase pressures on the environment. The main aim of sustainable waste management is to address long-term pressures through: recovery and recycling, resources reuse, waste streams to be reduced, and managing the resources in a sound environment and in an economically effective manner [23].

7 Discussion: Comparison of Criteria and Scoring

The comparison of criteria and scoring of BREEAM, LEED, IGBC, and GRIHA is shown in Fig. 4. Considering the comparison among rating system from the first priority. Table, it shows energy condition is having. Rating systems IGBC, GRIHA, LEED, and BREEAM have given importance for energy condition above 30% than other conditions. But LEED has highest priority to energy of about 39.75 of the total percent. The important point for causing enormous of the GB rating systems is because the future is going to suffer a greater energy demand crisis [25]. After comparison among LEED, BREEAM, GRIHA, and IGBC, among these, LEED is having a rigorous and comparatively lesser flexible than remaining GB rating tools. Based on the observation, it is known that “energy” criteria are approximately equivalent in considered rating tools.

The next most pressing matter here is “Water” condition. Among all, IGBC acquires about 20.22% of final score for water criteria. Water criteria are least in GRIHA showing 13% of total score. Main aspect in this criterion is to maintain a controlled usage of water which is attained by focusing on the implementation of water saving indicators and also innovative water technology; these can be viewed in LEED [25]. Here comes the next concern toward “IEQ” condition and in LEED, this condition is well maintained by securing of about 19.77% of ultimate score. Further [26], eliminates the relation of the LEED rating attained between the comfortable performance state attained in occupant state with the construction state. Consequently, this emerges as the cause to know more about conditions following IEQ criteria. Major Green rating systems consider “energy” and “IEQ.” Identically a comparative study was established among rating tools for refurbishment projects where a conclusion was attained stating that most strongly considered regions are “energy” and “IEQ” [27]. Materials are the basis for construction for anything in

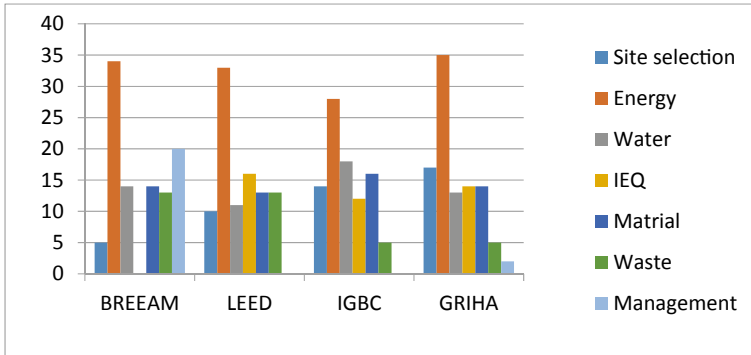


Fig. 4 Comparison of criteria

general. So efficient utilization of materials and also after its usage life, reuse of destroyed materials is the main aspect focused in green buildings concept. Regarding materials, transferring them from the market to site is the bigger deal. All these aspects are pointed for credit allocation in “Material” condition for IGBC [25]. Likewise, remaining rating tools also focus on materials used. “Site selection” condition is considered in all rating system but comparatively it’s been seeking greater significance of 17.97% of net score than the rest of rating tools. The product after its utility period is considered as waste. This leads to the condition of “waste.” BREEAM and LEED gives a higher importance for waste management among the four rating system compared. Where GRIHA and IGBC give the least importance for waste. “Maintenance and management” is the least considered component in the above compared rating system criteria. Only BREEAM and GRIHA have considered maintenance in the criteria of rating system. LEED and IGBC have not even considered maintenance as criteria. In BREEAM, maintenance is considered as the second most important component, but as in other rating systems it’s considered the least and mostly not taken under consideration.

8 Conclusion

Origin of green buildings concept leads to requirement of evaluation tool. Here comes the GBRS, according to various aspects, many GBRS are available. From that, a small scaled comparison is been established. Based on topography, globally LEED and BREAM are chosen and locally available IGBC and GRIHA are considered. Overall their evaluation is being studied based on the available manuals and journals, from which a solid criterion is fixed and comparison is produced. This shows energy is the aspect considered in all evaluation to a greater extent. Criteria which must be improved are waste management in local GBRS and in global scenario, site selection requires some importance. Overview of evaluation process in various rating system

is being evaluated. Theoretical comparison is done for considered green building rating system. Considered theoretical comparison is done based on the process and criteria for evaluation. This theoretical study is for better understanding and evaluation process. This evaluation consists of collecting data from various sources, establishing criteria and distribution of score for criteria using which comparison is being established. Based on this comparison, overall working process is explained. This shows the importance of evaluation sequence and required developments can be recommended.

References

1. Ali HH, AlNsairat SF (2009) Developing a green building assessment tool for developing countries—case of Jordan. *Build Environ* 44:1053–1064. <https://doi.org/10.1016/J.BUILDENV.2008.07.015>
2. Wong JKW, Kuan KL (2014) Implementing ‘BEAM Plus’ for BIM-based sustainability analysis. *Autom Constr* 44:163–175. <https://doi.org/10.1016/J.AUTCON.2014.04.003>
3. Stadel A, Eboli J, Ryberg A, Mitchell J, Spatari S (2011) Intelligent sustainable design: integration of carbon accounting and building information modeling. *J Prof Issues Eng Educ Pract* 137:51–54. [https://doi.org/10.1061/\(ASCE\)EI.1943-5541.0000053](https://doi.org/10.1061/(ASCE)EI.1943-5541.0000053)
4. Wong JKW, Li H, Wang H, Huang T, Luo E, Li V (2013) Toward low-carbon construction processes: the visualisation of predicted emission via virtual prototyping technology. *Autom Constr* 33:72–78. <https://doi.org/10.1016/J.AUTCON.2012.09.014>
5. Wong JKW, Zhou J (2015) Enhancing environmental sustainability over building life cycles through green BIM: a review. *Autom Constr* 57:156–165. <https://doi.org/10.1016/J.AUTCON.2015.06.003>
6. Wang N (2014) The role of the construction industry in China’s sustainable urban development. *Habitat Int* 44:442–450. <https://doi.org/10.1016/J.HABITATINT.2014.09.008>
7. Pulselli RM, Simoncini E, Pulselli FM, Bastianoni S (2007) Energy analysis of building manufacturing, maintenance and use: Em-building indices to evaluate housing sustainability. *Energy Build* 39:620–628. <https://doi.org/10.1016/J.ENBUILD.2006.10.004>
8. Yudelson J (2008) *The green building revolution*. Island Press, Washington, DC
9. Venkatarama Reddy BV, Jagadish KS (2003) Embodied energy of common and alternative building materials and technologies. *Energy Build* 35:129–137. [https://doi.org/10.1016/S0378-7788\(01\)00141-4](https://doi.org/10.1016/S0378-7788(01)00141-4)
10. Saunders MNK, Lewis P, Thornhill A (2019) *Research methods for business students*. Pearson Education Limited, New York
11. Cullen Howe J, Gerrard M (2010) *The law of green buildings regulatory and legal issues in design, construction, operations, and financing*. American Bar Association, Section of Environment, Energy, and Resources
12. Yoon SW, Lee DK (2003) The development of the evaluation model of climate changes and air pollution for sustainability of cities in Korea. *Landsc Urban Plan* 63:145–160. [https://doi.org/10.1016/S0169-2046\(02\)00186-X](https://doi.org/10.1016/S0169-2046(02)00186-X)
13. AII, IBEC (2005) *Architecture for a sustainable future: all about the holistic approach in Japan*. Institute for Building Environment and Energy Conservation
14. Anandh KS, Irshad M, Murali A, Priya MGS (2022) Energy-efficient educational building design based on green building concept and its stability analysis. In: *AIP Conference Proceedings*. pp. 040001-1–040001-7. <https://doi.org/10.1063/5.0102967>
15. Cole R (2003) Building environmental assessment methods: a measure of success. *Spec Issue Artic Futur Sustain Constr*

16. Vierra S (2011) Green building standards and certification systems. Steven Winter Associates. Inc., Washington, DC
17. Green Rating for Integrated Habitat Assessment. <http://www.grihaindia.org/>. Accessed 09 Aug 2018
18. Doan DT, Ghaffarianhoseini A, Naismith N, Zhang T, Ghaffarianhoseini A, Tookey J (2017) A critical comparison of green building rating systems. *Build Environ* 123:243–260. <https://doi.org/10.1016/j.buildenv.2017.07.007>
19. Bennet G (2005) Multicriteria environmental assessment: a practical guide. *J Hazard Mater* 119:261–262. <https://doi.org/10.1016/j.jhazmat.2004.11.027>
20. Bernardi E, Carlucci S, Cornaro C, Bohne R (2017) An analysis of the most adopted rating systems for assessing the environmental impact of buildings. *Sustainability* 9:1226. <https://doi.org/10.3390/su9071226>
21. Komeily A, Srinivasan RS (2015) A need for balanced approach to neighborhood sustainability assessments: a critical review and analysis. *Sustain Cities Soc* 18:32–43. <https://doi.org/10.1016/j.scs.2015.05.004>
22. Illankoon IMCS, Tam VWY, Le KN, Shen L (2017) Key credit criteria among international green building rating tools. *J Clean Prod* 164:209–220. <https://doi.org/10.1016/j.jclepro.2017.06.206>
23. Mattoni B, Guattari C, Evangelisti L, Bisegna F, Gori P, Asdrubali F (2018) Critical review and methodological approach to evaluate the differences among international green building rating tools. *Renew Sustain Energy Rev* 82:950–960. <https://doi.org/10.1016/j.rser.2017.09.105>
24. Bon-Gang H (2018) Performance and improvement of green construction projects. Butterworth-Heinemann
25. Zhang Y, Wang J, Hu F, Wang Y (2017) Comparison of evaluation standards for green building in China, Britain, United States. *Renew Sustain Energy Rev* 68:262–271. <https://doi.org/10.1016/j.rser.2016.09.139>
26. El Asmar M, Chokor A, Srour I (2014) Occupant satisfaction with indoor environmental quality: a study of the LEED-certified buildings on the Arizona State University Campus. In: ICSI 2014. American Society of Civil Engineers, Reston, VA, pp 1063–1070. <https://doi.org/10.1061/9780784478745.100>
27. Kamaruzzaman SN, Lou ECW, Zainon N, Mohamed Zaid NS, Wong PF (2016) Environmental assessment schemes for non-domestic building refurbishment in the Malaysian context. *Ecol Indic* 69:548–558. <https://doi.org/10.1016/j.ecolind.2016.04.031>

Integrating BIM with Energy Analysis and Green Building Certification System to Design Sustainable Building



G. S. Mahaaraja and S. M. Renuka

1 Introduction

BIM is used in the AECOO industry to reduce the time needed to complete projects, improve communication among designers, contractors, and other parties involved, to minimize errors, improve the accuracy of the design, optimize the use of resources, and decrease costs. Furthermore, BIM technology helps to improve sustainability, health and safety, and quality of construction projects. In conclusion, BIM is a valuable tool for the AECOO industry, as it offers an effective and efficient way to manage, design, and construct infrastructure. BIM offers a number of advantages that can be used to improve the quality, reduce costs, and increase sustainability. The building industry is seeking more attention to the design and construction of environmentally friendly structures that can achieve excellent performance and cost-effectiveness. Once the architectural and technical documentation have been produced, energy analysis is often carried out. This comprises both the operating energy (direct energy needed to use, maintain, and demolish the building) and the embodied energy (indirect energy needed to produce, transport, and install the building's materials). Architects and designers can make a building as efficient and sustainable as possible by considering energy demands in the early stages of a project. To reduce energy use and its negative effects on the environment, the main goal nowadays is to design energy-efficient structures. BIM-based simulations also reduce the amount of time and effort needed to model architectural geometries, as the three-dimensional model enabled by BIM eliminates the need for manual input of numerical data or the creation of a two-dimensional model. Systems for green building rating and certification are crucial for

G. S. Mahaaraja (✉) · S. M. Renuka
Division of Structural Engineering, Department of Civil Engineering, CEGC, Anna University,
Chennai 600025, India
e-mail: maharajasubramani@gmail.com

S. M. Renuka
e-mail: renuka@annauniv.edu

developing sustainable structures that are planned and built with consideration for the environment and resource efficiency. These systems offer evaluation standards for determining how a building’s siting and design, as well as its construction, operation, maintenance, refurbishment, and demolition, will affect people’s health and the environment. They make it possible for architects to set up criteria for green design, gauge a building’s predicted performance, and assess how well it is accomplishing sustainability objectives. Rating systems are available for all project kinds, from single-family homes to entire neighborhoods, for both new and existing buildings. With these systems, architects can ensure that their projects are designed and built with the long-term sustainability of both people and the planet in mind. India’s three major rating systems are, Figs. 1, 2 and 3 show the USGBC rating system for LEED India, IGBC rating system, and GRIHA rating system.

The purpose of the current study is to find the best material to enhance building performance, lower building energy use, and increase the annual cost savings of energy consumption. It will also assist designers in measuring and identifying potential energy loss or gain for various design alternatives, computing the potential green building points they might accrue and gain, and selecting the best option in the Green Building Studio. The study’s goals include developing a 3D BIM model of a commercial building, classifying LEED, IGBC, and GRIHA requirements that can



Fig. 1 LEED rating system



Fig. 2 IGBC rating system

GRIHA RATING THRESHOLD	RATING
25 – 40 Points	★
41 - 55 Points	★ ★
56 - 70 Points	★ ★ ★
71 - 85 Points	★ ★ ★ ★
86 or more Points	★ ★ ★ ★ ★

Fig. 3 GRIHA rating system

be quickly and cheaply adopted in construction, measuring a building’s energy efficiency, and assessing the building to obtain green certification. In this study, three Autodesk products are being used to create a 2D plan of an office building and 3D models of architectural, structural, and MEP models for energy analysis and green building rating systems.

Even with imperfect knowledge, Jalaei and Jrade [1] emphasized the value of the conceptual stage in developing ideas and making judgments. The article offered a revolutionary model with interconnected modules that were made possible by automated procedures and plug-ins. This model allowed for timely and affordable sustainable design at the outset of a building project. The model used the gbXML and IFC file formats to successfully import BIM data into ECOTECT. To get LEED points, the study used the Eco-Scorecard database. The Ferny Celina’s study [2] investigation emphasized a number of elements that affect how much energy is used in buildings, including wall and roof structure, window glass, building orientation, window shades, window-to-wall ratio, and lighting effectiveness. In order to improve energy efficiency and thermal comfort, the study especially looked at residential structures in Chennai and emphasized the need to decrease heat gain via the building envelope. According to the study, using the right technologies while creating the building envelope is essential for cutting down on energy use. In particular, the employment of shading equipment and glass in windows was beneficial in lowering energy consumption, although the influence of roof construction on energy benefits was relatively less. The results highlighted the necessity of policy-level interventions, such as adding comparable codes to building bye-laws and national building codes, to guarantee that new residential buildings in India fulfill the required minimum standards for thermal comfort and energy efficiency. Examining factors that affect the creation of energy-efficient components and energy use was the main goal of the study carried out by Maglad et al. [3] is to create new approaches for enhancing energy efficiency in new construction projects and promoting environmentally friendly energy consumption practices. The study emphasized the significance of best practices for energy utilization in reaching sustainability objectives. Ur Rehman et al. [4] emphasized to conserve energy and water in accordance with green construction principles. Energy use intensity was calculated both before and after implementing insulation using a parametric BIM model created on the Revit

platform. The integrated BIM strategy sped up and significantly reduced the cost of the LEED certification procedure. Prakash [5] explored BIM-based energy analysis, demonstrating its significance in achieving sustainability benchmarks and designing alternatives for energy harvesting and reducing environmental impact. Guo et al. [6] presented a BIM-based green building evaluation and optimization approach, emphasizing its ability to evaluate green building performance and achieve energy savings through building renovation measures.

From the above studies, the use of BIM reduces energy consumption and cost in pre-existing academic buildings. Autodesk Revit was used to perform energy simulations, and LEED and IGBC rating systems were used to identify and implement green measures. The integrated BIM method helps speed up and save time and resources during the LEED certification process. Renewable energy can be produced through the use of this BIM approach, which can reduce the negative impact on the environment.

2 Methodology

Currently, using BIM for energy analysis and green building certification systems necessitates a combination of software solutions, which should comprise both an energy analysis software program and a BIM software program for designing the project's 3D model. From Fig. 4, this research looks into using BIM with energy analysis and green building systems using Green Building Studio, Revit software. Data is collected by selecting a commercial building and site location and collecting alternate materials and their green building system points. A 3D energy model is then developed in Revit and perform energy analysis by simulating the building in GBS. The Energy Simulation Analysis Report is studied to assess the EUI, annual use of energy, and annual cost of energy. Based on the results, design alternatives are developed and green building points are calculated for both baseline and modified buildings. Prioritizing the green points criteria by conducting survey to the consultants, architects, and engineers by using Delphi technique [7].

3 Data Collection

3.1 Comparative Analysis Based on Credit Points

For a detailed comparative analysis of the specific points and criteria of these rating systems, it would be best to refer to the official documentation and guidelines provided by LEED [8], IGBC [9], and GRIHA [10]. Comparative analysis based on credit points Gour [11] is shown in Table 1.

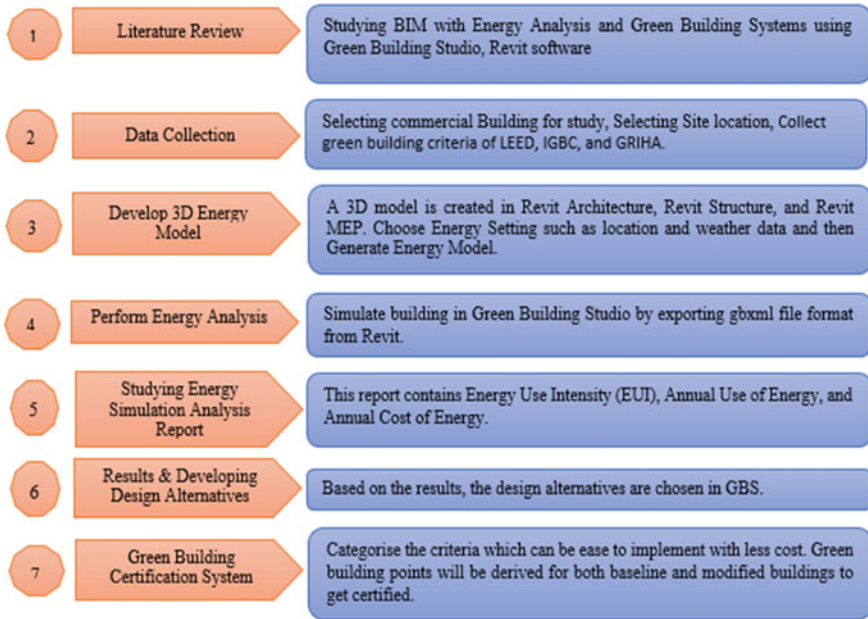


Fig. 4 Structure of methodology

Table 1 Credit point analysis of green criteria

Credit point analysis of LEED, IGBC and GRIHA						
Theme	LEED		IGBC		GRIHA	
	Maximum points	Weightage in percentage	Maximum points	Weightage in percentage	Maximum points	Weightage in percentage
Site selection, planning and design	25	22.7	19	19	16	15.2
Water efficiency	12	10.9	19	19	16	15.2
Energy efficiency	34	30.9	28	28	26	24.8
Building material	11	10	13	13	17	16.2
Waste management	2	1.8	3	3	6	5.7
Indoor environmental quality	16	14.5	11	11	12	11.4
Innovation and other	10	9.1	7	7	12	11.4
Total	110	100	100	100	105	100

From Table 1 analysis, the site selection, planning and design, and energy efficiency occupy more weightage; therefore, the minimum potential points are achieved by optimizing these factors.

3.2 Model Creation for the Study

The main study consists of the following steps,

- Creation of Architectural, Structural and MEP 3D models in Autodesk Revit.
- Creating Energy model in Revit.
- Exporting .gbxml file format for Energy Analysis.
- Importing .gbxml file format in Green Building Studio (GBS) cloud-based analysis [12] and choosing type of building, Schedule, Project location, cost of electricity in Rs. per kWh and run the analysis.
- Interpretation of results with green building certification system.

Project Details

Building Type: Office Building

Floor details: G + 5 Floors

Ground Floor Area: 1068 m²

1st to 5th Floor Area: 898 m²

Model Created: Architecture, Structural and MEP.

3.2.1 3D File Creation

There are a lot of softwares available for creating a 3D model, Revit Architecture by which makes it more user friendly is used here in this study. Revit Architectural elements such as walls, doors and windows, curtain walls, furniture and speciality equipments are shown in Fig. 5.

3.2.2 Revit Structure

Revit Structural elements such as footings, Columns, Beams, and Slabs are shown in Fig. 6.

3.2.3 Revit MEP

Revit MEP elements such as Air terminals, Ducts, Sprinkler pipes, Cable trays, and Conduits are shown in Fig. 7.

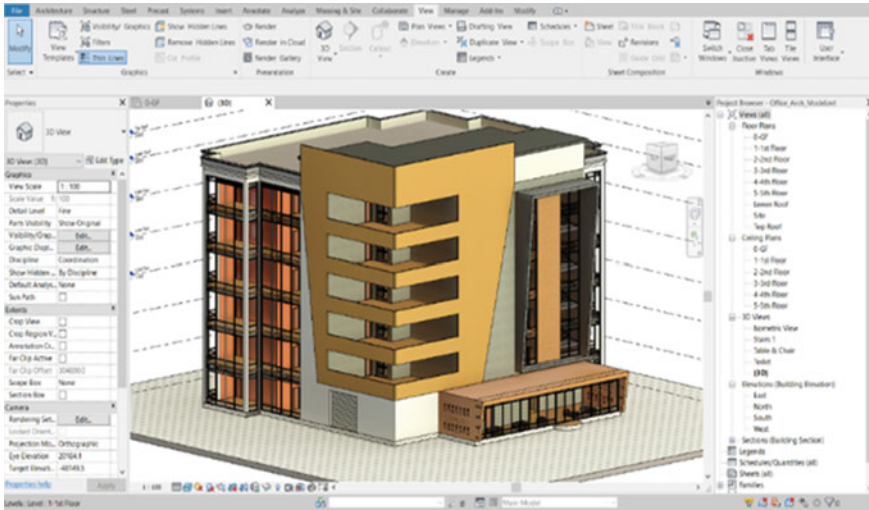


Fig. 5 Revit architecture

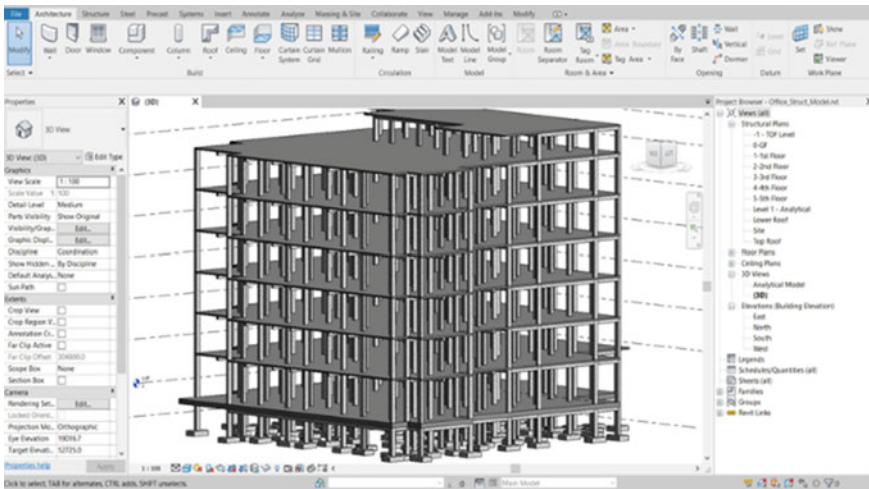


Fig. 6 Revit structure

3.2.4 Plan Layout

The ground floor plan layout is shown in Fig. 8.

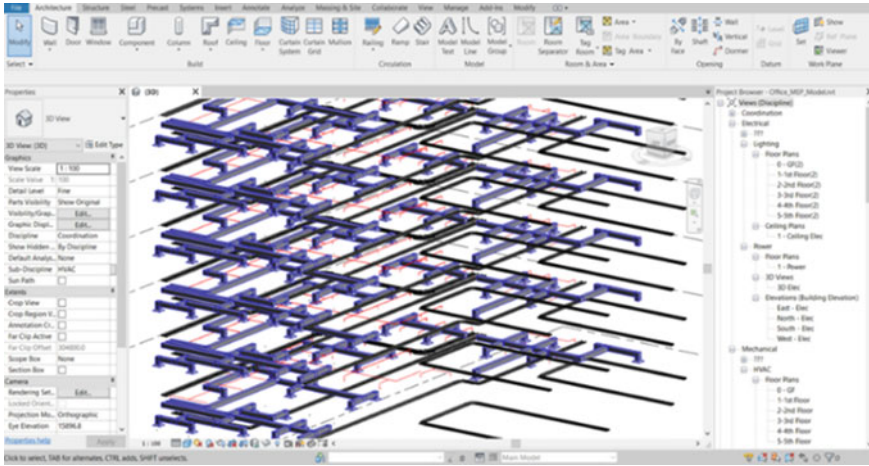


Fig. 7 Revit MEP

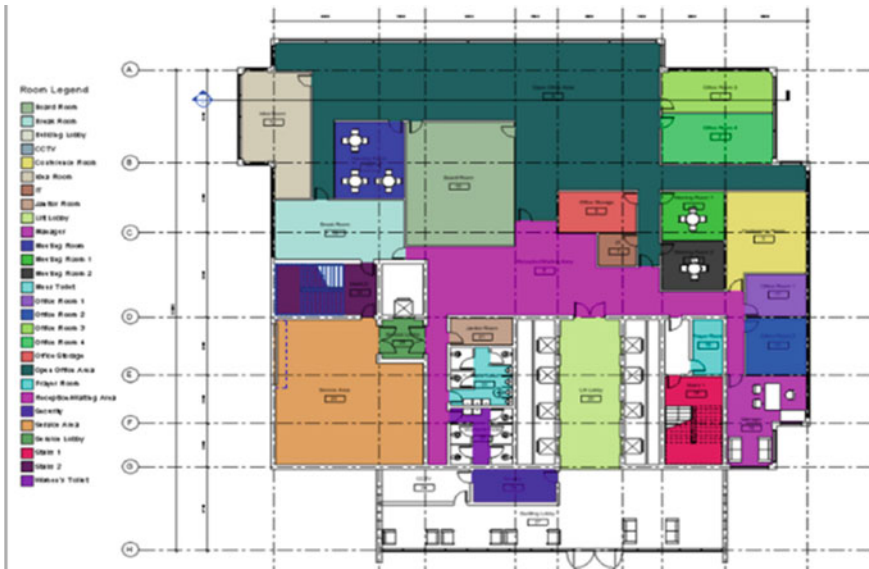


Fig. 8 Ground floor plan layout

3.2.5 MEP Network Plan Layout

The MEP layout is shown in Fig. 9.

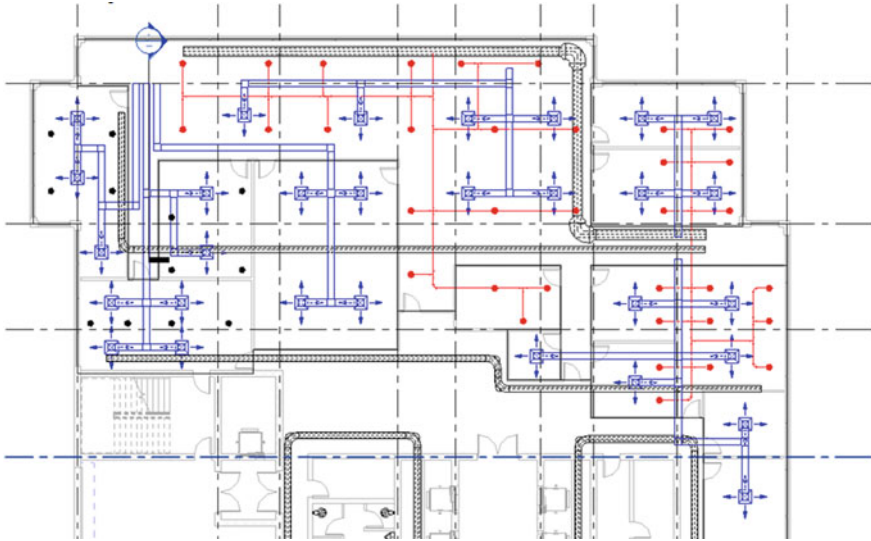


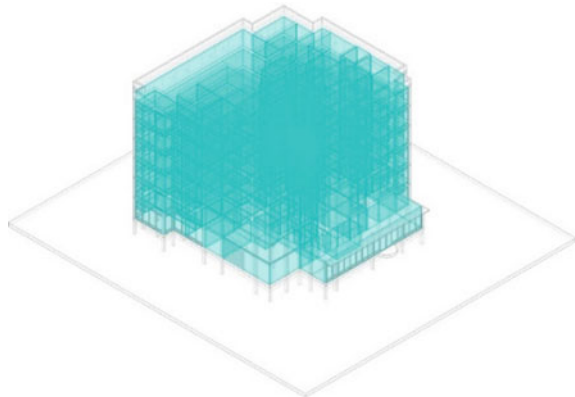
Fig. 9 Plan showing the MEP layout (ducts, conduits, and FFS)

3.3 Energy Model

The energy model created in Autodesk Revit is shown in Fig. 10. It shows that rooms and spaces to do energy analysis in cloud-based analysis of GBS. In order to perform energy analysis of the building, the created BIM model must be converted into an analytical model. We need to define zones in the BIM tool by converting all the spaces into rooms.

By putting the developed model to the test on a real five-story office building project, this section assesses its capabilities. The proposed structure is located in

Fig. 10 Energy model created for analysis



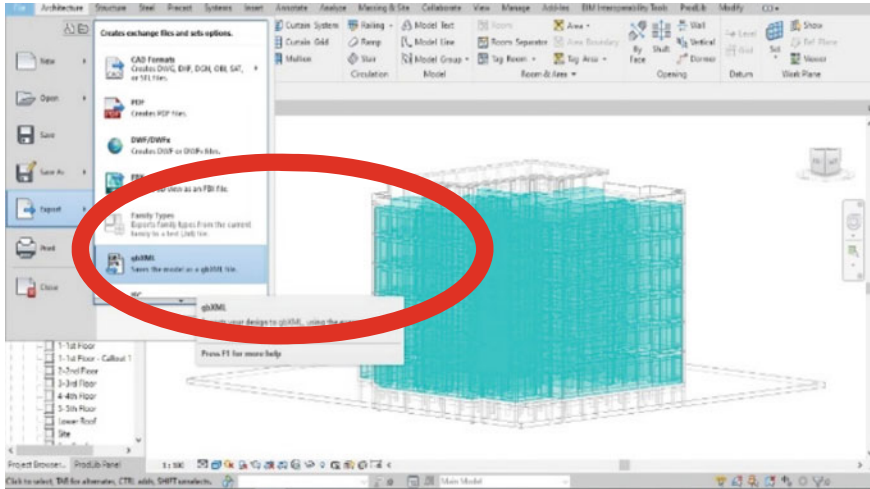


Fig. 11 Snapshot of exporting model Into.gbxml format

Solinganallur, Chennai, and has a ground floor area of 1068 m² and an area of 898 m² from the first to the fifth floors. The specifications of the parts used to create the office building’s design were fairly similar to those used in the final design.

It must be transferred to GBS in order to perform the energy analysis for design alternatives. The gbXML file format is the one used by GBS (Fig. 11).

4 Methodology Adopted to Run Energy Analysis in GBS

The methodology adopted to run energy analysis in GBS is shown in Fig. 12. GBS is an online simulation platform for assessing the energy efficiency of a building. It uses the DOE-2 simulation engine to power Autodesk Revit’s whole-building energy analysis tools. DOE 2 is the back end of GBS. GBS can analyze any gbXML file, thus making it compatible with any software that can export gbXML files. However, GBS does not have 3D modeling capabilities. The building type is office building which schedules of 24/6 facility and the electricity cost is Rs. 11 per kWh.

5 Results and Discussion

The energy costs of an office building with a floor area of 4275 m² can be calculated using the energy use intensity (1113.1 MJ/m²/year), electric cost (Rs. 11/kWh), and fuel cost (Rs. 0.007/MJ). The total annual electric energy used is 1,265,461 kWh and the total annual fuel energy used is 202.576 MJ. From Table 2, the total annual electric



Fig. 12 Autodesk GBS workflow

cost of Rs. 13,921,071 and a total annual fuel cost of Rs. 1498. Therefore, the total energy cost of the office building is Rs. 13,921,569. In conclusion, the energy costs for an office building of this size can be quite significant. It is important to consider energy efficiency measures to reduce energy costs and help the environment. The detailed annual electric and fuel end use in percentage is shown in Fig. 13.

The Annual electric end use of HVAC is 67.4%, other is 19.5% and Lights is 13.1% and the annual fuel end use of HVAC is 63.5%, other is 36.5% as shown in Fig. 14.

The default base run values i.e., building input specification of office building, as shown in Fig. 15, provided by Autodesk Revit, are indicated in terms of the *U*-values.

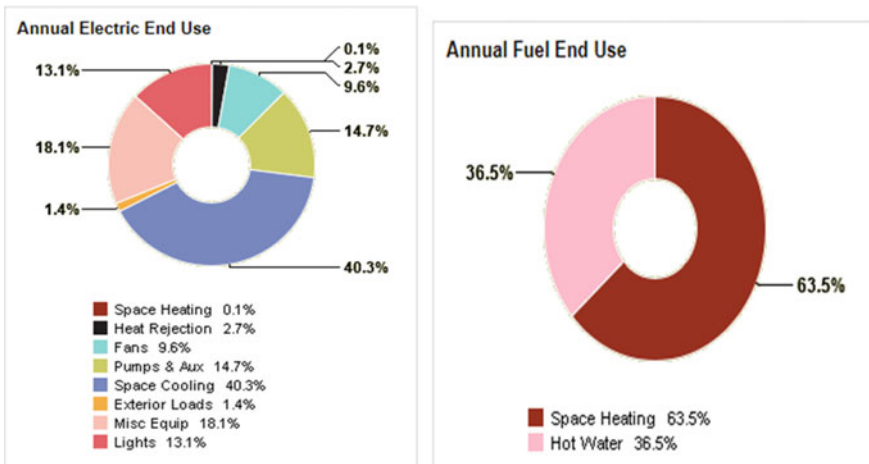


Fig. 13 Annual electric and fuel end use

Table 2 Energy analysis report

Name of building	Office building
Floor area (m ²)	4275
Energy use intensity (MJ/m ² /year)	1113.1
Electric cost (/kWh)	Rs. 11
Fuel cost (/MJ)	Rs. 0.007
Total annual electric energy (kWh)	1,265,461
Total annual fuel energy (MJ)	202.576
Total annual electric cost	Rs. 13,921,071
Total annual fuel cost	Rs. 1498
Total energy cost	Rs. 13,921,569

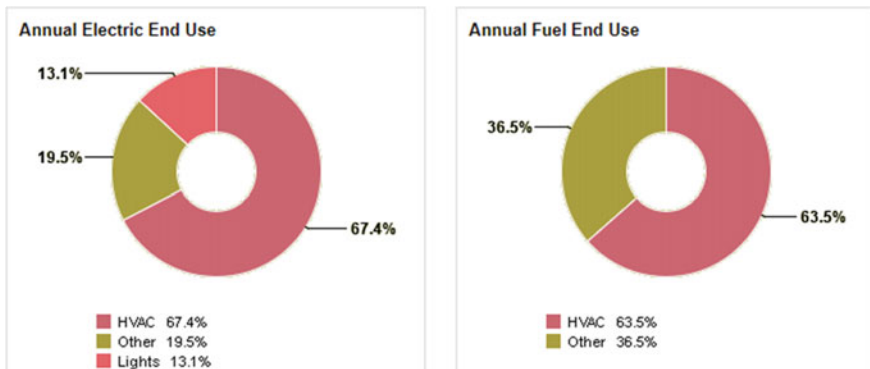


Fig. 14 Annual electric and fuel end use in terms of HVAC

If the efficiency with which a building element transfers heat is lower, it indicates lower *U*-value.

6 Summary

The Energy Analysis of an office building created in Revit is successfully done in GBS by analyzing in design stage. The use of the material in the model is basic material such as lighting fixtures, furniture, doors, windows, etc. From the base model study, based on the EUI, U-Value, SHGC Value, the energy usage of the building can be reduced to evaluate the green building certification criteria. GBS analysis helps the architects to design the energy-efficient building in easily and reduces time and cost. Future studies include, questionnaire for priorities the green point's criteria is created in google forms to response from the consultants, architects, and engineers. From the questionnaire, the responses of the consultants and architects for categorizing the

Base Run Construction		
Roofs	R20 over Roof Deck - Cool Roof U-Value: 0.26 (i)	3,365 m ²
Ceilings	4 in reinforced-concrete ceiling U-Value: N/A (i)	100 m ²
Exterior Walls	R13 Wood Frame Wall U-Value: 0.49 (i)	4,559 m ²
Interior Walls	R0 Metal Frame Wall U-Value: 3.25 (i)	3,988 m ²
Interior Floors	Interior 4in Slab Floor U-Value: 4.18 (i)	4,608 m ²
Air Walls	Air Surface U-Value: 15.32	128 m ²
Nonsliding Doors	R2 Default Door (227 doors) U-Value: 2.39 (i)	409 m ²
Air Openings	North Facing Windows: Unglazed opening (6 doors) U-Value: 0.00 W / (m ² -K), SHGC: 1.00 , Vit: 1.00	15 m ²
	Non-North Facing Windows: Unglazed opening (52 doors) U-Value: 0.00 W / (m ² -K), SHGC: 1.00 , Vit: 1.00	192 m ²
Fixed Windows	North Facing Windows: Pilkington RW33 double glazing (1/4 in + 1/4 in) (24 windows) U-Value: 2.86 W / (m ² -K), SHGC: 0.76 , Vit: 0.81	483 m ²
	Non-North Facing Windows: Pilkington RW33 double glazing (1/4 in + 1/4 in) (106 windows) U-Value: 2.86 W / (m ² -K), SHGC: 0.76 , Vit: 0.81	758 m ²

Fig. 15 Default base run values of office building

criteria are analyzed to evaluate green point’s criteria in building to get certified as green building. The 3D model for the main study will be created in Revit Architecture, Revit Structure, and Revit MEP and analyzed in GBS and the design alternatives are chosen to optimize. Evaluate the building to the criteria chosen to get certified as green building. Compare the base model and modified model to get the energy cost saving and to get minimum green points to get certified which is easy to implement with less cost.

Acknowledgements Thank construction professionals for providing data for doing research. This research doesn’t have any financial support.

References

1. Jalaei F, Jrade A (2014) Integrating building information modelling (BIM) and energy analysis tools with green building certification system to conceptually design sustainable buildings. *J Inf Technol Constr (ITcon)* 19:494–519. <http://www.itcon.org/2014/29>
2. Celina F (2020) Performance assessment via simulation with Revit insight and green building studio. Autodesk University, Autodesk article
3. Maglad AM et al (2022) BIM-based energy analysis and optimization using insight 360 (case study). *Case Stud Constr Mater.* <https://doi.org/10.1016/j.cscm.2022.e01755>
4. Ur Rehman HS et al (2022) A multi-facet BIM based approach for green building design of new multi-family residential building using LEED system. *Int J Constr Manag.* <https://doi.org/10.1080/15623599.2022.2033419>
5. Jadhav PP (2019) Assessment of building energy by performing simulation with BIM. *Ann Fac Eng Hunedoara Int J Eng Tome XVII*
6. Guo K et al (2021) BIM-based green building evaluation and optimization: a case study. *J Clean Prod.* <https://doi.org/10.1016/j.jclepro.2021.128824>

7. Norouzi D et al (2019) (2021) Investigating green hospital criteria using Delphi method for Fars Province, Southwest of Iran. *J Communal Health Res* 10(1):22–32
8. <https://www.usgbc.org/credits>
9. <https://igbc.in/igbc/redirectHtml.htm?redVal=showGreenNewBuildingsnosign>
10. <https://www.grihaindia.org/griha-rating>
11. Mishra P, Gour S (2018) Green building rating system. *Int J Res Eng Sci Manag* 1(10)
12. <https://gbs.autodesk.com/gbs>

Cost–Benefit Analysis of Adoption of Green Materials in Conventional Building to Improve Green Rating



Srihari Vedartham, J. S. Sudarsan, Vijay Narayan, K. Prasanna, and S. Mohanakrishna

1 Introduction

1.1 Description

In current years, India's ascent has been a crucial trend in the global economy. India's future prospects are excellent, thanks to growing investment and robust macroeconomic fundamentals. Infrastructure development in India is essential to the present growth and development to compete the rest of the world in GDP [1]. The Indian construction industry produces about 11–12 million tonnes of waste annually. Waste disposal has a vital impact on nature and can cause serious problems during the demolition stage. Therefore, green buildings are more important and relevant than conventional buildings [2].

Green building principles optimize the natural resources and improve our quality of life [3]. Rapid industrialization, infrastructure development, population growth, increase in carbon emissions and the destruction of natural resources are the reasons behind the concept of green buildings.

Important Features of a Green Building

Energy Efficiency: Energy-efficient buildings create comfortable living conditions in your home with the least energy consumption and maximum resource efficiency

S. Vedartham

NICMAR, 7-06, Jagannaguda, Shamirpet, Aliabad, Hyderabad 500101, India

J. S. Sudarsan (✉) · V. Narayan

NICMAR University, 25/1, Balewadi, N.I.A. Post Office, Pune 411045, India

e-mail: ssudarsan@nicmar.ac.in

K. Prasanna · S. Mohanakrishna

Department of Civil Engineering, Faculty of Engineering and Technology, SRM Institute of Science and Technology, Kattankulathur, Tamilnadu 603203, India

possible as energy-efficient buildings consume less operational energy. It can account up to 30% of the energy consumption of the entire life cycle [4]. Energy-efficient buildings keep the building fully functional and thermally comfortable for the occupants. Generating renewable energy on-site from solar, hydro, wind, or biomass can significantly reduce the impact on nature.

Water Efficiency: Of the absolute water accessible on Earth, only 0.3% is fresh water in the liquid state. As there is extensive use of water in building maintenance, we have several methods to conserve/reuse water. Having control over water consumption and protecting the quality of water are central goals of sustainable construction. Where possible, facilities should be made to increase the reliance on water collection, usage, filtration, and reusing. Conservation of water throughout the life cycle is achieved by designing a system that reuses water in flushing toilets, washing vehicles, and gardening needs [5].

Material Efficiency: Choosing materials and resources that can be easily reused or recycled at the end of their useful life, have low embodied energy, rapidly renewable materials, locally available, and manufactured in a resource-efficient process. Recycled materials used in the construction phase can also reduce the amount of demolition waste that goes to landfills. Locally available materials can reduce carbon emissions and embodied energy as it reduces the transportation distance.

Waste Reduction: Sustainable construction also seeks to reduce waste produced in the construction and utility phases. At the time of construction itself, the objective ought to be set to limit the construction wastage, following material waste management techniques to reduce the wastage of materials [6]. The demolition waste can be recycled and reused. Waste can also be reduced by increasing the overall lifespan of the structure.

Indoor Environmental Quality: It focuses on providing residents with an exciting and comfortable environment and reduces the risk of medical problems connected with the building. Indoor environmental quality includes conditions in the building, e.g. indoor air quality, usage of natural lighting to the fullest, thermal comfort, ergonomics, etc. Strategies of indoor environmental quality include protection of occupant's health, reducing stress and improving quality of life. A better quality of the indoor environment of the building can potentially improve the lives of the occupants.

Design Efficiency: The basis of construction is at the design stage. This stage is one of the most important parts of the building's life cycle, as it impacts the performance and cost. The goal of designing a green building is to minimize the overall environmental impact during the construction phase, operation and maintenance phase and demolition phase of the building [7]. Care should be taken in the selection of site, building orientation, and landscaping while designing a green building.

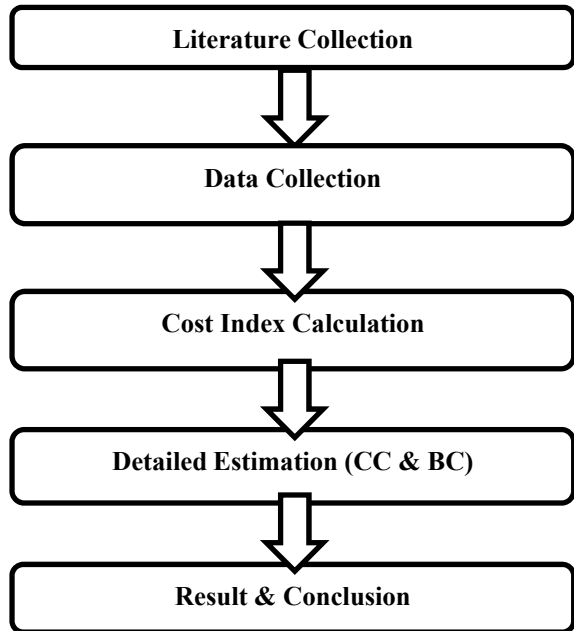
1.2 Importance of Sustainable Infrastructure

1. Many developing countries are aiming to accomplish long-term development in financial growth in all areas, as well as a more even handed dissemination of the benefits of development. The need for sustainable infrastructures is growing quickly in response to the building industry’s negative environmental impact. In their research publication “Sustainable Infrastructure,” Thomé and Ceryno [8] discuss the importance of sustainable design and green infrastructure in reducing adverse environmental effects. The working environment of a business, which includes air, water, land, and natural resources, is referred to as environmental sustainability in this study.
2. Unni and Anjali [1] in their research manuscript “Cost–benefit Investigation of Conventional and Modern Building Materials for Sustainable Development of Social Housing” discussed about the advantages of using sustainable building materials and a cost analysis is undertaken. The study demonstrates the need of reducing energy consumption wherever possible. The research focuses on strategies to make buildings more sustainable while keeping economic criteria by using green building materials that need less energy to manufacture and emit fewer greenhouse gases. According to the Global Building Alliance, buildings consume 40% of global energy in 2019, and the authors of this study seek to demonstrate how green materials may be used efficiently to reduce this consumption.
3. In their article “Cost Estimation Methods for Transport Infrastructure: A Systematic Literature Review” by Barakchia and Torp [4], the authors described the primary goal of their research, which was to examine various cost prediction techniques used in transportation projects. The study compared 12 cost estimation approaches to significant cost estimation parameters. Of the 12 ways, the parametric method was the most efficient. Given the enormous costs of transportation infrastructure building and the implications, it is vital that decision-makers receive reliable cost estimates.

1.3 Estimation in Infrastructure

A plan, specifications, and prices are required for estimation and BOQ preparation. SSR is used to compute the rates. Material, machinery, and labour will all be factored into the rates [9]. A complete station is used to conduct the survey. To compute slope distances from the instrument to a given point, the total station combines an electronic theodolite (transit) with an electronic distance metre (EDM) [10].

Fig. 1 Methodology flow chart



1.4 Objectives

- To study and compare the different components of a sustainable and unsustainable infrastructure.
- To optimize the application of resources and the financial factors of a project by adopting solar photovoltaic system.

2 Methodology

The obtainable comprehensive road plan is an excellent illustration of connectivity for an area along the sample building considered for the assessment (Fig. 1).

A thorough investigation and analysis is carried out. Data collection research is through secondary data source from reports and documents.

3 Results and Discussion

The cost for constructing the building with conventional building materials is Rs. 4,100,530.95 and the cost for constructing the building with sustainable and recycled materials is Rs. 3,971,384.64 as listed in Table 1. The percentage change in the

cost of construction after the replacement of sustainable materials reduced the cost of PCC by 24.46%, RCC up to plinth level by 2.1%, RCC above plinth level by 1.76%, full brickwork by 7.95%, half brickwork by 4.75%, plastering (12 mm) by 9.83%, plastering (15 mm) by 7.25%, and 3.15% of reduction in the total cost of construction. The detailed quantity estimation was represented in Table 1a and b and the cost comparison was discussed in Table 2.

As shown in Table 3, quantities and rates of the building with sustainable materials, to calculate the construction cost of this building, Delhi Analysis of Rates—2021 Volumes 1 and 2 was used and the details of the work and materials are as follows [10, 11].

Solar panel calculations are based on 75% of the available area of the total roof area of 75.52 m². The average electricity cost of the villa was assumed to be 8 Rs./kWh [12]. According to the Solar Rooftop Calculator's estimates, a 5.7 kW power plant is necessary to generate 8550 kWh of electricity annually and 213,750 kWh over the course of 25 years, assuming 5.5 sunny hours per kWh. The reduced carbon

Table 1 Quantities and rates of the building with conventional materials

S. No.	Description	UoM	Quantity	D.S.R code	Rate per unit	Cost
1	Excavation	cum	119.64	2.6.1	205.45	24,580.04
2	PCC	cum	5.27	4.1.8	6326.05	33,338.28
3	RCC up to plinth level	cum	21.05	4.20.1.3	8387.15	176,549.51
4	RCC—plinth level to V	cum	60.87	4.20.2.3	10,009.50	609,278.27
5	Backfilling	cum	96.71	2.25	253.95	24,559.50
6	Steel (handling)	kg	6204.21	5.22.6 and 5.22A.6	89.65	556,207.43
7	Brickwork 8"	m ²	67.43	6.29.2	8339.65	562,342.60
8	Half brickwork	m ²	46.23	6.13.2	1018.05	47,064.45
9	Plastering (1:4) 12 mm	m ²	1043.34	13.7.2	361.30	376,958.74
10	Plastering (1:4) 15 mm	m ²	754.63	13.8.2	406.10	306,455.24
11	Internal putty	m ²	946.04	13.80	123.85	117,167.05
12	Interior primer	m ²	946.04	13.43	64.45	60,972.28
13	Internal painting	m ²	946.04	13.83.2	121.55	114,991.16
14	External paint (with primer)	m ²	603.07	13.46.1	166.85	100,622.23
15	Texture paint	m ²	151.85	13.110.1	191.40	29,064.09
16	Flooring (granite 1:4)	m ²	245.69	11.56.1	3908.80	960,353.07
					Total cost	4,100,503.95

Table 2 Quantities and rates of the building with sustainable materials

S. No.	Description	UoM	Quantity	D.S.R code	Rate per unit	Cost
1	Excavation	cum	119.64	2.6.1	205.45	24,580.04
2	PCC	cum	5.27	4.1.8A	4715.6	24,851.21
3	RCC up to plinth level	cum	21.05	4.20A.1.3	8211.3	172,847.87
4	RCC—plinth level to V	cum	60.87	4.20A.2.3	9833.7	598,577.32
5	Backfilling	cum	96.71	2.25	253.95	24,559.50
6	Steel	kg	6204.21	5.22A.6	89.65	556,207.43
7	Brickwork (1:6)	m ²	67.43	6.34.2	7676.3	517,612.91
8	Half brickwork (1:4)	m ²	46.23	6.45.2	969.65	44,826.92
9	Plastering (1:4) 12 mm	m ²	1043.34	13.13	325.8	339,920.17
10	Plastering (1:4) 15 mm	m ²	754.63	13.14	376.65	284,231.39
11	Internal putty	m ²	946.04	13.80	123.85	117,167.05
12	Interior primer	m ²	946.04	13.43	64.45	60,972.28
13	Internal painting	m ²	946.04	13.83.2	121.55	114,991.16
14	External paint (with primer)	m ²	603.07	13.46.1	166.85	100,622.23
15	Texture paint	m ²	151.85	13.110.1	191.40	29,064.09
16	Flooring (granite 1:4)	m ²	245.69	11.56.1	3908.8	960,353.07
					Total cost	3,971,384.64

emissions are 175 tonnes, which is equivalent to planting 280 teak trees for a lifetime. This system costs Rs. 233,649 without subsidy and Rs. 162,325 with subsidy 40% up to 3 kW and 20% above 3–10 kW based on the current MNRE benchmark. The cost of construction of the building with sustainable building materials and solar panels is Rs. 4,133,709.64 as shown in Table 1. The percentage change in the addition of the cost of solar panels resulted in an increase of 0.81% in total cost.

Table 3 Percentage change in the cost of construction

S. No.	Description	Using conventional materials	Using sustainable materials	Difference in cost	% change in cost
1	PCC	33,338.28	24,851.21	– 8487.07	– 25.46
2	RCC up to plinth level	176,549.51	172,847.87	– 3701.64	– 2.10
3	RCC—plinth level to V	609,278.27	598,577.32	– 10,700.95	– 1.76
4	Brickwork (1:6) 10	562,342.60	517,612.91	– 44,729.69	– 7.95
5	Half brickwork (1:4)	47,064.45	44,826.92	– 2237.53	– 4.75
6	Plastering (1:4) 12 mm	376,958.74	339,920.17	– 37,038.57	– 9.83
7	Plastering (1:4) 15 mm	306,455.24	284,231.05	– 22,224.19	– 7.25
8	Total cost (including excavation, backfilling, steel, painting and flooring)	4,100,503.95	3,971,384.64	– 129,119.31	– 3.15
9	Solar panels	0.00	162,325	162,325.00	–
10	Total cost (including solar panels)	4,100,503.95	4,133,709.64	33,205.69	0.81

4 Conclusion

- The use of recycled resources for construction, such as fly ash bricks, recycled concrete aggregate, and stone dust decreases the cost of this G + 2 residential structure by 3.1%. Replacing 25% of coarse aggregate and fine aggregate with recycled aggregates in concrete and stone dust in cement mortar has no effect on strength.
- We may lower the overall cost, carbon emissions, embodied energy, ecological footprint, and reliance on natural resources by employing sustainable building materials, which are either industrial residue or recovered from construction and demolition debris.
- By installing solar panels while considering government subsidiaries and sustainable building materials, the cost of construction increases by 0.81%, which may be deemed minimal, and yearly energy generation is 8550 kWh, resulting in cost savings. The inclusion of solar panels may initially increase building costs, but over time, the money invested in solar panels can be offset by energy savings.

References

1. Unni A, Anjali G (2022) Cost-benefit analysis of conventional and modern building materials for sustainable development of social housing. *Mater Today: Proc* 51:1649–1657
2. John A, Aswathy Warriar D, Sabu HM, Mathew M (2018) Estimation of a reinforced building: a review. *Int Res J Eng Technol (IRJET)* 5(2):1680–1683
3. Sinha PC, Madaan J (2020) An analysis of challenges to infrastructure industry in India: concomitant impediments to growth prospects. *Indian J Projects Infrastruct Energy Law* 1(1):35–52
4. Barakchi M, Torp O (2017) Cost estimation methods for transport infrastructure: a systematic literature review. *Procedia Eng* 196:270–277
5. Baviskar RV, Devalkar RV (2018) Time-cost optimisation in road construction case study—Nashik Sinnar Highway. *Int J Eng Res Technol (IJERT)* 7(2):166–171
6. Tavakoli A, Masehiand JJ, Collyard CS (1990) FLEET: equipment management system. *J Manag Eng* 6(2):211–220
7. Gao T, Liu Q, Wang J (2013) A comparative study of carbon footprint and assessment standards. *Int J Low-Carbon Technol* 9:237–243
8. Thomé AMT, Ceryno PS, Scavarda A, Remmen A (2016) Sustainable infrastructure: a review and a research agenda. *J Environ Manag* 184:143–156
9. Lützkendorf T, Foliente G, Balouktsi M, Wiberg AH (2015) Net-zero buildings: incorporating embodied impacts. *Build Res Inf* 43(1):62–81
10. Kataria V, Salunkhe H (2016) Retrofitting of existing building as per IGBC existing building norms. *Int J Civ Struct Eng Res* 4(1):250–253
11. Yim S, Ng S, Hossain M, Wong J (2018) Comprehensive evaluation of carbon emissions for the development of high-rise residential building. *Buildings* 8:147
12. Zhao X, Huang G, Lu C, Zhou X, Li Y (2020) Impacts of climate change on photovoltaic energy potential: a case study of China. *Appl Energy* 280:115888

Impacts of Natural Disasters on the Performance of Residential Construction Projects of Kashmir, J&K



J. Rajprasad  and Hilal Ahmad Wani

1 Introduction

The construction industry had a significant impact on the country's development and growth [1]. The occurrence of any dangerous event is defined as a natural catastrophe, causing severe damage to both life and property [2]. Yearly worldwide mortality from natural disasters have averaged 106,000 per year over the last decade, with estimated annual losses of US\$165 billion [3]. Disaster's unpredictability and destructive force diminish social stratification, create physical and psychological suffering in society, and destroy the ecosystem. Natural disasters such as earthquakes, landslides, floods, cyclones, forest fires, volcanic eruptions, and severe accidents occur often around the world. These result in deaths, property damage, and socio-economic devastation. Natural catastrophes struck roughly 75% of the world's population at least once between 1980 and 2000, according to a United Nations Development Programme (UNDP) study from 2004 [4]. Inevitably, as the global population and infrastructure expand, so will the world's vulnerability to natural disasters. This is especially true because coastal areas (which are more vulnerable to floods, cyclones, and tidal waves) are experiencing the fastest population growth [5].

Natural disasters have a long history in Kashmir, J&K. Many natural disasters have struck the state, particularly in the nineteenth and early twentieth [6]. The state has suffered much in the past and is prone to many natural disasters due to its unique geography, difficult terrain, harsh weather conditions, and, most critically, a weak economy, particularly a deficient road and communication network [7]. Natural disasters like earthquake, floods, landslides, snow avalanche, etc., have negative impact on every sector including the construction industry [8]. Natural disasters have had

J. Rajprasad (✉) · H. A. Wani

Department of Civil Engineering, Faculty of Engineering and Technology, SRM Institute of Science and Technology, Kattankulathur, Tamilnadu 603203, India

e-mail: rajprasj@srmist.edu.in

a significant impact on the construction sector in Kashmir, leading to infrastructure damage, project delays, and increased costs [9]. The region has experienced devastating floods, earthquakes, landslides, and avalanches, posing numerous challenges for the construction industry. These challenges include a shortage of skilled labour and materials, delays in project completion, and hazardous working conditions. To address these issues, this research aims to explore and assess the effects of natural disasters on residential construction projects, identify related challenges, and analyze their impact using structural equation modelling (SEM). The findings of this study will assist project managers in recognizing, preventing, and managing natural disaster-related risks, as well as optimizing resource allocation in construction projects.

2 Literature Review

When a significant risk hits a community and renders it unable to function on a regular basis without outside assistance, inflicting damage, disruption, and fatalities, it is referred to be a natural disaster [6]. Kashmir, being a seismically active area, has been the site of many of the worst earthquakes in the past, and the frequency of such events is on the rise [10]. Large-scale disasters such as hurricanes, earthquakes, and cyclones all cause construction prices to surge [9]. When it comes to the time it takes to restore infrastructure to its pre-disaster operating levels, two things stand in the way of this: unexpected spikes in demand for services after catastrophes, and already-existing capacity supply limits [11]. Natural catastrophes provide a variety of obstacles to the construction sector. Reference [12] investigated of the availability of resources in post-disaster recovery efforts. The scarcity of resources available for post-disaster house reconstruction has a detrimental effect on the likelihood of a successful recovery. The inability to procure materials and labour slowed the recovery process greatly. Resources for recovery may be rapidly and efficiently accessed via a country's transportation infrastructure, including roads, airports, ports, and trains [13]. Research on post-disaster logistics found that the high cost of transporting resources and the absence of transportation options were significant obstacles to post-disaster recovery. Following a natural catastrophe, the Nepalese construction sector is plagued by labour shortages and inadequate site safety measures, according to a study by [14]. In the aftermath of a natural catastrophe, building projects have several problems that impact their schedule, cost, and scope [15]. Quality-related issues such as construction work quality, material quality increases the number of reworks and their cost. Construction clients usually face shortage of human resources after a natural disaster. This study aims to fill a research gap by examining the issues faced by residential construction projects in the Kashmir region due to natural catastrophes. By identifying key factors and their interactions through a theoretical structural model, and analyzing empirical data using a structural equation modelling approach, the study highlights the significant influence of manpower on project performance. The findings will assist project managers in recognizing, managing, and allocating

resources to mitigate risks associated with natural disasters in construction projects in Kashmir. Previous research has identified these factors emerging from natural catastrophes, as given in Table 1, laying the framework for attempts to identify factors influencing project performance (the study's first aim) based on a solid literature base.

Table 1 Project performance factors arising due to natural disasters in the construction industry of Kashmir, J&K

Latent factors	Code	Observed factors	References
Finance	F1	Price escalation of resources	[7, 13, 16–18]
	F2	Repairing costs	
	F3	Lack of funding	
	F4	Inflation of rates	
	F5	Cost of reworks	
Delays	D1	Logistics	[6, 16, 19]
	D2	Suspension of construction	
	D3	Extra time for reworks and debris removal	
	D4	Delays in transportation of resources	
	D5	Conflicts between project parties	
Labour	L1	Injuries	[6, 11, 19–21]
	L2	Loss of lives	
	L3	Shortage of labours and suppliers	
	L4	Shortage of experts	
	L5	Increased labour wages	
Material and equipment	M1	Damage to materials	[10, 12, 19, 21]
	M2	Shortage of materials	
	M3	Improper material storage	
	M4	Hindrances in material supply	
	M5	Damage/failure of equipments	
	M6	Loss of equipments	
	M7	Shortage of equipments and tools	
Environmental	E1	Air quality	[13, 15, 22]
	E2	Soil movements	
	E3	Adverse Weather and climate conditions	
	E4	Health and safety issues	
	E5	Volume of debris	
	E6	Damage to structures	
Project performance	P1	Estimated cost of the project	[19, 23]
	P2	Duration of the project	
	P3	Desired quality of the project	
	P4	Productivity of the project	

2.1 Theoretical Framework

There are five categories of factors arising due to the natural disasters that might impact construction project performance: financing, delays, manpower (labour), materials and equipments, and external, which constitute the theoretical basis for the paper's study model after a thorough examination of the relevant literature. The selection of factors in the theoretical framework was based on a thorough review of literature, industry reports, and expert consultations, considering their consistent mention and relevance in construction project management in disaster-prone areas. The final factors, including financial aspects, delays, manpower, material and equipment, and environmental considerations, were chosen for their significant impact on construction project performance during natural disasters in the Kashmir region.

3 Research Methodology

The first step in this investigation was to identify the factors influencing the performance of residential construction projects in Kashmir, J&K, as a result of natural catastrophes. The literature study highlighted finance-related factors, delays-related factors, manpower-related factors, material and equipment-related factors, and environmental-related factors. A questionnaire survey was then conducted in Kashmir, J&K. The questions were designed in such a manner that respondents could immediately understand and assess the relationship between those factors and project performance. Respondents were asked to express their thoughts on different degrees of influence on a five-point Likert scale ranging from "1 = strongly disagree" to "5 = strongly agree". Exploratory factor analysis (EFA) and structural equation model (SEM) have been used to analyze the data.

3.1 Data Demographics

Respondents were chosen from a diverse group of construction industry specialists in Kashmir, J&K (contractors, clients, and engineers). This study mainly focuses on the residential construction projects in Kashmir, J&K. As can be seen, the sample was well-balanced across fields. After an initial phone discussion and email exchange, the study's aims were described and clarified in order to elicit the greatest possible answer from each respondent. A total of 105 questionnaires were distributed in both hard copy and electronic format. Only 79 replies were found to be genuine, yielding a response rate of 75%. Because of relevant industrial experiences, personal interactions, and respondents' solid comprehension of survey questions, a small sample size was rated extremely trustworthy for analysis [10]. There was a 44% response rate among construction contractors, followed by engineers and managers

(35%). Clients made up little over a third of the overall number. More than 20% of respondents had more than 10 years of construction experience. Participants for this study were selected based on their involvement in residential construction projects in the Kashmir region, focusing on project managers and professionals. Potential biases include self-reporting bias in questionnaire responses, a bias towards individuals who have experienced severe natural catastrophes, and limitations in sample size and geographic coverage. Careful interpretation of the findings and acknowledgement of these biases is necessary for generalization beyond the specific sample.

3.2 Data Analysis

Using data from questionnaire surveys, exploratory factor analysis (EFA) and structural equation modelling (SEM) were utilized to evaluate a hypothetical model of construction project performance characteristics. The software used for EFA was SPSS and for SEM Smart PLS 3.0 software was used (IBM SPSS, 2019) (Smart PLS 3.0).

3.3 Exploratory Factor Analysis

EFA was used to figure out the structure of the model by looking at the correlations between variables and squeezing the data. A wider range of squared loadings may be seen when variables (factors) are rotated. This enables the loadings to be better understood depending on their significance. Unreliable construct indicators were ruled out by a large sample size, As a result, variables with loadings less than 0.40 were excluded from components [19]. Shortage of equipments and tools (M7), air quality (E1), and damage to structures (E6) were ruled out as a result of the low factor loading.

Table 2 lists the eigenvalues of each component, and Fig. 1 displays a screen plot that illustrates the distribution of eigenvalues for each component. The plot reveals that the eigenvalues decline rapidly until the fifth component, after which they stabilize and remain below the value of one. This suggests that the first five components explain a significant portion of the variance in the data, while subsequent components contribute less to the overall variance. According to the findings of the study, a total of 28 items were included in the initial data collection. The eigenvalue of a component is a reflection of how much variation it accounts for in the system. In this case, eigenvalues larger than one were maintained, while eigenvalues smaller than one were removed. Table 3 includes 25 variables that are organized into five categories, including finance, delays, manpower, material and equipment, and environmental.

Kaiser–Meyer–Olkin (KMO) test was also calculated to evaluate the sample validity of each model variable as well as the overall model. The KMO test is performed (how the variables explain each other). KMO levels close to 1.0 are

Table 2 Total variance

Initial eigenvalues				Rotated sums of squared loadings		
Component	Total	% of variance	Cumulative %	Total	% of variance	Cumulative %
1	9.335	32.189	32.189	4.957	17.092	17.092
2	5.288	18.236	50.425	4.679	16.133	33.225
3	2.974	10.256	60.681	4.614	15.911	49.136
4	2.348	8.095	68.776	3.827	13.197	62.333
5	1.786	6.159	74.935	3.654	12.602	74.935
25	0.001	0.002	100.00	–	–	–

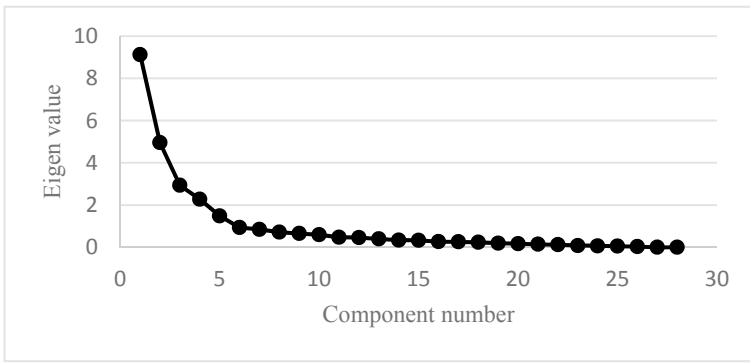


Fig. 1 Screen plot of the identified factors

considered optimal. For the sample size less than 100, KMO value greater than 0.6 is acceptable [6].

3.4 Structural Equation Modelling

SEM is a multivariate analytic tool for the analysis of quantitative correlations between independent variables, was developed by sociologists and psychologists [9]. In recent years, the usage of SEM in construction engineering and management has increased dramatically [12]. There is enough evidence to support using SEM to investigate and quantify how latent factors (such as finance, labour, materials and equipment, etc.) impact observable phenomena (i.e. project performance). As a result, the goal of this study is to discover the relationship of observed variables (finance, delays, manpower, material and equipment, and environmental) with the dependent variable (project performance). The proposed model was modified by removing the attributes having low values of correlations with their latent factor [17]. The model was stripped of M7, E1, and E6 due to low relationships between variables and

Table 3 Extracted factors and their loadings from SPSS

Factor	Item	Factor loading	KMO value
Finance	Price escalation of resources	0.814	0.783
	Repairing costs	0.773	
	Lack of funding	0.853	
	Inflation of rates	0.790	
	Cost of reworks	0.564	
Delays	Logistics	0.887	0.767
	Cancellation of construction	0.982	
	Extra time for reworks and debris removal	0.695	
	Delays in transportation of resources	0.881	
	Conflicts between project parties	0.851	
Labour	Injuries	0.803	0.809
	Loss of lives	0.879	
	Shortage of labours and suppliers	0.866	
	Shortage of experts	0.643	
	Increased labour wages	0.802	
Material and equipment	Damage to materials	0.755	0.888
	Shortage of materials	0.892	
	Improper material storage	0.865	
	Hindrances in material supply	0.908	
	Damage/failure of equipments	0.926	
	Loss of equipments	0.807	
Environmental	Soil movements	0.889	0.714
	Adverse weather and climate conditions	0.853	
	Health and safety issues	0.815	
	Volume of debris	0.703	

their latent factors. As a result of these adjustments, the SEM in Fig. 2 represents the modified model. Table 3 displays the final SEM's standardized path coefficients and square multiple correlation (R^2) for variables impacting project performance in Kashmir, J&K (all of which are positive and statistically significant at p 0.05).

3.5 Reliability and Validity

Cronbach's alpha is a method for determining the reliability of a questionnaire. The coefficient of Cronbach's alpha is used to measure how consistent each component was. Cronbach's alpha higher or equal to 0.7 is considered high internal consistency at the broad category level [19]. The average variance and composite reliability coefficients are used to assess the measurement's quality. In order to determine how much of a fluctuation in a concept is due to measurement error, an AVE calculation is performed [24]. To be more precise, AVE is an indicator of convergent validity.

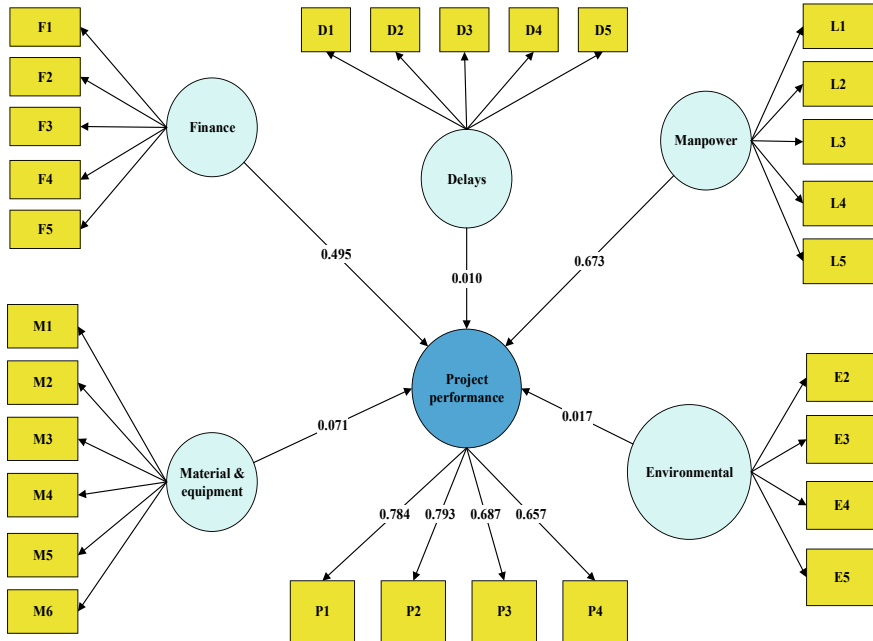


Fig. 2 Final structural equation model with factors affecting project performance

Convergent validity is confirmed if the value of AVE is more than 0.5. Composite reliability determines the overall dependability of an item [17]. Composite reliability levels of 0.6–0.7 are considered satisfactory. Convergent validity of a construct is also acceptable if AVE and composite reliability values are greater than 0.4 and 0.6, respectively [13].

4 Results and Discussion

Figure 2 shows the final SEM results, which show that manpower is the most significant factor impacting the performance of residential construction projects in Kashmir, J&K, with a β value of 0.673. The impact of manpower is regarded to be the most significant due to construction site accidents, loss of life in the case of catastrophic damage, labour shortages, shortages of experts, and rising labour expenses. Labour shortage was the most challenging factor in the reconstruction process after 2014 floods in Kashmir, J&K [14]. Construction project managers and specialists clearly play an important role in communicating activities and directions to the workforce. After a natural disaster, the most challenging issue faced by construction industry is the shortage of labours. Manpower expertise may be put to use in completing tasks and increasing productivity. A well-balanced labour force may help to stabilize

or even reduce wages. Natural disaster awareness and worker safety and evacuation training may help to prevent accidents on the construction site in the event of a natural catastrophe. Also, workers must wear the safety gears during working at the site. Good communication between project managers and workers will help to enhance performance of the project.

With a score of 0.495, finance is the second most significant element influencing project performance. Whenever a natural catastrophe strikes, the construction industry confronts financial difficulties, which causes project delays. The main financial problems arising in the construction during a natural disaster are price escalation of resources, repairing costs, lack of funding, inflation of rates, and cost of reworks. One of the most crucial issues is resource price inflation after a natural catastrophe. After 2014 floods, the cost of cement bags rises by 20% [19]. Financial problems arising due to the natural disasters can be avoided by proper financial management. Using more effective financial management strategies may help enhance profitability. As a result, enough funds for project financial management and planning must be set aside. The material and equipment latent variable were shown to have the third biggest impact on project performance (0.071). The following elements have been found to be associated with the material and equipment's influence: damage to materials, shortage of materials, improper material storage, hindrances in material supply, damage/failure of equipments, and loss of equipments. There is a shortage of materials after a natural disaster is strongly correlated to its latent factor. To avoid these challenges, materials and equipments should be stored at a safe and secure place during pre-disaster conditions. By establishing good coordination with the supplier, material shortages may be prevented. The environmental element has a statistically significant (0.017) influence on the model, despite the delay component having no effect on project performance. Poor weather and soil movement are strongly connected to the relevant latent factors. Project delays may arise because of weather-related damage.

5 Conclusion

The study highlights the increasing trend of natural disasters in Kashmir and their significant impact on the construction industry. It aims to identify the challenges posed by natural disasters in completing residential construction projects on time. The study collected 79 genuine responses through a questionnaire survey from construction experts in Kashmir, J&K, and analyzed the impact of latent variables such as finance, delays, manpower, materials and equipment, and the environment on project performance. The results emphasize the importance of construction manpower in project performance and suggest the need for thorough planning, coordination, and worker training. Finance is identified as the second most influential factor, while the environment also has a significant impact. The study recommends avoiding construction during the rainy season to mitigate delays caused by poor weather and soil movement. This study has certain limitations, including potential biases

in self-reported data, a limited sample size, and specific geographic coverage. The findings may not be fully generalizable to all residential construction projects in the Kashmir region or other sectors beyond construction. To overcome these limitations, future research can employ larger and more diverse samples, incorporate mixed methods approaches, conduct comparative analyses, and broaden the scope to include different sectors and project types. By addressing these areas, future studies can provide a more comprehensive understanding of the challenges posed by natural catastrophes, enhance generalizability, and contribute to effective risk management strategies in disaster-prone regions like Kashmir.

References

1. Ahady S, Gupta S, Malik RK (2017) A critical review of the causes of cost overrun in construction industries in developing countries. *Int Res J Eng Technol.* www.irjet.net
2. Apurva P, Sharareh K, Elnaz S (2020) Challenges in post-disaster housing reconstruction: analysis of urban vs. rural communities, pp 103–110. <https://doi.org/10.3311/ccc2020-061>
3. Abu Talib IF, Takim R, Nawawi AH, Hassan PF (2016) Impact of disaster to private construction organisations in Malaysia. *J Teknol* 78(5–2):91–97. <https://doi.org/10.11113/jt.v78.8497>
4. Benson C, Twigg J, Rossetto T (2007) Tools for mainstreaming disaster risk: guidance notes for development organisations. Tools for mainstreaming disaster risk reduction: guidance notes for development organisations. www.proventionconsortium.org
5. Chang Y, Wilkinson S, Brunson D, Seville E, Potangaroa R (2011) An integrated approach: managing resources for post-disaster reconstruction. *Disasters* 35(4):739–765. <https://doi.org/10.1111/j.1467-7717.2011.01240.x>
6. Choi J, Naderpajouh N, Yu DJ, Hastak M (2019) Capacity building for an infrastructure system in case of disaster using the system's associated social and technical components. *J Manag Eng* 35(4):04019013. [https://doi.org/10.1061/\(asce\)me.1943-5479.0000697](https://doi.org/10.1061/(asce)me.1943-5479.0000697)
7. Rajprasad J, Apparao GS, Pannirselvam N (2020) Financial assessment of construction industry in Chennai during demonetisation, p 240007. <https://doi.org/10.1063/5.0025306>
8. Döhrmann D, Gürtler M, Hibbeln M (2013) An econometric analysis of the demand surge effect. *Zeitschrift für die Gesamte Versicherungswissenschaft* 102(5):537–553. <https://doi.org/10.1007/s12297-013-0239-1>
9. El-Anwar O, Chen L (2014) Maximizing the computational efficiency of temporary housing decision support following disasters. *J Comput Civ Eng* 28(1):113–123. [https://doi.org/10.1061/\(asce\)cp.1943-5487.0000244](https://doi.org/10.1061/(asce)cp.1943-5487.0000244)
10. Field AP (2009) *Discovering statistics using SPSS: (and sex and drugs and rock “n” roll)*. SAGE Publications
11. Elnaz S, Sharareh K, Thahomina JN (2020) Analysis of cost performance indicators in reconstruction projects: a comparative study of low vs high level damages, pp 2–10. <https://doi.org/10.3311/ccc2020-049>
12. Enshassi A, Mohamed S, Abushaban S (2009) Factors affecting the performance of construction projects in the Gaza Strip. *J Civ Eng Manag* 15(3):269–280. <https://doi.org/10.3846/1392-3730.2009.15.269-280>
13. Habibi M, Asce SM, Kermanshachi S, Asce M, Safapour E, Student PD (2018) Engineering, procurement, and construction cost and schedule performance leading indicators: state-of-the-art review
14. Hassan R, Muslim M (2014) Disasters in Kashmir a satellite based rapid assessment of on floods in Jammu and Kashmir-September 2014. *IOSR J Hum Soc Sci (IOSR-JHSS)* 19(7). www.iosrjournals.org

15. Rajprasad J, Ummadisettisaisravan Pannirselvam N, Manivel S (2022) Influence of intellectual behaviour of labour in construction industry, pp 443–452. https://doi.org/10.1007/978-981-16-5839-6_39
16. Cho KM, Hong TH, Hyun CT (2009) Effect of project characteristics on project performance in construction projects based on structural equation model. *Expert Syst Appl* 36(7):10461–10470. <https://doi.org/10.1016/j.eswa.2009.01.032>
17. Fornell C, Larcker DF (1981) Evaluating structural equation models with unobservable variables and measurement error. *J Mark Res* 18(1)
18. Haider SA, Kayani UN (2021) The impact of customer knowledge management capability on project performance-mediating role of strategic agility. *J Knowl Manag* 25(2):298–312. <https://doi.org/10.1108/JKM-01-2020-0026>
19. J&K State Disaster Management Policy 2011. Department of Revenue, Relief and Rehabilitation (2011)
20. IBM Corp. Released 2019 (n.d.) IBM SPSS Statistics for Windows, version 26.0. IBM, Armonk, NY
21. Islam MDM, Faniran OO (2005) Structural equation model of project planning effectiveness. *Constr Manag Econ* 23(2):215–223. <https://doi.org/10.1080/0144619042000301384>
22. Chang-Richards Y, Wilkinson S, Seville E, Brunsdon D (2017) Effects of a major disaster on skills shortages in the construction industry: lessons learned from New Zealand. *Eng Constr Archit Manag* 24(1):2–20. <https://doi.org/10.1108/ECAM-03-2014-0044>
23. Jang H, Kim K, Kim J, Kim J (2011) Labour productivity model for reinforced concrete construction projects. *Constr Innov* 11(1):92–113. <https://doi.org/10.1108/14714171111104655>
24. Gunduz M, Birgonul MT, Ozdemir M (2017) Fuzzy structural equation model to assess construction site safety performance. *J Constr Eng Manag* 143(4):04016112. [https://doi.org/10.1061/\(asce\)co.1943-7862.0001259](https://doi.org/10.1061/(asce)co.1943-7862.0001259)
25. Apurva P, Sharareh K, Sanjgna K (2020) Impact of natural disasters on construction projects: strategies to prevent cost and schedule overruns in reconstruction projects, pp 49–57. <https://doi.org/10.3311/cc2020-054>
26. Byrne BM (2009) *Multivariate applications series structural equation modeling with Mplus*
27. Doloi H, Iyer KC, Sawhney A (2011) Structural equation model for assessing impacts of contractor's performance on project success. *Int J Project Manag* 29(6):687–695. <https://doi.org/10.1016/j.ijproman.2010.05.007>

Quantifying the Trends and Impacts of Solid Waste Generation in Chennai City: A Study of Current Management Practices and Future Needs



E. Mugesh and D. Justus Reymond

1 Introduction

The generation of solid waste is a growing problem in many urban areas, including Chennai, one of the largest cities in India. The increasing population, changing lifestyles and consumption patterns, and urbanization have led to a significant increase in the amount of solid waste generated in the city. The effective management of solid waste is essential to prevent environmental pollution and public health issues. This research paper aims to quantify the trends and impacts of solid waste generation in Chennai City and to study the current management practices and future needs [1–5].

Solid waste management has become a major challenge for the cities of developing countries including Chennai, India. The generation of solid waste in Chennai City has been increasing at a rapid pace due to the growing population, urbanization, and the changing lifestyle of its residents. The management of solid waste has become an increasingly important issue for the city, as improper disposal and management of solid waste can lead to environmental degradation, health hazards, and loss of valuable resources. In light of these concerns, this research paper aims to quantify the trends and impacts of solid waste generation in Chennai City and assess the current management practices and future needs [5–10].

E. Mugesh · D. J. Reymond (✉)

Department of Civil Engineering, Faculty of Engineering and Technology, SRM Institute of Science and Technology, Kattankulathur, Tamilnadu 603203, India

e-mail: justusrd@srmist.edu.in

1.1 Current Trends and Impacts of Solid Waste Generation in Chennai

Chennai generates approximately 5000 tons of solid waste per day, which is expected to increase to 15,000 tons by 2030. The city's current waste management system is inadequate and inefficient, resulting in the accumulation of waste in landfills and on the streets. The Greater Chennai Corporation (GCC) is responsible for solid waste management in the city and has introduced several initiatives to address the issue [11–13].

The majority of MSW in Chennai comes from homes (60%), with the remainder coming from businesses (15%), businesses in the food service industry (15%), and industries (10%) among others. Hospitals and other medical facilities have special waste disposal systems. After being collected, MSW is sent to one of two landfills, either Kodungaiyur (KDG) or Perungudi (PGD). KDG accepts garbage from zones 1 through 5 while PGD accepts garbage from zones 6 through 10 of Chennai. Even after prolonged periods of continuous dumping, the height of MSW deposits in landfills remains low because of the huge MSW dumping area. As quick degradation may occur in hot and rainy climates with shallow disposal sites, it was not envisaged that these areas would be major contributors of greenhouse gas (GHG) emissions [14–20]. The garbage that has been properly sorted is then either put to its intended use or disposed of in landfill sites, thanks to the implementation of the 3Rs, which stands for reduce, recycle, and reuse [21–24]. The solid waste generated in Chennai also has social impacts, including the health risks associated with the poor management of waste and the impact on the quality of life of the city's residents. The waste generated in the city also contributes to the spread of diseases and pests, affecting the health and well-being of the city's residents [25–27].

2 Methodology

To carry out this research, data was collected from various sources including government websites, academic journals, and reports from local organizations. The data collected was analyzed to quantify the trends and impacts of solid waste generation in Chennai City and to understand the current management practices and future needs.

Table 1 Composition of waste in Chennai

Physical composition	%Waste
Food waste	7.8
Organic waste	33.6
Timber	6.79
Consumable plastics	5.88
Industrial plastics	1.17
Steel and materials	3.55
Textiles and rags	7.01
Paper	6.55
Leather and rubber	1.37
Inert	26.28

3 Findings

The results of this research showed that the amount of solid waste generated in Chennai City has increased significantly over the past decade, with an average annual increase of 5%. This increase in waste generation is attributed to population growth, urbanization, and changes in consumption patterns.

The increasing amount of waste generated in Chennai has several impacts on the city and its residents. One of the most significant impacts is the environmental impact, which includes soil and water contamination, air pollution, and the emission of greenhouse gases. The city's landfills are also facing the challenge of limited capacity, leading to the need for additional landfill sites, which is a challenge in terms of finding suitable locations and obtaining necessary approvals [28, 29]. 14

The composition of waste of Chennai is shown in Table 1; Figs. 1, 2, 3, and 4 discuss about the waste processing across 15 zones, and the quantity has been shown in graphical representations on using Power BI.

4 Results and Discussions

4.1 Impacts of Solid Waste Generation in Chennai City

The impacts of solid waste generation in Chennai City are significant and include environmental pollution, public health issues, and reduced quality of life for residents. Improper waste management practices have resulted in the release of toxic chemicals into the environment, which can have negative impacts on air and water quality, as well as soil and food safety. In addition, the generation of solid waste has also led to an increase in the spread of vector-borne diseases, such as dengue and malaria, as well as respiratory problems in local residents.

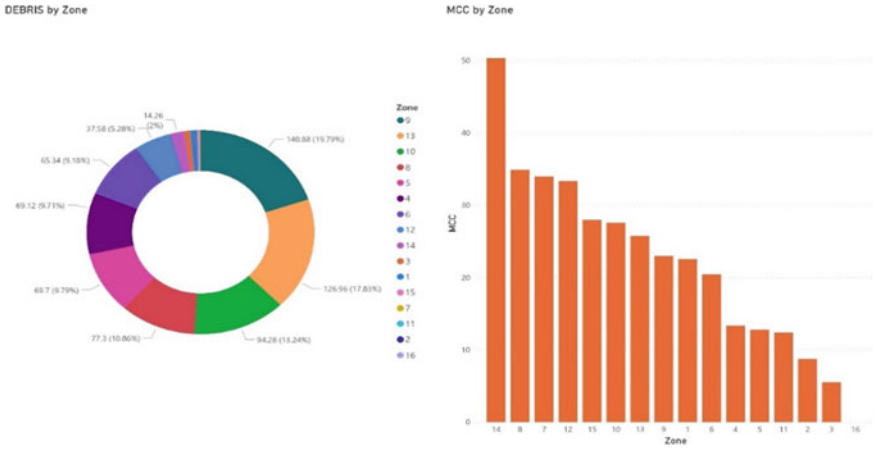


Fig. 1 Processing of waste using debris and microcomposting center for zones 1–15

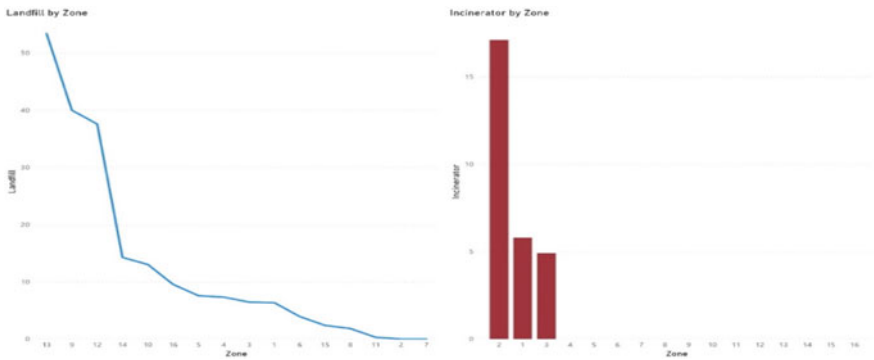


Fig. 2 Processing of waste using landfill and incinerator center for zones 1–15

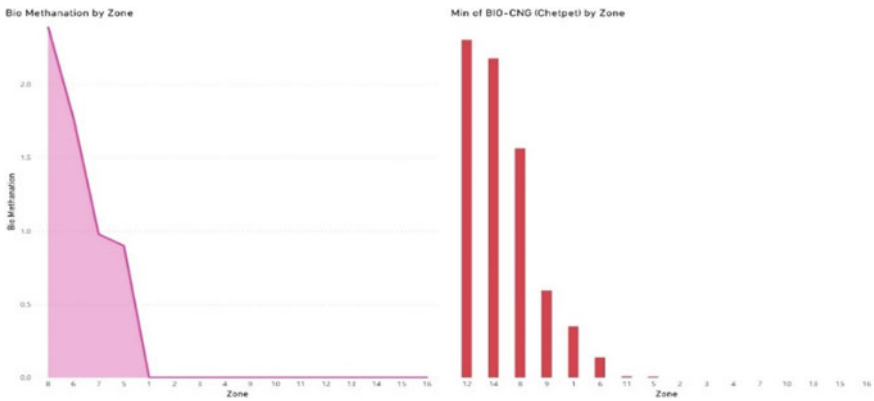


Fig. 3 Processing of waste using biomethanation and bio-CNG center for zones 1–15

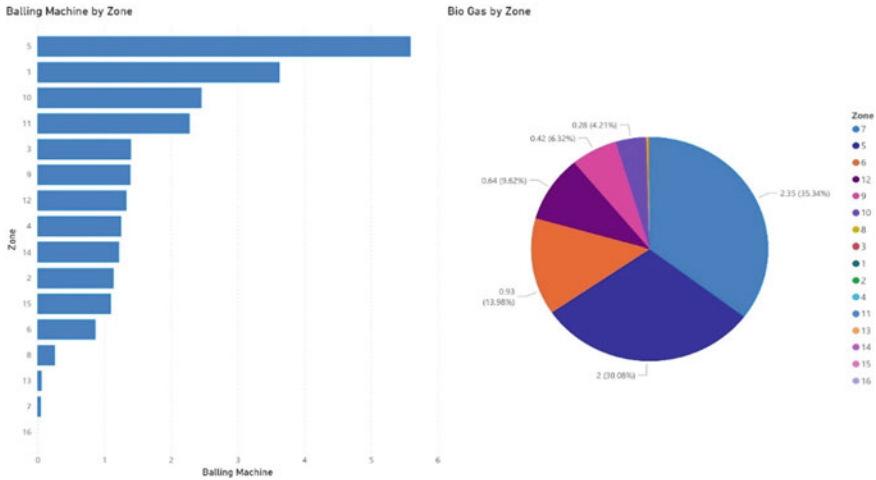


Fig. 4 Processing of waste using bailing machine and biogas center for zones 1–15

4.2 Waste-to-Fuel Projects

Waste-to-fuel projects involve converting solid waste into fuel, such as pellets, briquettes, and oil. These fuels can then be used as a substitute for traditional fuels like coal and wood. Waste-to-fuel projects have gained traction in India in recent years, with several private players investing in the development of these technologies.

4.3 Future Needs for Solid Waste Management in Chennai City

To address the challenges and impacts of solid waste generation in Chennai City, there is a need for improved solid waste management practices and infrastructure. This includes the implementation of effective waste segregation and recycling programs, the development of alternative waste management technologies, and the provision of adequate resources and funding for waste management authorities. In addition, there is a need for increased public education and awareness programs to encourage residents to adopt more sustainable waste management practices.

4.4 Future Needs of Solid Waste Management in Chennai

Additionally, Chennai could also implement the principles of circular economy in its solid waste management practices. Circular economy is an approach that prioritizes

the preservation and use of resources to maximize their value and minimize waste. It aims to keep products, materials, and resources in use for as long as possible and reduce waste generation. This can be achieved through various strategies such as waste reduction, recycling, and reusing materials. Implementing circular economy principles in Chennai's solid waste management could help reduce the volume of waste generated and reduce the burden on landfills.

Carbon capture technology (CCT) is an innovative solution to reducing greenhouse gas emissions, particularly carbon dioxide (CO₂), in the atmosphere. This technology captures and stores CO₂ emissions from various industrial processes, such as power generation and cement production, preventing them from entering the atmosphere and contributing to climate change. The implementation of CCT has been gaining traction in recent years, and it is expected to play a significant role in mitigating the impacts of climate change.

CCT involves three main steps: capture, transport, and storage. The capture step involves separating CO₂ from the flue gas generated by industrial processes, such as power plants or steel mills.

5 Conclusion

In conclusion, the latest trends in waste-to-energy concepts in India demonstrate a shift toward sustainable and innovative solutions that are economically viable and environmentally friendly. The adoption of these trends will be essential for India to manage its growing waste problem and meet its energy needs in a sustainable and responsible manner. Here are some of the most promising and cost-effective technologies for solid waste management. The best affordable waste-to-energy technologies for solid waste will depend on various factors such as the type and quantity of waste, local policies and regulations, energy demands, and available funding. While there is no one-size-fits-all solution, a combination of technologies such as incineration, gasification, anaerobic digestion, and pyrolysis can provide a comprehensive approach to solid waste management and energy generation.

References

1. Ramesh R, Purvaja R, Gupta PK, Jha AK, Sharma C, Singh N (2008) Greenhouse gas emissions from municipal solid waste management in Indian mega-cities: a case study of Chennai landfill sites. *Chemosphere* 71(4):750–758
2. Surya S (2016) Landscape ecological urbanism for restoration of Pallikarnai Marsh Land, Chennai, Tamil Nadu. *Proc Technol* 24:1819–1826
3. Hidalgo-Crespo J (2022) Quantification and mapping of domestic plastic waste using GIS. *Proc CIRP* 105:86–91

4. Abdallah M, Talib MA, Feroz S, Nasir Q, Abdalla H, Mahfood B (2020) Artificial intelligence applications in solid waste management: a systematic research review. *Waste Manage* 109(15):231–246
5. Ponti MG, Allen D, White CJ, Bertram D, Switzer C (2022) A framework to assess the impact of flooding on the release of microplastics from waste management facilities. *J Hazard Mater Adv* 7:100105
6. Biluca J, Rodrigues de Aguiar C, Trojan F (2020) Sorting of suitable areas for disposal of construction and demolition waste using GIS and ELECTRE TRI. *Waste Manage* 114:307–320
7. Rashmi BN (2015) Engineering landfill design for municipal solid waste management, Bangalore. *Int J Eng Res Technol* 4:1117–1120
8. Balasubramanian P, Chakraborty P (2019) Atmospheric polychlorinated biphenyls from an urban site near informal electronic waste recycling area and a suburban site of Chennai city, India. *Sci Total Environ* 710:135526
9. James NY, Derek H, Guhac MSNA (2022) Assessment of methane emissions from a California landfill using concurrent experimental, inventory, and modelling approaches. *Waste Manage* 154:146–159
10. Backab S, Sakanakura H (2022) Comparison of the efficiency of metal recovery from wet- and dry-discharged municipal solid waste incineration bottom ash by air table sorting and milling. *Waste Manage* 154:113–125
11. Choudhury S (2012) GIS and remote sensing for landfill site selection—a case study on Dharmanagar Nagar Panchayat. IOSR
12. Bai R (2001) The practice and challenges of solid waste management in Singapore. *Waste Manage* 22:557–567
13. Balakrishnan C (2016) A Survey of household solid waste management in Chennai. *ISBR Manage J* 1(2):71–83
14. Babalola A (2011) Selection of landfill sites for solid waste treatment in Damaturu town-using GIS techniques. *J Environ Prot* 2:1–10
15. John SE (2011) Design of incinerator for the treatment of bio medical solid waste in Chikmangalur city
16. Sumathi VR (2008) GIS-based approach for optimized siting of municipal solid waste landfill. *Waste Manage* 28:2146–2160
17. Jaafarzadeh N (2014) Municipal solid waste landfill site selection using analytical hierarchy process method and geographic information system in Abadan, Iran. *Iran J Health Sci* 2:37–50
18. Shekdar A (2009) Sustainable solid waste management: An integrated approach for Asian countries. *Waste Manage* 29:1438–1448
19. Giugliano M (2011) Material and energy recovery in integrated waste management systems. An evaluation based on life cycle assessment
20. Aswathy VV (2017) Characterization of solid waste management. *Int J Pure Appl Math* 116:431–49
21. Singh A (2014) Solid waste management—a case study of ultimate analysis and landfill design for NIT Calicut. *Int J Sci Eng Res* 5:174–182
22. Bilitewski B (2004). From traditional to modern fee systems. *Waste Manage* 28(12):2760–2766
23. Ahsan A (2014) Assessment of municipal solid waste management system in a developing country. Hindawi Publishing Corporation
24. Jain N (2016) Engineered landfill site design municipal solid waste of Jaipur, India. *SSRG Int J Civil Eng* 3:99–101
25. Nanda S (2020) Municipal solid waste management and landfilling technologies. *Environ Chem Lett* 19:1433–1456
26. Vikash T, Shreekrishnan TR (2008) Journal on municipal solid waste management in Delhi, The Capital of India. *Waste Manage* 28:1276–1287
27. Chen M, Jin Y (2022) Review of the current status and future perspectives of waste-to-energy technologies. *Renew Sustain Energy Rev* 152:111851

28. Demirbas A (2021) Waste-to-energy technologies: current status and future perspectives. *Energy Sour Part A Recov Utiliz Environ Effects* 43(6):715–730
29. Kumar V, Bhaskar T (2021) Overview of solid waste management with a focus on waste-to-energy technologies. *Sustain Cities Soc* 74:103223

A Path Towards Sustainable Transport Research and Policy: A Case Study from Metropolitan City in India



Ali Shkera and Vaishali Patankar

1 Introduction

The urban transportation situation in Indian metropolises is characterized by a severe crisis [1]. The transportation system, which comprises both motorized and non-motorized modes, suffers from overcrowding, unreliability, inefficiency, and unsafety [2]. Moreover, transport-related pollution and noise, along with other environmental impacts, have adversely affected the health of the urban population [3]. The challenge is further exacerbated by the high cost of new infrastructure, the scarcity of land for additional transportation infrastructure development, and public resistance to the potential negative consequences of new infrastructure projects in India [4].

Rapid sprawling development has led to an increase in the number and length of trips for many Indians, leading to a greater dependence on motorized transportation. Longer trip distances make walking less practical, while growing motor vehicle traffic makes walking less safe. However, a significant portion of travel in Indian cities still takes place on foot, primarily due to poverty, as many people cannot afford motorized transportation [5]. This complex transportation issue has contributed to unsustainable development. Given the limited resources and funding, it is crucial for policymakers to fully understand the complexities of the problem and find a sustainable solution [6].

Our research addresses the lack of a modelling framework to assess the benefits of pedestrian-oriented land use and transportation facilities in Greater Mumbai. By developing a framework to model pedestrian travel behaviour, we aim to identify factors influencing pedestrian behaviour and determine effective measures to promote

A. Shkera (✉) · V. Patankar
Department of Civil Engineering, Institute of Technical Education and Research, Siksha 'O'
Anusandhan (Deemed to be University), Bhubaneswar, Odisha 751030, India
e-mail: engalishkera@gmail.com

V. Patankar
e-mail: vaishalipatankar@soa.ac.in

walking. This framework will also evaluate the impact of future pedestrian-oriented infrastructure on travel patterns, providing valuable insights for sustainable transport research and policymaking. Additionally, we examine factors influencing the choice to walk, intending to develop strategies to enhance walking, personal health, and the environment, thereby mitigating the harmful impacts of car reliance.

2 Previous Research

The study of pedestrian travel behaviour has gained widespread attention in recent years, with many researchers exploring various aspects of it. Some studies delve into modelling pedestrian travel demand, using methods like linear regression models and the four-step approach. Others examine how the built environment, travel attitudes, and neighbourhood preferences affect walking behaviour. Challenges arise when considering the built environment and attitudinal factors, as they may be interrelated, leading to biased results. A few studies have focused on determining the defining characteristics and requirements of a walkable neighbourhood.

Walkable neighbourhoods encompass diverse mobility options and social connections, promoting physical, mental, and spiritual well-being. Different terms like traditional neighbourhood design, transit-oriented development, and new urbanism are used to endorse the concept of walkable neighbourhoods [7]. Factors affecting walking behaviour can be categorized into three main categories: individual and household demographics, personal attitudes and perceptions, and characteristics of the neighbourhood, including walking facilities and amenities. In Mumbai, individuals in the lowest income bracket had the highest proportion of walking trips, while factors such as age, employment status, education, and proximity to work also influenced walking frequency [8].

The relationship between walking-friendly environments and walking behaviour is complex. “Self-selection” plays a role, suggesting that people who enjoy walking are attracted to places designed for walking. However, improving the walking environment may not necessarily increase walking if residents who already walk prefer such environments. Enhancing infrastructure can enable more people who prefer walking to live in supportive neighbourhoods, potentially increasing active travel [9].

People tend to walk, bike, and make more trips for leisure or errands in cities that have diverse land use, high-density urban areas, and grid-like streets. Street trees make cities more livable by providing various benefits for the environment, society, and economy. Street trees are appreciated by residents for their beauty and usefulness, but their economic worth is often not fully recognized. To improve the health of street trees and prevent damage to pavements, some strategies such as using root barriers, structural soils, and previous pavements are being tested [10].

3 Methodology and Data Source

Based on a literature review of pedestrian travel behaviour and its factors, the study used a deductive approach and set research objectives and hypotheses. A structured survey questionnaire with closed-ended and open-ended questions was created to gather data on the respondents' and their households' activity-travel patterns, as well as their socio-demographic and built environment features. The questionnaire was pre-tested for clarity and validity. The main data for this analysis came from the 2010 Greater Mumbai Region Activity Travel Survey, which SSV Subbarao designed and executed for 15 days in the Greater Mumbai region. [11].

For 15 days, we collected detailed data on the activities and travels of about 126 households and all their members. We used a nine-category system to classify the activities by type and recorded their location type, start and end times, and geographic coordinates. We also noted the transportation mode and the trip duration for the travels. We calculated the dependent variable (walking frequency) from the daily number of walking trips reported by the respondents. We cleaned and processed the data with suitable software tools.

We used a sample of 261 pedestrians for this research. We classified 183 (70.1%) of them as "commuter pedestrians", who mainly walked to commute. They may also walk for other reasons, such as errands, exercise, socializing, or recreation. The other 78 pedestrians (29.9%) were "non-commuter pedestrians", who only walked for non-commuting reasons. We estimated an ordered response model with a maximum likelihood method to examine the factors influencing walking frequency for commuting and non-commuting purposes separately.

This study conducts two types of analyses: an exploratory descriptive analysis of pedestrians and their walking patterns, and an econometric analysis of walking frequency. The econometric analysis includes two models, one for commuters and non-commuter pedestrians. The dependent variable in these models is based on an ordered categorization, with commuter pedestrians being categorized as walking once, twice, thrice, four times, five times, or six times a day, and non-commuter pedestrians being categorized as walking once, twice, or thrice a day. The analysis period covers 15 days.

3.1 Exploratory Analysis

From the data collected [11], we found that the average trip length for commuting and non-commuting walk trips is 21.06 min. Among commuter respondents, 60.7% are males and 39.3% are females. It indicates that males walk more than females for commuting purposes. By age, 24.6% of those 5 to 15, 20.8% of those 16 to 24, 16.4% of those 25–34, 18.6% of those 35–44, and 19.6% of those 45–64 walk to work. The implication is clear; commuters in each age category are almost equally likely to walk to work. By occupation, 61.7% of the commuter respondents are workers, 1.6% are

non-workers, and 67% are students. 25.7% of the commuter respondents are in the low-income category, 52.5% are in the middle-income, and 21.8% are in the high-income category. 77.6% of the respondents own zero cars, 20.2% own 1 car, and 2.2% own 2 or more cars.

Among non-commuter respondents, 64.1% are females and 35.9% are males. It indicates that females walk more than males for non-commuting purposes. By age, 5.1% of those 5–15, 6.4% of those 16–24, 17.9% of those 25–34, 28.2% of those 35–44, 35.9% of that 45–64 and 6.4% of those 65 or older walk to work. Respondents in the middle age category are likely to walk more than children and old people for non-commuting purposes. By occupation, 21.8% of the commuter respondents are workers, 69.2% are non-workers, and 9% are students. 33.3% of the commuter respondents are in the low-income category, 44.9% are in the middle-income, and 21.8% are in the high-income category. 66.7% of the respondents own zero cars, 29.5% own 1 car, and 3.8% own 2 or more cars. Households having no cars tend to walk more for commuting and non-commuting.

3.2 Modal Structure

The mathematical model structures used in the framework are the ordered response mechanism discrete choice models. The ordered probability models are based on a latent regression [12–14]:

$$y_i^* = \beta' x_i + \epsilon_i. \quad (1)$$

According to Greene's notation, the unobserved variable y_i^* is modelled using a vector of parameters β and a random disturbance ϵ_i . The term $\beta' x_i$ is commonly referred to as the index function. The discrete and ordered observations y_i , with values ranging from 0, 1, 2, ..., J (where J is one less than the number of categories in responses), are generated by the following mechanism.

$$y_i = 0 \text{ if } y_i^* < \mu_0, \quad (2)$$

$$y_i = 1 \text{ if } \mu_0 < y_i^* \leq \mu_1, \quad (3)$$

$$y_i = 2 \text{ if } \mu_1 < y_i^* \leq \mu_2, \quad (4)$$

$$y_i = \dots \quad (5)$$

$$y_i = J \text{ if } y_i^* > \mu_{J-1}. \quad (6)$$

The threshold parameters μ are estimated alongside the vector of parameters β , forming a set of estimated parameters. The ordered probit model is the most widely used model within this category. It is based on the assumption that the disturbance term ϵ_i is normally distributed. The model parameters are estimated through the use of maximum likelihood estimation, with the constraint that the threshold parameters μ must be ordered in a monotonically increasing manner $\mu_0 < \mu_1 < \mu_2 < \dots < \mu_{J-1}$, and that the error term must have a mean of 0 ($E[\epsilon_i] = 0$) and a variance of 1 ($\text{Var}[\epsilon_i] = 1$). For identification, it is also required to impose an additional restriction that $\mu_0 = 0$.

With the above assumptions, the probabilities observing particular values of y_i are given by:

$$P(y_i = 0) = P(y_i^* \leq \mu_0) = \varphi(-\beta'x_i) \tag{7}$$

$$P(y_i = 1) = P(\mu_0 \leq y_i^* \leq \mu_1) = \varphi(\mu_1 - \beta'x_i) - \varphi(-\beta'x_i) \tag{8}$$

$$P(y_i = 2) = P(\mu_1 \leq y_i^* \leq \mu_2) = \varphi(\mu_2 - \beta'x_i) - \varphi(\mu_1 - \beta'x_i) \tag{9}$$

$$P(y_i = J) = P(\mu_{J-1} < y_i^*) = 1 - \varphi(\mu_{J-1} - \beta'x_i), \tag{10}$$

where φ is the standard cumulative normal distribution.

3.3 Empirical Analysis

We conducted an empirical analysis of the pedestrians' walking frequency. We experimented with different variable specifications (as described in the section on the exploratory analysis) and forms of variables. We chose the final variables for each model by eliminating those that were statistically insignificant, simplifying the variable effects, and taking into account intuition and prior studies.

Tables 1 and 2 show the empirical results of the walking frequency for commuting and non-commuting. The parameters show how the independent variables affect the walking propensity y_i^* of each individual (i). People who walk more have longer commute distances. Students and workers walk more for commuting than non-workers. Higher household income reduces walking for commuting. Workers walk less and students walk more for non-commuting. Higher household income also reduces walking for non-commuting. The constant and threshold parameters at the end of Tables 1 and 2 do not mean anything behaviourally; they just link the observed frequency categories to the underlying propensity to walk for commuting and non-commuting.

Table 1 Ordered response model of frequency of walking for commuting

Explanatory variables	Example	Font size and style
Commute distance	0.021	3.14
Worker	0.437	0.71
Student	0.755	1.23
Household income	-0.118	-2.61
<i>Constant and threshold parameters</i>		
Constant	0.755	1.16
Threshold 1	0.883	10.19
Threshold 2	1.226	13.76
Threshold 3	2.143	19.70
Threshold 4	2.771	19.23
Number of cases	183	
Log-likelihood at the convergence	-295.05	
Log-likelihood for constants-only model	-307.43	
McFadden pseudo R-squared	0.0402648	

Table 2 Results of the ordered response model for frequency of non-commuting walking

Explanatory variables	Parameter	t-Statistic
Worker	-0.459	-1.18
Student	0.042	0.08
Household income	-0.023	-0.30
<i>Constant and threshold parameters</i>		
Constant	-0.3240	-0.94
Threshold 1	0.851	4.56
Number of cases	78	
Log-likelihood at convergence	-6174	
Log-likelihood for constants-only model	-6263	
McFadden pseudo R-squared	0.0141138	

3.4 Model Fit

Table 1 displays a low pseudo R-squared value of (0.0402648) and Table 2 displays an even lower value of. (0.0141138), suggesting a mediocre fit for the model. Furthermore, Table 2 reveals that the log-likelihood of the model at the point of convergence is -61, while the log-likelihood of the model predicting walking frequency for commuting is -62.

A likelihood ratio test shows that these two models are very different. The test statistic is 2, which is much smaller than the chi-squared value with 3° of freedom,

for any significance level. This means that the independent variables in the model do not help much to predict the walking frequency for non-commuting. However, other factors like attitudes and perceptions, the built environment, and neighbourhood characteristics are very important for walking frequency. Adding these variables to the model can make it fit better and predict their effect on walking frequency more accurately.

4 Summary of the Results and Conclusion

This study explores the various factors that influence walking behaviour for commuting and non-commuting purposes, such as demographics, attitudes, preferences, perceptions, environmental factors, and neighbourhood characteristics. It collects data on the built environment and individual attitudes and perceptions to improve the model fit and predict the effect on walking frequency. It finds that walking is more common for commuting than for non-commuting purposes and that women, workers, students, and low-income households walk more frequently than others. It also finds that car owners walk less for both purposes. The study concludes that promoting walking can reduce traffic congestion, air pollution, and health issues related to sedentary lifestyles. It suggests considering factors such as gender, income level, and car ownership, creating walkable environments, addressing individual attitudes and perceptions, and tailoring initiatives based on different purposes of walking for effective policy implementation.

References

1. Kumar A, Poddar A, Nautiyal A (2022) Urban transportation system problems in context of the Indian conditions. *Lecture Notes in Civil Engineering*, vol 230 LNCE, pp 300–314. https://doi.org/10.1007/978-981-16-9963-4_24/COVER
2. B.V.-T.R.I.R. Journal, undefined 2015. Multimodal transport in India—issues and opportunities. *Theresearchers.Asia*. (n.d.). <https://www.theresearchers.asia/Papers/Vol-I,%20Issue-II/Multimodal%20Transport%20in%20India.pdf>. Accessed 24 May 2023
3. Kaur R, Pandey P (2021) Air pollution, climate change, and human health in Indian cities: a brief review, *frontiers in sustainable. Cities* 3:77. <https://doi.org/10.3389/FRSC.2021.705131/BIBTEX>
4. Nenavath S (2023) Does transportation infrastructure impact economic growth in India? *J Facil Manag* 21:1–15. <https://doi.org/10.1108/JFM-03-2021-0032/FULL/XML>
5. Su J, Sze NN (2022) Safety of walking trips accessing to public transportation: a Bayesian spatial model in Hong Kong. *Travel Behav Soc* 29:125–135. <https://doi.org/10.1016/J.TBS.2022.06.003>
6. Pucher J, Korattyswaropam N, Mittal N (2005) N.I.-T. policy, undefined 2005, Urban transport crisis in India. Elsevier. <https://doi.org/10.1016/j.tranpol.2005.02.008>
7. Brookfield K (2016) Residents’ preferences for walkable neighbourhoods. 22:44–58. <https://doi.org/10.1080/13574809.2016.1234335>

8. Built environment and nonmotorized travel: evidence from Baltimore city using the NHTS. Bureau of Transportation Statistics (n.d.). https://www.bts.gov/archive/publications/journal_of_transportation_and_statistics/volume_08_number_03/paper_04/index. Accessed 8 Feb 2023
9. Handy S, Cao X, Mokhtarian PL (2006) Self-selection in the relationship between the built environment and walking: empirical evidence from Northern California. *J Am Plann Assoc* 72:55–74. <https://doi.org/10.1080/01944360608976724>
10. Mullaney J, Lucke T, Trueman SJ (2015) A review of benefits and challenges in growing street trees in paved urban environments. *Landsc Urban Plan* 134:157–166. <https://doi.org/10.1016/J.LANDURBPLAN.2014.10.013>
11. Subbarao S (2013) Activity-based travel demand analysis for a mega city in a developing country
12. Greene W (2002) LIMDEP version 8.0: econometric modeling guide
13. Washington S, Karlaftis M, Mannering F (2020) Statistical and econometric methods for transportation data analysis. <https://www.taylorfrancis.com/books/mono/https://doi.org/10.1201/9780429244018/statistical-econometric-methods-transportation-data-analysis-simon-washington-matthew-karlaftis-fred-mannering-panagiotis-anastasopoulos>. Accessed 10 Feb 2023
14. Greene WH (2003) *Econometric analysis*. Prentice Hall

Scientometric Analysis of Building Energy Analysis in the Construction During 2005–2022



G. Nakkeeran and L. Krishnaraj

1 Introduction

Energy use in buildings is expected to rise as a result of population growth, increased housing stock, and improved living standards. It is estimated that global energy consumption grew by 2.3% in 2018, the fastest rate of growth for ten years [1]. The efficient use of energy within a built environment, through the application of innovative designs that use less energy and are environmentally friendly, can address this demand for energy. This energy demand, building information modelling (BIM) industries is because of this growing demand [2].

Building information modelling was first used in an article in the automation and construction journal in 1992, titled “Modelling multiple views on buildings” [3]. An entirely new approach to building information modelling was presented in this article. Since then, there has been a significant increase in BIM methodology research and discoveries of new applications are being made. Research into BIM began in the early stages, the majority of BIM’s novelty was covered in articles published in architecture magazines and scientific methods and how difficult adopting would be the best option [4].

BIM/BEM data transfer methods, such as design builder and virtual environment, have undergone some advancements in recent years, which are the only BIM tools that have developed their own plug-ins to facilitate the transfer of Revit data. Consequently, the paper’s goal is to evaluate the most prominent interoperability issues, data transfer quality between BIM models, as recommended, (a) location and geometry; (b) construction and space; (c) thermal zones; (d) occupancy, equipment, and lighting loads; and (e) HVAC systems. Additional to this is the validation of the results, which ensures the accuracy of the entire procedure [5]. Revit as BIM

G. Nakkeeran · L. Krishnaraj (✉)

Department of Civil Engineering, Faculty of Engineering and Technology, SRM Institute of Science and Technology, Tamil Nadu, Kattankulathur 603203, India

e-mail: krishnal@srmist.edu.in

was used to exchange information with design builder and virtual environment for a typical residential building in this regard.

The purpose of this review is to provide the reader with a thorough understanding of the most recent research in the BIM field [6, 7]. “An analysis of bibliometric data categorizes the papers into specific categories, discusses the selections from a collection, identifies keywords, determines the sources where most articles are published, lists the top 10 cited articles, and highlights the countries with the highest contributions.”

1.1 Bibliometric Software Tools

Many bibliometric analysis software tools are available, but many of these help researchers follow the recommended workflow. The important softwares are CitNetExplorer [8], VOSviewer [9], SciMAT, BibExce, Science of Science (Sci2) Tool CiteSpace, and VantagePoint R-packages in bibliometric analysis [10].

2 Material and Methods

This research aims to provide an overview of all studies on building energy analysis using BIM, specifically focusing on language and technology networks. To complete the examination of this article, the researcher observed the articles on “building energy analysis using BIM” distributed in the World Logical Diary through 2022 and considered their relevance. For the corresponding exploration, he described the relevant data set: Scopus. An examination of the substance of the entirety of the distributions (articles, book sections, and procedures papers) surfaced because of the hunt utilizing the questions “building energy analysis using BIM” [7]. In this bibliometric assessment, we examined segments: articles, writers, and references. Figure 1 shows a graphical representation of the methodology of the study.

3 Data Collection

The data collecting process is broken down into three steps. The first step is data extraction. These databases, which hold metadata about academic papers, may provide bibliographic information such as Scopus (<http://www.scopus.com>) [11, 12]. In the second sub-stage, researchers must import and transform data into a format that is compatible with the bibliometric tools they are using. Finally, data cleansing is a step in the process. The quality of the data is directly related to the quality of the ultimate output. Many preprocessing techniques may be used, e.g. to identify duplicate and misspelt items. Although most bibliometric data is trustworthy, cited references

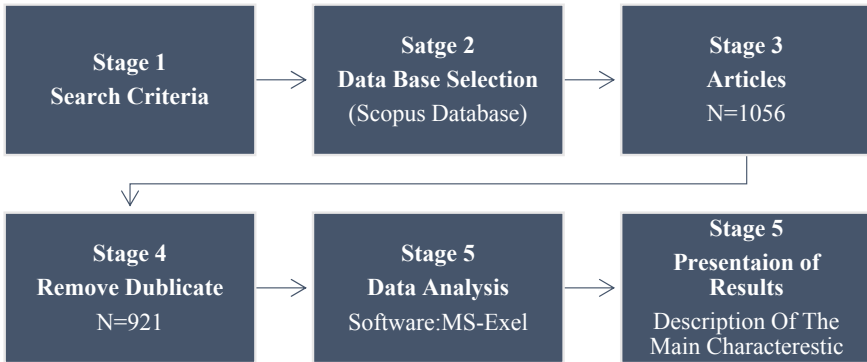


Fig. 1 Analytical procedure of the article

Table 1 Basic data

Description	Results
Duration of study	2005:2022
Sources of study	388
Documents of study	921

may include several variations and alternative as an author’s name in various forms. Since most writers are known by their surname and initials, a problem might occur when their names are too similar. Cited journals may also be found in a variety of ways. Basic data is shown in Table 1. Figure 2 shows an article published per year from 2005 to 2022. After 2014 building energy analysis research started increasing using BIM. Figure 3 shows an article published in source in a book chapter, research article, conference paper, etc.

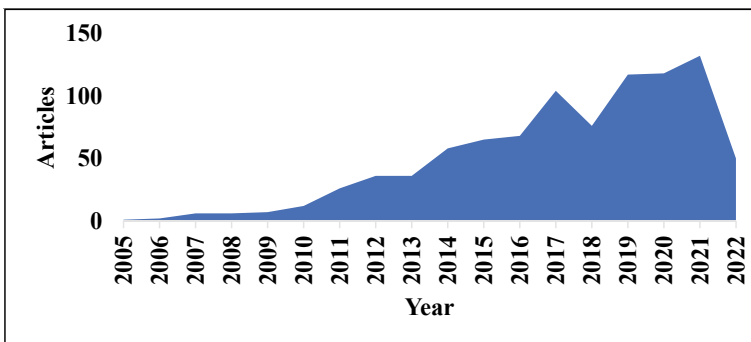


Fig. 2 Annual publications trend

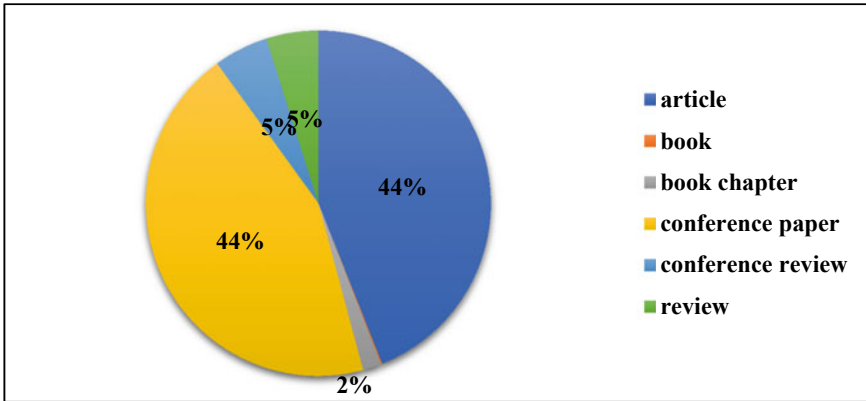


Fig. 3 Source of publication

4 Results and Discussion

4.1 Analysis of Article Keywords

In using a bibliometric analysis, most used keywords with occurring is a 30 frequency overall period [13]. It shows research it developing based on keywords, words architectural design-637, building information model-308, energy efficiency-284, energy utilization-222, information theory-192, buildings-168, sustainable development-156, life cycle-149, building information modelling-140, structural design-115, energy conservation-107, construction industry-93, energy management-86, construction-83, decision making-79, intelligent buildings-78, office buildings-69, environmental impact-61, information management-55, and interoperability-51. In this architectural design, BIM, energy efficiency is the most important keyword for building energy analysis. Figure 4 shows the top 10 relevant keywords.

4.2 Analysis of Article Source

Bibliometric analysis shows that the most frequently cited source is a journal article with an overall article [14]. It demonstrates that research is being developed based on the source, sources sustainability (Switzerland) articles 39, automation in construction articles 33, IOP conference series: Earth and environmental science articles 33, energy and buildings articles 21, Procedia engineering articles 21, journal of cleaner production articles 19, energies articles 16, buildings articles 14, IOP conference

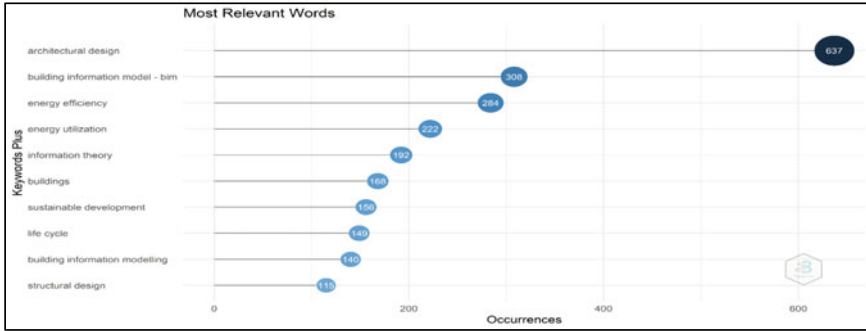


Fig. 4 Important keywords

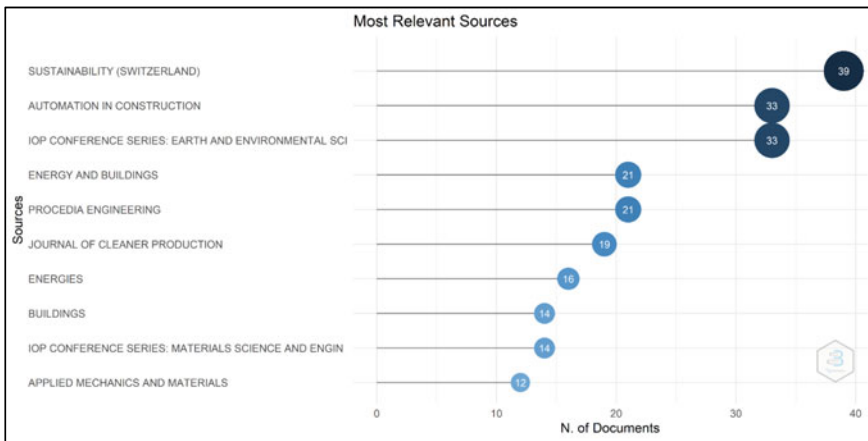


Fig. 5 Important source

series: materials science and engineering articles 14, applied mechanics and materials articles 12. This is 10 journal publishing an article related to your keyword shown in Fig. 5.

4.3 Analysis of Article Country

Bibliometric analysis shows the most frequent country contributing in research related to keyword [13]. Author contributing an first author, second author, or corresponding author region China Frequency of accuracy in article 430, USA accuracy in article 410, Italy accuracy in article 212, UK accuracy in article 168, Germany accuracy in article 131, Canada accuracy in article 109, South Korea accuracy in

article 108, Spain accuracy in article 107, Malaysia accuracy in article 104, India accuracy in article 95. Figure 6 shows an overall country contribution.

Figure 7 shows the list of keywords used by the author in order to familiarize with the current trends [15]. It shows lifecycle analysis, lifecycle assessment, building information modelling, and energy efficiency which are highly researched; the graph is based on the given keywords.

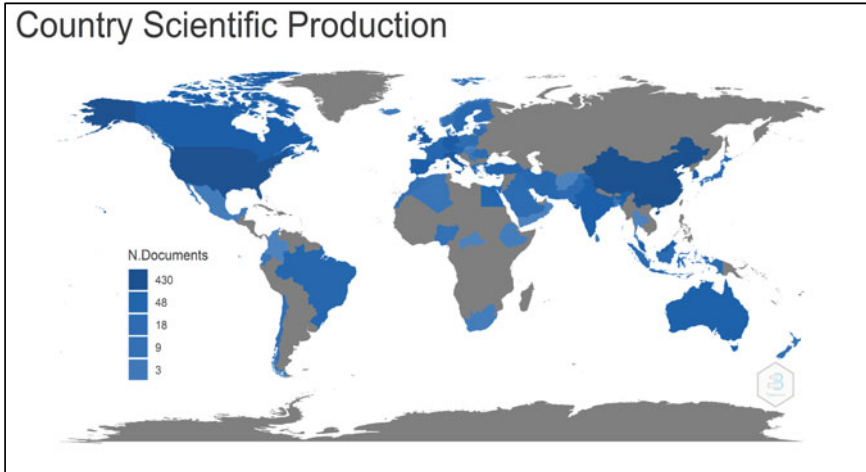


Fig. 6 Country contribution

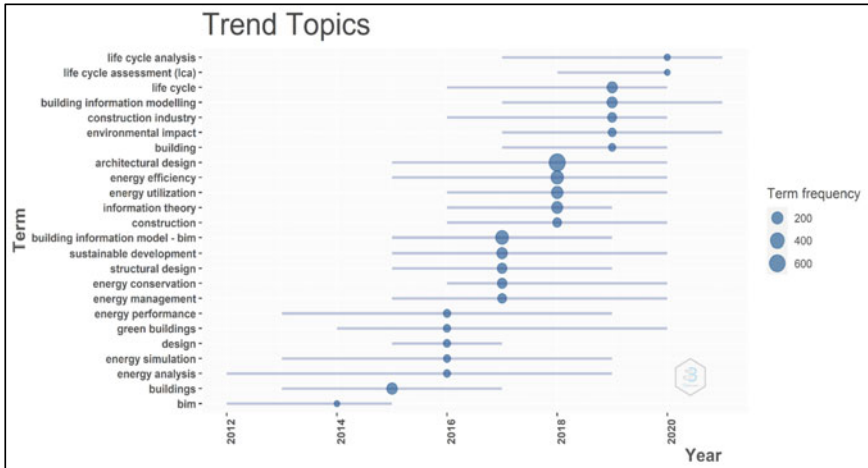


Fig. 7 Trend analysis

5 Conclusion

More than 90% of the papers published in the last few years in BIM research are currently under review. During the past few years, BIM research publications have been successful. Based on bibliometric analysis, results are given below:

- Regarding architectural design, BIM, energy efficiency is the most important keyword for building energy analysis.
- Sustainability (Switzerland), Automation in Construction, IOP Conference Series: Earth and Environmental Science, energy and buildings are the most important sources for articles for building energy analysis.
- China, USA, and Italy are the most important countries for building energy analysis research. India also contributes to the top 10 countries in building energy analysis.
- To analyze the top 10 articles with a total number of citations, year of publication, and normalized citations, it used for an author for future research.
- Shangkly diagram connection between a keyword, country, and source is shown in the results.

Limitation and Future direction: This study, Data collected from Scopus data base future planning to get an data from an web of science for Future study of BIM used in energy analysis.

References

1. Nakkeeran G, Krishnaraj L, Scholar R Optimization and performance analysis of residential building for sustainable energy design through BIM. *kuwaitjournals.org*. <https://doi.org/10.36909/jer.ACMM.16297>
2. Jayakeerti M, Nakkeeran G, Durai Aravindh M, Krishnaraj L (2023) Predicting an energy use intensity and cost of residential energy-efficient buildings using various parameters: ANN analysis. *Asian J Civil Eng* 1:1–17. <https://doi.org/10.1007/S42107-023-00717-Y>
3. van Nederveen GA, Tolman FP (1992) Modelling multiple views on buildings. *Autom Constr* 1(3):215–224. [https://doi.org/10.1016/0926-5805\(92\)90014-B](https://doi.org/10.1016/0926-5805(92)90014-B)
4. Sullivan CC (2005) Brace for BIM. *Architect* 94(4):77
5. Elnabawi MH (2020) Building information modeling-based building energy modeling: investigation of interoperability and simulation results. *Front Built Environ* 6:193. <https://doi.org/10.3389/FBUIL.2020.573971/BIBTEX>
6. Cerovsek T (2011) A review and outlook for a ‘Building Information Model’ (BIM): a multi-standpoint framework for technological development. *Adv Eng Inform* 25(2):224–244. <https://doi.org/10.1016/J.AEI.2010.06.003>
7. Santos R, Costa AA, Grilo A (2017) Bibliometric analysis and review of Building Information Modelling literature published between 2005 and 2015. *Autom Constr* 80:118–136. <https://doi.org/10.1016/J.AUTCON.2017.03.005>
8. van Eck N (2021) L. W.-J. of informetrics, and undefined 2014. *CitNetExplorer: a new software tool for analyzing and visualizing citation networks*. Elsevier. Accessed: 20 Dec 2021. [Online]. Available <https://www.sciencedirect.com/science/article/pii/S1751157714000662>

9. Ganasen N, Bahrami A, Loganathan K (2023) A scientometric analysis review on agricultural wastes used as building materials. *Buildings* 13(2):426. <https://doi.org/10.3390/BUILDINGS13020426>
10. van Eck N (2010) L. W.- scientometrics, and undefined 2010. Software survey: VOSviewer, a computer program for bibliometric mapping. Springer. <https://doi.org/10.1007/s11192-009-0146-3>
11. Makabate CT, Musonda I, Okoro CS, Chileshe N (2022) Scientometric analysis of BIM adoption by SMEs in the architecture, construction and engineering sector. *Eng Constr Archit Manag* 29(1):179–203. <https://doi.org/10.1108/ECAM-02-2020-0139>
12. Aravindh MD, Nakkeeran G, Krishnaraj L, Arivusudar N Evaluation and optimization of lean waste in construction industry. *Asian J Civil Eng* 1:3. <https://doi.org/10.1007/s42107-022-00453-9>
13. Oshodi OS, Awuzie BO, Akotia J, Ademiloye AS, Ngowi A (2020) A bibliometric analysis of recycled concrete research (1978–2019). *Built Environ Project Asset Manage* 10(5):725–736. <https://doi.org/10.1108/BEPAM-01-2020-0009>
14. Shikoh AS, Polyakov A (2020) A quantitative analysis of the research trends in perovskite solar cells in 2009–2019. *Physica Status Solidi (A) Appl Mater Sci* 217(23). <https://doi.org/10.1002/PSSA.202000441>
15. Cuccurullo C, Aria M, Sarto F (2016) Foundations and trends in performance management. A twenty-five years bibliometric analysis in business and public administration domains. *Scientometrics* 108(2):595–611. <https://doi.org/10.1007/S11192-016-1948-8/FIGURES/4>

Impact of Green Construction Management Study on the Quality of G+6 Offices Building at Kochi, Kerala



Balasubramanian Murugesan

1 Introduction

Environmental construction involves the planning, organizing, and implementing resource and environmentally conscious operations throughout the entire building life cycle, from conception to demolition. Construction of residential houses and environmental sustainability are balanced by green building design [1, 2]. The conventional building design concepts of economy, usability, durability, and comfort are expanded upon by the green building research. All aspects of green construction include energy and renewable energy, water efficiency, environmentally preferable building standards and materials, waste reduction, toxic reduction, indoor air quality, smart growth, and sustainable development. Buildings utilized around energy-related GHG emissions accounted for 19% of total world final energy in 2010 [3]. They also estimate that by the middle of the century, this form of energy use might have doubled, if not more. Green building, according to the World Green Building Council, reduces the negative impacts on our natural environment and climatic condition could promote beneficial changes. Green buildings conserve natural resources by using renewable energy and reducing pollution in the project design, construction, operation, and maintenance [4, 5]. While these facilities are initially costly, as demand grows, the cost of construction will certainly decrease. Any building that meets the requirements mentioned earlier, whether it be a house, office, school, hospital, or community center, qualifies as a green building [6]. It's crucial to remember, though, that not all green buildings are made equal regarding the quality of life for their inhabitants during design, construction, and operation. Climate, culture, traditions, building types, ages, environment, economic, and social concerns differ between nations and regions, which impacts how they approach green building [7, 8]. Green

B. Murugesan (✉)

Department of Civil Engineering, Faculty of Engineering and Technology, SRM Institute of Science and Technology, Kattankulathur, Tamil Nadu 603203, India
e-mail: balasubm1@srmist.edu.in

building design entails striking a balance between home construction and the long-term sustainability of the environment. Green building practice complements and enhances traditional building design principles such as economy, usability, durability, and comfort [9]. Energy efficiency and renewable energy, water efficiency, environmentally preferable building materials and specifications, waste reduction, toxic reduction, indoor air quality, smart growth, and sustainable development are a few elements of green construction [10, 11]. The building design's economic, utility, durability, and comfort aspects are extended and complemented by green building, commonly referred to as green construction or sustainable building. Compared with conventional constructions, green buildings consume less water, are more energy efficient, save natural resources, reduce wastage, and offer the occupants a healthier living environment [12].

2 Literature Review

Arif et al. [13] pointed out the drivers and obstacles of green construction in India. This article aims to provide the findings of a workshop organized in New Delhi to analyze the state of green building in India and outline the main challenges and drivers the sector is dealing with Lam and others [14]. The development of the new green specifications has been sparked by the addition of sustainability requirements and shifting priorities in construction management. The use of green construction criteria is influenced by various factors [15, 16]. Five independent factors for a functional green construction specification were found using factor analysis. They relate to (1) green technology and methodologies; (2) leadership and accountability; (3) specifications, consistency, and quality; (4) benchmarking and guideline systems; and (5) stakeholder participation. Shi et al. [17] studied the impact of construction on the neighborhood and the environment in which green construction became a popular solution to these problems.

In Shanghai, a questionnaire survey was undertaken with significant construction industry stakeholders to investigate difficulties related to green construction uptake. The findings revealed the high economic state, additional effort, and insufficient green construction materials and information are major roadblocks. Sofia Knapic studies the impact of cork as a natural, renewable, and long-lasting building material [18]. Cork has a unique set of features that make it ideal for use in buildings and infrastructures, including insulation, wear resistance, and durability. Designers, architects, and engineers can achieve some of the green building demands, thanks to the material qualities paired with a low ecological imprint. Lowering building energy consumption and attaining sustainable development, which has become a top priority in architectural research, are topics covered by Yongwang Zhang. These issues include the growing concerns about global warming, environmental damage, and energy resource shortages [19, 20]. Building owners and governments worldwide drive a higher focus on designing ecologically sustainable structures. The idea of green buildings for the general public is still in its infancy, although some top-notch

Fig. 1 Methodology flow chart



green buildings have recently been built in India [21–23]. The selection of materials for green construction is an extremely crucial step. Materials must be chosen after careful consideration of their cost and qualities.

3 Materials and Methodology

The methodology for the project includes case study site selection which was in Kochi, Kerala. The office building was examined and the required change that has to be made was noted down. Market study of the required materials was studied. Quality, cost, and quantity analysis of the required materials was studied. Energy analysis and thermal analysis of the conventional building was done and compared with the green building. It was brought to the conclusion that green building is more energy efficient and cost effective when compared with the conventional buildings. Figure 1 represents the overall methodology of this research work.

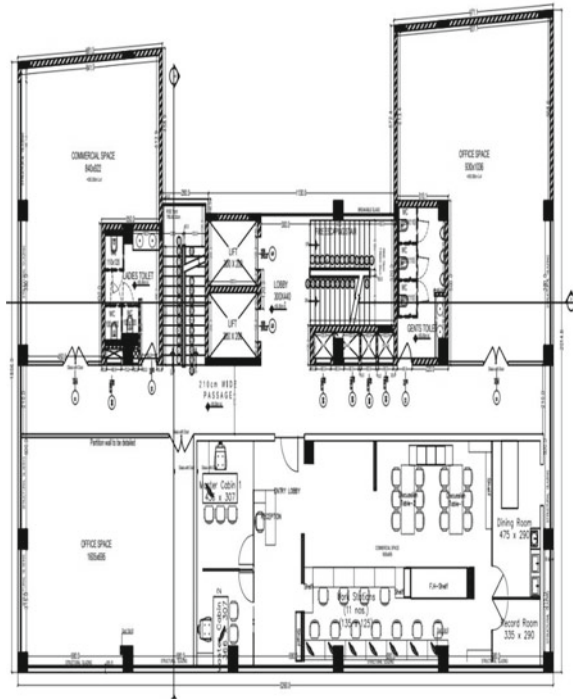
4 Results and Discussions

4.1 Planning

The site of the building is selected in Kochi, Kerala with the coordinate's 10.017 °N 76.344 °E. Kochi has a tropical climate, with wet months from April to November and dry months from December to March.

Kochi has high temperature throughout the year ranging between 29 °C (89 °F) and 33 °C (91 °F) and March is the warmest month of the year and has a maximum average temperature of 33 °C (91.4 °F). January has an average maximum temperature of 29.4 °C (84.92 °F) and is the coldest month of the year. In Kochi, the precipitation

Fig. 2 AutoCAD plan for ground floor up to second floor



amounts to 3015 mm, i.e., 118.7 inches per year. The rainfall ranges from 25 mm in the driest month (January, February) to 700 mm in the wettest month.

Floor plans: It is a typical plan from ground floor up to second floor. Each floor comprises of two master cabins, discussion room, record room, dining room, two washrooms, one fire escape, commercial space, conference hall, one normal staircase, and two elevators. Area of each floor is 554.55 SQM. And it is a typical plan from third floor up to sixth floor. Each floor comprises of two master cabins, discussion room, record room, dining room, two washrooms, one fire escape, one normal staircase, and two elevators.

Area of each floor is 206.79 SQM. Figure 2 shows the AutoCAD plan for the ground floor till second floor plan. Figure 3 contains the AutoCAD diagram for third floor up to sixth floor plan and Table 1 comprises of the brief details of area of each floor and the total area.

4.2 Analysis

Energy consumed by the conventional building is 310 kWh/m²/yr. Conventional materials are used in the building; therefore, the energy efficiency of the building

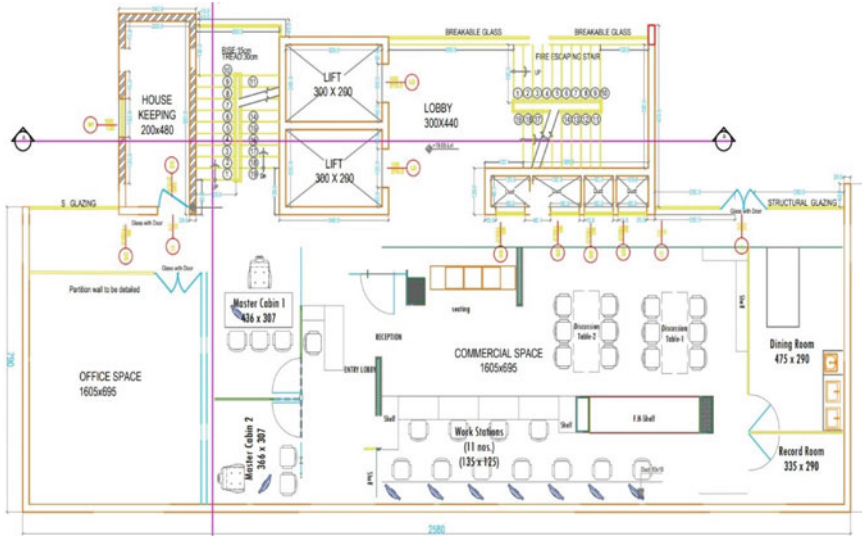


Fig. 3 AutoCAD plan for third floor up to sixth floor

Table 1 Area of each floor and total area

Floor	Area (SQM)
Ground floor	554.55
First floor	554.55
Second floor	554.55
Third floor	206.79
Fourth floor	206.79
Fifth floor	206.79
Sixth floor	206.79
Total	2284

is very low [22]. Energy consumed by the green building is 232 kWh/m²/yr. Green materials are introduced in the building which results in higher energy efficiency than the conventional building. Benchmark comparison helps to understand the building’s current energy consumption against industry benchmark such as ASHRAE 90.1 and Architecture 2030 as shown in Fig. 4.

HVAC system with ventilation, filtration, and thermal comfort, can significantly improve the indoor air quality. The installation of an HVAC system in a building raises the building’s energy efficiency to its maximum level. The visual representation of the energy comparison when HVAC system is introduced in office was represented in Fig. 5.

Introduction of solar panel helps in reducing cost savings and they are very less pollutant compared with the generators and other sources of electricity. They have

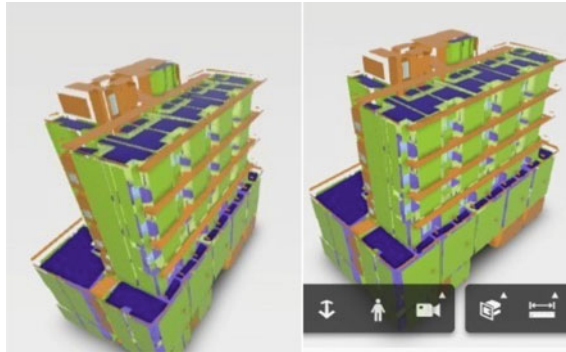


Fig. 4 Energy analyses of conventional building versus green building

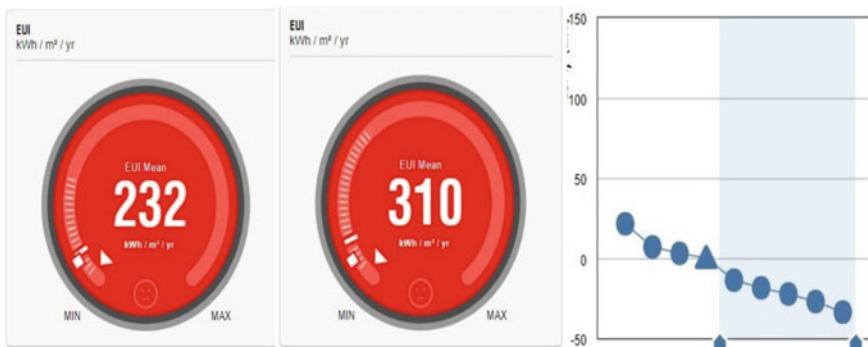


Fig. 5 Energy comparison when HVAC system is introduced and graph showing the energy efficiency

very less maintenance and have a life more than 20 years if properly maintained. The energy comparison when solar panel is introduced in office and the graphical representation was shown in Fig. 6. Energy paybacks ranging from one to four years and anticipated life expectancies of 30 years, 87–97% of the energy generated by PV systems will be free of pollution, greenhouse emissions, and resource depletion. The concept that PV can't pay back its energy investment is a fiction, according to models and real data as shown in Fig. 7. Lighting is one of the key factors that affect the energy consumption of a building. Introduction of light sensors and low-watt lighting increases the energy efficiency of the building. The energy comparison when efficient lighting is introduced in office and the graphical representation was shown in Fig. 8.



Fig. 6 Energy comparisons with the surface coverage of the solar panel and graph showing the energy efficiency

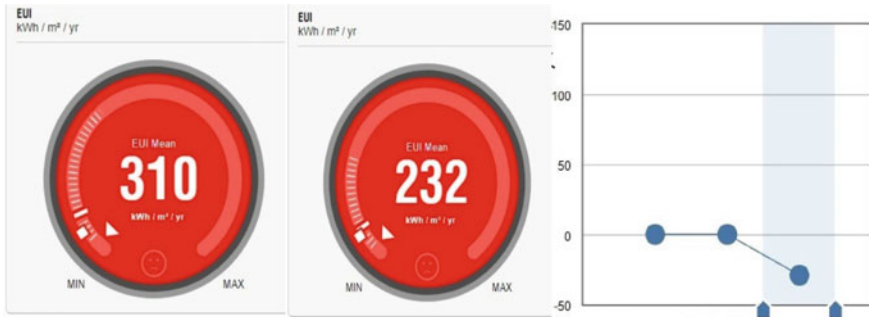


Fig. 7 PV—payback limit and graph showing the energy efficiency

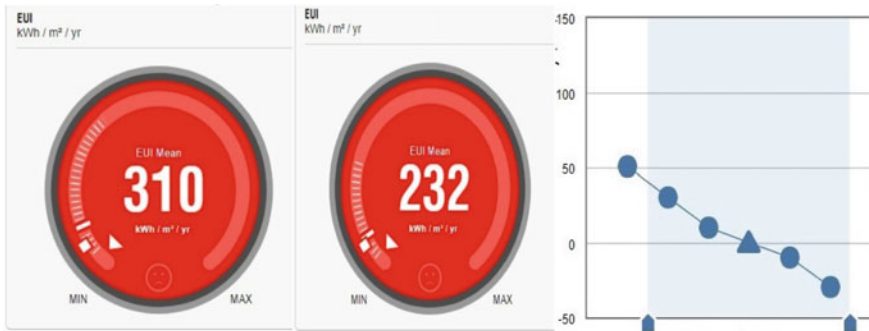


Fig. 8 Energy comparisons when the lighting efficiency and graph showing the energy consumption with respect to the lighting efficiency

4.3 Thermal Analysis

Thermal analysis helps us to choose the appropriate materials used in the building for energy conservation and how much difference does it make in the analysis when there is a change in the materials [24, 25]. Thermal analysis is a tool that basically optimizes the building potential. Thermal simulation report is determined by the data provided. The input data mainly consists of the building geometry, HVAC system, internal loads, weather data, operating strategies, and other specific parameters. Opaque walls can be simply modeled as parallel and homogeneous layers, with a mono dimensional thermal flux that permits analytical models to measure thermal transmittance [26]. When the wall performance is strong, this examination is more critical, as it is intimately tied to economic analyses. The report generated based on the thermal analysis are presented in Table 2. The details regarding the project summary was represented in Table 3 and the building summary was given in Table 4.

5 Conclusion

Even though there are lots of research on promoting green buildings, there is a lack on effective method of implementing them. Through the analysis, factors affecting the building is identified and changes are brought to overcome those factors for better energy efficiency and eco-friendly environment. Green construction is the way of the future. If we are to meet global climate targets, it must be. Overall project helped us in gaining knowledge about the materials used for green construction, their prices, and availability in the market. This project includes G+6 Office building in Kochi, Kerala and certain changes were made to make the building eco-friendly, energy efficient, and self-sustaining. It can be concluded that the efficiency of the green building using Revit (2019) is presented and the changes can be incorporated for better energy efficiency and thermal efficiency. The green building turned out to be more energy efficient, which in turn made the building more cost efficient. Green materials were added which helped in uplifting the thermal efficiency of the building and helped in reducing carbon footprints to a subsequent limit. Green material used in the building helped in increasing the air quality which helped occupants spending more pleasant and healthy time.

Table 2 Zone summary

Input	Corresponding values
Area (m ²)	2164
Volume (m ³)	8657.62
Cooling set point	23C
Heating set point	21C
Temperature of the air supply	12C
People in number	899
Infiltration (L/s)	0.0
Type of air volume calculation	VAV-single duct
Humidity relative	60.00%(Calculated)
<i>Psychro metrics</i>	
Psychro metric message	None
Dry-bulb temperature entering cooling coil	20C
Wet-bulb temperature entering cooling coil	21C
Leaving dry-bulb temperature after cooling coil	11C
Wet-bulb temperature after cooling coil	12C
Temperature of mixed air dry bulb	26C
<i>Calculated result</i>	
Maximum cooling load (W)	246,735
Month and hour of maximum cooling	May 16:00
Sensible load peak cooling (W)	134,476
Latent cooling peak load (W)	112,259
Peak airflow for cooling (L/s)	7993.7
Maximum heating demand (W)	-9124
Maximum heating airflow (L/s)	2712.1
Airflow at maximum ventilation (L/s)	2712.1
<i>Checksums</i>	
Density of cooling load (W/m ²)	114.00
Density of cooling flow (L/(s m ²))	3.69
Flow of cooling/load (L/(s KW))	32.40
Load/cooling area (m ² /KW)	8.77
Density of heating load (W/m ²)	-4.22
Flow density of heating (L/(s m ²))	1.25
Density of ventilation (L/(s m ²))	1.25
Person/ventilation (L/s)	3.0

Table 3 Project summary

Weather and location	Corresponding values
Project	Office building
Address	Kochi
The calculation time	03 May 2022 3:25 PM
The report type	Standard
The latitude	9.98
The longitude	76.30
Dry bulb for summer	32C
Wet summer bulb	26C
Dry bulb for winter	23C
Daily mean range	6C

Table 4 Building summary

Input	Corresponding values
The building type	Office
The area (m ²)	2284
The volume (m ³)	9136.21
<i>Calculation results</i>	
Total load peak cooling (W)	253,389
Month and hour of maximum cooling	May 16:00
Sensible load peak cooling (W)	139,311
Peak latent cooling capacity (W)	114,079
Cooling capacity maximum (W)	253,142
Peak airflow for cooling (L/s)	8344.3
Peak heating load (W)	-9492
Maximum heating airflow (L/s)	2760.3
<i>Check sums</i>	
Density of cooling load (W/m ²)	110.94
Density of cooling flow (L/(s m ²))	3.65
Flow of cooling/load (L/(s KW))	32.93
Load/cooling area (m ² /Kw)	9.01
Density of heating load (W/m ²)	-4.16
Flow density of heating (L/(s m ²))	1.21

References

1. Arif M, Egbu C, Haleem A, Kulon D, Khalfan M (2021, 10 July) State of green construction in India: drivers and challenges. *J Eng Des Technol*
2. Zhang Y, Wang W, Wang Z, Gao M, Zhu L, Song J (November 2021) Green building design based on solar energy utilization: kindergarten competition design as an example. *Energy Rep* 7(supplement 7):1297–1307
3. Knapic S, Oliveria V, Machodo JS, Pereira H (2016) Cork as a building material: a review. *Eur J Wood Wood Prod* 74:775–791
4. Perzan CP (2006) What you should know about green building. *Chicago Bar Assoc J* 20:38–43
5. Plessis CD (2001) Sustainability and sustainable construction: the African context. *Build Res Inform* 29(5):374–80
6. Mazor M, Mutto J, Russell D, Keoleian G (2011) Life cycle Green House gas emissions reduction from rigid thermal insulation use in building. *J Ind Ecol* 15:284–299
7. Shi Q, Zuo J, Huang R, Huang J, Pullen S (October 2013) Identifying the critical factors for green construction. *Habitat Int* 40:1–8
8. Lam PTI, Chan EHW, Poon CS, Chau CK, Chun KP (January–February 2010) Factors affecting the implementation of green specifications in construction. *J Environ Manage* 91(3):654–661
9. Costa A, Pereira H (2005) Quality characterization of wine cork stoppers using computer vision. *J Int Sci Vigne Vin* 39:209–218
10. Costa A, Pereira H (2006) Decision rules for computer vision quality classification of wine natural cork stoppers. *Am J Enol Vitic* 57:210–219
11. Costa A, Pereira H (2007) Influence of vision systems, black and white, colored and visual digitalization, in natural cork stopper quality estimation. *J Sci Food Agric* 87:2222–2228
12. Costa A, Pereira H (2009) Computer vision applied to cork stoppers inspection. In: *Cork Oak Woodlands and Cork Industry: present, past and future*. Ed. Santiago Zapata, Barcelona, Spain, pp 394–405
13. Fortes MA, Rosa ME, Pereira H (2004) *A Cortiça*. Ed. IST Press, Lisbon, Portugal, p 259
14. Gonzalez-Adrados JR, Pereira H (1996) Classification of defects in cork planks using image analysis. *Wood Sci Technol* 30:207–215
15. Gonzalez-Adrados JR, Lopes F, Pereira H (2000) Quality grading of cork planks with classification models based on defect characterisation. *Holz Roh Werkst* 58:39–45
16. Jordanov I, Georgieva A (2009) Neural network classification: a cork industry case. In: *IEEE international symposium on industrial electronics*. Ed. IEEE Computer Society, Seoul, Korea, pp 232–237
17. Lopes F, Pereira H (2000) Definition of quality classes for champagne cork stoppers in the high quality range. *Wood Sci Technol* 34:3–10
18. Melo B, Pinto R (1989) Análise de diferenças nos critérios de classificação qualitativa das rolhas. *Cortiça* 601:293–302
19. Xu W, Liu Z, Chen X et al (2016) Thoughts on the development of “near zero energy” building in my country. *Archit Sci* 32(4):1–5
20. Hao S, Song Y (2016) Differentiation and analysis of the concept of building climate adaptability under different building systems. *Archit J* 9:102–7
21. Huang L, Lan B (2011) From regionality to sustainability: the development and enlightenment of foreign vernacular architecture climate adaptability research. *Archit J* S1:103–7
22. Han D, Gu Z, Wu G (2019) Research on public building climate adaptability design method centered on spatial form. *Archit J* 04:78–84
23. Coria C, Li X, Yang S (1982) The architectural form follows the climate. *Trans World Archit* 1:54–58
24. Yi J, Xing W (2011) China should take its own real road of building energy conservation-Interview with Jiang Yi, academician of the Chinese Academy of Engineering. *Archit Tech* 11:46–49

25. Fu X, Lu L, Shi L (2019) Basic green building design—a formal space design strategy in response to climate. *Archit J* 01:100–4
26. Beijing Municipal Science and Technology Promotion Center for Housing and Urban-Rural Development. Green building evaluation standard: GB/T50378-2019. China Construction Industry Press, Beijing (2006)

Materials Science and Engineering

Regression Analysis on the Behaviour of Thin Spherical Shells with Various Parameters



G. Pennarasi, S. Sindhu Nachiar, and S. Anandh

1 Introduction

In the emerging field of construction and technology, there are various forms of structures that are designed to encompass large space. Those forms of constructions are developed from the structural systems of old age. In a building, a structural framework that covers the areas devoid of beams and columns are the thin shell structures. As a result, they are distinct from regular skin structures and are referred to as stressed-skin structures [1]. The structural behaviour of the shell depends on the geometric parameters and its configurations. Shells, when properly designed, can withstand heavy loads and enclose critical regions with the help of less consumption of material and thickness. Shells have an appealing lightness and elegance from an aesthetic sense [2]. There are various forms of structural roofing systems, in which thin shell structures are preferred for their less displacement and structural efficiency compared with flat roofs. Thin shell structures are formed by one or more curved plates or folded plated having less thickness compared to other dimensions [3]. Increase in thickness shall increase the self-weight and also the support area. To reduce the self-weight and the application of imposed loads, thin shell roofing systems are preferred in this modern-day technology [4]. Thin shells are structures that has radius of curvature to thickness ($\frac{R}{t}$) ratio less than 20. Some of the real-life examples of thin shell structures are shown in Fig. 1a, b [5, 6]. The major factors that affect the behaviour and efficiency of thin shells are its shape and thickness [7–9]. Optimization is an effective way of achieving the most suited shape and thickness using computational mechanics for determining the form of concrete shells [10–12].

Nachiar et al. [13] optimized that shape of spherical thin shell structure by varying the radius of curvature to thickness ratio and geometric parameters. Meng et al. [14]

G. Pennarasi · S. Sindhu Nachiar (✉) · S. Anandh
Department of Civil Engineering, SRM Institute of Science and Technology, Kattankulathur,
Tamil Nadu, India
e-mail: sindhus@srmist.edu.in



Fig. 1 a Haus der Kulturen der Welt, Germany. b L'Oceanographic, Spain [5, 6]

developed a new method for shape thickness topology for free form shells. Heygi [15] stated that it is necessary to utilize a membrane field in order to resist buckling load which is due to the out-plane slenderness of the arches. Hrvoje et al. [16] considered the geometric parameters, rotations, strains, and displacements for analysis and concluded that the structured mesh was more effective than the unstructured one. The shear deformation theory was used for analysing the static and transient response in cylindrical shells. The shells were analysed for its static and dynamic response of shells under localized loading and impulsive loading, respectively. It was concluded that the nonlinearity of the shell increases with increase in thickness of the shell [17].

Tahaseen [18] designed a reinforced cement concrete dome by calculating the meridional thrust and hoop stress. For any thin shell, the geometry has to be perfect so as to resist the buckling and post buckling load as any imperfections shall be very sensitive [19]. Many numerical methods were developed by researchers for resisting the buckling load and external pressure in domes such as Sanders theory and Donnell theory [20, 21]. The optimization methods studied by Antonia et al., 2010 underwent many objective functions, such as strain energy and structural weight. The optimization of the shape had a considerable effect on the mechanical behaviour of the shell. A minor imperfection in the shell geometry significantly affects the performance of the shell [22].

A statistical approach of linear regression analysis helps in identifying the degree of dependency between two variables: one being dependent (Y) and the other as explanatory variable (X) [23]. The regression analysis is a powerful statistical method in order to arrive at a dependency equation, coefficient of error with a confidence level of 95% [24]. The R^2 value represents the coefficient of determinacy (i.e.) percentage of variance between the variables. In the field of optimization and concrete technology, many researchers used regression analysis to predict the relationship between dependent and independent variables. Regression models were developed from the finite element analysis of glass fibre-reinforced polymer tubes [25]. Also, a probabilistic model was derived using a linear regression approach for the examination and prediction of bond strength between concrete and rebars [26]. Multiple regression analysis was used to predict the split tensile strength of concrete with zeolite and a

formula was arrived at for the same [27]. Similar type of analysis was performed to determine the strength of concrete with rice husk ash and compared with experimental investigation [28]. The regression technique was also adopted in the prediction of compressive strength of eco-friendly concrete and self-compacting concrete [29, 30]. The main advantage of using regression analysis in the prediction of the properties is the accuracy and arriving at a simplified equation for the same. Therefore, the scope of the paper includes the study on the dependency of geometric parameters of shell for different $\frac{R}{t}$ ratios of spherical shells from the previous study by Nachiar et al. [13] using the statistical approach of regression analysis.

2 Methodology

Nachiar et al. [13] studied on the optimization of spherical shell structure with three different $\frac{R}{t}$ ratios of 7, 13, and 20 (R7, R13, and R20). The authors varied the geometric parameters of the shell in order to study the most efficient form of shell structure using finite element software ANSYS based on stress, displacement, and self-weight. From the previous study, the equivalent stress, displacement, and self-weight were obtained, and regression analysis was performed to find the dependency between the geometric parameters like span and thickness. The R^2 value, coefficients, and standard error were obtained for the results dependent on the span and thickness of shell structure.

3 Regression Analysis

Linear regression analysis, a statistical method using least squares, was performed between the geometric parameters of shell and stress, where the geometric parameters are the independent variable (X) and stress being the dependent variable (Y) [31]. Also, the dependency of geometric parameters (X) with the stress and displacement (Y) was also analysed. The regression model adopted in this study has the equation of:

$$Y = aX + b, \tag{1}$$

In this equation, a represents the slope and b represents the intercept. Y and X are the dependent and independent variables [32], respectively.

4 Results and Discussions

4.1 Geometric Parameters Versus Equivalent Stress

The results of the linear regression analysis using least squares between the span, thickness, and stress are presented in Table 1 for the values of R^2 , intercept, slope, standard error, and the confidence index for thin spherical shells of R7, R13, and R20. Also, the regression equation with the predicted values for the stress and obtained stress values versus span and thickness is represented in the graphical representation in Fig. 2a, b for R7, Fig. 3a, b for R13 and Fig. 4a, b for R20, respectively.

From the results of the linear regression analysis using least square between the stress and geometric parameters, the R^2 value represents about 99% of variation of stress about span and thickness, the slope and the intercept forms the regression equation, and this equation can be used for predicting the stress for span and thickness. The confidence index provides the lower and the upper limit of the stress.

Table 1 Regression analysis results for stress

Description		Span versus stress			Thickness versus stress		
		R7	R13	R20	R7	R13	R20
R^2		0.99	0.99	0.99	0.99	0.99	0.99
Slope (a)		1.35	2.11	2.50	-5.08	-4.53	-24.95
Intercept (b)		1.86	0.94	1.78	31.35	29.62	54.08
Standard error (a)		0.02	0.02	0.02	0.09	0.10	0.67
Standard error (b)		0.24	0.26	0.18	0.22	0.13	0.58
Confidence index (a)	Lower limit	1.30	2.05	2.46	-5.27	-4.75	-26.47
	Upper limit	1.40	2.17	2.54	-4.90	-4.31	-23.43
Confidence index (b)	Lower limit	1.32	0.37	1.39	30.91	29.33	52.77
	Upper limit	2.40	1.50	2.17	31.80	29.90	55.39

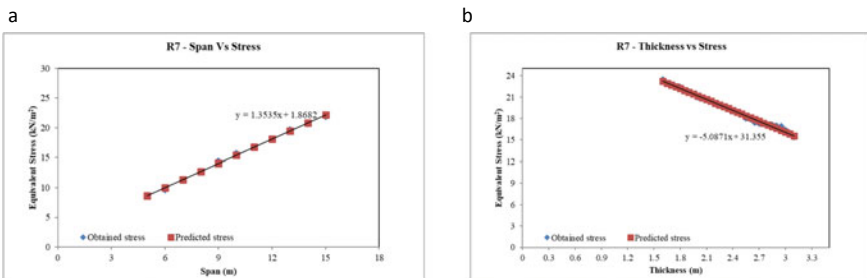


Fig. 2 Regression equation for the predicted stress for R7 **a** span versus stress, **b** thickness versus stress

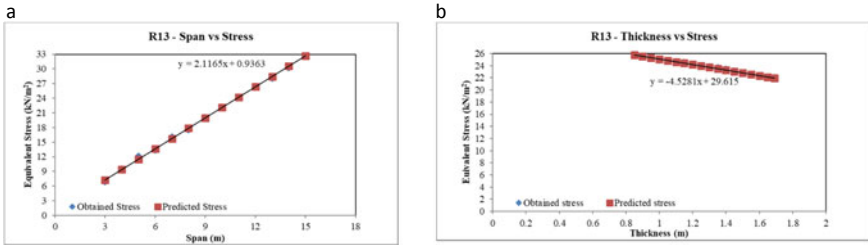


Fig. 3 Regression equation for the predicted stress for R13 **a** span versus stress, **b** thickness versus stress

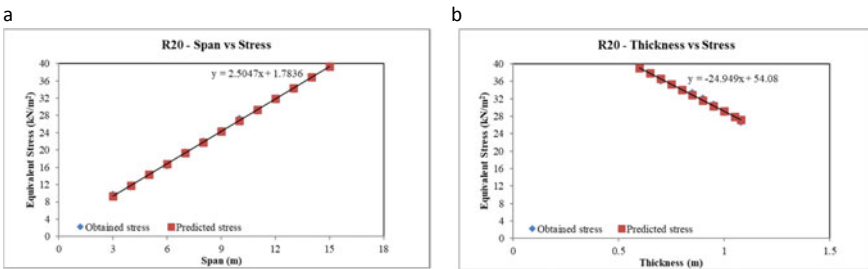


Fig. 4 Regression equation for the predicted stress for R20 **a** span versus stress, **b** thickness versus stress

4.2 Geometric Parameters Versus Displacement

The results of the linear regression analysis using least squares between the span, thickness, and displacement are presented in Table 2 for the values of R^2 , intercept, slope, standard error, and the confidence index for thin spherical shells of R7, R13, and R20. Also, the regression equation with the predicted values for the displacement and obtained displacement values versus span and thickness is represented in the graphical representation in Fig. 5a, b for R7, Fig. 6a, b for R13 and Fig. 7a, b for R20, respectively.

From the results of the linear regression analysis using least square between the displacement and geometric parameters, the R^2 value represents about 97% and 98% of variation of displacement about span and thickness, respectively, the slope and the intercept forms the regression equation, and this equation can be used for predicting the displacement for span and thickness. The confidence index provides the lower and the upper limit of the stress.

Table 2 Regression analysis results for displacement

Description	Span versus displacement			Thickness versus displacement			
	R7	R13	R20	R7	R13	R20	
R^2	0.9700	0.9669	0.9742	0.9924	0.9744	0.9806	
Slope (a)	0.0003	0.0006	0.0008	-0.0019	-0.0046	-0.0101	
Intercept (b)	-0.0018	-0.0024	-0.0033	0.0072	0.0116	0.0179	
Standard error (a)	2.1E-5	3.4E-5	4.3E-5	3.0E-5	0.0018	0.0004	
Standard error (b)	0.0002	0.0003	0.0004	7.3E-5	0.0002	0.0004	
Confidence index (a)	Lower limit	0.0003	0.0005	0.0007	-0.0019	-0.005	-0.0112
	Upper limit	0.0004	0.0006	0.0009	-0.0018	-0.0042	-0.0091
Confidence index (b)	Lower limit	-0.0023	-0.0031	-0.0042	0.0070	0.0111	0.0170
	Upper limit	-0.0013	-0.0016	-0.0023	0.0073	0.0121	0.0189

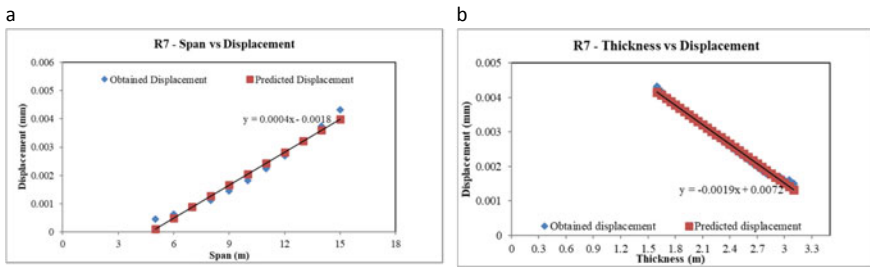


Fig. 5 Regression equation for the predicted displacement for R7 **a** span versus displacement, **b** thickness versus displacement

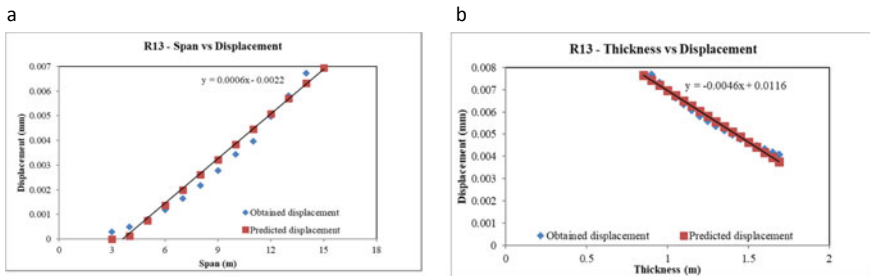


Fig. 6 Regression equation for the predicted displacement for R13 **a** span versus displacement, **b** thickness versus displacement

4.3 Geometric Parameters Versus Displacement

The results of the linear regression analysis using least squares between the span, thickness, and self-weight are presented in Table 3 for the values of R^2 , intercept,

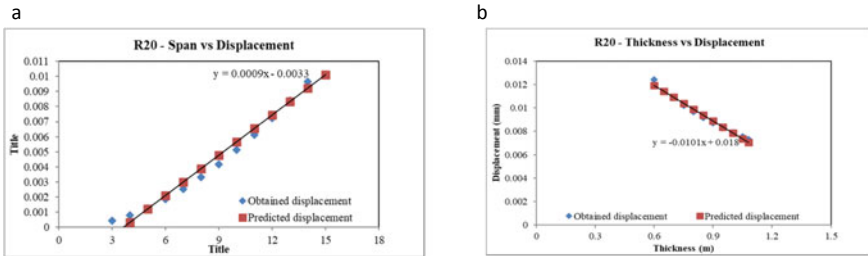


Fig. 7 Regression equation for the predicted displacement for R20 **a** span versus displacement, **b** thickness versus displacement

slope, standard error, and the confidence index for thin spherical shells of R7, R13, and R20. Also, the regression equation with the predicted values for the self-weight and obtained self-weight values versus span and thickness is represented in the graphical representation in Fig. 8a, b for R7, Fig. 9a, b for R13 and Fig. 10a, b for R20, respectively.

From the results of the linear regression analysis using least square between the self-weight and geometric parameters, the R^2 value represents about 97% and 99% of variation of self-weight about span and thickness, respectively, the slope and the intercept forms the regression equation, and this equation can be used for predicting the displacement for span and thickness. The confidence index provides the lower and the upper limit of the stress.

Table 3 Regression analysis results for self-weight

Description		Span versus self-weight			Thickness versus self-weight		
		R7	R13	R20	R7	R13	R20
R^2		0.98	0.97	0.97	0.99	0.99	0.99
Slope (a)		574.42	270.80	172.97	6910.89	5089.88	5007.68
Intercept (b)		-1939.47	-853.84	-579.75	-4349.99	-1142.94	-554.06
Standard error (a)		21.81	13.16	8.77	67.79	45.56	68.96
Standard error (b)		228.71	128.30	85.55	160.75	59.24	59.46
Confidence index (a)	Lower limit	525.09	241.83	153.65	6773.46	4993.29	4851.68
	Upper limit	623.75	299.77	192.29	7048.33	5186.46	5163.68
Confidence index (b)	Lower limit	-2456.85	-1136.21	-768.06	-4678.76	-1268.53	-688.58
	Upper limit	-1422.08	-571.46	-391.45	-4021.22	-1017.34	-419.55

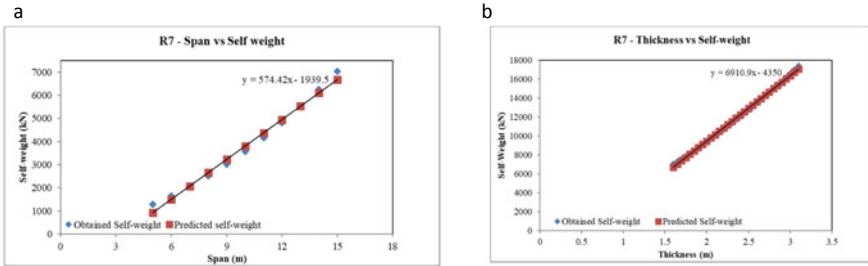


Fig. 8 Regression equation for the predicted displacement for R7 **a** span versus displacement, **b** thickness versus displacement

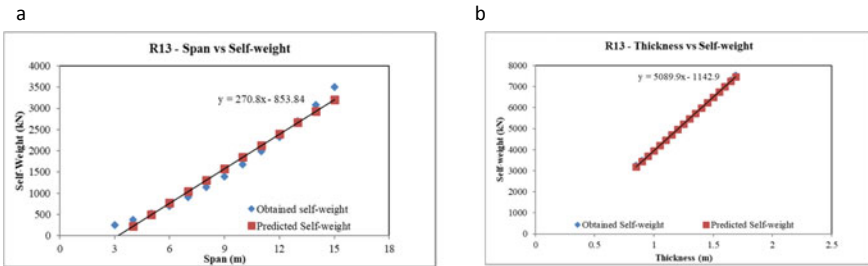


Fig. 9 Regression equation for the predicted displacement for R13 **a** span versus displacement, **b** thickness versus displacement

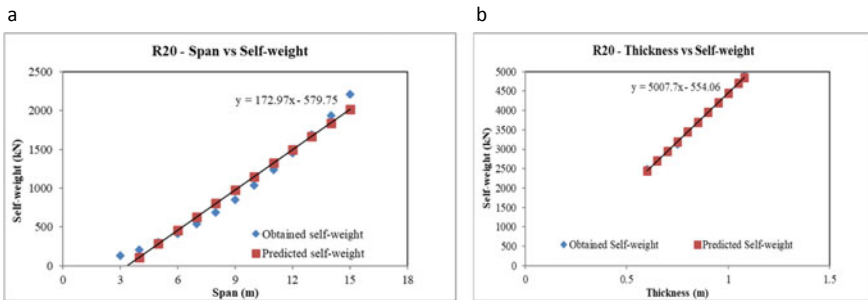


Fig. 10 Regression equation for the predicted displacement for R20 **a** span versus displacement, **b** thickness versus displacement

5 Conclusions

The following are the conclusions made from this regression analysis on the behaviour of thin spherical shell structure:

- From the regression analysis, the predicted stress and the obtained numerical stress were comparable, and the standard of error was found to be negligible.
- The R^2 value was found to be 0.99 for the predicted stress value for both the span and thickness of the spherical shell structure. This signifies that the stress of the shells depends mainly on the geometric parameters like span and thickness.
- Similarly, the predicted and the obtained numerical displacement were comparable, and the standard of error was found to be negligible.
- The R^2 value was found to be 0.97 and 0.98 for the predicted displacement for both the span and thickness of the spherical shell structure respectively. This signifies that the displacement also depends mainly on the geometric parameters like span and thickness.
- Similar results were obtained for the self-weight of the shell structures.
- This statistical result confirms that the behaviour of the shell structure depends on the shape and the geometric parameters of the shell structure.

References

1. Varghese PC (2010) Design of reinforced concrete shells and folded plates. PHI Learning Pvt. Ltd.
2. Ramm E, Wall WA (July 2002) Shells in advanced computational environment. In: V world congress on computational mechanics, pp 7–12
3. Bandhopadhyay JN (1986) Thin shell structures classical and modern analysis. New Age International Publishers, New Delhi
4. Abraham RA, Chandran GK (2008) Study of dome structures with specific focus on monolithic and geodesic domes for housing. [Online]. Available <https://www.Researchgate.Net/Publication/349138511>
5. https://de.wikipedia.org/wiki/Haus_der_Kulturen_der_Welt. Retrieved at 16.02.2023
6. <https://aehistory.wordpress.com/1996/10/09/1996-loceanografic/>. Retrieved at 16.02.2023
7. Chatterjee BK (1988) Theory and design of concrete shell, 3rd edn. Chapman & Hall, New York
8. Ramaswamy GS (1986) Design and constructions of concrete shell roofs. Cbs Publishers and Distributors, New Delhi
9. Timoshenko SP, Woinowsky S, Krieger Theory of plates and shells, 2nd ed. Tata Mcgraw Hill Edition
10. Bletzinger KU, Ramm E (2001) Structural optimization and form finding of lightweight structures. *Comput Struct* 79(22–25):2053–2062
11. Ramm E (2004) Shape finding of concrete shell roofs. *J Int Assoc Shell Spat Struct* 45(1):29–39
12. Ding Y (1986) Shape optimization of structures: a literature survey. *Comput Struct* 24(6):985–1004
13. Nachiar SS, Anandh S, Swathi K, Pennarasi G (2022) Optimization of thin spherical shell structure using fem. *Mater Today Proc* 68:17–25. <https://doi.org/10.1016/J.Matpr.2022.05.072>

14. Meng X, Xiong Y, Xie YM, Sun Y, Zhao Z-L (2022) Shape–thickness–topology coupled optimization of free-form shells. *Autom Constr* 142:104476. <https://doi.org/10.1016/J.Autcon.2022.104476>
15. Hegyi D (2021) Numerical stability analysis of arch-supported membrane roofs. *Structures* 29:785–795. <https://doi.org/10.1016/J.Istruc.2020.11.025>
16. Smoljanović H, Balić I, Trogrlić B, Živaljić N, Munjiza A (2021) Finite strain numerical model for the nonlinear analysis of thin shells. *Eng Struct* 234:111964. <https://doi.org/10.1016/J.Engstruct.2021.111964>
17. Bhimaraddi (1987) Static and transient response of cylindrical shells. *Thin-Walled Struct* 5(3):157–179. [https://doi.org/10.1016/0263-8231\(87\)90018-8](https://doi.org/10.1016/0263-8231(87)90018-8)
18. M. Tech (2015) Reinforced Cement Concrete (RCC) Dome Design Shaik Tahaseen. [Online]. Available www.researchpublish.com
19. Maali M, Aydın AC, Showkati H, Sağıroğlu M, Kılıç M (2018) The effect of longitudinal imperfections on thin-walled conical shells. *J Build Eng* 20:424–441. <https://doi.org/10.1016/J.Jobe.2018.08.005>
20. Błachut (1997) Minimum weight of internally pressurised domes subject to plastic load failure. *Thin-Walled Struct* 27(2):127–146. [https://doi.org/10.1016/S0263-8231\(96\)00036-5](https://doi.org/10.1016/S0263-8231(96)00036-5)
21. Salahshour S, Fallah F (2018) Elastic collapse of thin long cylindrical shells under external pressure. *Thin-Walled Struct* 124:81–87. <https://doi.org/10.1016/J.Tws.2017.11.058>
22. Tomás A, Martí P Shape and size optimization of concrete shells. *Eng Struct* 32(6):1650–1658
23. Ansari S, Nassif AB (2022) A comprehensive study of regression analysis and the existing techniques. In: 2022 Advances in science and engineering technology international conferences, Aset 2022. <https://doi.org/10.1109/Aset53988.2022.9734973>
24. Nasir M, Gazder U, Maslehuddin M, Baghabra Al-Amoudi OS, Syed IA (2020) Prediction of properties of concrete cured under hot weather using multivariate regression and ANN models. *Arab J Sci Eng* 45(5):4111–4123. <https://doi.org/10.1007/S13369-020-04403-Y>
25. Ramesh Babu C, Suresh S (2022) Finite element modeling and regression analysis of concrete filled—glass fibre reinforced polymer tubes. *Mater Today Proc* 64:956–963. <https://doi.org/10.1016/J.Matpr.2022.04.210>
26. Hassanzadeh M, Nazarpour H, Dehestani M (2022) A probabilistic framework to model bond strength between concrete and GFRP rebar using Bayesian linear regression. *Structures* 45:2173–2184. <https://doi.org/10.1016/J.Istruc.2022.10.021>
27. Waghmare S, Katdare A, Patil N (2022) Studies on application of multiple regression analysis for prediction of split tensile strength of concrete with zeolite. *Mater Today Proc* 59:1148–1154. <https://doi.org/10.1016/J.Matpr.2022.03.182>
28. Jha P, Pathak A (2022) Strength prediction of sustainable concrete incorporating rice husk ash by using regression technique. *Mater Today Proc*. <https://doi.org/10.1016/J.Matpr.2022.08.404>
29. Naser H, Badr AH, Henedy SN, Ostrowski KA, Imran H (2022) Application of multivariate adaptive regression splines (Mars) approach in prediction of compressive strength of eco-friendly concrete. *Case Stud Constr Mater* 17. <https://doi.org/10.1016/J.Cscm.2022.E01262>
30. Rajakarunakaran SA et al (2022) Prediction of strength and analysis in self-compacting concrete using machine learning based regression techniques. *Adv Eng Softw* 173. <https://doi.org/10.1016/J.Advengsoft.2022.103267>
31. Kumari, Yadav S (2018) Linear regression analysis study. *J Prac Cardiovascular Sci* 4(1):33. https://doi.org/10.4103/Jpcs.Jpcs_8_18
32. Gupta, Sharma A, Goel A Review of regression analysis models. [Online]. Available www.ijert.org

Parametric Study of Steel Pipe rack



Jatan Patel, Aditi Sheth, and Yogesh Kulkarni

1 Introduction

Structural steel pipe racks generally support pipes, power cables and instrument cable trays in petrochemical, chemical and power plants. Sometimes, pipe racks may also support mechanical equipment, vessels, and valve access platforms.

Pipe racks may also be of RCC up to first tier and structural steel for above tiers depending on project requirement, time and cost restrictions given by client. Pipe racks consist of series of transverse beams and longitudinal beams that run along the length of the pipe system [1]. A typical 3D view of steel pipe rack is shown in Fig. 1.

2 Need of Study

In any oil and gas or petrochemical industry, the quantum of structural steel of pipe racks contribute around 20–50% of the overall structural steel of the project based on the process unit. Therefore, it was found necessary to study the design of

J. Patel (✉)

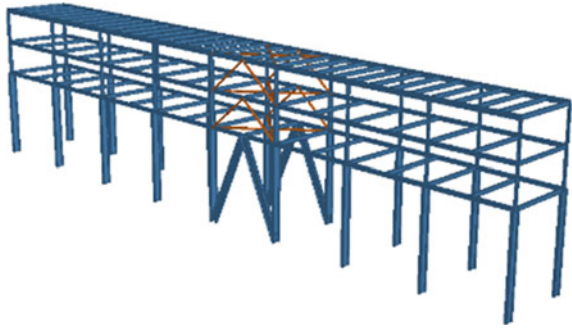
Civil Engineering Department, Dharmsinh Desai University, Nadiad 387001, Gujarat, India
e-mail: jatanpatel51@gmail.com

A. Sheth

Assistant Professor, Civil Engineering Department, Dharmsinh Desai University, Nadiad 387001, Gujarat, India
e-mail: aks.cl@ddu.ac.in

Y. Kulkarni

Assistant General Manager, Civil, Structural and Building Department, Larsen & Toubro Chiyoda Limited, N.H.8, Vadodara, Gujarat, India
e-mail: yuk24@rediffmail.com

Fig. 1 3D view of pipe rack

steel pipe racks to optimize the consumption of the structural steel [2]. For developing countries like India, such study will help to reduce consumption of structural steel which will lead to saving in fabrication cost, erection cost of the project. Further such study will also help in reducing national requirement of structural steel for various projects being executed simultaneously.

3 Scope of Study

- In this study, analysis and design of total 32 pipe racks are carried out by using STAAD.Pro software. Refer Table 1.
- 16 pipe racks are analyzed and designed for pinned base condition and 16 pipe racks for fixed-based condition.
- Pipe rack is designed by Limit State Method of Design by IS 800: 2007.
- Objective of this parametric study is to find whether fixed base condition is economical or hinged base condition is economical.
- Design of foundation is excluded from the present study (Figs. 2, 3 and 4).

4 Load Consideration

The following loads are considered in the design of pipe rack superstructures:

- DL: Dead Load
- LL: Live Load
- PO: Operating Pipe Load
- PE: Empty Pipe Load
- PT: Test Pipe Load
- PF: Pipe Friction Force
- AF: Anchor Force
- WL: Wind Load

Table 1 Cases considered for the study

S. No	Fixed base condition		Hinged base condition	
	Width of pipe rack	Height of first tier	Width of pipe rack	Height of first tier
1	5	5	5	5
2	5	5.5	5	5.5
3	5	6	5	6
4	5	6.5	5	6.5
5	6	5	6	5
6	6	5.5	6	5.5
7	6	6	6	6
8	6	6.5	6	6.5
9	7	5	7	5
10	7	5.5	7	5.5
11	7	6	7	6
12	7	6.5	7	6.5
13	8	5	8	5
14	8	5.5	8	5.5
15	8	6	8	6
16	8	6.5	8	6.5

Fig. 2 Typical cross section of pipe rack

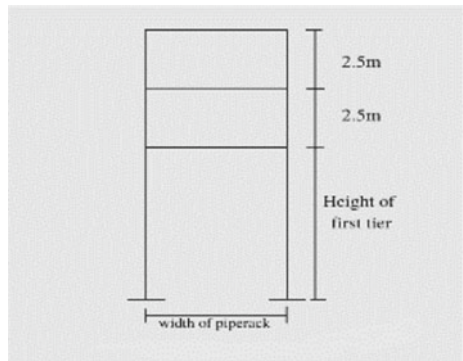


Fig. 3 Typical longitudinal section of pipe rack

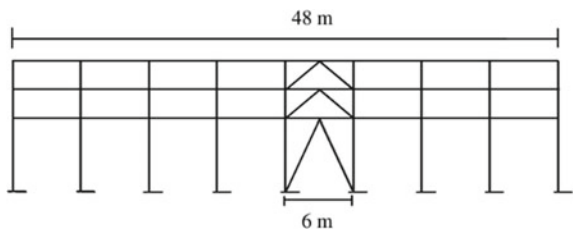
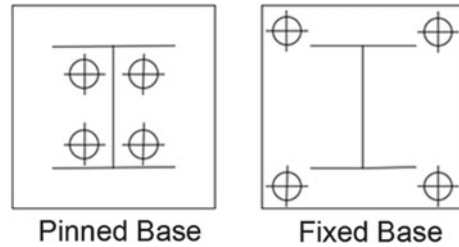


Fig. 4 Typical arrangement of pinned base and fixed base



- EQ: Earthquake Force.

4.1 Dead Load (DL)

The dead load (DL) is the load due to the weight of the structure and the components that make up the structure, such as beams and columns. Cable tray and its support loads are considered in dead load [3].

4.2 Live Load (LL)

In a steel pipe rack, a “live load” may include the weight of materials or equipment temporarily placed on the rack and the weight of people who may be accessing or working on the rack.

4.3 Operating Pipe Load (PO)

The operating load on a steel pipe rack refers to the maximum amount of pipe weight or force that the rack is designed to support during normal operation [4].

4.4 Empty Pipe Load (PE)

An “empty pipe load” on a steel pipe rack refers to the weight of the pipes when they are not filled with any fluid or material. The weight of the empty pipes is a principal factor to consider when designing a pipe rack, as it determines the load that the rack will be subjected to. Normally, 60% of the operating pipe load for piping levels is typically considered as empty load.

4.5 Test Pipe Load (PT)

A test pipe load on a steel pipe rack refers to a load applied to a pipe rack structure considering pipe filled with water. In absence of any data, test pipe load is considered to be equal to operating load [5].

4.6 Thermal Loads

Wind load is the force exerted by the wind on a structure. The wind load on a steel pipe rack will depend on several factors, including the location of the structure, the size and shape of the pipes, and the type of wind. In India, the Indian Standard (IS) 875 (Part 3)—2015, “Code of Practice for Design Loads (Other Than Earthquake) for Buildings and Structures,” provides guidelines for determining the wind load on buildings and other structures, including steel pipe racks [6]. These loads are acting on the transverse beams either by friction or by anchors.

4.6.1 Friction Force (FF)

The friction force opposes the relative motion of two surfaces in contact. In the case of a steel pipe rack, there are several factors that can affect the friction force on the rack, including the type of material the pipes are made of, the surface roughness of the pipes and the rack, the weight of the pipes, and the angle at which the pipes are resting on the rack.

The friction force on the pipe rack is 10% of the total piping weight (PO). It is assumed that the thermal movements on the individual pipes do not happen simultaneously.

4.6.2 Anchor Force (AF)

Anchor force is the force exerted on a pipe or piping component by an anchor or support. Pipe anchors prevent the pipe from moving in one or more directions and allow expansion movement to occur at appropriate points in a piping system.

4.7 Wind Load (WL)

Wind load is the force exerted by the wind on a structure. The wind load on a steel pipe rack will depend on several factors, including the location of the structure, the size and shape of the pipes, and the type of wind. In India, the Indian Standard (IS)

875 (Part 3)—2015, “Code of Practice for Design Loads (Other Than Earthquake) for Buildings and Structures,” provides guidelines for determining the wind load on buildings and other structures, including steel pipe racks. For present study, following wind parameters are considered:

Type: IndianIS 1893 (Part 4):2015 Include Accidental Load

Parameters	Value	Unit
Zone Factor	0.16	
Response reduction Factor (RF)	3	
Importance factor (I)	1.5	
Rock and soil site factor (SS)	1	
*Spectral Acceleration Coefficient (Sa/g)	0	
Category of Structure	2	
Damping ratio (DM)	0.02	
*Multiplying Factor for Zone Factor (DF)	0	
*Period in X Direction (PX)		seconds
*Period in Z Direction (PZ)		seconds

4.7.1 Wind Load Calculation According to IS 875 (Part 3): 2015

Basic wind speed V_b , = 39 m/s	Considered for Vadodara
Design wind speed $V_z = V_b \times k_1 \times k_2 \times k_3 \times k_4$	Cl 6.3 of IS 875 (Part 3): 2015
Risk coefficient (K_1) = 0.92	Cl 6.3.1 Table 1 of IS 875 (Part 3): 2015
Terrain, height factor (K_2)	Cl 6.3.2.2 Table 2
Topography factor (K_3) = 1	Cl 6.3.3 of IS 875 (Part 3): 2015
Importance factor for cyclonic region (K_4) = 1.15	Cl 6.3.4 of IS 875 (Part 3): 2015
Wind pressure $P_z = 0.6 V_z^2$	Cl 7.2 of IS 875 (Part 3): 2015
Design wind pressure $P_d = P_z \times K_d \times K_a \times K_c$	Cl 7.2 of IS 875 (Part 3): 2015
(Here $K_d = K_a = K_c = 1$, Therefore $P_d = P_z$)	

4.8 Earthquake Force (EQ)

Earthquake force on pipe rack refers to the force that are exerted on the structure during an earthquake event. The magnitude of these forces will depend on factors such as the location of pipe rack, category of structure and damping ratio of structure. For present study, following earthquake parameters are considered:- value Zone Factor-0.16, Response reduction Factor (RF)-3, Importance factor (I)-1.5, Rock and soil site factor (SS)-1, *Spectral Acceleration Coefficient (Sa/g)- 0, Category of Structure 2-2, Damping ratio (DM)-0.02.

Static method of design is considered for present study.

Table 2 Load combination for strength design

Load condition	Load combination
Erection	1.5 (DL + LL + PE)
	1.5 (DL + PE) ± 1.5 WL
	0.9 (DL + PE) ± 1.5 WL
	1.2 (DL + LL + PE) ± 1.2 WL
Operating	1.5 (DL + LL + PO + PF ± AF)
	1.5 (DL + PO + AF ± WL]
	0.9 (DL + PO + AF) ± 1.5WL
	1.5 (DL + PO + AF + EQ)
	0.9 (DL + PO + AF) ± 1.5 EQ
	1.2 (DL + LL + PO + AF ± WL)
	1.2 (DL + 0.5LL + PO + AF + EQ]
Test	1.5 (DL + LL + PT)
	1.5 (DL + PT) ± 1.5 (0.25 WL)
	1.2 (DL + 0.5LL + PT) ± 1.2 (0.25 WL)

5 Load Combinations

Following load combinations are considered for the strength design and serviceability design [7] (Table 3).

Table 3 Load combination for serviceability design

Load condition	Load combination
Erection	DL + 0.8LL + PE
	DL + PE ± WL
	DL + PE ± WL
	DL + 0.8 * LL + PE ± 0.8 * WL
Operating	DL + 0.8 * LL + PO + PF ± AF
	DL + PO + AF ± WL
	DL + PO + AF ± WL
	DL + PO + AF + EQ
	DL + PO + AF ± EQ
	DL + 0.8*LL + PO + AF ± 0.8 * WL
	DL + 0.8LL + PO + AF + 0.8 * EQ
Test	DL + LL + PT
	DL + PT ± 0.25(0.8 * WL)
	DL + 0.5LL + PT ± 0.25 WL

6 Results and Discussion

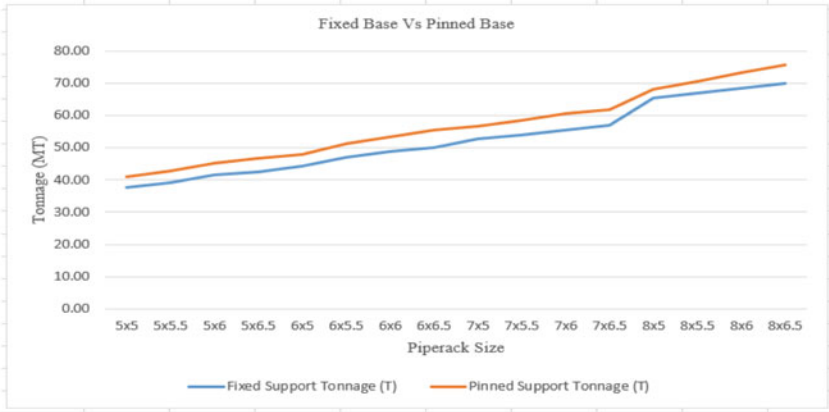
STAAD.Pro analysis and design have been carried out for 32 pipe racks as demonstrated above, and structural steel tonnage has been given as shown in Table 4. Utility ratio for strength design and serviceability design is restricted up to ~ 0.95.

Various graphs have been plotted to study the behavior and draw the conclusion (Figs. 5, 6, 7, 8 and 9).

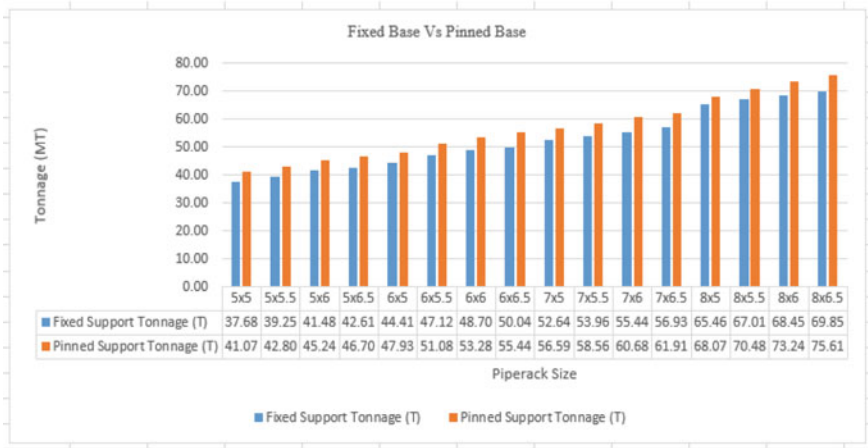
Table 4 Structural steel tonnage for fixed base condition and pinned base condition

S. No	Pipe rack details	Fixed support	Pinned support	%
	($W \times H$)	Tonnage (T)	Tonnage (T)	Difference
1	5 × 5	37.68	41.07	8.25
2	5 × 5.5	39.25	42.80	8.29
3	5 × 6	41.48	45.24	8.31
4	5 × 6.5	42.61	46.70	8.76
5	6 × 5	44.41	47.93	7.35
6	6 × 5.5	47.12	51.08	7.76
7	6 × 6	48.70	53.28	8.60
8	6 × 6.5	50.04	55.44	9.75
9	7 × 5	52.64	56.59	6.99
10	7 × 5.5	53.96	58.56	7.86
11	7 × 6	55.44	60.68	8.65
12	7 × 6.5	56.93	61.91	8.05
13	8 × 5	65.46	68.07	3.84
14	8 × 5.5	67.01	70.48	4.92
15	8 × 6	68.45	73.24	6.53
16	8 × 6.5	69.85	75.61	7.61

Note Tonnage mentioned in above table is without connection weight



a Graph Showing difference in Structural Steel Tonnage for Pinned Base & Fixed Base



b Graph Showing difference in Structural Steel Tonnage for Pinned Base & Fixed Base

Fig. 5 a Graph showing difference in structural steel tonnage for pinned base and fixed base.
b Graph showing difference in structural steel tonnage for pinned base and fixed base

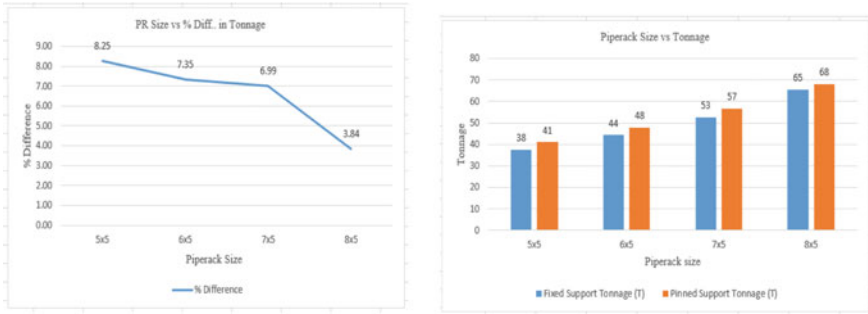


Fig. 6 Graph for 5 M height (1st tier) versus pipe racks of width 5, 6, 7 and 8 M

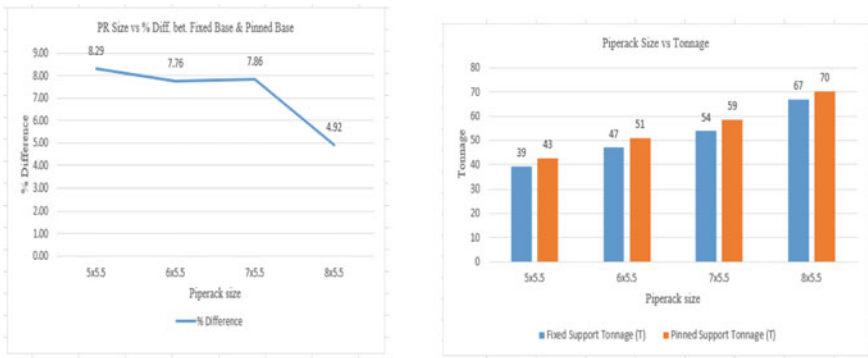


Fig. 7 Graph for 5.5 M height (1st tier) versus pipe racks of width 5, 6, 7 and 8 M

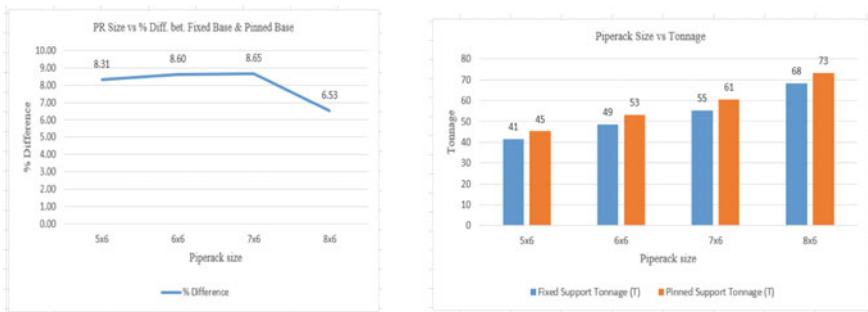


Fig. 8 Graph for 6 M height (1st tier) versus pipe racks of width 5, 6, 7 and 8 M

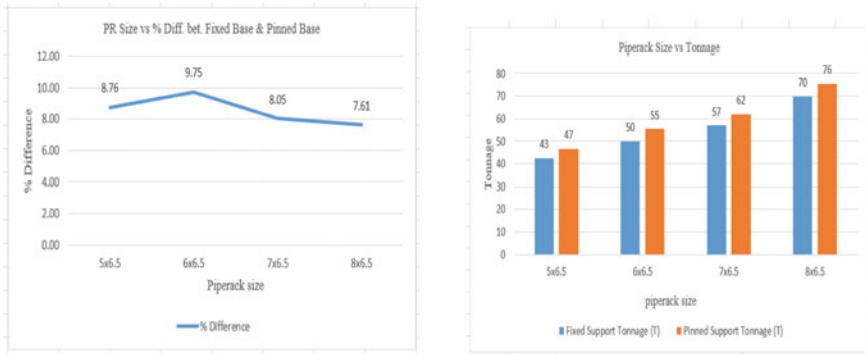


Fig. 9 Graph for 6.5 M height (1st tier) versus pipe racks of width 5, 6, 7 and 8 M

7 Conclusion

- Structural steel tonnage required for pipe rack members is more for hinged base condition as compared to fixed base condition.
- The structural steel tonnage for pinned base condition is 3–10% more than fixed base condition.
- As the height of first tier of pipe rack increases, percentage difference in structural steel increases.
- For same height of first tier, as the width of pipe rack increases, percentage difference in structural steel decreases.
- As far as structural steel tonnage is concerned, fixed base condition is economical. However, final decision shall be taken considering foundation cost also.

Acknowledgements The author wishes to thank Mr. K. N. Sheth (HOD, Civil Engineering, Dharm-sinh Desai University, Nadiad), Mr. Kiran M Patel (HOD, Civil and Structural Department, L&T Chiyoda LTD, Vadodara) and Mr. Ketan V Patel (Divisional Head, Civil and Structural Department, L&T Chiyoda LTD, Vadodara) for their valuable guidance and support.

References

1. Bendapudi KV (2010) Structural design of steel pipe support structures. Struct Mag 1–3
2. Manoharan R, Srivastava A (2020) Rational hybrid analytical model for steel pipe rack quantification in oil & gas industries. Civil Eng J 6(4):1–10
3. Drake RM, Walter RJ (2010) Design of structural steel pipe rack. Eng J (4):241–252
4. Singh NJ, Ishtiyaque M (2016) Optimized design & analysis of steel pipe racks for oil & gas industries as per international codes & standards. 5(10):16–28

5. Arya AS, Kumar A, Ajmani JL (1982) Design of steel structures, 6th ed. (The Limit State Method), pp 1–888
6. IS 800 (2007) Indian standard for general construction in steel—code of practice
7. IS 1893 (Part 1 & 4) (2015) Indian standard for criteria for earthquake resistant design of structures

Experiment Investigation of Protecting the R.C. Structure from Heat Exposure by Using Composite Materials



K. Sandhya, S. Barath Raj, and S. Muthu Kumar

1 Introduction

Fibre-reinforced polymers (FRP) are utilized for RC beams as a retrofitting material and as an externally bonded confinement. They have the potential to address a variety of concrete durability issues, including reinforcement corrosion, fire, acid attack, freezing and thawing and so on [1]. This is due to their excellent strength, low weight to strength ratio, corrosion resistance and endurance in a variety of challenging situations. Due to the tremendous improvements in architectural technology, modern buildings are more complex and composed of stronger and lighter materials. Numerous insulating materials, whether organic, inorganic, synthetic or natural, are easily flammable or ignite when exposed to high fire temperatures. In contrast, non-combustible substances like concrete and metals (apart from aluminium and magnesium) won't burn and will actually promote combustion when subjected to a fire state. It is important to keep in mind that these materials can only withstand a fire for a few amount of time [2]. In this regard, the strength and deformation of these materials substantially decrease at high temperatures and longer durations. As a result, when exposed to fire conditions, structural components could disintegrate. Fires can't always be totally avoided, but we can stop them from spreading. A significant percentage of the allowable or additional time in a fire situation is determined by the expected temperature growth of the fire, which is impacted by the type and quantity of combustible materials present as well as the ventilation condition. Influence of strain rate on concrete under high temperature. The results revealed that after being exposed to high temperatures, there was a significant strain rate dependency. Although coatings cannot completely fend off fire, they can prevent it from spreading or keep a structure from being destroyed, giving materials time to flee [3]. Thermal

K. Sandhya · S. Barath Raj · S. Muthu Kumar (✉)

Department of Civil Engineering, College of Engineering and Technology, SRM Institute of Science and Technology, Kattankulathur, Tamil Nadu 603203, India

e-mail: muthukus1@srmist.edu.in

insulation materials can be thought of as a way to reduce energy losses in both residential and commercial structures. The bulk of insulating materials are composed of composite materials, also referred to as polymer materials or fillers and other additives. There are numerous types of thermal insulation for buildings, but the majority of them fall into one of two categories: inorganic materials or biological materials. Polymers are well known for being good insulators due to their stable physical and chemical properties. Contrarily, the addition of inorganic fillers can be enhanced or adjusted to change the mechanical properties, hence enhancing the strength of the composite. Innovative thermal insulation materials as aerogels [4], gas-filled panels and vacuum insulation panels are being developed in addition to traditional thermal insulation materials.

1.1 Fibre-Reinforced Polymer (FRP) Material

FRP sheets are circumferentially or longitudinally mounted to the exterior of reinforced concrete (RC) structural components in this method to provide increased flexural capacity. Externally bonded reinforcement (EBR) is one of the primary techniques for strengthening reinforced concrete structures utilizing FRP near-surface mounted (NSM). One or more FRP laminates are adhered to the tensile surface of reinforced cement concrete members using the externally bonded reinforcement. The usage of FRP composite materials for structural strengthening and repair is growing. FRP's key benefits are its light weight and ease of handling. It is not susceptible to corrosion and won't corrode. Reinforced fibres are combined with a polymer matrix to form composites. It enables the transfer of loads between resin matrix and fibres that have a chemical bond. There are four types of FRP that are frequently utilized in the sector. Typically, glass, carbon, aramid and basalt fibres are used [5].

1.2 Insulation

Both organic and inorganic materials are typically used as insulation. Insulation is a term used to describe a protective material. Any form, size or surface can be covered using these materials. Building insulation is used to keep the interior at a constant temperature. The wool, wood fibre, calcium silicate and glass cellulose are all good insulation materials. These materials were selected based on whether they are combustible or not. When subjected to fire conditions, combustible materials can cause structural elements to collapse. When exposed to a fire, non-combustible materials won't any harm. Flammable substances like wool and wood fibre. Non-combustible substances as glass cellulose and calcium silicate [6, 7].

2 Literature Review

2.1 General

This section discusses a variety of subjects, such as general temperature research and various studies on insulation layers used to buildings.

2.2 Thermal Study on Insulation Materials

Panahi et al. [3] utilizing the computational finite element programme ABAQUS, it was determined whether externally bonded, near-surface mounted and combination externally near-surface mounted FRP composites could effectively strengthen reinforced concrete beams flexurally.

Zach et al. [2] have looked at the fibrous materials, which trap air within their fibres, restricting gaseous heat conduction by reducing gas molecule collisions and decreasing heat transmission by convection. As a result, they form excellent thermal insulation materials. Natural fibres have several advantages over synthetic fibres, including being environmentally friendly and renewable.

2.3 Literature Study on FRP Materials

Correia et al. [8] FRP materials are often wrapped around or fastened to reinforced concrete (RC) elements to increase their strength or deformability. Due to the loss of their tensile and binding properties at high temperatures, FRP reinforcement systems are frequently used in buildings where fire danger ratings are necessary. The fire resistance of RC structural elements that have been reinforced with FRP is currently evaluated in this article. The review analyses its main themes after a discussion of the crucial elements that control the mechanical behaviour of FRPs at high temperatures and how overheating impacts their relationship with concrete. The study gives a summary of experimental and numerical studies on the fire behaviour of RC beams, slabs and columns reinforced with FRP.

2.4 Literature Study on Concrete Beam

Yang et al. [9] in this study, it is investigated using the rigorous solution how the distributions of intermediate shear stress are impacted by equal loading settings. It is found that, despite the shear forces on the same cross section only making a small contribution, the flexural moments on the cross sections at the plate ends have a

substantial impact on the stress concentration. The shear stress along the interface between concrete and the adhesive layer is approximated in this work based on an observation.

Bisby et al. [10] the findings of three insulated FRP-fortified reinforced concrete (RC) columns' full-scale fire resistance tests are presented in this study, it is conceivable to achieve suitable fire resistance ratings for FRP-wrapped concrete columns by properly incorporating significant fire prevention devices into the entire FRP-strengthened structural system.

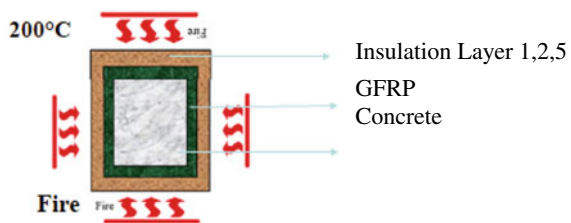
2.5 Summary of Literature Review

Forecasts of the behaviour of FRP concrete beams under extreme heat are accurate and dependable in the investigation governing equations to predict stresses and deflection based on the behaviour of the beam and FRP. From the study more research work is on the stiffness, strength, and other material properties at high temperatures of FRP materials. Debonding and other negative behaviours at the FRP/concrete contact point. At higher temperatures, simulations of the material and binding are more accurate. An examination of the tension stiffening stress–strain relationship for FRP reinforced or strengthened RC beams.

2.6 Concept for Fire Protection

It has been taken in reality case which is exposed by fire with four sides of the outer layer of the RC beam given in Fig. 1.

Fig. 1 Development of heat at 4 sides of the beam



2.7 Inorganic Materials

Thermal conductivity diminishes at relatively low temperatures according to the linear temperature-dependent law. It has occasionally been hypothesized that inorganic expanding materials like fibreglass or rock wool exhibit this phenomenon. Slurry is frozen to create alumina foams, which are then utilized to make refractory bricks. Alumina used as insulation in refractory bricks becomes less thermally conductive as temperature rises. The organic insulation material, which has a very low conductivity, will benefit from a protective layer provided by this type of non-combustible property [8]. Bricks with vertical holes have more thermal resistance as advantage to the addition of perlite to porous clay.

2.8 Bonding Agents

Tie constraint was used for interaction purpose between beam and GFRP shown in Table 1.

Table 2 displays the thermal properties of insulation materials, such as thermal conductivity, thermal resistance, specific heat capacity and density.

Table 1 Bonding efficiency

Material	Connection property
Concrete to steel	Embedded region
Concrete to GFRP	Tie connection
GFRP to insulation layer	Surface to surface contact

Table 2 Review of insulation material properties

Material	Thermal conductivity (w/m k)	Thermal resistance at 100 mm (km ² /w)	Specific heat capacity (J/(kg k))	Density (kg/m ³)
Wood fibre [14]	0.038	2.5	2100	160
Glass cellulose [15]	0.035	2.632	2020	27–65
Wool [15]	0.038	2.63	1800	23
Calcium silicate	0.058	3	2500	232

Table 3 Mechanical traits of several FRP material classes [16]

Reinforcing material	Yield strength (Mpa)	Density (g/cm ³)	Tensile strength (MPa)	Specific gravity	Elastic modulus (GPa)	Strain at break, %
Steel	500	7.75–8.05	–	7.8	200	–
Glass FRP	600–1400	2.11–2.70	480–1600	1.5–2.5	35–51	1.2–3.1
Basalt FRP	1000–1600	2.15–2.70	1035–1650	2.7–2.89	45–59	1.6–3.0
Aramid FRP	1700–2500	1.39–1.45	1720–2540	1.38–1.39	41–125	1.9–4.4
Carbon FRP	1755–3600	1.55–0.76	1720–3690	1.0–1.1	120–580	0.5–1.9

2.9 Strength Enhancement in FRP

A new technology for strengthening is near-surface mounting that is externally bonded. By enhancing one another, they aid in overcoming the limitations of the externally bounded reinforcement (EBR) and near-surface mounted (NSM) techniques in this strategy. The most likely failure modes for reinforced concrete beams as well as reinforced concrete beams with flexural and shear strengthening were both outlined in an experimental investigation for strengthening existing structures with FRP technology. These results are displayed in Table 3. It is possible to conclude that combining EBR with NSM is a useful strategy for dispersing the overall stresses brought on by increased loadings [16]. The un-strengthened beam's lower range of 71–105% had a larger range of flexural resistance above the control beam of about 350%. MPa and GPa stand for megapascals and gigapascals. The pascal is a unit of pressure given in Table 3.

3 Analytical Study

3.1 Modelling, Assigning Property and Assembly

Models for various layers, including GFRP and insulation material, were first built. Wool, wood fibre, calcium silicate and glass are the four different insulating materials. The layers are all varied sizes with a constant thickness of 1.2 mm. The material property was assigned to the models after they had been made, and they were put together. The beam is 2 m long, 200 mm wide and 300 mm deep.

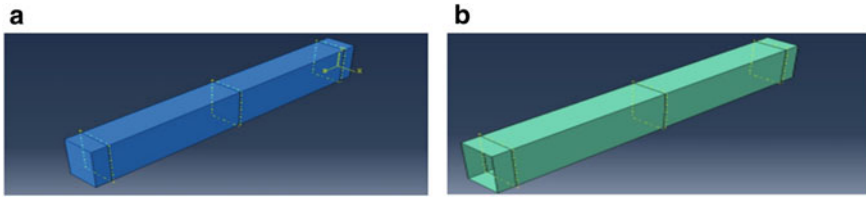


Fig. 2 a RC Beam model. b GFRP layer model

3.2 Analysis of Beam

ABAQUS, a finite element analysis (FEA) programme, was used to design the insulation layer and conduct the relevant experiments. The dimensioned of beam is 2.0 meter long, 202.40 millimetre wide and 302.40 millimetre deep layer were modelled and used with varying applications of loading and temperature at various points along the beam shown in Fig. 2. When FRP is wrapped around a beam, the 1.2 mm layer thickness increases strength. The analyses were carried out using FEA models with various diameters and a constant length of 2 m. 30 °C was the predetermined temperature. Thermal properties including density, thermal conductivity, and specific heat were required in order to conduct the required FEA tests. The temperature-dependent fluctuations in value, the appropriate temperatures and the different loadings made available for the beam pinned support was offered, and it was placed 100 mm from the beam's ends. Because temperature was a factor, a transient state analysis was conducted. Analysis of various layers, including GFRP and wood fibre, was conducted under a variety of loading scenarios, including 10, 20, 30, 40 and 50%. The specifics of the load applied as pressure to the beams. In order to determine the critical temperature, a temperature of 1000 °C was chosen based on earlier studies.

3.3 Deflection of Insulated RC Beam with Insulation

For each solid component, the programme builds a solid mesh with 3D solid elements. Because temperature was involved, the analysis type was transient state. Analysis was performed on a variety of layers, including GFRP and wood fibre, under various loading scenarios, including 10, 20, 30, 40 and 50% [9] shown in Fig. 5. Based on earlier studies, a temperature of 1000 °C was chosen to determine the critical temperature. In order to conduct the analyses, beam was used as a model for applications at various points of the beam with outside dimensions. Details of the load applied to the beams in the form of pressure, as per the predetermined done on segments 20, 30 and 50. There was a surface to surface relationship. The support supplied was of the kind that was shown at the bottom of Fig. 3. 2 kN of load due to the change in loading and temperature at various places along the beam, corresponding deflection

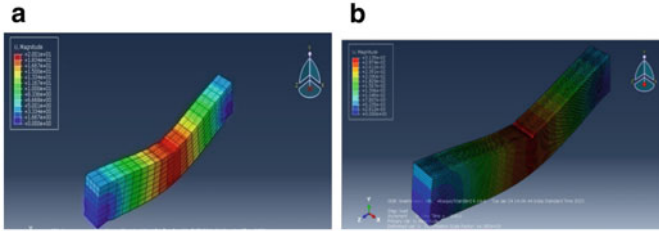


Fig. 3 **a** Deflection of RC beam with insulation, **b** deflection of insulated beam

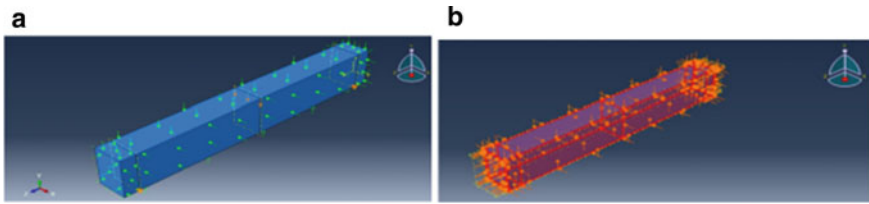


Fig. 4 **a** Thermal load on beam, **b** thermal load on insulation beam (magnitude is 30)

of 2.2 mm was predicted [9]. The analyses were carried out using FE models with constants that had external dimensions of 200 mm × 300 mm and a thickness of 1.2 mm for GFRP.

Room temperature applied on RC beam as predetermined temperature after that increased the degree of temperature which is increased by 200 °C shown in Fig. 4.

Tie constraint was used for interaction between these 2 layers such as GFRP and insulation layer when exposed to fire condition was found delamination case shown in Fig. 5.

4 Results and Discussion

4.1 Effect of Temperature on Beam

The deflection of concrete and GFRP as a function of temperature and beam deflection when load was applied is indicated in Table 4. Load is treated as constant in this case and load value taken from literature. Only when the magnitude increased, which happened every 30 min, the temperature was changed [10].

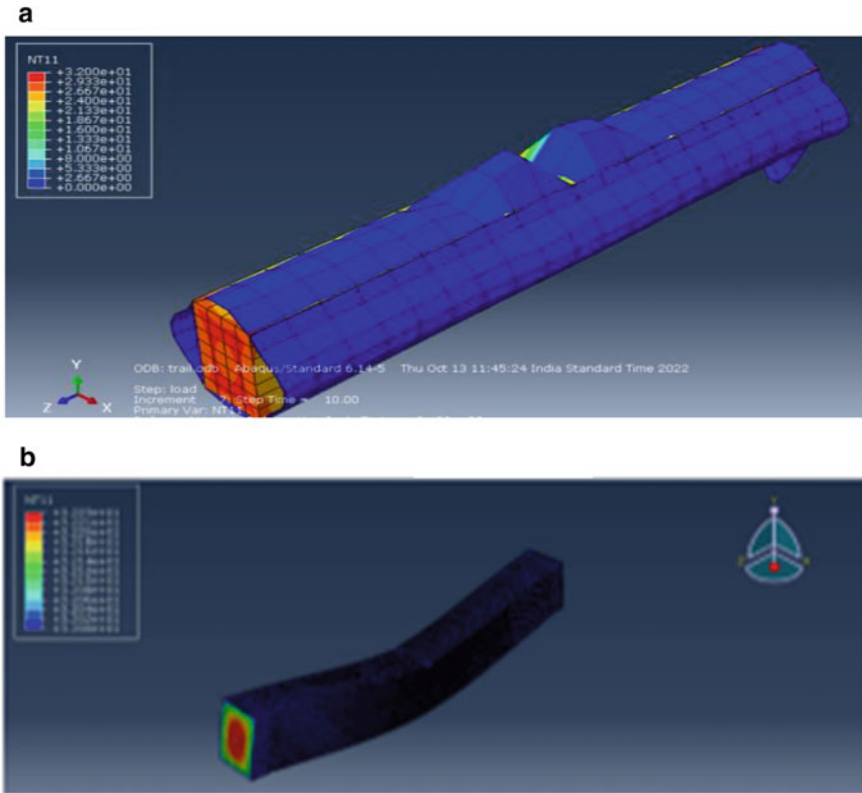


Fig. 5 **a** Temperature effect on FRP-strengthened beam, **b** temperature effect on Insulated beam (thermal load = 32°)

Table 4 Temperature effect on beam

Model	Input			Output		
	Load (kN)	Time (s)	Magnitude	Temperature (°C)	Deflection (mm)	
					Concrete	GFRP
1.a	2	180	20	32	1.7	58
1.b	2	3600	20	44	1.83	59
1.c	2	5400	20	60	1.89	59.7
2.a	2	180	30	30	1.7	58
2.b	2	3600	30	60	1.8	59.7
2.c	2	5400	30	83	2	60
3.a	2	180	50	50	1.8	58.4
3.b	2	3600	50	101	2.1	60
3.c	2	5400	50	139	2.7	61

4.2 One Case Insulation

The models for different layer were first created such as GFRP and insulation material. The five different insulations are wool, wood fibre, calcium silicate, glass cellulose and aerogel. Each insulation chosen based on combustible, non-combustible category and natural, artificial category. First case has considered only one insulation material such as wood fibre which is wrapped on RC beam when exposed to fire condition was found temperature as well as deflection given in Table 5. Further remaining insulation considered to wrapping on RC beam.

The stiffness profile at the location of concentrated loading on the middle portion of the beam is shown in Fig. 6 after the beam was subjected to concentrated loading and temperature. It was found that with increase in temperature, the deflection got reduced. The maximum deflection of 2.7 occurred at a time of 1.5 h from the time of heating.

Table 5 One insulation on RC beam

Model	Types of cases	Input			Output	
		Magnitude (°C)	Load (kN)	Time (h)	Temperature (°C)	Deflection (mm)
A	BGF	200	100	1	60	1.8
B	BGW	200	100	1	83	2.0
C	BGC	200	100	1	39	2.7
D	BGG	200	100	1	41	2.2
E	BGA	200	100	1	43	1.8

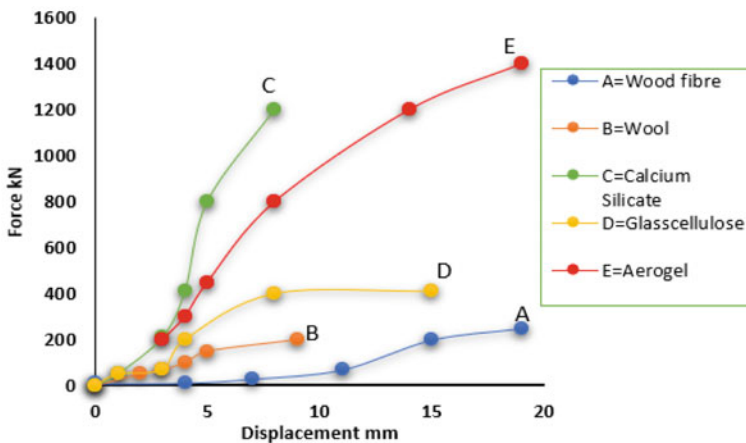


Fig. 6 Stiffness profile of concrete beam without thermal load

After the beam was subjected to combined stress and temperature, this graph displays the stiffness profile of the GFRP wrapping on the beam at the site of concentrated loading on the left portion of the beam (see Fig. 6). This graph displays a wrapped beam's nonlinear curve.

5 Conclusion

- From this study, it found that the deflection got reduced with decrease in the temperature. This may be due to the expansion of the section during the rise in temperature when wrapped combination insulation case. In one case, insulation was found less and high deflection.
- When wrapping FRP on RC beam was found delaminate of layer from concrete under thermal condition. To address, this insulation layer was created based on combustible and non-combustible category to add on beam when exposed to fire condition were found less deflection as well as less temperature transfer and there is no delaminate.
- Study extended for single layer of insulation material. At first insulation case which gives initially good on reduction of temperature. Similar cases have considered with only one non-combustible insulation material added at outer layer. When exposed to fire condition was found outer layer which is wrapped by calcium silicate got reduced with temperature as maximum.
- The multiple insulation layers case under fire were found gradually reduces the temperature to the core concrete beam. It found a choice of an insulation a system with minimum quantity and reduce the cost as well as enhance the safety of the building against fire.

Acknowledgements I wish to express my sincere thanks to Department of Civil Engineering, College of Engineering and Technology, SRM Institute of Science and Technology for giving this opportunity.

References

1. Al-Homoud DMS (2005) Performance characteristics and practical applications of common building thermal insulation materials. *Build Environ* 40:353–366
2. Zach J, Hroudová J, Brožovský J, Krejza Z, Gailius A (2013) Development of thermal insulating materials on natural base for thermal insulation systems. *Procedia Eng* 57:1288–1294. <https://doi.org/10.1016/j.proeng.2013.04.162>
3. Izadi A, Panahi M, Zareei SA (2020) Flexural strengthening of reinforced concrete beams through externally bonded FRP sheets and near surface mounted FRP bars. *Case Stud Constr Mater* 15:e00601
4. Hung LD, Pasztory Z (2021) An overview of factors influencing thermal conductivity of building insulation materials. *J Build Eng* 44:102604

5. Steau E, Mahendran M (2021) Elevated temperature thermal properties of fire protective boards and insulation materials for light steel frame systems. *J Build Eng* 43:102571
6. Firmo JP, Correia JR, Bisby LA (2015) Fire behaviour of FRP strengthened reinforced concrete structural elements: a state-of-the-art review. *Compos Part B Eng* 80:198–216
7. Hollaway LC (2010) A review of the present and future utilisation of FRP composites in the civil infrastructure with reference to their important in-service properties. *Constr Build Mater* 24:2419–2445
8. Lam L, Teng JG, Chen JF, Smith ST (2003) Behaviour and strength of FRP strengthened RC structures: a state-of-the-art review. *Proc Inst Civil Eng Struct Build* 156:51–62
9. Yang J, Ye J, Niu Z (2007) Interfacial shear stress in FRP-plated RC beams under symmetric loads. *Cem Concr Compos* 29:421–432
10. Kodur VKR, Bisby LA, Green MF (2006) Experimental evaluation of the fire behaviour of insulated fibre-reinforced-polymer-strengthened reinforced concrete columns. *Fire Saf J* 41:547–557
11. Liu Q, Zhang Y, Xu H (2008) Properties of vulcanized rubber nanocomposites filled with nanokaolin and precipitated silica. *Appl Clay Sci* 42:232–237
12. Shokrieh MM, Omid MJ (2009) Tension behavior of unidirectional glass/epoxy composites under different strain rates. *Compos Struct* 88:595–601
13. Abbood IS, Odaa SA, Hasan KF, Jasim MA (2021) Properties evaluation of fiber reinforced polymers and their constituent materials used in structures—a review. *Mater Today Proc* 43:1003–1008
14. Sun L et al (2020) The influence of double-layered distribution of fire retardants on the fire retardancy and mechanical properties of wood fiber polypropylene composites. *Constr Build Mater* 242:118047
15. Lemougna PN et al (2020) Utilisation of glass wool waste and mine tailings in high performance building ceramics. *J Build Eng* 31:101383
16. Mugahed Amran YH, Alyousef R, Rashid RSM, Alabduljabbar H, Hung CC (2018) Properties and applications of FRP in strengthening RC structures

The Impact of Glass Fiber on Controlled Permeable Formwork Self-Compacting Concrete



S. Kandasamy , S. Syed Ibrahim, and N. Pannirselvam

1 Introduction

The building demolition (C&D) waste is the main problem to the environment, nearly 35% of the world's trash is made up of C&D wastes [1]. In most nations, C&D waste is illegally discarded, and this is common in India. Therefore, it is crucial to stress how much the creation of sustainable structures will contribute to the preservation of our ecosystem. The caliber of a concrete structure's surface skin serves as a measure of its durability. The formwork system is also affecting the quality of surface skin of concrete [2].

The regular formwork system is impermeable to air and water; therefore, increased water to cement ratio at the concrete/formwork contact zone. This is main reason for decrees the strength of cover concrete. A good resistance surface concrete is needed for durable concrete. Many researchers [3–17] reported that by use of controlled permeable formwork (CPF) liner, the quality of cover concrete enhanced by 5–30 mm.

In general, stress and brittleness are two of concrete's weaknesses. As soon as the concrete is laid, cracks will begin to appear before it has properly grown stronger or hardened. The structures' service life and durability are reduced by the cracks.

S. Kandasamy (✉)

Department of Civil Engineering, Vel Tech Rangarajan Dr. Sagunthala R&D Institute of Science and Technology, Chennai, Tamil Nadu 600062, India

e-mail: drskandasamy@veltech.edu.in

S. Syed Ibrahim

Department of Civil Engineering, Ilahia College of Engineering and Technology, Mulavoor, Kerala, India

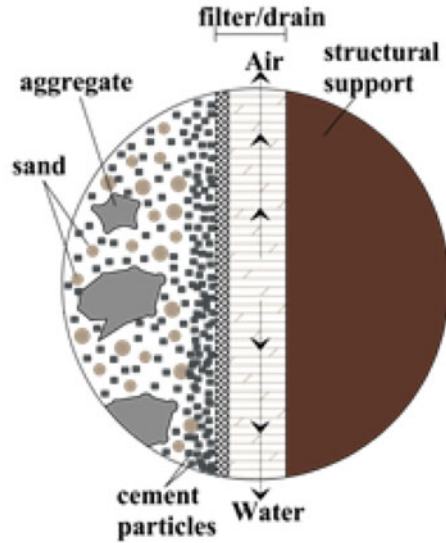
e-mail: syed_ibms@yahoo.co.in

N. Pannirselvam

Department of Civil Engineering, SRM Institute of Science and Technology, Kattankulathur, Chengalpattu District, Tamil Nadu 603203, India

e-mail: pannirsn@srmist.edu.in

Fig. 1 Working principle of CPF liner



The most recent advancements in concrete technology use fibers as reinforcement, particularly glass fibers, with the goal of controlling cracks [18–20]. However, there is no research on how glass fiber affects self-compacting concrete cast with CPF liners (Fig. 1).

2 Experimental Program

2.1 Materials

A OPC (grade 43) that complied with IS: 8112-2013 [21] was used in this study. Zone II river sand, per IS: 383-2016 [22], was employed. Coarse aggregate of 20mm was used as per IS: 383-1970 [22]. The concrete laboratory's use of water complies with IS: 456-2000 [23]. Fly ash that complied with IS: 3812-2013 was obtained for this inquiry from the Thermal Power Station in Ennore, Chennai [24]. In compliance with IS: 9103-1999 [25], a super plasticizer (SP) based on polycarboxylate ether polymer was also employed. Additionally, cohesion and segregation resistance were improved by using the viscosity modifying admixture (VMA).

2.2 Concrete Mixture Proportions

The precise mix ratios were given in Table 1.

Table 1 Concrete mix details

Mixture designation	Cement (kg/m ³) (C)	Fly ash (kg/m ³) (FA)	Glass fiber (%) (GF)	Coarse aggregate (kg/m ³) (CA)	Fine aggregate (kg/m ³) (FA)	Water (l/m ³) (W)	Super plasticizer (l/m ³) (SP)	Viscosity modifying admixture (l/m ³) (VMA)
IMF	400	90	0	840	850	190	4.5	2.0
CPF	400	90	0	840	850	190	4.5	2.0
CPF + 0.5%GF	400	90	0.5	840	850	190	4.5	2.0
CPF + 1.0%GF	400	90	1.0	840	850	190	4.5	2.0
CPF + 1.5%GF	400	90	1.5	840	850	190	4.5	2.0
CPF + 2.0%GF	400	90	2.0	840	850	190	4.5	2.0

2.3 CPF Liner

In this study, a type II CPF liner was used. This liner has a filter on one side and a drain on the other [3].

2.4 Glass Fiber (GF)

As shown in Fig. 2, the glass fibers used in this investigation are readily accessible for purchase (Zart, India). A percentage of the overall volume of CPF concrete is supplemented with glass fibers.

Fig. 2 Glass fiber



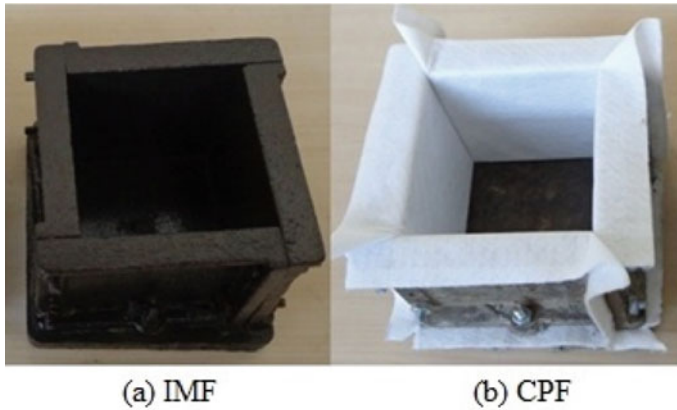


Fig. 3 Concrete cube specimen preparations

2.5 Preparing and Curing Samples

The steel mold was used to create the samples of self-compacting concrete. As seen in Fig. 3b, the CPF liner was affixed to the plate.

To achieve a homogeneous dispersion, the superplasticizer and viscosity modifying additive are first mixed with water. The ingredients were combined for one minute in a dry state before the addition of 50% of water. After three minutes of continuous mixing, the glass fibers were added gradually while under running water to prevent clumping. For five minutes, the fibers were continuously mixed to ensure even distribution. The mold was filled with concrete. After 24 h, the concrete specimen was taken out of the mold.

2.6 Specimen Testing

Compressive strength was carried out using 150 mm size cube specimens in accordance with IS: 516-1959) [26]. The splitting tensile strength was carried out on the cylindrical specimen (200 mm long and 100 mm dia.) in accordance with IS: 5816-1999 [27]. The flexural tensile test was carried out on the prism specimens (100 mm × 100 mm × 500 mm) in accordance with IS: 516-1959 [26]. A 100 mm cube specimens were used for rebound hammer, dynamic hardness, and rockwell hardness test in accordance with IS: 13311: Part 2-1999 [28], ASTM A 956 [29], and ASTM E 18 [30], respectively.

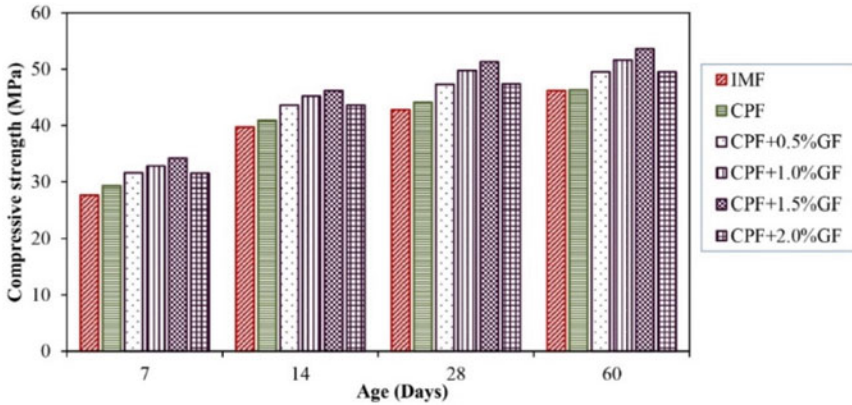


Fig. 4 Compressive strength versus age

3 Results and Discussion

3.1 Compressive Strength

Figure 4 shows that at all ages, CPF specimens showed higher compressive strength than IMF specimens. The improvement was rather minimal, falling between 3 and 6%. Additionally, GF addition of 0.5, 1.0, and 1.5% resulted in an additional enhancement in compressive strength of roughly 10, 15, and 19% relative to IMF specimens in CPF-lined self-compacting concrete. It is shown that the compressive strength significantly increases with an increase in GF percentage from 0.5 to 1.5%. This might be because GF delays the onset of early cracks in concrete specimens made with CPF. In contrast, an addition of 2.0% GF to CPF walled self-compacting concrete resulted in an improvement of roughly 10% over IMF sample. According to the data, the compressive strength starts to decline at a GF percentage of 2.0%. The results show that after 1.5% GF increase, no additional improvements were seen.

3.2 Flexural Strength

The flexural strength data are shown in Fig. 5. The development was significant and varied between 21 and 28%. The lowest portion of the beam faces the maximum tensile stresses during the flexure test. A thin (shell) layer was created to CPF specimens. This solid cover zone retards the formation of the first fracture. As a result, concrete now has greater flexural strength. Additionally, flexural strength was improved in self-compacting concrete with GF additions of 0.5, 1.0, and 1.5% by approximately 36, 44, and 51% relative to IMF specimens. Flexural strength is discovered to significantly increase with an increase in GF percentage from 0.5

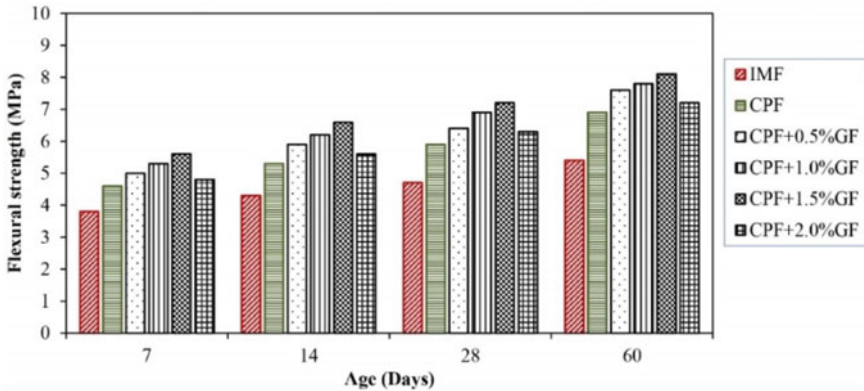


Fig. 5 Flexural strength versus age

to 1.5%. This might be because GF delays the onset of early cracks in concrete specimens made with CPF. The improvement over IMF specimens was only approximately 31% with a 2.0% GF increment in CPF concrete. It has been shown that the flexural strength begins to decline with a GF percentage increase of 2.0%. When GF was added in excess of 1.5%, the flexural strength decreased as seen in the prior characteristics.

3.3 Split Tensile Strength

The split tensile strength of the IMF specimens was lower than the CPF specimens as shown in Fig. 6. The improvement was significant and varied between 11 and 21%. A thin (shell) layer was created to CPF specimens. While the shell breaks, the specimen quickly ruptures, while the internal concrete provides no resistance. The tensile strength of the (split) material is greatly boosted as a result of this failure progression. Additionally, split tensile strength was improved in self-compacting concrete with GF additions of 0.5, 1.0, and 1.5% by approximately 32, 38, and 56% relative to IMF specimens. It is discovered that the tensile strength significantly upsurges with an increase in GF percentage from 0.5 to 1.5%. This might be the result of GF delaying the onset of early cracks in specimens of CPF-lined self-compacting concrete. However, the improvement was about 26% compared to IMF specimens when 2.0% GF was added to CPF-coated self-compacting concrete. The split tensile strength appears to begin to decline with a GF percentage increase of 2.0%.

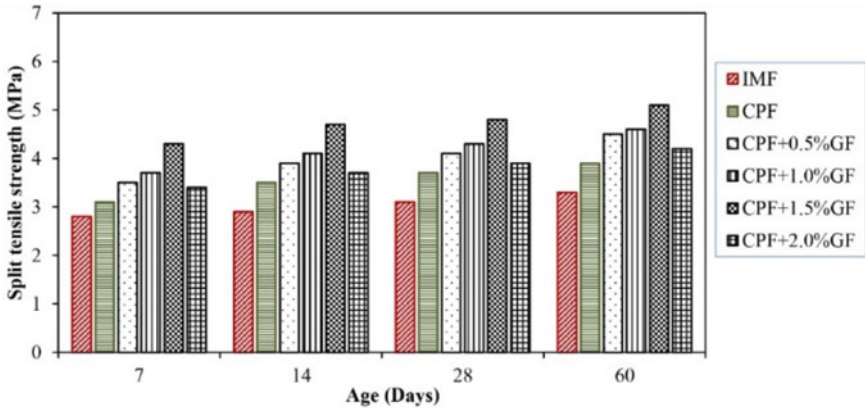


Fig. 6 Split tensile strength versus age

3.4 Rebound Number

The rebound number data are shown in Fig. 7, and it can be seen that the rebound number for CPF specimens has significantly increased. The improvement was substantial and fell between the ranges of 42 and 55%. Additionally, an additional improvement in rebound number of around 57, 66, and 75% with regard to IMF specimens was seen with GF addition of 0.5, 1.0, and 1.5% in CPF-lined self-compacting concrete. It is discovered that the rebound number increases significantly when the GF percentage rises from 0.5 to 1.5%. In contrast, an addition of 2.0% GF to CPF-lined self-compacting concrete resulted in an improvement of roughly 60% over IMF sample. It appears that as the GF percentage rises to 2.0%, the rebound number begins to fall.

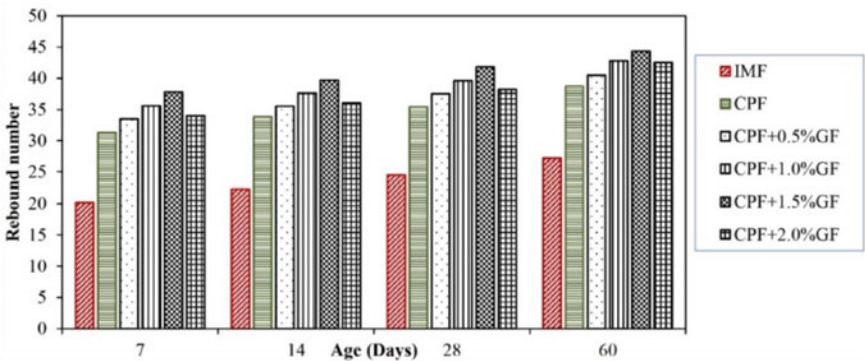


Fig. 7 Rebound number versus age

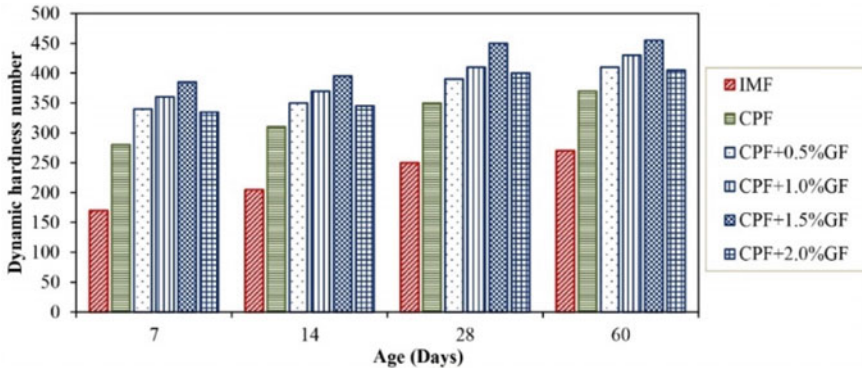


Fig. 8 Hardness number versus age

3.5 Hardness Number (Dynamic)

The hardness number of various concrete mixtures is shown in Fig. 8. The results showed that CPF specimens had a higher dynamic hardness number than IMF specimens at all ages. The improvement was remarkable and ranged from roughly 37–65%. Additionally, an additional improvement in dynamic hardness number of about 70, 79, and 92% with regard to IMF specimens was seen with GF addition of 0.5, 1.0, and 1.5% in CPF concrete. It is discovered that the rebound number increases significantly when the GF percentage rises from 0.5 to 1.5%. The improvement over IMF specimens was only about 69% with a 2.0% GF increment in CPF concrete. It is shown that the dynamic hardness number begins to decrease as the GF percentage rises to 2.0%.

3.6 Superficial Hardness Number (Rockwell)

The hardness of various concrete mixtures is depicted in Fig. 9. The results revealed that CPF specimens had a higher rockwell hardness number than IMF specimens at all ages. The improvement was substantial and fell between the range of roughly 23–35%. Additionally, an extra improvement in the superficial hardness number of roughly 40, 54, and 71% compared to IMF specimens was seen with GF additions (0.5, 1.0, and 1.5%) in CPF concrete. It is shown that the superficial hardness number increases with an increase in GF percentage from 0.5 to 1.5%. The improvement over IMF specimens was only about 59% with a 2.0% GF increment in CPF concrete. It is seen that the hardness number begins to decrease as the GF percentage increases to 2.0%.

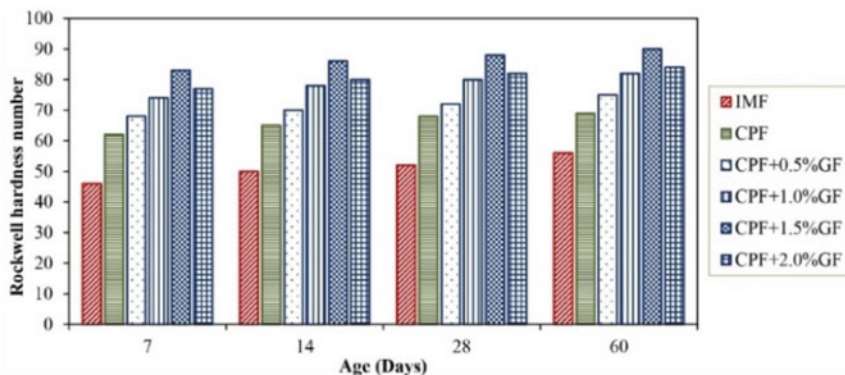


Fig. 9 Superficial hardness number versus age

4 Conclusion

The current experimental inquiry led to the following conclusions.

1. The compressive strength of CPF concrete was slightly improved (by about 3–6%) when compared to regular concrete. The performance of CPF concrete with GF, however, was notable and ranged from 10 to 19%.
2. The split tensile strength of CPF concrete was much higher (by roughly 11–20%). The incremental improvement in the CPF concrete with GF was found to be between 32 and 56%.
3. The flexural tensile strength of CPF concrete was much higher (21–28%) than that of regular concrete. CPF concrete with GF showed improvements of between 36 and 51%.
4. In comparison to conventional concrete specimens, the rebound number of CPF concrete was much higher (by roughly 42–55%). The incremental improvement in the CPF concrete with GF was between 57 and 75%.
5. Compared to normal concrete specimens, CPF concrete had a significantly higher dynamic hardness number (approximately 37–65%). CPF concrete with GF showed improvements of between 70 and 92%.
6. The rockwell hardness number of CPF concrete was considerably increased by 23–35% as compared to specimens of conventional concrete. The incremental improvement in the CPF concrete with GF was found to be between 40 and 71%.

References

1. Solis-Guzman J, Marrero M, Montes-Delgado M, Ramirez-De-Arellano A (2009) A Spanish model for quantification and management of construction waste. *Waste Manage* 29:2542–2548
2. Kwasny J, Sonebi M, Plasse J, Amziane S (2015) Influence of rheology on the quality of surface finish of cement-based mortars. *Constr Build Mater* 89:102–109
3. Price WF (2000) Controlled permeability formwork. CIRIA Report, C 511
4. Law DW, Molyneaux T, Aly T (2017) Long term performance of controlled permeability formwork. *Aust J Civ Eng* 15:117–125
5. Liu J, Miao C, Chen C, Liu J, Cui G (2013) Effect and mechanism of controlled permeable formwork on concrete water adsorption. *Constr Build Mater* 39:129–133
6. Brueckner R, Williamson SJ, Clark LA (2012) Rate of the thaumasite form of sulphate attack under laboratory conditions. *Cement Concr Compos* 34:365–369
7. Ye J, Yu L, Chen Y (2019) Study on the mitigative effect of controlled permeability formwork liner on early-age shrinkage of box-girder concrete. *J Adv Mater Sci Eng* 1–8. Article ID 4150279
8. Figueiras H, Nunes S, Sousa J, Figueiras J (2009) Combined effect of two sustainable technologies: self compacting concrete and controlled permeability formwork. *Constr Build Mater* 23:2518–2526
9. Kothandaraman S, Kandasamy S (2016) The effect of controlled permeable formwork liner on the mechanical properties of concrete. *Mater Struct* 49:4737–4747
10. Kothandaraman S, Kandasamy S, Sivaraman K (2016) Studies on the effect of controlled permeable formwork liner on the properties of self compacting concrete. *Constr Build Mater* 118:319–326
11. Aissoun BM, Gallias JL, Khayat KH (2017) Influence of formwork material on transport properties of self-consolidating concrete near formed surfaces. *Constr Build Mater* 146:329–337
12. Garg S, Nim KS, Bajpai KK, Misra S (2019) Enhancement in the quality of near surface concrete using some formwork liners. *Constr Build Mater* 207:722–733
13. Guo BL, Wang BM, Han Y, Jiang R (2020) Improvement of concrete property with controlled permeability formwork. *Rev Rom Mater* 50(3):379–386
14. Megid WA, Khayat KH (2020) Variations in surface quality of self-consolidation and highlyworkable concretes with formwork material. *Constr Build Mater* 238. Article ID 117638
15. Sørensen HE, Poulsen SL (2018) Effect of curing regime and controlled permeability formwork on early chloride penetration into fly ash concrete. In: *High tech concrete: where technology and engineering meet*. Springer, Cham, January
16. Tahmoorian F, Nemati S, Soleimani A (2020) A state of the art on the structural performance of fabric formwork systems. *Eng Solid Mech* 8(1):49–62
17. Kothandaraman S, Kandasamy S (2017) The effect of controlled permeable formwork (CPF) liner on the surface quality of concrete. *Cem Concr Compos* 76:48–56
18. Afroughsabet V, Biolzi L, Özbakkaloğlu T (2016) High-performance fiber-reinforced concrete: a review. *J Mater Sci* 51:6517–6551
19. Soong WH, Raghavan J, Rizkalla SH (2011) Fundamental mechanisms of bonding of glass fibre reinforced polymer reinforcement to concrete. *Constr Build Mater* 25:2813–2821
20. Tassew ST, Lubell AS (2014) Mechanical properties of glass fiber reinforced ceramic concrete. *Constr Build Mater* 51:215–224
21. IS:8112: 2013 (2013) Specification for ordinary Portland cement—43 Grade. Bureau of Indian Standards, New Delhi
22. IS:383: 2016 (2016) Specification for coarse and fine aggregate for concrete. Bureau of Indian Standards, New Delhi
23. IS:456: 2000 (2000) Plain and reinforced concrete. Code of Practice. Bureau of Indian Standards, New Delhi
24. IS: 3812: 2013 (2013) Pulverized fuel ash-specification: part 2-for use of admixture in cement mortar and concrete. Bureau of Indian Standards, New Delhi

25. IS: 9103: 1999 (1999) Specification for concrete admixtures. Bureau of Indian Standards, New Delhi
26. IS:516: 1959 (1959) Methods of tests for strength of concrete. Bureau of Indian Standards, New Delhi
27. IS:5816: 1999 (1999) Method of test for splitting tensile strength of concrete. Bureau of Indian Standards, New Delhi
28. IS:13311: Part 2: 1992 (1992) Methods of test for non-destructive testing of concrete. Bureau of Indian Standards, New Delhi
29. ASTM A 956-2002 (2002) Standard test method for LEEB hardness testing of steel products. Am Soc Test Mater
30. ASTM E 18-2008 (2008) Standard test method for Rockwell hardness of metallic materials. Am Soc Test Mater

Ramifications of Payment Delays on Contractors in the Construction Industry



B. Hemanth Sai Kalyan, S. Anandh, and S. Sindhu Nachiar

1 Introduction

Infrastructure development has many facets that contribute to the successful completion of a project. Proper planning, seamless execution, and adequate contingency plans to face unforeseen circumstances are among the few aspects which help in a hassle-free construction process [1]. Similarly, there are many other characteristics that hamper progress. As it involves many stakeholders, and often the confined thought of their responsibilities, their aspirations and their well-being might persuade them from not being a team player [2, 3]. During a discussion or argument between the collaborators, time and again, responsibilities are not stressed as much as rights do. It is the classical case of not what one brings to the table, but rather what one gets from the table. One of the unavoidable things in the construction industry is risk. Contractual provisions which do not define enough risk allocations can be a major hurdle in the dispute resolution process. Bestowing responsibilities based on contractual agreements will ensure smooth analysis in the post-mortem stage [4–7]. This is one of the major causes of conflict. The mismanagement in the initial stages of conflict is a direct result of the manifestation of a dispute.

Often it is misunderstood that disputes and conflicts are one and the same. But, with respect to the current interactionism theory, in certain situations and circumstances, for the development of an organization, conflicts can be considered as a constructive factor [3, 8]. Having said that, it is to be noted that this is not true in all the scenarios.

B. Hemanth Sai Kalyan · S. Anandh (✉) · S. Sindhu Nachiar
Department of Civil Engineering, Faculty of Engineering and Technology, SRM Institute of Science and Technology, Kattankulathur, Tamil Nadu 603203, India
e-mail: anandhs@srmist.edu.in

B. Hemanth Sai Kalyan
e-mail: hb0040@srmist.edu.in

S. Sindhu Nachiar
e-mail: sindhus@srmist.edu.in

But conflict management with strong evidential based backing as well as smooth communication can always be helpful for dispute resolution [3, 9–11].

According to many researchers, disputes in the construction industry have several reasons, but they can mostly be attributed to delays. Delays caused are of various types such as payment delays, performance delays, and working delays. Delays cannot be only confined to time as many other parameters in a construction process are associated with them [12–14]. For example, a time delay in handing over the project may result in a delay in the clearance of bills, and sometimes, interest for the same is also added [15, 16]. Such examples are many in number in the sector. While having several cases with similarities it is to be noted that there are other cases with different/peculiar combinations of dispute causes [17].

As nothing can be generalized, it is unfair to say that the industry as a whole is responsible but rather a victim of this. The consequences of the disputes on the stakeholders, especially contractors and consultants are to be considered as these are the major participants in the industry [18, 19]. It is important to identify the aftermath of the disputes as it affects in many ways most commonly being lack of funds to cater to new projects and also to repay interests to the loans taken either by banks or financiers. Many researchers have studied the causes of disputes in the construction sector and using various frameworks and models, suggested some dispute-mitigating solutions [20–30]. The objective of this research is to identify the major causes of disputes in the construction industry along with identifying the subcategories to understand the intricate causes of dispute which affect the stakeholders, especially contractors.

2 Methodology

It is evident that no dispute occurs due to a single cause. Among the many multiple causes for a dispute, one particular cause might have a significantly higher importance than the others. But is always a combination of 2–3 causes or rather factors for a dispute [17, 31]. In this study, the major identified causes for disputes are categorized into four types: non-payment, poor performance, contractual changes and compensation. Furthermore, each cause is divided into sub-causes which makes it easier to analyze and narrow down to the root cause. For the purpose of this study, judicial cases with pronounced judgments have been taken as primary data. It is to gather information from both sides of the disputed parties as to what is the actual cause of disputes. Petition from one party as well response from the other along with the final judgment comprises a wholesome data required for the intrinsic analysis. Identification of sub-causes is done in this analysis which helps in narrowing down the root cause.

It is to be noted that the occurrence of each cause represents the repetitions of sub-causes in each case while other causes might also be contributing to that particular dispute. For example, in a particular case, the major cause of the dispute is due to non-payment because of changes in contractual agreements. But it also means it can

be categorized into the contractual changes category as well. Thus, it a combination of payment related issues and contractual issues. Similarly, there are other cases as well that might have even three or more common categories combined. Therefore, it is essential to consider each sub-cause before finalizing the data set for analysis. Table 1 presents the major disputes and their sub-causes.

Different sub-causes and their occurrence in the case studies are depicted in Fig. 1. Among payment-related issues, deductions had highest number. Similarly, unsatisfactory work quality in poor performance and insufficient documents in contractual changes, had the highest occurrences. Delays in compensation had the least occurrence while the rest were same.

Table 1 Cause and sub-causes of disputes with occurrences

S. no	Causes	Sub-causes	Occurrence	Total
1	Non-payment	Changes in contractual agreements	6	30
		Adamant non-payment	4	
		Deductions	12	
		Non-releasing of deposits	4	
		Unjustified delays in payment by owner	4	
2	Poor performance	Delays on part of the contractor	8	41
		Unsatisfactory work quality	18	
		Changes incorporated apart from contractual agreements	5	
		Material discrepancies	10	
3	Contractual changes	Intermediate changes in contract	8	36
		Delays in approvals	10	
		Insufficient documents	11	
		Ambiguities in contracts	7	
4	Compensation	Denial of compensation	5	18
		Delays in compensation	3	
		Compensated amount is not satisfactory	5	
		Increase interest rates for compensation	5	
Total			125	

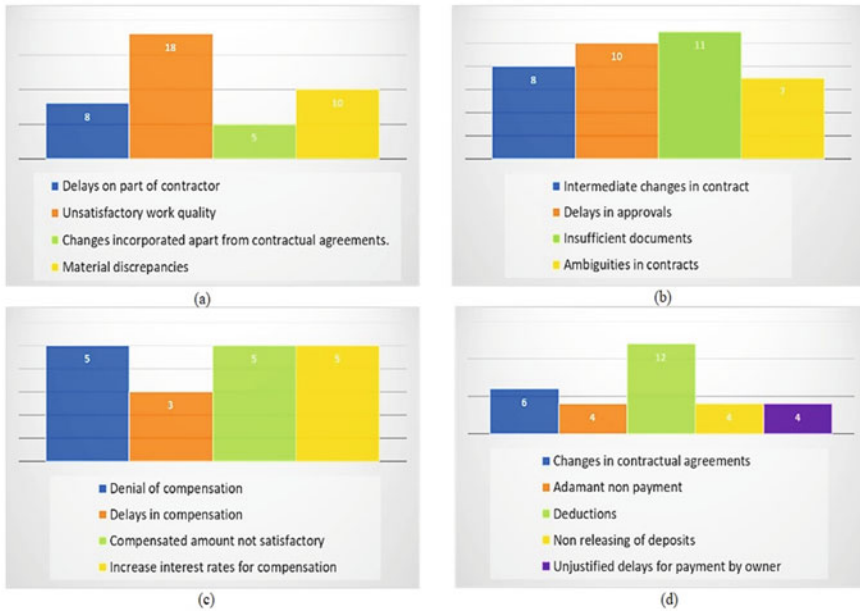


Fig. 1 a Poor Performance; b Contractual Changes; c Compensation; d Non-payment

3 Results and Discussions

3.1 Ramification Based on Sub-cause

Each cause of dispute has a particular effect on the contractor or owner or the project on the whole. Stakeholders’ risk allotment and control over the project have a major part to play in these attributions of causes. It is thus important to know the importance of one another and understand the consequences of disputes.

3.2 Non-payments

Payments are delayed and denied citing certain reasons from time to time. One of the most frequent causes of dispute is that of non-clearance of bills during or after work execution. Project progress suffers because of this as it is imperative to keep the money rolling in any case for the smooth flow of work. Due to the fact that most projects require heavy capital investments, it is usually done in batches and depends on how much percentage of the project completion is achieved at that point in time. Based on the contractual clauses, certain projects have the flexibility of bill clearance based on the percentage of work completed and these are in phases. Often these can

be seen in loan sanctions and phase-wise release of funds. With this audit scenario happening periodically, the work execution is monitored. Deduction during such phases or even after the completion stage due to various trivial reasons puts a heavy burden on the contractors. But some cases are peculiar that have no reason to halt the payments, even after the work is completed according to the clauses prescribed in the contract. The worst part is there is no proper reasoning given by the defaulter as to why the payment is put on hold.

3.3 Poor Performance

Delays in work progress is one of the main reasons for poor performance. It involves improper planning as well as irregular allocation of resources which halt the process. Delaying the process of construction as well as the idle of labor situation can easily be avoided, but this control and responsibility lie entirely on the contractor. Adequate contingency plans need to be pre-defined in an event of unforeseen delays. Delays is not only confined to time, but also it affects the quality of construction as every phase of construction has to have certain continuity aspects which does not allow unsatisfactory work. Also to save the costs of construction and get away with minimum effort spent on site, usually materials are used in apart from those that have been agreed upon during the contract drafting stage. It is the biggest mistake which a contractor does, and the worst part is, it is done in all awareness. Material quality cannot be altered with and it is the reason the work quality is blatantly exposed. It does affect the profile of the contractor, and in this case, the blame cannot be put onto others. With such a reputation, it also makes it difficult to acquire collaborative projects which this might even lead to black listing of the contractor for future projects.

3.4 Contractual Changes

When a contract is awarded to a particular bidder, it is an impetus that all the necessary documentation is done prior to it, and similarly, when the project is being handed over to the owner, all the documentation works are complete. Sometimes due to trust of goodwill or delays or communication gaps, etc., this process is delayed, and it causes serious damage to the project. In cases observed where in the pre-planning and initiation stage, the construction work is commenced without proper drawings, detailing, and approvals. Any one of these may be catastrophic as in the case of lack of drawing, it is difficult to carry out the work as is the case without detailing. Without prior approvals and necessary No Objection Certificates (NOC), it is illegal to carry forward construction and it is the responsibility of the owner as well as the contractor to make sure it is properly done.

3.5 Compensation

Compensation-related disputes can have significant consequences for civil contractors. These disputes can impact a contractor's cash flow, damage their reputation, increase their legal costs, and lead to a loss of productivity. As such, it is important for contractors to take steps to avoid compensation-related disputes and to resolve them quickly and efficiently if they do arise. This can help to protect the contractor's financial stability, reputation, and ability to compete in the marketplace. One of the most immediate consequences of compensation-related disputes is a negative impact on cash flow. When payments are delayed or withheld, contractors may struggle to cover their operating costs and pay their suppliers and employees. This can lead to cash flow problems that can make it difficult for contractors to continue working on the project. Compensation-related disputes can also damage a civil contractor's reputation. When disputes become public, it can create a perception that the contractor is unreliable or unprofessional. This can make it more difficult for the contractor to win future contracts and could harm their ability to attract and retain talented employees.

4 Conclusion

Major ramifications identified due to these causes are the stoppage of cash flow, the reputation of the contractor being spoiled, and a decline in the working standards of the contractor. Although consequences due to disputes do not change with respect to each type of dispute, but the process of analyzing the causes of disputes might help in finding a probable mitigating solution for the same. If the dispute cannot be resolved through negotiation or mediation, it may be necessary to involve lawyers and go to court. This can be a costly and time-consuming process, and the outcome is not always guaranteed. In addition, even if the contractor ultimately prevails in court, they may still have to pay significant legal fees. Therefore, future research in this prospect can be carried out in which the problem identification is done by analyzing the causes of disputes and a dispute resolution with respect to the significance of the disputes as well as the consequences is proposed.

References

1. Kappagomtula CL (2017) Overcoming challenges in leadership roles—managing large projects with multi or cross culture teams. *Eur Bus Rev* 29:572–583. <https://doi.org/10.1108/EBR-12-2015-0177/FULL/HTML>
2. Powell WW (1987) Hybrid organizational arrangements: new form or transitional development. *Calif Manage Rev* 30:67–87. <https://doi.org/10.2307/41165267.d>
3. Amoah C, Nkosazana H (2022) Effective management strategies for construction contract disputes. *Int J Build Pathol Adapt*. <https://doi.org/10.1108/IJBPA-01-2022-0004>

4. Yao H, Chen Y, Zhang Y, Du B (2021) Contractual and relational enforcement in the aftermath of contract violations: the role of contracts and trust. *Int J Manag Proj Bus* 14:1359–1382. <https://doi.org/10.1108/IJMPB-06-2020-0202>
5. Kandil O, Yehia N, Hamed T (2022) Threats to contractor's cash flow under remeasured public works contracts. *J Legal Affairs Dispute Resol Eng Constr.* [https://doi.org/10.1061/\(asce\)la.1943-4170.0000507](https://doi.org/10.1061/(asce)la.1943-4170.0000507)
6. Seneviratne K, Michael GV (2018) Disputes in time bar provisions for contractors' claims in standard form of contracts. *Int J Constr Manag.* <https://doi.org/10.1080/15623599.2018.1484854>
7. Akal AY (2022) What are the readability issues in sub-contracting's tender documents? *Buildings* 12:839. <https://doi.org/10.3390/buildings12060839>
8. Padhy J, Jagannathan M, Kumar Delhi VS (2021) Application of natural language processing to automatically identify exculpatory clauses in construction contracts. *J Legal Affairs Dispute Resol Eng Constr* 13:04521035. [https://doi.org/10.1061/\(asce\)la.1943-4170.0000505](https://doi.org/10.1061/(asce)la.1943-4170.0000505)
9. Fenn P (2008) Conflict management and dispute resolution. In: Lowe D (eds) *Commercial Management of Projects: Defining the Discipline*, pp 234–269. <https://doi.org/10.1002/9780470759509.ch11>
10. Singh A, Vlatas DA (1991) Using conflict management for better decision making. *J Manag Eng* 7:70–82. [https://doi.org/10.1061/\(asce\)9742-597x\(1991\)7:1\(70\)](https://doi.org/10.1061/(asce)9742-597x(1991)7:1(70))
11. Mohamed H, Ibrahim A, Soliman A (2014) Reducing construction disputes through effective claims management. *Am J Civil Eng Architect* 2, 186–196. <https://doi.org/10.12691/ajcea-2-6-2>
12. Ansah RH, Sorooshian S (2018) 4P delays in project management. *Eng Constr Archit Manag* 25:62–76. <https://doi.org/10.1108/ECAM-09-2016-0199/FULL/HTML>
13. Alaghbari W, Kadir MRA, Salim A (2007) The significant factors causing delay of building construction projects in Malaysia. *Eng Constr Archit Manag* 14:192–206. <https://doi.org/10.1108/09699980710731308/FULL/H>
14. Wang TK, Ford DN, Chong HY, Zhang W (2018) Causes of delays in the construction phase of Chinese building projects. *Eng Constr Archit Manag* 25:1534–1551. <https://doi.org/10.1108/ECAM-10-2016-0227/FULL/HTML>
15. Hashem M, Mehany MS, Grigg N (2016) Delay claims in road construction: best practices for a standard delay claims management system. *J Legal Affairs Dispute Resol Eng Constr* 8:1–5. [https://doi.org/10.1061/\(asce\)la.1943-4170.0000186](https://doi.org/10.1061/(asce)la.1943-4170.0000186)
16. Adamu PI, Akinwumi II, Okagbue HI (2019) Reactive project scheduling: minimizing delays in the completion times of projects. *Asian J Civil Eng* 20:1189–1202. <https://doi.org/10.1007/s42107-019-00177-3>
17. Hemanth B, Kalyan S, Sekar A, Nachiar SS, Ravichandran PT (2022) Discerning recurrent factors in construction disputes through judicial case studies—An Indian perspective. *MDPI.* <https://doi.org/10.3390/buildings12122229>
18. Marzouk M (2014) *Analyzing delay causes in Egyptian construction projects.* Elsevier, Amsterdam
19. Elawi GSA, Algahtany M, Kashiwagi D (2016) Owners' perspective of factors contributing to project delay: case studies of road and bridge projects in Saudi Arabia. *Proc Eng* 145:1402–1409. <https://doi.org/10.1016/j.proeng.2016.04.176>
20. Tayeh BA, Alaloul WS, Alkurdi MH, Abu Aisheh YI, Musarat MA (2022) Evaluation of biases in construction project dispute resolution: case study. *J Legal Affairs Dispute Resol Eng Constr.* [https://doi.org/10.1061/\(asce\)la.1943-4170.0000525](https://doi.org/10.1061/(asce)la.1943-4170.0000525)
21. Chou JS (2012) Comparison of multilabel classification models to forecast project dispute resolutions. *Expert Syst Appl* 39:10202–10211. <https://doi.org/10.1016/j.eswa.2012.02.103>
22. Lu W, Zhang L, Pan J (2015) Identification and analyses of hidden transaction costs in project dispute resolutions. *Int J Project Manage* 33:711–718. <https://doi.org/10.1016/j.ijproman.2014.08.009>
23. Elziny AA, Mohamadien MA, Ibrahim HM, Abdel Fattah MK (2016) An expert system to manage dispute resolutions in construction projects in Egypt. *Ain Shams Eng J* 7:57–71. <https://doi.org/10.1016/j.asej.2015.05.002>

24. Kalyan BHS, Prakash AA (2019) Case studies on dispute resolutions in construction projects for framing an expert solution. *Int J Recent Technol Eng* 8:476–483
25. Wind Y, Saaty TL (1980) Marketing applications of the analytic hierarchy process. *Manage Sci* 26:641–658. <https://doi.org/10.1287/MNSC.26.7.641>
26. El-Sayegh SM (2009) Multi-criteria decision support model for selecting the appropriate construction management at risk firm. *Constr Manag Econ* 27:385–398. <https://doi.org/10.1080/01446190902759009>
27. Lam KC, Lam MCK, Wang D (2008) MBNQA-oriented self-assessment quality management system for contractors: fuzzy AHP approach. *Constr Manag Econ* 26:447–461. <https://doi.org/10.1080/01446190801965350>
28. Doloi H (2008) Application of AHP in improving construction productivity from a management perspective. *Constr Manag Econ* 26:841–854. <https://doi.org/10.1080/01446190802244789>
29. Darko A, Chan APC, Ameyaw EE, Owusu EK, Pärn E, Edwards DJ (2019) Review of application of analytic hierarchy process (AHP) in construction. *Int J Constr Manag* 19:436–452. <https://doi.org/10.1080/15623599.2018.1452098>
30. Ravi S, International KS-G (2022) Delineation of groundwater potential zone by integrating groundwater quality parameters using geospatial techniques and multi-criteria decision analysis—a case. Taylor & Francis, Milton Park. <https://doi.org/10.1080/10106049.2022.2115152>
31. Alshihri S, Al-Gahtani K, Almohsen A (2022) Risk factors that lead to time and cost overruns of building projects in Saudi Arabia. *Buildings* 12:902. <https://doi.org/10.3390/buildings12070902>

Mechanical Properties and Microstructural Analysis of Banana Stem Fibre in M40 Grade Concrete



S. Prakash Chandar, D. Murugan, and R. Ramasubramani

1 Introduction

In India, bananas are widely grown. After the fruits and leaves have been consumed, banana fibre can be easily retrieved from the pseudo stem. It is self-evident that ecological materials meet basic requirements such as pollution control and cost reduction. The use of environmentally friendly agricultural by-products such as rice husk, coconut fibres, sisal, and banana reduces energy consumption, conserves non-renewable natural resources, reduces pollution, and helps to maintain a healthy environment. It as chemical composition of cellulose (60–65%), hemicellulose (5–19%), lignin (5–10%). This paper mainly focusses on mechanical properties of the concrete. For investigating the mechanical properties of the cube compression, a 100 mm standard cube is prepared, cylinder tensile strength is tested with 100 × 200 mm specimen, flexural beam is prepared with 100 × 500 mm length, and the impact strength is tested with the 153 mm disc with the thickness of 65 mm. These specimens' mechanical behaviour was tested at various intervals. The characterization study was made for the concrete samples which shows the C–S–H formation and the voids present inside the specimen.

2 Basic Properties of Materials

The materials taken for this study are OPC-53 grade cementitious material, M-sand as a fine aggregate, blue metal as coarse aggregate, and banana stem fibre which were used in this work.

S. Prakash Chandar (✉) · D. Murugan · R. Ramasubramani
Department of Civil Engineering, Faculty of Engineering and Technology, SRM Institute of Science and Technology, KTR Campus, Kattankulathur, Tamil Nadu 603203, India
e-mail: prakashs2@srmist.edu.in

2.1 Cement

The OPC-53 was used, which met IS 12269 requirements. It is a powdered dry substance formed by lime and clay and mixing it with liquid to make cement that is added in the concrete. It serves as a binding agent. Cement, once cured, offers the required strong point for the building of enormous manufacturing structures. Lime (63.1%), silica (21.7%), alumina (1.34%), and sodium oxide (0.41%) are the primary chemical components of OPC cement [1]. A good cement should be free of lumps, which are caused by moisture in the air and can compromise the strength of the concrete.

2.2 Fine Aggregate

This research work focussed, M-sand as the fine aggregate in the production of concrete. Manufacturing sand should not exceed 4.75 mm in size. By adding precipitate as a grout, the capacity of concrete can be enhanced. The fine aggregate has passed IS: 2386 (Part-I), [2], demonstrating that it complies the codal provision of IS 383 [3]. The specific gravity of manufacturing sand is discovered to be 2.69. The particle size curve is shown in Fig. 1.

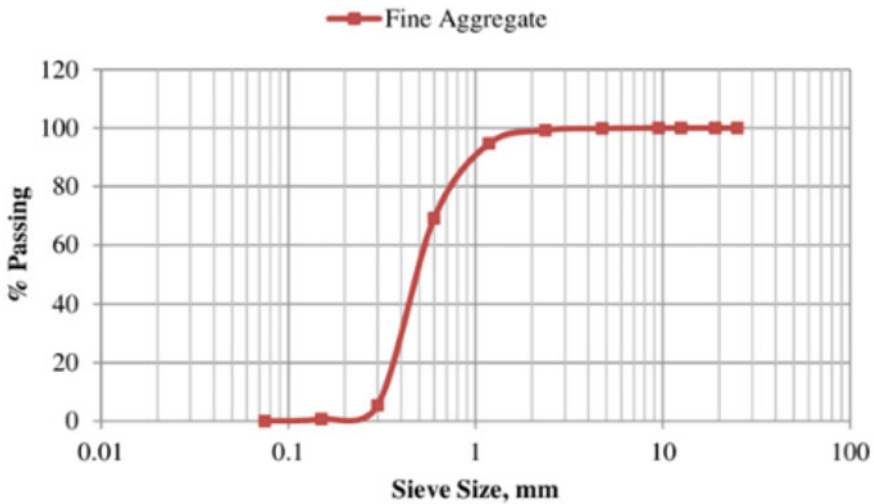


Fig. 1 Particle distribution of fine aggregate

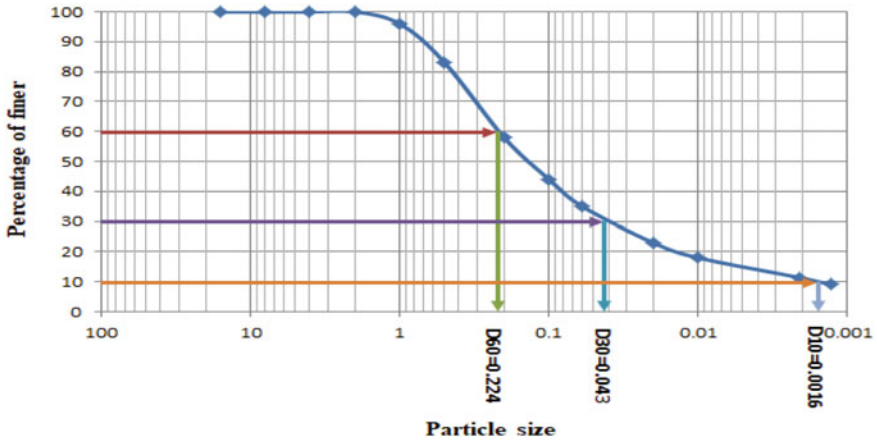


Fig. 2 Particle size distribution of coarse aggregate

2.3 Coarse Aggregate

The blue metal used in this study is of size 10 mm for preparing the concrete mixture. The aggregates which possess the size of more than 4.75 mm are taken as a coarse aggregate material, in which the 10 mm coarse aggregates are taken for this study and the basic properties of the material are tested. The blue metal aggregates used in this study achieve 2.87 of specific gravity, and it is assured that the aggregates are free from powders and waste muds. The material should enhance the crushing strength which directly improves the strength of the concrete and the distribution curve as shown in Fig. 2.

2.4 Banana Stem Fibre

This is the one of the maximum strength fibres when compared all other natural one. This fibre was collected from the banana stem and also biodegradable [4]. The physical properties of banana fibre are listed in Table 1 and the samples are shown in Fig. 3.

Table 1 Physical properties of banana fibre

Sl. no	Properties	Value
1	Density	1300 kg/m ³
2	Moisture content	12%
3	Tensile strength	5.8 N/mm ²
4	Young's modulus	3.6 N/mm ²

Fig. 3 Banana stem fibre

3 Experimental Setup

The testing setup is made for test the concrete specimen like cubes, cylinders, and beams as per the Indian Standard.

3.1 Design Mix

M40 grade concrete is developed according to IS10262-2009 [5] standards. For this study, a water cement ratio of 0.40 was assumed. With a cement content of 492.9 kg, the ratio was 1:1.23:2.26. The amount of banana stem fibre added varies depending on the percentage of bananas used (0.25, 0.50, 0.75, and 1). The concrete specimens were examined for mechanical strength after 3rd, 7th, and 28th days of casted.

3.2 Compressive Strength

The concrete to withstand the loads before failing is referred to as compressive strength. Because it proposals evidence on the concrete's possessions, among the various concrete tests, the compression test is the most important. The cube measuring 100 mm × 100 mm × 100 mm is casted by mixing the concrete in a mixer machine and then compacted with a table vibrator. After 24 h, the samples were demoulded and positioned in a curing tank to cure at various ages. Using the 3rd, 7th, and 28th days, the cubes are tested on a compression testing equipment in accordance with IS 516 (1959) [6].

3.3 Split Tensile Strength

Concrete is not normally anticipated to bear direct force due to its poor tensile strength and brittle nature. A load at which concrete specimens may breakage must be calculated from the split tensile test of concrete. When compared to other tensile tests, the concrete test on tensile test is straightforward to execute, and the most essential aspect is that it consistently delivers proper results. A cylinder with dimensions of 100 mm × 200 mm is casted to enhance the tensile performance. Using the cubes which are cured in various curing ages like 3, 7, and 28 days, the cylinders are tested on a compression testing equipment in accordance with IS 516 (1959) [6].

3.4 Flexural Strength

The beam specimen which is not reinforced with bars having some ability to withstand the load applied is known as flexural strength. The concrete specimens have necessity to withstand flexural loads. The bending performance is determined by beam measuring 100 mm × 500 mm. The specimen is tested on the 3rd, 7th, and 28th days, as specified in IS 516 (1959) [6].

3.5 Impact Resistance

The capacity of concrete to endure frequent hits and intake the loads without failure is determined using an impact cylinder. ACI committee 544.1R-96 [7] specifies the criteria for determining the concrete's impact factor.

3.6 SEM Analysis

A scanning of electron microscope was used to evaluate the microstructure of the materials used in this study. For testing, models are extracted at tested samples at various time breaks. The mixture of cement and aggregates samples taken for SEM analysis. The samples of cement-replaced concrete were examined in this study [8].

Table 2 Compressive strength test results

Materials	Percentage (%)	Compressive strength N/mm ²		
		3rd day	7th day	28th day
Conventional concrete mix	0	12.6	17.2	43.6
Banana stem fibre	0.25	12.8	18.3	44.2
	0.50	13.1	18.7	44.8
	0.75	14.8	15.6	44.6
	1	11.5	14.3	45.3

4 Results and Discussions

The key findings are described in the results' section of a research paper, and discussion section interprets the findings for readers and discusses their significance points.

4.1 Compressive Strength Test

The specimens were tested for compressive strength. Table 2 shows the result of the compressive strength. The strength is obtained at maximum of 1% when banana stem fibre is added in the concrete. The comparison of compressive strength values at various percentages added at different time intervals. Figures 4 and 5 show the test results on compressive strength [6].

4.2 Split Tensile Strength

Table 3 shows the values of the split tensile strength and the maximum strength obtained at 0.50% addition of banana stem fibre in the concrete. The comparison of strength values at various percentages added at different time intervals is shown in Fig. 6. Figure 7 shows the graph image of the split tensile strength [9].

4.3 Flexural Strength

Table 4 shows the values of the flexural strength. It is evident that the performance is increased to 1%. The comparison of flexural strength values at various percentages replaced at different time intervals [6] is shown in Fig. 8, and the graphical representation for the flexural strength is shown in Fig. 9.



Fig. 4 Compressive strength test

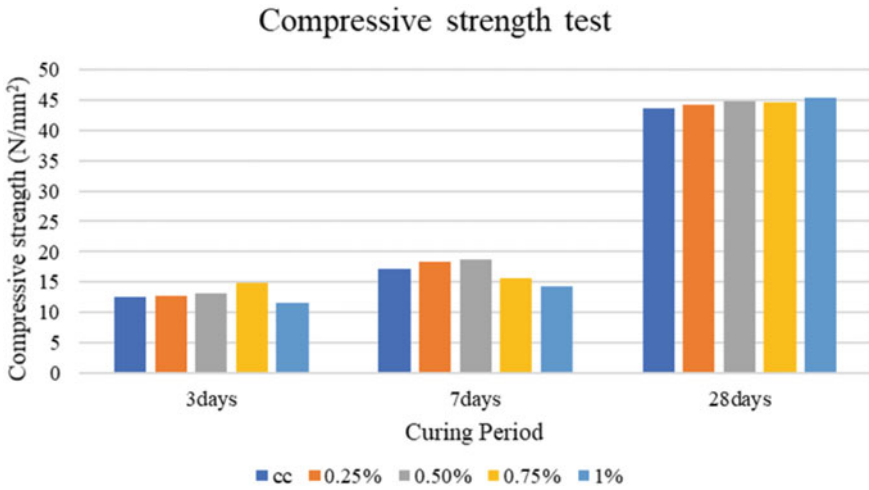


Fig. 5 Compressive strength value

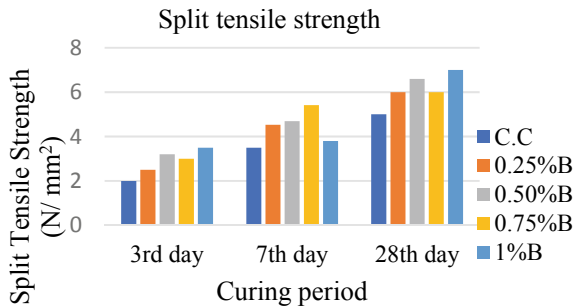
Table 3 Split tensile strength test results

Materials	Percentage (%)	Split tensile strength (N/mm ²)		
		3rd day	7th day	28th day
C.C	0	2.29	3.40	4.16
Banana stem fibre	0.25	2.67	2.96	3.91
	0.50	3.21	3.53	4.29
	0.75	3.01	3.50	3.69
	1	3.86	4.28	4.0



Fig. 6 Split tensile strength test value

Fig. 7 Split tensile strength value



4.4 Impact Resistance

The impact resistance of the concrete specimens is shown in Table 5. It is evident that the initial cracks are increased at 0.75% and final cracks are increased at 0.75%.

Table 4 Flexural strength value

Materials	Percentage (%)	Flexural strength (N/mm ²)		
		3rd day	7th day	28th day
C.C	0	2.0	3.50	5.0
Banana stem fibre	0.25	2.50	4.53	6.0
	0.50	3.20	4.69	6.60
	0.75	3.0	5.41	6.0
	1	3.50	3.80	7.0

Fig. 8 Flexural strength test



Fig. 9 Flexural strength value

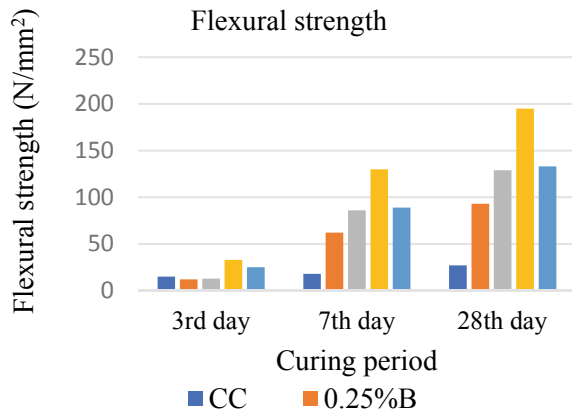


Figure 10 shows the impact strength testing; the comparison of impact strength values at various percentages replaced at different time intervals [7] is shown in Figs. 11 and 12.

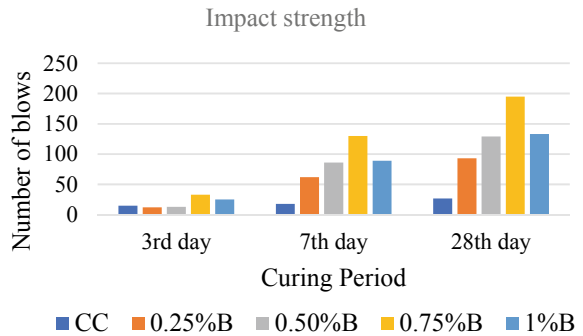
Table 5 Impact strength values

Materials	Percentage (%)	Impact resistant (N m)					
		3rd day		7th day		28th day	
		Initial crack	Final crack	Initial crack	Final crack	Initial crack	Final crack
C.C	0	11	15	15	18	22	27
Banana stem fibre	0.25	8	12	59	62	88	93
	0.50	8	13	72	86	108	129
	0.75	28	33	130	139	195	208
	1	21	25	74	90	111	135

Fig. 10 Impact strength test



Fig. 11 Initial cracks' values



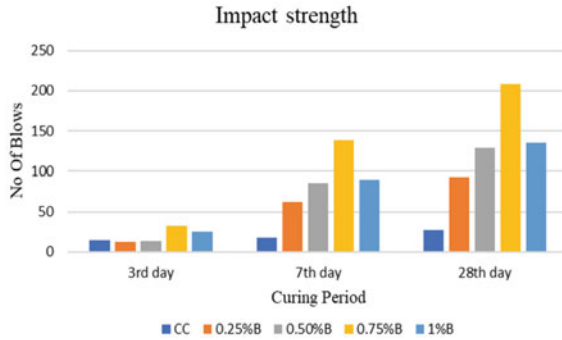


Fig. 12 Final cracks' values

4.5 SEM and EDS Analyses

The micrograph SEM is shown in Fig. 13, and it was measured that C-S-H gel was hydrated cement paste mixture which is the main cause for effective strength. The hydration process was observed using microstructural analysis on concrete with regular break, and it is obvious to have less voids and C-S-H gel was created at both the initial and later stages [10]. Figure 14 shows the raw banana stem fibre. Figure 15 shows conventional concrete of M40 grade. Figures 16, 17 and 18 shows the banana stem fibre concrete in M40 grade [11, 12].

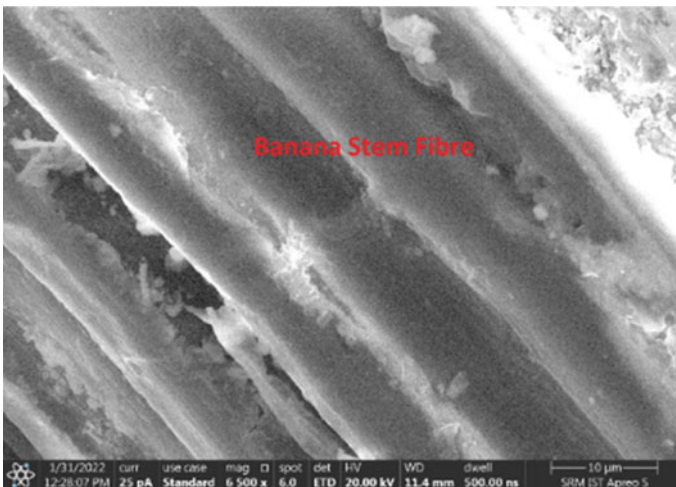


Fig. 13 Banana stem fibre

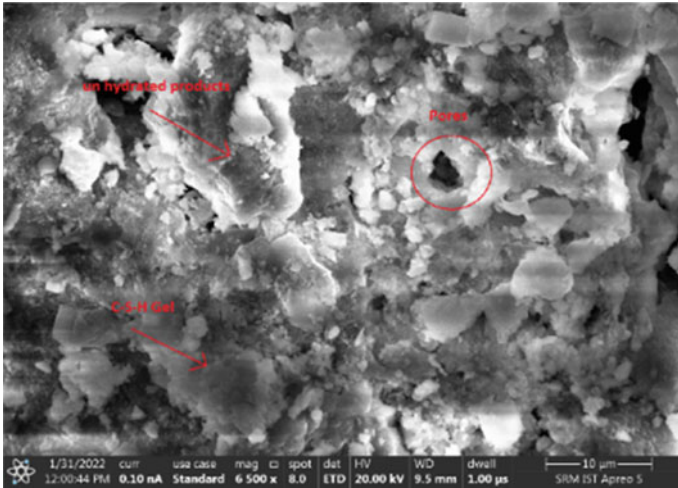


Fig. 14 Conventional concrete

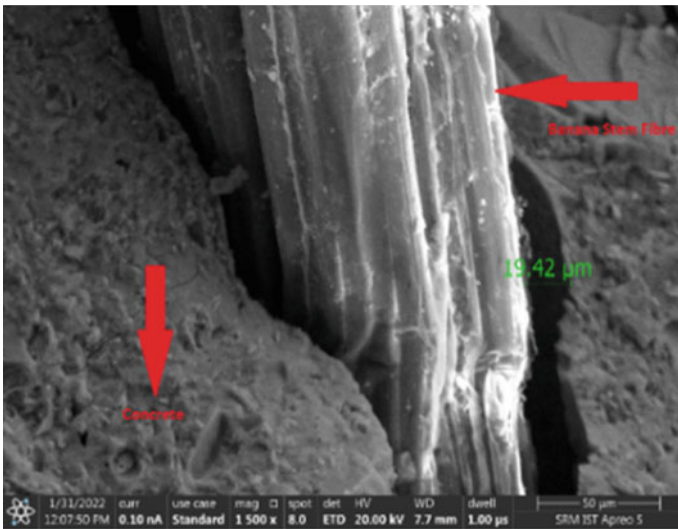


Fig. 15 M40 banana stem fibre concrete

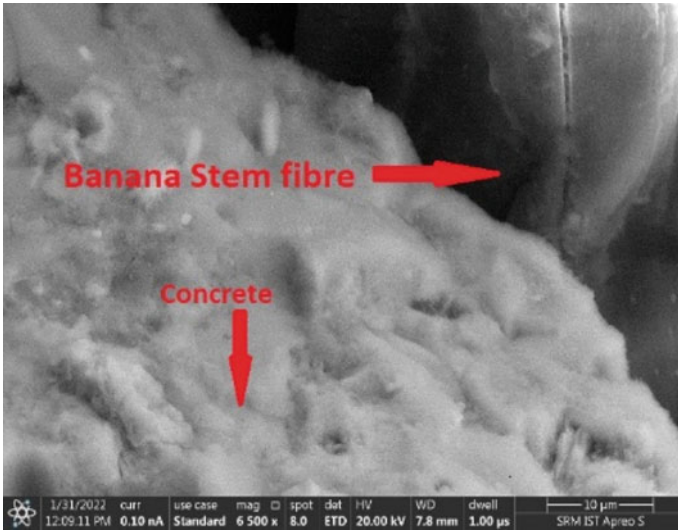


Fig. 16 Distance between the concrete and the banana fibre

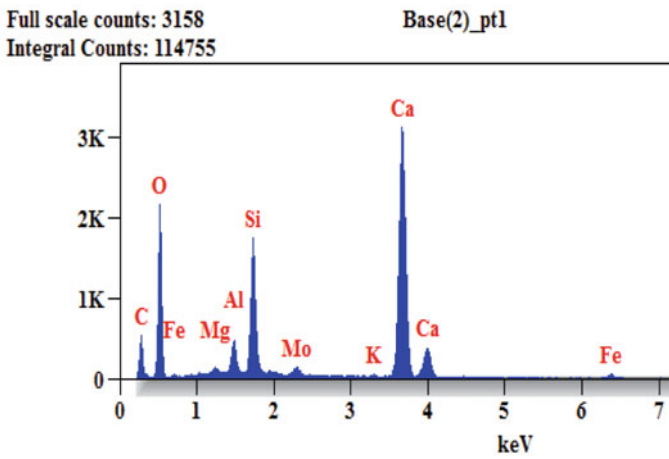


Fig. 17 M40 banana stem fibre concrete

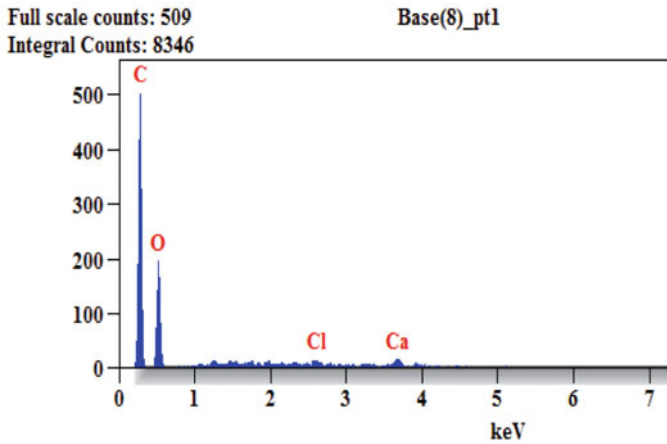


Fig. 18 Banana stem fibre

5 Conclusion

The conclusions are made with the points that are listed below for the comparison of mechanical properties with the characterization study for the addition of banana stem fibre.

- The banana fibre composite seems elastic with minimum plastic deformation.
- Addition of banana stem fibre in the concrete will slightly increase the compressive strength at 1% of banana stem fibre.
- Addition of 0.75% of banana stem fibre in the concrete we received the maximum strength for flexural strength.
- When banana stem fibre is increased in concrete, the cracks are reduced.
- The natural fibres are less non-harmful to the environment and biodegradable.
- From the SEM analysis, inclusion of banana stem fibre produces extra C–S–H gel formation which helps to reach more strength.

Acknowledgements Authors are very grateful thanks to SRM Central instrumentation facility (SCIF).

References

1. Ravichandran PT (2015) Investigations on Tensile properties of high strength steel fibre reinforced concrete. *Indian J Sci Technol* 8:1–6
2. IS:2386 (Part III) (1963) Methods of test for aggregates for concrete
3. IS 383 (2016) Coarse and fine aggregate from natural sources of concrete

4. Vidya Bharathi S, Vinodhkumar S, Saravanan MM (2021) Strength characteristics of banana and sisal fiber reinforced composites. *IOP Conf Ser Mater Sci Eng* 1055:012024
5. IS10262 (2019) Concrete mix proportioning—guidelines
6. IS 516 (2018) Method of tests for strength of concrete. Bureau of Indian Standard, pp 1–30
7. ACI Committee 544.3R-93 (2002) Guide for specifying, proportioning, mixing, placing and finishing steel fiber reinforced concrete
8. Chandar S, Gunasekaran K (2019) Study on the effect of quarry dust on deflection characteristics of coconut shell concrete slab. *Rasayan J Chem* 12(3):1038–1042
9. IS: 5816 (1999) Splitting tensile strength of concrete. Bureau of Indian Standard
10. Sapuan SM, Leenie A, Harimi M, Beng YK (2006) Mechanical properties of woven banana fibre reinforced epoxy composites. *Mater Des* 27(8):689–693
11. Lau K, Hung P, Zhu M-H, Hu D (2018) Properties of natural fibre composites for structural engineering applications. *Compos Part B Eng* 13(6):222–233
12. Ardanuy M, Claramunt J, Toledo Filho RD (2015) Cellulosic fiber reinforced cement-based composites: a review of recent research. *Constr Build Mater* 7(2):115–128

Comparative Study on the Performance of RC Frame Multistorey with Three Different FRP Reinforcements



Raj Dhruvkishor Patil and N. Pannirselvam

1 Introduction

Fibre-Reinforced Polymer also known as Fibre-Reinforced Plastic is a promising composite in various fields like aircraft, automobiles, sports gear, marine, construction industries, etc. In the construction industry, it is mainly used in rehabilitation techniques and there is limited use of FRP rods as a reinforcement bar in beams, columns, and slabs in place of steel [1]. Composite materials usually consist of two phases: one is the reinforcing phase and the other is the matrix phase. FRP was never a straight-out creation but evolved because of necessities. With many advantages of FRP over steel as reinforcing bar like resistance to corrosion, seismic resistant buildings/structures, cost-effectiveness, easy construction, durability, high tensile strength-to-weight ratio, low life cycle costs, the distant future is where FRP may even replace steel as a primary reinforcing bar.

A lot of work has been carried out in using Carbon Fibre-Reinforced Polymer (CFRP), Glass Fibre-Reinforced Polymer (GFRP), as sheets, rehabilitation bar, but there is limited work on using these FRPs as a primary reinforcing bar. With the aid of the pushover method, Peng et al. [2] conducted experimental research on the performance of beam–column joints using FRP reinforcement in the seismic zone. Following this, a comparison of the structure’s performance using the distribution of plastic hinges, target displacement, and pushover curve was made. Zadeh and Nanni [3] have worked on the guidelines for the members subjected to simultaneous flexure and axial load as the current guidelines have no provision for that. They have shown the theoretical for the basis of GFRP-RC subjected to simultaneous flexure and axial load, provided analysis provisions and revised designs for GFRP-RC, explained the rationale for the formulation that is consistent with the current guidelines. The

R. D. Patil · N. Pannirselvam (✉)

Department of Civil Engineering, Faculty of Engineering and Technology, SRM Institute of Science and Technology, Kattankulathur, Chengalpattu District, Tamil Nadu 603203, India
e-mail: pannirsn@srmist.edu.in

results of an investigation by Hasaballa et al. [4] into the viability of using GFRP to disperse energy during seismic loading revealed that the beam–column joints resisted more than 3% storey drift [5]. Amitshaha and Prakarsh [6] have studied the seismic performance of the multistorey building with GFRP reinforcements and have done a pushover analysis for the structure.

Sami et al. [7] investigated the design recommendations for the use of FRP for reinforcement and strengthening of concrete structures. The seismic behaviour of the structure with GFRP reinforcement bar has been examined by Apurv and Sunil [8] using the response spectrum approach. Results were obtained in terms of drift, storey displacement, shear, modal acceleration, stiffness, and modal time. So, in this study, we have used GFRP, CFRP, AFRP as a primary reinforcing bar in the analysis of a G + 7 reinforced concrete framed multistorey using STAAD.Pro software in earthquake zone using response spectrum analysis. The significance of the present paper is to check whether FRP with its many advantages can be used instead of steel.

2 Methodology

A G + 7 multistorey was planned in AutoCAD 2019 at first, and then, the model was made in Staad.Pro Advanced software for conducting response spectrum analysis in Zone V and soil type II with dead load, uniform floor load, lateral earthquake loads.

3 Material Properties

The material properties are furnished in Table 1.

Table 1 Material properties

Properties	GFRP	CFRP	AFRP
Young's modulus (kN/m ²)	3.5×10^7	1.2×10^8	1.1×10^8
Poisson's ratio	0.29	0.2	0.23
Density (kN/m ³)	24.51	17.26	14.122
Thermal coefficient (/°F)	5×10^{-7}	7×10^{-7}	7.7×10^{-7}
Critical damping	0.03	0.03	0.03
Shear modulus (kN/m ²)	247,979	8.33×10^7	1.24×10^9
Yield stress (N/mm ²)	500	500	500
Tensile strength (N/mm ²)	550	1000	2000

Table 2 Data used for multistorey buildings

Type of multistorey	Residential building
No. of storey	8
Floor to ceiling height	3 m
Number of bays along X-direction	3
Number of bays along Y-direction	4
Concrete grade	M30
FRPs used	GFRP, CFRP, AFRP
Soil type	Type II Hard soil
Zone	V; Z = 0.36
Importance factor	1
Response reduction factor	2.5
Damping ratio	5%

4 Data of the Multistorey

The data used for multistorey building are presented in Table 2.

5 Planning

AutoCAD 2019 was used to create the plan. During the planning stage of this project, many planning rules from the Pondicherry Planning Authority (PPA) and the National Building Code (NBC) were taken into account. The planned building borders an 18-m road; therefore, setback and floor space index (FSI) factors are taken into account. The following factors should be considered for a road width of 18 m:

1. A 7-m setback is required in all directions.
2. Covered area is < 50% of the entire area.
3. Maximum FSI equals 3.25.

For the intended location,

1. A setback of 7 m in all directions (minimum setback for road width of 18 m).
2. The whole area is 888.65 m².
3. The covered area is 240.18 m² (50% of 888.65 m²).
4. FSI = Floor Surface Indicator (all floors)/Plot Area = $(240.18 \times 8)/885.06 = 2.17 < 3.25$.

As a result, all design considerations are factored into the project plan. The building's ground floor, first to the seventh floor, and grid plan layout are depicted in Figs. 1, 2 and 3. Each level has three 2BHK units with dimensions that meet the PPA minimum plan requirements.

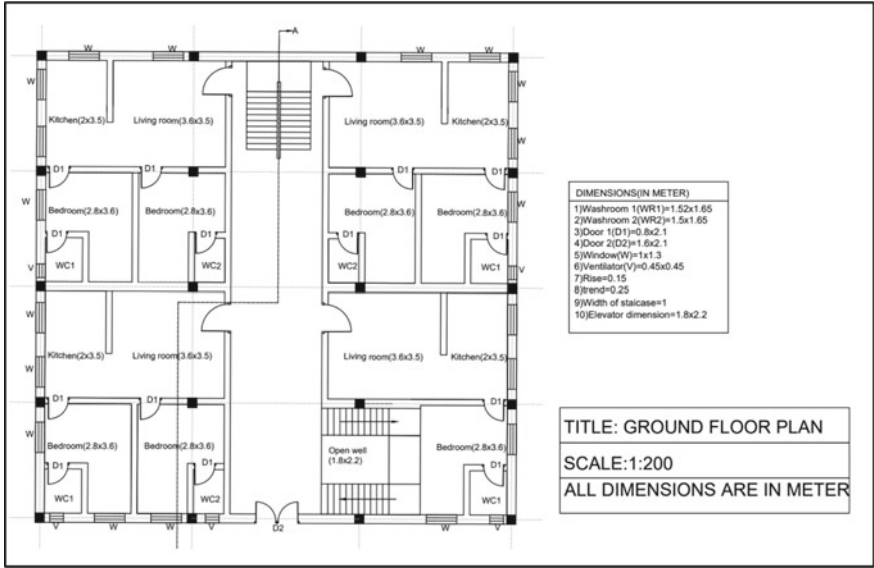


Fig. 1 Ground floor plan

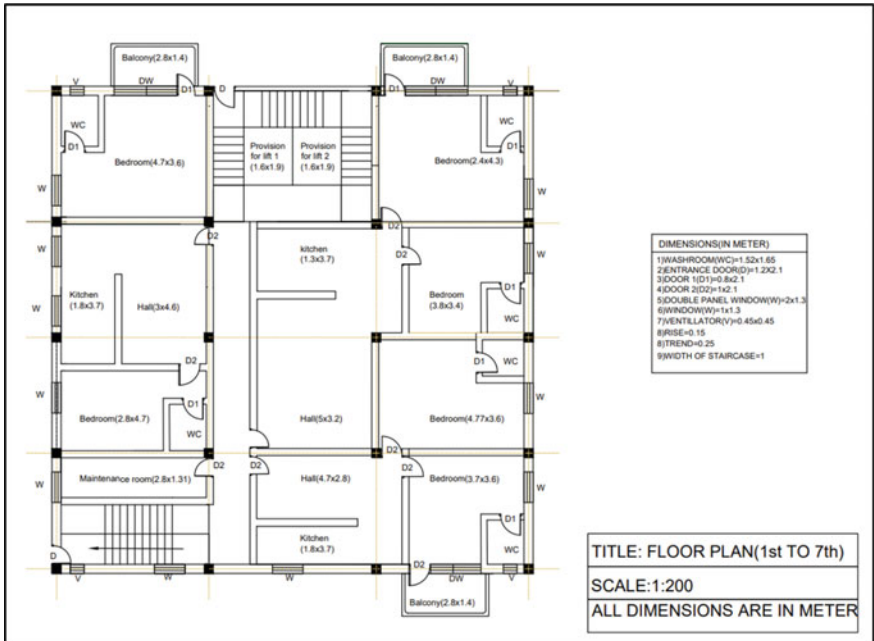


Fig. 2 First to seventh floor plan

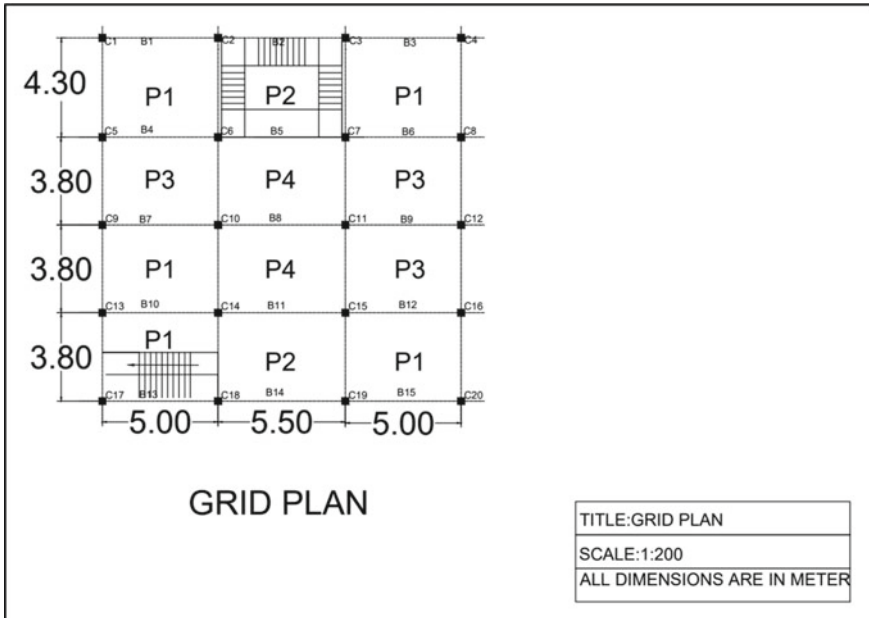


Fig. 3 Grid plan

5.1 Load Combinations

Load combinations that were applied to the structure were taken from IS: 456 (2000) [9]. The combinations of loads such as dead load, live load, and seismic load [10–12] are as follows:

- I. $1.5 (D.L. \pm E.L.)$.
- II. $1.2 (D.L. \pm L.L. \pm E.L.)$.
- III. $0.9 D.L. \pm 1.5 E.L.$

6 Analysis

Analysis was carried out for three models using three different FRPs, namely GFRP, CFRP, and AFRP. The model that was created is shown in Fig. 4.

The dimensions that were used for the slab, beam, and column are given in Table 3.

The loads that were applied on the structure are given below:

Data:

Beam thickness = 0.3 m.

Beam width = 0.23 m.

Fig. 4 Three-dimensional rendered view

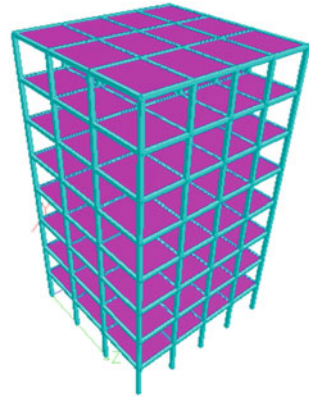


Table 3 Dimensions of the member

Component	Dimensions
Slab thickness	150 mm
Beam in metres	0.3 × 0.4
Column in metres	0.4 × 0.4

- Slab thickness = 0.15 m.
- Column width = 0.3 m.
- Column thickness = 0.3 m.
- Type of building = Residential.
- Unit weight of concrete = 25 kN/m³.
- Unit weight of brick work = 20 kN/m³.

1. Dead Load:

1.1 Floor load:

- a. Slab load = $0.15 \times 25 = 3.75 \text{ kN/m}^2$.
- b. Floor finishes = 1 kN/m²
- c. Furniture load = 1 kN/m².
- d. Total floor load = 5.75 kN/m².

2. Member load:

- a. Wall load = $(0.23 + 0.2) \times 1 \times 3.5 \times 20 = 30.1 \text{ kN/m}$.

2. Live Load:

- a. a. Uniform floor load = -2 kN/m in Y-direction.

3. Earthquake Load:

- a. Zone factor = 0.36 (zone V as per Table 3).
- b. Importance factor = 1.2 (Residential building as per Table 4).

- c. Response reduction factor = 3 (Ordinary Moment Resisting Frame as per Table 5).
- d. Percentage of imposed load = 25% (as per Table 6).
- e. Floor area = $15 \times (4.3 + 3.8 + 3.8 + 3.8) = 235.5 \text{ m}^2$
Seismic weight of each floor

$$f. = \text{Floor Area} \left(\text{Floor Load} + \left(\frac{\% \text{Imposed load}}{100} \times \text{Live load} \right) \right)$$

$$= 1471.875 \text{ kN}$$

- g. Total seismic weight of the structure = Seismic weight of floor $\times 7 = 10,303.13 \text{ kN}$.

$$T_a = 0.075 \times h^{0.75}$$

- h. Fundamental period = $0.075 \times 24.5^{0.75}$

$$= 0.825916 \text{ s}$$

- i. Soil type = Type II.

$$j. \frac{S_a}{g} = \frac{1}{T} = 1.646657.$$

- k. Design horizontal seismic coefficient $A_h = \left(\frac{Z}{2} \times \frac{S_a}{g} \right) \times \frac{R}{I}$
 $= 0.237119$.

- l. Design base shear $V_b = A_h \times W = 2443.062 \text{ kN}$.

Loading diagrams for dead, live, and earthquake loads are shown in Figs. 5 and 6.

Table 4 Lateral force at each storey

Storey level	W_i (kN)	h_i (m)	$(W_i \cdot h_i^2)/1000$	$\frac{W_i h_i^2}{\sum W_i h_i^2}$	Lateral force (kN)
1	1471.875	3.5	18.03046875	0.125	305.382788
2	2943.75	7	144.24375	0.2962963	723.870312
3	4415.625	10.5	486.8226563	0.421875	1030.66691
4	5887.5	14	1153.95	0.512	1250.8479
5	7359.375	17.5	2253.808594	0.5787037	1413.8092
6	8831.25	21	3894.58125	0.6297376	1538.48821
7	10,303.125	24.5	6184.450781	0.4375	1068.83976
			14,135.8875		

Table 5 Maximum and minimum values at critical section

	GFRP	CFRP	AFRP
Max F _x	640.07	573.28	547.02
Min F _x	-321.46	-259.031	-274.606
Max F _y	197.837	197.862	189.574
Min F _y	-197.837	-192.862	-189.574
Max F _z	306.45	243.45	194.885
Min F _z	-84.65	-88.73	-91.8
Max M _x	63.65	89.701	32.3
Min M _x	-64.54	70.0761	-32.3
Max M _y	171.6	155.876	146.319
Min M _y	-171.6	-155.88	-146.319
Max M _z	177.65	181.038	152.34
Min M _z	-157.84	-121.428	-116.6
Max X	3.063	0.247	0.45
Max Y	2.041	0.163	0.287
Max Z	3.3	0.282	0.428

7 Results and Discussion

Maximum storey displacement, drift, maximum and lowest bending moments, and shear force are used to depict the results of the response spectrum analysis in longitudinal and transverse directions. Maximum storey drifts in both X- and Z-directions for all the three FRPs are shown in the form of graphs in the following Figs. 7, 8, 9 and 10.

In the following table, we can see maximum and minimum shear forces and bending moments with maximum displacement values of the critical section for all the FRPs used.

Table 6 Cost analysis

Dia. of bar	Steel (kg)	Cost (₹)	CFRP (kg)	Cost (₹)	AFRP (kg)	Cost (₹)	GFRP (kg)	Cost (₹)
8	1198.06	87,781.86	0.00	0.00	0.00	0.00	49.56	4103.50
10	0.00	0.00	0.00	0.00	0.00	0.00	1380.43	114,293.0
12	3721.07	276,066.18	5124.90	401,786.52	4187.27	337,481.40	5497.61	455,175.1
16	675.70	50,130.18	209.61	16,433.19	31.31	2523.49	0.00	0.00
20	3211.41	238,254.51	37.28	2922.71	3120.74	251,522.28	0.00	0.00
25	5187.23	384,840.59	10,813.6	847,778.26	6203.87	500,013.31	4640.05	384,173.1
32	0.00	0.00	3727.91	292,264.04	0.00	0.00	0.00	0.00
		1,037,073.32		1,561,184.74		1,091,540.48		957,744.77

Fig. 5 Dead load loading diagram

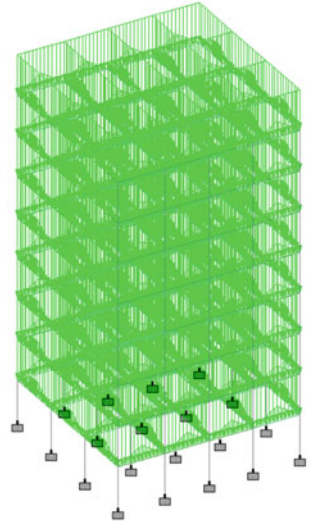
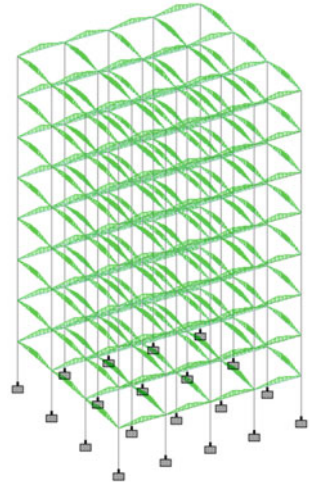


Fig. 6 Live load loading diagram



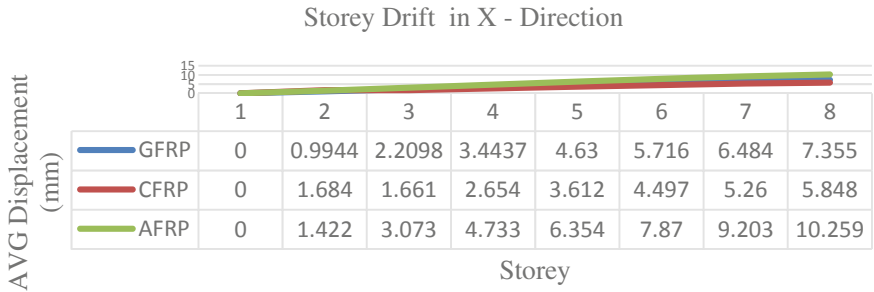


Fig. 7 Storey drift in X-direction

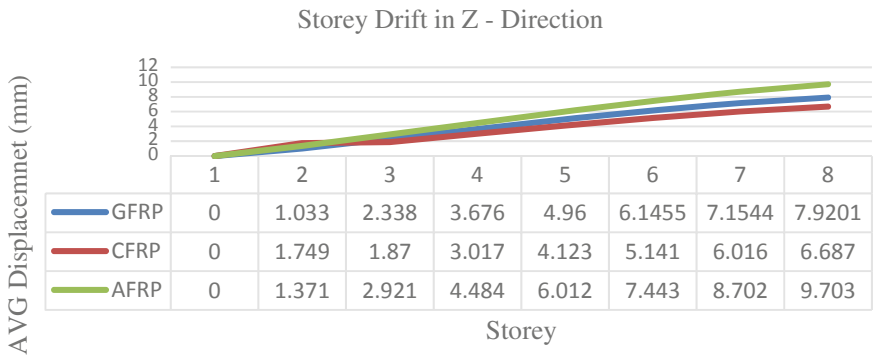


Fig. 8 Storey drift in Z-direction



Fig. 9 Storey stiffness in X-direction

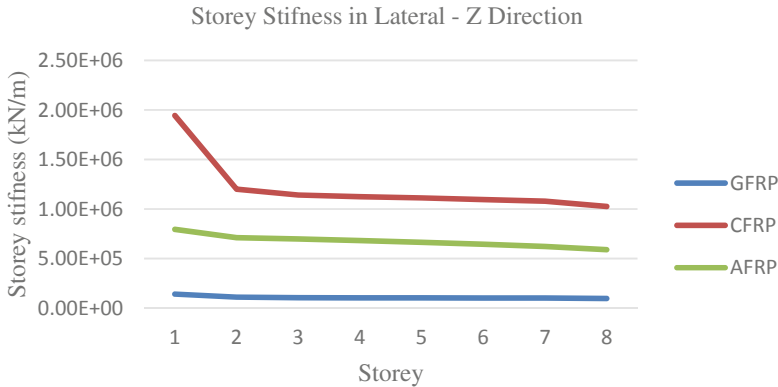


Fig. 10 Storey stiffness in Z-direction

8 Conclusion

- AFRP has the maximum storey drift and CFRP has the minimum of storey drift, whereas GFRP lies in the middle of these two.
- Comparing the three FRPs in terms of storey stiffness, then CFRP has the maximum and GFRP has the minimum storey stiffness, whereas AFRP lies in the middle of these two.
- After comparing maximum and minimum bending moments and shear forces and maximum displacement, we can conclude that CFRP better out in every respect than both the other FRPs.
- And comparing the cost of CFRP when compared with steel is almost equal. At the same time, AFRP is cost efficient than steel in cost analysis.
- But due to the easier availability of CFRP than AFRP, CFRP can be used as an alternative to steel as reinforcement bar.
- The fibres of GFRP, CFRP and AFRP as reinforcement cost from 0.92, 1.05, and 1.50%, respectively.

References

1. ACI 440.1R-15. Guide for the design and construction of structural concrete reinforced with fiber-reinforced polymer (FRP) bars
2. Peng Y, Ma M, Dong G (2010) Seismic performance analysis of FRP reinforced concrete frame structure. In: *CICE 2010—The 5th International Conference on FRP Composites in Civil Engineering*, vol 27, pp 4–5
3. Zadeh HJ, Nanni A (2013) Design of RC columns using glass FRP reinforcement. *J Compos Constr* 17(3):294–304

4. Hasaballa MH, El-Ragaby A, El-Salakawy EF (2014) Seismic performance of exterior beam-column joints reinforced with glass fibre reinforced polymer bars and stirrups. *NRC Res Press* 38:1092–1102
5. Cimilli ES, Saatcioglu M (2015) Seismic behaviour of FRP reinforced concrete frame buildings. In: *The 14th World Conference on Earthquake Engineering*, vol 32, pp 115–119
6. Amitshaha R, Prakarsh S (2016) Analysis and design of multistorey RC frame using FRP reinforcement. *Int J Appl Innov Eng Manage* 5(7):1–6
7. Rizkalla S, Hassan T, Hassan N (2019) Design recommendations for the use of FRP for reinforcement and strengthening of concrete structures. *Prog Struct Mat Eng* 5(1):16–28
8. Pol AA, Rangari SM (2021) Structural behaviour of RC multi-storey building with GFRP reinforcement subjected to seismic load by linear dynamic analysis. *Turk Online J Qual Inquiry* 12(6):414–426
9. IS 456 (2000) Plain and reinforced concrete code of practice. Fourth Revision, Bureau of Indian Standards, New Delhi, India
10. IS 1893 (Part 1) (2016) Criteria for earthquake resistant design of structures. Fifth Revision, Bureau of Indian Standards, New Delhi, India
11. IS 875 (Part 1) (1987) Code of practice for design load (Other than earthquake) for buildings and structures. Second Revision, Bureau of Indian Standards, New Delhi, India
12. IS 875 (Part 2) (1987) Code of practice for design load (Other than earthquake) for buildings and structures. Second Revision, Bureau of Indian Standards, New Delhi, India

Analytical Study of Plastic Hinge Formation in Beams Strengthened with CFRP Sheets



Anand Mehta, R. Ravi, and S. Sivakamasundari

1 Introduction

When the reinforced concrete member undergoes plastic deformation, it yields. This ascertains that the member has failed. The plastic deformation in flexural members is localized in a small zone which is called the zone of plastic hinge or the plastic hinge region [1] (Hines et al., 2004). Several attempts have been made to predict the location and the length of the plastic hinge zone and empirical equations were suggested. These empirical equations are summarized in Table 1 [2–13]. Using the commercial software DIANA, a sophisticated Finite Element Model is quite competent of modelling the plastic hinge behaviour in reinforced concrete beams [14]. Using the same Finite Element Modelling, investigation of plastic hinge region can be done analytically [15]. In order to analyze the fracture patterns, a 2D nonlinear finite element research is performed on a reinforced concrete beam that has been subjected to monotonic and cyclic loads. Flexural shear cracking was studied, and when the load–deflection data for experimental and analytical approaches were compared, the results were in good agreement [16]. Under reverse cyclic stress, the seismic behaviour of beam–column joint strengthened by integrating steel haunches and CFRP sheets is investigated [17]. Seismic performance of RC beam–column–slab joint which is strengthened with combining steel haunches and CFRP sheets under reverse cyclic loading is studied [17]. The retrofitting technique was successful in relocating the plastic hinge, and there was an average increase in strength of about 9% due to the retrofitting scheme [18]. FRP laminates improved the shear strength [19]. Shear failure tests were conducted and Mohr–Coulomb type failure envelope was derived to deduce the strength of the bond between the structure and the jacketing

Anand Mehta · R. Ravi (✉) · S. Sivakamasundari

Department of Civil Engineering, Faculty of Engineering and Technology, SRM Institute of Science and Technology (SRMIST), Kattankulathur 603203, India

e-mail: ravir2@srmist.edu.in

Table 1 Length of plastic hinge

References	Plastic hinge length (L_p)
Baker [2]	$c_0(z/d)^{1/4}d$ (for RC beams and columns)
I.C.E. Research Committee [3]	$c_1c_2c_3(z/d)^{1/4}d$
Sawyer [4]	$0.25d + 0.075z$
Corley [5]	$0.5d + 0.2\sqrt{d}(z/d)$ (for RC beams)
Mattock [6]	$0.5z + 0.05z$ (for RC beams)
Priestley and Park [7]	$0.08z + 6d_b$ (for RC columns)
Paulay and Park [8]	$0.08z + 0.022d_b f_y$ (for RC beams and columns)
Sheikh and Khoury [9]	$1.0h$ (for columns under high axial load)
Coleman and Spacone [10]	$G_f^c [0.6f_c(20 - c + 0.8f'_c/Ec)]$
Panagiotakos and Fardis [11]	$0.18z + 0.021d_b f_y$ (for RC beams and columns)
Bae and Bayrak [12, 13]	$h\{[0.3(p/pu) + 3(As/Ag) - 1](z/h) + 0.25\} \geq 0.25h$ (for columns)

[20]. Complete stress–strain behaviour of concrete under both tension and compression is simulated [21]. ABAQUS is used to validate the experimental flexural test results of an RC beam element [22]. A dynamic explicit model can be made in order to better understand the nonlinear behaviour of the element [23].

2 Methodology

Finite Element Modelling of RC beam is done by ABAQUS. Post-yield behaviour and plastic hinge formation in the beam are analyzed, and then, the beam is wrapped with Carbon Fibre-Reinforced Polymer wraps. Nonlinear finite element analysis of monotonic and non-reversed cyclic loaded RC beams was done by [16].

a. Modelling of Concrete

In this study, the concrete elements are triangular isoparametric plane stress elements having three nodes. The size of the mesh for the purpose of Finite Element Modelling is considered as 10 mm. Concrete damaged plasticity (CDP) is adopted for modelling the concrete elements. Compressive behaviour of concrete can be represented by plotting a graph between stress and strain when the specimen is subjected to axially compressive load and the corresponding strain is measured. Figure 1a shows the graph of yield stress on Y axis and corresponding inelastic strain in concrete on X axis. Mander et al.'s stress–strain model was adopted [24]. When concrete is subjected to tensile forces, due to nonlinear strain distribution, it fails at low average strain but high local strain as depicted in Fig. 1b. The softening curve is exponential and is evident in Fig. 1b. The softening depends upon the concrete tensile strength, tensile fracture energy, and the crack bandwidth [25] (Table 2).

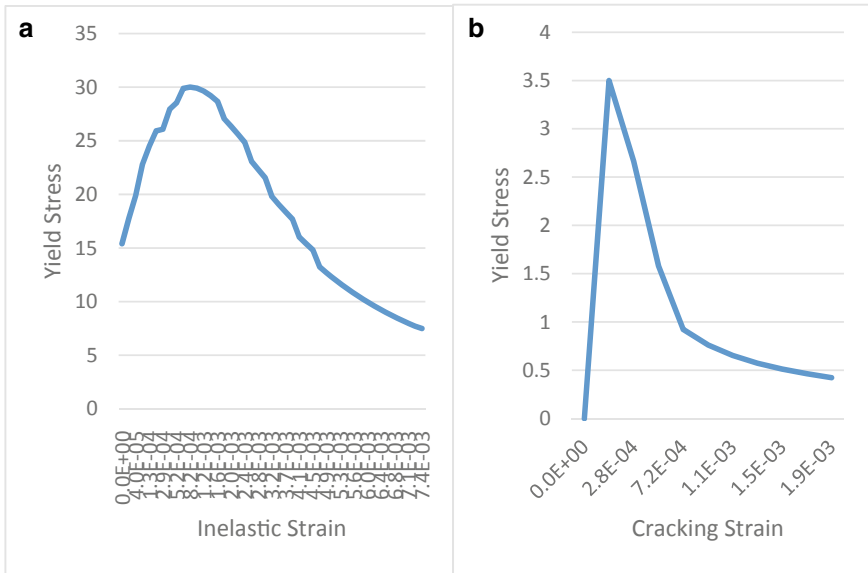


Fig. 1 a Compressive behaviour; b tensile behaviour

Table 2 Concrete damage plasticity properties

Dilation angle	Eccentricity	f_{b0}/f_{c0}	K	Viscosity parameter
30°	0.1	1.16	0.666	0.0001

b. Concrete Damaged Plasticity

The stress–strain curve shows no linearity, which means that there is no elastic modulus for the material. The Concrete Damaged Plasticity criteria is based on the Hognestad model of stress–strain. In 1951, Eivind Hognestad came up with a different model to estimate the stress–strain behaviour of plain concrete which is based on flexural tests. From zero stress to the maximum stress, the behaviour is described by Ritter’s parabola, then the concrete fails, and it follows a straight line. The two equations for this behaviour are shown below [26, 27].

$$\frac{\sigma_c}{f_{cm}} = \left(\frac{2\varepsilon_c}{\varepsilon_{c1}} - \left(\frac{\varepsilon_c}{\varepsilon_{c1}} \right)^2 \right), 0 \leq \varepsilon_c \leq \varepsilon_{c1},$$

$$\frac{\sigma_c}{f_{cm}} = 1 - 0.15 \left(\frac{\varepsilon_c - \varepsilon_{c1}}{\varepsilon_{cu} - \varepsilon_{c1}} \right), \varepsilon_{c1} \leq \varepsilon_c \leq \varepsilon_{cu}.$$

The stress–strain behaviour of concrete according to the Hognestad model is shown in Fig. 2.

Fig. 2 Stress–strain relation of concrete according to Hognestad criteria

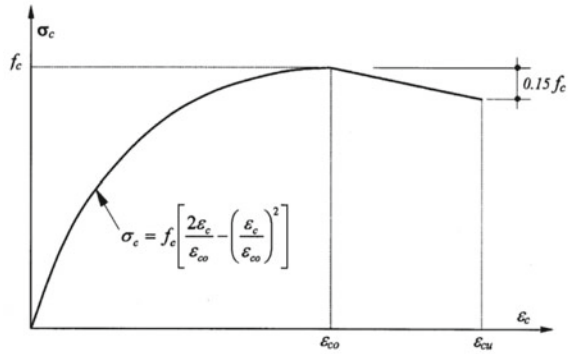


Table 3 Properties of steel

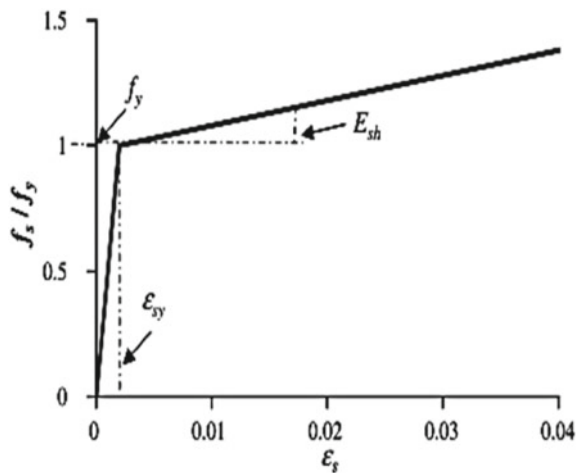
Mass density	Modulus of elasticity	Poisson's ratio
$7.8 \times 10^{-6} \text{ kg/m}^3$	210,000 N/m ²	0.3

c. Modelling of Steel

The reinforcing steel is modelled in the structure in accordance with the Indian Standards. The reinforcement is modelled as truss element in the software. Table 3 shows the property values taken and Fig. 3 shows the stress–strain model adopted in order to define the reinforcement section in the beam element. Strain hardening plasticity model is used for the purpose, and the following equation is employed to model the material properties of the reinforcing steel [15].

d. Modelling of CFRP Wrap

Fig. 3 Stress–strain model of steel



Carbon Fibre-Reinforced Polymer wraps are used to retrofit the yielded section of the reinforced concrete beam. CFRP is chosen for the wrapping purpose due to the material properties that are conducive to the requirements. Plastic hinge formed in the conventional RC beam without the wrap is strengthened by applying the CFRP coating over the beam. Comparisons are made between the two beams, viz. unwrapped conventional RC beam and the CFRP wrapped beam on various criteria such as load versus deflection curve, yielding stress, stress versus strain curve, rebar yielding zone, concrete crushing zone, crack patterns. The characteristics of CFRP are given in Tables 4 and 5 shows the CFRP properties applied to the model [28].

e. Model Geometry

The loads and the supports are applied to the beam over a span of 50 mm. Table 6 denotes all the geometric properties of the beam. Later, the beam is wrapped with a CFRP layer of 1 mm thickness. Comparative study is done with respect to various parameters such as load versus deflection, stress and strain, and crack pattern. The compression reinforcement, tensile reinforcement, and the stirrups are combined as reinforcement so that there is no bond-slip effect. Section properties for concrete and steel are assigned to the elements, respectively.

f. Loading and Step

Table 4 Properties of the CFRP material

Dry density of fibre	1.82 g/cm ³
Dry thickness of fibre	0.167 mm
Dry tensile strength of fibre	4000 N/mm ²
Tension modulus of elasticity	230,000 N/mm ²
Laminate thickness	0.167 mm
Tensile strength of laminate	3500 N/mm ²
Elasticity of laminate	225 kN/mm ²

Table 5 CFRP properties applied in model

Property	Symbol	Value
Longitudinal modulus	E_1	230 GPa
Transverse in-plane modulus	E_2	23 GPa
Transverse out-plane modulus	E_3	23 GPa
In-plane shear modulus	G_{12}	6.894 GPa
Out-of-plane shear modulus	G_{23}	4.136 GPa
Out-of-plane shear modulus	G_{13}	6.894 GPa
Major in-plane Poisson's ratio	V_{12}	0.3
Out-of-plane Poisson's ratio	V_{23}	0.25
Out-of-plane Poisson's ratio	V_{13}	0.25
Characteristic tensile strength	f_t	3400 MPa

Table 6 Geometric properties of the FEM model

Property	Value
Length	1500 mm
Height	250 mm
Width	230 mm
Length of reinforcement bar	1450 mm
Diameter of tensile reinforcement	12 mm
Diameter of compressive reinforcement	10 mm
Diameter of stirrups	8 mm

The beam that is modelled is a simply supported beam. Four-point loading is applied to the beam. The maximum number of increments applied to the model is 10,000. The initial size of increment is 0.01. Meshing is done to accurately quantify the values of various factors such stress, strain, displacement, deflection.

3 Results and Discussions

a. Paper Validation

When reinforced concrete beams are subjected to flexural loading, they frequently fail in compression at the top and tension at the bottom of the beam. Under monotonic loading, the plastic hinge area in reinforced concrete beams is investigated. Au and Bai [16] examine crack patterns in an effort to comprehend the post-yield behaviour of the beam (Fig. 4; Table 7).

Figure 5a shows the experimental and computed values using Finite Element Modelling of load applied and the corresponding deflection in the two dimensional RC beam. The comparison shows that the computed analytical values are fairly accurate when compared to the experimental data. Figure 5b shows the analytically

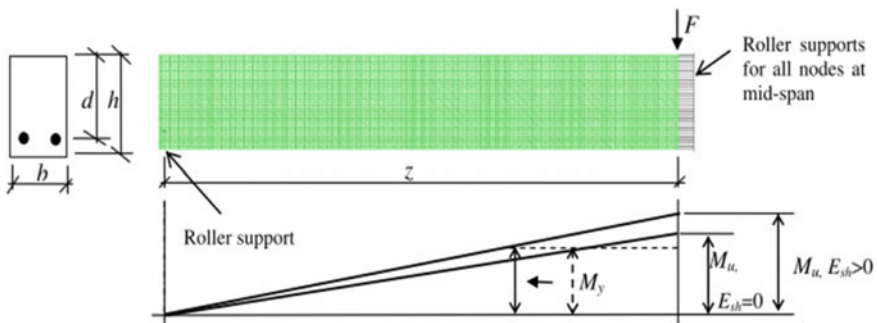


Fig. 4 Test setup as given in Au and Bai [16]

Table 7 Specimen properties

Specimen (reference)	f_c (MPa)	f_t (MPa)	E_c (GPa)	f_y (MPa)	E_s (GPa)	d (mm)	b (mm)	z (mm)	Tension steel $d_b \times$ Nos
B1 (Au and Bai)	52	4.5	27	488	200	260	200	1300	16 \times 3

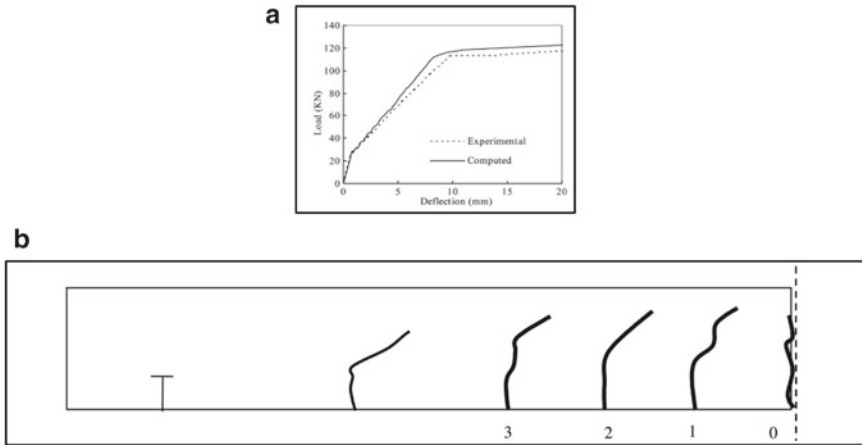


Fig. 5 a Load versus deflection curve computed by author [16]. b Crack pattern computed by Au and Bai

produced crack patterns of the beam under monotonic loading. The loading was symmetrical and modelled by the authors [16]. The experimental and the analytically produced crack patterns were compared and they showed a fair amount of similarity which infers that the analytical model was fairly accurate.

Figure 6 shows the analytically computed crack patterns in the beam on failure. Tensile as well as compressive damage parameters were included in the field output of the model in order to get the crack patterns. The crack patterns help to identify the mode of failure as well as to locate the exact location when modelling the structure so that the areas of potential failure can be either strengthened or retrofitted in order to improve the strength and the integrity of the structure.

b. Concrete Crushing Zone

Concrete crushing zone is the region where the concrete fails in compression, which is an indication of the formation of plastic hinge in the RC beam. In the compression region of the beam, the peak concrete strength is achieved when the strain exceeds 0.002 and the complete concrete crushing takes place when the strain in the concrete is greater than 0.006 in the compression region. In the conventional beam without the

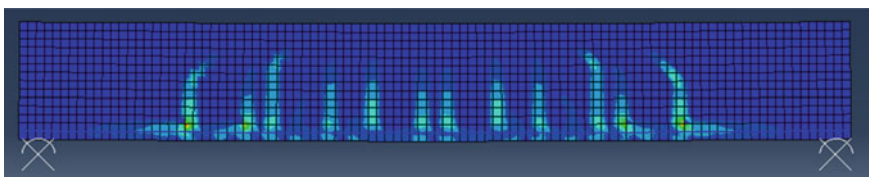
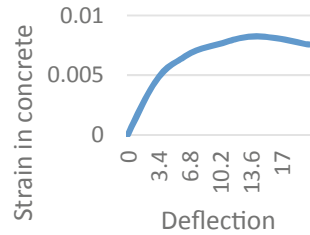


Fig. 6 Crack pattern computed using FEM

Fig. 7 Concrete crushing zone



wrapping, the strain in the compression region has exceeded the strain that causes complete concrete crushing as depicted in the graph in Fig. 7.

4 Conclusions

On a simply supported reinforced concrete beam, four-point loading is applied and the formation of plastic hinge is studied. Various parameters such as load versus deflection curve, rebar yielding zone of the reinforcement, concrete crushing zone in the compression region of the concrete as well as the crack pattern were analyzed in order to have a holistic idea of the formation of plastic hinge. Later, the reinforced concrete beam was wrapped with Carbon Fibre-Reinforced Polymer wraps for the purpose of strengthening of the beam and to prevent the formation of plastic hinge. An overall improvement in strength of about 15% was observed after the retrofit. The improvement in the strain in the reinforcement was found out to be about 8%. The failure of the beam wrapped with CFRP was extremely gradual which suggests that the beam will show clear indication of failure. Thus, it can be concluded that the CFRP wraps can be used to retrofit the flexural members to prevent plastic hinges' formation.

References

1. Hines EM, Restrepo JI, Seible F (2004) Force-displacement characterization of well- confined bridge piers. *ACI Struct J* 101:537–548
2. Baker ALL (1956) Ultimate load theory applied to the design of reinforced and pre-stressed concrete frames. Concrete Publications Ltd., London
3. I.C.E. Research Committee (1962) Ultimate load design of concrete structures. In: Proceedings of institution of civil engineers. London, p 399–442
4. Sawyer HA (1964) Design of concrete frames for two failure states. In: Proceedings of the international symposium on the flexural mechanics of reinforced concrete. ASCE-ACI, p 405–31
5. Corley GW (1966) Rotation capacity of reinforced concrete beams. *ASCE J Struct Div* 92:121–146
6. Mattock AH (1967) Discussion of rotational capacity of reinforced concrete beams by WDG Corley. *ASCE J Struct Div* 93:519–522

7. Priestley MJN, Park R (1987) Strength and ductility of concrete bridge columns under seismic loading. *ACI Struct J* 84:61–76
8. Paulay TP (1992) Seismic design of reinforced concrete and masonry buildings. John Wiley and Sons, New York, p 767
9. Sheikh SA, Houry SS (1993) Confined concrete columns with stubs. *ACI Struct J* 90:414–431
10. Coleman J, Spacone E (2001) Localization issues in force-based frame elements. *J Struct Eng* 127:1257–1265
11. Panagiotakos TB, Fardis MN (2001) Deformations of reinforced concrete members at yielding and ultimate. *ACI Struct J* 98:135–148
12. Bae SJ, Bayrak O (2008) Plastic hinge length of reinforced concrete columns. *ACI Struct J* 105:290–300
13. Bae SJ, Bayrak O (2008) Seismic performance of full-scale reinforced concrete columns. *ACI Struct J* 105:123–133
14. Zhao X et al (2011) Plastic hinge length in reinforced concrete flexural members. *Proc Eng* 14:1266–1274
15. Zhao, X-M, Wu, Y-F, and Leung, AYT (2012) Analyses of plastic hinge regions in reinforced concrete beams under monotonic loading. *Engineering Structures* 34, 466–482.
16. Au FTK, Bai ZZ (2007) Two-dimensional nonlinear finite element analysis of monotonically and non-reversed cyclically loaded RC beams. *Eng Struct* 29(11):2921–2934
17. Cai Z, Liu X, Li L, Lu Z, Chen Y (2021) Seismic performance of RC beam-column-slab joints strengthened with steel haunch system. *J Build Eng* 44(August):103250
18. Maheri MR, Torabi A (2019) Retrofitting external RC beam-column joints of an ordinary MRF through plastic hinge relocation using FRP laminates. *Structures* 22(May):65–75
19. Baggio D, Soudki K, Noël M (2014) Strengthening of shear critical RC beams with various FRP systems. *Constr Build Mater* 66:634–644
20. Ge EA, Onditioning ENC (2006) Behaviour of FRP reinforced panels subjected to. 126(June):692–699
21. Wahalathantri BL, Chan TH, Fawzia T (2008) A material model for flexural crack simulation in reinforced concrete elements using Abaqus. In: Proceedings of the first international conference on engineering, designing and developing the built environment for sustainable wellbeing, pp 260–264
22. Sinaei H (2012) Evaluation of reinforced concrete beam behavior using finite element analysis by ABAQUS. *Sci Res Essays* 7(21):2002–2009
23. Deng S, Qie Z, Wang L (2015) Nonlinear analysis of reinforced concrete beam bending failure experimentation based on ABAQUS. In: Proceedings of the First International Conference on Information Sciences, Machinery, Materials and Energy, vol 126(Icismme), pp 440–444
24. Mander JB, Priestley MJN, Park R (1988) Theoretical stress-strain model for confined concrete. *J Struct Eng* 114(8):1804–1826
25. He W, Wu Y-F, Liew KM (2008) A fracture energy based constitutive model for the analysis of reinforced concrete structures under cyclic loading. *Comput Methods Appl Mech Eng* 197:4745–4762
26. Zhao XM, Wu YF, Leung AYT (2012) Analyses of plastic hinge regions in reinforced concrete beams under monotonic loading. *Eng Struct* 34:466–482
27. Cheng YM (1995) Finite element modelling of reinforced concrete structures with laboratory verification. *Struct Eng Mech* 3(6):593–609
28. Daud R, Cunningham L, Wang Y (2015) Non-linear FE Modelling of CFRP-strengthened RC slabs under cyclic loading. *Athens J Technol Eng* 2(3):161–180

Influence of Basalt Fiber and Slag on the Moduli of Elasticity of Fine-Grained Concrete



Alein Jeyan Sudhakar and Bhuvaneshwari Muthusubramanian

1 Introduction

Considering the design and behavior of buildings, the elasticity of concrete is crucial and is the most fundamental parameter to be evaluated. It reveals the elastic performance of the material on loading by indicating its ability to deform practically. Dispersion of fibers in concrete plays a role and impacts the elasticity [1]. Instead, the fiber-reinforced concrete impacts the strain hardening and softening characteristics [2, 3]. The elastic characteristics such as dynamic and static are commonly assessed using destructive and non-destructive test (NDT). NDT is inexpensive experiments that do not damage the components that are being evaluated, which enables them to be repeated several times. In a non-destructive test, the material uniformity, strength, and modulus of elasticity (MOE) of concrete, the depth of concrete layers, structural defects are assessed, over time, such as curing and ageing [4]. Literature reveals modulus of elasticity of concrete which varies based on the materials used and curing duration, etc. [5, 6]. Adding GGBS to concrete influences the elastic properties based on the dosages added and improves the structure's long-term durability [7]. It is generally accepted that cement paste, aggregates, the interfacial transition zone (ITZ), and concrete capacity influence the MOE of concrete. As the cement paste stiffens over time, the modulus of elasticity of concrete also changes with age. The elasticity of mortar is lower than concrete [8–10]. Compared to other high-tech fibers, basalt fiber has distinct characteristics. As a result of the volcanic rock origin of basalt fiber, it possesses high chemical and thermal stability and does not emit any harmful gases [11]. Compared to natural and synthetic fibers, basalt fiber has a higher strength; it is green and meets environmental protection requirements [12–14]. There is an immediate need to lower the consumption of cement due to the emission of considerable

A. J. Sudhakar (✉) · B. Muthusubramanian

Department of Civil Engineering, Faculty of Engineering and Technology, SRM Institute of Science and Technology, Kattankulathur, Tamil Nadu 603203, India

e-mail: aj1024@srmist.edu.in

amounts of carbon dioxide during cement production. Slags are released from the steel industry as a by-product and are well-suited for structural and durable applications, in construction industry when added with cement by creating a little impact on the environment [15]. The effects of these materials on concrete properties vary based on material types used as cement substitution or mineral additives. Chemical, mineral, and particle compositions determine how much water they require, how well they pack, and how reactive they are when used as the concrete binder. Concrete pore structure has generally been refined by using such materials in concrete, and it may affect the strength, deformation, and durability characteristics of the matrix in its fresh and hardened states [16, 17]. Elastic modulus lowers with a higher dosage of GGBS by partially substituting the cement [18]. The silica and calcium oxide content in GGBS makes it set slower than cement [19–21].

From the referred literatures, it is vital to study the elastic modulus of any construction material to know its behavior before applying it in significant constructions. The moduli of elasticity vary depending on the type of fiber, raw materials used, and curing period. In general, the modulus of elasticity of mortar is less when compared to normal concrete. As fine-grained concrete resembles mortar in appearance but varies in its characteristics due to the particle size and is used in the construction industry as a matrix for thin construction elements with textile reinforcements, it is necessary to evaluate its elasticity. Fine-grained concrete is generally made using siliceous or quartz sand, but it is costly, and to overcome this in this study, M-Sand passing through 2.36 mm sieve is used. Only scarce studies have been reported on the MOE of FGC. From this concern, the present study concentrates on evaluating FGC dynamic moduli and static moduli with the influence of basalt fiber and GGBS. The relation between both static and dynamic moduli is evaluated in this study, and theoretical prediction is made based on different codal provisions. It does not require any coarse aggregate and helps in protecting mother nature.

2 Materials and Methods

2.1 Materials

The fine-grained concrete is prepared with 53 grade ordinary portland cement (OPC) of specific gravity and a fineness modulus of 3.14 and 6.82%, respectively. Manufactured sand (fine aggregate) penetrating through a 2.36 mm sieve is used. Fine-grained concrete does not require coarse aggregate, and thus, no coarse aggregate is used in this research. The basalt fiber used is of 12 mm length with aspect ratio 708, density 2660 kg/m³, and tensile strength of 2980 MPa. GGBS used is obtained from the local supplier with 2.83 as specific gravity, fineness modulus of 4.2, and density of 1235 kg/m³. A sulfonated naphthalene-based superplasticizer is used as a water-reducing agent to improve workability. It is added to the matrix by 1% cement content.

2.2 Specimen Preparation

The matrix is prepared based on trial and error method with ratio of water to cement as 0.45 [22, 23]. Cylindrical specimens are used to determine the static modulus of elasticity (SME). The 100 mm diameter cylinders with 200 mm in height are chosen for the current study. Prisms of $160 \times 40 \times 40$ mm are used for determining the dynamic modulus of elasticity (DME). Casted specimens are shown in Fig. 1. Basalt fiber and GGBS are added in different percentages to the composite matrix. The quantity of the materials involved in preparing this matrix is given in Table 1.



Fig. 1 Specimens. **a** Static modulus of elasticity. **b** Dynamic modulus of elasticity

Table 1 Details of the fine-grained concrete matrix

Matrix ID	Cement (kg/m ³)	GGBS (kg/m ³)	Fine aggregate (kg/m ³)	Superplasticizer (kg/m ³)	Water (kg/m ³)	Basalt fiber (kg/m ³)
BF0	479	–	1660	4.8	192	–
BF1						0.96
BF2						1.9
BF3						2.4
BF4						4.8
GBF1	430	48				1.9
GBF2	380	96				1.9
GBF3	335	144				1.9
GBF4	285	192				1.9

2.3 Methods

Static Modulus of Elasticity. The SME is tested by placing a compressometer with a gauge length of 105 mm around the cylinder under uniaxial compressive loading as shown in Fig. 2a. The compressometer should be placed at an equal distance from the top and bottom faces. The top surface should be even for uniform loading, and capping has to be done at the top face of the cylinder if it is uneven. In this research, all the faces of the cylinder are uniform, so no capping has been done. The SME is performed as per ASTM C 469 [24]. The cylinder is kept in the compressive testing machine, and load is given to make it seated. Then applied, the load till the longitudinal strain becomes 0.00005 (ε_1); the stress at this strain is calculated from the corresponding load as S_1 . Now 40% of the ultimate load of the cylinder is applied directly, and its stress is calculated as S_2 with corresponding strain (ε_2). The 40% of the ultimate load-carrying capacity to be applied is determined from the compressive strength of the cylinder. Then, Young's modulus of fine-grained concrete is determined using the formula as in Eq. 1.

$$E_C = \frac{S_2 - S_1}{\varepsilon_2 - 0.00005}, \quad (1)$$

where “ E = chord modulus of elasticity, S_2 = stress corresponding to 40% of ultimate load, S_1 = stress corresponding to a longitudinal strain ε_1 , $\varepsilon_1 = 0.00005$ and ε_2 = longitudinal strain produced by stress S_2 ”.

Dynamic Modulus of Elasticity. DME of concrete is performed as per ASTM C 597 [25]. The transducers are placed on two sides in the longitudinal direction of the prismatic sample, and the velocity is recorded as shown in Fig. 2b. Then, DME is calculated using the formula given in Eq. 2.

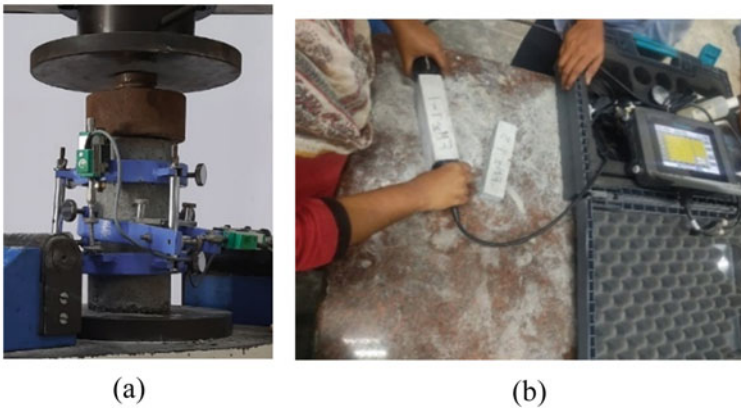


Fig. 2 Testing of (a) SMOE (b) DMOE

$$E_d = \rho v^2 \frac{[1 + \mu][1 - 2\mu]}{[1 - \mu]}, \quad (2)$$

where “ E_d —DME, ρ —density in kg/m^3 , μ —Poisson’s ratio and v —ultrasonic pulse velocity in m/s ”.

Codal Provisions. The SME obtained experimentally is compared with different codal provisions, and the difference between them is studied. The formulas followed to calculate the elasticity as per different standards are detailed in this section. The elastic modulus is determined from the compressive strength based on the equations Eqs. 3, 4, 5, and 6.

“According to IS 456: 2021 [26]

$$E_c = 5000\sqrt{f_{ck}} \quad (3)$$

where f_{ck} is the characteristic compressive strength (CS) in N/mm^2 ”.

According to ACI 318-14 [27],

$$E_c = 4700\sqrt{f'_c} \quad (4)$$

where f'_c is the characteristic CS in N/mm^2 .

According to BS 8110: Part II 1985 [28],

$$E_c = k_0 + 0.2\sqrt{f_{cu}}, \quad (5)$$

where f_{cu} is the characteristic CS in N/mm^2 , k_0 —20 kN/mm^2 for normal-weight concrete.

According to BS EN 1992-1-1: 2004 [29],

$$E_{cm} = 22 \left[\frac{f_{cm}}{10} \right]^{0.3} \quad (6)$$

where f_{cm} is the characteristic CS in N/mm^2 .

3 Results and Discussion

3.1 Static Modulus of Elasticity

It indicates the behavior of any material upon loading in the deformation stage.

The SME of all the fine-grained concrete matrixes is shown graphically in Fig. 3. The SME increases with the ages of curing. It improved by 6.63%, 10.8%, 5.12%, and 2.6% for FGC with 0.2%, 0.4%, 0.5%, and 1% inclusion of basalt fiber (BF) to the

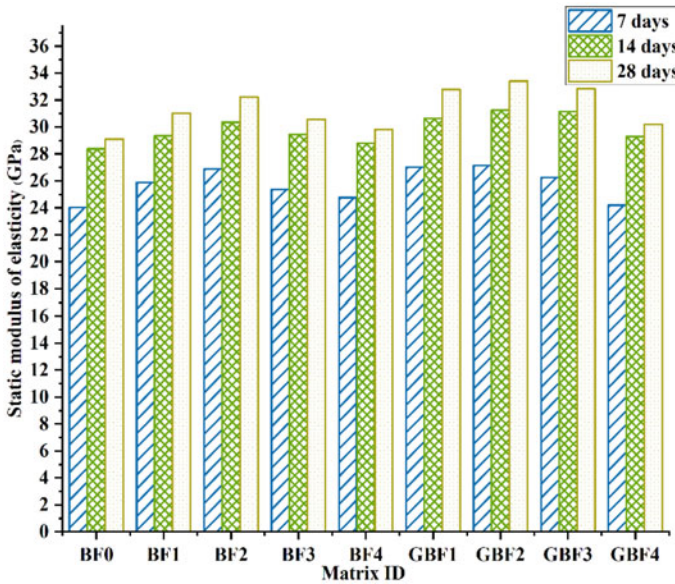


Fig. 3 Static modulus of fine-grained concrete

volume of matrix. It improved by 12.75%, 14.92%, 12.92%, and 3.89% when cement content is partially replaced with 10%, 20%, 30%, and 40% in FGC with 0.4% of basalt fiber inclusion. The SME improves with the ages of curing and with the incorporation of basalt fiber and GGBS. It is maximum for BF-reinforced FGC blended with 20% of GGBS content. As a result of the dilution effect, early strength consisted of less substantial replacement levels due to which the modulus of elasticity reduces on an elevated percentage of cement replacement by GGBS, and similar outcomes were inferred from Johari et al. [16, 30, 31]. Thus, static moduli are influenced by the fibers dispersed in the matrix and fineness of GGBS.

3.2 Dynamic Modulus of Elasticity

DME indicates the real-time monitoring of the structural element by passing vibrations. The DME of all the FGC matrixes is shown graphically in Fig. 4.

It has increased with ages of curing and with fiber addition. It has improved by 4.21% and 6.69% for FGC with 0.2% and 0.4%, and on further addition of 0.5% and 1% of basalt fiber, it has reduced by 12.71% and 17.38%, respectively.

It has still improved by 8.27% and 8.81% when cement content is partially replaced with 10%, 20%, in FGC with 0.4% of basalt fiber inclusion, and then reduced by 12.92% and 3.89% on further partial substitution of cement by 30% and 40% of GGBS. The DME improves with the curing duration, and the inclusion of basalt

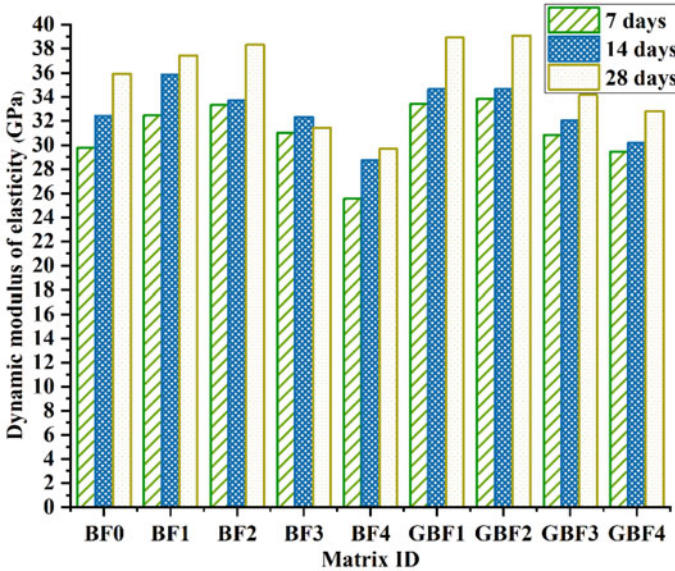


Fig. 4 Dynamic modulus of FGC

fiber and GGBS is reduced after optimum percentage addition. It is maximum for BF-reinforced FGC blended with 20% of GGBS. A fall in dynamic modulus with a higher percentage of slag content was reported by Tavasoli et al. [18] and is similar to the obtained data [30–32]. Thus, it is influenced by fibers and slag.

3.3 Relationship Between SME and DME

The moduli of elasticity of fine-grained concrete are lower for static than dynamic. The ratio between both moduli of different fine-grained concrete samples for various ages of curing is validated, and the ratio between them ranges between 0.79 and 0.85 as in Fig. 5.

The interrelation between different fine-grained concrete specimens is $R^2 = 0.8024$ and is of a good fit. The empirical relation generated is,

$$E_d = 1.056E_c + 8.946, \tag{7}$$

where E_d —DME and E_c —SME.

Different properties of composite elements cause dynamic and static moduli to behave differently, and it indicates why the DME is always larger than the SME [33, 34]. Aggregates in concrete make it stronger, affecting the linear relationship

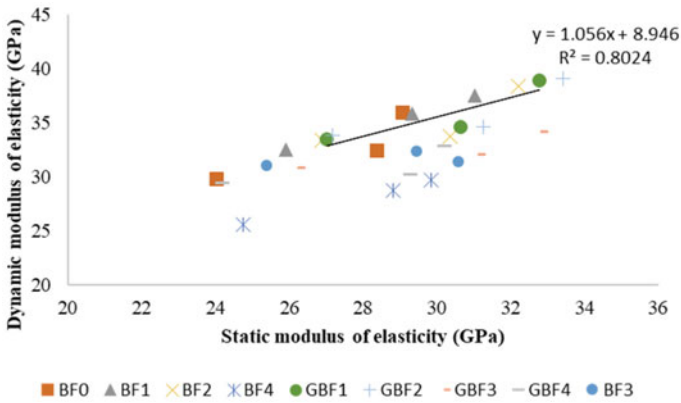


Fig. 5 Relation between SME and DME of fine-grained concrete

between E and E_d . The concrete type also influences the relation [35]. The DME is always larger than the SME [36].

3.4 The Difference in Elastic Modulus from Different Codal Provisions

The MOE of concrete determined per different codal provisions is given in Table 2. The experimentally obtained data vary from the predicted theoretical provisions, and its difference is given in Table 3. The elastic modulus predicted as per BS 8110-Part II [28] is higher than other codes, with a difference of 16–26%.

Table 2 Elastic modulus of concrete as per different codal provisions

Matrix ID	Compressive strength (MPa) [23]	Static modulus of elasticity (GPa)	Modulus of elasticity (GPa)			
			IS 456: 2021	ACI 318-14	BS 8110-Part II-1985	EN 1992-1-1: 2004
BF0	33.84	23.07	29.09	27.34	20.00	25.52
BF1	38.5	26.13	31.02	29.16	20.00	26.19
BF2	41.53	27.21	32.22	30.29	20.00	26.59
BF3	37.38	25.43	30.57	28.74	20.00	26.04
BF4	35.61	24.38	29.84	28.05	20.00	25.78
GBF1	43	27.56	32.79	30.82	20.00	26.77
GBF2	44.67	28.74	33.42	31.41	20.00	26.98
GBF3	43.13	27.85	32.84	30.87	20.00	26.79
GBF4	36.51	25.43	30.21	28.40	20.00	25.91

Table 3 Difference in elastic modulus of concrete between experimental and different codal provisions

Matrix ID	Difference in modulus of elasticity (%)			
	IS 456: 2021	ACI 318-14	BS 8110-Part II-1985	EN 1992-1-1: 2004
BF0	26.08	18.51	13.30	10.63
BF1	18.73	11.61	23.45	0.23
BF2	18.42	11.31	26.49	2.28
BF3	20.21	13.00	21.35	2.38
BF4	22.38	15.04	17.96	5.76
GBF1	18.97	11.83	27.43	-2.85
GBF2	16.28	9.30	30.41	-6.13
GBF3	17.91	10.83	28.18	-3.80
GBF4	18.80	11.68	21.35	1.90

Similarly, the difference in modulus of 9–18%, 13–30%, and 0–10% with reference to experimental and ACI 318-14 [27], BS 8110-Part II-1985 [28], and EN 1992-1-1: 2004, is found respectively. No significant difference in theoretical data was predicted as per BS 8110-Part II-1985 [28] for different mixes.

4 Conclusion

The modulus of elasticity varies in real time than from the laboratory study and is proven from the static and DME obtained. Adding BF and GGBS influences the elastic characteristics of fine-grained concrete. The SME and DME are higher by 14.92% and 8.81%, respectively, for FGC with 0.4% BF and 20% GGBS as a partial cement substitution. The difference between SME and DME is 1.05 times, and the variation is due to the loading condition. The greater difference in experimental and theoretical data is in determining the elastic modulus which is because the formulas used are for conventional concrete. This study proves that it is necessary to frame an equation for fine-grained concrete as the particle size of materials used, absence of coarse aggregate, and fibers have the major impact on the static moduli characteristics. The developed fine-grained concrete does not require coarse aggregate which is major source in construction industry thus, saves the mother earth, and can be considered as sustainable.

References

1. Suksawang N, Wtaife S, Alsabbagh A (2018) Evaluation of elastic modulus of fiber-reinforced concrete. *ACI Mater J* 115:239

2. Pliya P, Beaucour A-L, Noumowé A (2011) Contribution of cocktail of polypropylene and steel fibres in improving the behaviour of high strength concrete subjected to high temperature. *Constr Build Mater* 25:1926–1934
3. Bhargava P, Sharma UK, Kaushik SK (2006) Compressive stress-strain behavior of small scale steel fibre reinforced high strength concrete cylinders. *ACT* 4:109–121
4. Carrillo J, Ramirez J, Lizarazo-Marriaga J (2019) Modulus of elasticity and Poisson's ratio of fiber-reinforced concrete in Colombia from ultrasonic pulse velocities. *J Build Eng* 23:18–26
5. Swamy R, Bouikni A (1990) Some engineering properties of slag concrete as influenced by mix proportioning and curing. *Mater J* 87:210–220
6. Bakht B, Jaeger LG, Mufti AA (1989) Elastic modulus of concrete from compression tests. *Mater J* 86:220–224
7. Hale WM, Freyne SF, Bush TD, Russell BW (2008) Properties of concrete mixtures containing slag cement and fly ash for use in transportation structures. *Constr Build Mater* 22:1990–2000
8. Silva RV, de Brito J, Dhir RK (2016) Establishing a relationship between modulus of elasticity and compressive strength of recycled aggregate concrete. *J Clean Prod* 112:2171–2186
9. Neville AM (1995) Properties of concrete. Longman, London
10. Marques AI, Morais J, Morais P, Veiga MR, Santos C, Candeias P, Ferreira JG (2020) Modulus of elasticity of mortars: static and dynamic analyses. *Constr Build Mater* 232:117216
11. Alaskar A, Albidah A, Alqarni AS, Alyousef R, Mohammadhosseini H (2021) Performance evaluation of high-strength concrete reinforced with basalt fibers exposed to elevated temperatures. *J Build Eng* 35:102108
12. Zhou H, Jia B, Huang H, Mou Y (2020) Experimental study on basic mechanical properties of basalt fiber reinforced concrete. *Materials* 13:1362
13. Khan M, Cao M, Chaopeng X, Ali M (2022) Experimental and analytical study of hybrid fiber reinforced concrete prepared with basalt fiber under high temperature. *Fire Mater* 46:205–226
14. Sun X, Gao Z, Cao P, Zhou C (2019) Mechanical properties tests and multiscale numerical simulations for basalt fiber reinforced concrete. *Constr Build Mater* 202:58–72
15. Saranya P, Nagarajan P, Shashikala AP (2018) Eco-friendly GGBS concrete: a state-of-the-art review. *IOP Conf Ser Mater Sci Eng* 330:012057
16. Megat Johari MA, Brooks JJ, Kabir S, Rivard P (2011) Influence of supplementary cementitious materials on engineering properties of high strength concrete. *Constr Build Mater* 25:2639–2648
17. Güneysi E, Gesoğlu M (2008) A study on durability properties of high-performance concretes incorporating high replacement levels of slag. *Mater Struct* 41:479–493
18. Tavasoli S, Nili M, Serpoush B (2018) Effect of GGBS on the frost resistance of self-consolidating concrete. *Constr Build Mater* 165:717–722
19. Kalla J, Karri S, Sathi KV (2021) Experimental analysis on modulus of elasticity of slag based concrete. *Mater Today Proc* 37:2114–2120
20. Kumar DC, Vasanthi P (2022) Effect of coarse and fine GGBS in mechanical properties of concrete. *Mater Today Proc* 2022:S2214785322049318
21. Ganesh Babu K, Sree Rama Kumar V (2000) Efficiency of GGBS in concrete. *Cement Concr Res* 30:1031–1036
22. Sudhakar AJ, Muthusubramanian B (2022) Development of basalt fiber reinforced fine-grained cementitious composites for textile reinforcements. *J Compos Sci* 6(12):395
23. Sudhakar AJ, Muthusubramanian B (2023) Thermal Characteristics of fine grained concrete with various percentages of basalt fiber and GGBS. *J Therm Anal Calorim* 148(12):5217–5233
24. ASTM C 469: Test method for static modulus of elasticity and Poisson's ratio of concrete in compression. ASTM International
25. ASTM C 597: Test method for pulse velocity through concrete. ASTM International
26. IS 456 (2021) Plain and reinforced concrete—code of practice (reaffirmed 2021), p 114
27. ACI 318-19 (2019) Building code requirements for structural concrete and commentary. American Concrete Institute
28. BS 8110 (1985) Part II: structural use of concrete. Part 2: code of practice for special circumstances. British Standards Institution, London

29. Eurocode 2 (2015) Design of concrete structures—part 1–1: general rules and rules for buildings. British Standards Institution, London
30. Berndt ML (2009) Properties of sustainable concrete containing fly ash, slag and recycled concrete aggregate. *Constr Build Mater* 23:2606–2613
31. Nandanam K, Biswal US, Dinakar P (2021) Effect of fly ash, GGBS, and metakaolin on mechanical and durability properties of self-compacting concrete made with 100% coarse recycled aggregate. *J Hazard Toxic Radioact Waste* 25:04021002
32. Rao SK, Sravana P, Rao TC (2016) Experimental studies in ultrasonic pulse velocity of roller compacted concrete pavement containing fly ash and M-sand. *Int J Pavem Res Technol* 9(4):289–301
33. Zhang X, Chiu Y, Hao H, Cui J (2021) Free water effect on the dynamic compressive properties of mortar. *Cement Concr Compos* 118:103933
34. Lorenzi A, Tisbirek FT (2007) Ultrasonic pulse velocity analysis in concrete specimens. p 13
35. Koehler EP, Fowler DW, Foley EH, Rogers GJ, Watanachet S, Jung MJ (2007) Self-consolidating concrete for precast structural applications: mixture proportions, workability, and early-age hardened properties
36. Popovics JS, Zemajtis J, Shkolnik I (2008) A study of static and dynamic modulus of elasticity of concrete. ACI-CRC Final Report

Analytical Investigation of Cold-Formed Steel Build-Up Sigma-Shaped Section



A. Yogesh Kumar and S. A. Vengadesh Subramanian

1 Introduction

Cold-formed steels are the thin steel of smooth surface having a thickness of 0.3–6 mm. The cold-formed steel (CFS) construction is rapidly increasing day by day. These cold-formed steels are used in columns, beams, purlins, and some build-up sections. It leads the CFS member applications in which many single sections are connected to form “built-up” cross-sections. It can be used for both structural and non-structural members. Most of the countries like Germany, Great Britain, Japan, and the USA started the construction in cold-formed steels in different ways. Cold-formed steel has more advantages than hot-rolled steel sections. For example: different shapes can be adopted easily, the material requirement is small and easy for fabrication. The main properties of cold-formed steels are more strength, less weight, and more flexible. As a result, the stiffeners improve the material utilization efficiency. In this paper, by changing the shape of the cold-formed steel to get maximum strength and also find the effective configuration of cold-formed steel. Andrzej et al. [1] conducted the different geometric imperfections compared with its buckling failure mode. The overall stability of the specimen was affected by local instability. Young and Hancock [2] presented the comparison between NAS, NZS, AISI, and AS specifications with the experimental result values and failure mode. The specimens are channel sections with the inclined web at the flange. The compressive tests are carried out for the column sections. Young and Chen [3] noted that the specimen with end stiffener makes higher buckling stress leading to economic design. The design strength is applicable for the non-symmetric lipped section except for short columns. Liam et al. [4] reported that the load-bearing capacity of two sigma is 2.9 times higher than single sigma. Depending upon the section shape (by

A. Yogesh Kumar · S. A. Vengadesh Subramanian (✉)

Department of Civil Engineering, Faculty of Engineering and Technology, SRM Institute of Science and Technology, Kattankulathur, Tamil Nadu 603203, India

e-mail: vengades@srmist.edu.in

providing web stiffeners) different structural responses has been noted. Wang and Young [5] investigated moment capacities and failure patterns of the cold-formed steel built-up sections. The stiffeners are employed to reduce the buckling effect in the cold-formed steels. In four-point bending tests, the failure occurs at a moment. In point loading tests, the failure occurs at the loading point. Lateral–torsional buckling does not occur in any test results. The moment capacities in point loading are 13% higher than the two-point loading.

2 Numerical Analysis

The numerical analysis is completely worked out by using finite element software ABAQUS version 6.14. The models are simply supported with three-point bending and four-point bending. The CFS built-up beams are commonly used four-noded shell elements with six (three translational and three rotational) degrees of freedom for each node. Other researchers Wang and Young [6] have successfully used this element type in the numerical modelling of cold-formed steel built-up sections. Two sigma-shaped models are placed in the form of a hollow section. The holes are drilled at the interval of 100 mm for screws. The holes are drilled both at the top and bottom. In modelling, the partition circles are made around the screw holes to represent the washers of the screw.

The main property required to find out the capacity of the specimen is density, elasticity, and plasticity. The material properties of the specimen are listed in Table 1. The Young's modulus and Poisson ratio values are used in elasticity. The plasticity values are taken from the paper Kankanamge et al. [7]. The density and Poisson ratio of the specimen are the same for all the thicknesses except plasticity values. The properties are assigned to the modelled sigma specimen. In the assembly, separate sigma sections were placed together in the form of a hollow section.

The mesh-independent fastener option in the ABAQUS library was used to model the connection between the screws and plates. A validation model with two nodes and six degrees of freedom per node was used to model the self-driving screws with a higher degree of a factor of safety, assuming the linear elastic behaviour elastic stiffness value of 5kN/mm.

Table 1 Material properties

Specimen thickness (T)	Young's modulus (Mpa)	Poisson's ratio	Yield strength (Mpa)	Ultimate strength (Mpa)
0.6	214,000	0.3	675	700
1.0	205,000	0.3	616	634
1.2	213,500	0.3	569	589
1.6	204,300	0.3	544	568

3 Parametric Study of the Specimens

The created finite element model accurately forecasts the test beams' moment capacity and distorted forms. As a result, a thorough parametric analysis of 72 built-up beams subjected to a point loading and two-point loading was conducted using the validated model. The CFS-closed built-up beam section investigated in this work features a unique cross-section that combines the benefits of both the "I" and a closed-box section. There are nine different types of specimens that were investigated. The thickness of each specimen taken in the analysis are 0.6, 1.0, 1.2 and 1.6 mm. There are three different patterns which are investigated. For example: fully overlapped (FO), half overlapped (HO), and web stiffener are mentioned in Fig. 1. The shape of the specimen is also varied by means of three different types, based on the total number of stiffeners provided in the web region. They are one stiffener inwards, one stiffener outwards, and two stiffeners inwards which are mentioned in Fig. 2. The dimension of all the specimens is listed in Table 2.

The specimens are named to identify the details by its name. For example, the specimen is named as 3PFO1SIN1T which is described as follows: 3P refers to three-point loading, FO refers to fully overlapped, 1S refers to one stiffener in web, IN refers to inwards, 1 T refers to thickness in 1 mm. All the specimens were modelled for a length of 1400 mm and the supports are placed at 100 mm from both the ends. The screws are provided at every 100 mm spacing of the beam. The moment capacities, stiffness, and failure patterns are presented by FE analysis.

The material properties of the specimen are taken from the paper Kankanamge and Mahendran which are mentioned in Table 1 [7].

To check the optimized shape, the same dimensions of the previous shaped specimens are taken. The dimension of all the specimens was taken from Wang and Young [6].

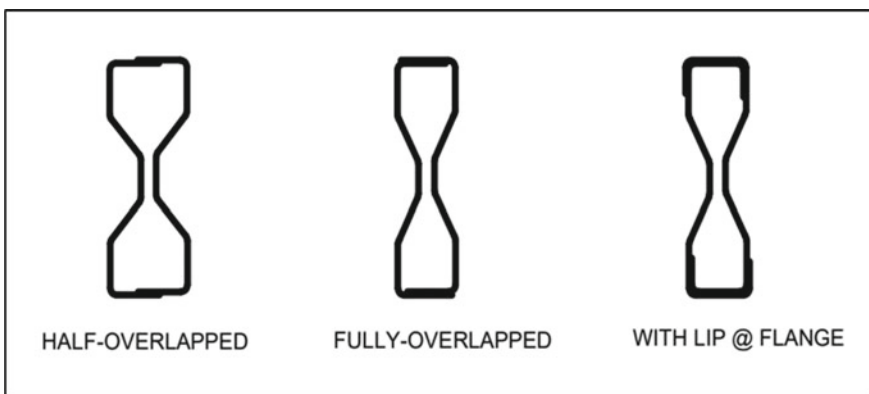


Fig. 1 Three different types of patterns

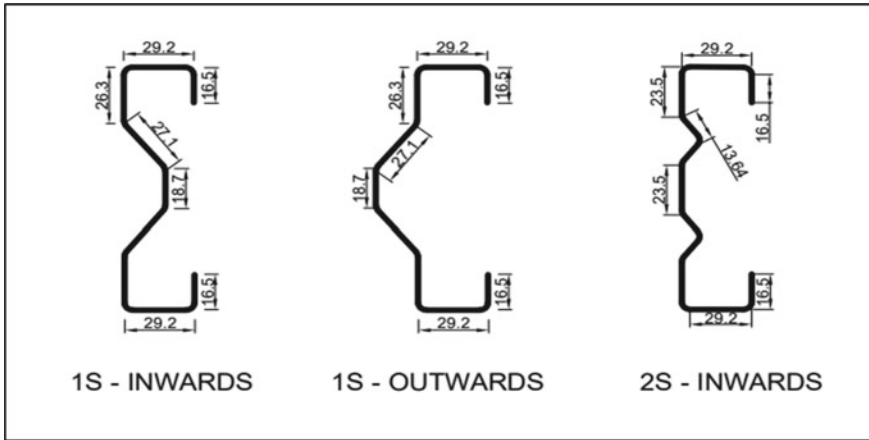


Fig. 2 Three different types of shapes

Table 2 Dimension of all the specimens

Specimens	bl (mm)	bf (mm)	L1 (mm)	L2 (mm)	L3 (mm)	t (mm)	r (mm)
HO1SIN	–	29.2	26.3	27.1	18.7	0.6–1.6	3.4
HO1SOUT	–	29.2	26.3	27.1	18.7	0.6–1.6	3.4
HO2SIN	–	29.2	26.3	13.64	–	0.6–1.6	3.4
FO1SIN	–	29.2	26.3	27.1	18.7	0.6–1.6	3.4
FO1SOUT	–	29.2	26.3	27.1	18.7	0.6–1.6	3.4
FO2SIN	–	29.2	26.3	13.64	–	0.6–1.6	3.4
FO1SINWL	16.5	29.2	18.84	27.1	18.7	0.6–1.6	3.4
FO1SOUTWL	16.5	29.2	18.84	27.1	18.7	0.6–1.6	3.4
FO2SINWL	16.5	29.2	18.84	13.64	–	0.6–1.6	3.4

4 Result and Discussion

4.1 Shapes' Deformation

There are three different types of failures which are discussed. They are local buckling, distortional buckling, and flexural buckling. Local buckling cause lateral displacement occurs at the point of loading. In most cases, it occurred at flanges or it will be high at flanges. The rotation of the specimen from the initial axis and translation that occurs at the flange or web section is called distortional buckling. In most cases, it occurred near the supports or corners of the beams. The combination of both rotation and bending that occurs at the beam is called flexural buckling. From the results of all the specimens, the failure mode of each specimen was studied. At the

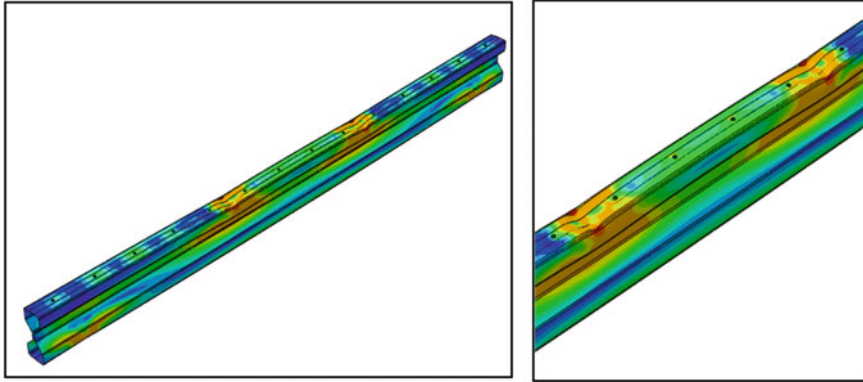


Fig. 3 Local buckling failure in four-point bending

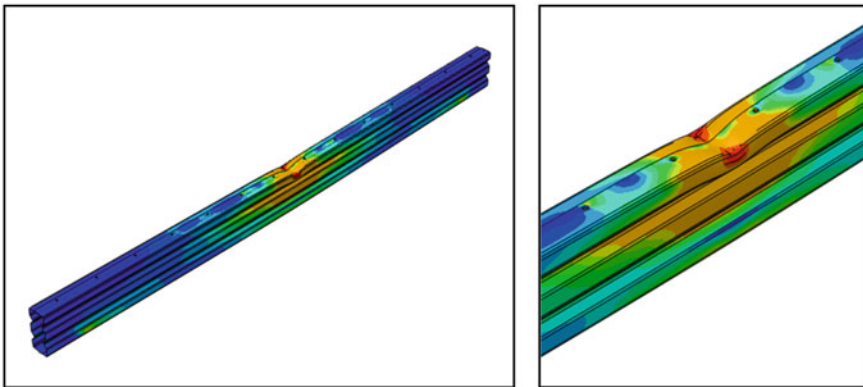


Fig. 4 Local buckling in three-point bending

compression flange, the local buckling was observed and also at the webs in moment span as shown in Figs. 3 and 4. Distorsional buckling occurred at both the supports of the specimen was observed as shown in Fig. 5.

4.2 Behaviour Study by Changing Thickness

To study the effect of thickness by comparing the ultimate load-carrying capacity of each specimen is compared and finalized the results. The varied thickness is 0.6, 1.0, 1.2, and 1.6 mm. The shape and pattern of the specimens are kept constant and changed the thickness, to check the capacity. The ultimate strength of the specimen

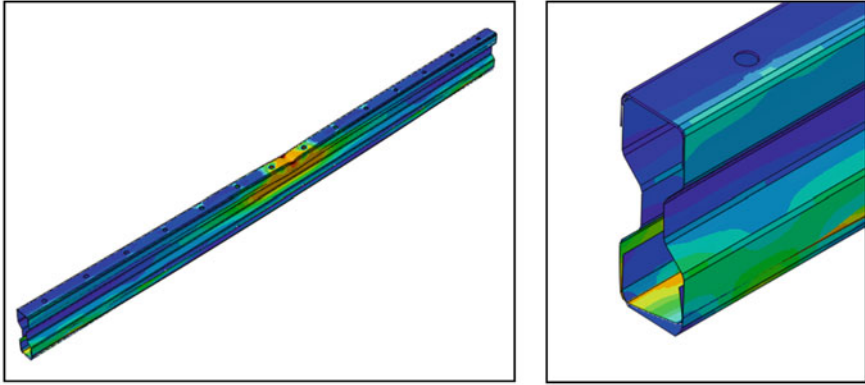


Fig. 5 Distorsional buckling at edges of the beam

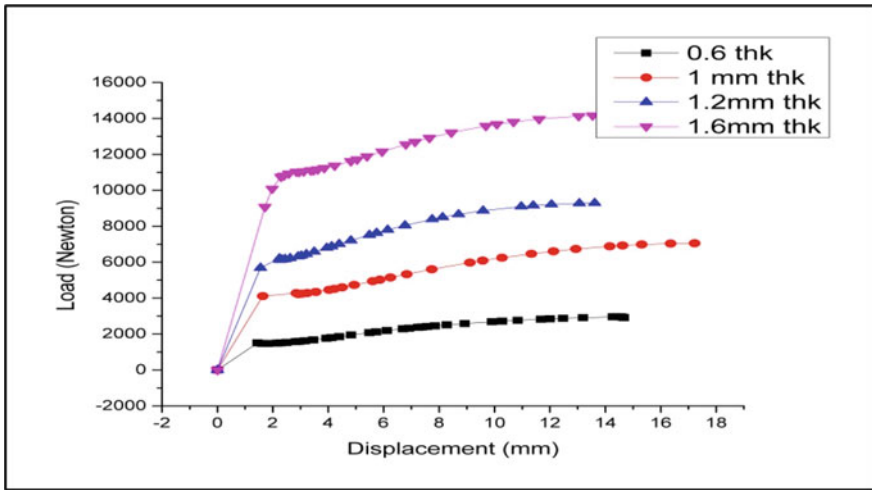


Fig. 6 Behaviour of specimens at different thicknesses

is increasing while increasing the thickness. Hence, it shows impact while changing the thickness (Fig. 6).

4.3 Pattern Variation Study

To find out the effective pattern which can carry maximum load-carrying capacity among the specimens result are calculated. The thickness and shape of the specimens are kept constant and change the pattern. To check the capacity of the specimens

while changing the pattern into half overlapped (HO), full overlapped (FO) and full overlapped with lips of each specimens are calculated. The maximum strength is achieved in full overlapped with lips. The minimum strength achieved in full overlapped (Fig. 7).

The specimen SPHO1S1T has failed by both local buckling and flexural buckling. The local buckling occurs at the point of loading. The displacement occurs at the point of loading. The overlapping regions of plates are compressed at the bottom flange of the specimen. The failure pattern of the specimen at loading and supports is mentioned in Fig. 8. The SPHO1S1T has 26.07% higher capacity than SPFO1S1T.

The specimen SPFO1S1TWEB has failed by both distortional buckling and flexural buckling. The distortional buckling occurs at the edge of the specimen. The displacement occurs at the point of loading. The failure pattern of the specimen at loading and supports is figured in Fig. 9. The SPFO1S1TWEB has a 41.62% higher capacity than SPFO1S1T.

The specimen SPFO1S1T has failed by both local buckling and flexural buckling. The local buckling occurs at the point of loading. The displacement occurs at the point of loading. The failure pattern of the beam at loading and supports is figured in Fig. 10. The specimen SPFO1S1T has a lesser load-carrying capacity comparing other specimens.

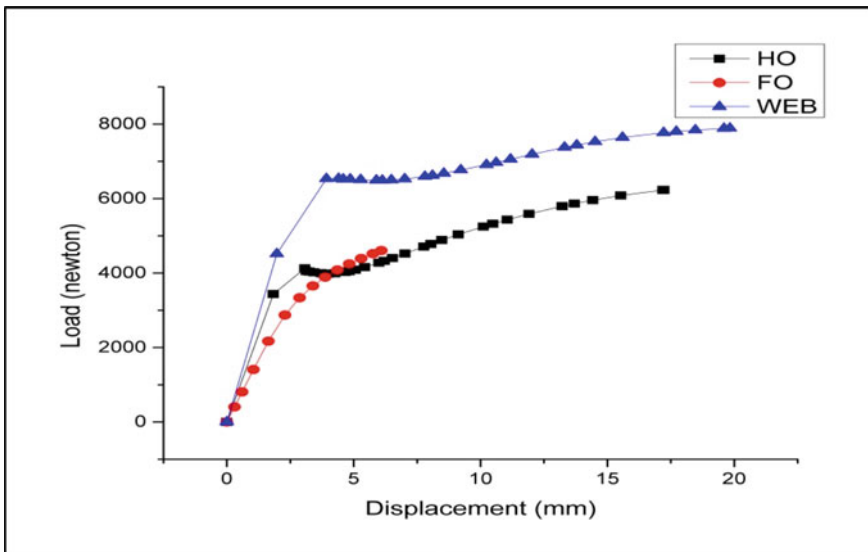


Fig. 7 The different patterns of the specimen

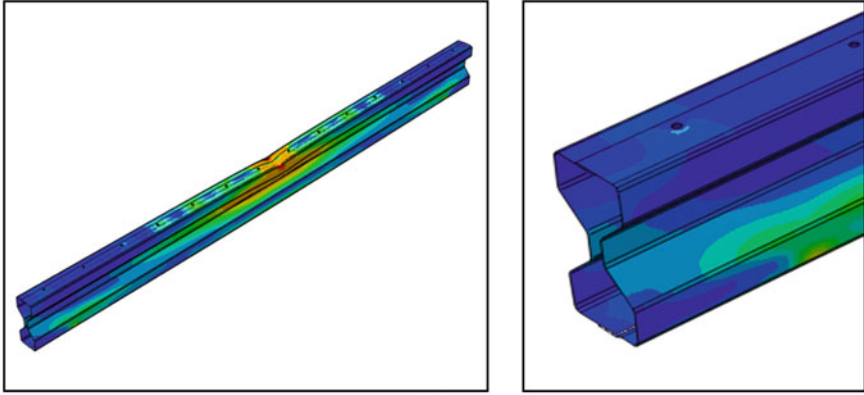


Fig. 8 Failure at loading point; failure at support of half overlapped (SPHO1S1T)

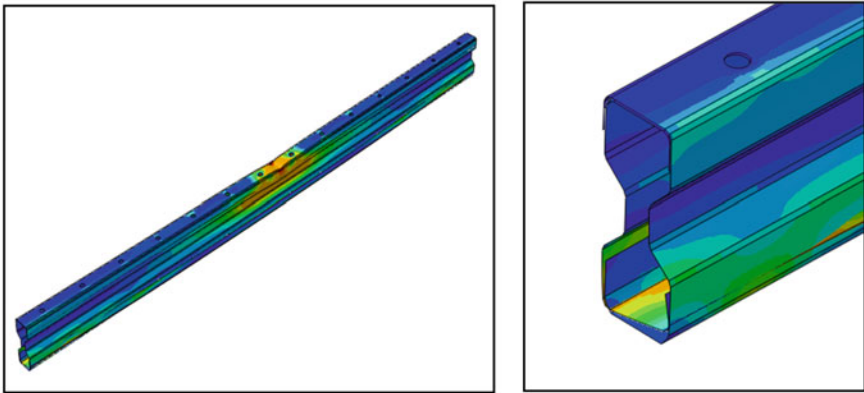


Fig. 9 Failure at loading point; failure at support of full overlapped (SPFO1S1TWEB)

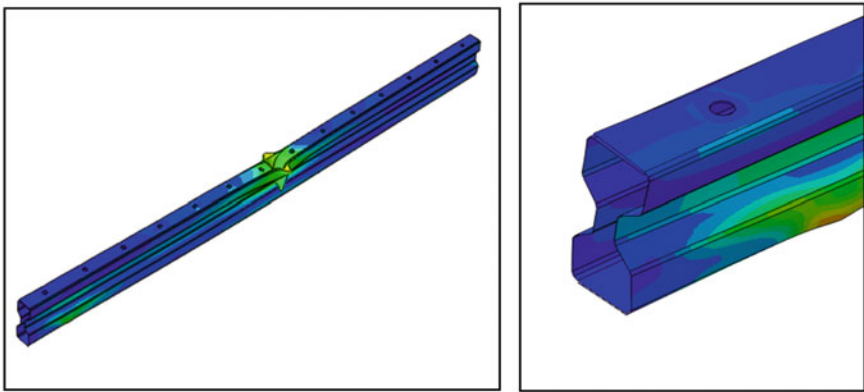


Fig. 10 Failure at loading point; failure at edge and support of full overlapped (SPFO1S1T)

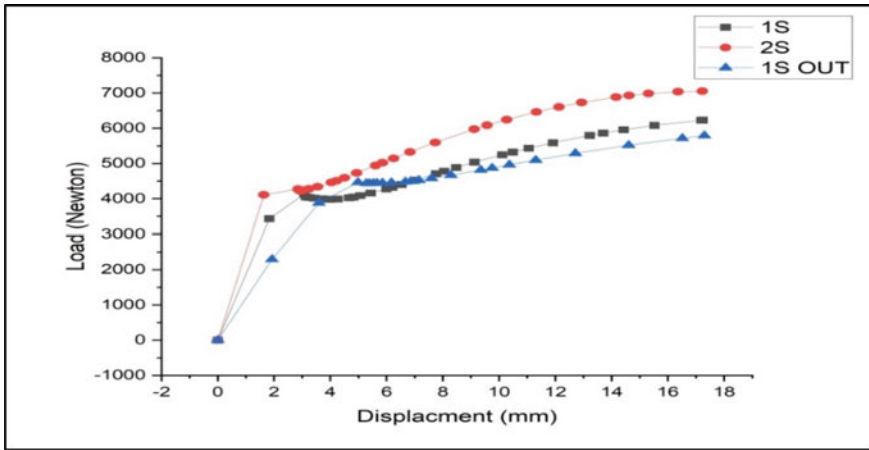


Fig. 11 The various shapes of the specimen

4.4 Shape Variation Study

To check the effect of changing the shape of the specimen by comparing their load-carrying capacities of the each specimens. The thickness and pattern of the specimens are kept constant and change the shape. The capacity of the specimens are checked while changing the shapes into 1S (IN), 1S (OUT), and 2S. The maximum strength was achieved in 2S (specimen with two stiffeners in web). The minimum strength is achieved in 1S (specimen with one stiffener inwards) (Fig. 11).

The specimen SPHO1S1T has failed by both local buckling and flexural buckling. The local buckling occurs at the point of loading. The displacement occurs at the point of loading. The overlapping regions of plates are compressed at the bottom flange of the specimen. The failure pattern of the specimen at loading and supports is figured in Fig. 12. The SPHO1S1T has a 6.98% higher capacity than SPHO1S1TOUT.

The specimen SPFO2S1T has failed by both local buckling and flexural buckling. The local buckling occurs at the point of loading. The displacement occurs at the point of loading. The overlapping regions of plates are compressed at the bottom flange of the specimen. The failure pattern of the specimen at loading and supports is figured in Fig. 13. The SPHO2S1T has a 17.83% higher capacity than SPHO1S1TOUT.

The specimen SPHO1S1TOUT has failed by both local buckling and flexural buckling. The local buckling occurs at the point of loading. The displacement occurs at the point of loading. The overlapping regions of plates are compressed at the bottom flange of the specimen. The failure pattern of the specimen at loading and supports is figured in Fig. 14. The specimen SPHO1S1TOUT has a lesser load-carrying capacity comparing other specimens.

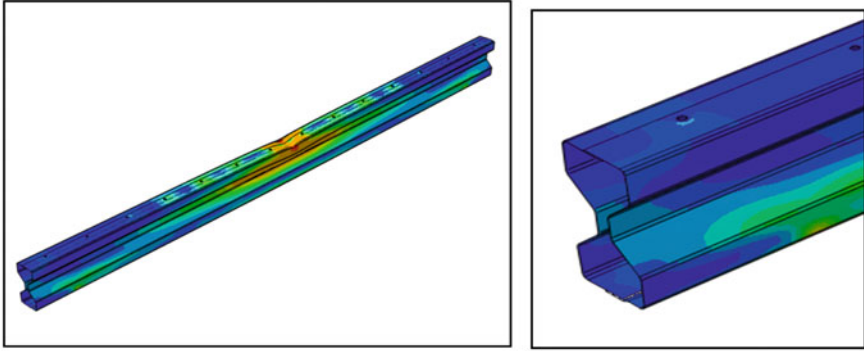


Fig. 12 a Failure at loading point; b failure at edge and support of half overlapped (SPHO1S1T)

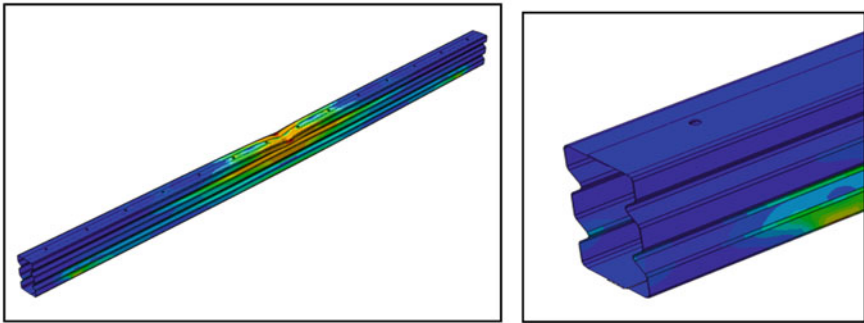


Fig. 13 Failure at loading point; failure at support of half overlapped (SPHO2S1T)

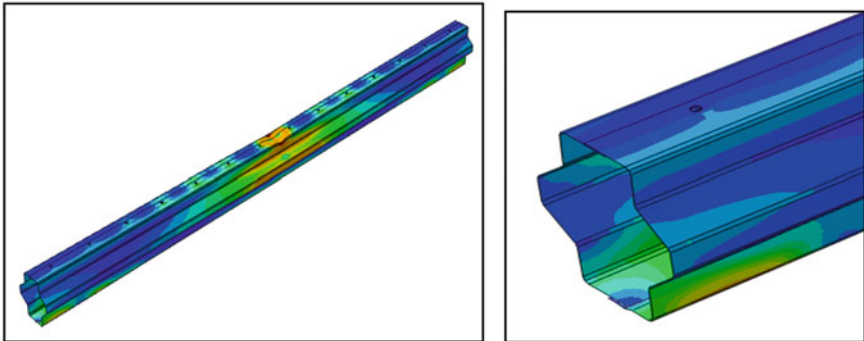


Fig. 14 Failure at loading point; failure at edge and support of half overlapped (SPHO1S1TOUT)

5 Conclusion

In this study, the behaviour of cold-formed steel built-up section with sigma is examined. The variation in thickness, pattern, and shape was investigated under three-point loading and four-point bending in this study. The maximum load-carrying capacity and the failure pattern of the specimen are discussed in this paper. The specimen with a lip specimen undergoes both flexural buckling and distortional buckling. The overlapping regions of plates are compressed at the bottom flange of the specimen with half overlapped. Other specimens are undergoing local buckling and flexural buckling. Most of the specimens has failed by local buckling or distortional buckling or a combination of both local and distortional bucklings. The specimen with lips and two stiffeners in the web performs well comparing other specimens. The increase of thickness of every specimen increases respective capacity strength.

References

1. Garstecki A, Kakol W, Rzeszut K (2002) Classification of local sectional geometric imperfections of steel thin-walled cold-formed sigma members. *Foundations of Civil Environmental Engineering*
2. Young B, Hancock GJ (2003) Compression tests of channels with inclined simple edge stiffeners. *J Struct Eng* 129(10):1403–1411
3. Young B, Chen J (2008) Column tests of cold-formed steel non-symmetric lipped angle sections. *J Constr Steel Res* 64(7–8):808–815
4. Laím L, Rodrigues JPC, Craveiro HD (2015) Flexural behaviour of beams made of cold-formed steel sigma-shaped sections at ambient and fire conditions. *Thin-Walled Struct* 87:53–65
5. Wang L, Young B (2014) Design of cold-formed steel channels with stiffened webs subjected to bending. *Thin-Walled Struct* 85:81–92
6. Wang L, Young B (2016) Behavior of cold-formed steel built-up sections with intermediate stiffeners under bending. I: tests and numerical validation. *J Struct Eng* 142(3):04015150
7. Kankanamge ND, Mahendran M (2011) Mechanical properties of cold-formed steels at elevated temperatures. *Thin-Walled Struct* 49(1):26–44

Innovation in Construction Materials

A Novel XGBoost and RF-Based Metaheuristic Models for Concrete Compression Strength



Manish Kumar , N. Zainab Fathima , and Divesh Ranjan Kumar

1 Introduction

Besides water, concrete is considered the most widely employed substance in the world. This is because it has many applications in civil engineering, where it excels. Fine aggregate, coarse aggregate, cement, admixtures, and other basic materials and additives make up concrete. It is no secret that cement is crucial to city buildings and transportation systems; however, production of carbon dioxide, a powerful greenhouse gas, is significant in the cement industry. Approximately 4 and 8 percent of total worldwide CO₂ emissions come from concrete, making it one of the most carbon-intensive materials in the world. The topsoil, the most nutrient-rich part of the soil, is harmed by the usage of concrete. A great deal of air pollution is produced during the cement making process, yet this process cannot be stopped. Imagining a planet devoid of cement is ludicrous. At this time, green cement is the only alternative accessible. Green cement is cement made with a carbon-negative production technique. Thus, it not only contributes in the reduction of carbon footprint and other environmental challenges associated with cement production but also enhances the performance of concrete [1]. Green concrete is created by using waste material as a

M. Kumar (✉)

Department of Civil Engineering, SRM Institute of Science and Technology (SRMIST),
Tiruchirappalli Campus, Deemed to be University, Tiruchirappalli, India
e-mail: manishk@srmist.edu.in

N. Z. Fathima

Department of ECE, SRM Institute of Science and Technology (SRMIST), Tiruchirappalli
Campus, Deemed to be University, Tiruchirappalli, India
e-mail: zn0615@srmist.edu.in

D. R. Kumar

Department of Civil Engineering, NIT Patna, Patna, India
e-mail: diveshk.ph21.ce@nitp.ac.in

partial replacement for cement or fine or coarse aggregate. While many environmentally preferable alternatives exist, they can only be utilized to partially replace the cement in concrete, rather than completely. Fly ash (FA) refers to the residual material that remains unburned in the burning zone of a boiler and is carried away by flue gases. It is typically collected using electrostatic or mechanical separators. On the other hand, silica fume (SF) is a fine particle material that can function as both a filler and a pozzolan in concrete. It mainly consists of aluminum oxide, iron oxide, and silicon dioxide. Silica fume is produced as a byproduct during the manufacturing of ferrosilicon alloys or silicon metal, owing to its highly reactive pozzolanic properties and distinctive physical and chemical characteristics.

The ability to forecast the compressive strength (CS) of concrete is particularly challenging since it depends on so many different variables, including the water–cement ratio, cement strength, the quality of the concrete’s raw materials, and quality control during production. Generally, the compressive strength of concrete is determined in lab by conducting the compressive strength test on a cube or cylinder. The standard test method used to access the compressive strength of cylindrical concrete specimen is specified in the code ASTM C39/C39M [2]. The compressive strength for any material is defined as the load applied on the point divided by the cross-section area of the applied load face. To obtain and maintain the specified CS in concrete design, which includes chemical admixtures, water, supplemental cementitious ingredients, fine and coarse aggregates, cement, and fibers, is a significant challenge. Finding trustworthy and cutting-edge machine learning techniques to uncover those links has been prompted by the lack of understanding regarding testing between concrete strength and its components. Trying all the different amounts and evaluating each one’s performance require a tremendous amount of time, effort, money and might be less accurate (experimental error). The technical staff must make intense attempts at numerous mix percentages over an extended period of time in order to capture a 28-day design CS with proper workability, increasing material waste and the expense of producing concrete. Significantly, it might be extremely challenging to adjust another test as previously in the event of concrete test failures after such a long waiting period. On the other hand, over the past few decades, the use of aggregates like silica fume, fly ash, and slag has been increasingly popular for enhancing the durability and strength of concrete. In this scenario, according to Abrahams Law, there exist multiple models that can predict and estimate the strength of concrete prior to the 28-day mark. However, the connection between concrete strength and its component materials is nonlinear in nature. Unfortunately, the Abrahams Law model struggles to accurately capture this complex relationship, thus lacking the ability to effectively generalize with unseen data. The laboratory work required to produce green concrete and ensure its strength is expensive, time-consuming, and labor-intensive.

As a result, linear and machine learning models were employed to forecast the CS. Machine learning (ML) and artificial intelligence (AI) are forms of intelligence displayed by machines as opposed to human and animal natural intelligence. Machine learning (ML) techniques can now be used to predict the mechanical properties of concrete, thanks to advancements in artificial intelligence (AI). Not only does this

assure the necessary proportions in mix design to produce strength, but it can also lower the amount of uncertainty involved in making predictions. Inferring the optimal model from a set of input variables, these supervised machine learning algorithms find strong correlations. Yaseena et al. [3] employed the MARS, SVR, M5 Tree, and ELM learning models to forecast the CS of lightweight foamed concrete; the conclusions of the study state that ELM was more accurate than the other four models. This research aimed to use artificial intelligence (AI) models to more accurately predict the CS of concrete subjected to fly ash and silica fumes. Although the adding of aggregates to concrete has been the subject of numerous studies, employing AI models is uncommon. AI has been shown to be an accurate and dependable technique for learning complex patterns while also saving time and resources. Various researchers have applied variety of machine learning techniques in the literature to predict the compressive strength of concrete [3–6]. Among AI algorithms, ANN is frequently recommended for predicting concrete strength by utilizing a backpropagation (BP) network. ANN and ELM were comparatively analyzed [7] for CS prediction of fly ash concrete where ANN was found to outperform ELM. However, BP fails because of the instability introduced by local minima in the formulated model. The ANN's multimodal optimization objective is the cause of the convergence to local minima. Biswas et al. [8] concluded that the ENN and RVM are robust models for predicting compressive strength of silica fume concrete. Though there is a recent surge in application of ML models for CS of concrete, most applications belong to basic models which are unable to capture the complex correlations or trained on very small dataset. For concrete mixed with fly ash and silica fume, there are even fewer applications. Several researches in literature [9, 10] established that XGBoost is a state-of-the-art simulation model for fly ash concrete. Li and Long [11] concluded that RF and XGBoost are robust to predict CS of fly ash silica fume concrete. Since the properties of the concrete and constituents vary from place to place, the ML needs to be checked for a variety of datasets from various locations before using it as a reliable alternative by construction engineers. The paper presents the comparative study of XGBoost and RF-based soft computing models for CS of fly ash and silica fume concrete.

2 Details of ML Models Used in the Study

XGBoost XGBoost is a well-known open-source gradient boosting machine learning package. Tianqi Chen created it in C++, and it eventually became a collaborative effort with numerous participants. XGBoost is a popular algorithm for classification and regression issues, as well as ranking and recommendation systems. The primary principle underlying XGBoost is to add weak models progressively to a final strong model. The approach trains a new model on the residual errors of the preceding model at each step, with the goal of minimizing the total error. This procedure is repeated until a preset stopping condition, such as a maximum number of models

or a minimal error level, is reached. One of the XGBoost's primary strengths is its capacity to tolerate missing data and outliers, as well as its efficient use.

Random Forest Random Forest (RF) is a highly versatile and efficient ensemble learning algorithm that distinguishes itself among the various types available. Random Forest is a machine learning algorithm that employs an ensemble of decision trees to make predictions by aggregating the results of multiple trees. Upon receiving training on a randomly selected subset of the training data, each tree provides its prediction to the ultimate outcome. The ensemble method serves to alleviate overfitting and enhance the precision and stability of the model. Several benefits are evident when comparing a Random Forest to a solitary decision tree. The technique of averaging across multiple trees mitigates the influence of any anomalous individual trees, thereby decreasing the method's vulnerability to overfitting.

3 Dataset for Model Simulation

A previous study [12] gathered a mix design of 24 mixes with 144 different sounds. In the study, eight input parameters were utilized: coarse aggregate (ca), high-rate water reduction agent (HRWRA), fine aggregate (ssa), fraction amount of fly ash (FA), sample age (AS), total cementitious material (TCM), fraction amount of silica fume (SF), and water content (W). The study also included a single output parameter, compressive strength of concrete (CS). Figure 1 visually represents the spreading of the dataset through a histogram and displays the confidence ellipse for the relevant parameters. To facilitate the analysis, the dataset was divided into a training dataset (70% of the data) and a testing dataset (30% of the data). The testing dataset was specifically used to evaluate the performance of the trained model.

4 Results and Discussion

All models were developed in the MATLAB environment using the PYTHON version on an i3-8130U CPU running at 2.20 GHz and with 12.00 GB RAM. The maximum number of features, the minimum number of samples required to divide a leaf node, the maximum depth of the tree, and the maximum number of leaf nodes are all artificially determined parameters that must be determined before the RF model can be established. The values of these parameters for the best-fitting RF and XGBoost models are shown in Tables 1 and 2. Trial and error are used to determine the hyperparameter values for the best fit model.

In this study, six performance statistical parameters were analyzed for the robustness appraisal of the simulated ML models: root mean square error (RMSE), coefficient of determination (R^2), variance account factor (VAF), weighted mean absolute

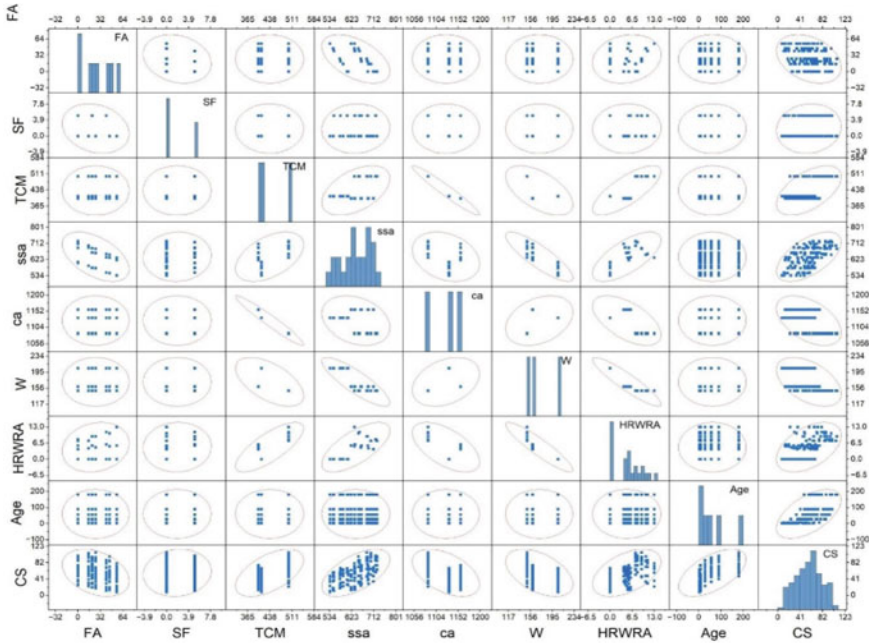


Fig. 1 Dataset visualized through a correlation plot, accompanied by histograms

Table 1 Summary of hyperparameters used in the RF model

Parameter	Brief explanation	Value
Num_Iter	It represents the total iterations' counts or cycles to be executed	5
Max_depth	This parameter defines the maximum depth allowed for a tree	1000
Bag size %	It determines the size of each bag, expressed in training set percentage	65
Seed	This is the seed value used for generating random numbers	120

Table 2 Summary of hyperparameters used in the XGBoost model

Parameter	Brief explanation	Value
Num_Iter	It represents the total number of iterations or cycles to be executed	10
Max_depth	Denotes the maximum number of split	10
Num_estimate	Number of estimators	100
Learn_rate	Learning rate	0.3
Seed	This is the seed value used for generating random numbers	123
N_round	It represents the number of round in the boosting phase	12

percentage error (WMAPE), Adj. R^2 , and mean absolute error (MAE). It is advisable to employ a variety of performance indicators in order to assess the predictive model's capacity for generalization. The details about the models can be studied from the literature [13, 14]. Remember that the above performance criteria are used to figure out how well a model works in different situations. However, rank analysis is used to decide what the final verdict will be. The concept of rank analysis was derived from existing scholarly works [15, 16]. On an individual basis, the technique assigned the highest rank to the model with the best value for each index and the lowest rank to the model with the poorest value for each index, for both the training and testing results. The cumulative score was computed by aggregating the individual ranks of the participants. Finally, the ultimate score for each model is determined by the collective rankings obtained from both the training and testing phases. For both the training and testing results, the procedure ranked the model with the best value for each index as the highest, and the model with the poorest value for each index as the lowest. Their final score was determined by adding their individual ranks together. At last, the combined ranks from the training and testing phases constitute the final score for each model (Table 2). Figure 2 represents the scatter plot between the actual and predicted values of the XGBoost and Random Forest for testing and training datasets separately. The performance of the proposed model is taken to be enhanced if the points fit closer to the regression line. The best model selected by these values is more or less equivalent to one in this chart indicating a relationship between both axes and R^2 . Based on the performance of this curve, the XGBoost hybrid model outperforms Random Forest.

From Table 3 result, it can be concluded that XGBoost model outperforms in both testing ($R^2 = 0.95$, WMAPE = 0.09, RMSE = 0.06, VAF = 94.57, Adj. $R^2 = 0.94$, NS = 0.94, MAE = 0.05) and training ($R^2 = 1.00$, WMAPE = 0.01, RMSE = 0.01, VAF = 99.63, Adj. $R^2 = 1.00$, NS = 1.00, MAE = 0.01) when compared to the Random Forest. Similar conclusion can be concluded from the rank analysis where the XGBoost leads Random Forest in both testing (12) and training (14) with the overall score of 26. It is evident that Random Forest is the lowest performing model in both testing (10) and training (7) with the overall score of 17. From the above results, it can be concluded that XGBoost has significantly improved performance compared to RF.

The effectiveness of the various models is also assessed via visual representations of the outcomes. A graphical depiction of findings is more apt to be deemed credible as it facilitates the audience's ability to promptly discern trends, patterns, and insights. Taylor diagrams are used to assess the efficiency of various proposed models used in this study; they are a simple graphical representation of the relationship between predicted and observed values [17, 18]. It plots statistical measures of variation, correlation, and RMS difference between models on a two-dimensional graph for easy comparison. The departure from the mean is represented by the radial distance from the center. The root-mean-square error is directly proportional to the standard deviation difference between the observed and anticipated fields. The correlation coefficient is shown as an azimuthal angle. The model's Taylor diagram is shown in Fig. 3. Figure 3 represents the Taylor diagram of XGBoost and Random Forest in

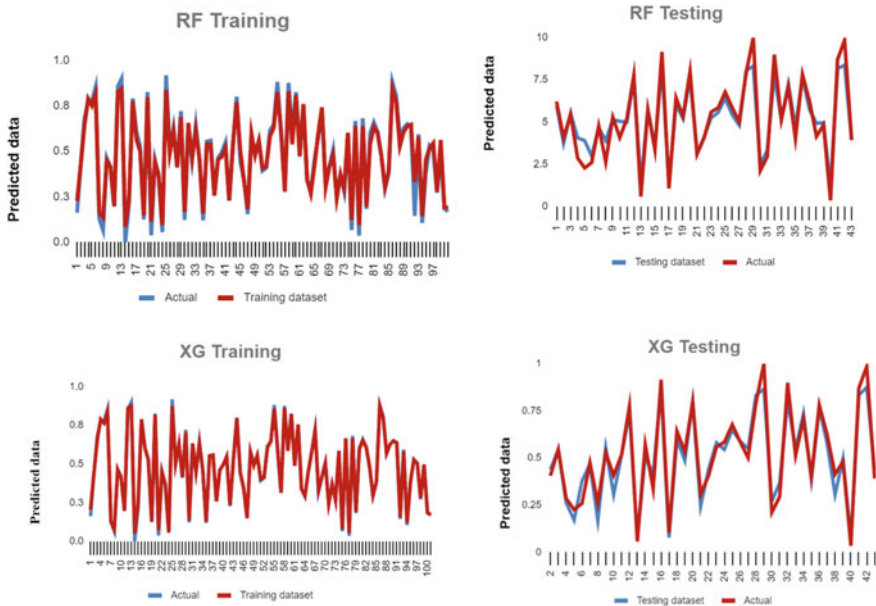


Fig. 2 Regression curve of the developed models

Table 3 Values of statistical parameters and rank analysis

Parameter		RF		XGBoost	
		TR	TS	TR	TS
R^2	Value	0.98	0.96	1.00	0.95
	Score	1	2	2	1
WMAPE	Value	0.06	0.09	0.01	0.09
	Score	1	1	2	2
RMSE	Value	0.04	0.07	0.01	0.06
	Score	1	1	2	2
VAF	Value	97.46	92.59	99.63	94.57
	Score	1	1	2	2
Adj. R^2	Value	0.98	0.95	1.00	0.94
	Score	1	2	2	1
NS	Value	0.98	0.93	1.00	0.94
	Score	1	1	2	2
MAE	Value	0.03	0.05	0.01	0.05
	Score	1	1	2	2
Sub total		7	10	14	12
Total score		17		26	

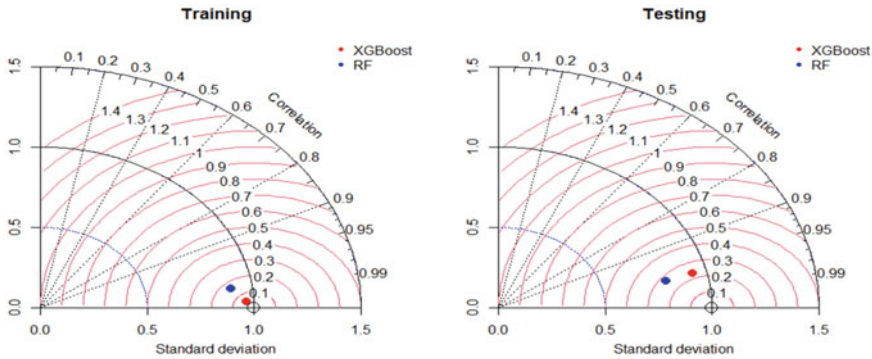


Fig. 3 Taylor diagram for the visual analysis of developed models

both testing and training. In training, the closest model is XGBoost followed by the Random Forest, while in testing, the same XGBoost model is the closest one. From the Taylor diagram, we can conclude that XGBoost is the best performing model in both testing and training and Random Forest is the most underperforming model.

5 Conclusion

The paper compares the XGBoost and RF models for predicting the bearing capacity of FA and SF concrete as a robust alternative to traditional methods of lab testing and empirical modeling, saving time, money, and labor and allowing proper mix proportioning of the constituents of concrete. The study concludes that both XGBoost and RF are reliable simulation models to predict the CS of fly ash and silica fume concrete; however, the performance of XGBoost ($R^2 = 0.95$, RMSE = 0.06 in testing) is slightly better than RF ($R^2 = 0.96$, RMSE = 0.07 in testing). In terms of performance parameters led rank analysis (12 for XGBoost and 10 for RF in testing) and visual interpretation of Taylor diagrams also, this conclusion is reinforced. In overall rank as well, RF (7) is outperformed by XGBoost (16). The model can be used for the variety of datasets at various locations after being trained and validated on the test data as future study.

References

1. Mazloom M, Ramezani-pour AA, Brooks JJ (2004) Effect of silica fume on mechanical properties of high-strength concrete. *Cem Concr Compos* 26:347–357. [https://doi.org/10.1016/S0958-9465\(03\)00017-9](https://doi.org/10.1016/S0958-9465(03)00017-9)
2. American Society for Testing and Materials, Standard Test Method for High-Strain Dynamic Testing of Deep Foundations, D 4945-08 (2010). www.astm.org. Accessed 11 Oct 2020.

3. Yaseen ZM, Deo RC, Hilal A, Abd AM, Bueno LC, Salcedo-Sanz S, Nehdi ML (2018) Predicting compressive strength of lightweight foamed concrete using extreme learning machine model. *Adv Eng Softw* 115:112–125. <https://doi.org/10.1016/J.ADVENGSOFT.2017.09.004>
4. Biswas R, Rai B, Samui P, Roy SS (2020) Estimating concrete compressive strength using MARS, LSSVM and GP. *Eng J* 24:41–52. <https://doi.org/10.4186/ej.2020.24.2.41>
5. Biswas R, Rai B, Samui P (2021) Compressive strength prediction model of high-strength concrete with silica fume by destructive and non-destructive technique. *Innov Infrastr Sol* 6:1–14. <https://doi.org/10.1007/S41062-020-00447-Z/METRICS>
6. Asteris PG, Skentou AD, Bardhan A, Samui P, Pilakoutas K (2021) Predicting concrete compressive strength using hybrid ensembling of surrogate machine learning models. *Cem Concr Res* 145:106449. <https://doi.org/10.1016/J.CEMCONRES.2021.106449>
7. Shariati M, Armaghani DJ, Khandelwal M, Zhou J, Khorami M (2021) Assessment of long-standing effects of fly ash and silica fume on the compressive strength of concrete using extreme learning machine and artificial neural network. *J Adv Eng Comput* 5:50–74. <https://doi.org/10.25073/JAEC.202151.308>
8. Biswas R, Samui P, Rai B (2019) Determination of compressive strength using relevance vector machine and emotional neural network. *Asian J Civil Eng* 20:1109–1118. <https://doi.org/10.1007/s42107-019-00171-9>
9. Nguyen NH, Abellán-García J, Lee S, Garcia-Castano E, Vo TP (2022) Efficient estimating compressive strength of ultra-high performance concrete using XGBoost model. *J Build Eng* 52:104302. <https://doi.org/10.1016/J.JOBE.2022.104302>
10. de Domenico D, Filipe L, Bernardo A, Shen Z, Farouk Deifalla A, Kamí Nski P, Dyczko A (2022) Compressive strength evaluation of ultra-high-strength concrete by machine learning. *Materials* 15:3523. <https://doi.org/10.3390/MA15103523>
11. Li QF, Song ZM (2022) High-performance concrete strength prediction based on ensemble learning. *Constr Build Mater* 324:126694. <https://doi.org/10.1016/J.CONBUILDMAT.2022.126694>
12. Pala M, Özbay E, Öztaş A, Yuce MI (2007) Appraisal of long-term effects of fly ash and silica fume on compressive strength of concrete by neural networks. *Constr Build Mater* 21:384–394. <https://doi.org/10.1016/j.conbuildmat.2005.08.009>
13. Bardhan A, Manna P, Kumar V, Burman A, Zlender B, Samui P (2021) Reliability analysis of piled raft foundation using a novel hybrid approach of ANN and equilibrium optimizer. *Comput Model Eng Sci* 128:1033–1067
14. Azam A, Bardhan A, Kaloop MR, Samui P, Alanazi F, Alzara M, Yosri AM (2022) Modeling resilient modulus of subgrade soils using LSSVM optimized with swarm intelligence algorithms. *Sci Rep* 12(1):14454
15. Biswas R, Kumar M, Singh RK, Alzara M, El Sayed SBA, Abdelmongy M, Yosri AM, Eldeen A, Yousef AS (2023) A novel integrated approach of RUNge Kutta optimizer and ANN for estimating compressive strength of self-compacting concrete. *Case Stud Constr Mater* 18:e02163
16. Thangavel P, Samui P (2022) Determination of the size of rock fragments using RVM, GPR, and MPMR. *Soils Rocks* 45(4)
17. Taylor KE (2001) Summarizing multiple aspects of model performance in a single diagram. *J Geophys Res Atmos* 106(D7):7183–7192
18. Kumar DR, Samui P, Burman A (2022) Prediction of probability of liquefaction using hybrid ANN with optimization techniques. *Arab J Geosci* 15(20):1587

Analytical Study on 3D-Printed Concrete Wall with Different Wall Configurations When Exposed to High Temperature



B. Vignesh and N. Parthasarathi

1 Introduction

Concrete is one of the most widely used modern building materials. Three-dimensional-printed concrete is a relatively new concept that has been getting more attention in recent times. The concrete mixture used here consists of water, cement, and aggregates, which is designed to be easily extruded through the nozzle of the 3D-printing equipment. The structures are built with the concept of layering where a layer will be deposited on a previously poured layer repeatedly until the required structure is formed. Firstly, a model will be created, and then, the co-ordinates will be converted into code and that will be fed into the 3D printer. Using 3D-printed concrete is cost-effective as it eliminates the need for casting concrete into molds or framework. The need for intensive labor is avoided in this process, and complex geometric structures can be easily created within a tight schedule with minimal chances of human error. It also helps in reducing construction waste, which makes it environmentally friendly. Three-dimensional-printed concrete can achieve a curing time as short as three days, allowing for the rapid construction of entire structures within hours, making it time efficient. These factors help us to understand that the 3D-printed concrete is a relatively quicker and cheaper alternative to conventional concrete. Paul et al. [1] talked about the advantages of the 3D-printed concrete and the materials that are used. One of the major advantages is that it is easier to design even the complex geometries rapidly. Fine particles are used significantly in 3DPC, but the coarse aggregates are not generally used. The most commonly used materials are cement, sand, water, fly ash, silica fume, super plasticizer, and fiber particles additionally to improve the tensile strength and toughness of 3DPC. Lyu et al. [2] explained the basic principles and process of concrete 3D-printing technology and

B. Vignesh · N. Parthasarathi (✉)

Department of Civil Engineering, Faculty of Engineering and Technology, SRM Institute of Science and Technology, Kattankulathur, Tamilnadu 603203, India

e-mail: parthasn@srmist.edu.in

also give detailed review of the material properties. The mechanical properties of the 3D-printed concrete are in research and development stage, and hence, it can be used for low-rise buildings but cannot be used for high-rise buildings in one print, but the parts can be printed separately and later assemble it, like pre-fabricated buildings. Only high strength concrete can be used in 3DPC for more strength, ordinary cement which cannot meet the requirements for the performance of the building. Adding fiber to the 3DPC will help in increasing the tensile strength and the toughness. A numerical model was developed by Wolfs et al. [3] to analyze the behavior of 3D-printed concrete. The model focused on studying the linear stress–strain relationship of the material until failure occurred. In order to obtain the necessary material properties, compression tests and direct shear tests were conducted. The findings revealed that as the fresh concrete ages, there is a linear increase in both Young’s modulus and cohesion. However, the Poisson’s ratio remained constant at 0.3, which was determined from the lateral deformations observed during the compression test, while the angle of internal friction also remained unchanged. In a study conducted by Suntharalingam et al. [4], the performance of different types of 3D-printed concrete walls, including solid, cavity, and composite walls, was examined in relation to their behavior under fire. The findings indicated that when exposed to standard fire conditions, non-load-bearing cavity walls made of 3D-printed concrete did not exhibit as good performance as solid 3D-printed concrete walls. EN 1992-1-2 [5] provides details about the thermal properties of concrete that incorporates siliceous and calcareous aggregates at elevated temperatures. This includes information on thermal conductivity, specific heat, and density. Marais et al. [6] analyzed the performance of high strength concrete and lightweight foam concrete under high temperatures. The results showed that the materials with high thermal conductivity perform well as 3DPC wall and the ones with lower thermal conductivity perform better as normal solid wall, and 3D-HSC wall performs better than HSC solid wall, whereas LWFC solid wall performs better than 3D-LWFC wall. Suntharalingam et al. [7] studied the fire performance of 20 different 3DPC wall configurations using finite element models, specifically evaluating their response under standard fire conditions. The study’s results highlighted that 3D-printed concrete (3DPC) non-load-bearing cavity walls show considerable resistance when exposed to standard fire loads. Notably, there was a noteworthy enhancement in fire performance by increasing the thickness of the walls arranged in parallel rows. These non-load-bearing cavity walls exhibited impressive resistance for a duration of four hours under standard fire load conditions.

2 Modeling

The dimension considered for the 3D-printed models has been provided in Table 1.

Table 1 Modeling and dimensions data

Description	Values
Length of the wall	1000 mm
Depth of the wall	100 mm
Height of the wall	500 mm
No. of layers	50 layers
Layer thickness	10 mm
Mesh size	25 mm

3 Finite Element Analysis

The finite element modeling for multiple 3D-printed concrete walls with and without openings was modeled using ABAQUS. The software was used to analyze the loaded 3D-printed concrete walls at high temperature, and the displacement and stresses were also studied by exposing the model to fire conditions.

3.1 Properties and Specimen Details

The dimensions of the 3DPC wall are 1000 mm length, 500 mm width, and 100 mm depth. The 3D-printed concrete wall has 50 layers with each layer having the 10 mm layer thickness. Properties such as conductivity, specific heat, Young's modulus, and mass density are given in Table 1 as per the EN 1992-1-2 [5] which provides the thermal properties at elevated temperature. The properties obtained were slightly modified as per Suntharalingam [7]. Totally, 16 sets of 3DPC walls are there with square, circular, rectangular, triangular, and hexagonal openings. The material and thermal properties are provided in Table 2, and the specimen details are provided in Table 3.

The top surface of the various types of 3D-printed concrete wall models is shown in Figs. 1, 2, 3, 4, 5, 6, 7, 8, 9, 10, 11, 12, 13, 14, 15 and 16.

3.2 Modeling and Meshing

The part was created and then assembled using the method of layering with 50 layers and layer thickness of 10 mm. Tie interaction and film coefficient were provided using EN ISO 6946 [8]. The model was analyzed for the time period of 2 h or 7200 s. Pressure was created on the top surface of the wall, and the surface heat flux was applied on the front surface of the wall as per ISO-834-10:2014 [9]. The bottom side of the 3DPC wall is fixed. In the fixed boundary condition, the displacement and the rotation in the x, y, and z directions (U1, U2, U3, UR1, UR2, UR3) are zero. The film

Table 2 Material and thermal properties

Temperature (°C)	Conductivity (W/m K)	Mass density (N/mm ²)	Specific heat (J/kg K)	Young's modulus (N/mm ²)
23	1.95	2.40E-09	600	27,368.16
100	1.77	2.40E-09	900	27,368.16
200	1.55	2.35E-09	1000	26,016.82
300	1.36	2.32E-09	1050	23,278.2
400	1.19	2.28E-09	1100	20,539.59
500	1.04	2.26E-09	1100	16,431.67
600	0.91	2.24E-09	1100	12,323.75
700	0.81	2.22E-09	1100	8215.83
800	0.72	2.20E-09	1100	4107.91

Table 3 Details of specimen

Model number	Model name	Opening name	No. of openings
1	Solid wall	-	-
2	BS1	Square	5
3	BS2	Square	10
4	BS3	Mini-square	10
5	BS4	Mini-square	20
6	BT1	Triangle	5
7	BT2	Triangle	10
8	BT3	Mini-triangle	10
9	BT4	Mini-triangle	20
10	BT5	Truss	21
11	BH1	Hexagon	5
12	BH2	Hexagon	10
13	BR1	Rectangle	5
14	BR2	Mini-rectangle	10
15	BR3	Mini-rectangle	20
16	BHT1	Hexagon and triangle	28

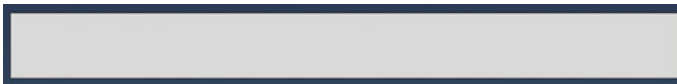


Fig. 1 Solid wall



Fig. 2 BS1 wall



Fig. 3 BS2 wall



Fig. 4 BS3 wall



Fig. 5 BS4 wall



Fig. 6 BT1 wall



Fig. 7 BT2 wall



Fig. 8 BT3 wall



Fig. 9 BT4 wall



Fig. 10 BT5 wall



Fig. 11 BH1 wall



Fig. 12 BH2 wall



Fig. 13 BR1 wall

coefficient was applied as per EN ISO 6946:2017 [8]. Here, coupled temperature–displacement analysis has been carried out in the transient state. By implementing the convergence study, optimum mesh size of 25 mm was determined and applied to all the models as shown in Fig. 2. Eight-node brick element has been used as it can yield more precise outcomes and handle irregular shapes with minimal compromise in accuracy (Figs. 17 and 18).



Fig. 14 BR2 wall



Fig. 15 BR3 wall



Fig. 16 BHT1 wall

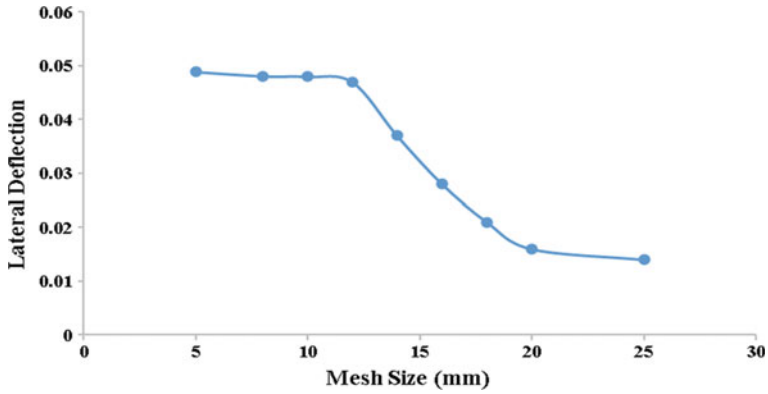


Fig. 17 Convergence study for optimum mesh size

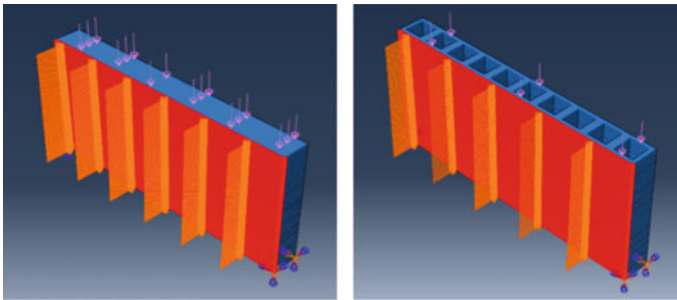


Fig. 18 Surface heat flux and pressure applied on solid wall and BS2

4 Results and Discussion

4.1 Results

The results of the finite element study on loaded 3D-printed concrete wall are provided below, and multiple graphs are modeled to study the behavior of the 3DPC wall under pressure and surface heat flux. The results obtained are provided in Table 4.

Table 4 Results obtained

Model name	Temperature (°C)	Displacement (mm)	Shear stress (N/mm ²)
Solid wall	922	3.2	1.8
BS1	891	2.78	1.46
BS2	877	2.02	1.01
BS3	811	2.04	1.57
BS4	839	2.6	1.76
BT1	826	2	1.43
BT2	759	1.37	1.62
BT3	784	1.72	1.8
BT4	806	1.87	1.77
BT5	836	1.57	0.98
BH1	837	2.41	1.44
BH2	792	1.72	1.26
BR1	909	1.65	0.92
BR2	878	2.65	1.17
BR3	867	2.1	1.06
BHT1	760	1.33	1.15

4.2 Discussion

The time versus temperature curve for 3DPC concrete wall is given in Fig. 19. This graph showcases the plotted values against time (minutes) and temperature (°C), following the ISO-834 [9] standard. The surface temperature and core temperature are plotted with respect to time (Fig. 20).

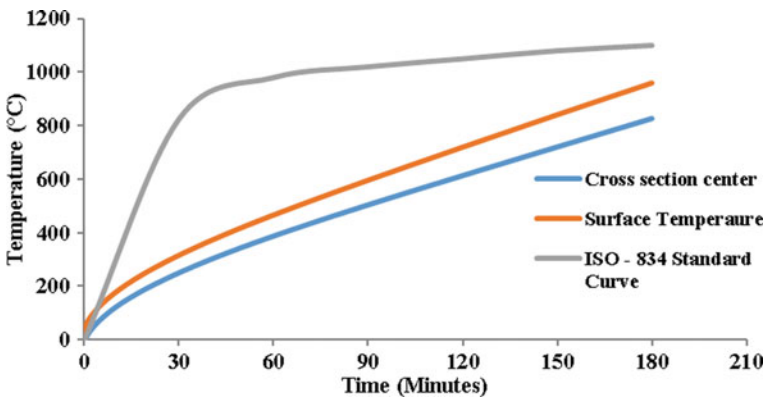


Fig. 19 Time vs. temperature curve as per ISO-834

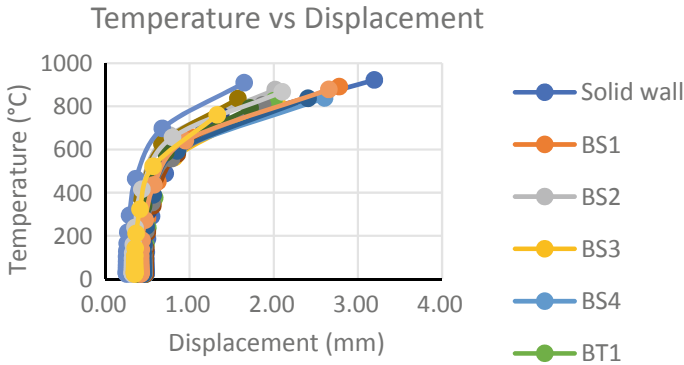


Fig. 20 Temperature vs. displacement graph

The temperature vs. displacement graph has been plotted based on the point at which the failure occurs, in order to understand the effect of the pressure and surface heat flux applied over the 3D-printed concrete walls (Fig. 21).

The temperature variance graph has been plotted to understand the behavior of various 3D-printed concrete walls with and without the openings when exposed to high temperatures (Fig. 22).

The displacement graph has been plotted to understand the displacement occurring on various 3D-printed concrete walls (Fig. 23).

The shear stress graph has been plotted to understand the shear stress occurring on various 3D-printed concrete walls (Fig. 24).

The time period graph has been plotted to understand the time required by various 3D-printed concrete walls with and without the openings to fail due to the pressure and surface heat flux applied over it.

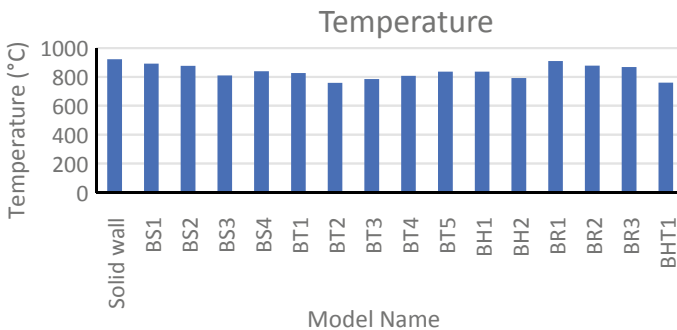


Fig. 21 Temperature variance graph

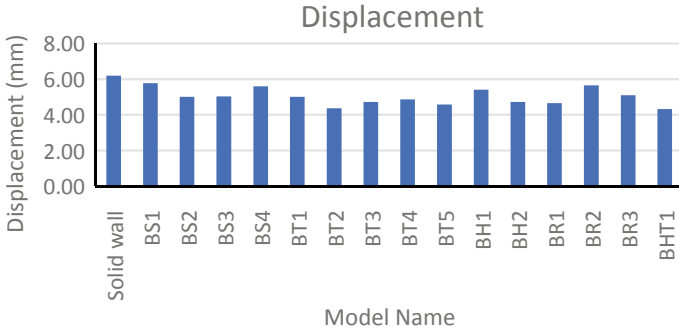


Fig. 22 Displacement graph

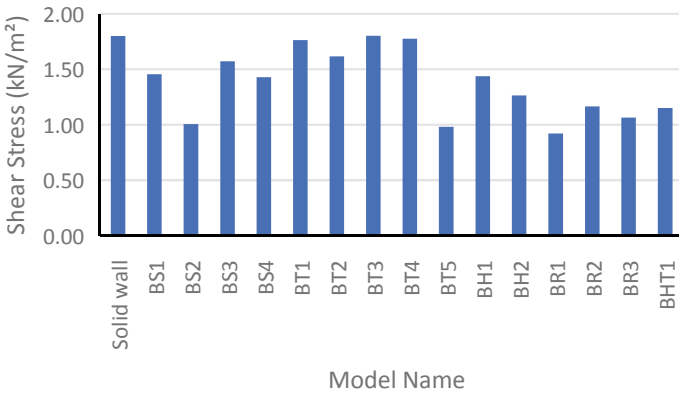


Fig. 23 Shear stress graph

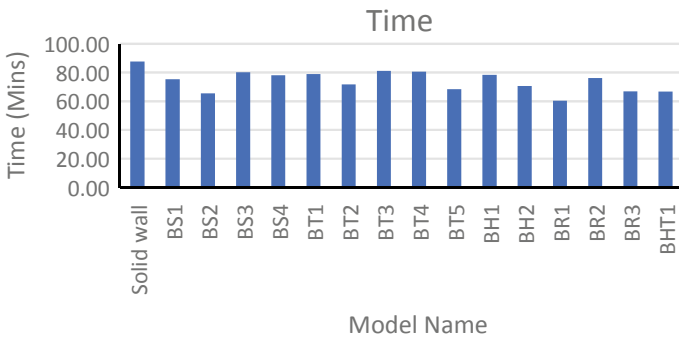


Fig. 24 Time period graph

5 Conclusion

With the results obtained from performing finite element research on the study of three-dimensionally printed concrete walls under high temperatures, a comprehensive analysis was conducted on 16 wall models, including variations with and without openings of different shapes. Based on these analyses, the following conclusions can be drawn:

- It can be observed that the maximum displacement of 6.20 mm was found in the 3DPC solid wall which has no openings. When the openings are provided in the wall, a maximum displacement of 5.78 mm can be observed in the BS1 wall which has been provided with five square-shaped openings.
- It can be observed that the minimum displacement of 4.33 mm was found in the BHT1 wall with 28 hexagonal and triangular openings.
- It can be observed that the 3DPC solid wall which has no openings can withstand the highest temperature of 922 °C when compared to the other walls. When the openings are provided in the wall, it can be observed in the BR1 with five rectangular openings which can withstand the highest temperature of 909 °C when compared to the other walls with openings.
- It can be observed that the BT2 wall with ten triangular openings withstands the lowest temperature of 759 °C when compared to the other walls with openings.
- It can be observed that the 3DPC solid wall displays the most shear stress of 1.80 N/mm² along with the BT3 wall with ten mini-triangular openings.
- It can be observed that the BR1 wall with five rectangular openings displays the lowest shear stress of 0.92 N/mm² when compared to the other walls.

References

1. Paul S, van Zijl G, Tan MJ, Gibson I (2018) A review of 3D concrete printing systems and materials properties: current status and future research prospects. *Rapid Prototyp J.* 24:784–798. <https://doi.org/10.1108/RPJ-09-2016-0154>
2. Lyu F, Zhao D, Hou X, Sun L, Zhang Q (2021) Overview of the development of 3D-printing concrete: a review. *Appl Sci* 11:9822
3. Wolfs RJM, Bos FP, Salet TAM (2018) Early age mechanical behaviour of 3D printed concrete: numerical modelling and experimental testing. *Cement Concr Res* 106:103–116
4. Suntharalingam T, Gatheeshgar P, Upasiri I, Keerthan P, Nagaratnam B, Corradi M, Perera D (2021) Fire performance of innovative 3D printed concrete composite wall panels—a numerical study. *Case Stud Constr Mater* 15. <https://doi.org/10.1016/j.cscm.2021.e00586>
5. Eurocode 2: Design of concrete structures—Part 1–2: general rules—structural fire design (EN 1992-1-2)
6. Marais H, Christen H, Cho S, De Villiers W, van Zijl G (2021) Computational assessment of thermal performance of 3D printed concrete wall structures with cavities. *J Build Eng* 41:102431. <https://doi.org/10.1016/j.jobe.2021.102431>
7. Suntharalingam T, Gatheeshgar P, Upasiri I, Keerthan P, Nagaratnam B, Rajanayagam H, Navaratnam S (2021) Numerical study of fire and energy performance of innovative light-weight

3D printed concrete wall configurations in modular building system. Sustainability 13:21. <https://doi.org/10.3390/su13042314>

8. EN ISO 6946:2017. Building components and building elements—thermal resistance and thermal transmittance—calculation methods
9. ISO 834-10:2014 Fire resistance tests—elements of building construction—part 10: specific requirements to determine the contribution of applied fire protection materials to structural elements

Seismic Response Analysis of Reinforced Concrete Chimneys with Tuned Mass Damper



Ashish Kumar Gupta, Sudhir Singh Bhadauria, and Aruna Rawat

1 Introduction

Tall chimneys are primarily employed in industries to expel harmful gases into the atmosphere. These chimneys endure various loads, including their own weight, wind, earthquakes, and temperature fluctuations. The chimney is damaged by the lateral forces applied on the structures such as wind, earthquake, etc. A huge amount of structural damage is caused by the earthquake. The vibration energy is produced during the earthquake on chimney which can be controlled by application of TMD [4, 6]. TMD is a device that is used to control vibrations and oscillations of structures by external forces, such as wind, earthquake, etc.

In the past researches on chimney done by Arunachalam and Lakshmanan [1], they introduced a semi-empirical technique for predicting the across-wind response of circular chimneys caused by vortex shedding during the lock-in range. This study explores the nonlinear relationship between the normalized root mean square (RMS) tip deflection and the fact parameter, providing further insights into this connection.

Brownjohn et al. [2] studied 183 m RC chimney at a coal-fired power station. The construction of a response monitoring system and TMD system was prompted by concerns over significant amplitude responses resulting from interference effects caused by the newly constructed chimney in the primary upwind direction. The study extensively examined various aspects, including the chimney itself, the monitoring system, its setup, data processing techniques, system identification methods, and performance data before, during, and after the TMD installation.

Chmielewski et al. [3] employed experimental and analytical models of the RC chimney to evaluate the natural frequencies and modes of 250 m chimney. A large-scale experiment was conducted using two geophone sensors. The study revealed

A. K. Gupta (✉) · S. S. Bhadauria · A. Rawat

Department of Civil Engineering, University Institute of Technology, RGPV, Bhopal 462033, India

e-mail: augupta2001@gmail.com

that the results of free vibrations were influenced by the flexibility of the soil beneath the base of the chimney. This finding emphasizes the significance of considering the soil's characteristics and flexibility when analyzing the free vibrations of the chimney.

Datta et al. [5] conducted an analytical investigation into the across-wind responses of tapered chimneys. They focused on the occurrence of periodic shedding of vortices under the lock-in condition. The study highlights the variation in chimney responses depending on the critical diameter used to calculate the critical velocity and aerodynamic lift coefficients.

Elias et al. [6] focused on the multimode regulation of along-wind responses in chimneys and proposed the implementation of distributed multiple tuned mass dampers (d-MTMDs). By installing a tuned mass damper, the researchers were able to regulate the chimney's response. Specifically, the dampers were positioned at locations with high amplitudes in the mode forms that required regulation, and they were tuned to the corresponding modal frequencies. The appropriate mass and damping ratios for the single tuned mass damper (STMD), additional distributed multiple tuned mass dampers (ad-MTMDs), and distributed multiple tuned mass dampers (d-MTMDs) were considered to achieve modified dynamic response control. The study concluded that the d-MTMDs were the preferred choice for designing the controller, considering the vibration modes.

Longarini and Zucca [9] conducted a review on the design of TMD to predict the seismic response of a historic masonry chimney 50 m high located in an Italian hydraulic facility. The seismic investigation involved a numerical analysis of two different scenarios: the chimney alone (referred to as Type A) and the chimney equipped with a TMD (referred to as Type B).

In the present study, the seismic analysis of RCC chimneys without and with TMD is carried out using lumped mass approximation approach. The 275 m, 180 m, and 120 m are the heights of the chimney. Model 1, Model 2, and Model 3 are analyzed having three different heights of chimneys, which represent varied thickness and diameter, constant thickness and varying diameter, and uniform thickness and diameter, respectively. A TMD is installed at the top of the chimney which absorbs the vibrational energy of the RCC chimneys. All the chimneys are examined for fundamental natural frequencies, maximum absolute acceleration, maximum absolute displacement, base shear, and bending moment.

2 Methodology

The lumped mass chimney models are created as cantilever beams where the multiple degrees-of-freedom system of the chimney is modeled without and with TMD. The fundamental natural frequency equation of motion is calculated by:

$$[M]\{\ddot{x}\} + [C]\{\dot{x}\} + [K]\{x\} = 0 \quad (1)$$

where $[M]$, $[K]$, $[C]$ are represented by mass, stiffness, damping matrices, and $\{\ddot{x}\}$, $\{\dot{x}\}$ and $\{x\}$ are acceleration, velocity, and displacement, respectively. In this matrix, $m_1, m_2, m_3 \dots m_i$ are represented as nodal masses and damper mass is taken at the top node with the one degree-of-freedom increased. The damper mass, damping, and stiffness are denoted by m_{TMD} , C_{TMD} , and K_{TMD} . Rayleigh's approach is used to calculate the damping matrices using damping ratio as 0.05.

$$[M]\{\ddot{x}\} = \begin{bmatrix} m_1 & 0 & 0 & \dots & 0 \\ 0 & m_2 & 0 & \dots & 0 \\ 0 & 0 & \ddots & \dots & 0 \\ \vdots & \vdots & \vdots & m_i & 0 \\ 0 & 0 & 0 & 0 & m_{TMD} \end{bmatrix} \begin{bmatrix} \ddot{x}_1 \\ \ddot{x}_2 \\ \vdots \\ \ddot{x}_i \\ \ddot{x}_{TMD} \end{bmatrix} \tag{2}$$

$$[C]\{\dot{x}\} = \begin{bmatrix} C_{11} + C_n & -C_{1,2} & 0 & \dots & 0 \\ -C_{2,1} & C_{2,2} & -C_{2,3} & \dots & 0 \\ 0 & -C_{3,2} & \ddots & \dots & 0 \\ \vdots & \vdots & \vdots & C_{n,n} + C_{TMD} & -C_{TMD} \\ 0 & 0 & 0 & -C_{TMD} & C_{TMD} \end{bmatrix} \begin{bmatrix} \dot{x}_1 \\ \dot{x}_2 \\ \vdots \\ \dot{x}_i \\ \dot{x}_{TMD} \end{bmatrix} \tag{3}$$

$$[K]\{x\} = \begin{bmatrix} K_{11} + K_n & -K_{1,2} & 0 & \dots & 0 \\ -K_{2,1} & K_{2,2} & -K_{2,3} & \dots & 0 \\ 0 & -K_{3,2} & \ddots & \dots & 0 \\ \vdots & \vdots & \vdots & K_{n,n} + K_{TMD} & -K_{TMD} \\ 0 & 0 & 0 & -K_{TMD} & K_{TMD} \end{bmatrix} \begin{bmatrix} x_1 \\ x_2 \\ \vdots \\ x_i \\ x_{TMD} \end{bmatrix} \tag{4}$$

3 Numerical Study

RCC chimney with TMD is having three different heights of the chimney 275 m, 180 m, and 120 m, respectively, where three models were considered. Model 1, Model 2, and Model 3 are denoted varied diameter and thickness, uniform thickness and vary diameter, and uniform thickness and diameter, respectively, as discussed in Table 1. For the analytical calculation of the chimneys have taken the lumped mass approximation methods as shown in Fig. 1. Bhuj earthquake (January 26, 2001) with PGA 0.782 m/sec² is considered for the dynamic analysis of the RC chimneys. Newmark's numerical integration technique [4] is used for the dynamic analyses of all chimney models. The properties of the RC chimneys are taken by references [6–8]. The 2 and 5% damping is considered for the TMD and chimney, respectively.

Table 1 Dimensions of different RCC chimneys

Dimension (in m)	Model	Bottom diameter (m)	Top diameter (m)	Bottom thickness (m)	Top thickness (m)
275	Model1	5.00	2.50	0.096	0.050
	Model2	5.00	2.50	0.096	0.096
	Model3	5.00	5.00	0.096	0.096
180	Model1	15.70	7.50	0.500	0.148
	Model2	15.70	7.50	0.500	0.500
	Model3	15.70	15.70	0.500	0.500
120	Model1	25.00	12.00	0.795	0.237
	Model2	25.00	12.00	0.795	0.795
	Model3	25.00	25.00	0.795	0.795

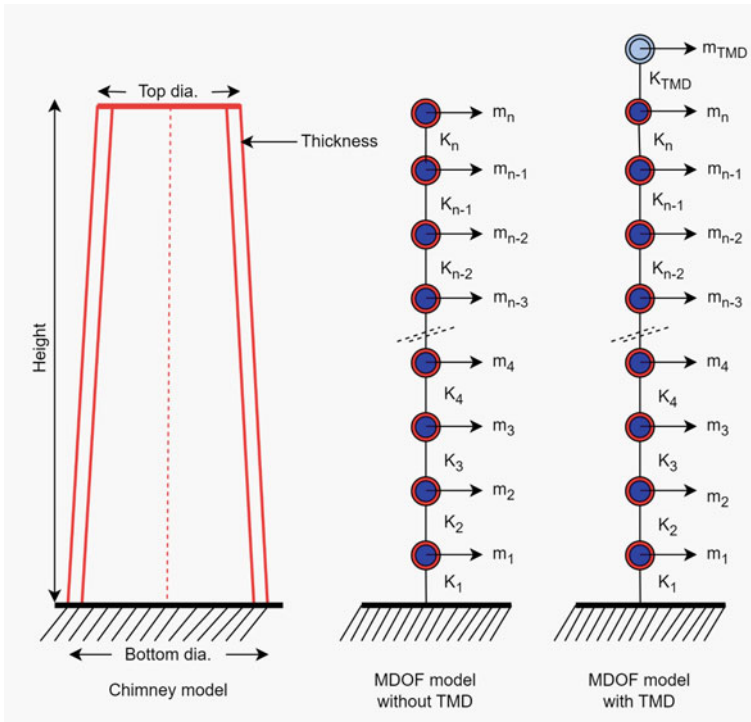


Fig. 1 Chimney model

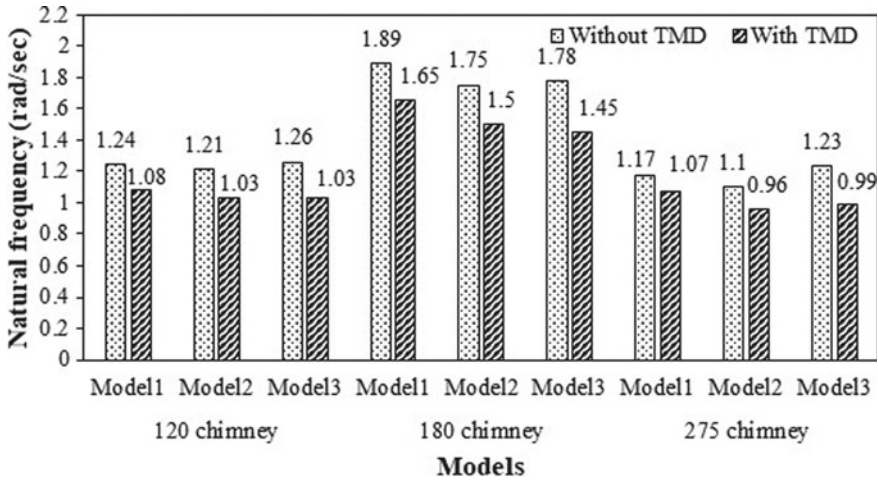


Fig. 2 Fundamental natural frequencies

4 Results

All chimney models are examined without and with TMD for their fundamental natural frequencies, maximum absolute acceleration, maximum absolute displacement, base shear, and bending moment.

4.1 Fundamental Natural Frequencies

The first fundamental natural frequencies are determined for all RC chimney models considered. It is observed that when a TMD is placed at the top node of the chimneys, the natural frequency is decreased as shown in Fig. 2. The primary cause for the decrease in natural frequency is the implementation of a TMD at the uppermost node of the chimney, which effectively mitigates vibrations and their effects.

4.2 Maximum Absolute Acceleration

The maximum absolute acceleration at top node of the chimney models is shown in Fig. 3. The top node of the chimneys is fitted with a TMD, which increases the maximum absolute acceleration compared to the other model of the chimney for 180 m height of the chimney. After installation of TMD at the top node of the chimney, absolute acceleration values are a few amounts of variations in the case

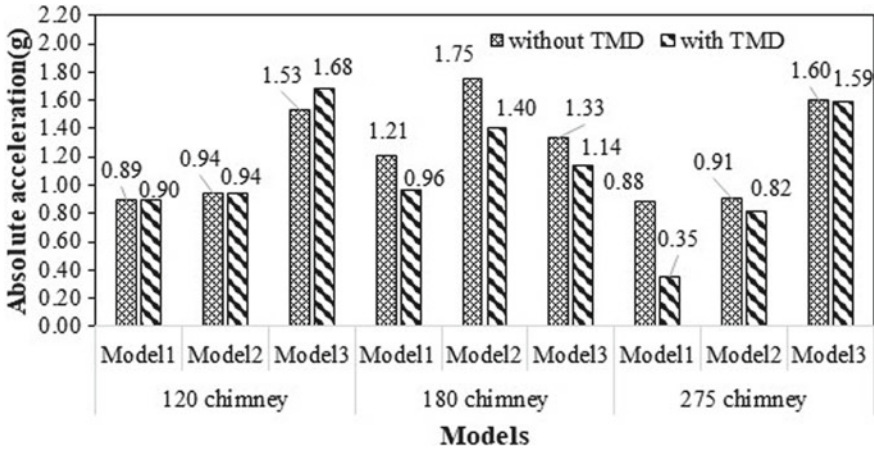


Fig. 3 Top node maximum absolute acceleration (g)

of 120 m height of the chimney and more reduction is observed in case of 180 and 275 m height of the chimneys.

4.3 Maximum Absolute Displacement

Figure 4 shows the maximum absolute displacement at the top node of the chimney models. The displacement is decreased with TMD chimney. The maximum absolute displacement is obtained at the Model 3 as compared to the other models. The TMD is reduced the absolute acceleration by 4–50% and more reduction is observed in case of Model 2.

4.4 Base Shear

Table 2 gives the base shear values for the chimney models. The base shear is the maximum for 275 m of the chimney in Model 3. It observed that base shear values are increasing with the increase in height of the chimney. The installation of a TMD at the top node of the chimney reduces the base shear in chimney.

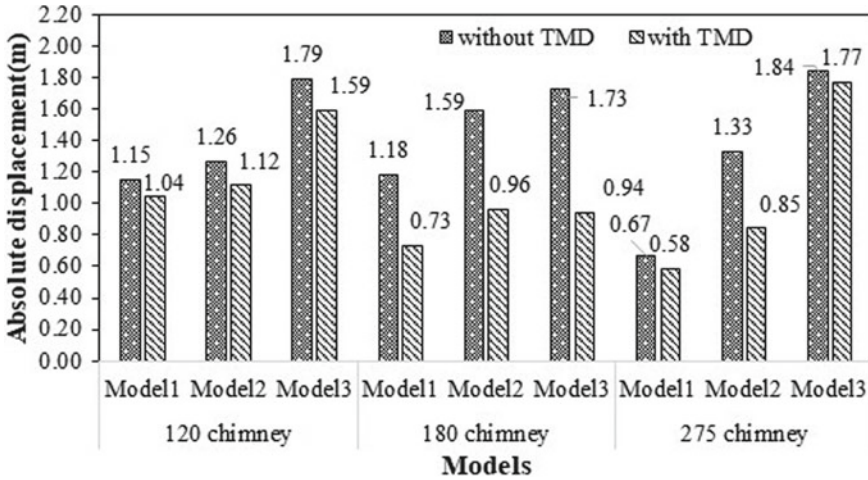


Fig. 4 Top node maximum absolute displacement (m)

Table 2 Base shear (MN)

Chimney Height (in m)		Model 1	Model 2	Model 3
120	Without TMD	2.16	2.85	4.60
	With TMD	2.18	2.88	4.62
180	Without TMD	47.41	78.72	96.03
	With TMD	42.75	72.77	95.08
275	Without TMD	117.00	244.00	416.00
	With TMD	119.00	240.00	409.00

4.5 Bending Moment

The bending moment for the chimney is given in Table 3. The maximum bending moments are observed in Model 3. The vibration energy of the chimney is reduced due to the installation of TMD at the top node of the chimney models.

4.6 Response of Time Histories

The seismic analysis of 120 m, 180 m, and 275 m heights of the chimney are obtained by the time history responses of all three models. The MATLAB program is used to analyze the dynamic analysis of the all chimney models. A total of nine displacement time history responses are shown in Fig. 5 for the Bhuj 2001 earthquake where TD1

Table 3 Bending moment (GN-m)

Chimney height (in m)		Model 1	Model 2	Model 3
120	Without TMD	0.17	0.22	0.34
	With TMD	0.17	0.21	0.33
180	Without TMD	6.21	9.65	11.00
	With TMD	5.25	8.29	10.10
275	Without TMD	22.13	41.10	68.30
	With TMD	22.10	39.10	65.90

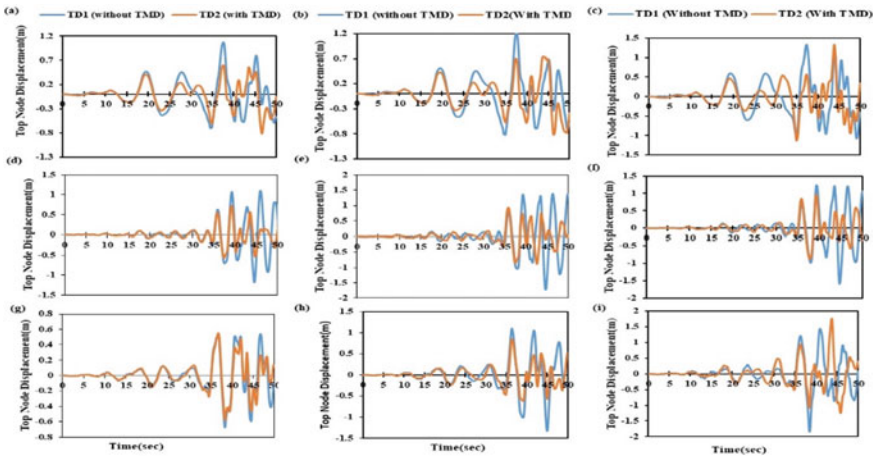


Fig. 5 Displacement time history responses. **a** 120 m height of Model 1, **b** 120 m height of Model 2, **c** 120 m height of Model 3, **d** 180 m height of Model 1, **e** 180 m height of Model 2, **f** 180 m height of Model 3, **g** 275 m height of Model 1, **h** 275 m height of Model 2, **i** 275 m height of Model 3

and TD2 represent the maximum displacement at the top node of chimneys without TMD and with TMD, respectively.

5 Conclusions

In the present study, the seismic analysis of 275 m, 180 m, and 120 m heights of the RCC chimneys without and with TMD is carried out using lumped mass approximation approach. Model 1, Model 2, and Model 3 are analyzed having three different heights of chimneys, which represent varied thickness and diameter, constant thickness and varying diameter, and uniform thickness and diameter, respectively. The following are the conclusions drawn from the present study:

1. By installing TMD at the top of the chimneys, the fundamental natural frequency is observed to decrease by 5–20%. Additionally, the absolute displacement of the chimney is significantly reduced by approximately 4–50%.
2. The implementation of the TMD leads to a reduction in both the base shear and bending moment experienced by the chimneys during an earthquake event.
3. Model 3 has the highest displacement among the other models due to its larger cross-sectional area for all three heights of chimneys.

Among the three models studied, Model 1 demonstrates superior performance due to its minimum displacement. The present study can further be extended for the experimental and numerical studies of chimneys for various intensities of earthquakes.

References

1. Arunachalam S, Lakshmanan N (2015) Across-wind responses of tall circular chimneys to vortex shedding. *J Wind Eng Ind Aerodyn* 145:187–195
2. Brownjohn JMW, Carden EP, Goddard CR, Oudin G (2010) Real-time performance monitoring of tuned mass dampers system for a 183 m reinforced concrete chimney. *J Wind Eng Ind Aerodyn* 98:169–179
3. Chmielewski T, Goeski P, Beirow B, Kretzschmar J (2000) Theoretical and experimental free vibrations of the tall industrial chimney with the flexibility of soil. *Eng Struct* 27:25–34
4. Chopra AK (2007) *Structural dynamics*, 3rd edn. Pearson Education India
5. Datta TK, Jain AK (1987) An analytical study of the across-wind response of cylinders due to vortex shedding. *Eng Struct* 9(1):27–31
6. Elias S, Matsagar V, Datta TK (2018) Along-wind response control of chimneys with distributed multiple tuned mass dampers. *Struct Control Health Monit* 26(1):1–25 (Wiley Online Library)
7. Elias S, Rajesh R, Olafesson S (2020) Tuned mass dampers for response reduction of a reinforced concrete chimney under near-fault pulse-like ground motions. *Front Built Environ* 6:1–9
8. Elias S (2019) Effect of SSI on vibration control of structures with tuned vibration absorbers. *Shock Vib* 2019:1–12
9. Longarini N, Zucca M (2014) A chimney's seismic assessment by a tuned mass damper. *Eng Struct* 79:290–296

Experimental Study on the Mechanical Properties of the Agro Waste as a Partial Replacement of the Binder Material



S. Vighash and L. Sabarigirivasan

1 Introduction

The growing population results a persistent lack of building materials that results in a significant increase in demand for building materials, especially during the past decade. Construction materials must be produced at an exponential rate to keep up with the housing demand [1]. Around the world, Ordinary Portland Cement (OPC) is acknowledged as the primary building material. The production requires more electrical and thermal energy which results in CO₂ emissions and environmental issues. Around 900 kg of CO₂ are released into the atmosphere per ton of OPC. According to predictions, the CO₂ emissions from cement manufacturing in India will peak at 835 million tons by 2050, a massive increase over current CO₂ emissions [2, 3]. Many research efforts have examined for cement replacements, including low-value, disposable wastes from agriculture and industry, whose advantages can be accomplished through the methods of recycling, reuse, and renewing. As a result, scientists have been looking into the usefulness, viability, and availability of pozzolanic wastes as alternatives to cement. The necessary components ought to come from a naturally occurring source which is abundant in aluminum (Al) and silicon (Si) [4]. Another considerations include the so-called “micro filler effect,” using the Portland cement with fine and ultrafine size range pozzolans in concrete mixture helps in achieving higher packing densities. Heterogeneous nucleation is the second physical consequence that might become significant with the decrease in particle size [5]. Numerous different cement alternatives involve industrial trash like fly ash, silica fume, and blast furnace slag. Further agricultural wastes being employed as pozzolanic materials include rice husk, hazel nutshell, wheat, peanut, and Sugarcane Bagasse Ash [6]. India is the second largest in sugarcane production, which is about

S. Vighash · L. Sabarigirivasan (✉)

Department of Civil Engineering, Faculty of Engineering and Technology, SRM Institute of Science and Technology, Kattankulathur, Tamilnadu 603203, India

e-mail: sabarigl@srmist.edu.in

500 million tons per year. Bagasse ash usage is low when it comes to its production, and appropriate waste management methods are lacking. One of the most effective approaches is the combustion of Sugarcane Bagasse to form Ash. As a result, a supplementary residue Sugarcane Bagasse Ash is produced (SCBA) [2, 7]. This ash has unique qualities that makes it a raw material source for the cement and concrete industries. As the silica (SiO_2) content in SCBA is higher, this ash possesses remarkable pozzolanic activity. Low carbon content, amorphous silica, and a significant amount of specific surface area all contribute to SCBA's improved pozzolanic characteristics. The properties of the agricultural ash may be defined based on the origin of the crop, environmental considerations, the burning time, temperature, cooling time, and the grinding of the ash and other technical considerations [8, 9]. Concrete properties including compressive strength during hydration have benefited from the inclusion of SCBA partly into cement in possible assistance. This pozzolanicity shall be used in conjunction with cement or to generate novel cements [10–13]. In addition to this, GGBS is also replaced at certain proportions to enhance the properties of the concrete. The residue left after burning iron ore, limestone, and coke at about 1500°C in a furnace is the GGBS and is capable of taking the place of cement in concrete [3]. By incorporating GGBS to concrete, long-term compressive and flexural strength properties are enhanced with only minor increases in elastic modulus. Furthermore, the use of GGBS can improve concrete durability by increasing resistance to abrasion, decrease in gas, water, and chloride ion permeability, and enhance great interaction between sulfate and alkali silica. The porosity of concrete is seen to be reduced due to the increased surface area of GGBS [12, 14, 15]. When SCBA and GGBS are added to cement, the fresh density of the concrete normally reduces in comparison to control concrete. Hence, the particles have a lower specific gravity and are lighter than cement [16, 17]. However, there needs a study on the influence of agro waste with the industrial waste in concrete. This paper evaluates the effect and its properties of SCBA as a replacement to concrete. Various trial mixes have been evaluated to obtain an optimum replacement percentage [18].

2 Materials and Methods

2.1 Materials

In the current experimental evaluation, GGBS and Sugarcane Bagasse Ash (SCBA) were utilized in various ratios to partially substitute cement. The following are the materials applied in this research.

Sugarcane Bagasse Ash (SCBA). Cement could be partly replaced by Bagasse Ash. Bagasse Ash was obtained by igniting the Sugarcane Bagasse, which had been sundried beforehand. (Fig. 1). The physical and chemical properties of the SCBA are determined by the laboratory test and microstructural study and are mentioned in Table 1.

Fig. 1 **a** Sugarcane Bagasse, **b** Sugarcane Bagasse Ash

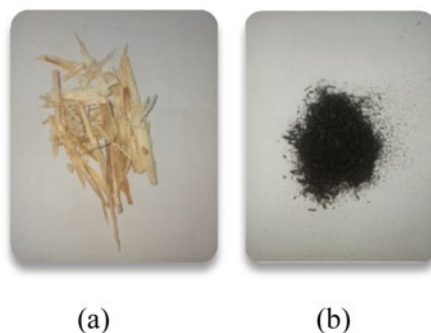


Table 1 Physical and chemical properties of SCBA

Physical properties	
Properties	Values
Density	575 kg/m ³
Specific gravity	1.65
Particle size	0.1–0.2 mm
Chemical properties	
Component	Percentage (%)
Silica	62
Alumina	31.5
Magnesium oxide	0.39
Calcium oxide	0.48
Manganese	0.004
Ferric oxide	1.79
Loss on ignition	0.71

Ground Granulated Blast Furnace Slag Cement (GGBS). The GGBS, a slag waste obtained from a steel factory, was used as cement substitution along with SCBA. The characteristics of GGBS were experimented in the laboratory as per standard procedures outlined in IS:12089-1987 [19]. The chemical and physical properties are tabulated in Table 2.

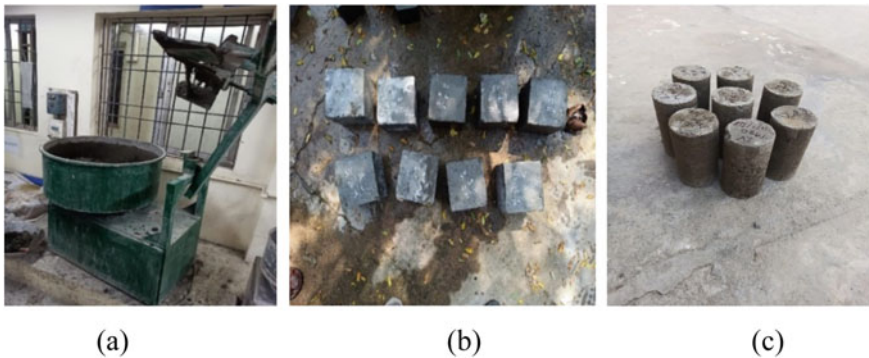
2.2 Casting of Specimens

The concrete mix of M30 grade with reference to IS 456-2000 and IS 10262-2019 is adopted for this experimental work [20, 21]. The SCBA has been replaced by 5, 10, 15, and 20% to the cement by means of weight of cement. In addition to it, GGBS is also replaced by 20, 30, and 40% to the cement by means of weight of the cement. The

Table 2 Physical and chemical properties of GGBS

Component	Percentage (%)
SiO ₂	32.7
Al ₂ O ₃	13.4
MgO	0.3
CaO	41.6
SO ₃	6.9
Fe ₂ O ₃	0.5
Loss on ignition	0.6
Specific gravity	2.64

Superplasticizer named Fosroc Conplast sp430 was used in the concrete mixtures. It is a sulfur-based SP. It has no chlorides and its density is of 1.08 g/cm³. A special care should be taken while mixing the concrete as it may affect the workability and strength properties of the concrete. In order to evaluate the characteristics of the materials, the required preliminary tests are done to prior mixing of concrete. Machine mixing is adopted to get an efficient and uniform mixing. The molds should be cleaned, dried, and greased. Following the mixing process, the concrete mixture is cast into specimens using different molds according to the needs. Cubical molds of 150 mm × 150 mm × 150 mm were utilized for compressive strength testing, while cylindrical molds measuring 150 mm × 300 mm were used for tensile strength testing. The hardened concrete after curing are then dried and are tested for compressive and tensile strength, and the results are obtained as shown in Fig. 2.

**Fig. 2** a Mixture machine, b cube specimens, c cylinder specimens

3 Microstructural Study

3.1 Scanning Electron Microscopy Analysis (SEM) and X-ray Diffractometer Analysis (XRD)

This study is done to determine about the particles, size, shape, and compositions of a material. Scanning electron microscopy with energy-dispersive X-ray spectroscopy (SEM–EDS) is a powerful analytical technique used in materials science, geology, chemistry, and other fields. The SCBA is dried and the sample is packed in an airtight bag in the form of fine powder. The SEM result supports the structure, morphology, and size of the elements. The energy-dispersive spectroscopy (EDS) and also the SEM simultaneously expose the chemical compositions of the elements. The SEM with EDS was done with magnification factor up to 5000 using Thermoscientific Apreo S machine. A non-destructive analytical method used to ascertain the crystalline structure of materials is X-ray diffraction (XRD). The XRD test produces a diffraction pattern, which is a series of peaks that correspond to specific crystal planes in the sample. By analyzing the diffraction pattern, scientists can determine the crystal structure, crystallite size, and orientation of the sample. The XRD test is also used to identify unknown materials by comparing their diffraction patterns to those of known materials in a database. The samples were assessed using a Bruker USA D8 advance, Davinci machine in the range of 10° – 90° angstrom.

4 Testing Methods

4.1 Compressive Strength Test

As per the codal recommendations, the cubes were tested for its maximum compressive strength as shown in Fig. 3.

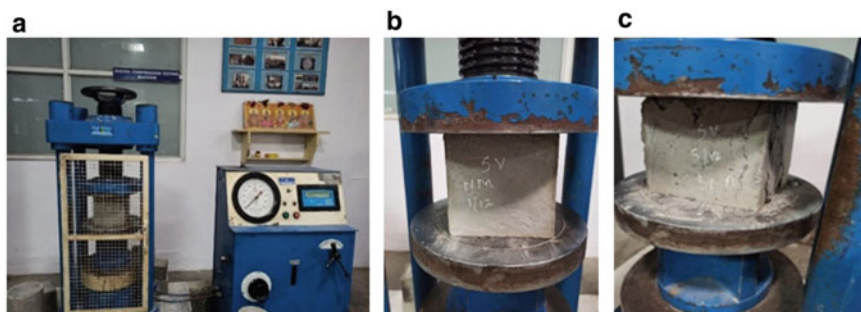


Fig. 3 a Compression testing machine, b cube before testing, c cube after testing

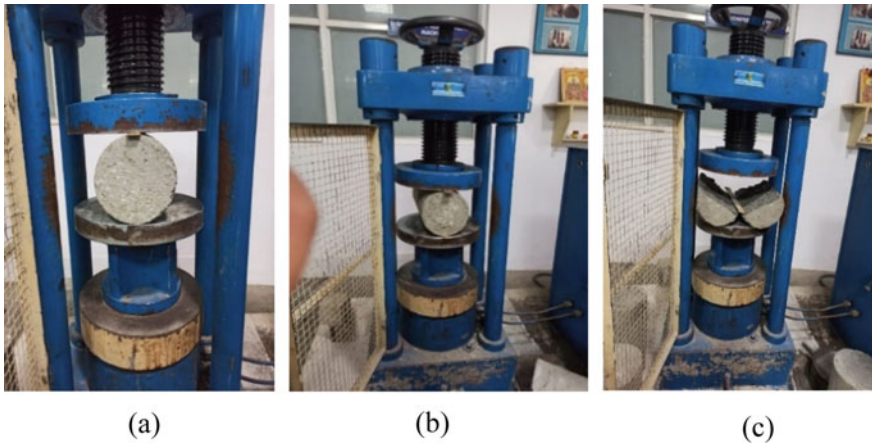


Fig. 4 **a** Compression testing machine (split tensile test), **b** cylinder before testing, **c** cylinder after testing

4.2 Tensile Strength Test

As per the codal recommendations, the cylinders were tested for its maximum tensile strength as shown in Fig. 4.

5 Results and Discussion

5.1 Scanning Electron Microscopy Analysis (SEM) and X-ray Diffractometer Analysis (XRD)

In this analysis, the particles are scanned by focused electron beams to obtain high-quality images of SCBA. The images obtained are at various magnifications ($250\times$ to $5.0\text{ K}\times$) as shown in Fig. 5. The image shows that the SCBA is of fibrous in nature, tetrahedral shape (prismatic), and crystalline character. Some cavities are also found there. EDS analysis exhibits the presence of the elements such as silicon, carbon, oxygen, and fluorine at various proportions in the SCBA as drawn in Fig. 6. The XRD pattern has been documented in the manner as described in Sect. 3.1. The XRD pattern was recorded from 10° to 90° in a 2θ range. Figure 7 displays the XRD spectrum. The maximum peak of silica is observed at 23.6° . The spectrum shows various peaks indicating various mineral phases with silica in abundance. Thus, the analysis reveals the presence of high silica that helps in better concrete strength.

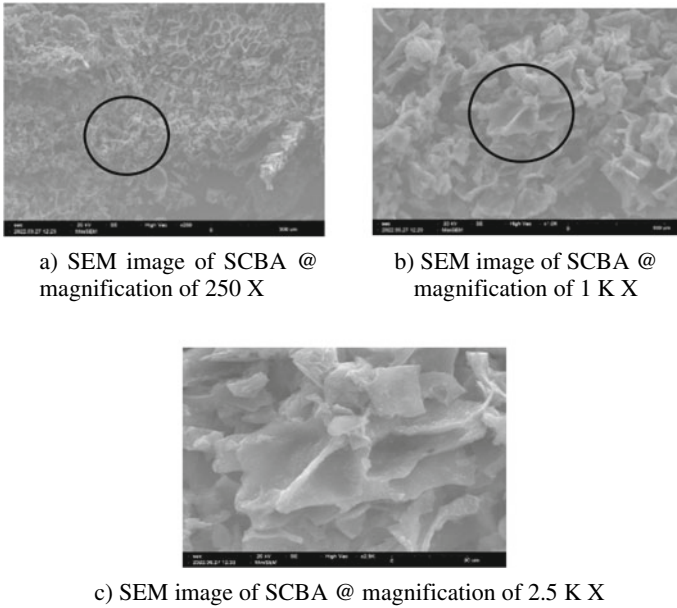


Fig. 5 SEM analysis of SCBA

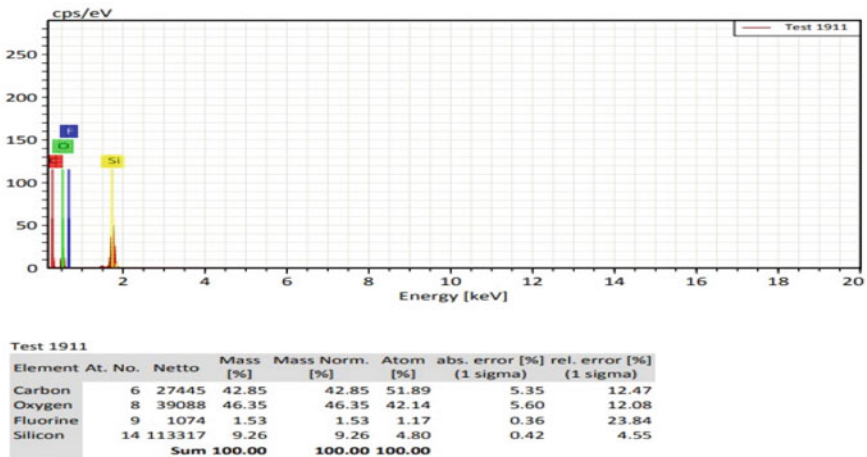
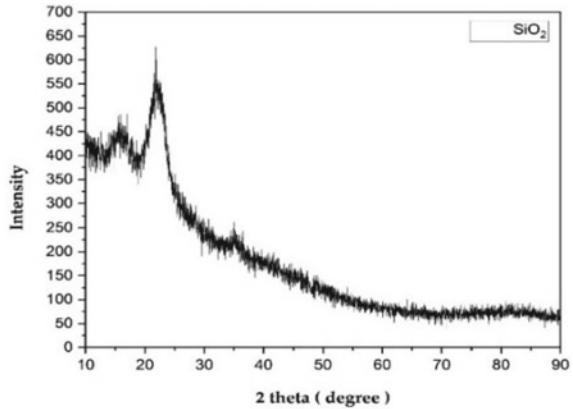


Fig. 6 EDS analysis of SCBA

5.2 Compressive Strength Test

The compressive strength test results of concrete with substitutions such as GGBS, SCBA, and GGBS to cement are shown in Figs. 8 and 9. First, the compression

Fig. 7 XRD analysis of SCBA



test of GGBS as a replacement to cement shows a better strength property with a proportion of 20% to the weight of cement than 30 and 40%. The 7-day test results show high strength of 27.1 N/mm² at 40% replacement than the other mix. But after days when it was tested for 28 days, the strength of the nominal was about 39 N/mm² which was the target strength, 20% addition of GGBS showed a better strength of 38.15 N/mm², where the 40% replacement was only about 33.5 N/mm². The result states that addition of GGBS higher than 20% affects the strength property. Now after the optimum value of GGBS to cement (i.e., cement—80% and GGBS—20%), the SCBA is added with 5, 10, 15, and 20% to the proportion. The maximum strength of 19.6 N/mm² was attained by 5% replacement proportion compared to the nominal mix. The 28-day test results conclude that the maximum strength of 34.5 N/mm² was also attained by 5% replacement mix than that of other proportions. The compression test data comparison states that the strength property is not much affected with the replacement of 5% of SCBA to the weight of the cementitious materials. As stated already, the addition of SCBA with higher proportions affects the strength property. The strength property may be due to the better pozzolanic reaction at certain proportions. Hence, an optimum replacement value of 5% of SCBA and 20% of GGBS to the weight of Cement has been obtained.

5.3 Tensile Strength Test

The results of the tensile strength of concrete with substitution to cement are shown in Fig. 10. The maximum strength of 1.9 N/mm² was attained by 5% replacement proportion compared to the nominal mix. The 28-day test results conclude that the maximum strength of 3.5 N/mm² was also attained by 5% replacement mix than that of other proportions. The tensile test data comparison states that the strength property is not much affected with the replacement of 5% of SCBA to the weight of the cementitious materials. As stated already, the addition of SCBA with higher

Fig. 8 Compressive strength of GGBS and cement

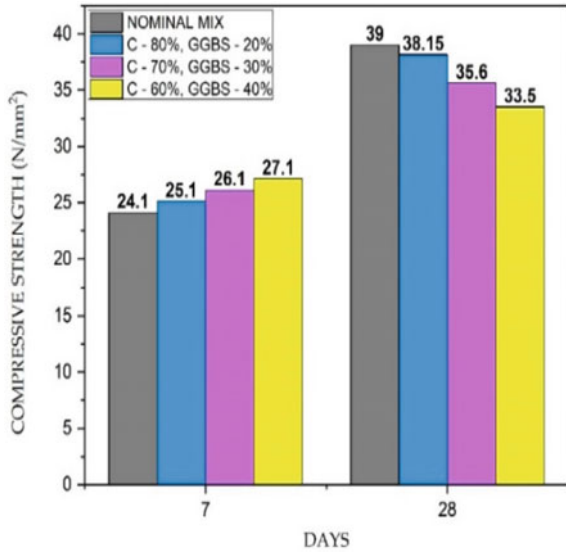
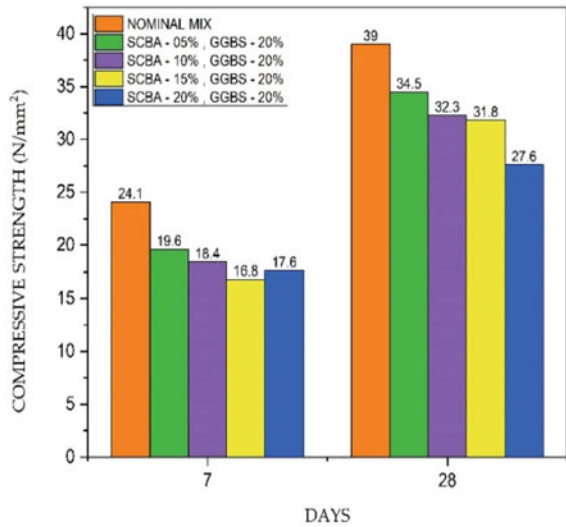
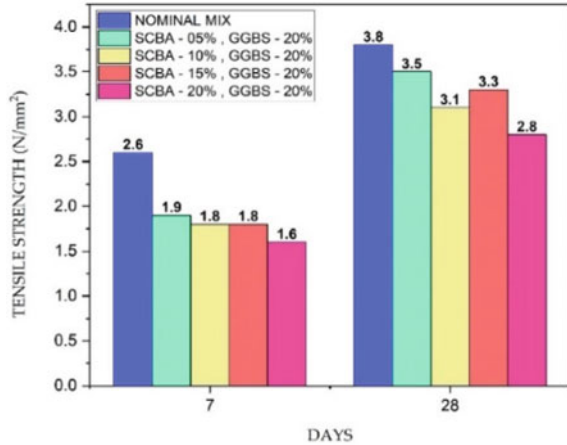


Fig. 9 Compressive strength of SCBA, GGBS and cement



proportions affects the strength property. The strength property may be due to the better pozzolanic reaction at certain proportions. Hence, an optimum replacement value of 5% of SCBA and 20% of GGBS to the weight of cement has been obtained.

Fig. 10 Tensile strength of SCBA and GGBS and cement



6 Conclusion

The investigation on the partial replacement of cement with Sugarcane Bagasse Ash (SCBA) combined with Ground Granulated Blast Furnace Slag Cement (GGBS) has been assessed. From the studies, the upcoming conclusions could be established.

1. The GGBS and SCBA has been replaced to cement in various proportions, and without affecting the property of the nominal concrete mix, an optimum percentage of 20% GGBS and 5% SCBA have been retrieved.
2. The material property study states that GGBS and SCBA has high silica content, which is a good pozzolanic property to act as a replacement aspects in cement.
3. Concrete with the partial replacement of cement with the optimum percentage yields better compressive and tensile strength properties.
4. The compressive strength of the cubes decreases with an increase in the proportion of SCBA beyond 5% and GGBS beyond 20%.
5. The tensile strength of the cylinder also decreases with an increase in the proportion of SCBA beyond 5% and GGBS beyond 20%.
6. The SEM–EDS along with XRD are the microstructural study that detects the shape, size, and composition of the elements present in the sample.
7. Concrete with the replacement of cement by SCBA and GGBS can be considered for real life practice. It also helps in eco-friendly aspects.

References

1. Madurwar MV, Ralegaonkar RV, Mandavgane SA (2013) Application of agro-waste for sustainable construction materials: a review. *Constr Build Mater* 38:872–878. <https://doi.org/10.1016/j.conbuildmat.2012.09.011>

2. Tripathy A, Acharya PK (2022) Characterization of bagasse ash and its sustainable use in concrete as a supplementary binder—a review. *Constr Build Mater* 322 (Elsevier Ltd). <https://doi.org/10.1016/j.conbuildmat.2022.126391>
3. Liu Z, Takasu K, Koyamada H, Suyama H (2022) A study on engineering properties and environmental impact of sustainable concrete with fly ash or GGBS. *Constr Build Mater* 316. <https://doi.org/10.1016/j.conbuildmat.2021.125776>
4. Aprianti E, Shafiqh P, Bahri S, Farahani JN (2015) Supplementary cementitious materials origin from agricultural wastes—a review. *Constr Build Mater* 74:176–187 (Elsevier Ltd). <https://doi.org/10.1016/j.conbuildmat.2014.10.010>
5. Cordeiro GC, Toledo Filho RD, Tavares LM, Fairbairn EMR (2009) Ultrafine grinding of sugar cane bagasse ash for application as pozzolanic admixture in concrete. *Cem Concr Res* 39(2):110–115. <https://doi.org/10.1016/j.cemconres.2008.11.005>
6. Ganesan K, Rajagopal K, Thangavel K (2007) Evaluation of bagasse ash as supplementary cementitious material. *Cem Concr Compos* 29(6):515–524. <https://doi.org/10.1016/j.cemconcomp.2007.03.001>
7. Payá J, Monzó J, Borrachero MV, Tashima MM, Soriano L (2018) Bagasse ash. In: *Waste and supplementary cementitious materials in concrete: characterisation, properties and applications*. Elsevier, pp 559–598. <https://doi.org/10.1016/B978-0-08-102156-9.00017-1>
8. Dhawan A, Gupta N, Goyal R, Saxena KK (2021) Evaluation of mechanical properties of concrete manufactured with fly ash, bagasse ash and banana fibre. *Mater Today Proc* 44:17–22. <https://doi.org/10.1016/j.matpr.2020.06.006>
9. Katare VD, Madurwar MV (2021) Process standardization of sugarcane bagasse ash to develop durable high-volume ash concrete. *J Build Eng* 39. <https://doi.org/10.1016/j.jobte.2021.102151>
10. Setayesh Gar P, Suresh N, Bindiganavile V (2017) Sugar cane bagasse ash as a pozzolanic admixture in concrete for resistance to sustained elevated temperatures. *Constr Build Mater* 153:929–936. <https://doi.org/10.1016/j.conbuildmat.2017.07.107>
11. Jha P, Sachan AK, Singh RP (2021) Agro-waste sugarcane bagasse ash (ScBA) as partial replacement of binder material in concrete. *Mater Today Proc* 44:419–427. <https://doi.org/10.1016/j.matpr.2020.09.751>
12. Le DH, Sheen YN, Lam MNT (2018) Fresh and hardened properties of self-compacting concrete with sugarcane bagasse ash–slag blended cement. *Constr Build Mater* 185:138–147. <https://doi.org/10.1016/j.conbuildmat.2018.07.029>
13. Quedou PG, Wirquin E, Bokhoree C (2021) Sustainable concrete: potency of sugarcane bagasse ash as a cementitious material in the construction industry. *Case Stud Constr Mater* 14. <https://doi.org/10.1016/j.cscm.2021.e00545>
14. Tanwar V, Bisht K, Ahmed Kabeer KIS, Ramana PV (2021) Experimental investigation of mechanical properties and resistance to acid and sulphate attack of GGBS based concrete mixes with beverage glass waste as fine aggregate. *J Build Eng* 41. <https://doi.org/10.1016/j.jobte.2021.102372>
15. Müllauer W, Beddoe RE, Heinz D (2015) Leaching behaviour of major and trace elements from concrete: effect of fly ash and GGBS. *Cem Concr Compos* 58:129–139. <https://doi.org/10.1016/j.cemconcomp.2015.02.002>
16. Minnu SN, Bahurudeen A, Athira G (2021) Comparison of sugarcane bagasse ash with fly ash and slag: an approach towards industrial acceptance of sugar industry waste in cleaner production of cement. *J Clean Prod* 285 (Elsevier Ltd). <https://doi.org/10.1016/j.jclepro.2020.124836>
17. IS-1727 (1967) IS 17127—method of test for pozzolanic materials. Bureau of Indian Standard, New Delhi
18. Indian Standards, IS 383 (2016): Coarse and fine aggregate for concrete-specification. Bureau of Indian Standard, BIS, New Delhi
19. IS:12089-1987 (1987) Specification for granulated slag for the manufacture of Portland slag cement. Bureau of Indian Standard, New Delhi, pp 1–14
20. IS 456 (2000) Plain concrete and reinforced. Bureau of Indian Standard, Delhi, pp 1–114
21. BIS, IS 10262:2019 Indian standard, concrete mix proportioning—guidelines (second revision)

Development of Sustainable Bricks by Industrial By-Product



Harresh Jagadeesan, R. Balaraman, and G. Senthil Kumar

1 Introduction

Various material production emits a huge amount of carbon emission; India emits 7.15% of carbon emissions by cement production globally [1]. These type of high carbon emission materials leads to greenhouse gases, and it is found that India is one of the major CO₂ contributors, as it is producing 20% of overall GHG occurring globally [2]. Cement production is not ending with CO₂ emission alone, it generates sulphur dioxide a colourless gas that is a major contributor to acid rain which creates an imbalance in the ecosystem, apart from this it also produces nitrogen oxides that cause air pollution which may create respiratory problem [3]. The CO₂ emission produced by cement manufacturing is almost 0.8–0.9 times of actual manufacturing rate, that is 800–900 kg of CO₂/T is produced, which may lead to a rapid increase in GHG emission [4]. In ancient days, we tend to use clay bricks for the construction of walls, which are made up of clay soil in this process initially the clay is dug, from the ground and later it is blended with a sufficient amount of water in it. The next stage is laying bricks in mould and the final stage is burning the bricks. During the burning, approximately 70–280 kg of carbon has been emitted for one ton of brick burning it also varies upon the type of fossil used for burning [4]. This was the procedure of clay brick manufacturing it is found that everyone started doing the same process for brick manufacturing, but at a later period due to the over usage of clay, it became an insufficient material, since it arrives from nature it was used as a fully sustainable material. When the material is forced under huge supply, it came under scarcity later to balance that cement bricks came into action [5–7]. In this paper, cement bricks are manufactured by adding cement, and sand together and

H. Jagadeesan (✉) · G. S. Kumar
Department of Civil Engineering, Easwari Engineering College, Chennai, India
e-mail: harreshjagadeesan@gmail.com

R. Balaraman
Department of Civil Engineering, Jerusalem College of Engineering, Chennai, India

placed in a mould once the brick attained its dry state, the comes curing here water curing takes place instead of burning the bricks. The compressive strength attained by cement bricks is high when compared to ideal clay bricks as this brick produces more strength it became the fastest connecting construction material that is used for wall construction. Cement bricks are classified as one of the best bricks for the construction of the wall in buildings, whereas clay bricks usage became half the initial usage, so it is found that the imbalance and demand in bricks are sorted out using cement bricks. Though it produces high strength on one side, the carbon emitted by cement bricks is getting increased on the other side. To reduce carbon emissions, cement should be partially replaced with some other binder that should undergo pozzolanic action, it is found that fly ash and GGBS can be partially replaced with cement to reduce that CO₂ emission, and at the same time, the industrial by-products were also utilized properly [8–10]. To reduce the CO₂ emission partial replacement for cementitious material such as fly ash, GGBS is implemented in general practices in the construction industry [11–15]. It is found that GGBS is a booming material that is used as a replacement for cement in concrete, almost 350 million tonnes of iron slag has been generated globally [16], so the same is taken into account here. Iron production is increasing rapidly, which poses an enormous amount of slag availability and still, there are places found with slag deposits on barren lands. Instead of depositing the slag as a waste material, it can be used as a properly reused material, so that it is treated as a valuable resource, on another hand, it is the best way to dispose the slag in a sustainable manner and it is also found that to grind the granulated blast furnace slag, only minimum amount of energy is required, that is 90% of energy is saved when its grinding is compared to Portland Cement production [17]. GGBS replacement is eventually placed with 50% as the replacement percentage takes action between 0.3 and 0.85 out of 1 [18]. GGBS won't produce a high strength in the early stage as its hydration is different from Portland cement, even though it's a sustainable replacement material for cement, the pores present inside the face at the centre affect the strength initially, but this slag replacement will produce a good strength in a later age that is approximately at 90-day strength. This replacement activity of slag in place of cement will reduce the amount of carbon emitted into the atmosphere, leading to the conservation of sustainable materials [19]. There are various factors that affect the cementitious property of GGBS, they are the fineness modulus, physical characterization, chemical characterization, amorphous content, etc. [14, 20]. Even though slag is a good cementitious replacement material, its optimum level of replacement should be properly studied because over-usage of GGBS will decrease the strength and durability of the overall material where slag is replaced [21–23]. It is found that unfired GGBS bricks will attain a high strength at a later age [24]. Based on the literature survey, it can be inferred that research under sustainable bricks has mostly consisted of fly ash and the partial replacement of GGBS in bricks is not commonly aware as same as fly ash. It is also found that GGBS is a proper cementitious material that can be replaced in place of Ordinary Portland Cement, which gives the same strength in case of a later age test apart from strength GGBS is a sustainable waste that has pozzolanic action in it. Hence, a combination of OPC, GGBS, and M-Sand is used to develop a sustainable brick in

order to reduce the carbon emitted by cement bricks. Here, three trials with different mix ratios were carried out and the experimental solutions are derived at the end which gave comparatively good results than ideal clay bricks.

2 Material and Experimental Approach

2.1 Materials

GGBS is partially replaced with cement with some percentage so that the amount of cement used can be reduced which results in less carbon emission. Cement is the first binder used here, which in addition to M-Sand gives good strength, cement used here is OPC 53 Grade. GGBS is used as a second binder material used here. GGBS is a slag that is obtained by the steel manufacturing industry, as its size is comparatively less than OPC it settles in between the cement particles which gives proper bonding that results in high compressive strength.

This study used OPC, GGBS, and M-Sand for developing a sustainable brick that gave high compression strength. GGBS used here were in size between 15 and 16 μm . The chemical composition of the GGBS and OPC powders obtained from the X-ray fluorescence (XRF) analysis from various literature is expressing that the predominant oxide constituents of OPC are SiO_2 (21.84%) and CaO (60.27%), whereas GGBS mostly consists of SiO_2 (39.22%), Al_2O_3 (10.15%), and CaO (32.62%) [25]. In the XRD pattern of GGBS, it can be noted that the crystalline peaks of Quartz (SiO_2), Calcite (CaCO_3), and Alumina (Al_2O_3) are observed in the GGBS sample. The morphological and elemental composition of the GGBS sample was acquired from scanning electron microscope (SEM) and energy-dispersive X-ray spectroscopy (EDX) analysis, respectively. The SEM micrographs of GGBS particles are mostly tetrahedron in shape with rough surface textures [26]. The preliminary test is carried out for all three samples, and the specific gravity of OPC, GGBS, and M-Sand was 3.15, 2.2, 2.67, respectively. Pycnometer apparatus is used to find the specific gravity of M-Sand, and a Le Chatelier's flask is used in the case of the other two cementitious materials mentioned above; these specific gravity plays a major role in calculating the volume of materials that need to be added.

2.2 Experimental Approach

In this study, three ratios are tried with raw materials of OPC, GGBS, and M-Sand, all three ratios were clearly mentioned in Table 1, and for all three variation volume of each material is calculated.

Table 1 Mix proportion of bricks

Trial specimen	OPC: GGBS: M-sand
SGBT1/1-SGBT1/3	1:1:2
SGBT2/1-SGBT2/3	1.2:0.8:2
SGBT3/1-SGBT3/3	1.2:1.2:1.4

Table 2 Mix proportion calculation of bricks

Parameter	OPC 53	GGBS	M-sand
Calculation quantity ratio of mix	(1.3/1)/4 0.325	(1.3/1)/4 0.325	(1.3/2)/4 0.650
	1	1	2

The mix proportion mentioned in Table 1 is used to develop a brick specimen, using this ratio bricks are laid as three bricks per variation, as totally three types of bricks were developed here, and exactly 9 bricks were cast as per IS 13757 [27]. Once the brick is taken from mould, it is then allowed for air curing for up to the next 24 h, after that, it is taken for water absorption, and compression tests. All the bricks are casted by weight batching it is derived by volume proportioning condition, details of it were tabulated in Table 2.

2.3 Test Methods

There are totally two tests carried out on the sustainable brick, they are compression and water absorption test, and the results of the following tests will be mentioned here; initially, water absorption test is carried out as per IS 3495 (Part 2):1992 [28] all the bricks are taken and immersed in water for 24 h and after that, it is taken out and wiped by cloth and specimen is taken for weighing within 3 min from the time of taking out from the water the weight of all the trial specimen is provided in Table 3. The model representation of the brick is shown in Fig. 1. In the water absorption test, dry and wet weight for all 9 specimens is taken, and the percentage of each is derived from guidelines as per IS 3495 (Part 2): 1992 clause 4.1.4, and the results were tabulated in Table 3 [28]. It is founded that the minimum and water absorption at 4.40 and 7.17% along with this an average of each set is calculated and it is ensured that the difference between the same samples is not more than 5%, so the average of 3 sets is within the exact limit (Figs. 2 and 3; Table 4).

Table 3 Water absorption test results

Trial specimen	Water absorption (%)
SGBT1/1	4.97
SGBT1/2	5.61
SGBT1/3	7.09

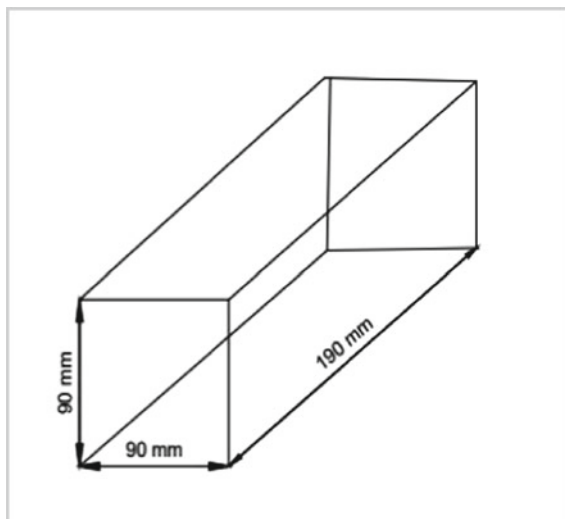


Fig. 1 Model of sustainable brick



Fig. 2 Water absorption test of sustainable brick a dry weight, b wiping of brick, and c wet weight

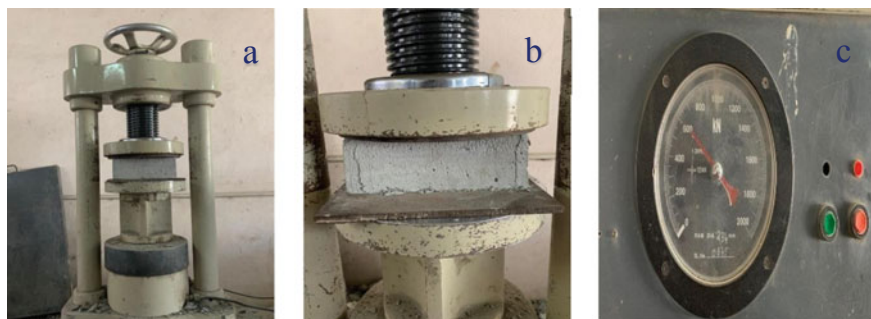


Fig. 3 Compression test a UTM with brick, b breaking point, and c dial gauge reading

Table 4 Compression strength test results

Trial specimen	Load (kN)
SGBT1	4.87
SGBT2	15.54
SGBT3	23.8

3 Result and Discussion

3.1 Compression Strength of Sustainable Brick

In this study, compression strength for all three trial bricks is carried out with the guidelines standard provided as per IS 1077:1992 and IS 3495 (Part 1): 1992 [28, 29]. This high strength is achieved due to a proper mix ratio and W/B ratio used in SGBT3, this high strength proves there are fewer voids present inside the brick, and apart from acting as a replacement material GGBS acted as an excellent filler material here. The proper filling is the main reason for the durability, as the filling material is properly bonded, the porosity level decreases, and as porosity decreases strength increases. It is not ended only with porosity even filling of cementitious material lead to proper hydration, on which the heat of hydration is controlled that reduces the shrinkage cracks during the setting of the top surface of the brick, usually shrinkage crack occurs due to the addition of Ordinary Portland Cement. Compression strength of all three bricks was plotted in a graphical manner in Fig. 4.

3.2 Water Absorption of Sustainable Brick

The water absorption tests for all three trial bricks are below 12%, which proves that all three are good, non-porous bricks. SGBT1 has a water absorption result of 4.06%, which is very low, the standard ideal bricks are classified as bad water absorbers; in this case, all trials proved that they are standard bricks that absorb less amount of water through the inner pores and cavity. There should be minimum content of water absorption because the small micropores that penetrate water ensure that there is a gap in between the molecules to exhale the heat present inside the room that is constructed by that brick. SGBT2 absorbed water up to 5.5%, this is due to the increase in addition of Ordinary Portland Cement, hydration takes place when OPC is treated with water that tends to change the wet state to a dry state at the inner face of the brick, thus due to the proper hydration, development of partially dried lumps is reduced that results in good water absorption standard. SGBT3 attained 7.3% of water absorption, which is exactly half the percentage mentioned in the codal reference, this is an accurate and appropriate result that proves that among three bricks, this is the perfect mix ratio and it also denotes that GGBS will reduce the water absorption pores when its optimum level is maintained exactly, in the same

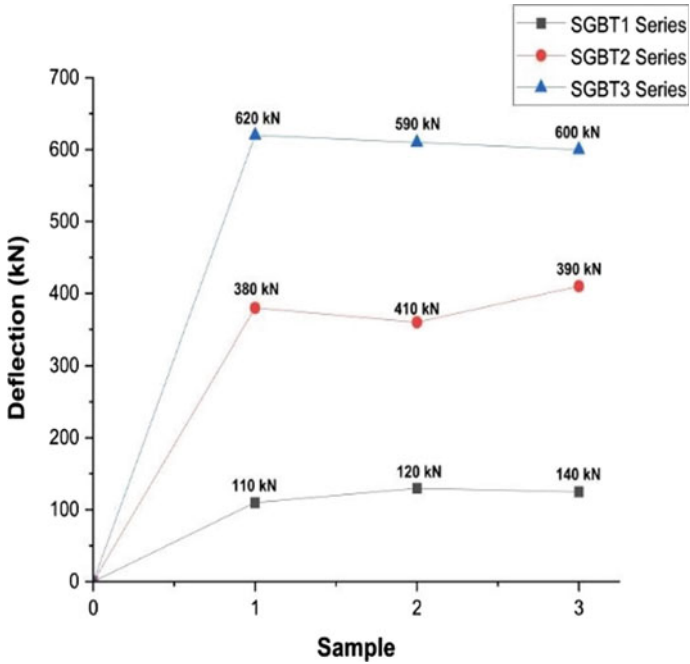


Fig. 4 Graphical representation compression strength of bricks

way, if it crosses the optimacy then it will just act as a filler material instead of acting as a cementitious material. All three variation bricks' water absorption results are plotted in a graphical presentation in Fig. 5.

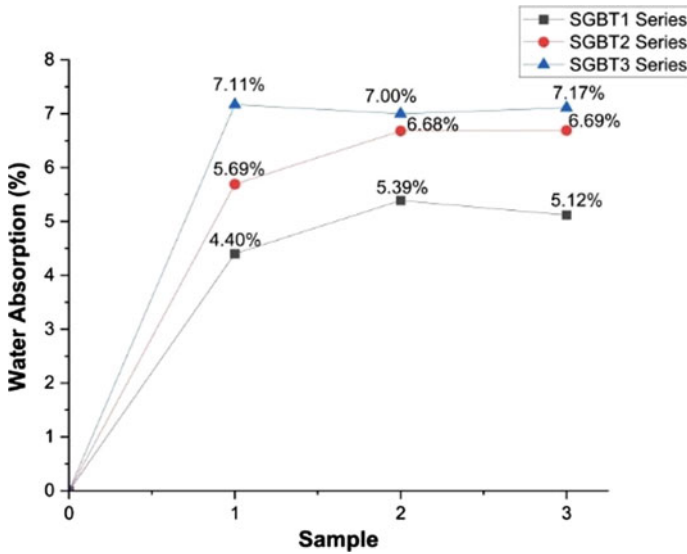


Fig. 5 Graphical representation of water absorption of bricks

4 Conclusion

- It is found that the partial replacement of cementitious material will increase the weight of the brick, from ideal clay brick, because the particle size of the replacement material is very less when it is compared to OPC53.
- There should be a proper limitation for the usage of any replacement materials, once this got more percentage in volume; then the amount of water consumption will get increase which will lead to the over addition of superplasticizers.
- Partial replacement of cement as GGBS of 30% gave a compression strength of 24 MPa, which is an average of three specimens cast with the same proportion.
- Water absorption is a maximum of 7.11% in sample SGBT3, this proved that the brick is a partial non-porous brick that only penetrated less water.
- Finally, the sustainable brick by industrial by-product gave expected results, within the expected time and the important learning from this study is, these types of work will increase the utilization of waste materials, which changes these dump materials into renewable materials

References

1. Venkatarama Reddy BV (2004) Sustainable materials for low carbon buildings. In: *Current science*, pp 899–907
2. Venkatarama Reddy BV, Jagadish KS (2003) Embodied energy of common and alternative building materials and technologies. *Energy Build* 35(2):129–137. [https://doi.org/10.1016/S0378-7788\(01\)00141-4](https://doi.org/10.1016/S0378-7788(01)00141-4)
3. Manikandan P, Vasugi V (2021) A critical review of waste glass powder as an aluminosilicate source material for sustainable geopolymer concrete production. *Silicon*. <https://doi.org/10.1007/s12633-020-00929-w>
4. Benhelal E, Zahedi G, Shamsaei E, Bahadori A (2013) Global strategies and potentials to curb CO₂ emissions in cement industry. *J Clean Prod* 51:142–161. <https://doi.org/10.1016/j.jclepro.2012.10.049>
5. Mckinley JD, Thomas HR, Williams KP, Reid JM (2001) Chemical analysis of contaminated soil strengthened by the addition of lime. *Eng Geol* 60(1–4):181–192. [https://doi.org/10.1016/S0013-7952\(00\)00100-9](https://doi.org/10.1016/S0013-7952(00)00100-9)
6. Rao SM, Shivananda P (2005) Role of curing temperature in progress of lime-soil reactions. *Geotech Geol Eng* 23(1):79–85. <https://doi.org/10.1007/s10706-003-3157-5>
7. Ktnuthia JM, Wild S (2001) Effects of some metal sulfates on the strength and swelling properties of lime-stabilised kaolinite. *Int J Pavement Eng* 2(2):103–120. <https://doi.org/10.1080/10298430108901720>
8. Rashad AM (2015) An investigation of high-volume fly ash concrete blended with slag subjected to elevated temperatures. *J Clean Prod* 93:47–55. <https://doi.org/10.1016/j.jclepro.2015.01.031>
9. Chaitanya M, Manikandan P, Prem Kumar V, Elavenil S, Vasugi V (2020) Prediction of self-healing characteristics of GGBS admixed concrete using artificial neural network. *J Phys Conf Ser* 1716:012019. <https://doi.org/10.1088/1742-6596/1716/1/012019>
10. Manikanta C, Manikandan P, Duraimurugan S, Elavenil S, Vasugi V (2020) Pozzolanic properties of agro waste ashes for potential cement replacement predicted using ANN. *J Phys Conf Ser* 1716:012018. <https://doi.org/10.1088/1742-6596/1716/1/012018>
11. Almeida FCR, Klemm AJ (2018) Efficiency of internal curing by superabsorbent polymers (SAP) in PC-GGBS mortars. *Cem Concr Compos* 88:41–51. <https://doi.org/10.1016/j.cemconcomp.2018.01.002>
12. Hooton RD (2008) Bridging the gap between research and standards. *Cem Concr Res* 38(2):247–258. <https://doi.org/10.1016/j.cemconres.2007.09.012>
13. Sales A, Lima SA (2010) Use of Brazilian sugarcane bagasse ash in concrete as sand replacement. *Waste Manag* 30(6):1114–1122. <https://doi.org/10.1016/j.wasman.2010.01.026>
14. Lothenbach B, Scrivener K, Hooton RD (2011) Supplementary cementitious materials. *Cem Concr Res* 41(12):1244–1256. <https://doi.org/10.1016/j.cemconres.2010.12.001>
15. Manikandan P et al (2022) An artificial neural network based prediction of mechanical and durability characteristics of sustainable geopolymer composite. *Adv Civ Eng* 2022:1–15. <https://doi.org/10.1155/2022/9343330>
16. Vinardell MP (2022) The potential use of waste glass powder in slag based geopolymer concrete—an environmental friendly material. *Int J Environ Waste Manag* 1(1):1. <https://doi.org/10.1504/ijewm.2022.10032507>
17. Shi C, Qian J (2000) High performance cementing materials from industrial slags—a review. *Resour Conserv Recycl* 29(3):195–207. [https://doi.org/10.1016/S0921-3449\(99\)00060-9](https://doi.org/10.1016/S0921-3449(99)00060-9)
18. Panesar DK (2019). Supplementary cementing materials. *Dev Formul Reinf Concr* 55–85. <https://doi.org/10.1016/B978-0-08-102616-8.00003-4>
19. Megat Johari MA, Brooks JJ, Kabir S, Rivard P (2011) Influence of supplementary cementitious materials on engineering properties of high strength concrete. *Constr Build Mater* 25(5):2639–2648. <https://doi.org/10.1016/j.conbuildmat.2010.12.013>

20. Siddique R (2014) Utilization (recycling) of iron and steel industry by-product (GGBS) in concrete: Strength and durability properties. *J Mater Cycles Waste Manag* 16(3):460–467. <https://doi.org/10.1007/s10163-013-0206-x>
21. Divsholi BS, Lim TYD, Teng S (2014) Durability properties and microstructure of ground granulated blast furnace slag cement concrete. *Int J Concr Struct Mater* 8(2):157–164. <https://doi.org/10.1007/s40069-013-0063-y>
22. Krivenko P, Drochytka R, Gelevera A, Kavalerova E (2014) Mechanism of preventing the alkali-aggregate reaction in alkali activated cement concretes. *Cem Concr Compos* 45:157–165. <https://doi.org/10.1016/j.cemconcomp.2013.10.003>
23. Klemczak B, Batog M (2016) Heat of hydration of low-clinker cements: part I. Semi-adiabatic and isothermal tests at different temperature. *J Therm Anal Calorim* 123(2):1351–1360. <https://doi.org/10.1007/s10973-015-4782-y>
24. Oti JE, Kinuthia JM, Bai J (2009) Compressive strength and microstructural analysis of unfired clay masonry bricks. *Eng Geol* 109(3–4):230–240. <https://doi.org/10.1016/j.enggeo.2009.08.010>
25. Manikandan P, Vasugi V (2022) Potential utilization of waste glass powder as a precursor material in synthesizing ecofriendly ternary blended geopolymer matrix. *J Clean Prod* 355(March):131860. <https://doi.org/10.1016/j.jclepro.2022.131860>
26. Manikandan P, Natrayan L, Duraimurugan S, Vasugi V (2022) Influence of waste glass powder as an aluminosilicate precursor in synthesizing ternary blended alkali-activated binder. *Silicon* 0123456789. <https://doi.org/10.1007/s12633-021-01533-2>
27. Bureau of Indian Standard (BIS) (1993) Burnt clay fly ash building bricks. IS 13757
28. Bureau of Indian Standards (1992) IS 3495 parts 1–4: methods of tests of burnt clay building brick, pp 1–7
29. I. 1077:1992 (1992) Building common burnt clay building bricks-specifications. Bureau Indian Standard

Experimental Investigation and Comparative Study on Self-healing Concrete with Superabsorbent Polymer and Bacteria



R. Kaviraja, N. Ganapathy Ramasamy, R. Suriyaprakash,
S. Prakash Chandar, and A. Siranjeevinathan

1 Introduction

Cement, fine aggregates, and coarse aggregates are combined with water to make concrete, a building material that hardens over time. Concrete cracks are unavoidable because it alternates between being fragile in tension and strong in tension. As a result, steel reinforcement bars are included into the material to enable the building of structures. Large permeability is caused by the formation of cracks in concrete buildings, which ultimately leads to durability issues [1]. The strength and sturdiness of concrete structures are impacted by cracks because they make the entire structure more susceptible to serious harm [2]. Contrarily, concrete is subjected to cracking, and these fractures, which are brought on by mechanical as well as environmental factors, significantly diminish the structure's usefulness, steel corrosion resistance, use, and resilience [3]. However, this affects the workability of the concrete, which may be assessed using the slump test [4]. In building applications, cracking is a

R. Kaviraja · N. Ganapathy Ramasamy (✉) · S. Prakash Chandar · A. Siranjeevinathan
Department of Civil Engineering, Faculty of Engineering and Technology, SRM Institute of
Science and Technology, Kattankulathur, Chennai, Tamilnadu 603203, India
e-mail: ganapatn@srmist.edu.in

R. Kaviraja
e-mail: kr6826@srmist.edu.in

S. Prakash Chandar
e-mail: prakashs2@srmist.edu.in

A. Siranjeevinathan
e-mail: sa7026@srmist.edu.in

R. Suriyaprakash
Research in Environment, Sustainability Advocacy and Climate Change, SRM Institute of
Science and Technology, Kattankulathur, Chennai 603203, India
e-mail: Suriyapr1@srmist.edu.in

significant concern. Shrinkage, freezing and thawing, structural strains, and other factors can all cause cracks. In concrete constructions, cracks significantly increase permeability, which in turn affects durability. The cracking of concrete structures is caused by changes in temperature and humidity, primarily when they are young, and by external loads, primarily when they are older. This opens a pathway for dangerous elements to enter the material and slowly deteriorate it over time [5].

1.1 Self-healing Concrete

Concrete that has a knack for self-heal fractures and other damages without human assistance is deemed to be self-healing. The healing agent used, the protective casing material, the dose, the depth and breadth of the cracks, the level of humidity and temperature, the mix design, and ultimately the healing time all have an impact on the self-healing activity [6]. During the self-healing process, the healing component takes moisture from the environment to patch up the crack. When fractures are less than 0.2 mm wide, concrete has been shown to heal itself over time, and when cracks are more than this, artificial restoration methods may be used [7]. The use of superabsorbent polymers (SAPs) as an additive may promote the self-sealing of fractures in cement-based materials such as concrete. Low cross-linking densities are necessary for SAPs to have a high fluid absorption capacity, and they frequently consist of ionic monomers [8]. One of their most vital qualities is their capacity to soak up and retain massive quantities of liquid, expand to produce an insoluble gel. SAPs are not only used as self-healing agent but also used for self-curing in concrete [9].

Bacteria is used in concrete mix to enhance its self-healing property. Calcite crystals are biologically developed by biologically self-healing concrete to stop cracks that emerge on the surface of the real building [9]. Recently, an alternative and environmentally conscious method for boosting the efficacy of concrete crack-healing has been put forward: bacteria-induced mineral precipitation [10]. Implementing a biotech technique based on calcite precipitation, the durability and reliability of reinforced concrete may be augmented [11]. These bacteria have the ability to affect the formation of precipitate of calcium carbonate through the generation of an enzyme called urease [12]. By hydrolysing urea into CO_2 and ammonia, this enzyme increases the bacterial environment's pH and carbonate concentration [12]. Because of the urea hydrolysis, bacteria becomes negatively charged, which causes the surrounding calcium ions to attract them quickly for biomineralization [13]. Certain species of bacillus produce urease, an enzyme that precipitates the calcite involved in biomineralization [14]. A user-friendly interface in self-healing concrete is made possible by the non-virulent microorganism *Bacillus subtilis* [15]. Temperatures between 25 and 35 °C are ideal for growing *Bacillus subtilis* [16]. By employing bacteria, 0.1-mm-wide cracks are completely repaired in 200 h [6]. Moreover, cracks 0.15–0.3 mm in width considerably contract in seven days and entirely mend in 33 days [6].

Table 1 Preliminary test findings

Description	Results obtained
Cement's specific gravity	3.1
Cement's fineness	4%
Specific gravity of fine aggregate	2.65
Fine aggregate sieve analysis	3.46 (zone II)
Coarse aggregate specific gravity	2.62
Sieve analysis of coarse aggregate	7.7

2 Materials and Methods

2.1 Materials Used

According to IS 12269:2013 [16], OPC grade 53 cement was used. The result of fineness of cement is shown in Table 1. This experiment utilised M-sand as a fine aggregate. The fine aggregate's specific gravity is displayed in Table 1. The coarse aggregate in this concrete mix has a nominal width of 20 mm. Table 1 depicts the coarse aggregate's specific gravity. Using IS 2386-1 [18] as a guide, the aggregates were tested [17]. This concrete mix contains a mineral additive called grey silica fume. Conplast SP430 is the superplasticizer employed here. In this experiment, both mixing and curing are accomplished with standard portable water. The SAP employed in this experimental study was sodium polyacrylate. *Bacillus subtilis*, a non-pathogenic kind of bacterium, was employed in this investigation.

2.2 Super Absorbent Polymer

A class of polymeric materials known as SAPs may absorb and hold a lot of liquid compared to their own mass. The chemical used as superabsorbent polymer here in this study was sodium polyacrylate. A class of polymeric materials known as SAPs may absorb and hold a lot of liquid compared to their own mass. Cross-linked polymers known as SAP have various distinctive properties that can be used in a variety of concrete technology applications. SAPs are water-entrained additives with the ability to take in large volumes of liquid, which then cause them to expand and solidify into waterproof, impenetrable gels [18]. Figure 1 shows the schematic diagram of self-healing mechanism of SAP [19]. Figures 2 and 3 show the dry form and wet form of SAP, respectively.

Fig. 1 Schematic diagram of self-healing

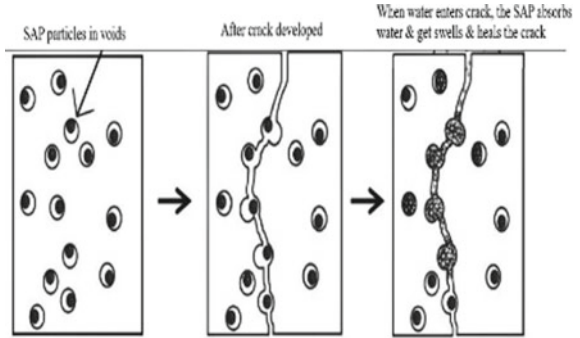


Fig. 2 Dry SAP



Fig. 3 Wet SAP of crack using SAP



2.3 Selection and Cultivation of Bacteria

Typically, bacteria are divided into three classes based on their morphology, gram stain, and oxygen consumption [20]. The absence of water and the high alkaline environment in concrete are the main challenges to bacterial survival; as a result, spore-forming bacteria that can survive adverse circumstances have become the main option for bacterial concrete [21]. The type of bacterium utilised during the present research is *Bacillus subtilis*. *Bacillus subtilis*, Gram-positive, ureolytic bacterium that produces spores, is commonly found in soil and vegetation [22]. *Bacillus subtilis* bacterium culture medium is obtained in a freeze condition from microbiology department, School of Bio-Engineering, SRM University. Its ideal temperature range is between 25 and 35 °C, this bacterium requires 24 h to grow in bio-reactor. Instead of water, bacteria medium is used while casting of concrete specimens. Nutrient broth is used for cultivation of wide varieties of microorganisms. Nutrient broth is a basic media composed of peptone, NaCl, yeast extract, beef extract, etc. Suspend 13 g of nutrient broth powder in 1000 ml of distilled water. *Bacillus subtilis* was cultured by adding 10% of inoculum to the culture media. The pH was altered to 7.0 and temperature was set to 37 °C with an rpm of 150, and 3 LPA pressure was maintained. The bacterial culture medium was collected after 24 h from the bio-reactor and stored at 4 °C.

2.4 Mechanism of Biologically Induced Self-healing

The ability of microorganisms to produce the urease enzyme has been utilised to cause calcium carbonate to precipitate [23]. The urease enzyme hydrolyses urea to release carbonate ions and ammonium in heterotrophic bacteria. This process causes the pH to rise and the carbonate ion to be enriched [24]. A single molecule of $\text{CH}_4\text{N}_2\text{O}$ undergoes internal hydrolysis that yields a single mole each of NH_3 and carbamate, which subsequently splits into a single mole each of NH_3 and H_2CO_3 [25]. Then, two moles of ammonium and hydroxide ions are created when NH_3 and carbamate equilibrate in water. After a particular amount of super-saturation is attained, Ca^{2+} present in the system causes CaCO_3 to precipitate [25]. The bacterial cell wall's outside is where CaCO_3 is developed. Formation of CaCO_3 on bacterial cell wall is shown in Fig. 4 [26]. And mechanism of CaCO_3 precipitation is shown in Fig. 5.

2.5 Concrete Specimens for Assessing Compressive, Split Tensile, and Flexural Strength

Using IS 10262-2019 as a guide, the M50 grade concrete mix was designed [27]. For 1 m³ of concrete and a water cement ratio of 0.34 under moderate conditions,

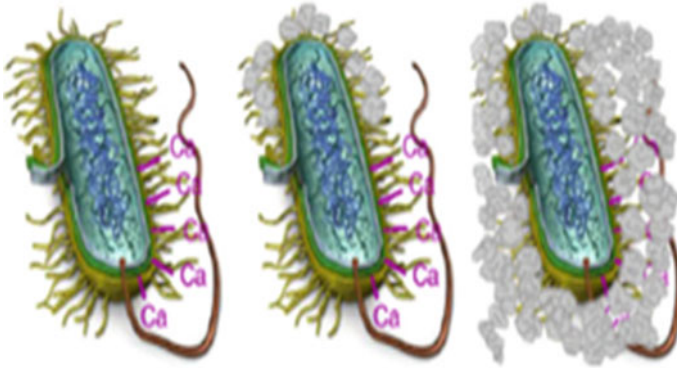
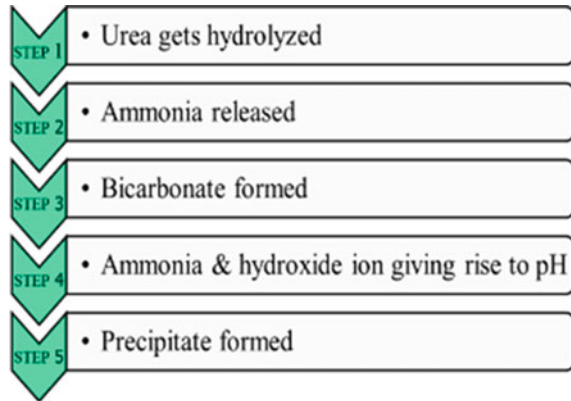


Fig. 4 Formation of CaCO_3 on bacterial cell wall

Fig. 5 Mechanism of CaCO_3 precipitation



the required amount of cement is 443.56 kg. Concrete’s mix ratio is 1:1.49:2.78 and its w/c ratio is 0.34. Concrete is formed into cubes with dimensions of 150 mm for compressive strength testing, cylinders with dimensions of 150 mm diameter and 300 mm length for split tensile strength testing, and concrete beams with dimensions of 500 × 100 × 100 mm for flexural strength testing.

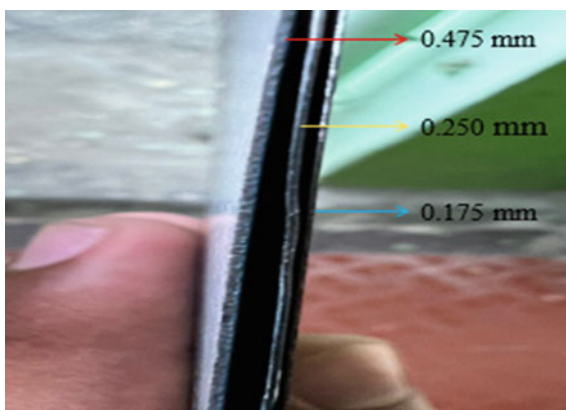
2.6 Preparation of Artificial Cracks

By placing GI sheets of three different thicknesses, the artificial cracks were made. The widths of all three GI sheets are 0.175, 0.250, and 0.475 mm, respectively. And depth of immersion of GI sheet was 75 mm approximately. This method of preparation of artificial crack was adopted from mentioned reference paper [28]. During casting, the sheets are placed in-between to form cracks artificially. And at the

Fig. 6 Preparation of artificial cracks in cubes



Fig. 7 Thickness of GI sheets



time of demoulding of specimens, the sheets should be removed. The preparation of artificial crack and thickness of GI sheets are displayed in Figs. 6 and 7, respectively.

2.7 Different Proportions of Concrete

1. Controlled concrete (CC).
2. Concrete made by 0.5% of superabsorbent polymer (SAP 0.5).
3. Concrete made by 1% of superabsorbent polymer (SAP 1).
4. Concrete made by 1.5% of superabsorbent polymer (SAP 1.5).
5. Concrete made by 1% of superabsorbent polymer and bacteria (SAPBC).

Table 2 Test outcomes for the compression strength test

S. No	Days	CC (N/mm ²)	SAP 0.5 (N/mm ²)	SAP 1 (N/mm ²)	SAP 1.5 (N/mm ²)	SAPBC (N/mm ²)
1	3rd	24.57	23.99	26.84	22.26	25.19
2	7th	39.64	38.95	40.21	37.72	40.47
3	28th	59.33	58.23	60.44	56.15	65.98

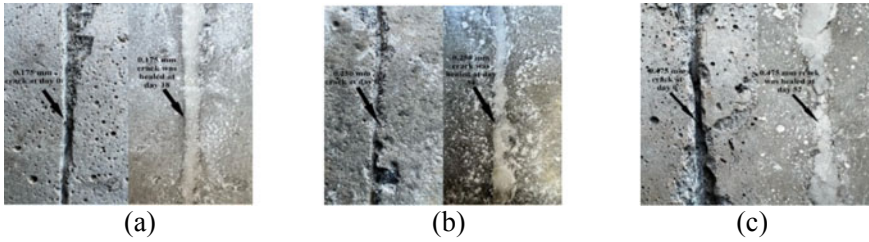


Fig. 8 Self-healing of different widths of crack using SAPBC **a** 0.175 mm; **b** 0.250 mm; **c** 0.475 mm

3 Experimental Study

3.1 Compressive Strength of Concrete

To determine concrete’s compressive strength, compression tests were performed on 150 mm cubes. On days 3, 7, and 28, the test was conducted, accordingly. Totally nine numbers of cube specimen were made for each proportion. The specimen’s target strength for M50 grade concrete was achieved in the 28th day. Table 2 includes the test findings. According to the compression test findings, the concrete cubes made by 1% of superabsorbent polymer and bacteria (SAPBC) have higher strength when compared to controlled concrete (CC). The 28th day compressive strength of SAPBC is higher than CC by 11.20% (Fig. 8). Comparison between compressive strengths of different mixes is shown in Fig. 9.

The similar trend of percentage increase was also found in one research paper [12], in which while comparing the bacterial concrete to their controlled concrete, the bacterial concrete exhibits a 10.80% improvement in compressive strength.

3.2 Split Tensile Strength of Concrete

Split tensile tests on cylindrical specimens 150 mm in diameter and 300 mm length were performed to ascertain the splitting strength of concrete. Table 3 includes the test findings.

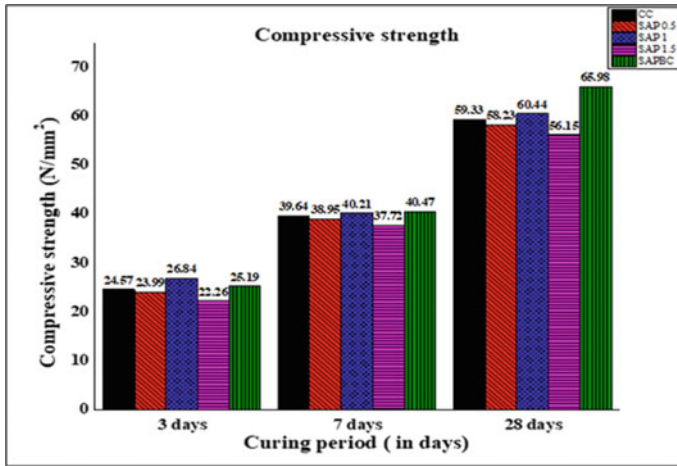


Fig. 9 Comparison between compressive strengths of different mixes

Table 3 Test outcomes for the split tensile strength test

S. No	Days	CC (N/mm ²)	SAP 0.5 (N/mm ²)	SAP 1 (N/mm ²)	SAP 1.5 (N/mm ²)	SAPBC (N/mm ²)
1	28th	6.22	6.14	6.52	6.06	7.25

The split tensile results indicate that the concrete made by 1% of superabsorbent polymer and bacteria (SAPBC) has higher strength when compared to controlled concrete (CC). SAPBC outperforms CC by 16.55% in terms of its 28th day split tensile strength. Comparison between split tensile strengths of different mixes is shown in Fig. 10. The similar trend of percentage increase was also found in one research paper [12], in which while comparing the bacterial concrete to their controlled concrete, the bacterial concrete exhibits a 29.30% improvement in split tensile strength.

3.3 Flexural Strength of Concrete

Concrete beams measuring 500 × 100 × 100 are tested to determine the flexural strength of the material. Table 4 includes the test findings. The flexural strength results indicate that the concrete made by 1% of superabsorbent polymer and bacteria (SAPBC) has higher strength when compared to controlled concrete (CC). The 28th day flexural strength of SAPBC is higher than CC by 8.21%. Comparison between flexural strengths of different mixes is shown in Fig. 11. The similar trend of percentage increase was also found in one research paper [12], in which while

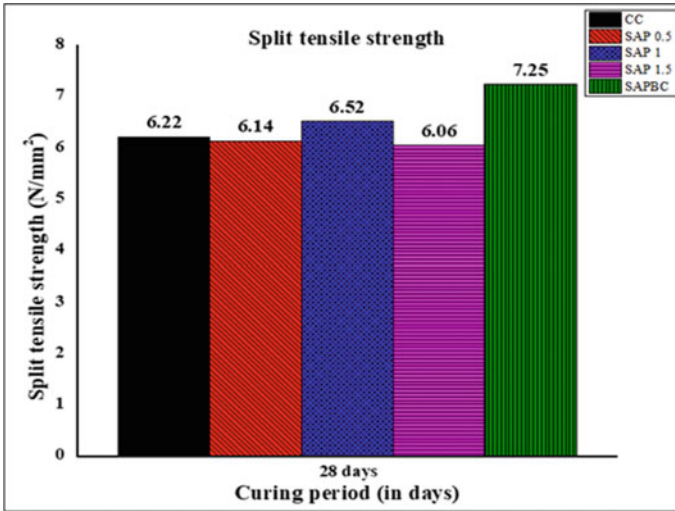


Fig. 10 Comparison between split tensile strengths of different mixes

comparing bacterial concrete to their controlled concrete, flexural strength increases by 5.10%.

Table 4 Test outcomes for the flexural strength test

S. No	Days	CC (N/mm ²)	SAP 0.5 (N/mm ²)	SAP 1 (N/mm ²)	SAP 1.5 (N/mm ²)	SAPBC (N/mm ²)
1	28th	8.16	8	8.66	7.66	8.83

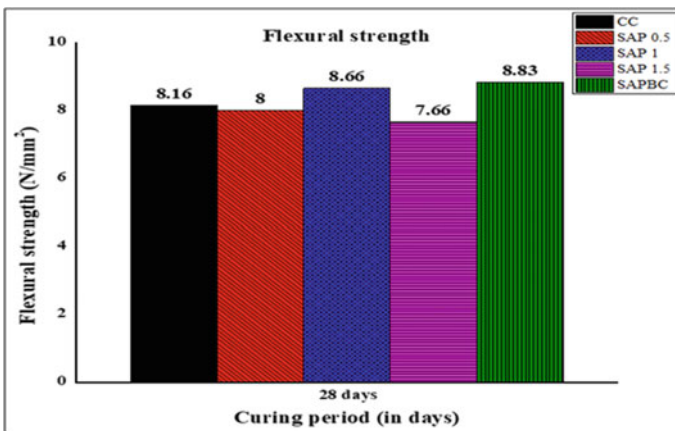


Fig. 11 Comparison between flexural strengths of different mixes

3.4 Self-Healing Analysis of SAPBC

For self-healing process, the concrete specimens are made up of 1% of SAP, and instead of required water quantity, bacterium media is replaced fully. About 1% of SAP gives significant values when compared with other mixes; thus, 1% of SAP is added along the bacteria for making self-healing bacterial concrete. The concrete specimen made of this combination is artificially cracked by placing a GI sheet of thickness 0.475, 0.250, and 0.175 mm and depth approximately of 75 mm, respectively. The GI sheets are inserted in-between the cubes while casting, and at the time of demoulding, the sheets were removed. After being cured in water for a period of fourteen days, the concrete cubes stay put at room temperature. Artificial cracks allow to study the behaviour of concrete structures under controlled conditions. They may assess the strength, durability, and performance of concrete in various conditions by adding cracks of specified sizes and orientations. Moreover, artificial cracks enhance the remediation of healing than the conventional concrete cracks [28]. There may still remain unhydrated cement compounds, such as calcium silicate hydrate gel, a crucial constituent of the cementitious matrix, within the hydrated cement particles. These unhydrated cement particles might keep interacting with water and assisting in the ongoing hydration process [29]. GI sheets are also taken off before the concrete's ultimate hardening period. Therefore, the prosthetic joint area may still contain bacteria and SAP. Therefore, self-healing can be achieved by making artificial cracks in concrete. The formation of white precipitate indicates the presence of CaCO_3 . The crack width of 0.475, 0.250, and 0.175 mm is healed within 52, 34, and 18 days, respectively. The SAPBC's capacity to create CaCO_3 precipitation is thus confirmed. The self-healing of various cracking widths employing SAPBC is depicted in Fig. 8.

4 Conclusion

In the current examination, an experimental investigation is conducted for a concrete mix of M50 grade to assess the compressive, split tensile, and flexural strength and also self-healing analysis of three various sizes of cracks. When 1% of SAP is added, compared to 0.5% and 1.5%, substantial results are obtained. Reduced strength values in mechanical properties are indicated by an increase in SAP content of greater than 1%. SAP functions as a self-curing agent in addition to being a self-healing agent. The compression strength test outcomes indicate that the SAPBC has higher strength than CC by 11.20%. The split tensile test outcomes indicate that the SAPBC has higher strength than CC by 16.55%. The flexural strength test outcomes indicate that the SAPBC has higher strength than CC by 8.21%. The hydrated cement particles may still contain unhydrated cement components, including C-S-H gel, which is a key component of the cementitious matrix and aids the self-healing process inside the artificially generated cracks/joints. Moreover, the development of white precipitate

due to hydrolysis of urea proves the existence of CaCO_3 precipitation. The 0.475 mm crack was healed within 52 days. The 0.250 mm crack was healed within 34 days. The 0.175 mm crack was healed within 18 days. Microcracks smaller than 0.5 mm heal quickly in a short amount of time when SAP and bacteria are incorporated together with the concrete mix. Thus, the combination of bacteria and superabsorbent polymer effectively fills up cracks without the need for human intervention, enhancing the concrete's lifespan.

References

- Schlangen E (2010) Super absorbent polymers to simulate self healing in ECC
- Chaitanya M, Manikandan P, Prem Kumar V, Elavenil S, Vasugi V (2021) Prediction of self-healing characteristics of GGBS admixed concrete using artificial neural network. *J Phys Conf Ser* 1716. IOP Publishing Ltd. <https://doi.org/10.1088/1742-6596/1716/1/012019>
- Mahmood F, Kashif Ur Rehman S, Jameel M, Riaz N, Javed MF, Salmi A et al (2022) Self-healing bio-concrete using bacillus subtilis encapsulated in iron oxide nanoparticles. *Materials*. <https://doi.org/10.3390/ma15217731>
- El-Tair A, Youssef P, El-Nemr A (2018) Using GLP as partial replacement in cement mortars. In: MATEC web of conferences, vol 199, EDP sciences. <https://doi.org/10.1051/mateconf/201819907005>
- Tziviloglou E, Wiktor V, Jonkers HM, Schlangen E (2016) Bacteria-based self-healing concrete to increase liquid tightness of cracks. *Constr Build Mater* 122:118–125. <https://doi.org/10.1016/j.conbuildmat.2016.06.080>
- Amran M, Onaizi AM, Fediuk R, Vatin NI, Rashid RSM, Abdelgader H et al (2022) Self-healing concrete as a prospective construction material: a review. *Materials*. <https://doi.org/10.3390/ma15093214>
- Iheanyichukwu CG, Umar SA, Ekwueme PC (2018) A review on self-healing concrete using bacteria. *Sustain Struct Mater*. <https://doi.org/10.26392/SSM.2018.01.01.012>
- Mignon A, Snoeck D, Dubruel P, Van VS, De Belie N (2017) Crack mitigation in concrete: superabsorbent polymers as key to success? *Materials*. <https://doi.org/10.3390/ma10030237>
- Tu W, Zhu Y, Fang G, Wang X, Zhang M (2019) Internal curing of alkali-activated fly ash-slag pastes using super absorbent polymer. <https://doi.org/10.1016/j.cemconres.2018.11.018>
- Danish P, Jessie A, Ganesh S, Jessie AJ, Ahmad Ganie M, Singh Raina C (2020) Experimental study on self-healing concrete with the effect of *Bacillus subtilis* bacteria to improve the strength and sustainability of the concrete
- Luo M, Qian CX, Li RY (2015) Factors affecting crack repairing capacity of bacteria-based self-healing concrete 87:1–7. <https://doi.org/10.1016/j.conbuildmat.2015.03.117>
- Vijay K, Murmu M, Deo SV (2017) Bacteria based self healing concrete—a review. *Constr Build Mater* 152:1008–1014. <https://doi.org/10.1016/j.conbuildmat.2017.07.040>
- Agannathan P, Satya Narayanan KS, Arunachalam KD, Annamalai SK (2018) Studies on the mechanical properties of bacterial concrete with two bacterial species. *Mater Today Proc* 5:8875–8879. <https://doi.org/10.1016/j.matpr.2017.12.320>
- Huynh NNT, Imamoto KI, Kiyohara C (2020) Compressive strength improvement and water permeability of self-healing concrete using *Bacillus subtilis* Natto, pp 113–20. <https://doi.org/10.23967/dbmc.2020.024>
- Andalib R, Abd Majid MZ, Hussin MW, Ponraj M, Keyvanfar A, Mirza J et al (2016) Optimum concentration of *Bacillus megaterium* for strengthening structural concrete. *Constr Build Mater* 118:180–193. <https://doi.org/10.1016/j.conbuildmat.2016.04.142>
- Rashmini Rathnayaka I, S B MH (2018) Review on self-healing concrete with *Bacillus subtilis*
- Indian Standards B. IS 12269 (1987) 53 grade ordinary Portland cement

18. Indian Standards B. IS 2386-1 (1963) Methods of test for aggregates for concrete, part I: particle size and shape
19. Chindasiriphan P, Yokota H, Pimpakan P (2020) Effect of fly ash and superabsorbent polymer on concrete self-healing ability. <https://doi.org/10.1016/j.conbuildmat.2019.116975>
20. Lee HXD, Wong HS, Buenfeld NR (2016) Self-sealing of cracks in concrete using superabsorbent polymers 79:194–208. <https://doi.org/10.1016/j.cemconres.2015.09.008>
21. Manvith Kumar Reddy C, Ramesh B, Macrin D, Reddy K (2020) Influence of bacteria *Bacillus subtilis* and its effects on flexural strength of concrete. Mater Today Proc 33:4206–4211. <https://doi.org/10.1016/j.matpr.2020.07.225>
22. Mondal S, Ghosh A (2021) Spore-forming *Bacillus subtilis* vis-à-vis non-spore-forming *Deinococcus radiodurans*, a novel bacterium for self-healing of concrete structures: a comparative study. <https://doi.org/10.1016/j.conbuildmat.2020.121122>
23. Pachaiyannan P, Hariharasudhan C, Mohanasundram M, Anitha Bhavani M (2020) Experimental analysis of self healing properties of bacterial concrete. Mater Today Proc 33:3148–3154 (Elsevier Ltd). <https://doi.org/10.1016/j.matpr.2020.03.782>
24. Bekheet IA, Syrett PJ (1977) Urea-degrading enzymes in algae. Brit Phycol J 12:137–143. <https://doi.org/10.1080/00071617700650151>
25. Hammes F, Verstraete W (2002) Key roles of pH and calcium metabolism in microbial carbonate precipitation, vol 1
26. Gupta SG, Rathi C, Kapur S (2013) Biologically induced self healing concrete: a futuristic solution for crack repair. <https://doi.org/10.3126/ijasbt.v1i3.8582>
27. Chahal N, Rajor A, Siddique R (2011) Calcium carbonate precipitation by different bacterial strains. Afr J Biotechnol 10:8359–8372. <https://doi.org/10.5897/ajb11.345>
28. Standard. IS 10262 (2019) Concrete mix proportioning-guidelines
29. Annamalai SK, Arunachalam KD, Sathyanarayanan KS (2012) Production and characterization of Bio Caulk by *Bacillus pasteurii* and its remediation properties with carbon nano tubes on concrete fractures and fissures. <https://doi.org/10.1016/j.materresbull.2012.07.024>

An Effective Approach on Implementation of Scrum in the Construction Industry for an Increased Productivity



S. Manikandaprabhu, Bommireddy Hruday Reddy, and Sachikanta Nanda

1 Introduction

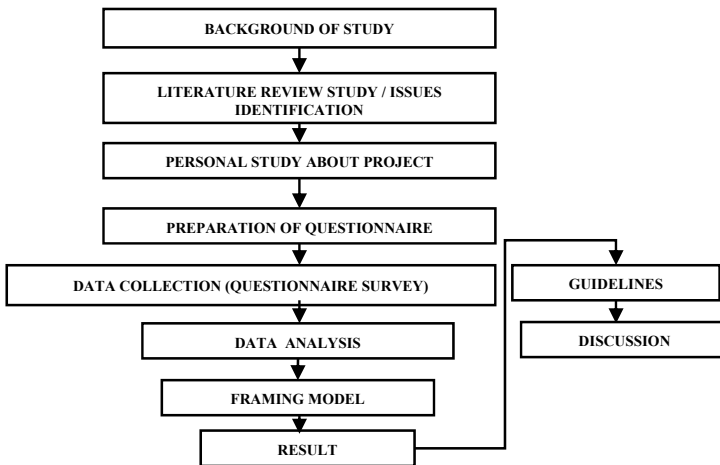
The construction procedure is a difficult task. From initial preparation to final execution, it encompasses a wide range of diverse activities and parties. The rare significant construction project that is built without encountering cost overruns and timetable delays. Bad time management is the main cause of poor results, although there are many other aspects as well [2]. It is well recognised that when work progresses more slowly, the cost or budget of the building project will increase and the quality of the project will decline. Managing the time element may be costly, stressful, and full of uncertainty. The owner, architect, engineers, construction managers, contractors, and subcontractors are the key decision-makers for the time extension factor [3]. Therefore, it is crucial to pinpoint the root cause and main contributing element of time overruns in construction projects in order to address them and improve the efficient management and administration of the contract time.

Ranking of delay factors in building projects following the Egyptian Revolution identifies the key responsibilities performed by the various parties engaged in the project and the time delays from the planned time [4–6]; the primary cause of time overruns in building projects is inadequate clarity in the schedule job information [7]. Traditional project management is often a process-oriented strategy that includes a series of tasks like initiating or starting; planning and designing; organising; implementing; monitoring and controlling; and closing [8–10]. Scrum is a powerful framework created to provide significant value continuously and early in a project. The product development process is adaptable and all-inclusive, and the development team collaborates to accomplish a common objective. Fixing the scope,

S. Manikandaprabhu (✉) · B. H. Reddy · S. Nanda
Department of Civil Engineering, Faculty of Engineering and Technology, SRM Institute of Science and Technology, Kattankulathur, Tamilnadu 603203, India
e-mail: saravanaprabhou@gmail.com

cost, and time, as well as managing those parameters, is the main focuses of traditional project management. Scrum promotes iterative, data-based decision-making. Delivering solutions that meet customer needs in brief iterative shippable increments is the main goal of the scrum methodology. The focus of traditional projects is on thorough planning in advance and adherence to the project plan developed by the project manager. At the end of the project, when the finished product is delivered, value is usually created by managing modifications through a formal change management system. Prior to the start of a scrum project, considerable long-term planning is not carried out. Before every sprint, planning is carried out iteratively. As a result, costs are reduced, leading to higher profitability and return on investment. This enables quick and effective response to change (ROI). The scrum framework’s core advantage of value-driven delivery, which offers substantially better prioritising and speedier business value realisation, is also a benefit. A minimum of one version of the product with minimum marketable features (MMF) is always available because of the iterative nature of scrum development. There are several fundamental distinctions between scrum and traditional approaches to planning in project delivery because even if a project is cancelled, there are typically some advantages or value provided prior to termination.

2 Methodology



3 Data Collection

The many selected individuals in the construction business were surveyed using a questionnaire to acquire the data for this project. Based on a literature review and an in-person interview, the questionnaire was created. Project managers, planning engineers, contractors, owners, and site supervisors with extensive expertise were among the people contacted to provide answers to the questionnaire that was distributed to various construction companies. As part of this project, a survey questionnaire was sent to the different categories of positions. The questionnaire was circulated to owner, project manager, contractor, site supervisor, and planning engineer of residential and commercial developments. Face-to-face interviews and the mail technique were used in the survey adoption. In a purposive sample, the components are chosen because it is anticipated that they will be useful for the research goal [11]. The questionnaire used in this survey was divided into two sections. Section 1 sought the respondent's demographic information. In Sect. 1, question consists of name of respondent, name of the firm, designation of the respondent, age, and experience in construction field. Section 2 is composing of 40 questions that were sought in nine major factors having the factors causing time overrun. Section 3 consists of 10 scrum factors that could be the possible solutions for reducing or to prevent cost and time delay in construction. These questions were based on two perspectives that are of the literature study and personal interview. All performance indicator variables found from the primary sources and secondary sources. All the questions are close ended questions with Likert scale. In this, all question are nominal questions. The different factors affecting time of construction project and the scrum factors were scored on a five point Likert scale with 1 expressing very low and 5 expressing very high.

3.1 Reliability Test

Internal consistency technique was used to calculate reliability for the four balanced scorecard perspectives [12]. Utilising the Cronbach alpha coefficient, scale internal consistency was evaluated. The most prevalent internal consistency indicator is Cronbach's alpha ("reliability"). It is most typically used to examine the reliability of a scale composed of numerous Likert questions in a questionnaire or survey. It also provides instructions on how to use Cohen's (k) kappa, which you might find helpful if you are worried about inter-rater reliability. Given that the value is in the range of 0.7–0.9, it is clear from Tables 1 and 2 that the questionnaire created for this project is trustworthy. The dependability for the key variables and overall is given in Table 1.

Table 1 Cronbach’s alpha value for time delay factors

Sl. No	Factors	Cronbach’s alpha value
1	Planning	0.474
2	Estimation	0.479
3	Labours cost	0.453
4	Material cost	0.465
5	Productivity	0.456
6	Construction	0.469
7	Others	0.485
8	Scrum method (overall 50)	0.499

Table 2 Cronbach alpha value for scrum methods

Scrum methods	Cronbach’s alpha value
Overall (10 methods)	0.469

3.2 Relative Importance Index for Time Overrun Factors

The relative relevance of the various delays’ causes was assessed using the RII technique by Kometa et al. [13] and Sambasivan and Soon [14]. The same method was adopted in this research for finding out for which attribute they used more frequently at the project formation. RII calculated for various variable as per below equation.

$$RII = \frac{\sum W}{(A \times N)} \tag{1}$$

where

- RII Relative importance index
- $\sum W$ Weightage provided for the factors by respondents (1 to 5 scale)
- A Maximum weight (5 in this case)
- N Total no. of respondents

Table 3 presents the rank of the various time overrun factors. Table 4 presents the rank of the major factors based on RII. Table 5 presents the top-10 time overrun factors based on their RII.

The RII value had a range 0–1. The higher the RII value means high frequency they used. It will be learned that which variables have the greatest influence on why construction projects go over budget and on schedule using RII. The most influencing factor causing time delay in construction projects is observed from Table 5 to be low labour productivity (rank1). The ranking of major factors based on the average RII value has been done, and it shows that the value has been obtained in range of zero to one. The higher the RII value means high frequency that the respondents have

Table 3 RII and rank of time delay factors

Sl. No	Factors	RII	Rank
	<i>Planning</i>		
1	Complex communication	0.447	R051
2	Lack of disciplined	0.447	R052
3	Incompetent team	0.446	R053
4	Lack of knowledge techniques	0.483	R054
5	Indecisive project team	0.462	R055
6	Poor site coordination	0.430	R056
7	In accurate estimation	0.451	R057
8	Insufficient support	0.439	R058
9	Lack of education	0.455	R059
10	Absence of schedule contingency	0.454	R060
	<i>Estimation</i>		
11	Trivial control and reporting system between management levels	0.474	R061
12	Cost of an construction estimating	0.482	R062
13	Cost estimation will help non-cost estimating	0.486	R063
14	Cost data generated by cost estimators	0.485	R064
15	Subjective estimates	0.434	R065
16	Office building project	0.458	R066
17	Proper standard	0.454	R067
18	Other trade masonry work	0.451	R068
19	Performance will be repeated in this future	0.465	R069
20	Manipulation occurs the estimator	0.467	R070
	<i>Labour cost</i>		
21	How much will be the contractor be required to pay for labour?	0.464	R071
22	The estimator must predict this cost	0.479	R072
23	Availability of skilled labour wage regulation	0.486	R073
24	This can be predicted with a fair degree of accuracy	0.481	R074
25	The material required must be accurately	0.479	R075
	<i>Material cost</i>		
26	Whether the factor can vary dramatically?	0.478	RO76
27	The amount will depend on company	0.491	RO77
28	Imagine very important to corporate	0.453	RO78
29	Construction project location	0.480	RO79
30	Consideration should be taken in to account	0.481	RO80
	<i>Productivity</i>		
31	The project location may be restricted city	0.439	RO81

(continued)

Table 3 (continued)

Sl. No	Factors	RII	Rank
32	Determine the project productivity challenges	0.431	R082
33	Your organisation's current problems	0.492	R083
34	Some problem has occurred in speed	0.458	R084
35	Efficiency and mainly in productivity	0.476	R085
36	Identify the traditional and productivity	0.456	R086
37	The most importance measures of labour productivity	0.451	R087
38	Labours and contractors organised	0.484	R088
39	The labour efficiency is the basis of most tender	0.478	R089
40	Relative growth in labour productivity	0.454	R090
	<i>Scrum</i>		
41	The techniques for effective product backlog management	0.454	R091
42	To understand the product planning	0.499	R092
43	The organisation in several ways including leading and coaching	0.462	R093
44	They organise the planning scrum implementation	0.472	R094
45	It is helping employees and stake holders understand	0.462	R095
46	It has the causing change that the increase the productivity of the scrum	0.469	R096
47	And working with scrum master to increase the effectiveness of the application of scrum	0.477	R097
48	How many participants completed a task	0.450	R98
49	Participants answered the three core question	0.457	R099
50	Application of scrum	0.470	R100
51	And facilities of scrum events as request	0.499	R101

Table 4 Rank of average RII for major time delay factors

Sl. No	Major factor	Average	Ranking
1	Planning	0.451	R054
2	Estimation	0.465	R057
3	Productivity	0.416	R055
4	Labour cost	0.476	R059
5	Material cost	0.475	R051
6	Construction	0.439	R056
7	Other	0.447	R053

Table 5 Top-10 time overrun factors

Sl. No	Major factor of scrum	Average value	RII
1	The techniques for effective product backlog management	0.454	R092
2	To understand the product planning	0.499	R093
3	The organisation in several ways including leading and coaching	0.465	R094
4	They organise the planning scrum implementation	0.472	R095
5	It is helping employees and stake holders understand	0.462	R096
6	It has the causing change that the increase the productivity of the scrum	0.469	R097
7	And working with scrum master to increase the effectiveness of the application of scrum	0.477	R098
8	How many participants completed a task?	0.450	R099
9	Participants answered the three core question	0.457	R0100
10	Application of scrum	0.470	R0101
11	And facilities of scrum events as request	0.499	R0102

responded. The most important major factor causing time overrun in construction projects is observed from Table 4 to be engineer and design.

3.3 Cause-and-Effect Diagram for Time Overrun

The cause-and-effect diagram demonstrates how the top major factors, such as planning, labour costs, productivity, material costs, and design, lead to additional subcategories of factors, such as payment delays, ineffective decision-making, improper planning and scheduling, low labour productivity, labour availability, natural disasters, improper fund flow, experience in designing and detailing work, and design changes made during project execution, which cause the construction project to take longer than expected to complete [14]. The Fig. 1 shows the cause and effect diagram for the time overrun in construction.

MANN–Whitney *U* test

The independent sample *t*-test and the Mann–Whitney *U* test are equivalent. The nonparametric Mann–Whitney *U* test is employed to compare two population or designation means that are drawn from the same population. Two population means are compared to see if they are equal. The nonparametric level test known as the Mann–Whitney *U* test does not call for a particular distribution of the dependent variable to be used in the analysis. As a result, it is better to compare responses when the dependent variable has an ordinal scale and is not regularly distributed. The contractor and owner’s median responses were compared for this study since they

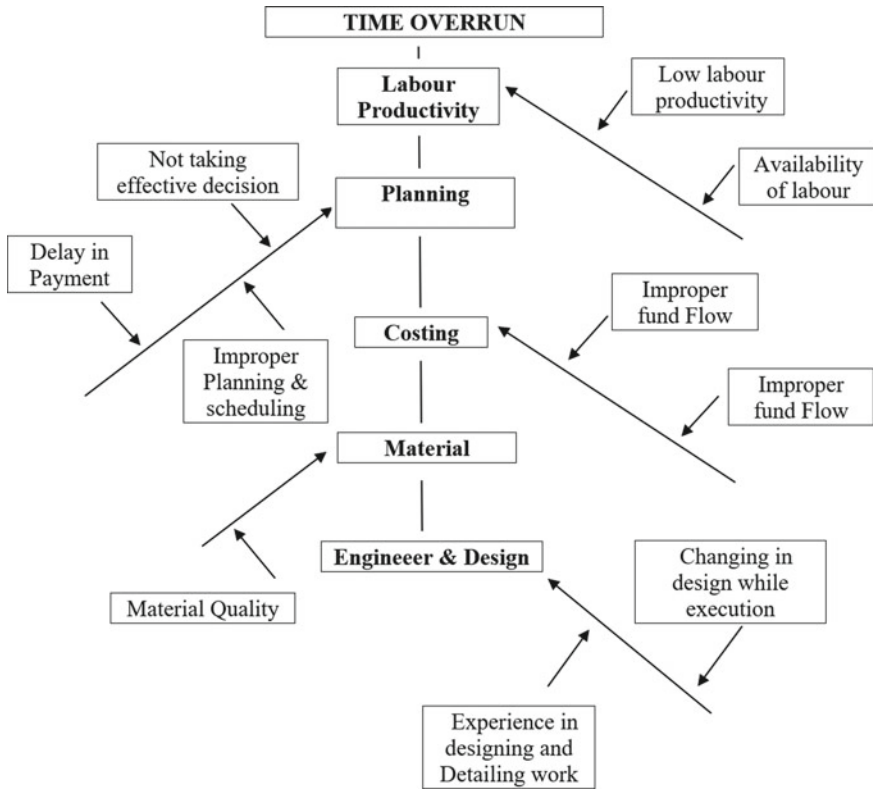


Fig. 1 Cause-and-effect diagram for time overrun in construction

are the two parties most crucial to the success of the building project. The Mann–Whitney *U* test uses the hypotheses H_0 (null hypothesis), which states that there is no significant difference between the two responses and H_A (alternate hypothesis), which states that there is a significant difference between the two responses. A comparison of the mean scores of the contractor and owner is given in Table 6 using the Mann–Whitney *U* test.

Table 6 Output of Mann–Whitney *U* test for top time overrun factors

Sl. No	Major factor of scrum	P value	Mean rank
1	The techniques for effective product backlog management	0.454	R092
2	To understand the product planning	0.499	R093
3	The organisation in several ways including leading and coaching	0.465	R094
4	They organise the planning scrum implementation	0.472	R095
5	It is helping employees and stake holders understand	0.462	R096
6	It has the causing change that the increase the productivity of the scrum	0.469	R097
7	And working with scrum master to increase the effectiveness of the application of scrum	0.477	R098
8	How many participants completed a task?	0.450	R099
9	Participants answered the three core question	0.457	R0100
10	Application of scrum	0.470	R0101
11	And facilities of scrum events as request	0.499	R0102

Relative importance index for mitigation methods using scrum

The mitigation methods for controlling the time overrun factors have been identified through literature study and direct interview with experts and based on that questionnaire prepared which has 25 methods to improve the effectiveness of the construction project, and this was ranked based on the response. Table 7 presents the rank of various mitigation methods. In Table 8, the top-10 mitigation methods based on their RII are listed.

Table 7 RII and rank of various mitigation methods using scrum

Sl. No	Mitigation method	RII	Rank
	<i>Planning</i>		R051
1	Complex communication	0.447	R052
2	Lack of disciplined	0.447	R053
3	Incompetent team	0.446	R054
4	Lack of knowledge techniques	0.483	R055
5	Indecisive project team	0.462	R056
6	Poor site coordination	0.430	R057
7	In accurate estimation	0.451	R058
8	Insufficient support	0.439	R059
9	Lack of education	0.455	R060
10	Absence of schedule contingency	0.454	R061

(continued)

Table 7 (continued)

Sl. No	Mitigation method	RII	Rank
	<i>Estimation</i>		
11	Trivial control and reporting system between management levels	0.474	R062
12	Cost of an construction estimating	0.482	R063
13	Cost estimation will help non-cost estimating	0.486	R064
14	Cost data generated by cost estimators	0.485	R065
15	Subjective estimates	0.434	R066
16	Office building project	0.458	R067
17	Proper standard	0.454	R068
18	Other trade masonry work	0.451	R069
19	Performance will be repeated in this future	0.465	R070
20	Manipulation occurs the estimator	0.467	R071
	<i>Labour cost</i>		
21	How much will be the contractor be required to pay for labour?	0.464	R072
22	The estimator must predict this cost	0.479	R073
23	Availability of skilled labour wage regulation	0.486	R074
24	This can be predicted with a fair degree of accuracy	0.481	R075
25	The material required must be accurately	0.479	R076
	<i>Material cost</i>		
26	Whether the factor can vary dramatically?	0.478	RO77
27	The amount will depend on company	0.491	RO78
28	Imagine very important to corporate	0.453	RO79
29	Construction project location	0.480	RO80
30	Consideration should be taken in to account	0.481	RO81
	<i>Productivity</i>		
31	The project location may be restricted city	0.439	RO82
32	Determine the project productivity challenges	0.431	RO83
33	Your organisation current problems	0.492	RO84
34	Some problem has occurred in speed	0.458	RO85
35	Efficiency and mainly in productivity	0.476	RO86
36	Identify the traditional and productivity	0.456	RO87
37	The most importance measures of labour productivity	0.451	RO88
38	Labours and contractors organised	0.484	RO89
39	The labour efficiency is the basis of most tender	0.478	RO90
40	Relative growth in labour productivity	0.454	RO92
	<i>Scrum</i>		
41	The techniques for effective product backlog management	0.454	RO93
42	To understand the product planning	0.499	RO94

(continued)

Table 7 (continued)

Sl. No	Mitigation method	RII	Rank
43	The organisation in several ways including leading and coaching	0.462	R095
44	They organise the planning scrum implementation	0.472	R096
45	It is helping employees and stake holders understand	0.462	R097
46	It has the causing change that the increase the productivity of the scrum	0.469	R098
47	And working with scrum master to increase the effectiveness of the application of scrum	0.477	R099
48	How many participants completed a task?	0.450	R100
49	Participants answered the three core question	0.457	R101
50	Application of scrum	0.470	R102
51	And facilities of scrum events as request	0.499	R103

Table 8 Top-10 ranks of mitigation methods using scrum

S. No.	Major factor of scrum	Average value	RII
1	The techniques for effective product backlog management	0.454	R092
2	To understand the product planning	0.499	R093
3	The organisation in several ways including leading and coaching	0.465	R094
4	They 'organise the planning scrum implementation	0.472	R095
5	It is helping employees and stake holders understand	0.462	R096
6	It has the causing change that the increase the productivity of the scrum	0.469	R097
7	And working with scrum master to increase the effectiveness of the application of scrum	0.477	R098
8	How many participants completed a task?	0.450	R099
9	Participants answered the three core question	0.457	R0100
10	Application of scrum	0.470	R0101
11	Facilities of scrum events as request	0.499	R0102

4 Conclusion

The most significant variable contributing to time overruns in building projects has been identified utilising the expert questionnaire survey. By calculating the relative importance index based on the respondents' frequency of responses, the main factor causing time overrun has also been discovered. Low labour productivity is seen as the main cause of time delays in construction projects, and the engineer and design factor are seen as the main causes of time overruns.

Additional research can be done by applying these mitigation strategies to actual projects and comparing them to similar projects to determine whether they have an effect on finishing construction projects on time. Research can also be done on individual time delay factors to determine how much of an impact they have on other types of construction projects.

References

1. Hamzah N, Khoiry MA, Arshad I, Tawil NM, Che Ani AI (2011) Cause of construction delay—theoretical framework. *Proc Eng* 20(Kpkt 2010):490–495
2. Abd El-Karim MSBA, Mosa El Nawawy OA, Abdel-Alim AM (2015) Identification and assessment of risk factors affecting construction projects. *HBRC J*
3. Alzara M, Kashiwagi J, Kashiwagi D, Al-Tassan A (2016) Using PIPS to minimize causes of delay in Saudi Arabian construction projects: university case study. *Proc Eng* 145(480):932–939
4. Aziz RF, Abdel-Hakam AA (2016) Exploring delay causes of road construction projects in Egypt. *Alex Eng J* 55(2):1515–1539
5. Enshassi A, Mohamed S, Abushaban S (2010) Factors affecting the performance of construction projects in the Gaza strip. *J Civ Eng Manag* 15(3):269–280
6. Marzouk MM, El-Rasas TI (2014) Analyzing delay causes in Egyptian construction projects. *J Adv Res* 5(1):49–55
7. Aziz RF (2013) Ranking of delay factors in construction projects after Egyptian revolution. *Alex Eng J* 52(3):387–406
8. Francis A (2015) Graphical modelling classification for construction project scheduling. *Proc Eng* 123:162–168
9. Siva Subramani G, Manikanda Prabhu S, Dey S (2016) Identifying the factors causing time overrun in construction projects in Chennai and suggesting for possible solutions. *Int J Civil Eng Technol* 7(6):660–668
10. Dey S, Manikanda Prabhu S, Siva Subramani G (2017) Identification and mitigation of factors affecting human resource productivity in construction. *Int J Civil Eng Technol* 8(1):123–131
11. Churchill GA, Lacobucci D (2002) *Marketing research: methodological foundations*. Harcourt College Publishers, San Diego, p 14
12. Nunnally JC (1978) *Psychometric theory*, 2nd edn. McGraw-Hill, New York
13. Kometa S, Harris F (1994) Attributes of UK construction clients influencing project consultants' performance. *Constr Manag Econ* 12:433–443
14. Sambasivan M, Soon YW (2007) Causes and effects of delays in Malaysian construction industry. *Int J Project Manage* 25(5):517–526

Investigation on the Mechanical Properties of Marine Algal Concrete in High Strength Concrete



R. Ramasubramani, M. Murali, and P. T. Ravichandran

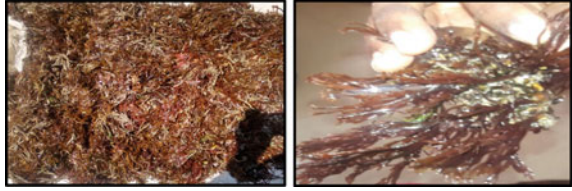
1 Introduction

1.1 General

Concrete is a commonly used and unavoidable construction material due to its versatility and low cost. Concrete is a homogenous material made up of a proportioned cementitious material, coarse aggregates, fine aggregates, and water. Cement is the binder in concrete, and it is manufactured in cement kilns. The other constituents of concrete, such as water, coarse aggregate, and fine aggregate, are also readily available natural commodities. Water is added to hydrate the cement and generate fresh concrete workability [1]. Aggregates are inert substances that give substantial bulk to the concrete. Concrete is an unavoidable construction material as it is used for multi-purposes. Annual usage of concrete throughout the world is almost 20 billion tonnes and cement required for concrete production is about 4.2 billion tonnes. Concrete is often used construction material as it is durable, easily moulded to any shape and as it possesses resistance to fire. Concrete protects the reinforcement from environment and prevent corrosion.

Algae is a basic photosynthetic organism found in plants. Their size ranges from micro to macro algae, and some species can grow up to 60 m in length. Algae are a varied group of organisms that can be found practically anywhere and serve a vital function in the environment. Algae may grow in a variety of environments, including the sea, waste water, and brackish water, all of which are unsuitable for cultivation. The pigment gives red algae, green algae, and brown algae their colours. There are 1500 species of brown algae in the phaeophyceae class. Fucoxanthin, pigment, is found in most brown algae, and it is this pigment that gives the word

R. Ramasubramani (✉) · M. Murali · P. T. Ravichandran
Department of Civil Engineering, Faculty of Engineering and Technology, SRM Institute of Science and Technology, Kattankulathur, Tamil Nadu 603203, India
e-mail: ramasubr@srmist.edu.in

Fig. 1 Marine brown algae

“algae” its name, derived from the algae’s unique greenish-brown tint [2]. There are many different sizes and forms of brown algae. The cementing ingredient, calcium carbonate, precipitates as a result of it.

1.2 Need for This Study

The use of brown seaweed in concrete mixes is the main focus of this study. The addition of brown seaweed to concrete makes it less expensive. There is a reduction in environmental impact by researching the characteristics of algae in concrete.

2 Marine Algae

Algae in the sea are separated into three groups: red, brown, and green algae. The phaeophyte group of marine brown algae is the largest and plays a significant sea environment plays. Three different forms of algae (rhodophyta) include red algae (phytoplankton), green algae (chlorophyta), and brown algae (phaeophyte). Figure 1 shows the sample of marine brown Algae [3].

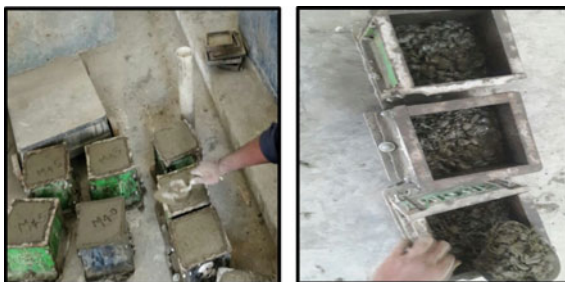
3 Marine Brown Algae Concrete

The marine algae was gathered in its wet condition (living algae). Seaweeds are a rich source of omega fatty acids, calcium (calcium carbonate, calcium silicate), phosphate, and minerals. Sea brown algae added on the concrete. The 53 OPC cement grade was employed. The water–cement ratios for the concrete classes M40, M45, and M50 are 0.40, 0.35, and 0.35, respectively [4]. The varying percentages of algae addition to the concrete are 5, 10, and 15 per cent. Figure 2 shows the casting of marine brown algae concrete.

Fig. 2 Marine brown algae concrete



Fig. 3 Cubes are cast in a mould



4 Experimental Investigation

The study focuses on the effects of marine algae put in the concrete at varying percentages. The study's main purpose is to figure out which concrete algae species have the most strength.

4.1 *Cube Samples*

Concrete cube specimen of size $150 \times 150 \times 150$ mm conformity to IS 516–1959 was used [5–8]. The specimens were taken out of curing tank for the specific days 3, 7, and 28 days. The crushing load is continuously applied throughout testing until failure was obtained. The $140 \text{ kg/cm}^2/\text{min}$ of loading occurred at a rate of 2.29 kN/s . Conventional concrete grades M40, M45, and M50 were used to cast the concrete in the moulds and with a 5%, 10%, and 15% adding of algae to the concrete. Figure 3 shows that the cubes are cast in a mould [9].

4.2 *Cylinder Specimens*

Casting a concrete cylinder of size 150×300 mm following the procedure recommended by ASTM C 496 was used. Rate of loading applied in this test was 0.70 kN/s (range suggested by ASTM C 496 was $0.56\text{--}0.75 \text{ kN/s}$). This test is done to

Fig. 4 Cylinders are cast in a mould



Fig. 5 Casting of flexure beams



find the tensile strength of concrete. The tensile strength is about 1/8th to 1/10th of compressive strength. Strips were placed at the top and bottom of specimen to distribute the load axially on the surface of cylinder. The concrete that is cast in moulds was with grades of M40, M45, and M50, both conventional and with a 5%, 10%, or 15% adding of marine algae to the concrete.

Figures 4 and 5 show that the cylinders and flexure beams are cast in a mould.

4.3 *Beam Specimens*

Used was a concrete beam with dimensions of 100 mm × 100 mm × 500 mm ASTM C78-84 [5–8]. This test is conducted using a two-point loading setup. The equipment is configured, and support structures and loading are positioned, so that they are L/3 apart. The beam is loaded and then subjected to a flexure failure test. A loading rate of 29.43 N/sec (180 kg/min) was used. Flexural strength was calculated from ultimate load using an equation. The standard concrete that is poured into moulds with the grade M40, M45, and M50 includes 5%, 10%, and 15% marine algae, respectively.

Fig. 6 Casting of long beams



4.4 Long Beams

For the flexural test, beams with dimensions of 150 mm in width, 230 mm in depth, and 1500 mm in length were chosen. To imitate an actual beam element and assure that failure in flexure is realised, this size was specifically chosen. Formwork was made with 25 mm thick plywood sufficiently fastened together with nails and screws. Figure 6 shows wooden moulds being used long beam casting [10].

4.5 Casting and Curing of Specimens

Cement, fine aggregate, coarse aggregate, and other materials were obtained according to the specifications. The components are combined in the mixer unit according to their mixing ratio. Concrete is poured into the moulds once the components have been mixed, and three levels of each layer are tamped with a tamping rod for adequate compaction. Placing the mould on the vibrating table is a good idea. The specimen is placed in the curing tank for 24 h after casting. The specimen must cure for 28 days to achieve the target's mean force, which varies depending on the concrete grades.

4.6 Deflection Test for Long Beams

For long beams, a cross-sectional dimension of 150 × 230 mm was employed, and a length measurement of 1500 mm was made. Both longitudinal and transverse reinforcing employed Fe415 steel [11]. To prevent failure, the beam was strengthened, especially at the centre. To make sure, it would not collapse under deflection, a beam's size and span breadth were selected. The structural laboratory at SRMIST has these testing facilities.

4.7 Conduct of Experiments

Here is a detailed explanation of where the research led. The test beam was raised and held inside the load step on the edge where simply since they were held up by straightforward beams, the steel bearings with rollers were changed to support those beams on either side. The 175 ordinary Indian bar (ISMB) was placed in line with any surface area of the beam. The 25 T utilised load limit for hydraulic jacks is set above ISMB I75 [12]. Over the 20 T maximum, a hydraulic jacket is positioned to provide ring proofing. By utilising pipe weaving, the beam can be measured until the centres of the rings of beams meet in the same line. The dial check is adjusted at the bar section, although the bases are spaced 5 cm apart on both sides of the handle. Beam packing is done in relation to the two-point packing, which is the assisted backbone. Now, the device is set to test and dialling settings are set to zero before the test starts. The hydraulic jack was always used to connect the weight. The load was also applied to the ISMB's borders. Before the final load was reached, beams were allowed and exposed to a steadily increasing load level [13].

5 Results and Discussions

Different tests were carried out on the material as part of the experimental programme to assess its features and to determine the concrete's strength. Compressive, tensile, and flexural strengths were all tested using a compression-testing machine. It is a powerful machine, with a maximum capacity of 2000 kN [14]. For all of the experiments, an average of three samples was collected for each value. For 7, 14, and 28 days of curing, test results for regular concrete and marine algal concrete were computed.

5.1 Compressive Strength

A universal testing machine was used to evaluate the concrete samples. For each test, three samples will be tested, each with varying amounts of common concrete and sea algae added. In Table 1, the cubes' average strength for the concrete slabs M40, M45, and M50 is displayed. Comparison of the M40, M45, and M50 marine algal concrete's compressive strength to that of conventional concrete is shown using a bar chart in Figs. 7, 8, and 9 [9]

With the addition of marine algae to the concrete, the compressive strength will improve as the number of curing days increases. With a grade of M40, M45, and M50, the maximum compressive strength of the concrete after 15% addition of marine algae is 45.55, 53.37, and 61.15 N/mm².

Table 1 Compressive strength results of M40, M45, and M50 grade of concrete

S. no	Curing period	Conventional concrete	Marine algae added as a proportion of grade of concrete M40, M45, and M50			
			5%	10%	15%	
1	7	M40	28.50	27.10	29.85	31.60
	14		31.50	30.70	32.65	34.80
	28		44.30	43.38	44.53	45.60
2	7	M45	31.25	30.25	32.58	35.48
	14		36.93	35.60	39.75	40.86
	28		47.11	48.10	50.50	53.39
3	7	M50	35.95	36.75	37.6	39.02
	14		39.64	40.75	43.82	45.73
	28		53.20	51.06	56.35	61.15

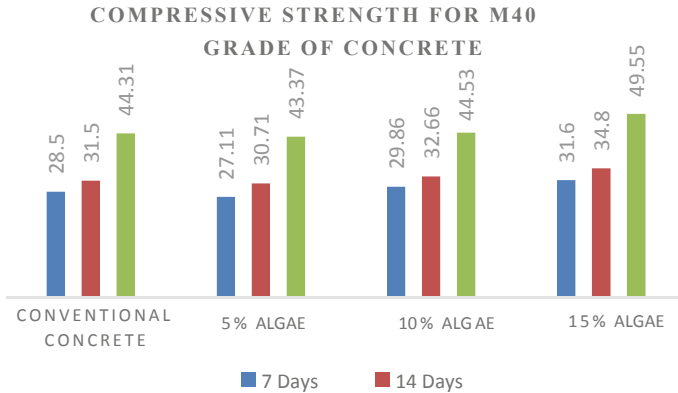


Fig. 7 Compressive strengths of traditional and marine algal concrete using M40 concrete grades

5.2 Split Tensile Strength

A split tensile test was performed on the concrete cylinder using a compression-testing machine. Three samples, each with a different percentage of marine algae added, as well as plain concrete, will be tested for each test. In Figs. 10, 11, and 12, the split tensile strength of regular concrete is compared to that of marine algal concrete in a bar chart. After a set number of days, adding marine algae to concrete boosted the strength of the split strength [12, 15, 16]. The highest split tensile strength of the concrete after 15 per cent addition of marine algae is 6.37N/mm², 6.89N/mm², and 7.56N/mm² with a grade of **M40, M45, and M50**. The average cylinder strength for **M40, M45, and M50** is given in Table 2.

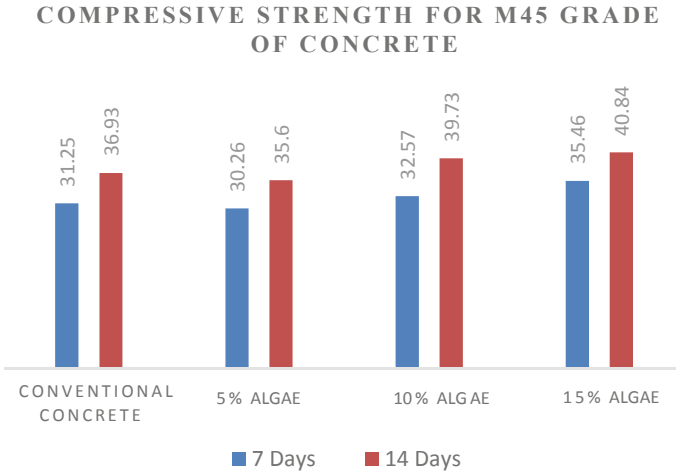


Fig. 8 Compressive strengths of traditional and marine algal concrete using M45 concrete grades

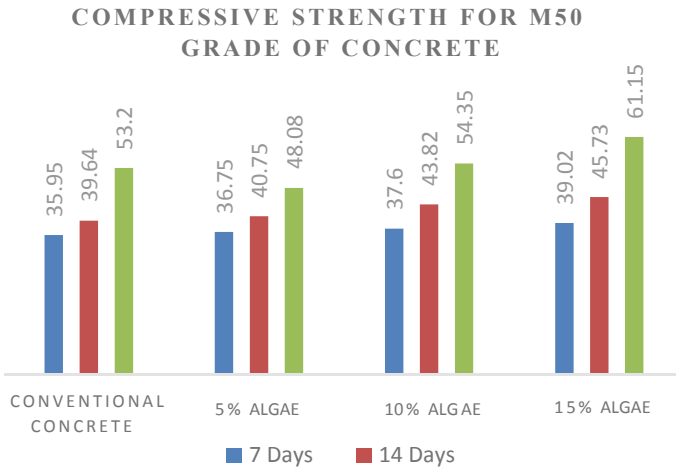


Fig. 9 Compressive strengths of traditional and marine algal concrete using M50 concrete grades

5.3 Flexural Strength

Three samples of flexural strength were tested in each concrete under the compression-testing machine for flexural strength testing. By stressing the beam at third locations, the flexible behaviour of the beam portion under simple bending was investigated. The arrangement of the loads was such that the area in-between the point loads could only be subjected to bending [17]. A hydraulic jack applied the weight gradually to the spreader beam. Table 3 presents the maximum flexural

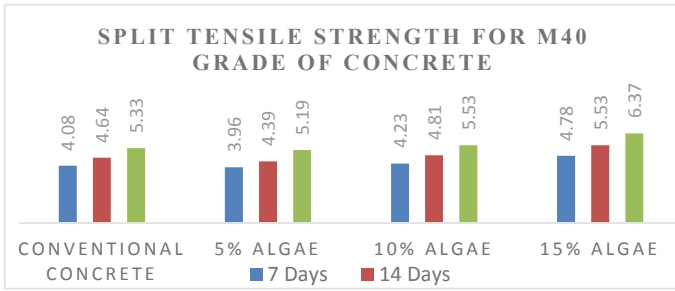


Fig. 10 Split tensile strength of traditional and marine algal concrete compared to M40 grade concrete

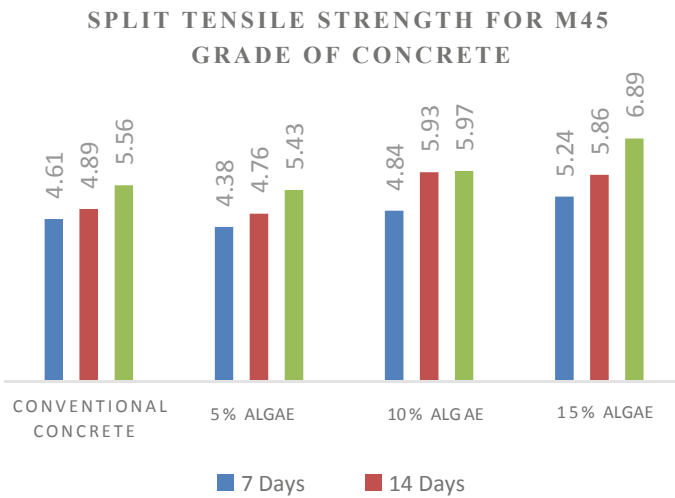


Fig. 11 Split tensile strength of traditional and marine algal concrete compared to M45 grade concrete

resistance of the beams for concrete grade M40, M45, and M50, and Fig. 13 uses a bar chart to compare the flexural strength of traditional concrete and marine algal concrete. The maximum flexural strength achieved for concrete grade M40, M45, and M50 was 5.36, 5.16, and 6.33 N/mm² with a 15% addition of marine algae to the concrete [18–21].

5.4 Deflection Characteristics

The deflection of long beams made of concrete grades such as M40, M45, and M50 is investigated using the crack that forms with the load applied with the resulting

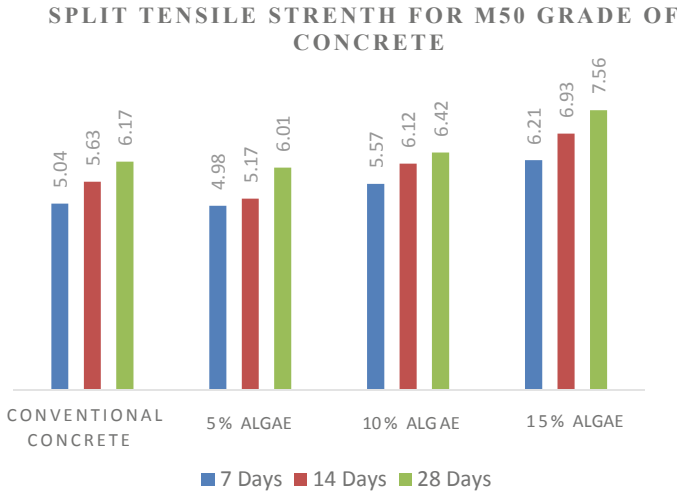


Fig. 12 Split tensile strength of traditional and marine algal concrete compared to M50 grade concrete

Table 2 Split tensile strength results of M40, M45, and M50 grade of concrete

S. no	Curing period	Conventional concrete		Marine algae added as a proportion of grade of concrete M40, M45, and M50		
				5%	10%	15%
1	7	M40	4.08	3.69	4.23	4.78
	14		4.64	4.39	4.81	5.53
	28		5.33	5.19	5.67	6.37
2	7	M45	4.61	4.38	4.84	5.24
	14		4.89	4.76	5.13	5.86
	28		5.56	5.43	5.97	6.89
3	7	M50	5.04	4.98	5.57	6.21
	14		5.63	5.17	6.12	6.93
	28		6.17	6.01	6.42	7.56

deflection of the beam in the centre of the beam [22]. The maximum displacement for appropriate blending is 4.97 mm at 13.2 tonnes of load with M40, compared to the average deflection of conventional concrete at 12 tonnes of load with M40. The average deformation of typical concrete in M45 is 5.42 mm at 13.6 tonnes, while the total deformation for optimal mixing is 6.38 mm at 14.4 tonnes. For ideal level mixing, the maximum displacement of typical concrete at 14.4 tonnes is 6.56 mm, and at 15.2 tonnes, the maximum displacement is 5.92 mm. In a conventional beam made of concrete grade M40, the initial fracture ends at 3.6 tonnes, but it starts at 4.4 tonnes

Table 3 Results for conventional concrete and marine algal concrete in terms of flexural strength with M40, M45, and M50 grade of concrete

S. no	Curing period	Conventional concrete		Marine algae added as a proportion of grade of concrete M40, M45, and M50 (N/mm ²)		
				5%	10%	15%
1	Summary 28 days	M40	4.66 N/mm ²	5.66	6.16	7
2		M45	5.16 N/mm ²	5.83	6.5	7.33
3		M50	6 N/mm ²	6.33	6.66	7.5

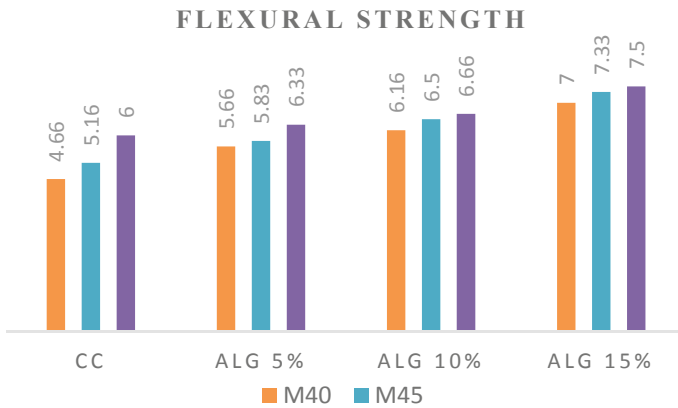


Fig. 13 Flexural strength of marine algal concrete versus traditional concrete

in an optimised mix beam. When utilising grade concrete M45, the first fracture in a normal beam starts at 4.8 tonnes, whereas it starts at 5.6 tonnes for an optimised mix beam. For concrete grade M50 in standard beams, the first fracture appears at 5.2 tonnes, while for optimised mix beams, it appears at 6.8 tonnes [23]. The usual beam fractures occur at the supports and in the beam’s shear region. This failure due to shear was prevented by the perfect level mixing beam. Even the perfect mixing beam, which has fractures all around it, is susceptible to this. Comparing specimens having crack formation to normal concrete beams (because of the emphasis on supports), the fracture growth in the specimens is not uniform (Fig. 14 shows the beam is under deflection testing). The evaluated beam specimen and the load versus deformation curve for the CC and improved mix beams are presented in Figs. 16, 17, and 18.

Fig. 14 Deflection testing of beam



Fig. 15 Tested beam specimens



6 Conclusions

The study's key findings are as follows: for concrete grades M40, M45, and M50, 15 per cent marine algae show the better concrete strength. In comparison with conventional concrete, the optimum mix has higher compression strength, split tensile strength, and flexural strength. The ideal concrete mixing beam can support 15% more density than a regular concrete beam.

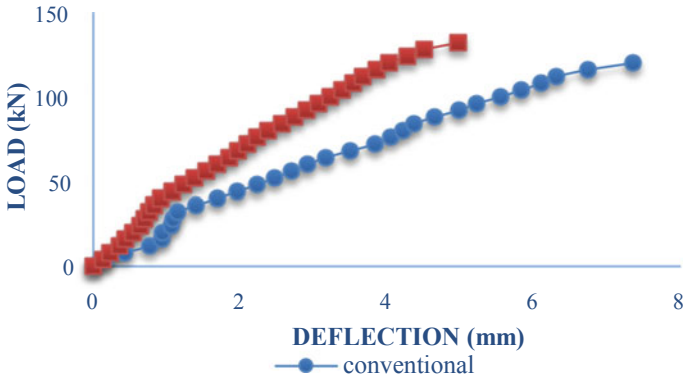


Fig. 16 Load versus deflection curves for M40 grade traditional and optimal mix

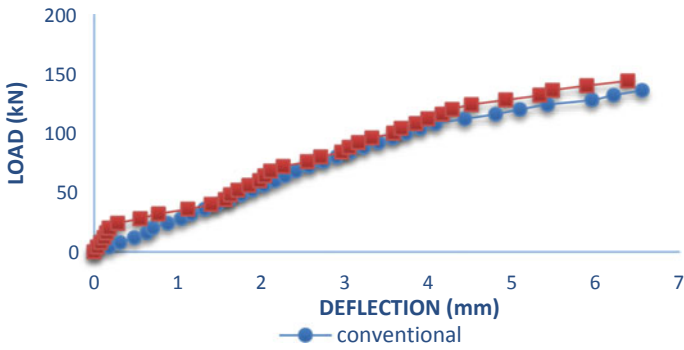


Fig. 17 Load versus deflection curves for M45 grade traditional and optimal mix

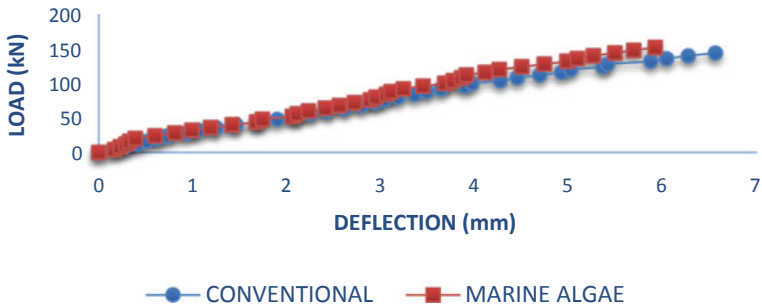


Fig. 18 Load versus deflection curves for M50 grade traditional and optimal mix

7 Conflicts of Interest

There are no conflicts of interest declared by the authors.

Acknowledgements The S.R.M Institute of Science and Technology Management helped the authors carry out this research, and they are appreciative of their assistance. Also, a big thank you to everyone who was directly or indirectly engaged in this study and assisted.

References

1. Ramasubramani R (2016) Study on the strength properties of marine algae concrete rasayan. *J Chem* 9(4):706–715
2. Ramasubramani R, Shakthivel V, Manikandaprabhu S, Ganapathy Ramasamy N (2019) The Influence of marine algae on the mechanical properties of concrete. *Int J Innov Technol Explor Eng* 8(11):536–543
3. ACI Committee 212 (1963) Admixtures for concrete. *J ACI* 60, 1481–1524
4. Collepari M (1998) Admixtures used to enhance placing characteristics of concrete. *Cement Concr Compos* 20(2–3):103–112
5. IS: 383 (1970) Indian standard for specification for coarse aggregates and fine aggregates from natural sources for concrete (second revision)
6. IS: 2386 (Part 1) (1963) Indian Standard for methods of test for aggregates for concrete (Part 1) particle size and shape
7. IS: 12269 (1987) Indian standard for specification for 53 grade OPC, reaffirmed January 1999.
8. IS: 10262 (1982) Recommended guidelines for concrete mix design. Indian Standard Institution, New Delhi
9. Dransfield J (2003) Admixtures for concrete mortar and grout. In: Newman J, Choo BS (eds) *Advanced concrete technology, constituent materials*. Oxford: Butterworth-Heinemann (2003)
10. Leon-Martinez FM (2014) Study of nopal mucilage and marine brown algae extract as viscosity-enhancing admixtures for cement based materials. *PF J Cano-Barrita* 65(9):1–11
11. Goaszewski J (2009) Correlation between rheology of super plasticized fresh mortars and fresh concretes (SP-262–16). In: Holland TC, Gupta P, Malhotra VM (eds) *Ninth ACI international conference on super plasticizers and other chemical admixtures*, Seville, pp 215–236
12. Schatzmann M, Bezzola GR, Minor H-E, Windhab EJ, Fischer P (2009) Large-particulated fluids: analysis of the ball measuring system and comparison to debris flow rheometry. *RheolActa* 48(8):715–733
13. Lachemi M, Hossain KMA, Lambros V, Nkinamubanzi P-C, Bouzoubaâ N (2004) Self-consolidating concrete incorporating new viscosity modifying admixtures. *CemConcr Res* 34(6):917–926
14. Malhotra VM (1976) No-fines concrete its properties and applications. *J Am Concrete Institute* 73–54, 628–644
15. Plank J (2004) Applications of biopolymers and other biotechnological products in building materials. *Appl Micro Biol Biotechnol* 66(1):1–9
16. Schneider M, Romer M, Tschudin MH (2011) Sustainable cement production present' and future. *Cem Concr Res* 41(7):642–650
17. Drew EA (1983) Halimeda biomass, growth rates, and sediment generation on reefs in the Great Barrier Reef Province. *Coral Reefs* 2:101–110
18. Goreau TF (1963) Calcium carbonate deposition by coralline algae and corals in relation to their roles as reef-builders. *Annu NY Acad Sci* 109:127

19. Hudson JH (1985) Growth rate and carbonate production in *Halimeda opuntia*: Marquesas Keys, Florida. In: Toomey DF, Nitecki MH (eds) *Paleoalgology: contemporary research and applications*. Springer, Berlin
20. Maxwell WGH (1968) *Atlas of the Great Barrier Reef*. Elsevier, Amsterdam
21. Merten MJ (1971) Ecological observations of *Halimeda macroloba* Decaisne (Chlorophyta) on Guam. *Micronesia* 7:27–44
22. Elliot GF (1960) Fossil calcareous algal floras of the Middle East with a note on a Cretaceous problematicum, *Hensonella eylandica*. *Q J Geol Soc* 115:217–232
23. Gilmartin M (1960) The ecological distribution of the deep-water algae of Eulwetok Atoll. *Ecology* 41:210–221

Feasibility Assessment on Electronic Waste (EW) as a Partial Reduction for Coarse Aggregate (CA) in Concrete



R. Padmapriya, J. S. Sudarsan, N. Sunmathi, and Srihari Vedartham

1 Introduction

The rapid growth of technology and its upgradation in various sectors results in producing EW in huge quantities. EW is generated in cities like Chennai, Bangalore, and Delhi in huge quantities. In recent years, many studies are being conducted to address this issue. EW products have become most important in day-to-day life, and its waste is very hazardous. Technological advancement introduces computers which were debuted in 1990, and each decade after then, many new gadgets have been introduced, rendering previous ones obsolete. Computers, laptops, and mobile phones are frequently replaced due to the advent of newer models with greater processing capability. Typically, outdated equipment is discarded, recycled, or predisposed of in dumping yard without proper secretion. This EW trash requires skilled disposal and reuse because not doing so or putting it in landfills poses a major danger to anthropological health as well as the purity of subsurface water. More than fifty million metric tonnes of EW are produced internationally each year, with an average of seven kilograms of e-waste per capita [1]. In developing countries, proper rules and facilities are lacking, making them more vulnerable to the detrimental effects of EW. Informal processing endangers both the people who labour in them and the environment. The developed world generates the vast majority of EW garbage. E-waste from developed countries is frequently exported to poor countries [2]. Poisonous components of e-waste may leak into the soil or subterranean water, causing long-term harm. Many metals can also be found in e-waste.

R. Padmapriya (✉) · N. Sunmathi
Department of Civil Engineering, Sathyabama Institute of Science and Technology, Chennai, India
e-mail: padmapriyar_77@yahoo.com

J. S. Sudarsan
School of Energy and Environment, NICMAR University, Pune, India

S. Vedartham
NICMAR, Jagannaguda, Shamirpet, Aliabad, Hyderabad 500 101, India

Almost 60 different metals are used in EW, and recovering them in both commercially and environmentally advantageous. It contains various metals, including gold, silver, and other valuable metals, as well as dangerous chemicals such as cadmium, mercury, and lead [3]. Nearly all nations are now working to combat this threat, and the Indian government has developed a structure for EW administration and is establishing producer accountability [4, 5].

This research focuses an alternate material for construction. [6, 7]. It was observed by one of the researcher in their research on utilisation of EW particle as CA in M20 strength concrete with fraction replacement of 0, 4, 8, 12, 16, 20, and 25% and addition of 10% fly ash [8, 9].

This type of project will yield a better result in terms of achieving sustainability, as well as assisting in the implementation of the reduce, reuse, and recycle 3R principle and effective waste management strategy [10]. This trivial initiative will fetch major leap in developing sustainable green material.

2 Methodology

2.1 Materials

Along with cement, fine aggregates, coarse aggregates, and water, additionally EW is also used as ingredient in concrete. The physical and chemical qualities of the materials indicated above were examined in a recognised laboratory to determine their appropriateness for use in concrete [11, 12].

2.2 Electronic Waste

Figure 1 shows the EW used in the concrete. The properties of EW are given in Table 1.

2.3 Methodology

Material testing, mix design, and testing procedures for this study are procured from various literature analysis. [13, 14] The workflow of this study is derived as a methodology flowchart, and it is shown in Fig. 2.

In the current investigational studies, M₃₀ concrete grade was implemented as per IS: 10262-2019 [15–17]. Around 45 cubes of size 0.15 m × 0.15 m × 0.15 m were tested for its compressive strength. The cube samples were tested at 7, 14, and

Fig. 1 EW**Table 1** Properties of e-waste

Element	Percentage (%)
Plastics	31.02
Refractory oxides	31.02
Copper	19.12
Iron	6.11
Tin	5
Nickel	3
Lead	3
Aluminium	3
Zinc	2
Silver	0.4
Gold	0.2
Palladium	0.05

28 days of curing period [18]. The organised samples were placed in compression-testing machine (CTM), and the test set up is shown in Fig. 3. The final load (P) at which concrete cube gets crushed is determined. Compressive strength (CS) of concrete cube is calculated using the formula suggested by IS 516:1959.

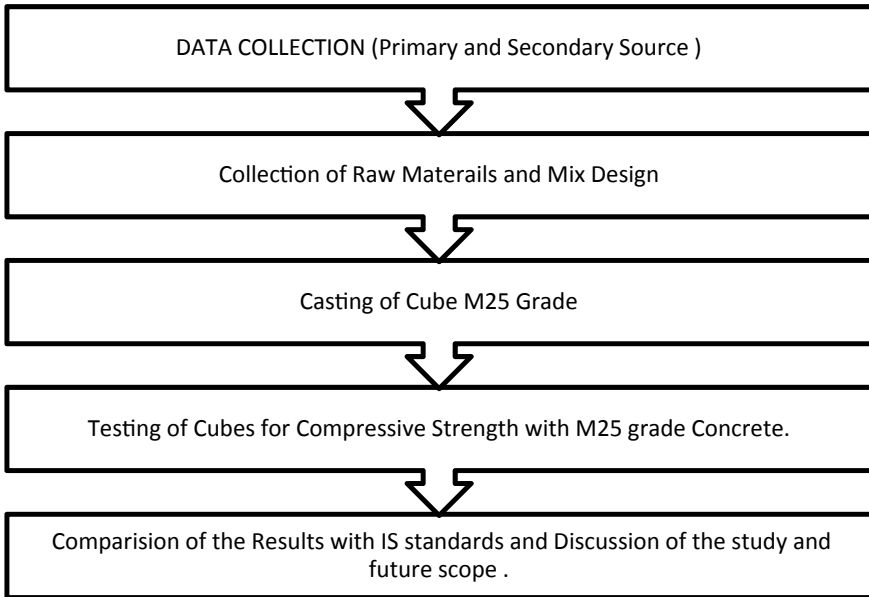


Fig. 2 Methodology

Fig. 3 Compressive strength on concrete cube



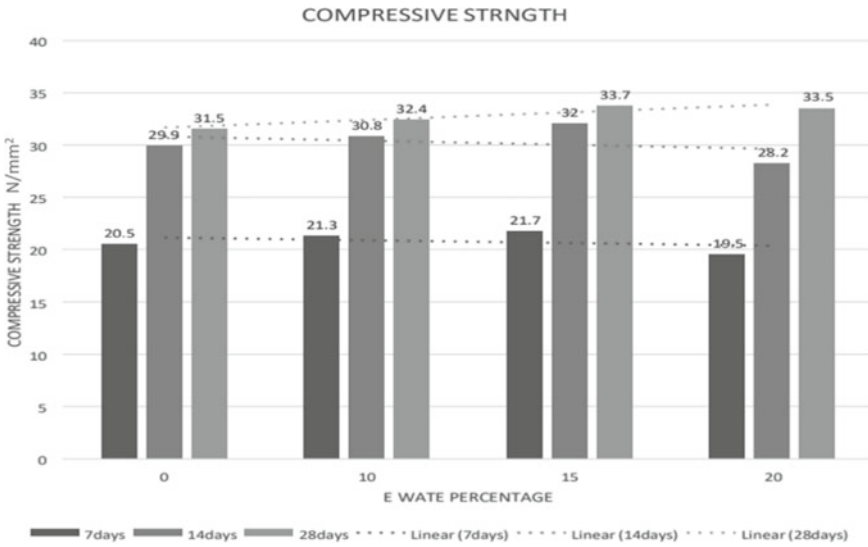


Fig. 4 Compressive strength

3 Result and Discussion

3.1 Compression Test (CT)

Figure 4 presents a CT results that was performed on cubes using part relief of CA with EW in the fractions of 0%, 10%, 20%, 30%, and 40% on the third, seventh, fourteenth, and twenty-eighth days [19, 20]. The CS of EW concrete increases with age, which demonstrates the consistency of e-waste plastic as a suitable CA replacement.

From Fig. 4 it is concluded that compressive strength of M30 grade concrete is maximum when CA is replaced by 20% e-waste [21–23]. Compressive strength decreases above 20% replacement due to poor bonding of e-waste.

3.2 Limitations

- (1) Huge quantity of electronic waste is needed for processing.
- (2) It mandatory to segregate the electronic waste before adding with concrete.
- (3) No standard guidelines are existing on the same.
- (4) It is mandatory to carry out leachate study of the casted material.
- (5) Health and safety of the stake holders need to be studied, and proper measures must be taken in utilising the electronic waste in concrete.

4 Conclusion

The Electronic waste samples were analysed, and it is observed that the composition of plastic and refractory oxides are found maximum 31.02%, whereas the proportion of copper is found as 19.12%. The other elements like tin, nickel, lead, aluminium, zinc, silver, gold, palladium, etc. are found in minimum proportion. Compressive strength of M30 grade concrete is maximum when CA is replaced by 20%. The higher percentage of refractory oxides and copper influences electronic waste as a potentially suitable material, and hence, it can be used as CA to produce durable concrete. This study demonstrate that it is possible to adopt electronic waste in concrete, but it needs detailed study and investigation. This study is the part of research study in adoption waste in concrete and other construction activities.

Scope for Future Study

The same electronic waste can be studied with different mix design and different applications, and leachate study needs to be carried out to check adaptability of the same with cost benefit analysis.

Acknowledgements The authors of this manuscript are very much grateful to management of Sathyabama University and NICMAR University for providing support in executing this research work successfully.

References

1. Balde CP, Kuehr R, Blumenthal K, Fondeur Gill S, Kern M, Micheli P, Magpantay E, Huisman J (2015) E-waste statistics-Guidelines on classification, reporting and indicators. United Nations University, IAS-SCYCLE, Bonn (Germany)
2. Widmer R, Oswald-Krapf H, Sinha-Khetriwal D, Schnellmann M, Böni H (2005) Global perspectives on e-waste. *Environ Impact Assess Rev* 25(5):436–458
3. Namias J (2013) The future of electronic waste recycling in the United States: obstacles and domestic solutions. Columbia University, Columbia
4. E-Waste in India (2011) https://rajyasabha.nic.in/rsnew/publication_electronic/E-Waste_in_india.pdf
5. Central Pollution Control Board (CPCB) (2016) <http://cpcb.nic.in/e-waste-rules/>. CPCB, New Delhi
6. Mandot V (2018) An overview of electronic waste. *JETIR* 5(5):334–337
7. Panwar RM, Ahmed S (2018) Assessment of contamination of soil and groundwater due to e-waste handling. *Curr Sci* 114(1):166
8. Lakshmi R, Nagan SJ (2010) Studies on concrete using e-plastic waste. *Int J Environ Sci* 1(3)
9. Gour MA, Sharma SK, Garg N, Das SK, Kumar S (2022) Utilization of plastic waste as a partial replacement of coarse aggregates in concrete. *IOP Conf Ser Earth Environ Sci*. <https://doi.org/10.1088/1755-1315/1086/1/012047>
10. Sunmathi N, Padmapriya R, Sudarsan JS (2021) Feasibility study of tannery waste as an alternative for fine aggregate in concrete. In: *Sustainable Construction Materials: Lecture Notes in Civil Engineering*

11. Liu H, Luo G, Wei H, Yu H (2018) Strength, permeability, and freeze-thaw durability of pervious concrete with different aggregate sizes, porosities, and water-binder ratios. *Appl Sci* 8(8):1217. <https://doi.org/10.3390/app8081217>
12. Krishna Prasanna P, Kanta Rao M (2014) Strength variations in concrete by using e-waste as coarse aggregate. *Int J Educ Appl Res* 4:82–84
13. Akram A, Sasidhar C, Pasha KM (2015) E-Waste management by utilization of e-plastics in concrete mixture as coarse aggregate replacement. *Int J Innov Res Sci Eng Technol* 4(7):5087–5095
14. Balasubramanian B, Gopal Krishna GVT, Saraswathy V (2016) Investigation on partial replacement of coarse aggregate using e-waste in concrete. *Int J Earth Sci Eng* 9:285–288
15. IS383 (1970) Specification for coarse aggregate and fine aggregate from natural sources for concrete. Bureau of Indian Standard, New Delhi
16. IS10262 (2019) Concrete mix proportioning. Bureau of Indian Standard, New Delhi
17. IS516 (1959) Method of tests for the strength of the concrete. Bureau of Indian Standard, New Delhi
18. Santhanam N, Ramesh B, Joshua Richard Prabu S (2020) Experimental study on use E-waste plastics as coarse aggregate in concrete with manufactured sand. *Mater Today Proc* 22(3):715–721. <https://doi.org/10.1016/j.matpr.2019.10.006>
19. Chen H-J, Tai P-H, Peng C-F, Yang M-D (2017) Concrete crack rehabilitation using biological enzyme. *Comput Concr* 19(4):413–417. <https://doi.org/10.12989/cac.2017.19.4.413>
20. Manjunath BA (2016) Partial replacement of E-plastic waste as coarse-aggregate in concrete. *Proc Environ Sci* 35:731–739
21. Shilpa B, Deshpande G, Nagarajan K, Narwade R (2019) E-waste: an alternative to partial replacement of coarse aggregate in concrete. *Int J Eng Res Technol* 8:7
22. Islam R, Nazifab TH, Yuniarto A, Shanawaz Uddin ASM, Salmiati S, Shahid S (2019) An empirical study of construction and demolition waste generation and implication of recycling. *Waste Manag* 95:10–21. <https://doi.org/10.1016/j.wasman.2019.05.049>
23. Suchithra S, Kumar M, Indu VS (2015) Study on replacement of coarse aggregate by E-waste in concrete. *Int J Tech Res Appl* 3(4):266–270

Information Technology in Civil Engineering

Review of Robotics' Role in Unsafe Site Conditions in the Construction Industry



Sourav Kumar, Balasubramanian Murugesan,
Aishwarya Sathyanarayanan, and Mukilan Poyyamozhi

1 Introduction

The construction sector is significant to national and global economies; however, it also faces numerous obstacles. Despite rapid economic growth and technology, the construction industry persists as one of the most significant sectors in the world. Construction-related injuries and fatalities are associated with financial costs. Accidents are caused by inherent dangers as well as the nature of the job performed by personnel. Large construction project frequently hires other subcontractors based on a contract to complete the project on time, with generally a small margin of the contract's price invested in occupational safety and health, which leads to the formation of unsafe conditions on the job site, increasing the risk of an accident, and putting the worker's life at risk. Major prevention steps are initiated by the project management level which plays a vital role in safety performance where support and commitment, management style, and competency are the main elements. According to various studies, management commitment to safety significantly impacts the maintenance of a safe workplace and the reduction of the accident/incident rate. Generally, the construction sector has not been a favorable location for robotics applications.

Stating to the technology used in construction, adopting a robot could resolve this challenge by working at vast heights and giving real benefits such as increased construction productivity, less personnel, shorter construction lead times, and lower construction costs [1]. Today, space research organizations are attempting to develop infrastructure without humans, while construction corporations are looking to robots to increase building quality, efficiency, and safety. Unmanned aerial vehicles (UAV) have widely been utilized in military applications, but their potential utility in engineering situations has recently gotten a lot of attention. In civil industry, UAVs have

S. Kumar · B. Murugesan (✉) · A. Sathyanarayanan · M. Poyyamozhi
Department of Civil Engineering, Faculty of Engineering and Technology, SRM Institute of
Science and Technology, Kattankulathur, Tamil Nadu 603203, India
e-mail: balasubm1@srmist.edu.in

been utilized for building inspection, damage monitoring and crack photogrammetric applications, pavement, and highway maintenance along with many other applications [2]. To secure the safety of personnel who operate in high-risk regions, such as near the building's edge, utilizing robots, new methods are needed [3]. With the advent of vertical development in the construction industry, the life risk to laborers has increased exponentially. It is the construction company's responsibility to secure the safety of its workers. There are countless regulations regarding the same from concerned departments. These issues can be better handled by using robots to automate. The purpose of this review is to explore the unsafe site conditions using UAVs for site safety inspections, with a focus on identifying requirements that can be checked and deviations from the specified safety criteria.

Unsafe site conditions refer to a potentially hazardous physical condition or set of circumstances that could lead to an accident. In 2018, the US Occupational Health and Safety Administration (OSHA) reported 1008 construction worker fatalities, the majority of which were occurred by on-site typical accidents like materials falling [4]. The stated accidents come under unsafe site acts and unsafe behavior. A combination of risky behaviors and unsafe site conditions brings on a significant number of accidents. Researcher must address the accident's core causes to achieve long-term improvement and adopt robots that can resolve the issue, and usage of robotics will undeniably increase.

2 Bibliometric Analysis: Citation

This research uses a systematic review to find ways to use robotics to improve hazardous site conditions. A systematic review, in contrast to a formal literature review, uses an explicit, stringent, repeatable, and auditable technique to evaluate and interpret all of the research that is currently available on a particular research question, topic area, or phenomenon of interest. By presenting the broader picture and merging discrete elements to synthesize data in an ordered manner, a systematic review can also overcome the drawbacks of a single-facet approach, frequently used in a literature review. Researchers can also synthesize existing evidence regarding a topic, discover research gaps, and justify new ideas and hypotheses by employing a systematic review approach.

Table 1 demonstrates the density distribution of all authors. It tracks research on the basis highest number of citations. The analysis includes five clusters with 54 authors as shown in Fig. 1. The top-ten authors on the basis of number of citations are given in Table 1. The analysis included authors having at least 30 citations. The maximum number of citations were 549 with 38 documents and 53 total link strength of Wang Y. Here, in the analysis, first 10 authors were discussed here.

The second ranked author is Zhang D. with 514 citations, 12 documents, and 12 total link strength. The third ranked is Li H. with 481 citations, 34 published articles with 34 total link strength; Zhang H. with 410 citations, 24 documents, and 20 total link strength; Wang J. with 406 citations, 33 documents, and 28 total link strength;

Table 1 Information of citations of authors

Number	Authors	Documents	Citations	Total link strength
1	Wang Y.	38	549	53
2	Zhang D.	12	514	12
3	Li H.	34	481	34
4	Zhang H.	24	410	20
5	Wang J.	33	406	28
6	Zhang X.	38	356	31
7	Wang C.	22	301	20
8	Zhang Y.	46	298	46
9	Wang S.	19	279	16
10	Li X.	30	266	32

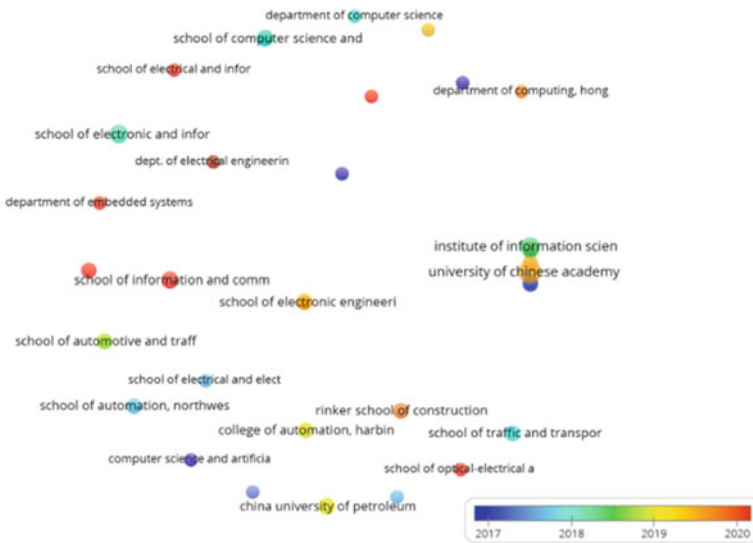


Fig. 1 Author analysis

Zhang X. with 356 citations, 38 documents, and 31 total link strength; Wang C. with 301 citations, 22 documents, and 20 total link strength; Zhang Y. with 298 citations, 46 documents, and 46 total link strengths; Wang S. and Li X. are last two authors with 279 and 266 citations respectively, followed by 19 documents for Wang S. and 30 documents for Li X. Investigation found that Wang Y. is clustered with cluster 4, which has the highest citation count. Figure 2 shows that Wang Y. has maximum number of meaningful citations in the civil sector. In the given analysis, authors identified the role of the unmanned aerial vehicle in the field of construction and to tend to identify the new technologies trends in this area.

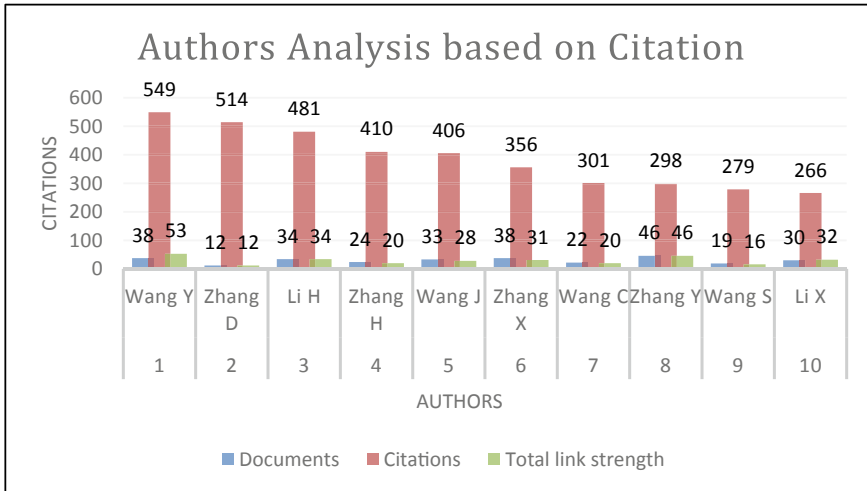


Fig. 2 Density visualization of all organizations

Table 2 demonstrates the information of citations of top 10 organizations. It tracks research on the basis highest number of citations. The analysis includes 50 organizations around the world. The top-ten organizations on the basis of number of citations are given in Table 2. The analysis included organizations having at least 30 citations. The maximum numbers of citations were 512 with 4 documents and 0 total link strength of School of Automation, Northwestern Polytechnical University, Xian, China. Here, in the analysis, first 10 organizations were discussed here. Rinker School of Construction Management University of Florida, Gainesville, United States, is the second-ranked organization, with 75 citations, 4 documents, and 0 overall link strength. Australia’s Deakin University, School of Architecture and Built Environment, is third on the list with 67 references, three papers, and zero total strength of links to other sources, followed by School of Electronic Engineering, Xidian University, Xian, China, with 65 citations, 5 documents and 1 total link strength, The Chinese University of Electronic Science and Technology’s School of Information and Communication Engineering has 55 citations, 4 documents, and 0 overall link strength; Institute of Information Science, Beijing Jiaotong University, Beijing with 44 citations,7 documents, and 1 total link strength; and 41 citations, 3 publications, and 0 overall link strength for the School of Electrical and Information Engineering at Tianjin University in Tianjin, China. Computer Science and Artificial Intelligence Laboratory, Massachusetts Institute, Cambridge, United States with 37 citations, 3 documents, and 0 total link strengths. Finally, with 36 and 30 citations each, Tianjin University’s School of Electrical and Information Engineering and Harbin Institute of Technology’s School of Computer Science and Technology are the only two institutions in China followed by 3 documents for School of Information Engineering, Chang’ an University, Xian, Shaanxi, China and 3 documents for School of Computer Science and Technology, Harbin Institute of Technology,

Table 2 Information of citations of top-ten organizations

Number	Organizations	Documents	Citations	Total link strength
1	School of Automation, Northwestern Polytechnical University, Xian, China	4	512	0
2	University of Florida, Gainesville, USA, Rinker School of Construction Management	4	75	0
3	School of Architecture and Built Environment, Deakin University, Geelong, Australia	3	67	0
4	School of Electronic Engineering, Xidian University, Xian, China	5	65	1
5	University of Electronic Science and Technology of China, School of Information and Communication Engineering	4	55	0
6	Institute of Information Science, Beijing Jiaotong University, Beijing	7	44	1
7	Tianjin University’s School of Electrical and Information Engineering, Tianjin, China	3	41	0
8	The Massachusetts Institute of Technology’s Computer Science and Artificial Intelligence Laboratory is located in Cambridge, Massachusetts	3	37	0
9	School of Information Engineering, Chang’an University, Xian, Shaanxi, China	3	36	0
10	Harbin Institute of Technology’s School of Computer Science and Technology, Heilongjiang, China	3	30	0

Heilongjiang, China. School of automation, Northwestern Polytechnical University has the highest number of citations in the analysis. Figure 3 shows the organizational analysis of top-ten organizations.

3 Drone Technology for Unsafe Site Conditions

In this study, the purpose is to identify the role of unmanned Aerial vehicle in the field of construction and to discover new technological trends in this industry. This includes an examination of the concerns, methodologies, and conclusions described

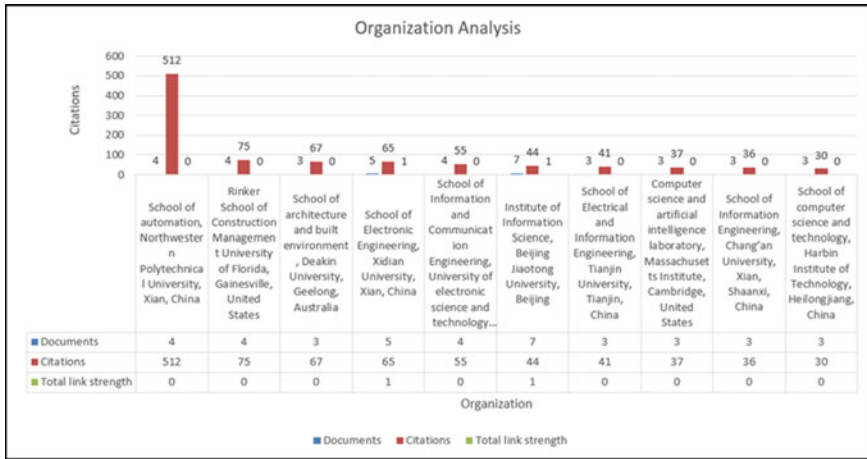


Fig. 3 Analyses of organizations

in the literature, both in the construction industry and in related domains. The articles and materials included in this study were obtained from several internet databases, including Science Direct and IEEE Xplore. There were two major categories in the literature search. The first was about unsafe site conditions in construction, while the second was about the adoption of UAVs in construction. “Construction” or “Unsafe site acts/conditions” or “Construction accidents” or “Unsafe conduct” are some of the terms used here along with “Unmanned aerial vehicle,” “Automated Construction,” “Drone in Construction Industry,” etc. The most relevant papers were utilized to build this state-of-the-art literature review as a consequence of this strategy. Siddiqui [5] utilized OSHA’s IMIS to collect and study 9141 cases of accidents due to materials fall in working sites for the past 20 years in order to investigate the primary reasons in the United States. Low-budget initiatives, frequent fall accidents on residential and commercial building construction sites, and inadequate fall safety precautions in construction work less than 30 feet deep were some of the causes he mentioned. Furthermore, 55% of all construction-related injuries occurred while working on the roof, ladders, or scaffolding. In the form of a conceptual model, Fig. 4 summarizes the groupings of the themes into contributing aspects of several factors which lead to accidents. Attitude and perception, age and experience, desired actions, competence and ability, and psychological characteristics are five of the individual factors that make up each participant. Several studies have found that these factors have a significant role in worker safety [6].

Because of the variety of activities that occur throughout the various stages of construction, a new category of site condition has been created, which includes hazardous operations, dangerous conditions, and welfare services. Work-related activities in construction are frequently dangerous, such as working at heights, outside operations in inclement weather, and the usage of diverse equipment. These factors are combined with workers’ attitudes toward safety [7]. Construction sites may be

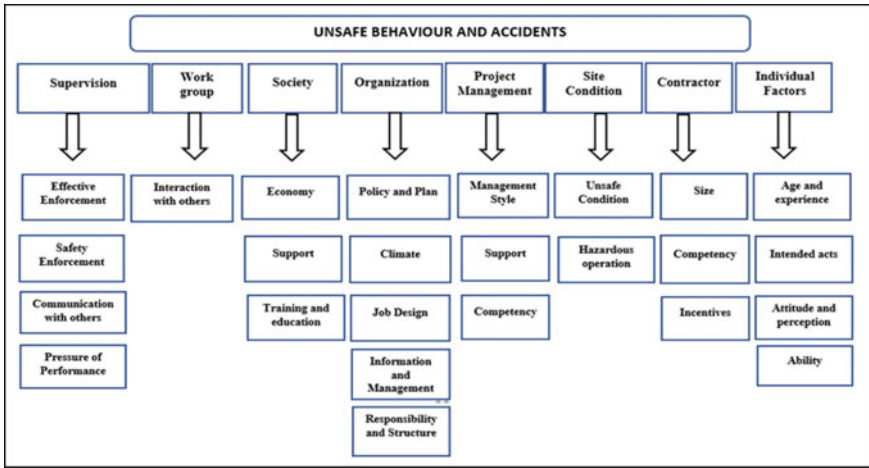


Fig. 4 Factors influencing unsafe behavior and accidents on construction site

open 24 h a day on occasion. During night shifts, workers may have difficulty seeing their surroundings if there is insufficient lighting or illumination. Due to a lack of illumination, employees may fall from high surfaces, increasing the risk of harm. The situation in night shifts is highly risky in terms of accidents in construction industry.

3.1 Current State of Drone in the Field of Construction

Use of drones, or unmanned aerial vehicles (UAVs), is becoming more commonplace in the construction business. Drones are used as tools for increasing communication among construction participants, site safety, and large-area topographic surveys, and producing structures, bridges, roads, and highways using aerial photogrammetry principles, reducing project time and costs, and so on [8]. de Melo [2] found that by the use of drone technology in the workplace which is one of the most serious issues facing construction management. The construction industry has taken note of the promising properties of unmanned aerial vehicles (UAVs) in research on transportation and jobsite monitoring [2]. The significant goal of this literature study is to determine if unmanned aerial vehicles (UAVs) can be used to inspect construction sites for safety, with a particular focus on identifying the requirements that might be inspected, as well as non-compliance with certain safety requirements. More study, however, is required to help guide the progress of workflow procedure for properly utilizing the drone technique, particularly for monitoring of safety on-site.

Innovative technologies are crucial to enhancing the performance of building processes and products, according to a recent study by Gamlath [9]. The use of cutting-edge technology can lead to considerable financial rewards. Robotics has not always been a suitable fit for the construction industry. The employment of robots is

projected to increase as new cost-effective uses and justifications emerge, such as a labor scarcity, aging qualified personnel, and safety concerns [10]. Aside from basic applications that are easy to understand and have clear benefits, the construction industry has not yet made fully-fledged, complex technical applications. A major goal of this article is to assess how robotics is being used in the local construction industry today.

According to the literature, comparing the other architecture, engineering, and construction (AEC) sectors, the construction business is now the most significant and fastest-growing UAV industry. Some major application areas in the construction domain looked at by various studies include progress monitoring, aerial construction, mapping, building inspection, surveying, safety monitoring, site communication, material handling, and security surveillance [11].

3.2 Unsafe Site Conditions

Unsafe conditions are defined as any circumstance or situation that enhances the risks and dangers of accidents. Unsafe activities can result in dangerous situations. Unsafe site conditions, such as moving objects above workers, are a common cause of construction site accidents. Figure 5a, b shows the various unsafe conditions and acts on construction site. There has been some progress in the development of sensors for detecting workers who have been hit by falling debris from cranes, but they are currently limited to the construction site [12]. As a result, new research necessitates the search for an ideal sensor with a wide sensing range that may be used to construct the system. According to the research of the literature, many sensors have been employed in proximity warning systems.

According to He [12], one of the most common causes of construction site accidents is moving goods above employees due to risky site circumstances. The dynamic

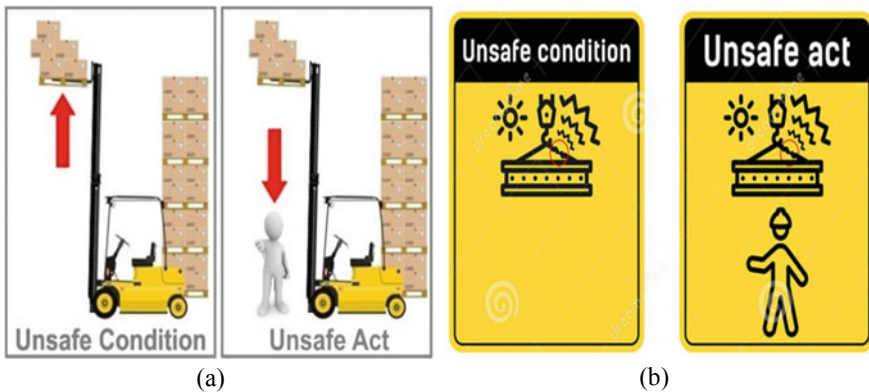


Fig. 5 a, b Unsafe conditions and acts found on construction site

and complicated character of building sites might result in the dangerous scenarios described above. As opposed to this, previous research has generated an accident detection sensor system that is limited to use on a crane prototype in the laboratory. In order to notify construction workers of potentially hazardous conditions, this study aims to formulate a SW system (sensor warning system). This research focuses on a tower crane lifting operation. As well as a GPS sensor and a server, the sensor warning system is based on the IoT technology (Internet of Things). The pilot test in this study was done using GPS devices in order to estimate the measurement inaccuracy and for calibrating the whole system. By using the SW system, the cause of accidents can be reduced. The subsequent sections discuss over some of the dangerous acts and conditions that were discovered.

Unsafe Act—Storage of equipment and materials in improper settings: Unsuitable storage of equipment and supplies is a workplace offence that can occur on a regular basis or infrequently, depending on the frequency of the event. This breach is mostly caused by physical environment characteristics (e.g., a lack of space in the office), and it is aided by a lack of workplace surveillance and supervision [13, 14]. *Unsafe Act—Lack of personal protective equipment (PPE):* An alarming number of people fail to use personal protective equipment (PPE). Incorrect crew management and a poor mental state are crucial issues; the latter can be traced back to the discomfort of the available PPE. In this unsafe act scenario, leadership training entails reminding responsibility in recognizing the necessity of personal protective equipment (PPE) and their responsibility in regulating PPE use [15]. *Unsafe Site condition—Hazardous operations and unsafe equipment:* The majority of construction activities take place in ever-changing environments with constantly altering site circumstances. Unsafe equipment, bad weather, welfare services, hazardous operations, and construction stage are all examples of unsafe site conditions. Unsafe circumstances, for example, show a moderately favorable correlation with unsafe actions and accidents [16].

4 Discussion

UAVs and unsafe construction site practices were both examined in-depth in this article. In this study of unsafe behaviors and conditions, a potentially hazardous physical state or a group of circumstances that could cause an accident is compiled. The majority of fatalities in the construction industry were determined to be due to routine accidents. Accidents resulting from falling from a height have been linked to the use of scaffolding and roofing [17]. The majority of accidents are brought on by several contributing factors and more than one dangerous action or circumstance, as seen in Fig. 4. There is no doubt that learning from accidents is important, and by using robots in construction, it can be reduced as much as possible in a variety of ways. Their use in the building sector will increase in the future since they can rapidly record high-quality data and considerably lower the danger to the safety of construction labors.

5 Conclusion

In the field of civil engineering, accidents are something which cannot be predicted and can occur any place, any time, and anywhere. Stating to the technology used in construction, adopting a robot could resolve this challenge by working at vast heights and giving real benefits such as increased construction productivity, less personnel, shorter construction lead times, and lower construction costs. Generally, only a small portion of the contract money is allocated to occupational safety and health, resulting in risky working conditions on the project site which leads to rise in accidents in construction industry. It is recommended that new novel research approaches and additional data sources be employed for unsafe site condition study in order to gain a better knowledge of these potentially hazardous physical circumstances that could result in an accident. The construction industry, which is rapidly expanding, will quickly embrace unmanned aerial vehicle technology as a tool that saves money, time, and improves safety and control. Construction companies are obtaining drones at a far faster rate than ever before due to their multiple benefits. Regardless of whether it is for topographic terrain mapping, building surveys, or something else, UAVs have shown to be a valuable tool throughout the construction project's life cycle. The industry is currently focusing on constructing ever more complex management systems in order to meet this issue. Individual operators may have to implement a unique method to drone use in search and rescue systems. A final finding was the fact that concerns about security and privacy are less prominent than in previous periods, with drones deployed in a variety of environments allowing researchers the opportunity to analyze their introduction and impact on persons with whom they will interact in coming future. As to conclude, the majority of accidents are brought on by several dangerous acts and conditions and a combination of contributing variables. It is mandatory to address the accident's core causes to achieve long-term improvement and adopt robots that can resolve the issue, and usage of robotics will definitely increase.

References

1. Jayaraj A, Divakar HN (2018) Robotics in construction industry. IOP Conf Ser Mater Sci Eng 376(1). <https://doi.org/10.1088/1757-899X/376/1/012114>
2. de Melo RRS, Costa DB, Álvares JS, Irizarry J (2017) Applicability of unmanned aerial system (UAS) for safety inspection on construction sites. Saf Sci 98:174–185. <https://doi.org/10.1016/j.ssci.2017.06.008>
3. Cambraia FB, Saurin TA, Formoso CT (2010) Identification, analysis and dissemination of information on near misses: a case study in the construction industry. Saf Sci 48(1):91–99. <https://doi.org/10.1016/j.ssci.2009.06.006>
4. Hou L, Chen H, Zhang GK, Wang X (2021) Deep learning-based applications for safety management in the AEC industry: a review. Appl Sci 11(2):1–18. <https://doi.org/10.3390/app11020821>

5. Kang Y, Siddiqui S, Suk SJ, Chi S, Kim C (2017) Trends of fall accidents in the U.S. construction industry. *J Constr Eng Manag* 143(8):1–7. [https://doi.org/10.1061/\(asce\)co.1943-7862.0001332](https://doi.org/10.1061/(asce)co.1943-7862.0001332)
6. Khosravi Y, Asilian-Mahabadi H, Hajizadeh E, Hassanzadeh-Rangi N, Bastani H, Behzadan AH (2014) Factors influencing unsafe behaviors and accidents on construction sites: a review. *Int J Occup Saf Ergon* 20(1):111–125. <https://doi.org/10.1080/10803548.2014.11077023>
7. Azhar S, Choudhry RM (2016) Capacity building in construction health and safety research, education, and practice in Pakistan. *Built Environ Proj Asset Manag* 6(1):92–105. <https://doi.org/10.1108/BEPAM-09-2014-0044>
8. Sawant R (2021) Drone technology in construction industry: state of art, Nov 2021
9. Gamlath M, Waidyasekara KGAS, Pandithawatta S (2020) Feasibility of robotic technology for the advancement of construction industry in Sri Lanka. In: *MERCon 2020—6th international multidisciplinary Moratuwa engineering research conference proceedings*, pp 54–59. <https://doi.org/10.1109/MERCon50084.2020.9185384>
10. Lee JH, Park JH, Jang BT (2018) Design of robot based work progress monitoring system for the building construction site. In: *9th international conference on information communication technology convergence. ICT Convergence. Powered by Smart Intelligence. ICTC 2018*, pp 1420–1422. <https://doi.org/10.1109/ICTC.2018.8539444>
11. Jeelani I, Gheisari M (2020) Safety challenges of UAV integration in construction: Conceptual analysis and future research roadmap. *Saf Sci* 144:105473. <https://doi.org/10.1016/j.ssci.2021.105473>
12. He V, Peansupap V (2018) Application of sensor technology for warning unsafe conditions from moving objects above construction workers. In: *2018 2nd international conference on engineering innovation. ICEI 2018*, pp 69–74. <https://doi.org/10.1109/ICEI18.2018.8448690>
13. Baldissoni G, Comberti L, Bosca S, Murè S (2019) The analysis and management of unsafe acts and unsafe conditions. Data collection and analysis. *Saf Sci* 119:240–251. <https://doi.org/10.1016/j.ssci.2018.10.006>
14. Tkáč M, Mésároš P (2019) Utilizing drone technology in the civil engineering. *Sel Sci Pap J Civ Eng* 14(1):27–37. <https://doi.org/10.1515/sspjce-2019-0003>
15. Fang Q et al (2017) Detecting non-hardhat-use by a deep learning method from far-field surveillance videos. *Autom Constr* 85:1–9. <https://doi.org/10.1016/j.autcon.2017.09.018>
16. Matus-Vargas A, Rodriguez-Gomez G, Martinez-Carranza J (2021) Ground effect on rotorcraft unmanned aerial vehicles: a review. *Intell Serv Robot* 14(1):99–118. <https://doi.org/10.1007/s11370-020-00344-5>
17. Nadhim EA, Hon C, Xia B, Stewart I, Fang D (2016) Falls from height in the construction industry: a critical review of the scientific literature. *Int J Environ Res Publ Health* 13(7). <https://doi.org/10.3390/ijerph13070638>

Perception of Proposed Bridge Using Augmented Reality of BIM in Educational Institute—Case Study



V. Kavithanjali, A. Meenachi, and M. Soundararajan

1 Introduction

Engineering has established and developed the building information modelling (BIM) technology in its new digitalization era, which is a relatively new idea in Indian business. Building information modelling (BIM), which is now considered as the industry's gold standard for project delivery, has the power to totally change the market [1]. Every phase of a facility's lifespan is covered by applications for BIM. Planning, design, pre-construction, construction, and post-construction are all phases of construction [2]. BIM also goes by the moniker computational BIM in addition to these uses. The architectural, engineering, and construction business has been significantly impacted by building information modelling (BIM), one of the most popular information and communication technologies used in recent years. Utilizing BIM has the potential to improve construction-related support tasks, team cooperation, and information exchange [3]. This paper highlights the perception study of students, faculty members, and others in an educational institution of using BIM to determine whether it is essential to construct a bridge connecting the buildings. The buildings were initially surveyed and span of the bridge is decided. The bridge was then designed and modelled using Revit software, and then, the modelled bridge was given as a view to the respondents using augmented reality techniques perception of proposed bridge using augmented reality of BIM in educational institution, and a bridge was analysed using AR and modelled using BIM, and it is shown in the picture. Therefore, a questionnaire was prepared and the respondents were among student, faculty members to collect their perspectives, and then learn more about the benefits and drawbacks of building the bridge between the departments. The bridge was proposed to connect bridges between second floor using an arch-type bridge.

V. Kavithanjali (✉) · A. Meenachi · M. Soundararajan
Department of Civil Engineering, Sona College of Technology (Anna University), Salem, Tamil Nadu 636005, India
e-mail: Kaviyacivil21@gmail.com

Using AR technology, engineers and technicians may see a real-time representation of the virtual design blueprint and actual construction site, improving accuracy and efficiency [4]. For AR, it is not required to thoroughly recreate the surroundings or the ongoing project process. The project's budget, process errors, and completion timelines may all be kept within reason by incorporating AR into the lifecycle planning of the construction site.

2 Tentative Augmented Reality Assessment of a Proposed Bridge

The general questions, such as if a bridge is required to connect second floor, what kind of bridge is required, what are the needs and specifications of the bridges, and what kind of bridges are suitable for placement, were posed to the participants. Participants were questioned about their perspectives on the bridges design and analysis, what are the best materials to use while building a bridge, according to many perspectives [5].

2.1 Augmented Reality

For a better understanding of the entire project through models, it builds and improves precise reproductions of the real environment. Before the project is completed, AR gives the team a walkthrough of the full project, complete with all the specifics and measurements. Augmented reality is used for design and product development, maintenance, operational control, and safety, employee and operator training and learning, and quality control [6].

2.2 AR in AEC Industry

Construction is gradually replacing technology despite its advancement. Whether they be little developments or major ones. Modern technologies have helped the sector grow. Although it is still in its infancy, augmented reality has already shown to be a highly helpful tool in the construction sector. Building information modelling (BIM), augmented reality (AR), and advanced 3D modelling software have all significantly improved the design and planning process. For instance, the user can see the construction before it is built, together with its actual surroundings and scale. Users can virtually walk around constructions that are still being built to look for conflicts or make improvements without creating problems or delays. This type of technology enables managers, contractors, and engineers to view the outcomes of any changes

in real time. As a result, project risk will be reduced because it will help identify flaws and quickly fix them.

3 Results and Discussion

In this study, the respondents were surveyed using a Likert scale to determine how much they agreed or disagreed with various claims regarding a fact, circumstance, design, or method. The survey data was converted into numerical scores, statistical analysis was performed on it, and then, it was displayed visually in a variety of ways [12].

3.1 Perception of BIM

The findings show that BIM as a new efficient tool has not yet received wide acceptance. The respondent's level of awareness was assessed using a five-point Likert scale, where 1 represents "not likely" and 5 represents "likely." The 53% of respondents said they were familiar with BIM. Twenty (20) respondents claimed that they had minimal to moderate BIM knowledge. A large number of people were discovered to be experts in this field. Three survey participants stated they had never heard of BIM. Apart from 22 respondents, the remaining respondents had more than a reasonable understanding of BIM, which is an important finding from the results regarding awareness of it.

3.2 BIM's Impact on the Analysis and Design of an Effective Bridge

The next section's goal was to assess the benefits of employing BIM. The required/not necessary category of the Likert scale in this survey section contains ten-point response scales. Each response was given a score on a Likert scale of 1 to 5, with 5 denoting strongly agree and 1 strongly disagree. The graphs below show a graph for each response category, representing the distribution of responses. Impact of BIM on effective bridge analysis and design, all five improvements presented as mean and standard deviation, followed by mean > 3. Design visualization improves from the usage of this technology, according to research bridge necessity (4.326 ± 0.786), bridge repetition (4.108 ± 0.760), deterioration effects (3.772 ± 0.960), variations in temperature (3.910 ± 0.740), how much do you analyse if any resistance to the movement of the bearings (3.821 ± 1.935), bridge swaying (3.396 ± 0.883), aware of

Fig. 1 Front view of the bridge



what building information modelling (3.831 ± 0.708), and do you believe BIM will be helpful in the construction industry.

4 Data Collection

4.1 Questionnaire Design

The key purpose of the questionnaire was to determine the advantages and disadvantages of a bridge that was analysed using BIM and was made of materials like steel or reinforced concrete, with the base of the arch structure being below the deck and the top rising above it is shown in Fig. 1. To determine the advantages and drawbacks of adopting BIM, six sets of Likert scale questions were employed. The conditions for the implementation of BIM, opinions on public sector, and the role of the government in supporting the use of BIM were also gathered using open-ended questions [7, 8].

4.2 Open Ended Questions on Questionnaire

Requirements for the use of BIM in the study and design of a successful bridge provide detailed replies and raise points that the closed questions did not address. Thoughts and opinions on how the current regime should support the use of BIM in the planning and construction of successful bridges an average level (44.7%) of replies was used to get the data from the open-ended questions [9]. All civil engineering students, faculty, and industry participants, including top management, were emphasized for their commitments. Few people opposed BIM, citing the excessive

time and expense requirements, and few others questioned if adopting BIM was wise. The following were a handful of the responders' most pertinent comments [10], providing effective lectures and training to explain BIM. People should be aware of the advantages and disadvantages of BIM since it is a novel approach to the study and design of an effective bridge which is shown in Fig. 2. In order to be taken seriously in the study and design of an effective bridge, using BIM must demonstrate that it is superior to the currently available alternative. The lack of data necessary to analyse cost, time, sustainability, etc., may act as an obstacle. Higher-level management's commitment is essential. To demonstrate the advantages and comprehend the needs and goals, pilot studies utilizing BIM are required. Before adoption, a benefit–cost analysis is required. The cost of the resources and software required for implementation should be considered in the analysis. Professional experts must carry out the implementation. Before adopting in the study and design of an excellent bridge utilizing BIM, the qualified experts must allot adequate time and resources and have well-defined parameters, rules, and processes [11]. On the role in encouraging the use of BIM in future projects, 27.7% of the 100 respondents (of 100) offered thoughts and opinions. Six respondents offered their support for the government's efforts to promote the use of BIM on these kinds of projects and welcomed BIM. The use of BIM was stated as being probably preferable to the other alternative approaches in the future (4.168 ± 0.693), quality of project delivery (4.168 ± 0.874), AR/VR in construction (4.069 ± 0.634), views from the bridge (4.089 ± 1.097), effective remedy (3.594 ± 0.762), BIM is clear and understandable (3.960 ± 1.542) Survey (3.930 ± 1.329).

Fig. 2 Autodesk BIM 360



4.3 Limitations on BIM

The final segment, which included five elements, highlighted the adoption of BIM's limits. The Likert scale in this section of the survey features four-point response scales, eliminating the category for "not sure/undecided." Each obstacle was evaluated on a five-point Likert scale, with 1 denoting "strongly disagree" and 5 denoting strongly agree [13]. Professional perspectives on building information modelling BIM's limitations and shortcomings in the study and design of a successful bridge. Each of the five activities was given a mean SD and a mean score. Five things made up the third portion, which focused on the adoption of BIM's drawbacks. The Likert scale in this section of the survey only accepts responses on a four-point scale, removing the category for "not sure/undecided." Each obstacle was scored on a Likert scale of 1–5, with 5 representing strong agreement. The distribution of replies is shown in the graphs below, with one bar representing each type of response [14]. Professionals' perspectives on building information modelling BIM have shortcomings and limitations when it comes to effective bridge analysis and design. The mean score for each of the five activities was reported as mean SD [17–20].

4.4 Rendering of a Bridge

See Figs. 1 and 2.

5 Results from Respondents

5.1 Perception with Using Bridges

For structures to be connected, erection of bridges is necessary as shown in Fig. 3. According to the survey results, half of the respondents said that using the stairs to get from one building to the next would take a lot of time and effort as shown in Fig. 4; however, using this bridge would make it extremely simple to stay linked to other bridges [15]. It is easy to interact with friends and to connect directly. It makes it easier for more people to go from one building to another. For linking the second-floor buildings in educational institutions, arch bridges are helpful.

5.2 The Influence of BIM and AR Technology in Bridges

In the design analysis of the bridge, augmented reality is introduced. Building analysis is done using Autodesk BIM 360 software. According to the respondents, the

Fig. 3 Erection of bridges

erect a bridge between two structures

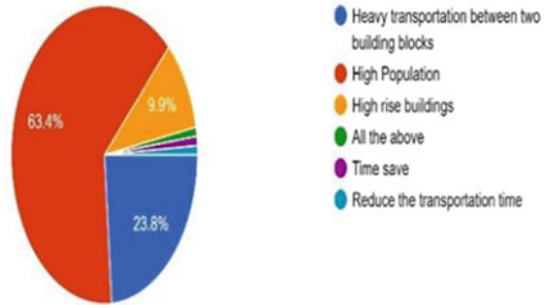
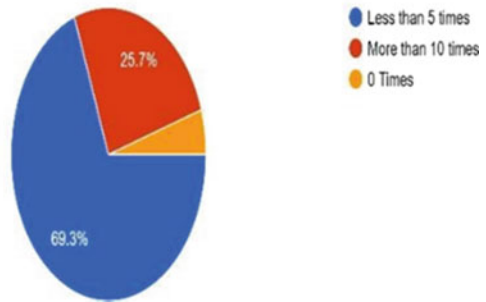


Fig. 4 Usage of bridges

How many times you use this Bridge in a day
sponses



respondents' ideas were based on the absence of information sharing [16]. Using this programme now will result in a successful future treatment. BIM is one of the programmes that might be suggested for usage in the future. Arch bridges have a superior appearance and can provide attractive architectural appearance (Figs. 5 and 6; Table 1).

Fig. 5 Usage of BIM

what do you think of the usage of a BIM as a tool in this case ?

responses

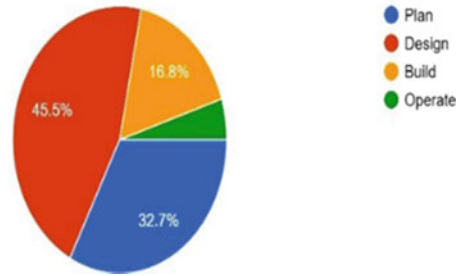


Fig. 6 Usage of AR/VR

Does AR/VR improve the processes used in construction?

responses

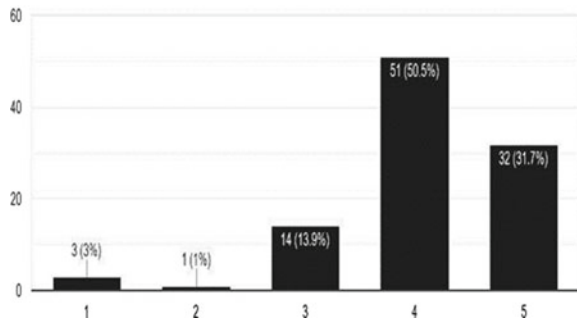




Table 1 Comments made from students and teachers in comparison with the highlighted topics

Research survey	Students	Faculty members
Bridges	According to students, using the stairs to get from one building to another involves a lot of time and effort, but thanks to the assistance of this bridge, staying connected to other bridges are quite simple	Building a bridge between two structures, in the opinion of the faculty, results in a high population density and high-rise projects
BIM	By combining network analysis with problem-based learning, we could make undergraduate built environment students become more proficient with BIM [18]	A redesigned framework for AEC education to enhance integration and cross-disciplinary cooperation
Technical/ technological skills	Students who saw how much time, work, and expertise it takes to construction model commented, "I have gained a new appreciation for architects."	Faculty members believe that at the very least, students should have a basic comprehension of the programme
Augmented reality/virtual reality	<p>In the perspective of students, augmented reality is more practical than virtual reality, which is excellent for constructions</p> 	 <p>AR combines the actual world and the virtual world in the faculties' perception</p>
Relevance to the industry	"How are we supposed to know what these other people do when we have no idea who we are?" Realize the effects their designs will have on cost and constructability	But in the enterprise, this never occurs

6 Conclusion

This study found that there has been a spike in BIM awareness and knowledge based on a review of the literature on BIM applications and benefits, the use of BIM in analyses and the design of a functioning bridge at the Sona Campus' second floor level, an analysis of BIM definitions, and a survey of the respondents. The 53% of respondents claimed to be specialists in this technology, whereas 22% of respondents said they knew little to a lot about it [19]. Better design visualization came out on top when experts were asked to rank the advantages of BIM, followed by improved cross-disciplinary collaboration, cost and time savings, and sustainable design. The majority of respondents (66%) approved of the public sector using BIM

for bridge design. The practitioners' aversion to change was the main impediment to the adoption of BIM on these kinds of projects. Other difficulties identified included the need for higher spending on software and technology, a shortage of technical support, and an increase in workload.

References

1. Ademci E, Gundes S (2018) Review of studies on BIM adoption in AEC industry. In: Review of studies on BIM adoption in AEC industry, 5th international project and construction management conference (IPCMC) proceedings
2. Alani Y et al (2019) An exploration of the owner's requirements for BIM in facilities management. In: CIB world building congress
3. Arayici Y et al (2009) Towards implementation of building information modelling in the construction industry. In: Proceedings of the fifth international conference on construction in the 21st century: collaboration and integration in engineering, management and technology
4. Bui N, Merschbrock C, Munkvold BE (2016) A review of building information modelling for construction in developing countries. *Procedia Eng* 164:487–494
5. Cao Y, Kamaruzzaman SN, Aziz NM (2022) Green building construction: a systematic review of BIM utilization. *Buildings* 12(8):1205
6. Garg C (2017) Review on detailed analysis of building information modelling process (BIM) and implementation based on a case study. *Int J Appl Res* 3(8):387–395
7. Gray M et al (2013) Building information modelling: an international survey. In: Proceedings of the 19th international CIB world building congress, Brisbane 2013: construction and society. Queensland University of Technology
8. Hire S, Sandbhor S, Ruikar K (2022) Bibliometric survey for adoption of building information modeling (BIM) in construction industry—a safety perspective. *Arch Comput Methods Eng* 29(1):679–693
9. Isac IA, Anoop CK (2019) Analysis of building information modelling and scope of BIM in India. *Int J Eng Res Technol* 8(11):72–76
10. John DD (2018) Building information modeling (BIM) impact on construction performance
11. Khan A et al (2018) Evaluating benefits of building information modelling (BIM) using a 5D model for construction project. Available at SSRN 3371434
12. Latiffi AA, Brahim J, Fathi MS (2017) Building information modelling (BIM) after ten years: Malaysian construction players' perception of BIM. *IOP Conf Ser Earth Environ Sci* 81(1)
13. Liu Z, Lu Y, Peh LC (2019) A review and scientometric analysis of global building information modeling (BIM) research in the architecture, engineering and construction (AEC) industry. *Buildings* 9(10):210
14. Moreno C, Olbina S, Issa RR (2019) BIM use by architecture, engineering, and construction (AEC) industry in educational facility projects. *Adv Civ Eng* 2019
15. Rocha G, Mateus L (2021) A survey of scan-to-BIM practices in the AEC industry—a quantitative analysis. *ISPRS Int J Geo Inf* 10(8):564
16. Shaaban K, Nadeem A (2015) Professionals' perception towards using building information modelling (BIM) in the highway and infrastructure projects. *Int J Eng Manag Econ* 5(3–4):273–289
17. Suermann PC, Issa RRA (2009) Evaluating industry perceptions of building information modelling (BIM) impact on construction. *J Inf Technol Constr (ITcon)* 14(37):574–594
18. Takim R, Harris M, Nawawi AH (2013) Building information modeling (BIM): a new paradigm for quality of life within architectural, engineering and construction (AEC) industry. *Procedia Soc Behav Sci* 101:23–32

19. Travaglini A, Radujković M, Mancini M (2014) Building information modelling (BIM) and project management: a stakeholders perspective. *Org Technol Manage Constr Int J* 6(2):1001–1008
20. Zalmai ML et al (2020) Implementation of building information modeling in Turkish government sector projects. *Int J Civ Environ Eng* 14(12):438–442

Machine Learning-Based Dynamic Cost Estimation Model for Construction Projects



Sheema Shah and S. Gopinath

1 Introduction

In the globalized world of today, construction industry is one of the biggest and most challenging. There has been an exponential rise in complex and mega construction where the aim is to complete projects in the allocated duration and time. However, the lucrative completion of construction projects is rare [1]. Despite improvements in the field practices and knowledge, construction industry is besmirched owing to enhanced complexity, scope creep, inefficient management, and involvement of different stakeholders [2]. All allies are required to work cooperatively for the successful accomplishment of the projects. Construction projects are considered successful when they are completed within the cost, time, and scope [3]. The accuracy of estimate of cost is essential for project success, as it affects the overall profitability of the project and ensures that resources are utilized effectively. Also, the main determinant of client trust and satisfaction is the cost of construction projects, and it stays at cutting edge of projects success as it influences the decision-making powers [4]. Before a project is started, the cost estimation is done in the planning stage; however, the accuracy is low due to ignorance, and issues crop up in the execution stage which are not considered when the budget is prepared. Hence, the estimate prepared without uncertainty consideration becomes unrealistic. Literature study has described the following factors that affect the cost performance of construction projects [5]:

- Lack of coordination
- Unsuitable climate
- Lack of knowledge
- Delay in payment

S. Shah (✉) · S. Gopinath
Department of Civil Engineering, Faculty of Engineering and Technology, SRM Institute of Science and Technology, Kattankulathur, Tamil Nadu 603203, India
e-mail: ss5309@srmist.edu.in

- Owner interference
- Delay in decision making
- Poor finance control
- Mistakes in construction
- Material/labor shortage
- Equipment failure.

A lot of statistical techniques and traditional approaches have been used in calculating the budget of the construction projects [6]. However, traditional cost estimation methods, such as expert judgment and comparative methods, have limitations and often result in cost overruns. To address this challenge, there has been a growing interest in the development of dynamic cost estimation models for construction projects [7]. These models provide real-time updates and can adjust the cost estimate as the project progresses. Dynamic cost estimation models are based on a combination of artificial intelligence, machine learning, and data analytics and can be applied at different stages of the project [8]. The use of these models can significantly improve the accuracy of cost estimation and reduce the risk of cost overruns, making construction projects more financially feasible and sustainable [9].

Dynamic cost estimation models can be applied at different stages of the construction project, from pre-design to post-construction. During construction, the model can be used to monitor the progress of the project and update the cost estimate based on changes in the project scope or schedule [10]. After construction, the model can be used to evaluate the actual cost of the project and compare it to the initial estimate. The use of dynamic cost estimation models has the potential to revolutionize construction project management [11]. By providing real-time updates and improving accuracy, these models can help ensure the success of construction projects and reduce the risk of cost overruns. This is particularly important in large-scale construction projects, where the cost of overruns can be substantial.

The construction of models can be done using a number of techniques. However, machine learning models are one of the promising options that can be used to construct prediction models. Machine learning is a branch of artificial intelligence that replicates the human brain functioning by using algorithms. The models are built on data, which is used to make decisions or predictions without being programmed explicitly to do so. It is used in a number of applications such as spam detection, computer vision, and speech recognition. In this work, machine learning-based dynamic cost estimation model is developed to estimate the project cost in the execution stage of the projects. The possible uncertainties like accidents, equipment breakdown, and unsuitable weather which are completely ignored in the traditional or statistical models will also be considered while making predictions. The developed cost estimation model produces reliable results.

2 Literature Review

Construction projects are complex and require careful planning and management to ensure their successful completion. In recent years, there has been an increased focus on the development of dynamic cost estimation models that can provide real-time updates and improve accuracy [12]. The traditionally used cost estimation models such as expert judgment, and comparative methods have limitations and often result in cost overruns [7]. To overcome this problem, dynamic models have been developed using a combination of artificial intelligence, machine learning, and data analytics. These models take into account changes in project variables such as scope, schedule, and resource allocation and use real-time data to estimate the cost of construction projects [13]. One of the earliest studies on cost estimation models was conducted in the early 2000s. This study compared the performance of traditional cost estimation methods with that of a dynamic model based on artificial neural networks (ANNs). The results showed that the ANN-based model was more accurate and able to adapt to changes in the project, reducing the risk of cost overruns. Likewise, a study which was conducted in 2010, focused on the application of data mining techniques in construction cost estimation. The researchers collected data on various construction projects and used regression analysis and decision tree algorithms to develop a dynamic cost estimation model. The results showed that the model was able to provide accurate and timely cost estimates, and was more effective than traditional cost estimation methods. Similarly a study proposed a support vector machine model for cost prediction. It was trained on a dataset of construction project and showed good performance in terms of accuracy and efficiency [1]. One more study proposed a dynamic cost estimation model based on a combination of artificial neural networks and decision tree analysis. This model was tested on a real-world construction project and showed improved accuracy compared to traditional cost estimation methods [12]. Another study proposed a hybrid cost estimation model that combined artificial neural networks with expert knowledge and was tested on a dataset of construction project data. The results showed that the hybrid model outperformed traditional cost estimation methods and was able to provide more accurate cost predictions [14]. Overall past studies have demonstrated the potential of artificial intelligence-based cost estimation models in terms of evaluating the cost for construction projects as compared to the traditional and statistical techniques used for cost prediction. These models are based on advanced technologies such as artificial intelligence, machine learning, and data analytics and can provide real-time updates and improve accuracy. Summarizing the literature, uncertain incidents were not included in the estimation of construction project cost as the probabilities of uncertainties were unknown. Therefore, the cost estimation models generated using neural networks or machine learning lacks in estimating or predicting the cost in a dynamic environment. The proposed machine learning-based cost estimation model consider the uncertainties and results in reliable cost estimation.

3 Methodology

The research methodology involves two stages. Collection of project information to develop the dataset in the first stage. The second stage, machine learning prediction model was developed. Finally, the machine learning model was validated with performance indicators (Fig. 1).

3.1 Data Collection

The aspects of cost estimation of two projects located in Srinagar, Kashmir, India. The scope of the commercial projects includes pile foundation, excavation, construction of RCC framed building components, block-work, cladding, and finishing. The information about work package, quantum of work, planned duration, planned cost, and uncertainties associated with the project work was continuously monitored and recorded. The uncertainties were categorized into low, medium, and high categories. The values of uncertainties were considered as 0.00, 0.25, and 0.50 for three categories, respectively. The uncertainties were categorized based on the exposure of working conditions, probability of an accident, shortage of resources, rework, improper supervision, and unawareness of laborers. Five work packages were included to develop the dataset considering the computational efforts. The work packages included in the dataset are presented in Table 1.

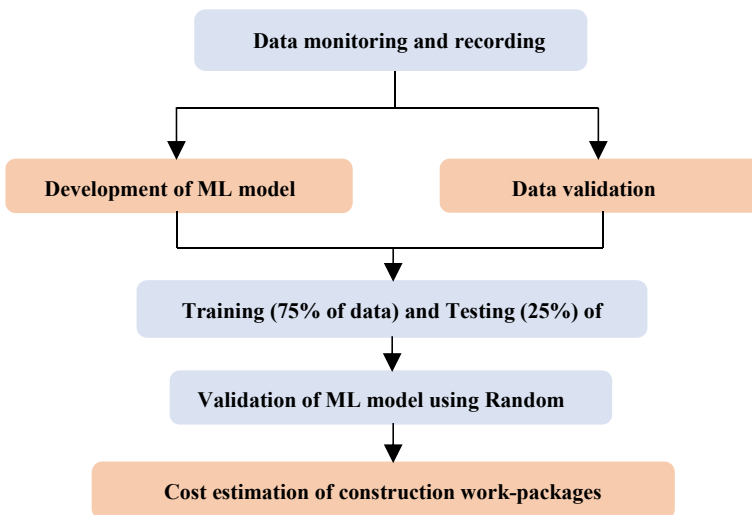


Fig.1 Methodology

Table. 1 Work package indices

S. No.	Task name	Task number
1	Earthwork	1
2	Brickwork	2
3	Concrete work	3
4	RCC work	4
5	Plaster work	5

3.2 Prediction Model

A prediction model was developed using Python programming application. A percentage of 75% of the data was used for training; the model 25% was used for testing. Several performance indicators such as linear regression, decision trees, random forest, and K neighbors regressor were used to evaluate the model. The performance indicators are a set of quantifiable measures that are used to evaluate the model. Linear regression is used for predicting values of variables based on other variables. The limitation of linear regression is that it is prone to over-fitting. Even though tough decision trees are like structured trees in which each node signifies testing attribute and each branch denotes an outcome for test and leaf node has a label for a particular class, it has a disadvantage of over-fitting and feature reduction. K neighbors regressor is another performance indicator that employs a non-parametric method that uses association between independent and continuous outcomes by taking an average of observations in the same neighborhood. It has a set-back of high memory storage requirements. Unlike other performance indicators, random forest has a particular number of decision trees for different subsets of dataset and takes average for improved predictive accuracy. The higher number of trees leads to better accuracy as the decision is based upon the majority of prediction votes. All the performance indicators can evaluate the model; however, random forest is better because of following reasons.

- Reduced over-fitting and improved accuracy.
- Works well with continuous as well as discrete.
- Handles missing values.
- Solves classification as well as regression.
- Efficient handling of nonlinear parameters.
- Less influenced by noise.
- Notable efficiency in handling large datasets.
- No feature scaling required in case of random forest.

4 Results and Analysis

The distribution of final cost for different work packages with different uncertainty constants is represented in Fig. 2. There is a significant increase in the final cost for both construction projects with an increase in uncertainty constant. The distribution of the planned cost of different work packages is presented in Fig. 3. Among all the work packages, the range of final cost in brickwork is significant in both construction projects.

The model was executed using dataset for different quantum of works and uncertainty constants for different work packages. The final cost is predicted considering the constant for uncertainty.

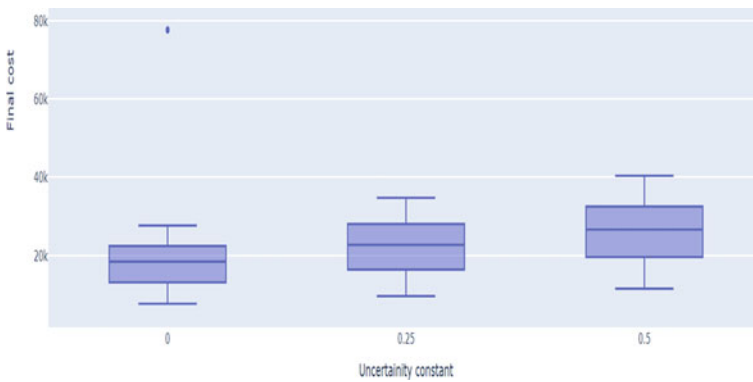


Fig. 2 Final cost and uncertainty constant box plot

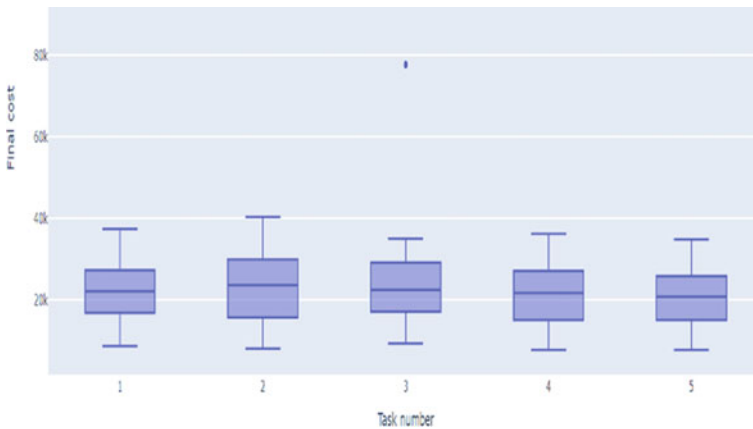


Fig. 3 Final cost and task number box plot

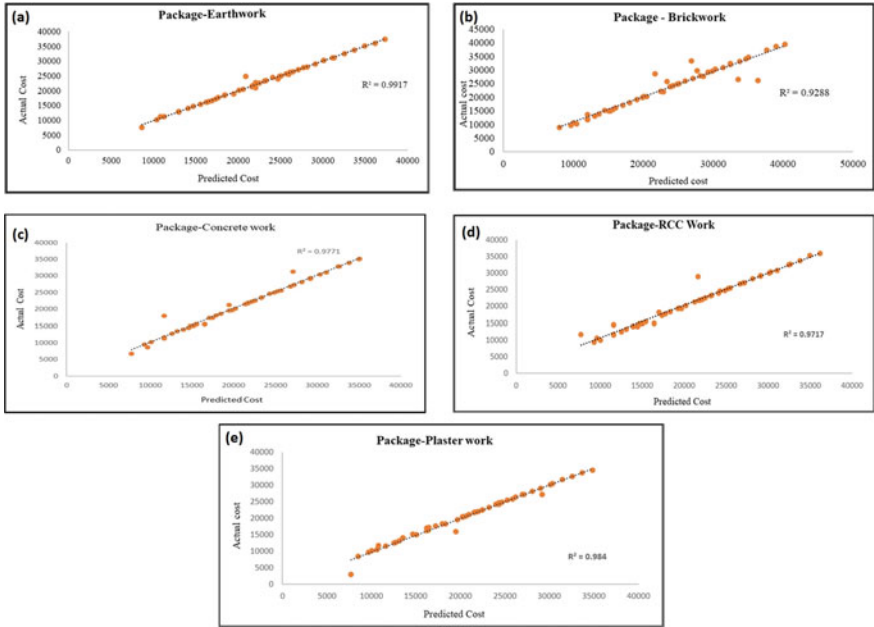


Fig. 4 Scatter plot of actual and predicted cost

The predicted cost corresponding to the actual cost for earthwork, brickwork, concrete work, RCC work, and plaster work is presented in Fig. 4. The R^2 value is used to meter the reliability of the trend line. It is used to quantify the goodness of the fit. The values of R^2 lie in the range of 0.92–0.99 for different work packages indicating a high-reliability value between the actual and predicted cost. All the work packages had a positive correlation between actual and predicted cost.

The range of training and testing accuracy for the earthwork package was observed and presented in Fig. 5. The testing and training accuracy varies in the range of 94–99% using random forest regression. This implies that the performance of model is good.

5 Discussion

The model can be used in construction projects to estimate the cost in the dynamic stage considering the uncertainties that may occur on site. According to the results shown in Fig. 2, the cost of construction has a range of 17,000–21,000 INR when the constant of uncertainty is low, 19,000–23,000 INR when the uncertainty constant is medium, and 20,000–26,000 INR when the uncertainty is high. This reflects that construction cost increases due to occurring uncertainties. The results in Fig. 3 indicate that the cost for earthwork package is 18,000–22,000 INR, 19,000–25,000 for

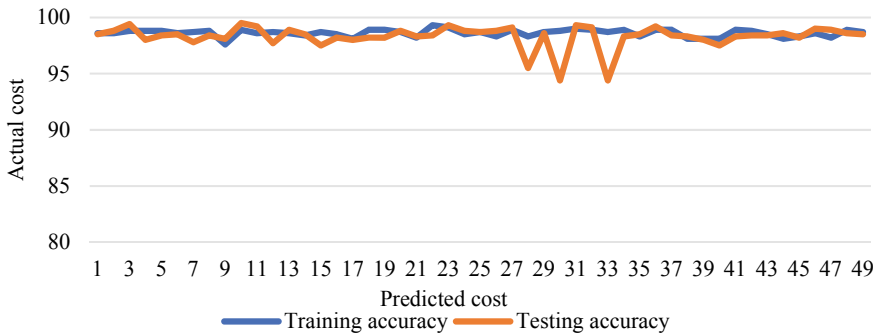


Fig. 5 Training and testing accuracy—random forest

brickwork INR, 19,000–24,000 INR for concrete work, 17,000–21,000 INR for RCC-work, and 17,000–20,500 INR for plastering work. The cost of brickwork is more due to requirement of skilled labor. The R^2 value was used to evaluate model performance. The value of R^2 score value is 0.99–0.92 indicating a very good performance. Other performance indicators used to evaluate the performance of the model are linear regression, K neighbours regressor, random forest, and decision tress. The main performance indicator is the random forest regressor because it does not get influenced by noise in the data. The noise is the additional non-significant values present inside the dataset. The random forest accuracy values have a range of 94–99%. This value indicates that the model evaluation is highly accurate. The performance indicators reflect that the model has efficient performance and can be effectively used in cost estimation during the execution phase.

6 Conclusion

When estimate is prepared in the planning stage of project, the occurrence of possible uncertainties like accidents, material shortage, and equipment breakdown are totally ignored. The uncertainties significantly influence the duration of the project and lead to cost overruns. The cost is one the important constrains for the client satisfaction. The inclusion of uncertainties can significantly improve the reliability of the cost estimation. The previously made models used statistical techniques for improving the predictions in the planning stage; however a machine learning model that predicts the cost overruns in the execution/build up stage considering the possible uncertainties occurring on site was never attempted. The developed machine learning model can predict the cost of construction based on the conditions of a site including the uncertainties. The model can be used in the execution phase of construction projects by substituting the dataset and making effective prediction without any high programming skills. The accuracy of the developed machine learning model was found to

be in the range of 0.92–0.98 indicating a good performance value, thereby outperforming the traditional statistical and traditional methods used for cost estimation. Also, the machine learning model can deal with the nonlinearities in the dataset in a better way. Thus, the proposed model could be a promising solution to the problem of inaccurate cost prediction.

References

1. Wang R, Asghari V, Cheung CM, Hsu SC, Lee CJ (2021) Assessing effects of economic factors on construction cost estimation using deep neural networks. *Autom Constr* 134:104080. <https://doi.org/10.1016/j.autcon.2021.104080>
2. Elmousalami HH (2020) Data on field canals improvement projects for cost prediction using artificial intelligence. *Data Br* 31:105688. <https://doi.org/10.1016/j.dib.2020.105688>
3. Matel E, Vahdatkhaki F, Hosseinalamdary S, Evers T, Voordijk H (2022) An artificial neural network approach for cost estimation of engineering services. *Int J Constr Manag* 22(7):1274–1287. <https://doi.org/10.1080/15623599.2019.1692400>
4. Elmousalami HH (2019) Intelligent methodology for project conceptual cost prediction. *Heliyon* 5(5):e01625. <https://doi.org/10.1016/j.heliyon.2019.e01625>
5. Zhao ZY, Lv QL, Zuo J, Zillante G (2010) Prediction system for change management in construction project. *J Constr Eng Manag* 136(6):659–669. [https://doi.org/10.1061/\(asce\)co.1943-7862.0000168](https://doi.org/10.1061/(asce)co.1943-7862.0000168)
6. Sayed M, Abdel-Hamid M, El-Dash K (2023) Improving cost estimation in construction projects. *Int J Constr Manag* 23(1):135–143. <https://doi.org/10.1080/15623599.2020.1853657>
7. Chakraborty D, Elhegazy H, Elzarka H, Gutierrez L (2020) A novel construction cost prediction model using hybrid natural and light gradient boosting. *Adv Eng Inform* 46. <https://doi.org/10.1016/j.aei.2020.101201>
8. Thongpeth W, Lim A, Wongpairin A, Thongpeth T, Chaimontree S (2021) Comparison of linear, penalized linear and machine learning models predicting hospital visit costs from chronic disease in Thailand. *Inform Med Unlocked* 26:100769. <https://doi.org/10.1016/j.imu.2021.100769>
9. Alshamrani OS (2017) Construction cost prediction model for conventional and sustainable college buildings in North America. *J Taibah Univ Sci* 11(2):315–323. <https://doi.org/10.1016/j.jtusci.2016.01.004>
10. Tayefeh Hashemi S, Ebadati OM, Kaur H (2020) Cost estimation and prediction in construction projects: a systematic review on machine learning techniques. *SN Appl Sci* 2(10):1–27. <https://doi.org/10.1007/s42452-020-03497-1>
11. Regona M, Yigitcanlar T, Xia B, Li RYM (2022) Opportunities and adoption challenges of AI in the construction industry: a PRISMA review. *J Open Innov Technol Mark Complex* 8(1):45. <https://doi.org/10.3390/joitmc8010045>
12. Shoar S, Chileshe N, Edwards JD (2022) Machine learning-aided engineering services' cost overruns prediction in high-rise residential building projects: application of random forest regression. *J Build Eng* 50:104102. <https://doi.org/10.1016/j.jobe.2022.104102>
13. Morid MA, Sheng ORL, Kawamoto K, Ault T, Dorius J, Abdelrahman S (2019) Healthcare cost prediction: leveraging fine-grain temporal patterns. *J Biomed Inform* 91:103113. <https://doi.org/10.1016/j.jbi.2019.103113>
14. Koc K, Ekmekcioğlu Ö, Gurgun AP (2021) Accident prediction in construction using hybrid wavelet-machine learning. *Autom Constr* 133:103987. <https://doi.org/10.1016/j.autcon.2021.103987>
15. Hsu PY, Aurisicchio M, Angeloudis P (2017) Investigating schedule deviation in construction projects through root cause analysis. *Procedia Comput Sci* 121:732–739. <https://doi.org/10.1016/j.procs.2017.11.095>

Effectiveness of Multicriteria Decision-Making for Ongoing Construction Projects—AHP Method



S. Antony Kevin and A. Arokiaprakash

1 Introduction

The construction projects in real time include several different stakeholders; each of them contributes overall complexity to the projects. Applying multicriteria decision-making (MCDM) helps to solve complex issues in the simplest form. MCDM is a computational process that sorts the criteria in order to indicate which alternative option is best. It is the pre-feasibility tool. The theory's use of computational methods incorporates several criteria and order of preference in evaluating and selecting the best option among many alternatives based on the desired outcome. It is a tool utilized in all areas, especially in the engineering field. It is used for evaluating/assessing/selecting alternative decisions. It acts according to the performance in cases when there is more than one complicated criterion. When analyzing the construction sector, it can be challenging to determine where to place the line because the final outcome of a project affects so many individuals, groups, organizations, and levels of government. Gould and Joyce [1] To solve an issue with MCDM, one must determine what kind of problem it is, what the requirements are, what the desired outcome is, what kind of solutions are, and so on. Some examples of MCDM techniques include analytical hierarchical process (AHP), technique for order preference by similarity to an ideal solution (TOPSIS), elimination and choice expressing reality (ELECTRE), best worst method (BWM), decision making trail and evaluation laboratory (DEMATEL), and grey relation analysis (GRA). When dealing with a complicated or advanced issue, the MCDM method is the way to go [1–5]. The analytical hierarchical process (AHP) method is used. It is systematic, analytical and combines both mathematics and psychology. While choosing a complicated situation, several factors must be

S. Antony Kevin · A. Arokiaprakash (✉)

Department of Civil Engineering, Faculty of Engineering and Technology, SRM Institute of Science and Technology, Kattankulathur, Tamil Nadu 603203, India

e-mail: arokiapa@srmist.edu.in

weighted in order to focus on alternative solutions. It arranges everything in a hierarchical structure, picks and ranks and shows the greatest possible option. The main contribution of this study is to suggest suitable decisions on the right time to get the work done on schedule, in addition to looking over the cost and time so far. The looking over responded that one should think from the executive point of view and client point of view [6, 7]. The extension of the study will have a major contribution to MCDM technique applications. The research refines and reforms the application of tools and methods, which helps the project completion effectively. The study gets extended for further work needed to develop refined methods to reach sustainable solutions in the MCDM method. Expanding the study brings on effectiveness to the development of MCDM methods to address the challenges with alternative decisions. Many Authors has reviewed the functions of MCDM in the initial stage of a project. Most of the research based on the delay in completion and financial crisis are focused on by many authors. AHP is a tool to sort out the raised issues in the ongoing project. The study was expanded in order to create refined strategies for reaching the optimal alternative solutions in the MCDM approach. The study improves the efficiency of developing MCDM methods to deal with the difficulties of making decisions among several alternatives. The majority of the study deals with completion on schedule and the financial crisis. AHP technique is a resolving issue in currently undergoing projects [2, 8].

2 Literature Review

The construction projects are usually expensive and call for a lot of human resources, equipment, and money. Large losses are frequently experienced when a construction engineering project fails. Prior research has concentrated on identifying risks, but strategic resource allocation for managing risk following risk identification has received insufficient attention. According to the literature, grey rhino risks are common in construction projects and have mutually reinforcing relationships, making it challenging for managers to allocate adequate resources to preventative measures. To that end, this research presents a novel multicriteria decision-making (MCDM) approach to risk ranking that takes into account the relative strength of eliciting relationships between different hazards. Five of the grey rhino risks encountered during the construction engineering project for the Chengdu-Chongqing Middle Line High-speed Railway were randomly selected for this study, and the results were used to create a detailed ranking. The breakdown of the supply chain, mistakes in making decisions, exposure to legal and policy risk, a slowing economy, and stakeholder disagreements are all potential problems. In other words, the results demonstrated that the other risks stemmed from the policy and legal risk and constituted symptoms rather than the underlying cause of the problem [9].

The construction industry concern over how to lessen the effects of construction has grown in the wake of the Goals for Sustainable Development. In this setting, modern methods of construction (MMC) have become a potent tool for mitigating

life-cycle impacts by maximizing material efficiency. This research compares the environmental impact of several up-to-date methods for building single-family homes out of concrete. The traditional reference design, the precast design, the lightweight slab design with pressurized hollow discs, and the design based on double-wall structural components are all evaluated and compared in terms of their life-cycle performance in terms of sustainability. The findings demonstrate that a comprehensive approach to sustainability, taking into account all three aspects, results in well-rounded designs, the preferences of which need not be identical to those generated from the various life-cycle perspectives [10].

Zhu [4] Making good decisions is crucial to the success of any business or project, but it is essential in the complex field of construction. Given the complexity of many decision problems, multiple criterion decision-making (MCDM) is a valuable technique. New forms of MCDM are constantly being developed and are increasingly being used to solve practical building issues. Thus, conducting a comprehensive literature review is strongly recommended to show the development of mainstream MCDM methods and their current status in building applications. Finally, the statistical study is applied to explain the current state of the study. After that, we analyze how MCDM techniques were put to use in the building through a thematic qualitative discussion. It is possible to identify potential obstacles (such as practical application, reliability, delay effect, evolving and upcoming challenges, and the level problem) to current studies through further discussion. As a bonus, it helps inform the discussion of where MCDM research and practice could go [8].

Buildings, roads, and other infrastructure are only things built as a nation progresses. In the past, building projects in the United Arab Emirates (UAE) had several issues, the most significant of which were cost and schedule overruns. There may be shareholder discord and discontent as a result. Because of this, research into the topic is necessary, as is an attempt to apply the “best value” notion to government building endeavors. To do this, the use of the notion of “best value” to help people understand what we mean, explain how it applies to the complicated public sector in the United Arab Emirates, and classify it so that it can be used effectively. Therefore, this study aims to offer a research approach for constructing an evaluation model for outcomes-based optimal value by using the multicriteria decision-making tool to rank the criteria in order of importance. A complete model may then be developed in subsequent investigations using the same process [11, 12].

2.1 Objectives

This study aims to propose suitable decision making in the site for completing the project in the scheduled time. In addition, the work done on program financial cost, materials arrived on site in time, and the productivity of effective team in both technical and non-technical and physical conditions. The extension of the study will have a major contribution to MCDM techniques applications. The research refines

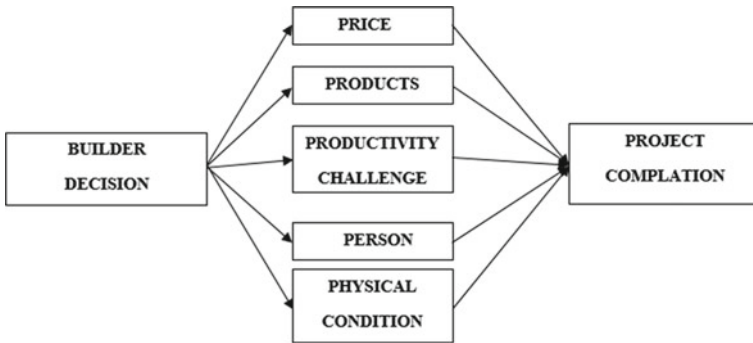


Fig. 1 Five Ps (price, products, productivity challenges, persons and physical condition significant issues that frequently arise in construction

and reforms the application of the AHP method, which effectively helps the project completion.

The primary objective of the study

- To analyze decision-making criteria for sustainable project completion.
- To evaluate the predictive ability of MCDM criteria by identifying the key indicators through expert decisions to complete the project’s scheduled time.

The secondary objective of the study

- To determine effective decision-making based on AHP method requirements in project completion.

2.2 Conceptual Framework

See Fig. 1.

2.3 Definition for All Variables

Price —It is deciding factor in considering the market for overall construction application
Product —Bringing materials to the workplace demands both quality and quantity
Productivity —Operation for preparing, managing, and supervising a building work
Persons —The company organizes work for people who involve in the project
Physical changes and Climatic challenges —Unfavorable impact during site activity
AHP —Applied to determine critical decisions based on arithmetic values

3 Research Design

The research methodology is based on the following steps: The literature survey based on MCDM concepts and construction management articles was presented to highlight the core idea of the study. This article aims to propose some suggestions for the construction projects facing the likely change through a case study. So, in the following section, the case study is presented: a plan with the problem of construction delay considered an MCDM problem. Possible alternatives for decision-makers are mentioned. The governing criteria in this MCDM problem are defined, and criteria weights are determined. AHP methods referred to some crises during the project in progress. Criteria values are determined, and alternatives are prioritized using grey decision-making tools. Discussions about the calculations and conclusions presented. The research design in this study was descriptive in nature. It has attempted to obtain information concerning the MCDM constructs in bringing about alignment between strategy and corporate strategy, which in turn results in a competitive advantage for construction firms in Chennai. Two types of data collecting can be used in any research, namely qualitative and quantitative. These two sorts of data each have their own set of advantages and disadvantages. In most cases, qualitative data obtained from interviews and observations is a massive corpus of unstructured textual materials that are difficult to analyze. It does, however, allow academics to explore a limited number of topics in considerable depth and complexity. Quantitative data, on the other hand, necessitates the use of standardized instruments in order to fit people's diverse perspectives and experiences into a small number of predetermined response categories to which numbers are allocated [13].

4 Hypothesis

H1—There is no significant association between price, product, productivity challenges, person, and physical conditions concerning experience.

H2—There is no significant relationship between price, product, productivity challenges, person, and physical conditions with respect to MCDM reconsideration.

5 Tools and Techniques Used for the Study

The study was conducted among the builders who are engaged in the construction field in Chennai city. Convenience sampling was adopted to choose the respondents' data collected with a structured questionnaire. Five points Likert scale was used, ranging from strongly disagree to 5 strongly agree, respectively. The sample size is 110 respondents. Correlation, regression, and ANOVA are used as statistical tools to analyze data with SPSS software.

6 Results

The results of the questionnaire survey are tabulated in Tables 1, 2, 3, 4, 5 and 6.

Table 1 Reliability statistics

Cronbach's alpha	No. of items
0.919	50

Interpretation

Cronbach's alpha value is $\alpha = 0.919$. It is excellent, the survey questionnaire is reliable, and items are within the constants

Table 2 KMO and Bartlett's test

Kaiser–Meyer–Olkin measure of sampling adequacy		0.721
Bartlett's test of sphericity	Approx. Chi-square	3493.731
	Df.	1225
	Sig.	0.000

Interpretation

In this Kaiser Meyer–Elkin Bartlett's test, construct validity is reliable. It has significant values

Table 3 Tests of normality

	Kolmogorov–Smirnov ^a			Shapiro–Wilk		
	Statistic	Df.	Sig.	Statistic	Df.	Sig.
Variable	0.112	110	0.002	0.968	110	0.009

Lilliefors Significance Correction

Interpretation

Data is normally distributed go for parametric tests

Table 4 Descriptive statistics

	N	Mean	Std. deviation
What kind of issues are solved by using MCDM	110	2.10	0.967
How do you be successful in implementing MCDM in your project	110	3.21	1.220
Give your ratings on MCDM	110	1.91	0.736
Would you like to reconsider MCDM again in your project	110	2.06	1.377
Valid N (listwise)	110		

Interpretation

The mean score and standard deviation value of the respondents used MCDM methods to take decisions in their projects

Table 5 Correlation test

	Price	Products	Productivity	Persons	Physical condition
Price	1	0.544**	0.428**	0.351**	0.384**
Products		1	0.599**	0.593**	0.482**
Productivity			1	0.586**	0.437**
Persons				1	0.409**
Physical condition					1

H1—There is no significant association between price, product, productivity challenges, person, and physical conditions concerning experience (**significance level)

Interpretation

The significance level indicates the relationship among the variables. If the significance level is more than 0.05, it is positive relation or else less than 0.05, and it is negatively correlated among the variables

7 Analytic Hierarchy Process (AHP)

The analytic hierarchy process (AHP) can be described as it is a concept and technique for measuring the comparison distances. When comparing, users are more concerned with the ratios among particular variables than their precise dimensions. It is challenging to create a measuring range for intangible characteristics of possibilities. Thus, employing relative measures helps the study. The primary objective of the main analytic hierarchy process (AHP) is to provide ranges for possibilities that line the concept of relative evaluation through pairwise comparison of possibilities. To demonstrate the importance of management study without proceeding much further, we may make use of certain criteria provided by “Saaty”. The founder of the analytic hierarchy process has published the study in publications. The analytic hierarchy process is utilized in investments such as accounting, construction, funding, quantitative, advertising, hybrid securities, plan layout, predicting the future, wealth (expenditure, planning, and mental well-being), regulations and standards, logistics, irrigation study, and optimization techniques. In political challenges like weapon management, disputes and settlement, legislative, risk analysis, military drills and global importance. In civil services like academics, challenging activity, sustainability considerations, healthcare, legal, medicines, and demographic trends (cross-border movements, birth rates). Industry management, investment strategies, and innovation are examples of engineering fields.

Following procedure involved in AHP:

1. Describe the issue
2. Choose the decision-making group
3. Determine the problems and goals
4. Create the hierarchical framework
5. Determine the reliability of variables
6. Possibilities must be evaluated
7. Prepare statement on observations

Table 6 Regression test

Model summary				
Model	R	R square	Adjusted R square	Std. error of the estimate
1	0.121 ^a	0.015	- 0.033	1.89443

^a Predictors: (Constant), e, a, d, c, b

^b Dependent Variable: variable

ANOVA ^a						
Model		Sum of squares	Df.	Mean square	F.	Sig.
1	Regression	5.519	5	1.104	0.308	0.907 ^b
	Residual	373.241	104	3.589		
	Total	378.760	109			

^a Dependent Variable: variable

^b Predictors: (Constant), e, a, d, c, b

Coefficients ^a						
Model		Unstandardized coefficients		Standardized Coefficients	t Sig.	
		B	Std. error	Beta		
	(Constant)	9.258	1.379		6.716	0.000
	Price	- 0.017	0.044	- 0.047	- 0.395	0.693
1	Products	0.003	0.043	0.011	0.073	0.942
	Productivity	0.035	0.036	0.130	0.975	0.332
	Persons	- 0.014	0.043	-0.042	- 0.321	0.748
	Physical condition	0.021	0.066	0.037	0.319	0.751

^a Dependent Variable: variable

H2—There is no significant relationship between price, product, productivity challenges, person, and physical conditions with respect to MCDM reconsideration

Interpretation

The value $p = 0.000 < 0.05$, the hypothesis is accepted, and the variables have a significant relationship. If not, there is no significant relationship between the variables hypothesis is rejected if it is more than 0.05 values

8. Verify for logic
9. Complete decision-making
10. Prepare paperwork for the final outcome.

8 Discussions

This study shows that (ref. Tables 1, 2, 3, 4, 5 and 6) applying and because of implying MCDM in their projects causes goodness. It is assistance in all kinds of sources. The test value Alpha and KMO test results are adequate. The constructs are

equally distributed, all the variables are correlated, and the result proves that there is a significant relationship among the variables. The hypothesis of the study is proven in their respective values.

9 Conclusion

This study concluded that solving the instantaneous crisis in projects helps solve various issues by using MCDM Price, Product, Productivity, Person, and Physical Conditions. It is the instantaneous crisis in projects following traditional methods, previous experiences, discussions with others in the same locality, experts' involvement, and MCDM. The concepts' AHP has been taken in as secondary objectives by conserving many review papers the author has proven the effectiveness of the application. The limitation of the study is that it does not work in AHP software due to scale development 1–9 level of rating; the study already implies a 5-point Likert scale for its development. An implication of MCDM already exists. Further research can take AHP methods to develop the matrix for the development of the study.

References

1. Gould, Joyce N (2009, 2014) Construction project management, 3rd ed. Pearson Prentice Hall
2. Sánchez-Garrido AJ et al (2022) Multicriteria decision-making applied to the sustainability of building structures based on modern methods of construction. *J Clean Prod* 330:129724
3. Emovon I, Ogheniyerovwho OS (2020) Application of MCDM method in material selection for optimal design: a review. *Results Mater* 7:100115
4. Zhu X et al (2021) Application of multiple criteria decision making methods in construction: a systematic literature review. *J Civ Eng Manage* 27(6):372–403
5. Górecki J, Núñez-Cacho P (2022) Decision-making problems in construction projects executed under the principles of sustainable development—bridge construction case. *Appl Sci* 12(12):6132
6. Navarro IJ et al (2020) life cycle sustainability assessment for multicriteria decision making in bridge design: a review. *J Civ Eng Manage* 26(7):690–704
7. Asadabadi MR et al (2019) Are MCDM methods useful? A critical review of analytic hierarchy process (AHP) and analytic network process (ANP). In: Zhou Z (ed) *Cogent engineering*, vol 6, no 1. Informa UK Limited
8. Ameri Shahrabi M, Mohammadi H (2013) Investigating different challenges in construction projects. *Manage Sci Lett* 3(7):1869–1872
9. Chiang F-Y et al (2017) Construction contractor selection in Taiwan using AHP. *Int J Eng Technol* 9(3):211–215
10. Haseeb M et al (2012) Problems of projects and effects of delays in the construction industry of Pakistan. *Austr J Bus Manage Res* 01(06):41–50
11. Hosani IA (2021) Developing of multicriteria decision making model in assessment of outcomes based best value in UAE public construction sector
12. Ahmed R, Afifi M, Nassar A (2019, June) Using multicriteria decision making (MCDM) methods in Egyptian construction projects. In: Canadian society for civil engineering annual conference, Laval, QC, Canada

13. Gunduz M, Khader BK (2020) Construction project safety performance management using analytic network process (ANP) as a multicriteria decision-making (MCDM) tool. In: Computational intelligence and neuroscience, vol 2020, Hindawi Limited, pp 1–11

House Price Prediction in Southern Chennai Using Machine Learning Algorithms



J. Prasanna Kumar, M. B. Sridhar, R. Sathyanathan, and B. Divya

1 Introduction

Housing has always been a crucial priority in India as it falls under the category of essential needs. Housing is an important for the country's economy, job opportunities, taxes, and salaries, and also, it contributes in improving the quality of life [1]. Investing in real estate involves various risks, like market risk, tenant risk, location risk, liquidity risk, and financial risk. The rapid urbanization of cities further complicates the prediction of real estate prices, making it difficult for buyers and sellers to understand the parameters that define the value of a property [2]. Investors, particularly retail investors, encounter a significant challenge in evaluating the value of real estate when considering investment opportunities. Determining the true value of a property can be a difficult task. Models that can assist individuals in predicting the value of a property are in demand. Hedonic price model is the statistical model aims to determine the price of a property based on the most relevant factors for predicting its value [3]. It involves a mathematical equation that enables the prediction of house prices. An artificial neural network (ANN) is a machine learning technique that emulates the structure and function of the human brain, allowing it to identify intricate patterns and connections within data which can be used for the prediction of house price. The evaluation of model has been done using the metrics like R-squared, mean absolute error (MAE), root mean squared error (RMSE), and mean absolute percentage error (MAPE). During the comparison, both models were evaluated using the same metrics, and the results indicated that the ANN model was more accurate than the HPM model [4]. An artificial neural network is a deep learning algorithm that utilizes a computerized model to predict house prices based on several parameters and datasets. This model is trained using the available data and then tested to

J. Prasanna Kumar · M. B. Sridhar (✉) · R. Sathyanathan · B. Divya
Department of Civil Engineering, SRM Institute of Science and Technology, Kattankulathur,
Tamil Nadu 603203, India
e-mail: sridharb@srmist.edu.in

accurately predict prices. Analyzing the predicted output using evaluation metrics such as R-squared, root mean squared error (RMSE), mean absolute error (MAE), and mean absolute percentage error (MAPE) enables us to obtain improved values [5].

Machine learning algorithms are another computerized model that can be employed to determine the different parameters that affect the cost of properties. This model can be of great benefit to buyers and sellers who wish to stay informed about the real estate market, and the accuracy of the model can be ensured through the use of error metrics. There are different machine learning algorithms available for predicting the price of real estate properties based on collected data, and the best algorithm can be identified by comparing the model-predicted value to the market value [6]. The dataset used for machine learning algorithms comprises crucial parameters that affect housing costs. These parameters include the area, location, amenities, number of bedrooms and bathrooms, condition, and age of the house. A literature survey was carried out to discover past research and surveys on real estate prices. This was done to identify the parameters covered in previous studies and the types of algorithms used to predict housing prices [7]. which was evaluated with some evaluation metrics.

Machine learning algorithms like support vector machine (SVM), back propagation (BP), and particle swarm optimization (PSO) were used to analyze and predict the prices of real estate houses as time series models. SVM provides better results than BP and PSO [8]. Australia's previous real estate transactions are examined using various machine learning techniques such as regression trees, neural networks, support vector machines (SVM), and principal component analysis (PCA) to develop helpful models for people interested in purchasing or selling homes [9]. Using machine learning algorithms such as decision tree, decision tree regression, and multiple linear regression, the price of a house can be predicted based on various parameters in which linear regression predicts with more accuracy than other models [10].

The techniques used in prediction of and analysis were logistic regression, support vector machine, Naive Bayes, stochastic gradient descent, extra trees, K-nearest neighbor, and voting classifier [11]. Decision tree algorithm, multiple linear regression has been used in the house price prediction model [10]. The models like particle swarm optimization and Support Vector Machine has been used to create the model for prediction of house price [8]. Machine learning techniques have been employed to predict the price of a house, Algorithms such as Artificial Neural Network, Support Vector Machine, and Random Forest were employed for this purpose. in which the Random Forest method outperforms the other models in terms of accuracy [12]. The price is considered as a dependent variable. The models were created and analyzed to predict the price of the house and compared along with each model [13].

There is a need for the prediction of house price in Southern Chennai by considering distance parameters and various amenities. The amenities have been combined all together as a ranking. The objective of the research is to develop models using linear regression, K-nearest neighbor, and random forest with the factors influencing the property's price in Southern Chennai. The house price using machine learning algorithms like multi linear regression and decision tree regression. Some of the

major inputs like area, rooms, baths, stories, driveway, and garage are considered for the prediction of house price [13] determines the price of the property.

2 Study Area

Chennai is the capital city of the state of Tamil Nadu, located on the eastern coast of India. Chennai stands sixth in the highly populated cities in India. Chennai district covers an area about 426 square kilometers. Southern Chennai has been selected as a study area as it was urbanizing rapidly with more numbers of IT parks, industries, educational institutions, and automobile companies. Southern Chennai includes the areas like Guindy, Perungudi, Velachery, Alandur, and Sholinganallur. Southern Chennai consists of important roads like East Coast Road, Old Mahabalipuram Road which connect the city internally and externally. Southern Chennai consists of airport and metro stations. It consists of the number of malls, beaches, and other entertainment centers in the area.

Figure 1 represents the study area which is highlighted in the image. The data collection contains information about the latitude and longitude coordinates for each data point, which enables one to determine the distance between each data point. The latitude and longitude were plotted on the dataset to provide an accurate distance between the parameters and the study points. The other parameters were also plotted in the shapefile using ArcGIS and Google Earth. Figure 2 represents the study points of houses which are ready for sales are plotted.

3 Methodology and Data Collection

The parameters which determine the value of the property are taken into consideration and col. Generally, the house price is determined by various factors that are categorized as physical and distance factors. The factors like area, number of bedrooms, number of bathrooms, number of floors, lift availability, parking availability, swimming pool availability, age of the building, CCTV availability, security availability, power backup facility, gym facility, sports facility, kids' play area availability, furnished status, number of balconies, distance from the national highway, MRTS, bus stops, central bus stands, airports, entertainment cities, colleges, schools, hospitals, central business district, IT companies, and industries are the factors considered for predicting the house price. Further the missing data and unnecessary data were removed from the dataset and provided in the algorithm for prediction [14]. The numerical and categorical parameters were normalized.

The physical characteristics such as number of floors, lift availability, parking availability, swimming pool availability, age of the building, CCTV availability, security availability, power backup facility, gym facility, sports facility, kids' play area availability, furnished status, and number of balconies are ranked based on

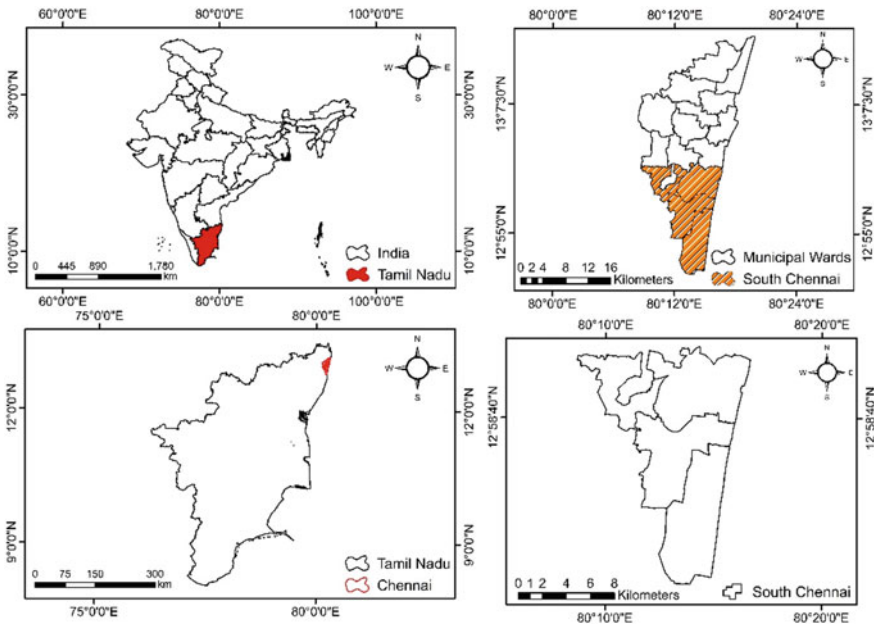


Fig. 1 Study area of southern Chennai

its availability. The amenities considered, the allotted for each amenity is given in Table 1 and the ranking has been given out of 11 for each property. The data has been collected from advertisements, site visits, and online advertisements. For each property every influencing factor have been collected in the data collection process. Data was collected for 330 houses from different areas located within the Southern Chennai boundary. The mean and the standard deviation calculated from the collected data for each parameter are given in Table 2. Figure 3 represents the methodology adopted for developing the models for predicting the price of the houses in the study area.

The collected data of 330 house prices and the value of the parameters are utilized to develop the price prediction models. The selected algorithms of KNN, random forest, and linear regression are trained with 70% of the collected data, and the remaining 30% of the data is utilized for testing of the trained models. By doing so, the accuracy of the machine learning model is improved, and its predictions are more reliable [15].

3.1 Linear Regression

The input data has been provided as an independent variable, and the output is considered as the dependent variable in linear regression analysis. This relationship

Fig. 2 Study points plotted in Southern Chennai

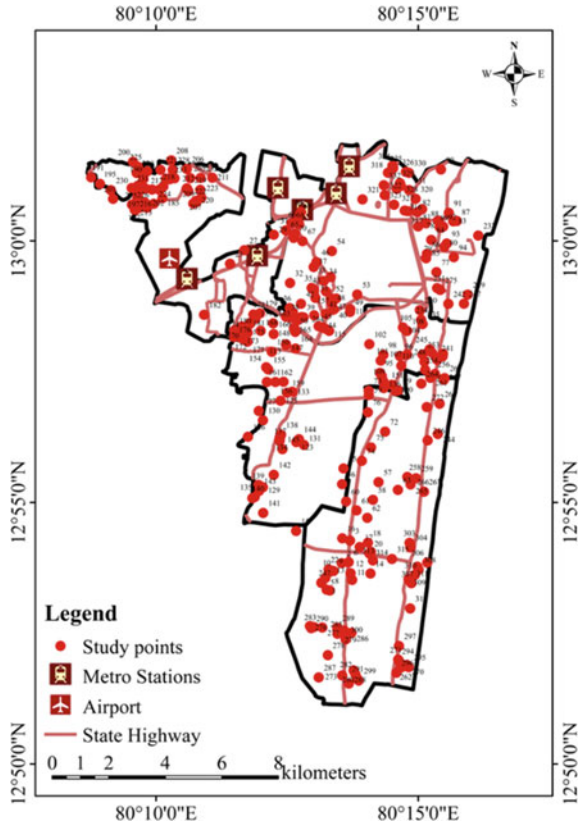


Table 1 Physical parameters as rankings

S. No.	Parameters	Description
1	Lift facility	Availability of lift in the apartment (1 = yes, 0 = no)
2	CCTV facility	CCTV availability in the apartment (1 = yes, 0 = no)
3	Security	Security availability in the apartment (1 = yes, 0 = no)
4	Pool availability	Swimming pool availability in the apartment (1 = yes, 0 = no)
5	Gym facilities	Availability of gym facility in the apartment (1 = yes, 0 = no)
6	Power backup	Availability of power backup in the apartment (1 = yes, 0 = no)
7	Sports facilities	Availability of sports facility in the apartment (1 = yes, 0 = no)
8	Kids play area	Availability of kids play area (1 = yes, 0 = no)
9	Furnished status	Furnished status of the house (1 = yes, 0 = no, 2 = semi)
10	Parking facility	Availability of parking in the apartment (1 = yes, 0 = no)

Table 2 Descriptive statistics of dataset

S. No	Parameters	Description	Mean	Standard Deviation
1	Price	Actual price of the house	9618.01	4387.70
2	Number of bedrooms	Number of bedrooms available in the house	2.74	0.85
3	Number of bathrooms	Number of bathrooms available in the house	2.61	0.93
4	Total area of the house	Total area of the house in sq. ft	1513.38	1124.41
5	Number of floors	Number of floors in the apartment	0.07	0.09
6	Number of balconies	Number of balconies available in the house	1.35	0.94
7	Age	Age of the building	4.88	4.83
8	Distance to MRTS	Distance from house to the railway station	8.68	49.37
9	Distance to CBD	Distance from house to the central business district	17.87	5.74
10	Distance to central bus stand	Distance from house to the Central bus stand	19.63	8.01
11	Distance to airport	Distance from house to the airport	13.93	5.79
12	Distance to nearby bus stop	Distance from house to the nearby bus stop	0.61	0.53
13	Distance to nearby schools	Distance from house to the nearby schools	1.02	0.64
14	Distance to nearby colleges	Distance from house to the nearby colleges	3.71	19.18
15	Distance to nearby IT companies	Distance from house to the nearby IT companies	3.51	3.29
16	Distance to Industries	Distance from house to the nearby industries	1.00	0.90
17	Distance to National highway	Distance from house to the national highway	1.34	1.20
18	Distance to entertainment cities	Distance from house to the entertainment cities	4.94	2.69
19	Distance to nearby hospital	Distance from house to the nearby hospital	1.61	1.49

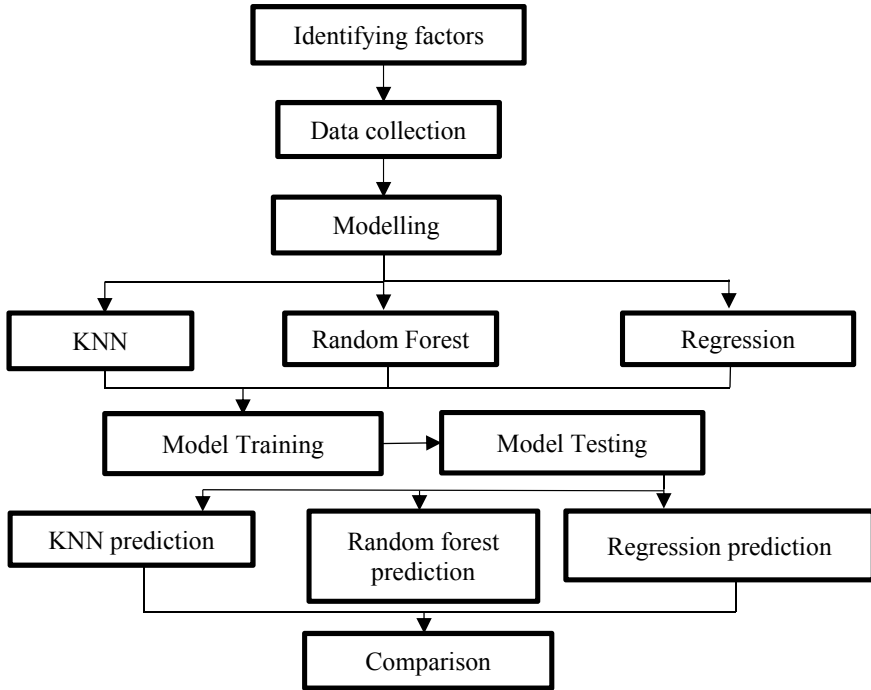


Fig. 3 Methodology adopted for the study

between the variables can be used for both classification and regression models, with the goal of accurately predicting the dependent variable’s value based on the independent variable [13].

3.2 *K-Nearest Neighbor*

The K-nearest neighbor (KNN) algorithm is a classification and regression tool. When the user specifies the value of *K*, the algorithm identifies the nearest point in the classified list. The *K* value is used to move the data point closer to the classified points. In KNN regression, distance calculation is used to classify the data points. Two types of distance calculation are commonly used—Euclidean distance and Manhattan distance. For regression problems, the closest point is determined by taking the mean of existing points. The algorithm calculates the distance in the same way. The purpose of KNN is to classify a data point in the classifier by calculating the distance between it and the classified points. The closest classifier is identified and used for classification. The most important aspect of this algorithm is determining the nearest point or distance between the new point and the classified points [16].

3.3 *Random Forest*

The random forest model blends many small decision trees to generate a prediction. These decision trees comprise decisions and predictions that are combined to yield the most precise forecast for a given dataset. This model is typically employed to predict complex sets of data and improves the dataset's accuracy [17].

3.4 *Evaluation Metrics*

In the field of machine learning, evaluation metrics are utilized to assess the performance of a model. The selection of these metrics is contingent upon the type of problem being addressed. For the price prediction, the metrics like root mean squared error (RMSE), mean absolute error (MAE), and mean squared error (MSE) are used [1].

3.4.1 *Mean Squared Error*

Mean squared error is the commonly used evaluation metrics which is the average of squared difference between actual value and the predicted value.

$$\text{MSE} = \frac{1}{n} \times \sum (y_i - \hat{y}_i) \quad (1)$$

3.4.2 *Root Mean Squared Error*

It is a variation of mean squared error (MSE) by which the square root of average of squared difference between actual value and predicted value.

$$\text{RMSE} = \sqrt{\frac{1}{n} \times \sum (y_i - \hat{y}_i)} \quad (2)$$

3.4.3 *Mean Absolute Error*

It is the average of absolute differences between actual price and the predicted price.

$$\text{RMSE} = \sqrt{\frac{1}{n} \times \sum (y_i - \hat{y}_i)} \quad (3)$$

4 Results and Discussion

The models to predict house prices were developed using three machine learning algorithms of linear regression, KNN, and random forests. These models were initially trained with 70% data and then tested with 30% of the collected the data. The developed model’s metrics were retrieved and presented in Table 3. The results showed that random forests had the highest accuracy, while linear regression had the lowest accuracy. The findings suggest that random forests are more suitable for this task than linear regression since they can handle complex nonlinear relationships between variables. Linear regression, on the other hand, assumes a linear relationship between input and output variables, limiting its ability to make accurate predictions. KNN, being a non-parametric algorithm, is useful when modeling underlying variable relationships is difficult. However, it requires extensive data and can be computationally expensive.

The developed models were used to predict the house price of 10 new houses. The predicted prices were compared with the actual prices, and evaluation metrics are calculated in represented in Table 4 [18].

The root mean squared error (RMSE) of the linear regression model is 87.152 rupees. Based on the k-nearest neighbor (KNN) model used to predict house prices,

Table 3 Evaluation metrics for the model

Evaluation metrics	Linear regression	K-nearest neighbor	Random forest
MAE	7595.53	2248.38	2205.37
MSE	77,246,843.71	6,975,740.4	9,220,512.26
RMSE	87.15	47.417	46.961

Table 4 Actual price and predicted price comparison

Actual price	Predicted price			Price deviation		
	Linear regression	KNN	Random forest	Linear regression	KNN	Random forest
12,909	12,101	12,474	12,729	808	435	180
4999	5528	4498	4789	529	501	210
6452	6000	6328	6242	452	124	210
5396	5000	5496	5576	396	100	180
8611	7999	8300	8877	612	310	266
10,000	9124	10,420	9734	876	420	266
10,000	9678	9399	9728	322	601	272
11,111	10,280	10,788	11,355	831	323	244
5988	6710	6880	9381	722	892	393
6000	5688	5998	6221	312	2	221

the root mean squared error (RMSE) of the model is 47.417 rupees. The values are similar with the previous results [19]. The random forest model used to predict house prices shows the root mean squared error (RMSE) of 46.961 rupees, indicating that the average difference between predicted and actual house prices is relatively small [20], which was also compared with previous researches [21]. The random forest model shows promise in its ability to predict house prices with reasonable accuracy.

5 Conclusion

Predicting the house prices is a complex and intricate task, but it is crucial for various entities and groups involved in the real estate sector. This research explored different approaches and models for prediction of house prices, such as linear regression, decision trees, and random forests. It is discovered that each method has its own strengths and weaknesses, and the selection of a model depends on the specific problem and the available data. The linear regression model predicted the prices with an RMSE of 87.15 rupees, KNN predicted the prices with an RMSE of 47.417 rupees, and random forest model predicted the prices with an RMSE of 46.96 rupees. It was found that more advanced models like random forests generally outperform traditional linear regression models. The price prediction models will be useful for the buyers and sellers to determine the price of the property. They are also useful for prediction of house price in large-scale data, unknown areas and can be useful for the real estate people to have a knowledge about how price is being fixed for the property. Further factors like interior design, construction materials can be considered in the future price prediction studies.

References

1. Tiwari P, Rao J (2016) Housing markets and housing policies in India, ADBI working paper 565. Asian Development Bank Institute, Tokyo
2. Bhat PA, Shafiq M, Mir A, Ahmed P (2017) Urban sprawl and its impact on land use/land cover dynamics of Dehradun City, India. *Int J Sustain Built Environ* 06(02):513–521
3. Limsombunchai V (2004) House price prediction: hedonic price model vs. artificial neural network. In: New Zealand agricultural and resource economics society conference, 25–26. New Zealand Agricultural and Resource Economics Society
4. Abidoye RB, Chan APC (2018) Improving property valuation accuracy: a comparison of hedonic pricing model and artificial neural network. *Pacific Rim Property Res J* 24(01):71–83
5. Stubnova M, Urbanikova M, Hudakova J, Papcunova V (2020) Estimation of residential property market price: comparison of artificial neural networks and hedonic pricing model. *Emerg Sci J* 04(06):530–538
6. Yu H, Wu J (2016) Real estate price prediction with regression and classification CS 229 autumn 2016 project final report
7. Rahadi RA, Wiryono SK, Koesrindartoto DP, Syamwil IB (2015) Factors influencing the price of housing in Indonesia. *Int J Housing Markets Anal* 08(02):169–188

8. Wang X, Wen J, Zhang Y, Wang Y (2014) Real estate price forecasting based on SVM optimized by PSO. *Optik (Stuttg)* 125(03):1439–1443
9. Phan TD (2019) Housing price prediction using machine learning algorithms: the case of Melbourne city, Australia. In: *Proceedings—international conference on machine learning and data engineering*. Institute of Electrical and Electronics Engineers Inc., pp 8–13
10. Thamarai M, Malarvizhi SP (2020) House price prediction modelling using machine learning. *Int J Inf Eng Electron Bus* 12(02):15–20
11. Modi M, Sharma A, Madhavan P (2020) Applied research on house price prediction using diverse machine learning techniques. *Int J Sci Technol Res* 09(04)
12. Banerjee D, Dutta S (2017) Predicting the housing price direction using machine learning techniques. In: *IEEE international conference on power, control, signals and instrumentation engineering*, house to be a very influential factor in determining the house 2998
13. Kaushal A, Shankar A (2021) House price prediction using multiple linear regression. In: *Proceedings of the international conference on innovative computing & communication*
14. Priya P, Mahalakshmi G, Manojkumar K, Kumararaja V (2022) Property price prediction and possibility prediction in real estate using linear regression. *Adv Appl Math Sci* 21(7):3805–3819
15. Rawool AG, Rogye DV, Rane SG, Vinayk DR, Bharadi A (2021) House price prediction using machine learning. *IRE J* 04(11):29–33
16. Wang L (2019) Research and implementation of machine learning classifier based on KNN. In: *IOP conference series: materials science and engineering*. IOP Publishing Ltd.
17. Varma A, Sarma A, Doshi S, Nair R (2018) House price prediction using machine learning and neural networks. In: *Proceedings of the international conference on inventive communication and computational technologies, ICICCT 2018*. Institute of Electrical and Electronics Engineers Inc., pp 1936–1939
18. Sridhar MB, Sathyanathan R (2022) A Comparison between artificial neural network and hedonic price model. *Int J Intell Syst Appl Eng Estimation Residential Land Price Suburban Region India*
19. Srour IM, Kockelman KM, Dunn TP (2002) Accessibility indices: connection to residential land prices and location choices. *Transp Res Rec* 1805(1):25–34
20. Mukhlishin MF, Saputra R, Wibowo A (2017) Predicting house sale price using fuzzy logic. In: *Artificial neural network and K-nearest neighbor. 2017 1st international conference on informatics and computational sciences (ICICOS)*
21. Adetunji AB, Akande ON, Ajala FA, Oyewo O, Akande YF, Oluwadara G (2021) House price prediction using random forest machine learning technique. *Procedia Comput Sci*: 806–813

Access the Prospect of Automation in Inventory Management of Construction Projects



B. Pavan Kumar and A. Arokiaprakash

1 Introduction

Construction industry is the one of the oldest industries in the world. Total 16% of nations population depends on the construction industry for the live hoods. Over 30 million of people are creating a more than 200 billion rupees worth of assets in India. That a total of 5% of nations GDP. Even the industry is oldest there were no much changes in the way of construction from the centuries.

1.1 Inventory Management

Inventory control is crucial to the timely and successful execution of building projects. The purpose of inventory is to keep materials on the site so it can also be made available as needed of their employ. Inventory always stores finished goods, spare parts, and tools in addition to the raw materials needed for construction. In the Indian construction business, it is fairly typical for projects to go over budget and behind schedule. With good inventory management implementation, issues like these may be resolved. It would improve on-site productivity and ensure steady project progress. Inventory management entails a number of steps, including material selection, purchase, and transportation costs. Inventory management has the budget of its own, which it uses to cover a variety of expenses for keeping and operating the inventories at the best level. The key expense incurred whenever a business places an order is the purchasing cost. Storage costs are incurred when items are kept off-site before being utilized. Expenses related to material storing or storage costs. These costs that

B. Pavan Kumar (✉) · A. Arokiaprakash
Department of Civil Engineering, Faculty of Engineering and Technology, SRM Institute of Science and Technology, Kattankulathur, Tamil Nadu 603203, India
e-mail: pb2266@srmist.edu.in

include the price of rent, power, and other expenses may be internal or external. If a project is also to be completed successfully, then all requirements must be met through communicating effectively, making crucial decisions, and maintaining a check on inventory and managing it appropriately.

1.2 Automation in Construction

Automation in the construction idea offers advantages and disadvantages, just like any new adjustments to the established approach of the project (Fig. 1).

Construction automation has the ability to revolutionize the way projects are carried out from beginning to end and advance the sector by empowering it with technology. When unforeseen delays like those caused by bad weather, design conflicts, and equipment failure would cause major delays in the project’s projected timeline and may be avoided by employing automated information management, project length must be reduced. There are issues that need to be resolved for successful use of automation in construction because of the significant shift that it demands. However, there are certain special obstacles that must be recognized and overcome in order for these new approaches to be implemented successfully. One of automation’s key advantages is the reduction of necessary effort and increased openness, which will lower corruption. All systems that profit from corruption will thus be opposed to these new techniques. The primary obstacles are the initial cost and transition period, especially for small businesses who cannot afford these sources despite the advantages. There are undoubtedly more difficulties that anyone employing this new way

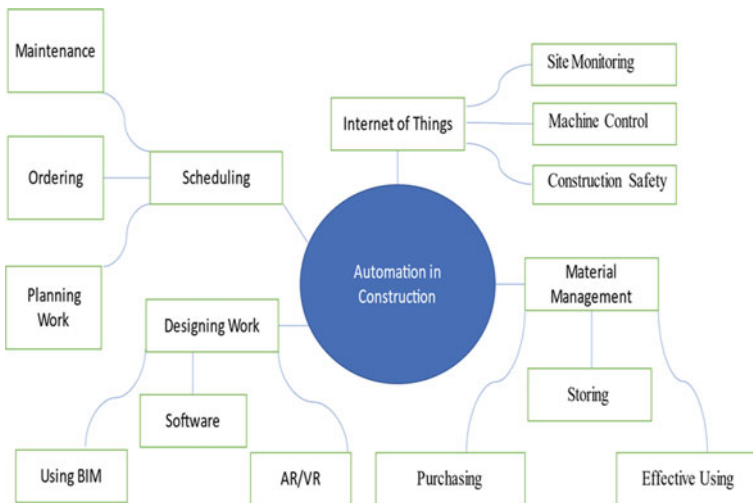


Fig. 1 Automation in construction

may encounter. To increase productivity, safety, and product quality, automation and robotic technology are widely seen as being important components of the construction industry's future. Construction work is occasionally carried out in hazardous conditions and circumstances; thus, robotics is required to optimize equipment functioning and enhance safety and job quality. Construction processes that are automated result in year-round productivity. The construction sector should employ machinery and equipment more and more in order to complete projects quickly, safely, and with high quality. By employing devices like machines and robots in the proper locations, human effort and danger are decreased. Given that India has the second-largest labour force in the world, automation is a necessary complement that meets the demands of mega-building and fast-track development. In India nowadays, new automation technologies are replacing human labour.

1.3 Advantages of Automation in Construction

By implementing the automation in the construction, there are many advantages for the productivity increasing and for improvement of quality of work.

Construction workers who use manual labour to create distinctive buildings and structures will have less work to do as a result of automation and robotization. Industrial robots offer significant social and economic advantages and enable a more logical use of labour resources. The removal of individual and subjective elements also leads to an improvement in work quality and a decrease in rejections in the manufacturing of construction materials and goods, which both contribute to an increase in labour productivity.

Save Time. The fact that automation helps save time is among its finest advantages. Consider the time required to analyse each item of inventory, manually update the stock levels on various platforms, and continue doing all of this every day for business as usual.

Accurate Inventory Level. The failure of sellers to maintain optimal stock levels in their inventory is a significant issue that they frequently encounter. For instance, the majority of the items will either continue to sell out on their Website or will be rotting in a warehouse owing to low demand. Such circumstances harm a company's reputation with consumers as well as its bottom line. Customers flock to your rivals when things on your Website run out of stock, so you miss out on a potential sale. When paired with the power of data analytics, automation aids in precisely anticipating demand. This implies that you will be alerted automatically to refill when your items are likely to run out of stock and client requests are anticipated.

Improves the Quality of Delivery. The success or failure of your business is greatly influenced by the amount of your product delivery. Despite this, even the slightest error can have a negative influence on the standard of delivery and, in turn, lower customer satisfaction. According to statistics, 81% of consumers encountered a "out

of stock” goods scenario, which left them unsatisfied and reduced a company’s earnings. Automation can assist by reminding vendors to replenish their stock levels and by offering a uniform tracking system. Since tracking enables the consumer to keep a close check on their package, it can enhance the quality of delivery.

Reduces the Risk for Human Error. Hand-completing jobs leave more possibility for human mistake. On the other hand, automation eliminates this necessity and lessens the reliance of inventory management on manual procedures. Statistics show that administrative mistakes resulting from human chores may be minimized by as much as 41% only by adopting the barcode system for tracking items. Furthermore, correct inventory management expenses make it easier to calculate costs for things like operational and sales.

1.4 Disadvantages of Automation

Employment Reduction. Worker displacement has already been mentioned as a major drawback of automation. Almost always, a person whose job has been replaced by a machine experiences a period of emotional stress, notwithstanding any potential societal advantages from retraining displaced employees for alternative employment. The worker may also be geographically displaced in addition to being uprooted from their place of employment.

High Initial Cost. Other drawback of automated equipment includes the high capital investment necessary to invest in automation (designing, fabricating, and installing an automated system can cost millions of dollars), the need for more maintenance than with a manually operated machine, and a general lack of flexibility in terms of the possible products compared to a manual system.

Need of Frequent Updating. Many issues can be conveniently solved by automation. However, if a modification is made that necessitates modifying the automation, this convenience may become unnecessary. These kinds of adjustments might end up costing the organization valuable time and resources while simply serving to increase burden.

1.5 ABC Analysis in Inventory

The ABC analysis serves as the foundation for managing materials and plays major role in defining stocking as well as the frequency of inventory inspections. It is a method of analytically regulating various inventory items. The ABC categorization system is based upon the Pareto’s law, which argues that even a relatively small number of products have a disproportionately high monetary worth. In this method, each content is divided into one of three groups, namely A, B, or C.

In the ABC classification of the materials, it is classified as

- For materials of A is 20% materials account for the 70% value of the money.
- For materials of B is 30% materials account for the 25% value of the money.
- For materials of C is 50% materials account for the 5% of money value.

All of the items that are in inventory are classified according to the factors as investment, material value used, and inventory items nature. Proper analysing the material through the ABC analysis and categorizing them accordingly will help in the better material and inventory management. After categorizing the material, the most important material can be tracked and monitored by using automation techniques (sensors and cameras) will help in saving the time and efforts for ordering and from running out from stocks.

1.6 Internet of Things

The construction business is undergoing a change because to technologies like artificial intelligence (AI), 3D printing, robotics, big data, and virtual reality. IoT is being utilized to address problems at many levels, from straightforward design changes to complex multifactorial problems. It could be simpler to define IoT by what it does not do than what it does. There are a wide variety of IoT applications. An equipment or a system joins a larger network if it is connected to the Internet.

Site Monitoring. Because of their size, construction sites are too large to depend entirely on manual security. A construction site's IoT security approach might focus on preventing entry, early detection, and recovery from undesirable actions. For site monitoring, autonomous vehicles and unmanned aerial vehicles are preferred. Drone-like UAVs are suitable for monitoring and keeping an eye on large areas. These drones are capable of collecting precise aerial photographs and survey maps of a location. It may also be utilized to remotely monitor the development of the construction project. Aerial photographs have been proven to be helpful for both monitoring and spotting possible issues that would not have been seen from the ground.

It takes a lot of time and is prone to human mistakes to manually monitor the placement and condition of heavy tools and equipment at a building site. Accuracy and convenience are increased when an IoT-enabled tracker is attached to such assets. These trackers' data collection is reliable and simply used. Real-time tracking and cloud-based analytics assist in reducing theft and boosting productivity. The wonderful thing about IoT is that even smaller locations and short-term initiatives may use it without breaking the bank. These IoT-enabled equipment, gadgets, and robots are accurate, practical, and profitable.

Machine Control. Construction work involves a lot of large, powerful machinery that are operated by people. By IoT, this work may be further made simpler. The construction process can become productive and self-sufficient. These devices can operate much more accurately and with less assistance from humans if they have

sensors. Information about equipment condition and maintenance needs may also be continually monitored using IoT sensors. This can avoid unforeseen failures or calibre faults. IoT-powered tools can speed up building without sacrificing quality.

Construction Safety. Everyone is worried about the safety of the workers at the construction site, including the owners, managers, and employees. Even though these locations have several safety precautions, they are among the riskiest workplaces. Impactful tools and technologies have been developed by IoT. It could aid in enhancing the security measures at building sites. Wearable technology gear is no longer just for the fitness sector. They have carved out a crucial place for themselves in the building sector. Many advantages are provided by these tools, such as labour tracking and safety. These tools can aid in staff counts and location. It can also monitor their health by monitoring their pulse rate and give safety alerts as needed. For instance, air quality monitors can notify staff members to hazard before they visit an area. IoT can predict problems at building sites and eliminate risks.

Building Information Modelling. Building information modelling, or BIM, is a process which involves the intelligent modelling of building. An engineer can design a structure digitally before building it physically using BIM software. This aids students in comprehending both the structural and functional elements of the building. Due to financial restrictions, labour shortages, competing demands, and deadlines, builders, engineers, and project managers frequently encounter a variety of difficulties. They can effectively pinpoint the disparities and identify problems early on thanks to this software.

2 Literature Review

- Rao et al. [1], are stating various cases studied by using these technologies and approaches for real-time problem detection, worker behaviour, and health inspection, and monitoring static and dynamic construction settings are covered through this chapter. In both indoor and outdoor locations, their perspective concentrates on sensor technologies and approaches for real-time mapping, scene interpretation, placement, and monitoring of construction operations. As it can assist overcome the difficulties and restrictions associated with each sensor, integrating many types of sensors frequently offers advantages over employing just one type of sensor. sensors for communication and positioning. Devices for tracking and identification, like barcodes and RFID, are examples. Real-time monitoring techniques include tracking, positioning, and scene interpretation.
- Ogunseiju et al. [2], are stating that sensing technologies gather data on the context and state of construction resources and processes throughout a facility's lifespan to increase participant communication, project 9 safety, and quality control. The shortage of skilled workers is a major obstacle to the broad deployment of these technologies. Understanding which sensing technologies are used by the business, how widely this are used, and what the industry believes CEM programs should

cover are all necessary for properly preparing this future workforce. Additionally, it is crucial to comprehend the amount of the sensing technology instruction provided by CEM programs.

- Madhavarao et al. [3], are stating the planning, buying, handling, stocking, logistics, and waste management phases of the material management process. What are inventory management techniques: ABC analysis is used for identify the items material that are going to have a high impact on the overall cost of the inventory. Here in the ABC analysis, the materials are been divided into three groups: A Group, B Group, and C Group. Materials for A group should be given the most attention, those for B group should be given moderate thought, and materials for C group should be given the least thought. The crucial project management technique is S-curve analysis. The projected and actual costs of material components were compared in this investigation. The overview of project performance in terms of cost and timeline is provided by an S-curve. The construction project team can identify industrial and construction and possible issues that might affect the project if the right corrections is not done by analysing the S-curves. Also, the cost variance is analysed using the S-curve, which is determined as the difference between the budgeted costs as well as the real costs of the job completed. The cost efficiency is determined by dividing the budgeted cost by the real price of the task completed.
- The successful construction project depends heavily on the delivery and availability of resources (such as materials) at the appropriate time and location. In order to gather all the necessary data and information, it is essential to monitor every item used during a building phase. Manual data collection relies on the abilities and motivation of the employees, which makes it unreliable and incomplete. Accurate data is required for construction projects not only to manage ongoing projects but also to update 10 the historical database. These improvements will make it possible to plan future projects more effectively in terms of costs, timetables, manpower allocation, etc. In the construction industry, where radio frequency identification will be used to gather work place data through automatically detecting resources and global navigation satellite system (GPS) in combined with GIS can be used track the location of their both internal and external transportation vehicles, the advantages of integrating RF-based techniques with geographical information systems (GIS) are evident. The GIS application will evaluate and support the historical tracing of the materials used in construction projects through the use of various technologies [1, 4].
- Kasim et al. [5], are stating managing resources well is essential for boosting productivity in construction projects. The overall construction budget, quality, and schedule are commonly impacted by poor material control. Several construction organizations employ manual processes, which involve paper-based methods and are problematic because they frequently lead to human mistakes in both the tracking of resources and in the material management as a whole. The bulk of the currently used manually, mainly paper based techniques for material tracking on construction projects material control issues [6].

- The technique that allows for product tracking is RFID tagging. On the building site, the technology has been used for a variety of purposes, including tracking inventory. As input for preventing future mishaps, specific building site locations. The performance monitoring of the material all through delivery at the construction area, transportation to something like a specific contracting company, and upcoming use, in addition to the monitoring of such price of material usage on the construction area, the checking of both the order of steel, and the tracking of the temperature of porous materials are all logistics-related issues that can be realized using radio frequency identification. A key component of construction is logistics, which has an impact 11 on how quickly a project moves forward. The transfer of supplies and tools necessary to support a building project is referred as construction management.
- The data gathering is crucial for management since building projects are dynamic and complicated. Trying to cut technologies like communication and digital construction sites are introduced by sensing technologies, and these new technologies improve in betterment of construction efficiency and safety. Despite significant scientific research in this field, the implementation of sensor technologies has indeed been delayed by technological and human-related issues. The current state of different sensors under development includes physical sensors, location-based sensing technologies, sight-based sensing technologies, wireless networks of sensors, and techniques and resources for existing literature.
- **AUTOMATION—A NEW MILLENNIUM TECHNOLOGY FOR CONSTRUCTION INDUSTRIES:** By this research paper, the author studied about the construction process. How the automatic machines are going to change the entire work of the construction is studied and what are all the machines which are being used for the automation work is clearly studied and mentioned in this paper. Different kind of robots which are used for the different work is mentioned and explained. Advantages like the safety of the workers and faster completion of project are discussed, and for the disadvantages the higher initial expenditure is mentioned as the primary aspect. The final conclusion of this paper work is how the robots and the automation in the construction are developed and which way they can be more developed is discussed Rajgor et al. (2013).
- **DRIVERS FOR THE APPLICATION OF AUTOMATION IN CONSTRUCTION ACTIVITIES:** By this research paper, the author studied about the automation techniques and where are the areas in the site they need to get improved has been studied. Different type of question is prepared for knowing the impact of the drivers in the automation. The questions include the training and site of the construction for implementing the automation, about the mindset of the construction companies and how to use the robots and what the barriers were discussed. In conclusion, it stated that by making the construction sector fully automated there are many advantages in the form of productivity and performance of the workers [7].
- **AUTOMATION IN CONSTRUCTION INDUSTRY IT IS APPLICATION AND BARRIERS TO IMPLIMENTATION ON CONSTRUCTION SITE:** The automation techniques that has been used and what are the barriers in the

implementing of the techniques were known by doing the questionnaire survey. Several aspects are taken for the questions and asked for knowing the impact of the automation techniques in the construction. After collecting the data, it has been analysed, and mean value has been determined. By that the place where it is lacking and need improvements is easily known. The questions are given on various sectors in the construction; it includes the designing, planning, management, etc.

- **EFFECTS OF AUTOMATION ON CONSTRUCTION INDUSTRY PERFORMANCE:** In recent scenario the researchers are tried to find what are all the effects that will be carried on the construction by using the automation in it. For the work the author chose the construction workers who works in the site are and the contractors and many more. What are all the problems faced by the automation and without automation technology is known by doing this work. The stress that workers are getting in the construction and the ways that can be mitigated is also the recent research interest. .
- **A REVIEW OF THE ADVANTAGES AND DISADVANTAGES OF THE USE OF AUTOMATION AND ROBOTICS IN THE CONSTRUCTION INDUSTRY:** In this review paper, the author is discussing about the hazardous and the dirt that caused by the construction and the ways how the automation work by using robots can be helpful. What is meant by automation and robotics in construction is explained in detail in this review paper. The advantages and the disadvantages of using the automation are discussed in this paper. The advantages cover the increase in safety, productivity, and sustainability of construction. Disadvantages are like the loss of jobs; high cost is mentioned [8].

3 Summary of Literature

- (i) The final summary of this literature review is that all the authors from the papers that have collected stating that implementing the sensor technology into the material or construction management can lead to save more amount of money for the client.
- (ii) The main problem that has noticed by studying all the papers is that the initial cost will be very high for implementing this sensor into the construction site. But once after installing this sensor not only for the material tracking but it can be used for many different purposes also like in the safety control at site and in the labour monitoring also.
- (iii) By studying and analysing the papers and the journals, it shows the places where the construction industry is lacking and what are all the necessary steps to be taken for the better improvement of the project.
- (iv) And also, how the smart construction is going to make the major changes in the industry in the future. The integrating of the sensors is also discussed in the papers and how this is going to improve the quality and safety in the construction is discussed.

- (v) Even though the construction industry started to implement the sensors but it is still lacking in some places and this has to be improved for the better quality and safety of project.

4 Conclusion

- (i) Still, after many years of implementing the sensors there is still many places where the sensors can be improved. Based on the studies there is only certain level of implementing sensors in construction majorly the sensors are been used in the big construction projects because of the cost of the sensors. If this is the case it will take even more time for the smaller projects to implement the sensors in their projects due to pricing and analysing the data.
- (ii) As mentioned, there are still several places in the construction sector where automation needs to be improved or still yet to be implemented. By doing the analysis work, it is clear that due to the high initial cost of implementing the automation technology, every contractor or owner is taking a back step.
- (iii) The high initial cost is very common in implementing this due to the advanced technology, and it is not very familiar to everyone in India. For some more upcoming years, it will be the same, once after getting familiar with the technology, the cost will automatically get down. And by the survey it is clear that there are still many areas in the construction where automation is not yet implemented at all and it has to end due to the generation change. For tendering works, some advanced technology like AR and VR can be used for a better understanding of the project, and tendering can be done which will make it very easy and simple.
- (iv) The more that automation techniques get implemented the faster the work will get done. Not only the faster completion of the project but also the safety will also be increased due to these techniques. A highly educated person needs to perform all these processes daily at the site area. By faster completion of the work, it will lead to saving a huge amount of money for the owner. For the ordering method, most of the contractors are preferring the daily ordering method because of the fewer budget issues and due to the owner. On a construction site or in the supply chain, the precise positioning of components is crucial. Only knowing or assuming to know that the items have arrived at the building site or are accessible in the marketplace based on an inaccurate or outdated written document not enough is a warehouse or a laydown area.

References

1. Rao A, Radanović M, Liu Y, Hu S, Fang Y, Khoshelham K, Palaniswami M, Ngo T (2022) Real-time monitoring of construction sites: sensors, methods, and applications. *Autom Constr* 136:104099. <https://doi.org/10.1016/j.autcon.2021.104099>
2. Ogunseiju O, Akanmu A, Bairaktarova D (2021) Sensing technologies in construction engineering and management programs: a comparison of industry expectations and faculty perceptions. National science foundation
3. Madhavarao B, Mahindra K, Asadi S (2018) A critical analysis of material management techniques in construction project. *Int J Civil Eng Technol* 9
4. Sardroud JM, Limbachiya M, Sardroud JM, Limbachiya MC, Saremi AA (2015) Ubiquitous tracking and locating of construction resource using GIS and RFID Sustainable construction using concrete. In: View project building information modeling and green building view project ubiquitous tracking and locating of construction resource using GIS and RFID
5. Kasim N, Latiffi AA, Fathi MS (2013) RFID technology for materials management in construction projects—a review. *Int J Constr Eng Manage* 2(4A):7–12
6. Kasim N (2015) Intelligent materials tracking system for construction projects management. *J Eng Technol Sci* 47(2):218–230
7. Oke A, Aigbavboa C, Mabena S (2017) Effects of automation on construction industry performance. In: Second international conference on mechanics, materials and structural engineering (ICMMSE 2017). Atlantis Press, pp 370–374
8. Llale J, Setati M, Mavunda S, Ndlovu T, Root D, Wembe P (2020) A review of the advantages and disadvantages of the use of automation and robotics in the construction industry. In: The construction industry in the fourth industrial revolution: proceedings of 11th construction industry development board (CIDB) postgraduate research conference 11. Springer International Publishing, pp 197–204
9. Vasilaki E, Rigakis I, Papadoulis T, Staridas A, Psaroudaki A, Frantzeskakis L, Makris Z, Lazari D, Antonidakis E (2022) Inertia sensor detecting materials using electromagnetic signals. *WSEAS Trans Syst* 21:140–146
10. Navon R (2007) Research in automated measurement of project performance indicators. *Autom Constr* 16(2):176–188
11. Nasir H (2009) A model for automated construction materials tracking. Master's thesis, University of Waterloo
12. Ahmed Z (2017) The impact of material management on construction project delivery in Maldives. Faculty of Engineering and Science, Universiti Tunku Abdul Rahman
13. Daniel CO (2019) Effects of materials management on the productivity of an organisation. *World J Innov Res (WJIR)* 6(1):16–22
14. Attaran M (2012) Critical success factors and challenges of implementing RFID in supply chain management. *J Supply Chain Oper Manage* 10(1):144–167
15. Karagiannaki A, Papakiriakopoulos D, Bardaki C (2011) Warehouse contextual factors affecting the impact of RFID. *Industr Manage Data Syst*
16. Ismail A-R (2009) Assessing the relationship between the Internet, radio frequency identifier (RFID), and information technology (IT) flexibility: a correlational study and findings. Ph.D. diss., Capella University
17. Hasan N, Saini S (2017) Survey of use and impact of RFID: a case study of IIT Delhi. In: Curation and management of cultural heritage through libraries, 563–577
18. Navon R, Berkovich O (2006) An automated model for materials management and control. *Constr Manag Econ* 24(6):635–646
19. Akinradewo OI, Aigbavboa CO, Okafor CC, Oke AE, Thwala DW (2021) A review of the impact of construction automation and robotics on project delivery. *IOP Conf Ser Mater Sci Eng* 1107(1):012011
20. Fadamiro OP, Oke AE (2019) The level of awareness of automation technology in the construction industry. *IOP Conf Ser Earth Environ Sci* 331(1):012013

21. Feldmann FG (2022) Towards lean automation in construction—exploring barriers to implementing automation in prefabrication. *Sustainability* 14(19):12944
22. Navon R, Berkovich O (2006) An automated model for materials management and control. *Constr Manage Econ* 24(6):635–646
23. Rajgor M, Dr. Pitroda J (2013) Automation: a new millennium technology for construction industries 2:79–81